INSTITUTE OF PHYSICS PUBLISHING REPORTS ON PROGRESS IN PHYSICS

Rep. Prog. Phys. **69** (2006) 2843–3067 doi:10.1088/0034-4885/69/11/R01

Supersymmetry facing experiment: much ado (already) about nothing (yet)

Luc Pape[1] **and Daniel Treille**[2]

[1] Institute of Particle Physics, ETH, 8093 Zurich, Switzerland
[2] PH Department, CERN, 1211 Geneva 23, Switzerland

Received 22 June 2006
Published 24 October 2006
Online at stacks.iop.org/RoPP/69/2843

Abstract

This report emphasizes the comparison between supersymmetric models and experiments. A minimal theoretical introduction is included as a guide to the interpretation of results. The existing constraints from low energy measurements, accelerator searches (LEP, Tevatron and HERA) and non-accelerator searches for neutralinos are presented. Prospects for upgrades of these facilities and for the LHC and linear collider are summarized. Most discussions are made in the framework of the minimal supersymmetric standard model inspired by supergravity (MSUGRA). But alternatives such as gauge mediated supersymmetry breaking (GMSB), anomaly mediated supersymmetry breaking (AMSB), models with R-parity violation and even alternatives to supersymmetry are also briefly considered.

(Some figures in this article are in colour only in the electronic version)

This article was invited by Professor G Barbiellini.

Contents

1. Why supersymmetry

There exist many excellent reviews and lecture notes on supersymmetry. The present review emphasizes the comparison between model predictions and experiments. Formulae are kept to a minimum and are given without derivation. For a more rigorous presentation of the theory, the reader is referred to the primer of Martin [1] or other lecture notes and reviews [2], to mention only some of them. Our main purpose is to develop an intuitive understanding of the physics involved, mostly by examples, and to confront the largely different predicted signatures with experimental tests, present or future. This review attempts, in the first chapters, to give some explanations of the main ideas and scenarios of supersymmetry. However, readers can also enter its content at any item of their choice to get information about the corresponding results and bibliography up to 2005.

The unavoidable starting point is the so-called standard model (SM) [3], rebaptized by Wilczek as the 'Theory of Matter' [4], a more adequate name for such a successful theory. It combines the weak, electromagnetic and strong interactions into a single framework, where the physical laws are invariant under the local gauge transformations $SU(3)_c \times SU(2)_L \times U(1)_Y$. The $SU(3)_c$ component leads to quantum chromo dynamics (QCD) with colour as conserved quantum number [5] and the $SU(2)_L \times U(1)_Y$ to the electroweak theory with the weak isospin and the hypercharge as conserved quantum numbers before it is broken. The source particles are the spin 1/2 fermions, leptons and quarks organized in three families, and the mediators of the interactions are the vector bosons. The electroweak symmetry is supposed to be spontaneously broken by the vacuum expectation value of a spin-zero field, its remnants being the $U(1)_{em}$ symmetry of quantum electro dynamics (QED), with the conserved electric charge quantum number, and a physical particle, the Higgs boson [6]. The SM has been shown to describe to high accuracy all present results from precision measurements at the LEP and SLC accelerators and from low energy measurements, such as $(g-2)$, electric dipole moments and rare decays of K and B mesons. Crucial to this was the ability to compute and test the theory at the level of quantum corrections, which are sensitive to the mass of unobserved particles through virtual effects [7]. An example was the measurement of the top-quark mass from the LEP/SLC electroweak radiative corrections, well before it was directly detected at Fermilab, as illustrated in figure 1. The presently achieved accuracy of the electroweak measurements at LEP/SLC even brings evidence that, once the top contribution is accounted for and if no new particles besides the Higgs boson contribute to the radiative corrections, this boson should be light, below ∼250 GeV at the 95% confidence level (CL). Some caveat on the consistency of results is given below. Unfortunately, the Higgs boson has escaped direct detection, even at the highest energies of LEP.

In spite of its impressive successes, the SM cannot be the final theory. In addition to its many unexplained parameters, a fundamental limitation is that it does not contain gravity. At present, the best candidate to reconcile quantum physics with gravity is string theory [9, 10]. Its natural energy scale is around 10^{18}–10^{19} GeV, which makes direct experimental tests sound like foolish dreams. It has been demonstrated that string theory embeds both the above gauge theories and gravity, unifying all known forces of nature. But, equally important for an experimentalist, it also predicts departures from the SM picture. Some of its implications might be subject to experimental measurements: first, it makes supersymmetry (SUSY) a likely symmetry of nature (see, e.g. Schwarz [11]); second, it requires additional spatial dimensions and it has been conjectured that some of them could correspond to energy scales of the order of TeV. Supersymmetry extends the SM with new particles carrying masses of at most 1–10 TeV (if one sticks to solving the hierarchy problem, see below) and requires the existence of several Higgses, one of which is predicted to have a mass below

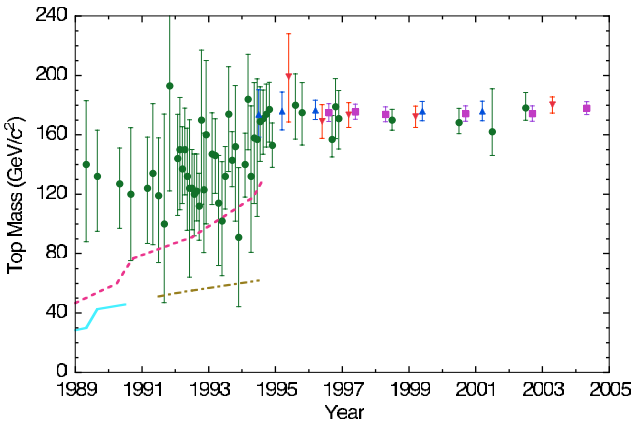

Figure 1. Evolution of the top mass measurements. The circles are the LEP predictions from radiative corrections; the squares and triangles are the direct measurements from Tevatron. From [8].

about 130 GeV. Clearly, had the Higgs exploration been pushed ∼10–15 GeV higher at LEP, the present review would certainly have a quite different content. The path to follow for experiments, from our current energy scale towards the strings, therefore seems to be to (1) discover the lightest Higgs (highest priority); (2) look for SUSY particles; (3) find some signs revealing the existence of extra space dimensions (the latter is briefly discussed in section 2.1).

The SM keeps a clear distinction between the matter constituents (fermions) and the mediators of the interactions (vector bosons). Supersymmetry [12] introduces symmetry vector-bosons by associating each fermionic state of the SM to a bosonic state in the same multiplet and vice versa. If supersymmetry were an exact symmetry, the associated fermionic and bosonic states would have identical masses. This situation is analogous to the symmetry of particles and antiparticles or of two spin projection states of the same particle. In this sense, supersymmetry does not really introduce new particles, but only new states (superpartners) of the SM particles. In the simplest SUSY version, called the minimal supersymmetric standard model (MSSM) [13], a scalar superpartner is associated with each SM fermion and a fermionic superpartner to each vector boson. An important consequence of this doubling of states is that it tames the divergences of quantum corrections to the Higgs mass. At the quantum level the SM Higgs mass involves loop corrections, which diverge quadratically with a cut-off scale and hence destabilize the mass (**the hierarchy problem**). In supersymmetry, the contributions from SM fermionic loops are exactly compensated by opposite sign contributions from their bosonic superpartners and vice versa, cancelling the quadratic divergences. The remaining contribution diverges only logarithmically with the cut-off scale and is proportional to the squared-mass difference of the fermion and boson. The non-observation of superpartners at LEP or Tevatron experiments forces their masses to be well above the corresponding SM particles, except the stop which may be lighter than the top quark. On the other hand, to prevent the hierarchy problem from reappearing, a crude upper limit on their masses of 1–10 TeV can be derived.

An unbroken SUSY theory is very constrained. Although it introduces many superpartners, making many new interactions possible, **the structure of these interactions is fully defined by the same gauge invariances and the same coupling constants as in the SM**. This, however, leads to a theory where all particles are massless (similarly to the SM without spontaneous symmetry breaking). **The mechanism which breaks supersymmetry and yields**

the superpartners their masses is, unfortunately, unknown. In its most general form [14], the SUSY breaking potential introduces 105 parameters, in addition to the 19 of the SM. Some of them are severely limited, as they would induce flavour changing neutral currents (FCNC) or CP violation at an unacceptable level. Nevertheless, the most general MSSM remains untractable. More restrictive models with fewer parameters have been developed, the most popular being inspired from supergravity [15] and hence called MSUGRA [16]. It contains, depending on the assumptions, 1 to 5 free parameters and is the model most extensively used to derive experimental implications.

All three coupling 'constants' of the SM gauge groups have been known since 1991 to high accuracy at the Z^0 scale, owing to the precision measurements of the Z^0 mass and of the strong coupling α_S, performed at LEP (and further improved since then by LEP and SLC). Once loop corrections to the vector boson propagators are included, the effective couplings vary with the energy scale at which they are evaluated. The energy dependence is described by a differential equation, the renormalization group equation (RGE), whose coefficient depends on the nature and number of particles circulating in the loop. It was conjectured by Georgi *et al* in 1974 [17] that this energy dependence might make the couplings unify at some high energy scale, leading to a grand unification of the gauge groups. The precise values from LEP showed clearly that in the SM, although the couplings converge, their crossing in a single point is ruled out at the level of 8–12 standard deviations and no unification is achieved. On the other hand, if superpartners with masses in the TeV region are included, the slopes of the evolution are changed accordingly and the couplings meet at a scale of about 2×10^{16} GeV [18]. This lends support to **the hypothesis of a grand unified theory (GUT), realizable within the supersymmetric SM**.

In the MSSM, it is usually assumed that the supersymmetry breaking defines the mass parameters at the GUT scale. These parameters are then evolved down to the electroweak scale, by means of their RGEs, which determine the superpartner masses as a function of the original parameters. In particular, the mass-squared parameter of the Higgs field which couples to up-type fermions receives large negative corrections dominated by the large top-quark Yukawa coupling. This may naturally drive the mass-squared parameter negative near the electroweak scale and consequently **trigger the spontaneous breaking of the electroweak symmetry** [19]. This possibility was actually a first hint that the top quark should be heavy [20]. One of the virtues of SUSY is that the mechanism of electroweak symmetry breaking (EWSB) occurs at the level of perturbation theory, without the need for any new strong interaction. **Compared with the SM which explains only 'how' the symmetry is broken, its supersymmetric extension tells 'why' the Higgs mechanism takes place**. Some questions have been raised in the past concerning unwanted effects of symmetry breaking, namely a violation of $U(1)_{em}$ symmetry making the photon massive. Considering the Higgs sector, while some two-doublet models may present such problems, the MSSM is free of them [21]. However, the role of other scalars, which may lead to charge and/or colour breaking (CCB) minima, should be closely watched (see section 8.4).

A strong prediction, quite generally valid within the MSSM, is that, as we said, the lightest Higgs should have a mass below approximately 130 GeV. This value is compatible with the indirect upper bound obtained from the electroweak precision measurements. The direct search for such a particle was very actively pursued at LEP but, due to the energy limitation imposed on the machine, only a lower limit on its mass of about 114 GeV could be obtained. Searches for superpartners, carried out at LEP and Tevatron, were also unsuccessful and put lower bounds of 100 to ∼300 GeV on their masses. In view of the 1–10 TeV upper range mentioned earlier, the latter may not be very worrying. But (a solid chance exists that), if the MSSM makes sense, the light Higgs and at least some of the superpartners will be discovered at the

future LHC machine or even, if much progress is made, the Tevatron. Moreover, some low energy experiments are now reaching a precision such that they could also become sensitive to new particles via the loop corrections. Might they discover SUSY, even before the LHC?

The SM particles are distinguished from their superpartners by a multiplicative quantum number, called R-parity [22], which is +1 for ordinary particles and −1 for the superpartners. If it is assumed that R-parity is conserved in the interactions, superpartners can only be produced in pairs, their decay will always involve another superpartner, and finally the lightest SUSY particle (LSP) has to be stable. From cosmological arguments [23], this is likely to be a neutral particle, which is easily satisfied in the MSSM. It could be an excellent candidate for the dark matter in the universe.

A review of the daily evolving literature concerning supersymmetry illustrates the quasi-infinite variety of the considered scenarios. One of the *raison d'être* of SUSY is the assumed existence of a desert between the electroweak and some very high scale. If, for instance, because of the existence of large extra dimensions, such a desert does not exist, the usefulness of SUSY can be reconsidered, as is dicussed in section 2.3. Similarly one can give up the hope of solving the problem of the fine tuning which guarantees the mass hierarchy, considering that this is too ambitious and/or premature (anyhow we must live with the even more dramatic problem of the cosmological constant [24]). Then one can push the scalar superpartners to arbitrary high mass as in the split supersymmetry version [25]. However, besides the mere fact that such a symmetry exists as a mathematical reality and allows gravity to be brought into the game, there are good phenomenological reasons to keep the SUSY frame. The first one is the problem of dark matter. As we just said, a light SUSY partner such as the LSP is still the most promising candidate offered by particle physics. For instance, the inventors of split supersymmetry stick to that idea and keep to low mass, besides the lightest Higgs h^0, the SUSY partners of gauge and Higgs bosons, hence the name of the scenario. But even in this perspective, since the nature of the LSP is not precisely known, one can think of splitting the split supersymmetry and push the Higgs superpartners to high mass [27]. On the other hand, the tenants of R-parity breaking versions (see [26]) have given up the idea of solving the dark matter problem within supersymmetry.

Another phenomenological fact quoted above is the indication obtained at LEP, in the frame of the SM, of a light Higgs boson, <250 GeV. This is compatible with SUSY, but not a compelling argument in its favour. As we said, the MSSM predicts such a light boson, <130 GeV, likely to be SM-like. Even more complicated versions, such as the next-to-MSSM (NMSSM, see section 3.5.2), still lead to relatively light bosons, well below the LEP upper limit, but the increased number of parameters in their Higgs sector allows one to play quite complicated games and to prove what one wants.

These examples illustrate the versatility of SUSY scenarios and show that for experimentalists it is a moving target, difficult if not impossible, to falsify. Potential indirect indications of low energy programmes will likely be insufficient to unambiguously demonstrate its existence. We hope therefore that, if SUSY is a reality, the next programmes and especially LHC will provide some direct 'smoking gun' evidence of its existence.

It is also clear that SUSY, in spite of the progress it would bring compared with the SM, is still an effective theory since its parameters, in particular the ones controlling the symmetry breaking, have to be introduced from outside. Nevertheless it is a useful framework: if superpartners would be discovered, the measurements made at LHC and/or a future lepton collider would allow its parameters to be extrapolated to high energy in the same way as was done for the gauge couplings. This might open a window on a more fundamental theory.

The present review starts with a more theoretical part including a brief presentation of alternatives to SUSY in section 2, the basic ingredients of MSSM in section 3, supersymmetric grand

unification in section 4 and an overview of the various SUSY breaking mechanisms and the ensuing sparticle spectroscopy in section 5. Section 6 presents the status and potential impact of low energy measurements. The existing and future accelerators and detectors, as well as the SUSY generator programs, are summarized in section 7. The existing limits on the Higgs mass, from LEP and Tevatron, and the expectations from the future accelerators, LHC or a linear collider, are presented in section 8. After a discussion of sparticle decays in section 9 and production in section 10, the present limits from HERA, Tevatron and LEP are reviewed in section 11. The resulting limit from LEP on the LSP mass, its impact on neutralino dark matter and the current searches and future prospects of non-accelerator experiments are summarized in section 12. Sections 13 and 14 are devoted to the results from searches for gauge mediated SUSY and R-parity violation, respectively. Finally, the expectations from future searches at the Tevatron, LHC and a linear collider are summarized in section 15 and the connection between the sparticle mass spectra and GUT scale physics in section 16. Section 17 contains the conclusions.

Note on references: the literature on supersymmetry is extremely abundant. Many references have been included to guide the reader who wants to study a given subject more deeply. In general, preference was given to recent papers and didactic presentations (reports or lecture notes). We apologize for the numerous missing references to the original material. The literature scan was stopped in May 2005.

2. Brief survey of alternatives to SUSY

Before we deal in depth with SUSY, we would like to underline that alternative scenarios beyond the SM do exist, even if for various reasons (apparent conflict with electroweak measurements, lack of maturity because of their recent birth, maybe simply the effect of fashion) they did not receive as much attention as supersymmetry. We summarize their main features and predictions.

2.1. Strong electroweak symmetry breaking

If to go beyond the SM one chooses the composite way instead of SUSY; the most general possibility, derived from the Goldstone boson equivalence theorem [28], is to consider new strong interactions between the intermediate vector bosons, more exactly between their longitudinal components V_L [29]. To reveal these, one can study the production of vector–boson pairs in e^+–e^- or q–$\bar{q}$ scattering: this is the high energy analogue of the measurement of the time-like pion form factor, as performed in the good old days. Another way is to study boson–boson scattering, where the bosons are emitted from incident $e^\pm$ or quarks: this is the high energy analogue of pion−pion scattering. Such interactions may be resonant or not. In the non-resonant case, one is still guided by low energy theorems (LETs) [28], as in the pion–pion case.

If no light Higgs or other low lying resonance exists, unitarity requires that the interaction among gauge bosons becomes strong at high energy. The expected symmetry breaking scale is $\Lambda = 4\pi\sqrt{2}v \sim 3\,\text{TeV}$ (with $v \simeq 175\,\text{GeV}$). Below this scale the physics of longitudinal bosons is described by an effective Lagrangian, whose parameters α_i [30] can be probed by measuring the V_L interactions. Since the ρ parameter has been found to agree with the SM expectation, such interactions should first respect a $SU(2)$ 'custodial' symmetry which guarantees such an agreement.

A naive dimensional approach says that, if no resonance exists below Λ:

$$\alpha_i/(8\pi^2) = (v/\Lambda_i)^2, \tag{1}$$

where Λ_i, the scale of new physics, is of the order of Λ. Hence the α_i are of order one. From 4-fermion final states one can measure the triple gauge couplings (TGCs). The corresponding

α_i ($i = 1, 2, 3$) are related to the usual (g_1^Z, κ_Z, κ_γ), already measured at LEP and found to agree with the SM expectations at the few% level. From 6-fermion final states one measures the quartic gauge couplings (QGCs), labelled $\alpha_{3,4,5}$. An introduction to these scenarios and a comparison of the potentials of various machines can be found in [31,32]. An explicit example of a model having resonances below Λ is the BESS Model [33] (which stands for 'breaking electroweak symmetry strongly').

2.2. Technicolour

Technicolour [34,35] is probably the most studied theory of dynamical EWSB. It stems from the QCD analogy of spontaneous chiral flavour symmetry breaking by quark condensates: these also break electroweak symmetry, but the Z mass is predicted to be 60 MeV! The idea is to emulate this mechanism at a much higher scale: one assumes a new asymptotically free gauge interaction called technicolour, introduced in 1979 by Weinberg and Susskind [36]. It has a gauge group G_{TC}, and a coupling α_{TC}, which becomes strong at a few hundred GeV. N_{D} is the number of doublets of L and R technifermions (TFs). They form condensates which break the chiral flavour symmetry, giving masses to the Z and the W.

However, the quarks and leptons are still massless. One has to go to extended technicolour (ETC): quarks, leptons and TF are put into the same representation of a new gauge group, with Λ_{ETC} much larger than Λ_{TC}. ETC still has problems with the rate of flavour changing neutral currents and its confrontation to accurate measurements. The reason is that it is just a scaled-up version of QCD: asymptotic freedom sets in too fast. If two matrices of the ETC group link quarks to techniquarks the commutator of these matrices links quarks with quarks and this is the origin of unwanted FCNC effects, as long as no way to cure them is added.

One has therefore to invent 'walking technicolour' (WTC), a version of the theory in which the evolution of couplings is very slow. The flavour changing direct effect of ETC on light quark physics is reduced. The problems with accurate measurements disappear because in WTC one cannot compute the observables reliably! This is not a strong point of the theory, but it saves it temporarily.

Practically, the search for technicolour is quite analogous to the Higgs search. One looks for techni-vector mesons (ρ_T, ω_T) produced in e^+–e^- or q–$\bar{q}$ collisions. A technirho can decay into technipion pairs, W_L-technipion or W_L pairs. A neutral technipion (π_T^0) decays into b–$\bar{b}$ (it acts like a Higgs boson), a charged one into b–$\bar{c}$. LEP and Tevatron have already put substantial limits on their masses [37].

2.3. Extra-dimensions

These models stem from the idea required in string theory that extra space dimensions, which are compactified and usually considered to be of the size of Planck length, could after all be much larger, i.e. down to the TeV scale [38], without violating any established fact. A large variety of models exist [39–41], depending on which particles are allowed to propagate in the 'bulk' of the δ extra dimensions (ED).

If only gravitons can do so, one can still distinguish models where the hierarchy problem is taken care of by a large volume of the ED space (Arkani-Hamed, Dimopoulos, Dvali: ADD model) [42] from those where it is generated by a large curvature of the extra dimension (Randall, Sundrum: RS model) [43].

A common feature of the extra dimensional models is that, if a particle propagates in the bulk, its mass in $4 + \delta$ dimensional space-time is given by

$$m_0^2 = E^2 - p_1^2 - p_2^2 - p_3^2 - p_4^2 \cdots - p_{3+\delta}^2 \tag{2}$$

and, if measured in our 4-dimensional space-time, will appear as

$$m^2 \equiv E^2 - p_1^2 - p_2^2 - p_3^2 = m_0^2 + p_4^2 \cdots + p_{3+\delta}^2. \tag{3}$$

The quantification of the fields in an extra dimension requires the momentum to be a multiple $p = n/R$ of the inverse radius R. The 4-dimensional mass then appears as

$$m^2 = m_0^2 + \sum_{i=1,\delta} \left(\frac{n_i}{R_i}\right)^2 \tag{4}$$

with a zero mode mass m_0 followed by an infinite series of recurrences, called a Kaluza–Klein (KK) tower, which is the signature of the extra dimensions.

In the ADD model the scale M_{D} at which gravity becomes strong in $4 + \delta$ space-time is given by:

$$M_{\mathrm{Pl}}^2 = V_\delta M_{\mathrm{D}}^{2+\delta}, \tag{5}$$

where V_δ is the volume of compactified dimensions. Hence, the Planck scale M_{D} in $4 + \delta$ dimensions can be of the order of the electroweak scale, eliminating the hierarchy problem. In the four-dimensional space-time it appears large, due to the large volume of the extra dimensional space. For $M_{\mathrm{D}} = 1$ TeV, $\delta = 1$ is excluded by the validity of Newton's law at the astronomical scale. For $\delta = 2$ (R_c is a fraction of a millimetre) and $\delta = 3$ one still must take into account, in the case of flat ED, strong astrophysical and cosmological constraints [41,44]. The phenomenology of these models at colliders is essentially due to the possibility of real gravitons escaping to the ED (i.e. non-standard missing energy-momentum processes) and of the exchange of virtual gravitons [45] (i.e. slight modifications to the rates of SM processes: one should proceed with care in determining the actual limits). In this model, the radii of the extra dimensions range usually from μm to fm and thus to very small mass splittings between the KK states, giving rise to an almost continuous graviton mass spectrum. As a similar situation would occur for other particles propagating in the extra dimensions, which is experimentally excluded, the gauge bosons and fermions are confined to the four-dimensional space-time.

A quite distinct version of ED postulates TeV^{-1}-sized ED (we recall that 1 fermi $=$ 1/200 MeV). In such a case SM fields may also propagate in the bulk and should have Kaluza–Klein excitations in the TeV region. The scenario where all can do so, called universal ED (UED) [46], has a special phenomenology. In UED (4+δ)-dimensional momentum is conserved at tree level. Kaluza–Klein states can only be pair produced. Their exchange intervenes only at the loop level. The lightest Kaluza–Klein state is stable and a candidate for cold dark matter. The phenomenology is thus quite similar to the SUSY case. Finding ways to distinguish them is a challenging exercise [47]. LHC should be able to confirm or rule out UED at the TeV scale.

In the first version of RS models, gravity is in the 5D bulk of finite extent limited by two rigid branes. One brane is trapping gravity while on the other brane gravity is not trapped. On that second brane gravity is weak and that is the brane where the SM fields are located. There is the possibility of direct resonant production of the spin-2 states of the graviton Kaluza–Klein tower, with a first excitation at the TeV scale [43]. The existence of the radion, quantum excitation of the brane separation which is directly coupled to the energy-momentum tensor, could offer an interesting phenomenology [48]. It may be the lightest new field predicted by the RS model. It would then be very similar to the SM Higgs boson except for its couplings to gluons and photons. For instance, for $m_\phi \leqslant 150$ GeV, the decay mode $\phi \to gg$ dominates, while hadronic production is essentially from gg initial state. The relevant LEP limit is then the one from the 'flavour-blind' Higgs search, $m_h \geqslant 112.5$ GeV. At LHC one could look, for instance, at [49]

$$gg \to \phi \to ZZ \text{ or } WW \text{ or } \gamma\gamma. \tag{6}$$

Mixing of the radion with the SM Higgs boson can also modify the Higgs properties [50].

Such an eventuality, which has naturally to be fully explored, would be an extraordinary chance for LHC and its prospective study also contributes to agreeably diversify the phenomenology. However, before dreaming too much, it is important to appreciate correctly the existing limits, drawn either from accelerators or from astrophysics. Astrophysical bounds severely limit the possibility of observing collider signals in the case of less than 3 flat extra dimensions. But [51] small distortions of the compactified space can lift the masses of the lightest graviton excitations, evading astrophysical bounds without affecting collider signals. For the ADD scenario, one should also consider the impact of dedicated tests of Newtonian gravity at small scale, which, besides micro-mechanical experiments [52], may in the future use sophisticated methods involving Bose–Einstein condensates [53] or ultra-cold neutrons [54] and build interesting bridges between particle physics and other sectors of physics.

2.4. Solving the 'small' hierarchy problem

SUSY helps to solve the 'large hierarchy problem' between the Fermi and the GUT scales. But one can choose to focus first on the '**small hierarchy problem**', namely to reconcile the indication of a light boson ($\lesssim$250 GeV) on one hand and the evidence that the SM seems to be valid up to a cut-off of several TeV on the other hand [55, 41]. The resulting scenarios can either still use [56, 57] or ignore [58–60] the idea of supersymmetry. Solutions to the large hierarchy problem are 'left for later'.

In the first reference, the authors take the benefit of a fifth compact dimension. An interesting prediction of theirs, besides a quite light boson (<130 GeV), is that the LSP could be a heavy stable charged particle, an incentive for future experiments to implement a performant time-of-flight measurement. We will come back to such models in section 5.1.

The scenario described in the second reference, called the little Higgs and which wants to avoid SUSY, has also an interesting phenomenology [58–60]. It contains a light Higgs boson, but not so tightly bound in mass as in the MSSM, and new states, the role of which is to cancel the effects of the SM particles loops. These are

- a new vector-like up-type quark, cancelling the top loop divergence,
- new heavy gauge bosons $W_H(\rightarrow t\bar{b})$ and $Z_H(\rightarrow Zh, Zf\bar{f})$ in the TeV or few TeV region, cancelling the gauge and Higgs loops and having well predicted couplings.

A strongly interacting sector exists above ~10 TeV. **As one can see, the divergences due to particles of one type, fermion or boson, are cancelled by particles of the same type**. LHC has a good chance of revealing such new states and, if accurate measurements of branching ratios can be performed, of identifying the corresponding scenario.

Obviously these new approaches, like others, have to cope with the constraints of electroweak precision observables [61]. A recent paper [62] insists on the need for such models to keep custodial symmetry in the Higgs sector. The little Higgs is an example of a newborn scenario which will certainly develop into a rich and diversified phenomenology [59, 63, 64].

2.5. A combination of these scenarios?

Actually these approaches need not be exclusive and many extensions built on the co-existence of more than one scenario have been proposed. In particular one can combine the idea of supersymmetry with the various models considered above. However in general some of the original motivations which led to the introduction of SUSY are lost or modified.

The author of [65] proposes consideration of a supersymmetric version of technicolour. The secondary goal of TC which is to eliminate scalar bosons is thus abandoned. However, while TC achieves EWSB in an elegant and natural way, the supersymmetric version helps to solve several problems of usual TC, listed above. In the particular model of [65], there is no light elementary Higgs boson and EWSB is fully dynamical. The e^+e^- production of technistates is calculable, but not the electroweak precision observables.

Concerning the small hierarchy problem, which in the MSSM can be expressed by a requirement of fine tuning (between the bare $m^2_{H_u}$ and/or μ against the radiative corrections to the Higgs mass), a calculable supersymmetric theory of a composite 'fat Higgs' model has been recently devised [66]. Electroweak symmetry is broken dynamically through a new gauge interaction that becomes strong at an intermediate scale. The Higgs boson mass can be raised beyond the LEP limit and the supersymmetric small hierarchy problem can be solved.

Combining extra dimensions with SUSY allows a number of games to be played. We will mention a few in section 5.1

Concerning all these scenarios and probably others not yet invented, a very interesting feature is that, true or not, they offer alternatives to conventional SUSY and rejuvenate the phenomenology at future machines. The message to the experimentalists is that they should explore all accessible channels, optimize the heavy flavour tagging devices and procedures, in particular with the aim of separating b from c, be as quantitative as possible, in case new physics appears in non-resonant channels. Furthermore one should watch as a priority the V_L component of vector bosons and, when possible, enhance its contribution by appropriate projections.

3. Basics of supersymmetry

3.1. Taming of divergences

It is assumed in the SM that there exists a single Higgs doublet and that its mass is obtained at tree level by minimization of a simple potential. This leads to the estimate of a Higgs mass roughly of the same order as the electroweak scale, ∼100 GeV. Furthermore, the requirement that the scattering amplitude of longitudinal W-bosons does not exceed the unitarity bound imposes an upper limit to the Higgs mass of about 600–800 GeV [67]. The tree value of the Higgs mass is affected by very large radiative corrections from loops involving all particles coupling to the Higgs, as seen in figure 2(*a*). To prevent the radiative corrections from going to infinity, a cut-off scale Λ on the momentum integral can be introduced. The value of Λ can, however, be chosen anywhere between the electroweak scale and the Planck scale, $M_{\rm Pl} \equiv (8\pi G_{\rm Newton})^{-1/2} = 2.4 \times 10^{18}$ GeV, at which gravity has a strength comparable to the other interactions and can no longer be neglected. This requires the SM to be extended and will, most likely, introduce new heavy particles. This enormous disparity of scales is at the origin of the hierarchy problem, discussed in more detail in [1] or, for example, the lecture notes of Drees [68] or Murayama [69].

More quantitatively, loop corrections in the SM involve fermions, coupling to the Higgs via the Yukawa interaction term $-\lambda_f H \bar{f} f$ in the Lagrangian (the minus sign is conventional). Each Dirac fermion type contributes with a correction in which the dominant terms are

$$\Delta m^2_H|_f = \frac{\lambda_f^2}{8\pi^2}\left[-\Lambda^2 + 6m_f^2 \ln\frac{\Lambda}{m_f}\right]. \tag{7}$$

The leading term diverges quadratically. The Higgs radiative correction is not proportional to its mass, which shows that the symmetry of the Lagrangian is not increased when the Higgs mass

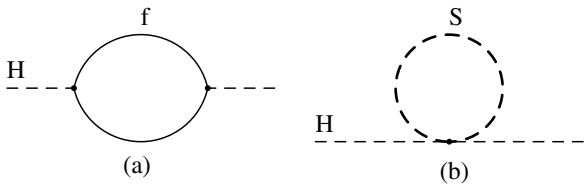

Figure 2. Loops affecting the squared Higgs mass from (*a*) fermion trilinear couplings, (*b*) scalar quartic couplings. From [1].

goes to zero. If no physical meaning is attached to the scale Λ, the quadratic divergence can be removed by renormalization (e.g. it does not appear when using dimensional regularization). But even so, if new particles exist at some scale below the Planck mass, they will induce large corrections through the second term in (7). **Altogether, the Higgs mass is extremely sensitive to the heaviest particle to which the H couples and its most 'natural' value is close to the largest mass scale in the theory**.

Now, assuming that there also exists a scalar which couples to the Higgs by a quartic interaction of the form $-\lambda_S|H|^2|S|^2$ (see figure 2(*b*)), the corresponding loop correction contributes to the Higgs mass by

$$\Delta m_H^2|_S = \frac{\lambda_S}{16\pi^2}\left[\Lambda^2 - 2m_S^2 \ln\frac{\Lambda}{m_S}\right]. \tag{8}$$

It also generates a quadratic divergence, but its sign is opposite to the one of the fermions (which is related to Fermi statistics). It is seen that if every fermion is accompanied by two scalars with couplings $\lambda_S = \lambda_f^2$ the quadratic divergences cancel exactly. **Such relation between the couplings could be the result of a symmetry and is actually achieved by imposing supersymmetry to the Lagrangian.**

The contribution remaining after the cancellation can also be evaluated. The term in the quartic interaction where the Higgs field is replaced by its vacuum expectation value also needs to be included. This yields a contribution without quadratic divergence and with leading term in $m_f^2 \ln(\Lambda/m_S)$. If the two scalars are assumed to have the same mass, and in the approximation where the mass difference between the fermion and the scalars is small, the total correction is reduced to

$$\Delta m_H^2|_{\text{tot}} \simeq \frac{\lambda_f^2}{4\pi^2}(m_S^2 - m_f^2)\ln\frac{\Lambda}{m_S}. \tag{9}$$

The resulting radiative correction is **logarithmic and proportional to the mass-squared difference, reflecting the additional symmetry imposed on the couplings**. The particles running in the loops can now be very heavy: provided their mass differences are of the order of the electroweak scale, the correction itself also remains of the order of the electroweak scale. The hierarchy problem can be solved in a theory with nearly degenerate fermions and scalars and adequately chosen couplings.

This is exactly what happens in supersymmetry, which postulates the existence of supersymmetric partners for every SM particle. Doubling the spectrum of states does not sound like an economic step. However, it is reminiscent of what happened when the concept of antimatter was introduced by Dirac [69]. The problem then concerned the self-energy of the electron, due to photon emission and reabsorption. This $\Delta E_{\text{Coulomb}}$ is divergent as $\sim 1/r_e$, where r_e is the radius of the electron. Since we know that the radius is smaller than 10^{-17} cm, $\Delta E_{\text{Coulomb}}$ is larger than 10 GeV, and to obtain the physical mass of 0.5 MeV one would have to postulate an absurd cancellation between $\Delta E_{\text{Coulomb}}$ and an hypothetical large bare mass of

the electron (negative). However, introducing the positron one gets additional processes with electron–positron loops, whose effect appears already at the scale of 10^{-11} cm or so. The sum of their effects is

$$\Delta E_{\text{tot}} = \Delta E_{\text{Coulomb}} + \Delta E_{\text{pair}} = \frac{3\alpha}{4\pi} m_{\text{e}} c^2 \ln \frac{\hbar}{m_{\text{e}} c r_{\text{e}}}. \tag{10}$$

There too, the power divergence becomes a logarithmic one and the overall effect is proportional to the electron mass and would vanish with it, which reflects the existence of a symmetry (chiral symmetry) which 'protects' the electron mass from acquiring large radiative corrections.

3.2. Superpartners

A supersymmetry transformation turns a fermion state $|F\rangle$ into a boson $|B\rangle$ and vice versa

$$Q|F\rangle = |B\rangle, \qquad Q|B\rangle = |F\rangle. \tag{11}$$

The operator, Q, which performs such transformation has to carry spin 1/2. In supersymmetry, the single particle states fall into irreducible representations of the supersymmetry algebra, called *supermultiplets* [12]. Hence a supermultiplet consists of both fermions and bosons differing by 1/2 unit in spin. All members of a supermultiplet have the same four-momentum, hence the same mass.

The supersymmetry generators commute with the generators of gauge transformations. Therefore, all members of a supermultiplet are in the same representation of the gauge group and have identical charge, weak isospin and colour. In summary, **they are identical particles, except for their spin.**

Furthermore, the number of bosonic degrees of freedom, n_{B}, and the number of fermionic degrees of freedom, n_{F}, in a supermultiplet are equal:

$$n_{\text{B}} = n_{\text{F}}. \tag{12}$$

An on-shell SM fermion corresponds to a Weyl spinor[3] with two real components. It is, via supersymmetry, accompanied by two scalars (which will be written as a single complex scalar field), one associated with each helicity state. This is called a **chiral or matter supermultiplet**. By convention, they are expressed in terms of left-handed particles only. For singlet (right-handed fermion) states, the left-handed charge conjugate particle is used, e.g. U_{L}^{C} instead of U_{R}. The left- and right-handed fermions have different gauge transformation properties and correspond to separate two-component real Weyl spinors which belong to different supermultiplets. Therefore, each has its own complex scalar partner, with the same name preceded by 's' (e.g. selectron). In the notation, they are referred to by the subscripts 'L' and 'R', like their fermionic partners, although they have spin zero.

Higgs bosons are defined as complex spin 0 fields and also reside in chiral supermultiplets. Their fermionic partners are called 'higgsinos'. In fact, **supersymmetry requires the existence of at least two Higgs doublets in order to provide masses for both up- and down-type particles (this is also required for the cancellation of the triangle gauge anomaly).** The Higgs field H_{d} couples to down-type particles and H_{u} to up-type particles.

A SM gauge boson corresponds to a vector field. If the gauge symmetry is unbroken, this spin-1 boson is massless and has only two helicity states. Its superpartner is therefore a spin 1/2 Weyl fermion with two degrees of freedom. Gauge bosons transform as the

[3] A four-component Dirac spinor can be represented as two two-component Weyl spinors, each corresponding to a given chirality. As the SM is chiral (i.e. distinguishes between left- and right-handed fermions), the Weyl representation is very convenient and commonly used.

Table 1. Particle content of MSSM.

Vector supermultiplet		Chiral supermultiplet	
$J = 1$	$J = 1/2$	$J = 1/2$	$J = 0$
g	$\tilde{g}$	$Q_{\rm L}\ U_{\rm L}^{\rm C}\ D_{\rm L}^{\rm C}$	$\tilde{Q}_{\rm L}\ \tilde{U}_{\rm L}^{\rm C}\ \tilde{D}_{\rm L}^{\rm C}$
$W^{\pm}W^0$	$\tilde{W}^{\pm}\tilde{W}^0$	$L_{\rm L}\ E_{\rm L}^{\rm C}$	$\tilde{L}_{\rm L}\ \tilde{E}_{\rm L}^{\rm C}$
B^0	$\tilde{B}^0$	$\tilde{H}_{\rm d}\tilde{H}_{\rm u}$	$H_{\rm d}H_{\rm u}$

Table 2. MSSM scalar particle quantum numbers.

Superfield	Charge	Scalar component (1st family)
Q_i	(3,2,+1/3)	$Q = (\tilde{u}_{\rm L}, \tilde{d}_{\rm L})$
$U_i^{\rm C}$	(3,1,–4/3)	$U^{\rm C} = \tilde{u}_{\rm L}^{\rm C}$
$D_i^{\rm C}$	(3,1,+2/3)	$D^{\rm C} = \tilde{d}_{\rm L}^{\rm C}$
L_i	(1,2,–1)	$L = (\tilde{\nu}_{\rm L}, \tilde{e}_{\rm L})$
$E_i^{\rm C}$	(1,1,+2)	$E^{\rm C} = \tilde{e}_{\rm L}^{\rm C}$
$H_{\rm d}$	(1,2,–1)	$H_{\rm d} = (H_{\rm d}^0, H_{\rm d}^-)$
$H_{\rm u}$	(1,2,+1)	$H_{\rm u} = (H_{\rm u}^+, H_{\rm u}^0)$

Table 3. MSSM gaugino quantum numbers.

Fermion	Vector boson	Charge
$\tilde{g}$ (gluino)	g	(8,1,0)
$\tilde{W}$ (Wino)	W	(1,3,0)
$\tilde{B}$ (Bino)	B	(1,1,0)

adjoint representation of the gauge group[4] and their fermion superpartners must be in the same representation. Since the adjoint representation is its own conjugate, the left- and right-handed components of these fermions must have the same gauge transformation properties, hence not allowing for chiral fermions. This is called a **vector or gauge supermultiplet** and the superpartners are called gauginos which include the gluinos, the winos and the bino.

The minimal supersymmetric standard model (MSSM) contains the minimum extension of the SM particles [13], as summarized in table 1.

Taking the first family as example, the scalar superfields are listed in table 2, where the charge is for $SU(3)_c$, $SU(2)_{\rm L}$, $U(1)_Y$, with the convention $Q = I_3 + Y/2$. The vector supermultiplets consist of the vector bosons and their partner fermions (gauginos), see table 3.

After breaking of the electroweak symmetry, the W^0 and the B^0 mix to give Z^0 and γ. The corresponding mixtures of their superpartners $\tilde{W}$ and $\tilde{B}$ are called the zino ($\tilde{Z}^0$) and the photino ($\tilde{\gamma}$). Moreover, the gauginos will mix with the higgsinos and give rise to mass eigenstates which are called

- charginos from mixing of $\tilde{W}^{\pm}$ and $\tilde{H}^{\pm}$, leading to two states $\tilde{\chi}_{1-2}^{\pm}$,
- neutralinos from mixing of $\tilde{W}^0$, $\tilde{B}^0$, $\tilde{H}_{\rm d}^0$, $\tilde{H}_{\rm u}^0$, leading to four states $\tilde{\chi}_{1-4}^0$.

The SM particles can be distinguished from their superpartners by a **multiplicative quantum number, called R-parity**, which is defined for each particle inside a supermultiplet by

$$R_{\rm p} = (-1)^{3B-L+2s}, \tag{13}$$

[4] The adjoint representation can be viewed as the traceless part of the product of the basic vector of the group by its conjugate.

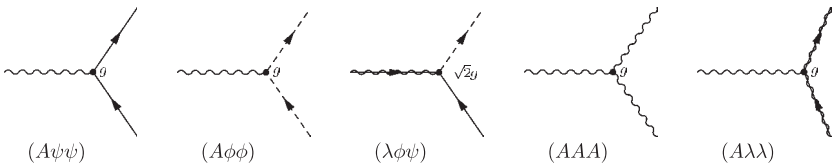

Figure 3. MSSM trilinear gauge interactions. Full lines represent fermions, dashed lines scalars, wiggly lines vector bosons and wiggly+full lines gauginos.

where s represents the particle spin. The R-parity is $R_{\rm p} = +1$ for all SM particles (including the Higgses) and $R_{\rm p} = -1$ for their supersymmetric partners.

In this review, we will ignore **extended supersymmetry**, namely having more than one supersymmetry generator in the theory ($N > 1$) and where the number of superpartners rapidly proliferates. While $N = 1$ SUSY preserves important properties of the SM, such as chirality, $N \geqslant 2$ **would imply a L–R symmetry which, together with other arguments, makes it unlikely to be a realistic symmetry of the four-dimensional world.**

3.3. The couplings in the SM and the MSSM

The gauge interactions in the MSSM can be simply derived from the SM ones in the following heuristic way. **The SM particles and their superpartners belonging to the same supermultiplet have the same gauge properties and hence should couple with the same strength**. The MSSM interaction terms can be inferred from the SM ones by replacing SM particles by their superpartners. However, as they differ by 1/2 unit in spin, the resulting interaction term can only remain a scalar in spin space if the replacement is done in pairs.

The convention used for the fields is that chiral supermultiplets consist of the fields (ψ, ϕ), where ψ is the fermion and ϕ the complex scalar; vector supermultiplets contain (A, λ), where A stands for the gauge boson and λ for the gaugino. The interaction vertices will be labelled by the fields only, ignoring their space-time structure as it will not be needed in the following.

3.3.1. Gauge couplings. The SM gauge coupling between a boson and a fermion pair is then written as $(A\psi\psi)$ and, using the above replacement rule, is complemented in the MSSM by the couplings $(A\phi\phi)$ and $(\lambda\phi\psi)$ with the same coupling constant (within a factor $\sqrt{2}$). For example, the $(W^{\pm}e_{\rm L}\nu)$ vertex in the SM is accompanied in the MSSM by the $(W^{\pm}\tilde{e}_{\rm L}\tilde{\nu})$, $(\tilde{W}^{\pm}\tilde{e}_{\rm L}\nu)$ and $(\tilde{W}^{\pm}e_{\rm L}\tilde{\nu})$ vertices. Similarly, the SM vertex (AAA) gives rise to a $(A\lambda\lambda)$ coupling. The complete set of trilinear gauge couplings is illustrated in figure 3.

For electroweak interactions, the coupling strengths in the diagrams of figure 3 are summarized as

$$\begin{aligned} &W^{\pm}(\tilde{W}^{\pm}) \propto g_2 I^3, \\ &\gamma(\tilde{\gamma}) \propto eQ = g_2 Q \sin\theta_W, \\ &Z^0(\tilde{Z}^0) \propto g_2(I^3 - Q\sin^2\theta_W). \end{aligned} \tag{14}$$

The charged wino, such as the $W^{\pm}$, couples to the third component of the weak isospin; the photino, such as the photon, couples to the electric charge; the zino couples to the same combination of isospin and charge as the Z^0. Some examples are as follows:

- the $(A\psi\psi)$ coupling to SM fermions, which contains $(Wf\bar{f}')$ and $(Zf\bar{f})$, has a strength defined by $I^3 = \pm 1/2$ for $f_{\rm L}$ and $I^3 = 0$ for $f_{\rm R}$;

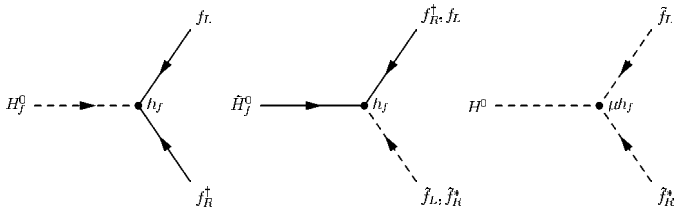

Figure 4. MSSM trilinear Yukawa interactions.

- but in the MSSM it also leads to the coupling $(Z\tilde{H}\tilde{H})$ where $I^3 = \pm 1/2$ for both L and R components;
- the (AAA) and $(A\lambda\lambda)$ vertices give rise to $(Z^0W^+W^-)$ and $(Z^0\tilde{W}^+\tilde{W}^-)$ couplings with strength determined by $I^3 = \pm 1$ and $Q = \pm 1$. However, $(Z^0W^0W^0)$ or $(Z^0\tilde{W}^0\tilde{W}^0)$ coupling strengths are zero.

3.3.2. Yukawa couplings. The same replacement rule can be applied to SM Yukawa interactions. For example, the $(h_e e_L e_L^C H_d^0)$ coupling, which induces a mass for the electron in the SM, leads to couplings $(h_e \tilde{e}_L e_L^C \tilde{H}_d^{\,0})$ and $(h_e e_L \tilde{e}_L^C \tilde{H}_d^{\,0})$ in the MSSM, defined by the same Yukawa coupling. It could be naively expected to also give a vertex such as $(h_e \tilde{e}_L \tilde{e}_L^C H_d^0)$. This, however, does not exist as such, as it has the wrong mass (or energy) dimensionality. It is easily seen (e.g. from the kinetic terms) that the dimensionality of fermions is $(E)^{3/2}$ and that of scalars and vector bosons is $(E)^1$. The above term would have canonical dimension $(E)^3$, whereas a Lagrangian density is of dimension $E/L^3 = (E)^4$. Such a term could enter the Lagrangian, provided it is multiplied by a constant with dimension of mass, which is actually the case in the MSSM (see later). The trilinear Yukawa interactions are illustrated in figure 4. Weak isospin invariance also implies the existence of a $(-h_e \nu_L e_L^C H_d^-)$ term. Supersymmetry then requires the terms $(-h_e \tilde{\nu}_L e_L^C \tilde{H}_d^{\,-})$ and $(-h_e \nu_L \tilde{e}_L^C \tilde{H}_d^{\,-})$.

After electroweak symmetry is broken, both Higgs fields H_d and H_u acquire vacuum expectation values (vev), respectively v_d and v_u. The masses of up- and down-type fermions are obtained from the Yukawa terms $(h_d v_d d_L d_L^C)$ and $(h_u v_u u_L u_L^C)$. The vev $v = \sqrt{v_d^2 + v_u^2}$, which plays the same role as the SM Higgs vev, is determined by the vector boson mass, $v = \sqrt{2}(M_W/g_2) \simeq 175\,\text{GeV}$. The remaining free parameter is defined as $\tan\beta = v_u/v_d$, the ratio of Higgs vacuum expectation values. The Yukawa couplings are then given in terms of the particle masses by

$$h_u = \frac{m_u}{v \sin\beta}, \qquad h_d = \frac{m_d}{v \cos\beta}. \tag{15}$$

Unlike in the SM, the Yukawa couplings of the MSSM are not uniquely determined by the fermion masses, but depend also on the parameter $\tan\beta$.

3.3.3. Magnitude of the couplings. It is interesting to compare the relative magnitudes of the above trilinear couplings. For the gauge couplings, choosing as measure $\alpha_i = g_i^2/4\pi$, in analogy with the fine structure constant, leads to $\alpha_{em}(M_Z) \simeq 1/129$, $\alpha_1 \simeq 1/100$, $\alpha_2 \simeq 1/30$, $\alpha_3 \simeq 0.12$. For comparison, the magnitude of Yukawa couplings can be taken as $Y = h^2/4\pi$. For $\tan\beta$ values in the range $\tan\beta = 1$–35, the Yukawas are $Y_t = 1/6$–$1/13$, $Y_b = 1\cdot10^{-4}$–$6\cdot10^{-2}$, $Y_\tau = 2\cdot10^{-5}$–$1\cdot10^{-2}$, $Y_\mu = 6\cdot10^{-8}$–$5\cdot10^{-5}$, $Y_e = 1\cdot10^{-12}$–$1\cdot10^{-9}$. Hence, **the top Yukawa is never negligible compared with gauge couplings and the bottom**

and tau Yukawas are not negligible for large $\tan\beta$**. In all other cases the Yukawas can safely be neglected in comparison with the gauge couplings**.

These trilinear couplings will be of utmost importance for the study of production and decay processes, as they **define the *selection rules* to be applied**.

3.4. The MSSM Lagrangian

Once the supermultiplets and their gauge transformation properties are defined, the gauge interactions in the Lagrangian are determined. But not all quadratic divergences have been eliminated and one still needs to specify the form of the potential containing the Yukawa couplings. In this somewhat more formal section, the basic formulae will be stated without justification. The curious reader may be interested to look at the more rigorous derivation in [1].

3.4.1. Kinetic terms and gauge interactions. The part of the Lagrangian density describing the kinetic terms and the interactions of matter fields with gauge and gaugino fields is given by

$$\begin{aligned}\mathcal{L}_{\text{kin}} = & -D^{\mu}\phi^{*i}D_{\mu}\phi_i - i\psi^{\dagger i}\bar{\sigma}^{\mu}D_{\mu}\psi_i \\ & -\tfrac{1}{4}F^a_{\mu\nu}F^{\mu\nu a} - i\lambda^{\dagger a}\bar{\sigma}^{\mu}D_{\mu}\lambda^a \\ & -\sqrt{2}g[(\phi^{*i}T^a\psi_i)\lambda^a + \lambda^{\dagger a}(\psi^{\dagger i}T^a\phi_i)],\end{aligned} \tag{16}$$

where the conventions follow the ones of Martin [1]. The indices i label the various flavours and chiralities of the fermions and sfermions and a the vector bosons and gauginos of the gauge groups. The first line, with covariant derivatives defined by

$$\begin{aligned}D_{\mu}\phi_i &= \partial_{\mu}\phi_i + igA^a_{\mu}(T^a\phi)_i, \\ D_{\mu}\psi_i &= \partial_{\mu}\psi_i + igA^a_{\mu}(T^a\psi)_i,\end{aligned} \tag{17}$$

where T^a are the generators of the gauge group (for $SU(2)$ they are 1/2 times the Pauli matrices), contains the kinetic terms for the complex scalar and the two-component fermionic matter fields, as well as their interactions with the gauge bosons. The latter include the trilinear couplings called $(A\psi\psi)$ and $(A\phi\phi)$ in section 3.3, together with a quartic interaction $(AA\phi\phi)$ between the scalars and gauge bosons. The second line contains the usual Yang–Mills field strength

$$F^a_{\mu\nu} = \partial_{\mu}A^a_{\nu} - \partial_{\nu}A^a_{\mu} - gf^{abc}A^b_{\mu}A^c_{\nu}, \tag{18}$$

with f^{abc} being the totally antisymmetric structure constants, defined by the commutators $[T^a, T^b] = if^{abc}T^c$ (for $SU(2)$ they are $f^{abc} = \epsilon^{abc}$). It leads to the kinetic terms of the gauge fields, the trilinear interactions called (AAA) in section 3.3 and a quartic interaction of the gauge bosons. The second term, with covariant derivative

$$D_{\mu}\lambda^a = \partial_{\mu}\lambda^a - gf^{abc}A^b_{\mu}\lambda^c, \tag{19}$$

yields the kinetic term for the gauginos and their trilinear interactions called $(A\lambda\lambda)$ in section 3.3. The third line corresponds to the trilinear interactions called $(\lambda\phi\psi)$ in section 3.3.

3.4.2. MSSM superpotential. The potential of the MSSM Lagrangian can be **derived from a function called *superpotential*. Its form is constrained by the requirement of invariance under supersymmetry transformations**, which allows it to be written as a polynomial of at

most order 3 in the scalar fields and with no complex conjugate fields (i.e. an analytic function of the fields), with the general form

$$W = \tfrac{1}{2}M^{ij}\phi_i\phi_j + \tfrac{1}{6}h^{ijk}\phi_i\phi_j\phi_k \tag{20}$$

and of dimension 3 in mass; [5] hence, it is not a potential in the ordinary sense. Its expression in the MSSM is of the form:

$$W = \epsilon_{ij}(-\tilde{L}^i_{\mathrm{L}}h_{\mathrm{L}}\tilde{E}^{\mathrm{C}}_{\mathrm{L}}H^j_{\mathrm{d}} - \tilde{Q}^i_{\mathrm{L}}h_{\mathrm{D}}\tilde{D}^{\mathrm{C}}_{\mathrm{L}}H^j_{\mathrm{d}} + \tilde{Q}^i_{\mathrm{L}}h_{\mathrm{U}}\tilde{U}^{\mathrm{C}}_{\mathrm{L}}H^j_{\mathrm{u}} + \mu H^i_{\mathrm{u}}H^j_{\mathrm{d}}) \tag{21}$$

with i, j being isospin indices, $\epsilon_{ij} = -\epsilon_{ji}(\epsilon_{12} = 1)$ and where

- $h_{\mathrm{L}}, h_{\mathrm{D}}, h_{\mathrm{U}}$ are dimensionless Yukawa coupling constants, expressed as 3×3 matrices in family space (as seen in section 3.3, only the third generation Yukawa couplings are of practical relevance);
- μ is a Higgs mixing parameter, **the only parameter with dimension** (mass) **in the superpotential**. This is the first appearance of this parameter [6].

In the SM a single Higgs field is sufficient to describe the Yukawa couplings by coupling down fermions to H and up fermions to H^*. In supersymmetry, the analyticity of the superpotential requires two Higgs doublets with opposite hypercharge to be present, one coupling to down particles and another to up particles (the same doubling of Higgses is also required to avoid triangle anomalies).

Some comments may help to clarify the structure of the superpotential. **Invariance under the gauge transformations imposes all terms to be singlets under all gauge groups**. Hence, the $I = 1/2$ fields must appear in antisymmetric combinations, to form an $I = 0$ term. For example, $\epsilon_{ij}(\tilde{Q}^i_{\mathrm{L}}H^j_{\mathrm{d}}) = \tilde{u}_{\mathrm{L}}H^-_{\mathrm{d}} - \tilde{d}_{\mathrm{L}}H^0_{\mathrm{d}}$ (note that both terms have charge $-1/3$). All terms should be neutral to conserve charge; the previous term can then only be multiplied by $\tilde{D}^{\mathrm{C}}_{\mathrm{L}}$. Hypercharge will then also be automatically zero. The colour indices are implicitly supposed to be summed to make singlets. Note that although a term of first order in the fields would be allowed in (20), it cannot be present in the MSSM as all fields carry non-zero quantum numbers[7].

For example, this yields for the first family (ignoring the off-diagonal elements of the Yukawa matrices)

$$\begin{aligned} W = {} & h_e(\tilde{e}_{\mathrm{L}}\tilde{e}^{\mathrm{C}}_{\mathrm{L}}H^0_{\mathrm{d}} - \tilde{\nu}\tilde{e}^{\mathrm{C}}_{\mathrm{L}}H^-_{\mathrm{d}}) + h_{\mathrm{d}}(\tilde{d}_{\mathrm{L}}\tilde{d}^{\mathrm{C}}_{\mathrm{L}}H^0_{\mathrm{d}} - \tilde{u}_{\mathrm{L}}\tilde{d}^{\mathrm{C}}_{\mathrm{L}}H^-_{\mathrm{d}}) \\ & + h_{\mathrm{u}}(\tilde{u}_{\mathrm{L}}\tilde{u}^{\mathrm{C}}_{\mathrm{L}}H^0_{\mathrm{u}} - \tilde{d}_{\mathrm{L}}\tilde{u}^{\mathrm{C}}_{\mathrm{L}}H^+_{\mathrm{u}}) + \mu(H^+_{\mathrm{u}}H^-_{\mathrm{d}} - H^0_{\mathrm{u}}H^0_{\mathrm{d}}). \end{aligned} \tag{22}$$

The minus signs in the superpotential (21) were chosen to produce positive contributions to the mass terms of down-type particles.

This is the most general form consistent with gauge invariance and conserving R-parity, defined in (13). R-parity conservation implies conservation of B and L numbers. It also imposes the superpartners to always appear in pairs in the superpotential. The extension to the case of R_{p} violating terms will be discussed in section 3.6.

Once the superpotential is specified, it is possible to derive the contribution to the potential in the MSSM Lagrangian.

[5] That the dimension is at most 3 is easily verified from the relation between the superpotential and the Lagrangian, see sections 3.4.3 and 3.4.4 below.

[6] Note that the sign of the μ-term is arbitrary and both conventions appear in the literature. Here, we follow Martin [1] and Haber [70]. See [71] for the convention used by various authors.

[7] But, as will be seen later, such a term multiplied by a constant of dimension mass-squared can be introduced in models beyond the MSSM, such as in NMSSM.

3.4.3. MSSM Lagrangian for chiral fields. The contribution to the Lagrangian for *chiral fermions* is

$$\mathcal{L}_{\text{chir}} = -\frac{1}{2}\frac{\partial^2 W}{\partial\phi_i\partial\phi_j}\psi_i\psi_j + h.c., \tag{23}$$

with ϕ_i the spin 0 partner of the ψ_i fermionic field. It generates Yukawa interactions and fermion mass terms. The first term in the above example, equation (22), gives rise to the interaction terms:

$$\begin{aligned}\mathcal{L}_{\text{chir},e} = & -\frac{h_e}{2}[(e_{\text{L}}e_{\text{L}}^{\text{C}})H_{\text{d}}^0 + (e_{\text{L}}^{\text{C}}\tilde{H}_{\text{d}}^0)\tilde{e}_{\text{L}} + (e_{\text{L}}\tilde{H}_{\text{d}}^0)\tilde{e}_{\text{L}}^{\text{C}} \\ & - (\nu e_{\text{L}}^{\text{C}})H_{\text{d}}^- - (e_{\text{L}}^{\text{C}}\tilde{H}_{\text{d}}^-)\tilde{\nu} - (\nu\tilde{H}_{\text{d}}^-)\tilde{e}_{\text{L}}^{\text{C}}] + \text{ h.c.}\end{aligned} \tag{24}$$

It contains the trilinear Yukawa interactions between fermions, scalars and a Higgs or higgsino. The first term reproduces **the familiar standard model Yukawa interaction** and will generate a mass for the fermions after electroweak symmetry is broken. The others correspond to **new interactions, but do not introduce new parameters**. The terms in equation (24) are the ones discussed previously in section 3.3.

In addition, there is a contribution from the μ-term in the superpotential:

$$\mathcal{L} \supset \mu(\tilde{H}_{\text{u}}^0\tilde{H}_{\text{d}}^0 - \tilde{H}_{\text{u}}^+\tilde{H}_{\text{d}}^-) + \text{ c.c.}, \tag{25}$$

providing off-diagonal elements in the mass matrices for the higgsino fermions. In consequence, the physical states will be mixtures of the higgsino fields $\tilde{H}_{\text{u}}$ and $\tilde{H}_{\text{d}}$.

3.4.4. MSSM scalar potential. It is also possible to derive the *scalar potential*. This includes two contributions

$$\begin{aligned}F_i &= \frac{\partial W}{\partial\phi_i}, \\ D^a &= -g\phi_i^* T_{ij}^a \phi_j.\end{aligned} \tag{26}$$

The first term is the 'chiral contribution', called *F-term*, the second one is the 'gauge contribution', called *D-term*, with T_{ij}^a being the generators of the gauge groups. The index a runs over all gauge groups and their generators. The indices i and j in the D-term imply a summation over all scalar fields (and chiralities). For the $U(1)$ contribution, $T_{ij} = Y/2$ connects two fields of same chirality and flavour, whereas for $SU(2)$, $T_{ij}^a = \tau^a/2$ (the Pauli matrices τ^a) connects two chiralities of fields with the same isospin. The full scalar potential is then written in the compact form (summation implied):

$$V(\phi) = F_i^* F_i + \tfrac{1}{2}D^a D^a. \tag{27}$$

An example of the D-terms for Higgs fields will be given below.

Without attempting to give a derivation of formulae (26) and (27), which can be found in [1], it is nevertheless useful to clarify somewhat the notions involved. The fields F_i and D^a are called 'auxiliary fields'. They originate from the fact that the matching of degrees of freedom discussed in section 3.2 holds only when the particles are on-shell, whereas the theory should be able to cope with the off-shell case as well. In the chiral supermultiplet, the off-shell fermion spinor is a complex two-component object, so it acquires two more fermionic degrees of freedom than on-shell. The matching of degrees of freedom is achieved by the introduction of another two real scalar degrees of freedom, a complex scalar field called F_i. In the gauge supermultiplet, the fermion also acquires two more degrees of freedom, while the vector field acquires only one more, its longitudinal spin component. The matching is obtained by introducing an additional real scalar field D^a. **These auxiliary fields should**

only be a bookkeeping device and they should not affect the physics on-shell. This is achieved by not giving them a kinetic term in the Lagrangian, so that they do not propagate, but introducing them only in the potential according to (27). Note that, unlike the ordinary scalar fields, the auxiliary scalar fields are of canonical dimension $(E)^2$. After working out the classical equations of motion, the auxiliary fields F_i and D^a can be expressed in terms of the scalar fields, given in equation (26), so that **the scalar potential becomes a function of the physical fields only**. The auxiliary field formulation is especially useful when treating the spontaneous breaking of supersymmetry.

The *F-term contribution* from the Yukawa interactions to the scalar potential leads to quartic terms, for example:

$$\begin{aligned} -\mathcal{L} \supset V_e = {} & |h_e \tilde{e}_{\mathrm{L}}^{\mathrm{C}} H_{\mathrm{d}}^0|^2 + |h_e \tilde{e}_{\mathrm{L}}\, H_{\mathrm{d}}^0|^2 + |h_e \tilde{e}_{\mathrm{L}}\, \tilde{e}_{\mathrm{L}}^{\mathrm{C}}|^2 \\ & + |h_e \tilde{e}_{\mathrm{L}}^{\mathrm{C}} H_{\mathrm{d}}^-|^2 + |h_e \tilde{\nu}_{\mathrm{L}} H_{\mathrm{d}}^-|^2 + |h_e \tilde{\nu}_{\mathrm{L}} \tilde{e}_{\mathrm{L}}^{\mathrm{C}}|^2, \end{aligned} \tag{28}$$

which do not have their equivalent in the standard model. The first two contribute to $(\mathrm{mass})^2$ terms for the left and right scalars. They are also the couplings which cancel the trilinear $f_{\mathrm{L}} f_{\mathrm{L}}^{\mathrm{C}} H^0$ couplings from equation (24) in the loop contributions to the Higgs mass, mentioned in section 3.1. The third one introduces quartic interaction between the left and right scalars. By comparing (28) and (24), it is also observed that **the scalars and the fermions are mass degenerate**.

The F-term contribution from only the μ-term in the superpotential yields

$$-\mathcal{L} \supset V \supset |\mu|^2(|H_{\mathrm{d}}^0|^2 + |H_{\mathrm{u}}^0|^2 + |H_{\mathrm{d}}^-|^2 + |H_{\mathrm{u}}^+|^2) \tag{29}$$

giving rise to a quadratic term in the Higgs fields. As this potential is positive definite, it is clear that **in an unbroken supersymmetric theory the electroweak symmetry breaking does not occur**. The minimum of the Higgs potential is located at $v_{\mathrm{d}} = v_{\mathrm{u}} = 0$, so that all particles remain massless.

In addition, the $\partial W/\partial H_i$ also contributes with a product of the μ and Yukawa terms, leading to trilinear interactions of scalars:

$$\begin{aligned} \mathcal{L} \supset {} & \mu^*(h_e \tilde{e}_{\mathrm{L}} \tilde{e}_{\mathrm{L}}^{\mathrm{C}} H_{\mathrm{u}}^{0*} + h_{\mathrm{d}} \tilde{d}_{\mathrm{L}} \tilde{d}_{\mathrm{L}}^{\mathrm{C}} H_{\mathrm{u}}^{0*} + h_{\mathrm{u}} \tilde{u}_{\mathrm{L}} \tilde{u}_{\mathrm{L}}^{\mathrm{C}} H_{\mathrm{d}}^{0*} \\ & + h_e \tilde{\nu} \tilde{e}_{\mathrm{L}}^{\mathrm{C}} H_{\mathrm{u}}^{+*} + h_{\mathrm{d}} \tilde{u}_{\mathrm{L}} \tilde{d}_{\mathrm{L}}^{\mathrm{C}} H_{\mathrm{u}}^{+*} + h_{\mathrm{u}} \tilde{d}_{\mathrm{L}} \tilde{u}_{\mathrm{L}}^{\mathrm{C}} H_{\mathrm{d}}^{-*}) + \text{ c.c.}, \end{aligned} \tag{30}$$

with coupling strength $(\mu.h)$ with dimension of mass. **They connect left to right scalars and play an important role in determining the mixing between left and right sfermions**.

The *D-term contribution* is entirely determined by supersymmetry and gauge invariance. In particular, it does not depend on the assumptions underlying the specification of the superpotential (nor on supersymmetry breaking). It introduces in the scalar potential quartic interactions with coupling strength g^2 of sfermions and of Higgses; for example, the piece containing the Higgs fields reads

$$-\mathcal{L} \supset V \supset \frac{1}{2} g_2^2 \left(H_{\mathrm{d}}^* \frac{\vec{\tau}}{2} H_{\mathrm{d}} + H_{\mathrm{u}}^* \frac{\vec{\tau}}{2} H_{\mathrm{u}} \right)^2 + \frac{1}{8} g_1^2 (|H_{\mathrm{u}}|^2 - |H_{\mathrm{d}}|^2)^2, \tag{31}$$

where g_1 and g_2 refer to the gauge groups $U(1)$ and $SU(2)$ and $\vec{\tau}$ are the Pauli matrices. **They generate quartic terms in the neutral Higgs potential with strength fixed by the gauge couplings. This is a fundamental difference with respect to the SM where this coupling constant remains a free parameter**. The contribution from the neutral Higgses is given by

$$V(H_{\mathrm{d}}^0, H_{\mathrm{u}}^0) \supset \frac{g_1^2 + g_2^2}{8} (|H_{\mathrm{u}}^0|^2 - |H_{\mathrm{d}}^0|^2)^2. \tag{32}$$

The full expression including charged Higgses can be found in [1]. **The fact that the D-terms are entirely determined by symmetry principles explains the robustness of the prediction of m_h in supersymmetry**.

3.4.5. Conclusion. The full Lagrangian density for an unbroken supersymmetry is given by

$$\mathcal{L} = \mathcal{L}_{\text{kin}} + \mathcal{L}_{\text{chir}} - V(\phi), \tag{33}$$

where the three terms are defined, respectively, by equations (16), (23) and (27).

Altogether, unbroken supersymmetry is a very constrained theory. It doubles the number of states and introduces a large number of new interactions, but it does not require more free parameters than in the standard model. In fact, whereas the SM Higgs potential contains two free parameters, the MSSM contains only one, the parameter μ.

In addition, the MSSM with the assumption of **R-parity conservation requires the superpartners to appear in pairs in all interactions. As a consequence, the lightest supersymmetric particle (called LSP) is predicted to be stable.** This has far-reaching implications for the phenomenology. A stable LSP should be neutral for cosmological reasons [23] and is likely to be the lightest neutralino. The latter interacts very weakly and escapes detection, leading to missing energy, the typical signature of supersymmetry. It is also a respectable candidate for cold dark matter.

3.5. SUSY breaking

In unbroken supersymmetry, the superpartners are expected to be degenerate in mass with the SM particles of the same supermultiplet and massless. The non-observation of superpartners, therefore, requires supersymmetry to be broken. However, to avoid that the radiative corrections to the mass of scalar particles generate quadratic divergences (the hierarchy problem[8] of the SM), the breaking must take a specific form, called 'soft supersymmetry breaking'. The list of allowed terms was established by Girardello and Grisaru [14]. The parameters of soft breaking have to be dimensionful and with positive mass dimension (e.g. this forbids the introduction of a quartic Higgs coupling by soft breaking).

To break supersymmetry softly, a piece is added to the Lagrangian:

$$\delta\mathcal{L}_{\text{soft}} = -\sum_{\tilde{q}\ ,\tilde{l}\ ,H_{\text{d,u}}} m_{0,i}^2|\Phi_i|^2 + (-\tfrac{1}{2}m_{1/2,a}\lambda_a\lambda_a - A_{0,i}W_{3,i} - B_0\mu H_{\text{u}}H_{\text{d}}) + \text{h.c.}, \tag{34}$$

where $m_{0,i}$ introduces a mass for the scalars and $m_{1/2,a}$ for the gauginos. In principle, $m_{0,i}$ is a matrix in generation space. It is also allowed to introduce the superpotential terms, multiplied by a mass parameter: $A_{0,i}$ and B_0 are parameters with dimension of mass and $W_{3,i}$ represents the trilinear terms (with their sign and Yukawa couplings) of the superpotential. Antisymmetrization of the isospin components in (34) is implied. **As no convincing mechanism of supersymmetry breaking is known so far, this should be merely viewed as 'a parametrization of our ignorance' [1] and can be used as an effective Lagrangian from which to derive the phenomenology**.

In this general form, **a large number of free parameters are introduced**. In total 124 were counted [76] including the ones of the SM, hence the name MSSM-124 [77]. However, several could induce flavour changing neutral currents (FCNC) or CP violation at an unacceptable level. More restrictive models satisfying these requirements and relying on fewer parameters have been developed and will be considered later.

The mass parameters introduced by the soft SUSY breaking lift the mass degeneracy of the members of the supermultiplets. They contribute to the radiative corrections, shown in expression (9), affecting the Higgs mass. **To avoid recurrence of the hierarchy problem, their values can be at most a few TeV**.

[8] We do not consider here variants such as the 'small or no hierarchy', to be mentioned in section 5.1, and adhere to the usual, hierarchical, version.

3.5.1. The Higgs potential. Collecting the relevant terms from section 3.4, the neutral Higgs potential takes the form

$$V(H_{\rm d}^0, H_{\rm u}^0) = \frac{g_1^2 + g_2^2}{8}(|H_{\rm d}^0|^2 - |H_{\rm u}^0|^2)^2 + \mu_1^2|H_{\rm d}^0|^2 + \mu_2^2|H_{\rm u}^0|^2 - \mu_3^2(H_{\rm u}^0 H_{\rm d}^0 + \text{ c.c.}), \tag{35}$$

where the scale dependent mass coefficients are $\mu_1^2 \equiv m_{H_{\rm d}}^2 + \mu^2$, $\mu_2^2 \equiv m_{H_{\rm u}}^2 + \mu^2$, $\mu_3^2 \equiv B\mu$. The first term is the D-term contribution of equation (31), the other terms originate from the F-term in (29) and the soft breaking pieces in (34). **It is a noteworthy feature of supersymmetry that the coefficient of the quartic term is fixed by the gauge couplings, unlike the SM where it is arbitrary**.

When electroweak symmetry is broken, the Higgs fields $H_{\rm d}$ and $H_{\rm u}$ acquire vacuum expectation values $v_{\rm d}$ and $v_{\rm u}$, whose ratio defines $\tan\beta = v_{\rm u}/v_{\rm d}$, as mentioned earlier. The minimization of the tree level neutral Higgs potential with respect to $H_{\rm d}$ and $H_{\rm u}$ leads to two equations. The first one

$$\sin 2\beta = \frac{2\mu B}{m_{H_{\rm d}}^2 + m_{H_{\rm u}}^2 + 2\mu^2} \tag{36}$$

relates the value of $\tan\beta$ to the SUSY breaking parameter μB. The second one is

$$\frac{M_Z^2}{2} = \frac{m_{H_{\rm d}}^2 - m_{H_{\rm u}}^2 \tan^2\beta}{\tan^2\beta - 1} - \mu^2. \tag{37}$$

As $m_{H_{\rm d}}$ and $m_{H_{\rm u}}$ are soft SUSY breaking parameters, their magnitude is expected to be of the order of the electroweak scale. In consequence, μ is also expected to be of that scale. This is at the origin of the so-called μ problem.

3.5.2. The μ problem and the NMSSM. We saw that the μ parameter appears as a basic one in the expression of the superpotential, equation (21). Since it has the dimension of mass, one would expect $\mu = 0$ or $\mu = M_{\rm Pl}$. However, μ appears also in the MSSM scalar potential and for a correct electroweak symmetry breaking (i.e. W and Z masses), the preferred value is $\mu \simeq$ few 100 GeV. The question **why μ is so small and not zero is referred to as the μ problem**. In supergravity models a μ term of the correct magnitude is generated and $B \cdot \mu$ (see section 3.5) are naturally of the same order as the other supersymmetry breaking terms [72].

If one wants to address it, one answer is to postulate that μ originates from the vacuum expectation value of a new Higgs singlet field. This would lead to an extension of the MSSM, called NMSSM (for a recent review, see [73,74]). In its minimal version, the NMSSM assumes the existence of a single scalar, S, which transforms as a singlet under the gauge groups. A piece is added to the MSSM superpotential (without μ term) which is

$$W_S = \lambda\epsilon_{ij} H_{\rm u}^i H_{\rm d}^j S + \tfrac{1}{3}\kappa S^3, \tag{38}$$

where S is the gauge singlet superfield. It is scale invariant, i.e. there is no μ-term. Instead, two Yukawa couplings λ and κ appear. Once the electroweak symmetry is broken, the scalar component of S acquires a vacuum expectation value $\langle S\rangle$, thus generating an effective μ term $\mu = \lambda\langle S\rangle$. The second term breaks an unwanted Peccei–Quinn (PQ) symmetry. It is shown in [75] that the qualitative features of the Higgs system are dependent on how strongly this PQ symmetry is broken. If it is left explicitly unbroken in the Lagrangian ($\kappa = 0$), there should exist a massless PQ axion which was not observed. The domain of the parameter space left does not provide a natural solution to the μ problem. **But the NMSSM with slightly broken PQ symmetry is still a valid scenario.** New Higgs states appear, as well as an additional neutralino, which usually mix with the corresponding MSSM states. A strongly broken PQ symmetry may lead to decoupled scenarios more difficult to distinguish from the MSSM.

The tree level potential for the neutral Higgs states is of the same form as (35): the D-term is unaffected (the field S is a gauge singlet) and in the other terms μ is replaced by $\lambda\langle S\rangle$. There are additional terms due to the presence of the field S,

$$V_{\mathrm{NMSSM}} = V(H_{\mathrm{d}}^0, H_{\mathrm{u}}^0) + \lambda^2 |H_{\mathrm{d}}^0 H_{\mathrm{u}}^0|^2 + \lambda\kappa[S^{*2} H_{\mathrm{d}}^0 H_{\mathrm{u}}^0 + \text{ h.c.}] + \kappa^2 |S|^4 + m_S^2 |S|^2 + \left[\frac{\kappa}{3} A_\kappa S^3 + \text{ h.c.}\right], \tag{39}$$

of which the first three contributions are F-terms and the last two are soft breaking terms. The free parameters are the couplings λ and κ, the three soft masses $m_{H_{\mathrm{d}}}$, $m_{H_{\mathrm{u}}}$ and m_S and the trilinear couplings A_κ and $A_\lambda (= B_0$ of equation (34) in our previous discussion). After electroweak symmetry breaking, this potential needs to be minimized with respect to H_{d}, H_{u} and S. It is customary to use the three minimization equations to eliminate the soft masses in favour of M_Z, $\tan\beta$ and $\mu = \lambda\langle S\rangle$, leaving the parameters

$$\lambda, \kappa, \tan\beta, \mu, A_\lambda, A_\kappa \tag{40}$$

in addition to the soft masses of the other scalars and gauginos and the trilinear coupling parameters of the MSSM. The signs can be chosen such that λ and $\tan\beta$ are positive, but the other parameters can have either sign.

The requirement of perturbativity up to the GUT scale imposes a bound on the NMSSM couplings

$$\lambda^2 + \kappa^2 \leqslant 0.5. \tag{41}$$

The original phenomenology of the NMSSM in terms of Higgs bosons and of neutralinos will be described later.

3.6. R-parity?

The couplings introduced in the superpotential (21) conserve both lepton number and baryon number. **It is permitted in the MSSM to include additional terms which are gauge- and supersymmetry-invariant, but violate lepton or baryon number** [22]. Most terms are easily derived after observing that the H_{d} has the same gauge quantum numbers as the $\tilde{L}$ isospin doublet, see table 2. The most general superpotential would also include

$$W_{\mathrm{RPV}} = \lambda_{ijk} \tilde{L}_i \tilde{L}_j \tilde{E}_k^{\mathrm{C}} + \lambda'_{ijk} \tilde{L}_i \tilde{Q}_j \tilde{D}_k^{\mathrm{C}} + \lambda'_{ijk} \tilde{U}_i^{\mathrm{C}} \tilde{D}_j^{\mathrm{C}} \tilde{D}_k^{\mathrm{C}} + \mu'_i \tilde{L}_i H_{\mathrm{d}}. \tag{42}$$

The indices i, j, k represent the three generations and the antisymmetrization of the isospin 1/2 fields is implicitly assumed. The first, second and fourth terms violate the total lepton number, $\Delta L = 1$, while the third term violates the total baryon number, $\Delta B = 1$. The possible types of Yukawa couplings are limited to

- λ_{ijk}: the term is antisymmetric in i and j by $SU2$ invariance, leaving 9 independent couplings, and the usual convention adopted is that $i < j$ (which introduces a factor 2 in the superpotential),
- λ'_{ijk} has no symmetry constraints, hence 27 terms,
- λ'_{ijk}: the term is antisymmetric in j and k by invariance under colour $SU(3)$, leaving 9 couplings, with again the usual convention that $j < k$ (and the factor 2).

Altogether, there are 45 new couplings from the trilinear terms. The last, bilinear, term is basis dependent but cannot be rotated away simultaneously from the superpotential and from the symmetry breaking Lagrangian by a redefinition of the Higgs fields [78]. Bilinear terms will induce a non-zero vacuum expectation value for the sneutrinos. The vacuum expectation values induce mixing between neutrinos and neutralinos which give mass to one neutrino,

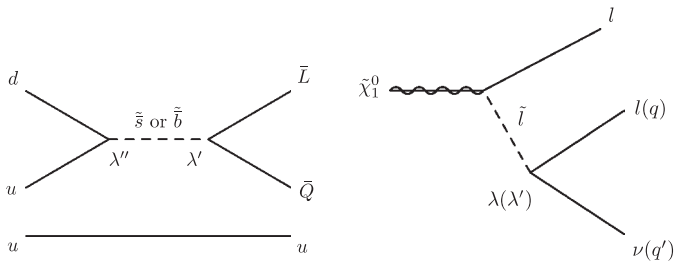

Figure 5. (left) R_p violating couplings leading to proton decay. (right) R_p violating decay of a neutralino.

while the second mass is induced by loop effects. The same parameters, which give ν masses and mixings, lead also to the decay of the LSP. One can therefore under various assumptions derive correlated features between neutrino physics and R-parity violating SUSY [79], for instance between the atmospheric ν mixing angle and the ratio of semi-leptonic branching ratio of the LSP into μ and τ. See for instance [80] and references therein for an analysis of neutrino oscillation results within this context. The relationship between the origin of neutrino properties and R-parity violation is only an assumption, perhaps marginal, and the present trend is rather to search for their origin at much higher scales and invoke a seesaw mechanism.

The presence of such terms in the superpotential is usually forbidden by assuming the conservation of R-parity. The R-parity is $R_p = +1$ for all SM particles and $R_p = -1$ for their supersymmetric partners. Therefore, its conservation forces the superpartners to appear in pairs in all interactions. The superpotential (21) conserves R-parity, while the terms in (42) are R_p violating (RPV).

The superpotential in its general form above contains potentially dangerous terms, as simultaneously non-zero λ' and λ'' couplings may lead to fast proton decay through, for instance, the diagram in figure 5 (left). The proton lifetime, which is experimentally known to exceed 10^{33} years (see section 6), puts stringent limits on the products $\lambda'\lambda''$. For reasons of simplicity, the experimental analyses frequently assume that only one term is non-zero at a time.

The main consequence of RPV is that the lightest neutralino is no longer stable. It can decay into a pair (possibly virtual) $l\tilde{l}$ or $q\tilde{q}$, followed by the RPV decay of the $\tilde{l}$ or $\tilde{q}$ as illustrated in figure 5 (right). The celebrated missing energy signature of MSUGRA no longer exists, except for final states involving neutrinos. **But new signatures appear**, as RPV decays lead to additional leptons and/or jets, depending on which Yukawa couplings dominate. It is also worth mentioning that, if the LSP is unstable, the requirement from cosmology that it be neutral no longer persists. In the RPV framework, the LSP can as well be a charged particle, such as a slepton. With RPV, **there is no longer a natural supersymmetric candidate for dark matter**.

Finally, non-zero Yukawa couplings λ or λ' allow respectively the s-channel resonant production of sneutrinos at LEP or squarks (looking like scalar leptoquarks) at HERA.

Section 14 will deal in detail with R-parity violation.

4. SUSY and grand unification

A problem with the SM is its large number of parameters. The introduction of (unbroken) supersymmetry does not increase this number, but does not reduce it either. A possible road

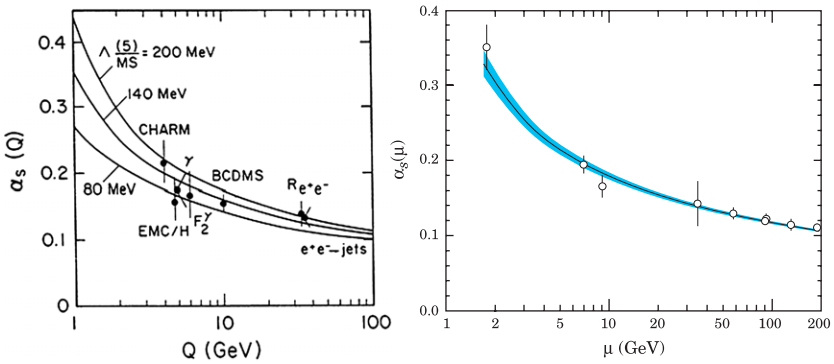

Figure 6. Evolution of the α_S couplings, from [82].

to address this problem is to embed the SM gauge groups into a larger group, called grand unification theory (GUT) [81]. A very exciting possibility would be to combine the ideas of SUSY with GUT and, as we said, there is indeed some experimental support from the extrapolation of the gauge couplings to higher energies that this might work.

4.1. Evolution of coupling constants, example of α_S

Due to the effect of virtual particles in loop diagrams, **coupling constants evolve with the scale at which they are measured**. The precise knowledge of the evolution of the fine structure 'constant' α from the static limit to the Z^0 scale is a key to the electroweak tests. Such behaviour has been clearly observed by the measurement of the strong coupling α_S as function of energy [5], illustrated in figure 6. The left figure summarizes the knowledge of the running of α_S before the start of LEP (in 1989) and gave an average value at the Z^0 mass scale $\alpha_S(M_Z) = 0.11 \pm 0.01$. After the LEP measurements, the accuracy was significantly improved, as seen in figure 6 (right), and its value was determined [83] to be $\alpha_S(M_Z) = 0.1187 \pm 0.002$. For a review, see [85].

Also observed, but much less spectacular, the running of α between its static value and the Z scale is a key effect since what matters for accurate SM testing is $\alpha(M_Z)$. The problem is related, but not identical, to the determination of the hadronic contribution to $g-2$, discussed in section 6.5.

The experimentally determined values of the EW couplings at the Z^0 mass are (in the $\overline{MS}$ renormalization scheme) as follows [84]: $\alpha_{em}^{-1}(M_Z) = 127.918 \pm 0.018$; from the measurement of $\sin^2\theta_W(M_Z) = 0.23120 \pm 0.00015$ the U(1) and $SU(2)$ couplings are obtained using the relations $\alpha_1^{-1} = (3/5)\alpha_{em}^{-1}\cos^2\theta_W$ and $\alpha_2^{-1} = \alpha_{em}^{-1}\sin^2\theta_W$. The factor $3/5$ is required for the correct embedding of the SM gauge groups into the unification groups $SU5$ or $SO(10)$.

4.2. Grand unification

The values of the three SM coupling constants, α_a, are known with high accuracy, especially after the measurements from LEP/SLC which allowed an improvement of the precision on $\sin^2\theta_W$ by a factor ~50. Their values determined at the scale of the Z^0 mass can be extrapolated to higher energies by means of RGEs. At 1-loop level, they lead to the relations:

$$\frac{\mathrm{d}}{\mathrm{d}t}\alpha_a^{-1}(t) = -\frac{b_a}{2\pi}, \tag{43}$$

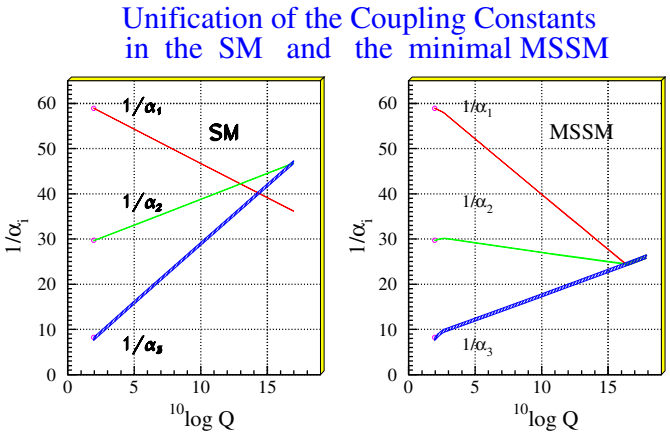

Figure 7. Evolution of the gauge couplings as a function of the scale Q (in GeV), from [87].

showing that the inverse couplings evolve linearly with the scale parameter $t \equiv \ln(q/q_0)$. The constants b_a are determined by the particles entering in the loops and by their charges for the gauge groups $U(1)$, $SU(2)$, $SU(3)$. In the SM, they take the values $b_a = (41/10, -19/6, -7)$, while in the MSSM they are $b_a = (33/5, 1, -3)$. The values for b_1 for the SM and the MSSM assume the correct normalization of the coupling constant g_1 for the embedding into the unification groups $SU5$ or $SO(10)$. The unification of α_1 and α_2 corresponds to $\tan\theta_W = \sqrt{3/5}$ at the GUT scale. Apart from this normalization factor, the evolution does not depend on assumptions about the unification group until one reaches the GUT scale.

Unification would require that, at some energy scale, all couplings become equal, $\alpha_1 = \alpha_2 = \alpha_3 = \alpha_{\mathrm{GUT}}$ [17]. Difficulties with the SM were initially observed in 1987 [86], before the start of LEP. But after the start of LEP, unification was totally ruled out for the SM. The evolution, including 2-loop effects, is illustrated in figure 7 (from [87]). It is seen that, for the particle content of the SM, some convergence occurs but no true unification is obtained (it is missed by about 12σ [88]). On the contrary, if the evolution is started with the SM particle content and, at a scale M_{SUSY} around 1 TeV, the MSSM particles are included, the slopes change drastically and the gauge couplings unify at approximately $M_{\mathrm{GUT}} \simeq 2 \times 10^{16}$ GeV [18].

- **The unification occurs below the Planck scale.** This is important because above the Planck scale gravitational interactions could no longer be neglected.
- The unified coupling amounts to $\alpha_{\mathrm{GUT}} \simeq 1/25$, **well inside the perturbative regime**.
- **The energy scale of $\sim 10^{15}$ GeV at which the couplings 'meet' in the SM is in conflict with the present bounds on the proton lifetime. With SUSY, it is raised by an order of magnitude and can be compatible with proton decay results** (see section 6.1).

This might be a first experimental hint that something exists beyond the SM. The unification is, however, not very sensitive to the exact value of the SUSY masses, as a range $100\,\mathrm{GeV} \leqslant M_{\mathrm{SUSY}} \leqslant 10\,\mathrm{TeV}$ can be accommodated.

To check the idea of coupling constant unification, an alternative presentation is to use the precisely measured weak angle and the extrapolated fine structure constant $\alpha(M_Z)$ to predict the Z-pole strong coupling and the unification scale and compare the predicted with the observed value. Model dependent corrections are typically of order 10% and need to be included consistently [89]. Such corrections come from

- using the correct spectrum of superpartners and heavy Higgs particles to evaluate $M_{\rm SUSY}$ as a weighted sum of all mass logarithms, instead of a mere generic mean,
- GUT threshold corrections, depending on the details of the theory and
- non-renormalizable operator corrections gravitationally induced and generic, see e.g. [90].

The estimate of their magnitude and uncertainty is discussed in [89]. They are expected to be small, provided gauge couplings remain perturbative and the GUT scale is sufficiently below the string and Planck scales. Assuming no conspiracies among the different model-dependent corrections, the assumption of coupling unification with SUSY requires $\alpha_S(M_Z) \simeq 0.129 \pm 0.010$. The observed value of $\alpha_S(M_Z)$ is thus on the low side of the prediction, but quite compatible with it. In contrast, the prediction $\alpha_S(M_Z) \sim 0.07$ of non-supersymmetric gauge unification would require much larger corrections. It can be noted that in the case of the gauge coupling unification with supersymmetry the effect of massive neutrinos is small but of the right sign to improve the agreement with experiment [91].

In the above mechanism leading to unification of the gauge couplings, it is assumed that no new particles exist between the superpartners, in the 1–10 TeV region, and the unification scale. This assumption of a 'desert' can, however, be evaded. For example, provided new particles appear in complete representations of the unification group, they contribute equally to all constants b_a and the unification will still take place at the same scale but for a different value of the unified coupling [17, 93]. Other models with intermediate scale and not necessarily SUSY (e.g. [92]) can also lead to unification. Adding new particles in incomplete GUT multiplets at intermediate scales or multiple GUT breaking scales, one can certainly achieve GU without invoking SUSY. An example is the breaking sequence $SO(10) \to SU(4)_C \times SU(2)_L \times SU(2)_R \to SM$ with the second breaking at an intermediate scale [94]. In the case of large extra dimensions, grand unification depends on the assumed scenario. We refer to [95] for the ADD scenario and to [96] for the case of warped extra dimensions. Symmetry breaking in extra dimensions can also be applied to breaking SUSY. The case of extra dimensions of GU scale will be alluded to later. Several other possibilities of grand unification are discussed in [97].

4.3. Particle contents in GU groups

Grand unification is a most important idea in particle physics [88], which may resolve at once several of its puzzles. It explains the quantification of charge. It clarifies the observed structure within a family. While in the SM the fermions of a family are scattered among five multiplets, $SU(5)$ groups them in two multiplets, $\bar{\mathbf{5}}$ and $\mathbf{10}$ [81]. The minimal extension of the SM symmetry required to group a family into a single multiplet is the Pati–Salam conjecture [98]

$$G \equiv SU(4)_{\rm C} \times SU(2)_{\rm L} \times SU(2)_{\rm R}, \tag{44}$$

where the lepton number is treated as a fourth colour. It requires that there are sixteen two-component fermions in each family, as opposed to fifteen for the SM. This symmetry is embedded in $SO(10)$ which preserves the 16-plet family structure. Besides offering, as we saw, the meeting of the three gauge couplings, supersymmetric GU such as G or $SO(10)$ offers heavy right-handed neutrinos $\nu_{\rm R}$ as a compelling feature to fill the vacant position in the 16-plet.

However, two notable pieces needed to validate the idea are still missing. On one hand, supersymmetry has still to be discovered. On the other hand, the quark-lepton symmetry thus introduced, and their transformability, induces proton decay which has not yet been observed. The latter will be considered in section 6.1.

4.3.1. Unification in $SU(5)$. In the original scheme proposed in 1974 by Georgi and Glashow [81], the quarks and leptons of a given family are allocated to a $\bar{\mathbf{5}} = [d^c, L]$ and a $\mathbf{10} = [Q, u^c, e^c]$ of $SU(5)$. The Higgs doublet(s) is part of a $\mathbf{5_H}$ or/and $\bar{\mathbf{5}}_\mathbf{H}$, the other three states being colour triplet Higgs scalars. The latter are supposed to be heavy ($\sim 10^{10-11}$ GeV) to avoid too fast proton decay, which they can mediate via effective operators of dimension 5 ($\propto 1/M_U$). The doublet–triplet splitting problem and its solutions have been abundantly discussed, e.g. [99]. In supersymmetric $SU(5)$ [100], both Higgs multiplets are required.

With these multiplet assignments, the Yukawa couplings in the superpotential (21) are of the form

$$W \supset h(\mathbf{10}\,\bar{\mathbf{5}}\,\bar{\mathbf{5}}_\mathbf{H}) + h'(\mathbf{10}\,\mathbf{10}\,\mathbf{5_H}) \qquad (45)$$
$$= -h(\tilde{L}_\mathrm{L}\tilde{E}^\mathrm{C}_\mathrm{L}H_\mathrm{d} + \tilde{Q}_\mathrm{L}\tilde{D}^\mathrm{C}_\mathrm{L}H_\mathrm{d}) + h'(\tilde{Q}_\mathrm{L}\tilde{U}^\mathrm{C}_\mathrm{L}H_\mathrm{u}).$$

They yield at tree level the relation $h_b = h_\tau = h$ (see section 4.3.3), but also wrong relations for the 1st two generations (see Georgi and Jarlskog [101] for a possible solution).

A variant is the so-called 'flipped $SU(5)$' [102], where the unification group is $SU(5) \times U(1)$ and non-abelian unification occurs, but part of the hypercharge $U(1)_Y$ appears in the external $U(1)$ factor. The particle assignment is in this case $\bar{\mathbf{5}} = [u^c, L]$ and $\mathbf{10} = [Q, d^c, \nu^c]$ of $SU(5)$ (hence the term 'flipped') and the singlet $\mathbf{1} = [e^c]$. This structure implies the existence of a right-handed neutrino.

4.3.2. Unification in $SO(10)$. In the case of unification in the group $SO(10)$ [103], all quarks and leptons of a family are put in a 16-dimensional spinor representation. As shown, for example, in [4], there exists an elegant description of the 16-dimensional representation as a tensor product of five spin 1/2 states. The connection with $SU(5)$ is $\mathbf{16} = [\mathbf{10} + \bar{\mathbf{5}} + \mathbf{1}]_{SU(5)}$. The singlet can be assigned to ν^c, which is therefore sterile. The Higgs doublets can be put in a $\mathbf{10}_H = [\mathbf{5_H} + \bar{\mathbf{5}}_\mathbf{H}]_{SU(5)}$.

For $SO(10)$ unification, the Yukawa couplings are simply

$$W \supset h(\mathbf{16}\,\mathbf{16}\,\mathbf{10_H}), \qquad (46)$$

which lead to the expectation $h_t = h_b = h_\tau = h$.

There are two maximal breaking patterns of $SO(10)$. The first is $SO(10) \to SU(5) \times U(1)_X$, which leads to the usual $SU(5)$ if the electromagnetic charge originates entirely from the $SU(5)$ generators or to flipped $SU(5)$ if the charge comes partly from $U(1)_X$. The second is $SO(10) \to SU(4)_\mathrm{C} \times SU(2)_\mathrm{L} \times SU(2)_\mathrm{R}$, leading to the Pati–Salam symmetry.

The existence of 3 heavy singlets allows the three known neutrinos to acquire naturally small Majorana masses through the seesaw mechanism. The decay of the lightest of them may generate a lepton asymmetry in the early universe which gets converted by sphalerons during the electroweak phase transition to the presently observed baryon asymmetry of the universe.

4.3.3. Unification of Yukawa couplings. The equations (15) allow the quark and lepton masses to be related to their Yukawa couplings for a fixed value of $\tan\beta$. Starting from the running masses, after including radiative corrections, evolving the Yukawa couplings up to the GUT scale by means of RGEs allows the Yukawa unification hypothesis to be checked. The results of the analysis from [104] in the MSSM are displayed in figure 8, where the relative deviation from unification $\epsilon_b = (h_b - h_\tau)/h_\tau$ at the GUT scale is shown as function of $\tan\beta$. As has been known for years, there are two regions where b–τ unification is possible, namely at small $\tan\beta \simeq 1.2$–1.7 and high $\tan\beta \simeq 20$–50. The 1-loop RGEs of the Yukawa couplings contain terms proportional to the Yukawa couplings themselves and terms proportional to the gauge couplings, the two being of opposite sign. For low $\tan\beta$, this leads to a cancellation of

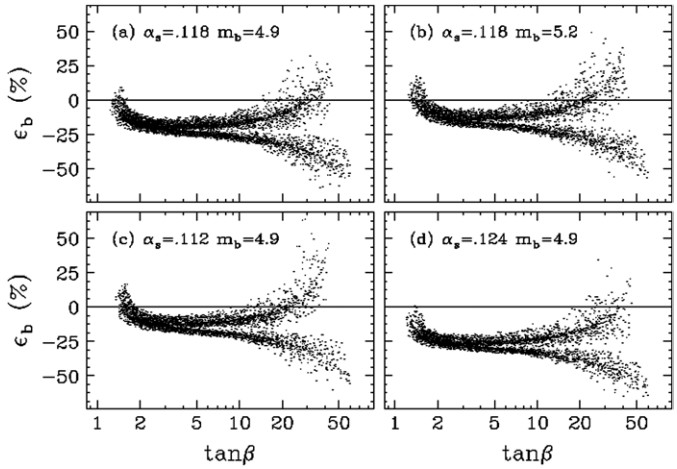

Figure 8. Unification of the Yukawa couplings, reprinted from [104]. Copyright 1997, with permission from Elsevier. The relative deviation from unification is shown as function of tan β for several values of α_S and m_b. The two branches correspond to opposite signs of the parameter μ.

the contribution of α_S to the evolution of the bottom Yukawa coupling which allows it to unify with the τ Yukawa coupling at the GUT scale. The Yukawa of the top quark remains large at the GUT scale and is at the origin of the large disparity of masses for the top and the other fermions. At large tan β, the Yukawa couplings of the b and τ are both enhanced compared with the top and allow unification of t, b and τ. In this case, the large disparity of the masses is related to the large value of tan β. The low tan β region is presently disfavoured by the LEP searches for the light Higgs (unless m_t is substantially higher than its present determination). The two branches at high tan β correspond to different signs of μ, the upper (lower) one being for $\mu < 0 (\mu > 0)$ [9]. The high tan β region is still acceptable and overlaps with the region tan $\beta \simeq 40$–50 of $t - b - \tau$ unification expected in $SO(10)$, but only for $\mu < 0$. This is not the region favoured by $b \to s\gamma$ results nor by the present but controversial discrepancy on $g - 2$ of the muon, as will be seen in section 6. For the preferred sign, $\mu > 0$, the discrepancy in Yukawa unification is of -24 to -60%. But the unification at large tan β depends very sensitively on the parameters, especially m_b, which receives very important threshold corrections at the weak scale. Also see [105].

An interesting approach is described in [106]. The authors proceed from top to bottom, imposing an $SO(10)$ unification for the third generation Yukawa couplings at high scale. They find that consistency of this assumption with low energy data is limited to a narrow region of soft SUSY breaking parameters with definite predictions for $m_h (114 \pm 5 \pm 3\,\text{GeV})$ and for the SUSY spectrum, as will be discussed in section 5.5.

4.4. Provisional conclusion

Before entering the complexity of SUSY breaking scenarios, it is worth pausing a moment and summarizing our main conclusions so far.

We have seen up to now that supersymmetry, compared with the SM, has some outstanding virtues. It allows the divergences of the scalar masses to be tamed and reduces them from a

[9] The sign convention for μ in [104] is opposite to the one we use and has been flipped here to make it consistent with the rest of the text.

quadratic to a logarithmic dependence on the cut-off scale Λ, the latter being innocuous as long as the superpartner masses are not too large.

SUSY offers also the possibility of an accurate grand unification (GU) at a scale of a few 10^{16} GeV. Grand unification brings in further clues, as is well known, for instance an explanation of the equality of electron and proton charges, as well as potential experimental clues, such as non-zero neutrino masses and nucleon instability, to which we return later.

A third **bonus from SUSY, when R-parity is conserved, is the existence of a stable neutral lightest superpartner (LSP), which is an excellent candidate for cold dark matter (CDM)**.

Owing to the structure of SUSY, no new coupling is introduced as long as the theory is unbroken, and the only expense is the doubling of states. Unfortunately, SUSY is a broken symmetry and we saw that the breaking is the step through which new parameters, possibly a huge number of them, creep in. In the following chapters, we will consider three possible scenarios of SUSY breaking, make explicit the set of parameters they introduce and give the main features of their respective phenomenologies.

Yet another interesting feature of SUSY is that, owing to the large mass of the top quark, the breaking of the electroweak symmetry occurs quite naturally through radiative corrections.

A very important remark that the reader should keep in mind, before delving into the complexity of the scenarios, is that at least one feature of SUSY is nearly independent of the variety of SUSY breaking scenarios: **the existence of a very light Higgs boson (<130 GeV in the MSSM). This is the hard core of the MSSM phenomenology**.

The problems of the SM that SUSY has cured were linked to the existence of a large gap and a desert between the electroweak scale and the GU or Planck scale. If these assumptions are relaxed, one can reach different conclusions. It is even more true if, because of the existence of large compact extra dimensions, the effective Planck scale is actually next door, so that there is no large energy gap or a desert (see section 8.2). However, **a last crucial bonus that SUSY brings in is the possibility to introduce gravity into the game, which is ignored in the SM. This is at the root of superstring theory and therefore a strong incentive to keep focusing on SUSY.**

The SM is clearly an effective theory, valid within a certain domain and not beyond, which needs many inputs from outside. **SUSY, in spite of the progress it brings, would still also be an effective theory**. One does not know yet what superstring theory will lead to, but one may hope that it turns out to be a much more fundamental one.

5. Physical idea and gross features of the scenarios

5.1. SUSY breaking mechanisms

Although the effective theory, defined by the soft supersymmetry breaking contribution to the Lagrangian (34) is sufficient (with some additional conditions) to derive the phenomenology, it is nevertheless interesting to discuss a bit more the question of the origin of the SUSY breaking masses. This will allow for instance a better understanding of the very distinctive properties of gauge mediated supersymmetry breaking (GMSB), compared with the MSUGRA scenario outlined above. Readers more interested in the general features of the scenarios and the list of their parameters can go directly to section 5.2.

It is shown in the primer by Martin [1] that **the communication of SUSY breaking to the MSSM particles is very difficult to achieve in a phenomenologically acceptable way if one deals only with renormalizable interactions at tree level** (problem of giving masses

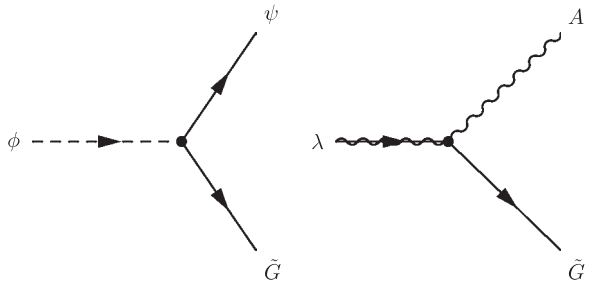

Figure 9. Goldstino interactions with supermultiplets.

to the gauginos, some sfermion masses unacceptably light due to the existence of a sum rule, etc). For these reasons, one expects that the MSSM soft terms arise indirectly or radiatively, rather than from a tree level coupling to the SUSY breaking order parameter. It is assumed that there is a 'hidden sector' of particles with no (or very weak) direct couplings to the MSSM supermultiplets of the 'observable sector'. **The breaking of supersymmetry, which is supposed to occur in the hidden sector, is transmitted via a 'messenger sector' to the visible sector**, resulting in the soft terms of expression (34). One usually assumes a hierarchy $M_{\rm ew} \ll$ messenger scale $\ll$ hidden scale. Models have been proposed where this transmission is mediated by gravitational interactions (SUGRA) or by gauge interactions (GMSB), or by an anomaly (anomaly mediated supersymmetry breaking, AMSB). The following presentation relies heavily on the lecture notes of Zwirner [107].

5.1.1. SUSY breaking in the hidden sector. It is a general feature, well-known from field theory, that the spontaneous breaking of a global symmetry gives rise to massless Goldstone bosons. The vector bosons associated with an exact local symmetry remain massless and have only transverse spin components. But **if the local symmetry is broken by the vacuum expectation value of a scalar field, the 'would be' Goldstone bosons are absorbed as the missing (longitudinal) spin component and make the vector bosons massive. A similar mechanism is invoked for the breaking of supersymmetry**.

The spontaneous breaking of a **global** supersymmetry requires that the vacuum is not invariant under supersymmetric transformations. This requires in turn that the SUSY scalar potential has a non-zero vacuum expectation value. From its form, given in equation (27), it appears that at least one of the auxiliary fields must acquire a non-zero vacuum expectation value, which gives the potential a positive vacuum energy. An unavoidable consequence (see e.g. [1] for an explanation) of the spontaneous breaking of a global supersymmetry is the existence of a massless spin 1/2 fermion, the goldstino $\tilde{G}$, in complete analogy with the spontaneous breaking of ordinary global symmetries. For simplicity, we assume that the goldstino is a member of a chiral multiplet. **If the auxiliary scalar field associated with the goldstino in the same supermultiplet acquires a vev $\langle F \rangle$, of dimension** $(\text{mass})^2$**, supersymmetry will be spontaneously broken**. The interaction of the goldstino with the other supermultiplets is defined by the Lagrangian

$$\mathcal{L}_{\rm goldstino} \supset -\frac{1}{\langle F \rangle} j^{\mu\alpha} \partial_\mu \tilde{G}_\alpha + \cdots, \tag{47}$$

where the supercurrent $j^{\mu\alpha}$, of dimension $(\text{mass})^{7/2}$, involves fermion-scalar and gaugino-gauge boson products, leading to interactions pictured in figure 9.

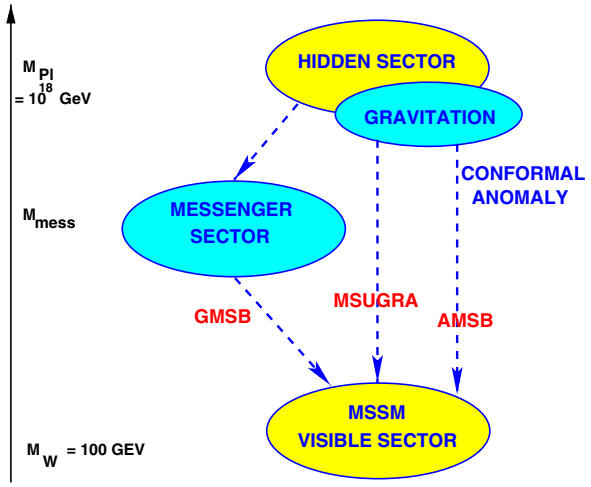

Figure 10. Supersymmetry breaking scenarios.

If gravity is taken into account, supersymmetry must be a local symmetry, called supergravity, which unifies the space-time symmetries of general relativity with local supersymmetry transformations. Invariance under supergravity transformations requires the spin-2 graviton to have a superpartner, the gravitino with spin 3/2, and if supersymmetry were unbroken both would have zero mass and only two helicity states. Once supergravity is spontaneously broken, the gravitino absorbs the goldstino, hence acquiring its mass $m_{3/2}$ and its two longitudinal helicity components $\pm 1/2$ (superhiggs mechanism) [108]. After including gravitational interactions, the scalar potential (27) is replaced by [107]

$$V = |F|^2 + |D|^2 - |H|^2, \tag{48}$$

where the expressions of F and D are different from (26) but play the same role. The third term is particular to supergravity and has the universal property that $\langle |H|^2 \rangle = 3m_{3/2}^2 M_{\mathrm{P}}^2$, where M_{P} is the reduced Planck mass, given in terms of the gravitational constant by $M_{\mathrm{P}} = (8\pi G_N)^{-1/2} = 2.4 \times 10^{18}\,\mathrm{GeV}$. A non-zero $\langle V \rangle$ contributes to the cosmological constant and to satisfy the existing experimental bounds requires that $\langle V \rangle \simeq 0$, which reflects the fine-tuning problem. This leads to a relation between $\langle |F|^2 \rangle$ and the gravitino mass (we assume that $\langle |D|^2 \rangle \simeq 0$ for simplicity). The gravitino mass resulting from this superhiggs mechanism is then

$$m_{3/2} = \frac{\langle F \rangle}{\sqrt{3} M_{\mathrm{P}}} \simeq 2.5 \left(\frac{\sqrt{\langle F \rangle}}{100\,\mathrm{TeV}} \right)^2 \mathrm{eV}. \tag{49}$$

As seen from equations (47) and (49), **an increase in the vev $\langle F \rangle$ leads to an increase in the gravitino mass, but to a decrease in its coupling strength**. Moreover, the SUSY breaking generates mass splittings (Δm), controlled by an effective coupling of strength λ,

$$\Delta m^2 \sim \lambda \langle F \rangle, \tag{50}$$

in all the sectors to which the goldstino supermultiplet couples. Depending on the magnitude of the coupling λ, several situations may arise, as illustrated in figure 10.

5.1.2. SUSY breaking in SUGRA. The first model for the generation of the supersymmetry breaking masses, dating back to the 1980s, is based on supergravity [15]. **In SUGRA,**

the messenger is supposed to be gravity itself through direct coupling of the goldstino supermultiplet to the MSSM states with gravitational strength [16]. Hence the coupling is small and, for a rough order of magnitude calculation, it can be expressed as $\lambda \simeq \langle F\rangle/M_{\rm P}^2$. This yields soft mass terms (or mass splittings) for superpartners

$$m_{\rm soft}^2 = \Delta m^2 \sim \frac{\langle F\rangle}{M_{\rm P}^2}\langle F\rangle. \tag{51}$$

In the limit $\langle F\rangle \to 0$, supersymmetry is unbroken and $m_{\rm soft}$ vanishes as it should; in the limit $M_{\rm P} \to \infty$, $G_N \to 0$ and gravity becomes irrelevant to generate $m_{\rm soft} \neq 0$. But if we keep $m_{3/2}$ constant for $M_{\rm P} \to \infty$ it is seen from (49) that we keep $m_{\rm soft} \neq 0$. For gravity to induce a reasonable value for the soft mass, such as $m_{\rm soft} \simeq M_W \sim 100$ GeV, the vev should be of order $\sqrt{\langle F\rangle} \sim 10^{10}$–$10^{11}$ GeV. **In the MSUGRA scenario the gravitino is heavy, of the same order as $m_{\rm soft}$, and its interaction is extremely weak, so that it plays no role in collider phenomenology. In particular, the LSP is most likely a neutralino**.

The breaking of supersymmetry through gravitational interactions does not ensure universality of the soft terms, as is discussed in some detail by Martin [1]. This so-called 'flavour problem' of SUGRA is the main incentive for searching alternative scenarios of SUSY breaking. The above statement, which sounds *a priori* counter-intuitive will be developed in section 5.10.

5.1.3. SUSY breaking in GMSB. An alternative proposal, the gauge mediated supersymmetry breaking, appeared in 1993 [109]. **In GMSB, there is no tree level coupling of the goldstino to the MSSM visible sector states, but the hidden (or secluded) sector particles couple to a messenger sector**. The messenger fields consist of chiral supermultiplets with quantum numbers of l, $\bar{l}$, q, $\bar{q}$, where $\bar{l}$ and $\bar{q}$ are the complex conjugate of the fields l and q (called a vector-like representation). They are supposed to appear in complete representations of the GUT group, in order to preserve the unification of the gauge couplings. In a $SU5$ GUT, they belong, for example, to a $5 + \bar{5}$ and/or to a $10 + \bar{10}$ representation.

Masses are generated for the messengers through their Yukawa coupling to a field X from the hidden world, which is a singlet under the SM gauge groups, e.g. the goldstino superfield (but any singlet field would do). The superpotential of the messengers has the form of a Yukawa coupling

$$W = yX\bar{\Phi}\Phi, \tag{52}$$

and it is assumed that both the scalar component of the field X and its auxiliary field acquire vacuum expectation values $\langle S\rangle$ and $\langle F_S\rangle$, respectively[10]. Then, the chiral contribution of equation (23) generates a mass term for the fermions

$$V \supset y\langle S\rangle\bar{\psi}\psi, \tag{53}$$

whereas the scalars obtain mass through their F-term, given by equation (27), after shifting the field F_S by its vev. This yields the quadratic terms for the scalar fields

$$V \supset |y\langle S\rangle|^2(|\phi|^2 + |\bar{\phi}|^2) + y\langle F_S\rangle\bar{\phi}\phi + (y\langle F_S\rangle)^*(\bar{\phi}\phi)^* \tag{54}$$

so that the scalars have mass eigenvalues $m_\phi^2 = |y\langle S\rangle|^2 \pm |y\langle F_S\rangle|$. The first term is the same as for the fermions, but the SUSY breaking is introduced through the $\langle F_S\rangle$ contribution. It is customary to simplify the notation by absorbing the Yukawa coupling in the field definitions

[10] To simplify the presentation, we use here a single field Φ and its complex conjugate, although several such fields are normally introduced, as mentioned above. The more general derivation can be found in [1].

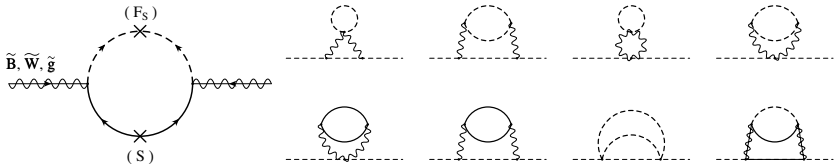

Figure 11. Loop diagrams generating soft mass terms for gauginos (left) and for scalars (right). From [1]. Wavy, full and dashed lines represent gauge bosons, fermions and scalars, respectively. Gauginos are shown as superposed wavy and full lines.

putting $M = y\langle S\rangle$ and $F_S = y\langle F_S\rangle$. The messenger masses for the fermions and scalars are then

$$m_\psi = M, m_\phi^2 = |M|^2 \pm |F_S|. \tag{55}$$

Note that this mass splitting is of the same form as relation (50). But, at the other extreme, compared with gravitation, it could be assumed that the coupling is stronger, y near 1, which generates mass splittings in the messenger sector of order

$$\Delta m^2 \sim \langle F\rangle \simeq m_{3/2} M_{\rm P}, \tag{56}$$

where the last equality assumes that the messenger mass splitting originates from the goldstino superfield. As the average messenger mass is M, and the splitting of the scalars is F_S, to avoid tachyonic scalars it is necessary that $M \geqslant \sqrt{F_S}$.

The messenger fields couple in turn to the particles from the observable sector via the usual gauge interactions and their mass splittings induce soft mass terms by loop diagrams displayed in figure 11, which introduce typically a loop factor $\alpha/4\pi$. The loops are of first order for the gauginos and of second order for the scalars. But, as they determine the mass for the gauginos and the mass-squared for the scalars, the soft mass is in both cases of order

$$m_{\rm soft} \sim \frac{\alpha}{4\pi}\sqrt{F_S}. \tag{57}$$

To yield a soft mass of the order of the weak scale, the scale of supersymmetry breaking should be as low as $\sqrt{F_S} \sim 10^4$–10^5 GeV. This implies a small gravitino mass, of order $m_{3/2} \sim 1$ eV and a non-negligible interaction strength. **The GMSB scenario is therefore characterized by a gravitino as LSP, to which the sparticles will ultimately decay**.

5.1.4. SUSY breaking in AMSB. In anomaly mediated models of SUSY breaking, introduced in 1998 [110, 111], **the source of the breaking resides in a single field of the supergravity Lagrangian, the chiral compensator field (CC)**. Its properties stem from the requirement that supergravity can be formulated as a conformal theory [112], with its Lagrangian being invariant under super-Weyl (also called conformal or scale invariant) transformations. If the observable sector does not have an explicit mass scale, the Lagrangian is scale-invariant at the classical level. However, the scale invariance is broken at the quantum level, because of the need to regulate the theory. This non-invariance can be compensated by the transformation of a chiral compensator super-field. If the observable sector had no explicit mass scale, the CC could be eliminated from the Lagrangian by a redefinition of the fields. But as it has one, the chiral compensator remains and has **couplings to the observable sector** (including supersymmetric) fields which are completely fixed by the super-Weyl invariance.

When the auxiliary field of the CC takes on a vacuum expectation value this leads to supersymmetry breaking terms in the observable sector. When the classical invariance of the Lagrangian is broken at the quantum level leading to physical effects, this is generically called

an anomaly, hence the name given to this SUSY breaking mechanism. In such models, the only communication of SUSY breaking effects from the hidden to the observable sector **occurs through the supergravity multiplet, and thus through this vacuum expectation value**. The consequent breaking terms in the observable sector are highly constrained. **A distinctive feature of AMSB is that gravitinos are much heavier than any of the superpartners**. This is due to the fact that the soft masses are loop-suppressed relative to the gravitino mass.

The anomaly contributions will always be present if supersymmetry is broken. But in the MSUGRA or GMSB scenarios, they may be negligible compared with the other contributions. **In AMSB, it is assumed that the anomaly-induced masses are dominant**.

Recent studies [113] have shown that, even when the anomaly-mediated terms are not the sole contributors to the soft SUSY breaking Lagrangian, they can still have an important influence over the resulting phenomenology, in particular in the gaugino sector.

5.1.5. SUSY breaking with superstrings or extra dimensions. The introduction of extra dimensions in SUSY scenarios allows one to play a number of games. In particular, coordinate-dependent compactifications of higher-dimensional theories provide a mechanism for electroweak symmetry breaking and mass generation. It can also be used for breaking supersymmetry. See [114] for an excellent introduction. The mechanism was first proposed by Scherk–Schwarz [115]. The idea is to 'twist' the periodicity conditions in the compact extra dimensions by a symmetry of the action or of the equations of motion. If instead of having strict periodicity in the 5th dimension y, one has periodicity up to a global $SU2$ transformation ('twisted' periodicity conditions)

$$\Psi(y + 2\pi R) = \mathrm{e}^{\mathrm{i}\vec{\beta}\cdot\vec{\sigma}}\Psi(y),$$

where $\vec{\beta}$ is a triplet of real parameters (β is the modulus), then the 4D modes have a classical spectrum characterized by a universal shift of the KK levels

$$m = \frac{n}{R} - \frac{\beta}{2\pi R}.$$

From a 4D point of view this twist induces mass terms that break the symmetries with which it does not commute. However if one looks at small distances, smaller than R, symmetry breaking effects should disappear.

The general features of the 'traditional' and 'new' versions of the Scherk–Schwarz mechanism are explained and illustrated in [114, 116]. The superHiggs effect, i.e. the spontaneous breaking of supersymmetry in 5D supergravity compactified on the orbifold S^1/Z_2 (S^1 is a circular symmetry and Z_2 a reflection symmetry about a diameter, so that the physics is defined on a segment between 0 and πR), is explained and the connection with brane-induced supersymmetry breaking and gaugino condensation in M-theory is made. Similarly to the formula given above, the resulting gravitino mass spectrum is typically given by

$$m_{3/2} = \frac{n}{R} + \frac{\delta}{2\pi R}(n = 0, \pm 1, \pm 2), \tag{58}$$

where δ is a parameter that takes into account the modified boundary conditions and R is the compactification radius. One finds also in [114] a list of references of applications of the mechanism to the subject of supersymmetry breaking in M-theory and in 5D field theory orbifolds.

Supersymmetry breaking obtained in simple classes of superstring compactifications has been studied in, e.g. [117]. These heterotic models have a natural hidden sector built in, made of gauge singlet fields, the complex dilaton field, S, which arises from the gravitational sector of the theory, and the complex moduli fields, T_i, which parametrize the size and shape of the

compactified variety. The assumption is then that **the auxiliary fields of these multiplets are the seed of SUSY breaking** and interesting predictions are obtained, briefly discussed in section 5.2.

In traditional models, the hidden sector in which SUSY breaking originates is hidden from the visible MSSM fields by the weakness of the direct couplings, for instance Planck-scale suppressed couplings in gravity mediated models. **In contrast, extra-dimensional theories provide a geometrical way to separate the two sectors**. This can be in the context of higher-dimensional models involving parallel branes, inspired by the Horava–Witten set-up [118], such as in the model by Randall and Sundrum [111] or in more elaborate situations [119].

As we said, a long list of proposals for the breaking of the electroweak symmetry and of supersymmetry by applying different versions of the mechanism described above is given in [114]. Rather than reviewing them, which is well beyond our scope and competence, we would like to give a couple of examples illustrating the variety of resulting phenomenologies [120].

A scenario [56] already quoted in section 2.4 and aiming at solving the LEP paradox [55], is based on the extension of SUSY into five dimensions, one of which is compactified on a circle with two orbifold projections, $S^1/(Z_2 \times Z_2)$. In 5D there are two supersymmetries. Each boundary of the orbifold breaks one of them and the low energy theory is not supersymmetric. It becomes so at energies larger than $1/R$, leaving only a finite contribution to the Higgs mass, predicting

$$m_h = 127 \pm 10\,\text{GeV}. \tag{59}$$

In this model only one Higgs doublet exists. But each SM particle has two superpartners. The LSP is a degenerate doublet of stable (or metastable) stops. Their mass is approximately $(1/R) - m_t$, with a lowest preferred value in the 200 GeV range. This fact should be a strong incentive (amongst others) to implement accurate TOF measurements in future experiments. Several problems encountered by the model, in particular concerning the contribution to the ρ parameter, motivated the study of variants in order to alleviate them.

Another set of examples [121], which however do not specifically refer to the supersymmetric case, investigate the nature of **gauge symmetry breaking by boundary conditions** (orbifold conditions or a wider set of consistent conditions) and show that such theories seem to have a good high energy behaviour, just as gauge theories broken by the Higgs mechanism would. This may lead to speculation that the breaking of gauge symmetries via boundary conditions could replace the usual Higgs mechanism, although there is still a long way to go to find a fully realistic implementation. Presently one expects KK excitations for the W and Z bosons with masses too low to satisfy the bounds. Warping the ED is a possible way to lift the masses of the excited KK modes and make them phenomenologically acceptable. Another obstacle for Higgsless ED theories also comes from electroweak precision data.

5.1.6. Small hierarchy. In the conventional view on SUSY, it is admitted that a hierarchy exists between the scale of SUSY mediation M, the SUSY breaking scale $\sqrt{F}$ and M_W

$$M \gg \sqrt{F} \gg M_W \tag{60}$$

justifying the encoding of SUSY breaking through the soft terms introduced earlier. If however, in analogy with what low scale extra dimensions offer, one assumes that such hierarchy is small or nonexistent [122], the resulting effective theory may be quite different. Non standard soft terms or even hard-breaking terms can emerge. Specific interactions between the MSSM multiplets and the sector where SUSY breaking occurs are no longer negligible (the 'hidden' sector is not that hidden anymore). Goldstinos, sgoldstinos, gravitinos play a

role in phenomenology. The Higgs sector is also modified and looks more like that of two-Higgs-doublet models, with an additional singlet: it therefore escapes to the usual MSSM mass limits.

It is clear that, given the weak experimental constraints, a quasi infinite number of games can be played within the SUSY line of thinking. A long list of such phenomenological variations has been advocated in the past as the most convincing (as e.g. the low tan β version of the low scale MSSM) and have turned out to be disproved. For many years at LEP time, the predicted Higgs mass was the current limit plus a few GeV. **The main point is that experimentalists, in SUSY searches like in any other, should avoid to focus on any *a priori*, keep their minds open and exploit at best the possibilities offered to them**.

5.2. Scenarios and their parameters

5.2.1. MSUGRA: reducing the number of parameters. In its general form (34), the soft SUSY breaking of the **MSSM** introduces a large number of free parameters. However, several could induce too large flavour changing neutral currents (FCNC) or CP violation. A simple assumption to avoid such catastrophe is 'mass universality': it imposes a common scalar mass, $m_{0,i} = m_0$, a common gaugino mass, $m_{1/2,a} = m_{1/2}$ and a common $A_{0,i} = A_0$ (multiplying the Yukawa couplings) at the grand unification scale [16]. This leaves the 5 GUT scale free parameters:

$$m_0, m_{1/2}, A_0, B_0, \mu, \tag{61}$$

making the model much more predictive. As such a situation can be realized in some supergravity models, it will be called **SUGRA** in the following[11]. It should be emphasized, however, that supergravity does not, in general, imply the mass universality relations. For example, the scalar masses could be flavour-dependent and include mixing terms and phases (the 'flavour problem' in SUGRA). An arbitrary choice of the values of the 5 SUGRA parameters does not, however, warrant radiative electroweak symmetry breaking and hence the correct value of the Z^0 mass.

Still the possibility to decrease further the number of parameters has been actively explored. An example is the **no-scale supersymmetry** [123] which requires particular forms of the 'Káhler' function such that the vacuum energy vanishes and the potential has flat directions which leave the gravitino mass undetermined. Minimization of the electroweak scale scalar potential with respect to the gravitino mass then determines its value. Most of the string models explored [123] do not satisfy these requirements. An example of a string no-scale supergravity model has been proposed [124], in which

$$m_{1/2} = A_0 = B_0 = m_{3/2}, \qquad m_0 = 0. \tag{62}$$

The low energy theory depends on only one parameter, $m_{3/2}$. However, the predictions of this model ($m_{\tilde{l}_R} < 50\,\text{GeV}$, $m_{\tilde{\chi}^\pm} < 90\,\text{GeV}$, $m_{h^0} < 90\,\text{GeV}$) were not met by experiment. Another example is a no-scale SUGRA model [125] inspired from M-theory: again it predicts light objects which have not been seen. A conclusion [126] was that, when no-scale boundary conditions are given at the GUT scale and universal gaugino masses are postulated, LEP200 results severely constrain the model. However, relaxing one or both of these assumptions can lead to a variety of sparticle mass spectra [127].

[11] As there is no generally accepted naming convention for some of the more constrained scenarios, we define here the terms we will use throughout this paper. The reader is warned, however, that the same names may have a different meaning in other publications.

An alternative scenario is the **dilaton-dominated model** [128]. The dilaton appears in superstring models as a flat direction of the effective potential. When its corresponding F-term takes a vacuum expectation value, it induces soft supersymmetry breaking terms which, because of the universal couplings of the dilaton, can all be parametrized at the unification scale by the gravitino mass $m_{3/2}$ [129]

$$m_{i,0} = m_{3/2}, \qquad m_{a,1/2} = \pm\sqrt{3}m_{3/2} = -A_{i,0}, \tag{63}$$

and B_0 is not restricted further, as its value is model dependent. It provides a natural justification of universality and features a very constrained model with only three free parameters, $m_{3/2}$, μ and B_0($|\mu|$ can be determined from radiative electroweak symmetry breaking, as described below, leaving two free parameters and a sign). Typical values for the spectrum (except the third generation sfermions) are $m_{\tilde{g}} : m_{\tilde{q}_L} : m_{\tilde{u}_L^c} : m_{\tilde{d}_L^c} : m_{\tilde{l}_L} : m_{\tilde{e}_L^c} \simeq 1 : 0.94 : 0.92 : 0.92 : 0.32 : 0.24$ at the electroweak scale. A dilaton-dominated scenario would be attractive for its simplicity and the natural explanation it offers to the universality of the soft terms. However, a pure dilaton model seems to be excluded by requiring the absence of low energy charge and/or colour breaking (CCB) minima and by the measured value of m_t once one requires consistency with electroweak symmetry breaking. One must, therefore, turn to mixed dilaton/moduli SUSY breaking. The low energy phenomenology predictions of this SUSY breaking are generally

$$m_{\tilde{l}} < m_{\tilde{q}} \simeq M_{\tilde{g}}, \tag{64}$$

but exceptions to that pattern can arise in several situations, when SUSY breaking is mainly moduli dominated. The results of [117] refer to simple perturbative heterotic compactifications and the assumption that the goldstino is a fermionic partner of some combination of the dilaton and/or the moduli fields. This model (as well as the no-scale model) suffers, as we said, from problems of stability of the vacuum [130] and we will, for the phenomenology, treat m_0, $m_{1/2}$, A_0 and B_0 as independent parameters in the following.

The values of the mass parameters and couplings can then be evolved down from the GUT scale to the electroweak scale, by means of renormalization group equations (RGE), where they determine the mass spectrum, the production cross-sections and the decay branching ratios of the supersymmetric particles.

It is customary to replace the high scale parameter B_0 of SUGRA (61) by the low energy parameter $\tan\beta = v_u/v_d$, the ratio of vacuum expectation values of the Higgs fields H_u and H_d, leaving as free parameters

$$m_0, m_{1/2}, A_0, \tan\beta, \mu. \tag{65}$$

Furthermore, some analyses assume that the electroweak symmetry is 'correctly broken'. This means that they assume explicitly that the spontaneous gauge symmetry breaking is induced by radiative corrections. The requirement that the SUSY parameters evaluated at the electroweak scale, more precisely the expression $v_d^2 + v_u^2$, reproduce correctly the value of the Z^0 mass introduces an additional constraint. This constraint allows μ^2 to be expressed in terms of the other parameters, as we will see in section 5.3. The sign of μ remains, however, free and the parameters are

$$m_0, m_{1/2}, A_0, \tan\beta, \text{sign}(\mu). \tag{66}$$

This will be called the **MSUGRA** scenario. Sometimes, additional constraints are imposed, for instance from cosmology by requiring that the amount of cold dark matter in the universe is accounted for by neutralinos. This will be called constrained MSUGRA or **CMSUGRA**.

The opposite attitude is also sometimes taken, namely to relax the assumption of universality between the Higgs mass parameters and the sfermion masses. The correct breaking

Table 4. Summary of SUGRA scenarios. Also shown is whether radiative EWSB is imposed or not.

Scenario	Parameters	Rad. EWSB
SUGRA	$m_0, m_{1/2}, A_0, \tan\beta, \mu$	No
MSUGRA	$m_0, m_{1/2}, A_0, \tan\beta, \text{sign}(\mu)$	Yes
CMSSM	$m_0, m_{1/2}, A_0, \tan\beta, \mu, m_A$	Yes

of electroweak symmetry is still required, but the constraint determining the absolute value of μ is lost. Furthermore, the value of the CP-odd Higgs mass, m_A, is introduced as free parameter, rather than the GUT scale Higgs mass parameters. Altogether, the free parameters for this constrained MSSM, **CMSSM**, scenario are chosen as

$$m_0, m_{1/2}, A_0, \tan\beta, \mu, m_A, \tag{67}$$

where m_0 now only applies to sfermions.

The naming conventions and corresponding parameters are summarized in table 4.

5.2.2. GMSB parameters. A didactic introduction to the theory of gauge mediated supersymmetry breaking (GMSB) is given in the primer by Martin [1]. A more extensive presentation is found in the review paper by Giudice and Rattazzi [131].

It was seen in section 5.1 that in gauge mediated supersymmetry breaking, the messenger fields consist of chiral supermultiplets with quantum numbers of q, $\bar{q}$, l, $\bar{l}$. They occur in complete representations of the GUT group, for example a $5+\bar{5}$ and/or a $10+\bar{10}$ representation for an $SU5$ GUT.

The parameters which govern the sparticle spectroscopy of a GMSB model are the following.

- **The messenger scale**, M, which represents the average mass of the messengers. This scale determines the amount of RGE evolution and, therefore, enters only logarithmically in the values of the masses.
- The scale $\Lambda = F_S/M$, related to **the mass splitting of the scalar components of the messenger supermultiplets**. This parameter sets the scale of the entire superpartner spectrum.
- The existence of the messengers modifies the RGEs of the gauge couplings and increases the value of the unified gauge coupling constant α_{GUT}. The extra contributions depend on a parameter, called **messenger index** N, which is the sum $N = \sum n_i$ of constants determined by the group representations with $n_i = 1$ for $5 + \bar{5}$ and $n_i = 3$ for $10 + \bar{10}$. The requirement that the gauge couplings remain perturbative up to the GUT scale limits the messenger index to values $N \leqslant 5$–10 for messenger scales $M = 10^5$–10^{10} GeV, respectively.
- Values for the supersymmetry breaking **trilinear parameters** A_i do not arise at the one-loop level. To a good approximation, they are set to zero at the messenger scale, but become non-zero at the electroweak scale due to the RGE evolution proportional to the gaugino masses and Yukawa couplings. They are mostly relevant for third family squarks and sleptons. The parameter B is quite model dependent and is also often taken to be zero at the messenger scale. Under the assumption of correct breaking of the electroweak symmetry the absolute value of the parameter μ and the value of B can be obtained from the gauge boson mass and the parameter $\tan\beta$.

In summary, the free GMSB parameters which determine the sparticle spectrum are

$$\Lambda, M, N, \tan\beta, \text{sign}(\mu), \tag{68}$$

with the condition that $\Lambda < M$ to avoid that scalar messengers get a negative squared mass and break gauge symmetry at the messenger scale.

A very attractive feature of GMSB is the fact that **soft masses are generated by gauge interactions, which guarantees flavour universality**.

These five parameters are, however, not sufficient to determine completely the GMSB phenomenology. Even when the messenger mass splitting is generated by the goldstino superfield ($\langle F\rangle = \langle F_S\rangle$) the sparticle coupling to the gravitino (hence the decay width or lifetime) is determined by $\langle F\rangle = \Lambda M/y$ and depends on the Yukawa coupling. A frequent convention is to define an additional parameter

$$C_{\text{grav}} \equiv \langle F\rangle / F_S \geqslant 1, \tag{69}$$

which then determines the lifetime.

5.2.3. AMSB parameters. The anomaly mediated models of SUSY breaking are very constrained. In pure AMSB, a single parameter, **the gravitino mass** $m_{3/2}$, determines the soft masses of the gauginos, the scalars and the A-terms. Unfortunately, it turns out that the squared masses of sleptons are negative, making them tachyonic. In the minimal AMSB, this is cured by introducing **a universal scalar mass parameter** m_0 **at the GUT scale**. In addition, there are the usual supersymmetric parameter μ and the parameter B entering the soft SUSY breaking. Assuming a correct breaking of the electroweak symmetry, the free parameters are

$$m_{3/2}, m_0, \tan\beta, \text{sign}(\mu). \tag{70}$$

5.2.4. Phases. So far, it is implicitly assumed that all parameters are real. In MSUGRA only two new sources of CP violation appear, in addition to the CKM phase of the SM. They may be represented as the phases of the complex parameters $m_{1/2}$ and A_0 relative to that of μ. Their values are constrained in particular by the upper limits on electric dipole moments (e, n and mercury atom), see section 6.8. Such large phases in $m_{1/2}$ and in the third generation trilinear couplings are still possible. More light may come from B-factories. The effect of phases in SUSY is described in section 8.5 for the Higgs sector. Other sectors may be affected as well, such as the phenomenology of neutralinos, charginos and the third generation squarks [401]. The relevant studies will be described in due time. However, **a thorough treatment of the problem does not seem to exist**.

5.3. MSUGRA spectroscopy

Under the assumption of mass universality, the particle spectrum can be predicted as a function of the MSUGRA parameter values at the GUT scale by the use of the RGEs. An example is given in figure 12. The following qualitative features emerge

- The sfermion masses start from a common value m_0 at the GUT scale. The squark masses increase fast, due to the contributions proportional to α_3 in the RGEs. The slepton masses increase slowly, as the only contributions in the RGEs are from the couplings $\alpha_{1,2}$.
- The gaugino masses start from a common value $m_{1/2}$. The gluino mass increases fast (for the same reason as for the squarks), whereas the $\tilde{B}$ and $\tilde{W}$ masses remain low.

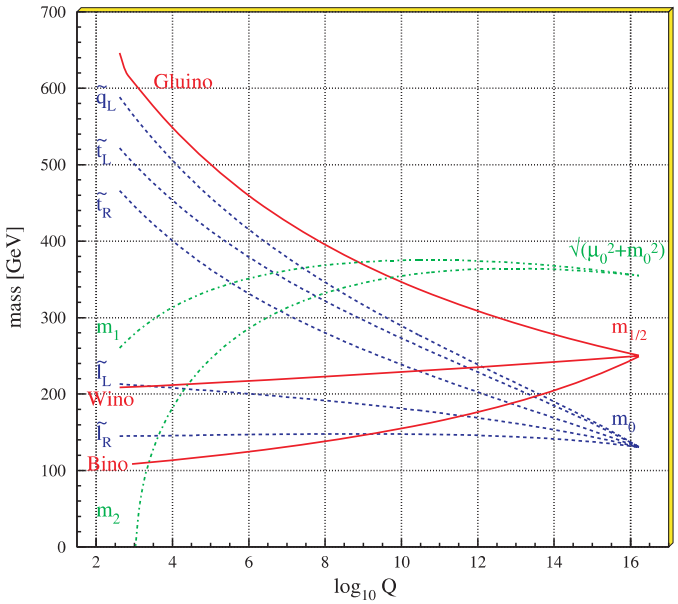

Figure 12. Evolution of the mass parameters in MSUGRA, from [87].

It is thus expected that the strongly interacting particles, the squarks and gluinos, will generally be heavy compared with the sleptons, winos and bino (but the latter two are not physical states, as they will mix).

The Higgs (mass)^2 parameters start from the value $(m_0^2 + \mu^2)$, determined by the soft breaking mass for scalars and the μ-term in the superpotential (the F-term in equation (29)). The large Yukawa coupling of H_u to the top quark drives the (mass)^2 parameter of H_u negative. In consequence, the coefficient of the quadratic term in the Higgs potential becomes negative, which allows the breaking of the electroweak symmetry (at least if some conditions are fulfilled, see [1]). The MSSM therefore incorporates a quite natural mechanism for breaking the electroweak symmetry.

Moreover, the minimization of the neutral Higgs potential, which will be discussed in section 8.4, induces a constraint among the weak scale parameters which is frequently used to determine the absolute value of μ as a function of the remaining parameters and which reads at tree level as

$$\mu^2 = \frac{m_{H_\mathrm{d}}^2 - m_{H_\mathrm{u}}^2 \tan^2\beta}{\tan^2\beta - 1} - \frac{M_Z^2}{2}. \tag{71}$$

In the MSUGRA model, where $m_{H_\mathrm{d}} = m_{H_\mathrm{u}} = m_0$ at the GUT scale, the value of μ at the weak scale for intermediate to large $\tan\beta$ is almost independent of m_0. It depends little on $\tan\beta$, as the relation (71) shows that the main contribution to μ becomes $\mu^2 \simeq -m_{H_\mathrm{u}}^2$. It becomes almost linear in $m_{1/2}$, which is introduced through the loop effects in the running of m_{H_u}, as illustrated in figure 13 (left). Approximate analytical expressions are found in [134]. However, for large values of m_0, the value of μ^2 decreases very rapidly and becomes eventually negative, as seen in figure 13 (right), signalling that radiative EWSB is no longer possible. This region is quite sensitive to the value of the top quark mass and may give rise, at the present status of the calculations, to instabilities or non-convergence of the RGEs, as is clearly observed in the figure for $m_t > 176\,\mathrm{GeV}$.

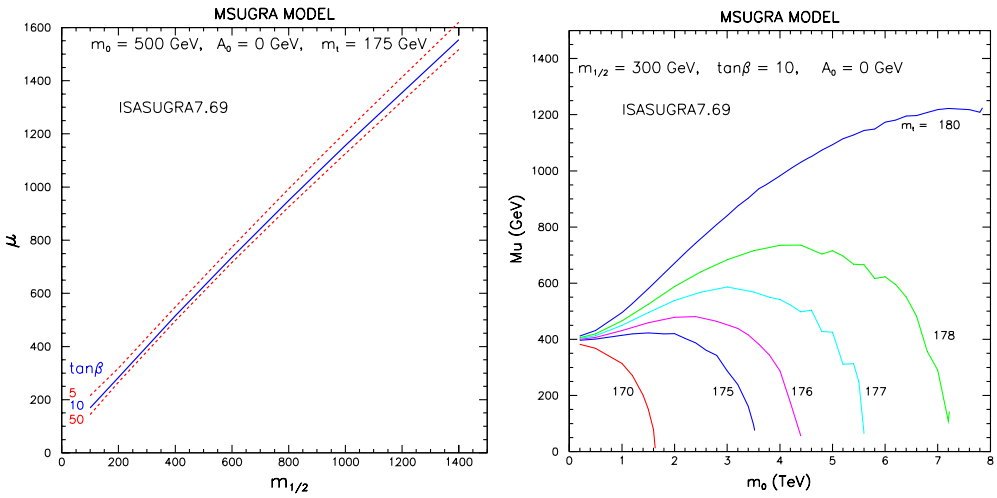

Figure 13. (left) Dependence of the parameter μ on $m_{1/2}$ and $\tan\beta$ in the MSUGRA model. (right) Dependence of the parameter μ on m_0 in MSUGRA, for several values of the top quark mass, showing the region where no radiative EWSB takes place. Both figures are computed with ISASUGRA 7.69 [133].

In this picture, with a desert between the electroweak scale and the GUT scale, **the measurement of the superpartner spectrum provides via the RGEs a window on the high scale parameters**. There are, however, also quantities which are insensitive to the values of the GUT scale parameters. These will be discussed now.

5.3.1. Infrared quasi-fixed points. The most common way to reduce the set of parameters of the MSSM is to assume universality of the soft terms. Further reduction has been discussed using the concept of **infrared quasi-fixed points (IRQFP) which shows insensitivity of some low energy MSSM parameters to their value at high energy** [135]. In the past, this scenario has been considered mainly in the low $\tan\beta$ regime, which was then theoretically preferred, for instance at the top quark mass IRQFP solution [136]. In [137] the dependence of the particle spectrum on two free parameters, m_0 and $m_{1/2}$, has been discussed. However, the LEP limits on the Higgs mass have excluded the low $\tan\beta$ scenario and the interest has shifted to larger values. For large $\tan\beta$, the reduction of the parameter space is also possible. But the situation is more complicated because one must deal with the whole set of Yukawa couplings of the third generation and one is limited to a numerical investigation. In [138] the quasi-fixed points of some of the SUSY soft breaking parameters are used to evaluate masses. All the Higgs boson masses, except as usual the lightest one (<130 GeV), are found to be quite heavy (>600–1100 GeV), as well as stops and sbottoms (>1 TeV).

5.3.2. Focus points. In focus point supersymmetry [139] all sfermions, including those of the third generation, have masses well above 1 TeV. Their naturalness arises from correlations among SUSY parameters. Assuming a hierarchy $m_i \gg M_i, A_i$, the weak scale value of $m^2_{H_u}$ and therefore the scale of electroweak symmetry breaking is determined primarily by gaugino masses M_i and trilinear couplings A_i. Sufficient conditions have been presented in [139]. For any value of $\tan\beta \gtrsim 5$ and $m_t \simeq 175$ GeV, a universal scalar mass guarantees focus point supersymmetry: whatever its value at the GUT scale, the family of renormalization equation

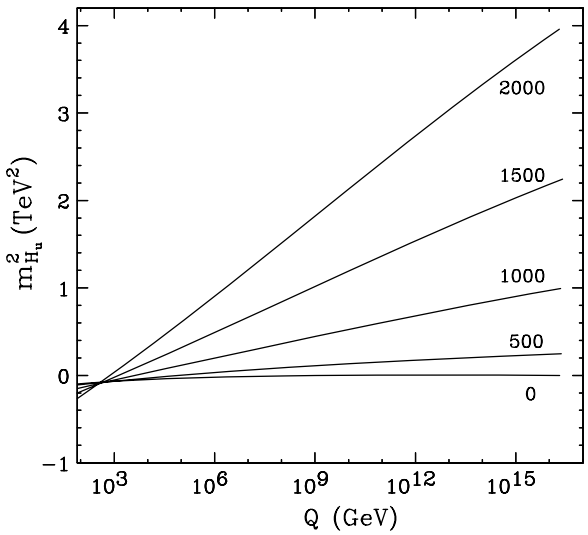

Figure 14. Evolution of the Higgs mass parameter in focus point supersymmetry, reprinted with permission from [139]. Copyright 2000 by the American Physical Society.

trajectories of $m^2_{H_u}$ meet at a point, at a scale of about 1 TeV, as illustrated in figure 14, a highly non-trivial occurence requiring in particular that the top mass is within ∼2% of its value of 175 GeV.

The cosmological and astrophysical implications of fixed point supersymmetry have been explored [140]. The stable neutralino stays as a good dark matter candidate, however as a gaugino–higgsino mixture, a fact which enhances the rates of many indirect detection signals. This will be developed in section 12.2.1.

Low energy constraints (proton decay, electric dipole moments) are less stringent [141]. A Higgs boson mass at or above 115 GeV is naturally expected without requiring heavy gauginos.

5.3.3. Fine tuning. The amount of fine tuning of the SUSY parameters required to obtain the electroweak scale increases rapidly for sparticle masses ≫1 TeV. A usual definition of the fine tuning is the value of the quantity [142]

$$\Delta \equiv \sqrt{\sum_i (\Delta_i)^2}, \qquad \Delta_i \equiv \frac{a_i}{M_Z}\frac{\partial M_Z}{\partial a_i}, \tag{72}$$

where the a_i are the fundamental parameters of the theory under consideration.

In the past, fine-tuning arguments were used to show that, especially due to the steadily increasing lower limit on the lightest Higgs mass at LEP, the MSSM appeared as more and more contrived [55]. However, the substantial effect of the limit on the Higgs mass is lifted if one considers large tan β scenarios, as in [143]. It is true, nevertheless, that the domain of MSSM parameters still open seems to present some appreciable degree of fine tuning. For instance, in the benchmarks [143] presented in section 15.4, one finds that the electroweak fine tuning ranges from few tens to several hundreds. It roughly scales with $m_{1/2}$ and is nearly independent of m_0. This is seen from the approximate relation

$$\mu_0^2 \simeq 3.3m_{1/2}^2 + 0.2m_0^2 - 0.4A_0m_{1/2} + 0.1A_0^2 - 0.56M_Z^2, \tag{73}$$

derived from [144] for universal soft masses at $\tan\beta = 5$ and where all parameters are defined at the unification scale.

The extent to which one cares about the amount of fine tuning depends on the underlying measure in the parameter space, which is unknown. Correlations between input parameters may reduce it radically [145], an example being the focus point scenario. Nevertheless, it was argued in [144] that cancellations among the other MSSM parameters are not a generic feature, which leads the authors to expect rather light gluinos, charginos and neutralinos.

However, as we saw, some authors have chosen to consider, instead of MSSM, alternative scenarios [56, 58] aiming at solving this 'little hierarchy' problem raised by the LEP limits on the Higgs mass and on SUSY particles on one hand, on a new physics scale on the other hand.

5.3.4. Split supersymmetry. An alternative, rather drastic proposal, was recently put forward and named split supersymmetry [25]. Here it is decided to discard the hierarchy problem and its associated fine tuning of the Higgs mass on the basis that this is dwarfed by the enormous fine tuning required for the cosmological constant. In these circumstances, SUSY may be broken at a high energy scale, m_S, far above the TeV scale. The scalars would have masses of order m_S, except for one combination of the Higgs doublets which is fine tuned to remain light. The gauginos and higgsinos can be protected by symmetries and can come out naturally as rather light objects (although their lightness is not fully guaranteed). The low energy theory is, therefore, non supersymmetric, with a single light Higgs and the gauginos and higgsinos possibly in the TeV range. Such splitting of the SUSY spectrum allows several MSUGRA problems mentioned above to be solved: it eliminates excessive flavour and CP violation and relieves the constraints on proton decay by dimension 5 operators (see section 6.1). On the other hand, it retains the possibility of a dark matter candidate and the unification of the gauge couplings. Actually, it was shown in [51] that among the few consistent choices allowing unification in a single step is the one of the split supersymmetry spectrum.

The relatively light gluinos are expected to be long lived, as their decay always involves a squark, which is heavy (of order m_S) in this case. Their lifetime is given approximately by the formula [146]

$$\tau \simeq \left(\frac{m_S}{10^9\,\mathrm{GeV}}\right)^4 \left(\frac{1\,\mathrm{TeV}}{m_{\tilde{g}}}\right)^5 \mathrm{s} \tag{74}$$

If stable, they would bind to atomic nuclei and would exist today in the form of anomalously heavy isotopes. The existence of stringent limits on heavy hydrogen isotopes [147] limits their lifetime to less than the age of the universe and hence the mass scale m_S to less than about 10^{13} GeV.

The split spectrum scenario has a strong impact on the phenomenology [146, 148]. Its consequences for the chargino and neutralino searches will be discussed in section 9.5. Given the potentially long lifetime of the gluino, it is expected to hadronize before decaying to form bound states called R-hadrons, whose experimental signature we will present in section 9.4.

5.4. Gaugino masses and composition

5.4.1. Gaugino mass evolution. The gaugino masses are determined in the MSSM by three parameters M_a for which the one-loop renormalization group equations are

$$\frac{\mathrm{d}}{\mathrm{d}t} M_a = \frac{1}{8\pi^2} b_a g_a^2 M_a, \tag{75}$$

where the coefficients ($b_a = 33/5, 1, -3$) are the same as in the RGE for the gauge couplings and t is defined as $t = \ln(Q/Q_0)$. It is worth noting that, if M_a is zero at the scale Q_0, it

remains zero over its entire evolution. From this equation, it follows that the three ratios M_a/g_a^2 are constant. Assuming universality of the gaugino masses at a scale Q_0, the RGE is simple :

$$M_a(t) = \left(\frac{\alpha_a(t)}{\alpha_{a,0}}\right) m_{1/2}, \tag{76}$$

for any value $Q < Q_0$. This equation is valid up to small two-loop effects ($\mathcal{O}(10\%)$) and possibly larger threshold effects near $M_{\rm GUT}$. Q_0 is presumably close to M_P, but is most often taken as $M_{\rm GUT}$, the value where the coupling constants are seen to unify. In this case:

$$\frac{M_1}{\alpha_1} = \frac{M_2}{\alpha_2} = \frac{M_3}{\alpha_3}. \tag{77}$$

In MSUGRA models, the common value is also equal to $m_{1/2}/\alpha_U$, α_U corresponding to the unified gauge coupling constant. Furthermore, the same equation is also the solution of the one-loop RGE in the context of gauge mediated SUSY breaking, although there is no unified mass $m_{1/2}$ in this case. This equation implies the hierarchy $M_1 < M_2 < m_{1/2} < M_3$.

- M_3 is the physical mass of the gluino, $M_3 = M_{\tilde{g}}$, at least up to QCD corrections, as $SU(3)$ is unbroken.
- After breaking $SU(2) \times U(1)$, the Higgs vev produces a mixing of M_1 and M_2 with higgsino mass parameters to give physical chargino and neutralino states.

  At the weak scale, the following approximate relation holds:

$$M_1 \simeq \frac{5}{3}\tan^2\theta_W M_2 \simeq 0.5 M_2. \tag{78}$$

Explicit values at the electroweak scale ($t = -66$) are

$$\begin{aligned} &M_3 \equiv M_{\tilde{g}} \simeq 2.7 m_{1/2}, \\ &M_2(M_Z) \simeq 0.8 m_{1/2}, \\ &M_1(M_Z) \simeq 0.4 m_{1/2}. \end{aligned} \tag{79}$$

This makes the gluino mass $M_{\tilde{g}} \simeq m_{\tilde{q}_{\rm L}}$, unless m_0 is large, in which case $m_{\tilde{q}_{\rm L}} > M_{\tilde{g}}$ can be expected.

Small departures from these relations can be expected due to threshold effects near $M_{\rm GUT}$. They can, however, be more drastically modified if the fields at the origin of SUSY breaking are non-singlet, as shown by Gunion [149]; for instance $M_1 \simeq M_2$ would be possible.

5.4.2. Chargino masses and composition. Contributions to the masses of winos and of higgsinos arise, respectively, from soft SUSY breaking terms ($M\lambda\lambda$) and from the chiral contributions of the superpotential in the form ($\mu \tilde{H}_{\rm d}^- \tilde{H}_{\rm u}^+ +$ c.c.). In addition, there are mixing terms generated by the ($\lambda\phi\psi$) vertex leading to ($\tilde{W}^\pm H_{\rm d,u}^0 \tilde{H}_{\rm d,u}^\mp$) contributions. After breaking of $SU(2) \times U(1)$ the H^0 acquires a vev which provides for off-diagonal elements $v_{1,2}\tilde{W}^\pm \tilde{H}_{\rm d,u}^\mp$ in the mass matrix and mixes the charged wino and higgsino states. The mass matrix in the ($\tilde{W}^+ \tilde{H}^+$) basis is [1]

$$\begin{pmatrix} M_2 & \sqrt{2}M_W \sin\beta \\ \sqrt{2}M_W \cos\beta & +\mu \end{pmatrix}. \tag{80}$$

M_2 is positive and μ can be either positive or negative and is here assumed to be real. Note that in CP non-invariant theories, the mass parameters are complex. However, by reparametrization

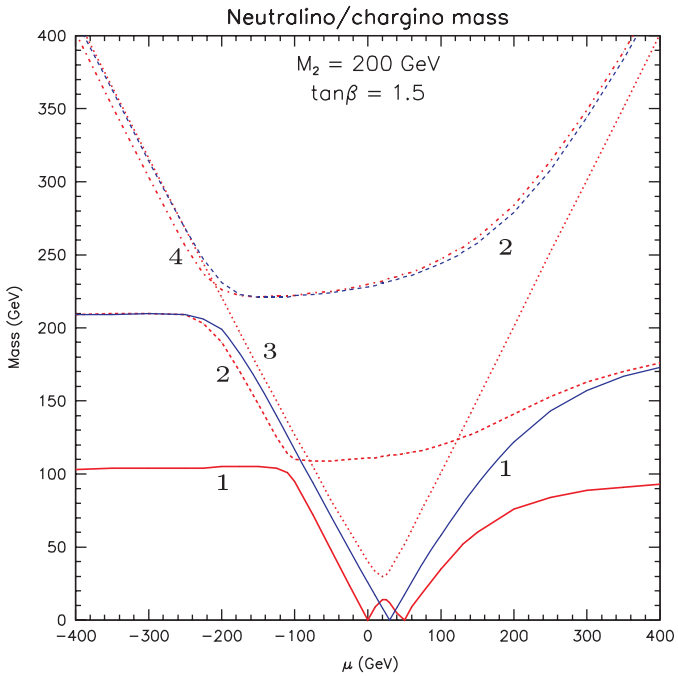

Figure 15. Chargino and neutralino mass solutions as function of μ for $M_2 = 200\,\mathrm{GeV}$ and $\tan\beta = 1.5$. The neutralino mass solutions are labelled from 1 to 4 on the left and the chargino solutions 1 and 2 on the right. The curves become more symmetric with respect to the sign of μ when $\tan\beta$ is increased.

of the fields, M_2 can be assumed real and positive and the only non-trivial phase may be attributed to μ. Mass eigenstates $\chi_1^\pm$ and $\chi_2^\pm$ are obtained after diagonalizing this matrix:

$$M(\tilde{\chi}_{1,2}^\pm)^2 = \frac{1}{2}(M_2^2 + \mu^2 + 2M_W^2) \mp \frac{1}{2}\left[(M_2^2 + \mu^2 + 2M_W^2)^2 - 4(\mu M_2 - M_W^2 \sin 2\beta)^2\right]^{1/2}. \quad (81)$$

The chargino masses depend on three SUSY parameters, M_2, μ and $\tan\beta$. Moreover, they are invariant under the substitution $|\mu| \leftrightarrow M_2$. They depend, however, on the sign of μ, except for large values of $\tan\beta (\sin 2\beta \simeq 0)$ where they become symmetrical in $\pm\mu$. An example of chargino masses is displayed in figure 15.

Gaugino-like or higgsino-like regions. A useful approximation is obtained in the limit where the electroweak symmetry breaking effects can be viewed as small perturbations, namely $M_Z \ll |\mu \pm M_2|$. The chargino masses then take the approximate values:

$$M(\tilde{\chi}_1^\pm) \simeq M_2 - \frac{M_W^2(M_2 + \mu \sin 2\beta)}{\mu^2 - M_2^2},$$
$$M(\tilde{\chi}_2^\pm) \simeq |\mu| + \frac{M_W^2(|\mu| + \epsilon M_2 \sin 2\beta)}{\mu^2 - M_2^2}, \quad (82)$$

where ϵ is the sign of μ. This applies to the deep gaugino or higgsino regions. If $M_2 \ll |\mu|$ the lightest chargino is gaugino-like (wino-like) with mass $M(\tilde{\chi}^\pm) \simeq M_2$ and the heavier chargino is higgsino-like with mass $M(\tilde{\chi}^\pm) \simeq |\mu|$. For $\mu \ll M_2$ the situation is reversed.

Diagonal region for negative μ. Another interesting case occurs when $\mu \simeq -M_2$, then the chargino masses are

$$M(\tilde{\chi}^{\pm}_{1,2})^2 = (M_2^2 + M_W^2) \mp [(M_2^2 + M_W^2)^2 - (M_2^2 + M_W^2 \sin 2\beta)^2]^{1/2}, \tag{83}$$

and for $\tan\beta \simeq 1$ both charginos become degenerate with masses $M(\tilde{\chi}^{\pm}_1)^2 \simeq M(\tilde{\chi}^{\pm}_2)^2 \simeq M_2^2 + M_W^2$ and nearly degenerate with the W if M_2 is small.

5.4.3. Neutralino masses and composition. Due to the same reasons as seen for charginos, mixing between the neutral gaugino and higgsino states occurs when the $SU(2) \times U(1)$ symmetry is broken. The mass matrix, expressed in terms of the basis $(\tilde{B}, \tilde{W}, \tilde{H}_{\rm d}, \tilde{H}_{\rm u})$, takes the form

$$\mathbf{Y} = \begin{pmatrix} M_1 & 0 & -M_Z \cos\beta s_W & M_Z \sin\beta s_W \\ 0 & M_2 & M_Z \cos\beta c_W & -M_Z \sin\beta c_W \\ -M_Z \cos\beta s_W & M_Z \cos\beta c_W & 0 & -\mu \\ M_Z \sin\beta s_W & -M_Z \sin\beta c_W & -\mu & 0 \end{pmatrix}, \tag{84}$$

where the abbreviations $s_W = \sin\theta_W$ and $c_W = \cos\theta_W$ have been used. In this matrix one can recognize

- a 2×2 block with parameters M_1 and M_2 originating from the supersymmetry breaking terms $(M_a \lambda\lambda)$,
- a 2×2 block depending on μ whose source is in the unbroken MSSM Lagrangian and
- off-diagonal entries proportional to M_Z coming from the $(\lambda H \tilde{H})$ couplings, similar to the ones encountered for charginos.

Since the mass matrix is symmetric, it can be diagonalized by a single unitary matrix N transforming the interaction eigenstates to the mass eigenstates

$$\tilde{\chi}^0_i = N_{i,1}\tilde{B} + N_{i,2}\tilde{W} + N_{i,3}\tilde{H}_{\rm d} + N_{i,4}\tilde{H}_{\rm u}.$$

Analytical solutions for the mass eigenvalues can be computed, see for example [150], but we will here concentrate on some special cases.

Gaugino-like or higgsino-like regions. In the limit where electroweak symmetry breaking effects are small compared with the MSSM parameters, namely $M_Z \ll |\mu \pm M_1|, |\mu \pm M_2|$, approximate values for the neutralino masses are

$$\begin{aligned} M(\tilde{\chi}^0_1) &\simeq M_1 - \frac{M_Z^2 s_W^2 (M_1 + \mu \sin 2\beta)}{\mu^2 - M_1^2}, \\ M(\tilde{\chi}^0_2) &\simeq M_2 - \frac{M_Z^2 c_W^2 (M_2 + \mu \sin 2\beta)}{\mu^2 - M_2^2}, \\ M(\tilde{\chi}^0_3) &\simeq |\mu| + \frac{M_Z^2 (1 - \epsilon \sin 2\beta)(|\mu| + M_1 c_W^2 + M_2 s_W^2)}{2(|\mu| + M_1)(|\mu| + M_2)}, \\ M(\tilde{\chi}^0_4) &\simeq |\mu| + \frac{M_Z^2 (1 + \epsilon \sin 2\beta)(|\mu| - M_1 c_W^2 - M_2 s_W^2)}{2(|\mu| - M_1)(|\mu| - M_2)}, \end{aligned} \tag{85}$$

where ϵ is the sign of μ. The mass eigenstates are then $\tilde{\chi}^0_1 \simeq \tilde{B}^0$, $\tilde{\chi}^0_2 \simeq \tilde{W}^0$ and $\tilde{\chi}^0_3, \tilde{\chi}^0_4 \simeq (\tilde{H}^0_{\rm d} \pm \tilde{H}^0_{\rm u})/\sqrt{2}$. In this approximation, the chargino $\tilde{\chi}^{\pm}_1$ is degenerate with the neutralino $\tilde{\chi}^0_2$.

If universality of gaugino masses is assumed, M_1 can be eliminated as $M_1 \simeq 0.5 M_2$ at the weak scale. The following cases can be envisaged

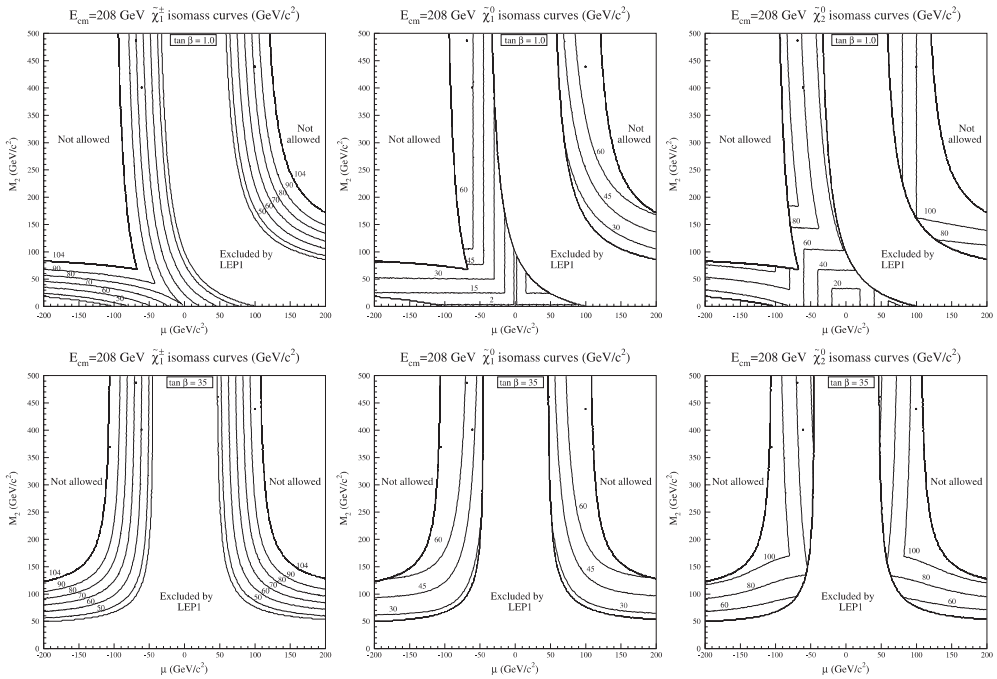

Figure 16. Chargino and neutralino isomass curves in the (μ, M_2) plane for $\tan\beta = 1.0$ and 35. The line delimiting the region labelled 'not allowed' is the kinematic limit for chargino production at LEP with 208 GeV. From [151].

- If $M_2 \ll |\mu|$, the LSP is bino-like. In this case, the lightest chargino and two lightest neutralinos are gaugino-like and $2M(\tilde{\chi}_1^0) \simeq M(\tilde{\chi}_2^0) \simeq M(\tilde{\chi}_1^\pm) \simeq M_2$. The heavier chargino and neutralinos are higgsino-like and $M(\tilde{\chi}_3^0) \simeq M(\tilde{\chi}_4^0) \simeq M(\tilde{\chi}_2^\pm) \simeq \mu$.
- If $M_2 \gg |\mu|$ the LSP would be higgsino-like and nearly degenerate with the $\tilde{\chi}_1^\pm$ and $\tilde{\chi}_2^0$. The heavier chargino and neutralinos are gaugino-like, with masses $2M(\tilde{\chi}_3^0) \simeq M(\tilde{\chi}_4^0) \simeq M(\tilde{\chi}_2^\pm) \simeq M_2$.
- In the intermediate region (the so-called mixed region), the situation is rather complex and the states are not as pure gaugino- or higgsino-like as above. For not too small M_2, e.g. $M_2 \geqslant 100$ GeV, the region given approximately by $M_1 \leqslant |\mu| \leqslant M_2$ is characterized by a dominantly bino LSP, nearly degenerate higgsino-like $\tilde{\chi}_1^\pm$, $\tilde{\chi}_2^0$ and $\tilde{\chi}_3^0$ and nearly degenerate gaugino-like $\tilde{\chi}_2^\pm$ and $\tilde{\chi}_4^0$.

These features are more outspoken for negative μ than for positive μ.

The regions where $|\mu| \gg M_2$ and $M_2 \gg |\mu|$ will be called, respectively, **gaugino-like** and **higgsino-like** in the following, according to the composition of the lightest chargino and neutralinos. The region between these two extremes is called **mixed**.

The masses of the lightest chargino and of the two lightest neutralinos are displayed in the (μ, M_2) plane in figure 16 for $\tan\beta = 1.0$ and 35.

5.4.4. Radiative corrections to gaugino masses. The complete corrections to the chargino and neutralino masses, including the gauge, Higgs, gaugino and higgsino sector, are found in [104]. They are typically 3–10% for the lighter states $\tilde{\chi}_1^0$ and $\tilde{\chi}_1^\pm$, the largest relative corrections arising for low masses. These corrections are relevant when determining the values of the underlying parameters from a set of physical χ masses.

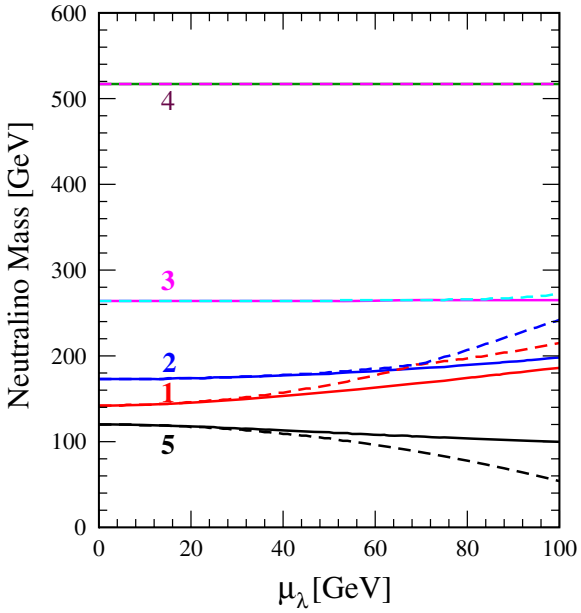

Figure 17. Neutralino masses as a function of μ_λ, the other parameters being fixed to $\mu_\kappa = 120\,\text{GeV}$, $M_1 = 250\,\text{GeV}$, $M_2 = 500\,\text{GeV}$, $\mu = 170\,\text{GeV}$ and $\tan\beta = 3$. The exact numerical solutions are shown as solid and the approximate solutions as dashed lines. Reprinted from [154]. Copyright 2005, with permission from Elsevier.

The LEP constraints for the search of charginos and neutralinos, taking into account the radiative corrections, have been analysed in [152]. They do not alter the excluded domain in $m_{\tilde{\chi}^\pm}$ as a function of the chargino–neutralino mass difference, but they alter its mapping in the $\mu, m_{1/2}$ plane. These effects are taken into account in the final LEP analyses.

The radiatively generated mass for a gluino which is massless at tree level ($m_{1/2} = 0$ at the GUT scale) falls usually in the light gluino window, $m_{\tilde{g}} \leqslant 3\,\text{GeV}$ [153]. The correction to the mass of a massive gluino arise from $g\tilde{g}$ and $q\tilde{q}$ loops and can be large [104]. They vary from about 30% for $m_{\tilde{g}} \ll m_{\tilde{q}}$ to about 4% for gluinos masses above the quark/squark threshold.

5.4.5. Neutralinos in the NMSSM. The introduction of an additional singlet field in the NMSSM (see section 3.5.2) does not affect the chargino sector. However, the neutralino mass matrix is extended to a 5×5 matrix

$$\mathbf{Y_5} = \begin{pmatrix} M_1 & 0 & -M_Z\cos\beta s_W & M_Z\sin\beta s_W & 0 \\ 0 & M_2 & M_Z\cos\beta c_W & -M_Z\sin\beta c_W & 0 \\ -M_Z\cos\beta s_W & M_Z\cos\beta c_W & 0 & -\mu & -\mu_\lambda\sin\beta \\ M_Z\sin\beta s_W & -M_Z\sin\beta c_W & -\mu & 0 & -\mu_\lambda\cos\beta \\ 0 & 0 & -\mu_\lambda\sin\beta & -\mu_\lambda\cos\beta & \mu_\kappa \end{pmatrix}, \tag{86}$$

which cannot be solved analytically. Here $\mu_\kappa = 2\kappa\langle S\rangle$, $\mu_\lambda = \lambda v$ and $\mu = \lambda\langle S\rangle$. The parameter μ_λ determines the mixing between the MSSM neutralino doublet and the singlet called singlino. Approximate analytical expressions for the neutralino spectrum have been derived in [154] for small mixing μ_λ.

A novel feature of the NMSSM is the possibility for that, small μ_κ, the LSP is the singlino. An example spectrum is presented in figure 17, where both the approximate solutions and the exact numerical solutions for the masses are displayed. The latter are computed with the program NMHDECAY [155].

5.5. *Squark and slepton masses*

At some energy scale M_X, usually assumed to be $M_{\rm GUT}$, squark and slepton masses are defined by the soft breaking terms $m_{i,0}$. The physical mass spectrum is obtained after running down the high scale parameters by means of RGEs [1]. In the MSUGRA scenario, the scalar masses are all equal to a common mass m_0, but in many of the cases below such strict scalar mass universality will not be required. Instead, relaxed assumptions are made, such as for conditions (67), or no scalar mass universality is assumed at all.

5.5.1. First two families. As discussed in section 3.3, the Yukawa couplings of the first two families are very small. They can safely be neglected in the RGEs governing the evolution of the scalar masses, so that only the gauge interactions need to be taken into account. At lower energy the following hold.

- The SUSY breaking mass, $m_{i,0}$, is not renormalized at the level of one-loop RGE when Yukawa couplings can be neglected,
- The one-loop RGEs induce a term due to fermion–gaugino loops, proportional to gaugino masses.

$$\frac{{\rm d}\tilde{m}_\phi^2}{{\rm d}t} = -\frac{2}{\pi}\sum_a C_a \alpha_a M_a^2, \tag{87}$$

where t is defined as $t = ln(Q/M_X)$ and the C_a are group constants. This introduces a dependence on $m_{1/2}$ and α_is, increasing the mass. As in equation (87) the contributions from the 3 gauge groups evolve independently (at 1-loop), the resultant contributions to scalar masses are encoded in 3 functions, K_a. After performing the integration, these are proportional to

$$K_a(t) = -\kappa_a \frac{2M_a^2(t)}{b_a}\left[1 - \frac{\alpha_a^2(0)}{\alpha_a^2(t)}\right], \tag{88}$$

where the constants $\kappa_a = (3/5, 3/4, 4/3)$ and the b_a have been defined in section 4.2.

- A D-term of the form $\sum_a g_a^2(\phi^* T^a \phi)^2/2$, see equation (26), leads to quartic interactions (squark)^2(Higgs)^2 or (slepton)^2(Higgs)^2. When $SU(2) \times U(1)$ is broken, it induces a contribution to the (mass)^2 given by

$$\Delta_i = (I_i^3 - Q_i \sin^2\theta_W)\cos 2\beta M_Z^2. \tag{89}$$

This term is model-independent and, in particular, does not depend on the mechanism of supersymmetry breaking, as discussed in section 3.4.

We will assume that, at the scale M_X, the scalar masses are diagonal in family space, to avoid potentially large FCNC. Then, they will remain diagonal after running the RGEs to any other scale.

The general form of the running masses of sfermions is

$$\tilde{m}_i^2 = m_{i,0}^2 + c_{a,i} K_a + \Delta_i = m_{i,0}^2 + c_i m_{1/2}^2 + \Delta_i, \tag{90}$$

where the coefficients should be evaluated at the scale of the running mass, $Q = m(Q)$ (and radiative corrections, e.g. from QCD, will need to be included to obtain the pole masses). The second equation in (90) assumes universality of the gaugino masses.

Table 5. Coefficients for the masses of the first two families of sfermions. The values of the c_i are determined from 1-loop RGEs, without including QCD corrections to the squark masses. The range of values quoted corresponds to a variation of $m_{1/2}$ from 50 GeV (higher value) to 1000 GeV (lower value), corresponding to a scale Q_{EWSB} from about 100 to 1800 GeV, respectively. The coefficients c_i are computed with SUSPECT2.0 [156].

Particle		c_i	$p_i = I_i^3 - Q_i \sin^2\theta_W$	
$\tilde{u}_{\mathrm{L}}$	$K_3 + K_2 + \frac{1}{36}K_1$	3.8–5.9	$+(1/2) - (2/3)\sin^2\theta_W$	$= +0.35$
$\tilde{d}_{\mathrm{L}}$	$K_3 + K_2 + \frac{1}{36}K_1$	3.8–5.9	$-(1/2) + (1/3)\sin^2\theta_W$	$= -0.42$
$\tilde{u}_{\mathrm{R}}$	$K_3 + \frac{4}{9}K_1$	3.4–5.5	$+(2/3)\sin^2\theta_W$	$= +0.15$
$\tilde{d}_{\mathrm{R}}$	$K_3 + \frac{1}{9}K_1$	3.4–5.4	$-(1/3)\sin^2\theta_W$	$= -0.07$
$\tilde{e}_{\mathrm{L}}$	$K_2 + \frac{1}{4}K_1$	0.45–0.49	$-(1/2) + \sin^2\theta_W$	$= -0.27$
$\tilde{\nu}$	$K_2 + \frac{1}{4}K_1$	0.45–0.49	$+1/2$	$= +0.50$
$\tilde{e}_{\mathrm{R}}$	K_1	0.14–0.15	$-\sin^2\theta_W$	$= -0.23$

For the 1st and 2nd generations, the expressions for the masses and the values of the coefficients c_i evaluated at a scale $Q_{\mathrm{EWSB}} \equiv \sqrt{m(t_{\mathrm{L}})m(t_{\mathrm{R}})}$ are summarized in table 5. As there are 7 physical masses and 4 parameters, the universal m_0 and the 3 values K_a, there exist three independent relations, or sum rules, between the masses. The D-term determines a model-independent sum rule for the left slepton or squark 'hyperfine' mass splitting

$$m^2_{\tilde{e}_{\mathrm{L}}} - m^2_{\tilde{\nu}_{\mathrm{L}}} = m^2_{\tilde{d}_{\mathrm{L}}} - m^2_{\tilde{u}_{\mathrm{L}}} = -M_W^2 \cos 2\beta, \tag{91}$$

from which it follows (note: $\cos(2\beta) \leqslant 0$) that $m_{\tilde{e}_{\mathrm{L}}} > m_{\tilde{\nu}_{\mathrm{L}}}$ and $m_{\tilde{d}_{\mathrm{L}}} > m_{\tilde{u}_{\mathrm{L}}}$. In addition to these two sum rules, a third one can be written as [157]

$$2(m^2_{\tilde{u}_{\mathrm{R}}} - m^2_{\tilde{d}_{\mathrm{R}}}) + (m^2_{\tilde{d}_{\mathrm{R}}} - m^2_{\tilde{d}_{\mathrm{L}}}) + (m^2_{\tilde{e}_{\mathrm{L}}} - m^2_{\tilde{e}_{\mathrm{R}}}) = \frac{10}{3}\sin^2\theta_W M_Z^2 \cos 2\beta. \tag{92}$$

This relation assumes a universal m_0, but does not rely on any assumptions on gaugino mass parameters.

If particles are discovered and identified, the relations (91) may allow the determination of $\tan\beta$, independently from the universality assumptions. The sum rule (92) then tests the universality of m_0.

As the evolution is entirely determined by gauge couplings, the sparticles of the first two generations are degenerate if m_0 is universal. Rather different values may be found in the literature for the coefficients c_i of $\tilde{Q}_{\mathrm{L}}$, $\tilde{u}_{\mathrm{R}}$ and $\tilde{d}_{\mathrm{R}}$ in table 5. This is due to their high sensitivity to uncertainties on $\alpha_3(M_X)$ and to the exact scale at which they are evaluated, as α_3 varies strongly near the electroweak scale. Nevertheless, the coefficients of $m_{1/2}$ are larger for squarks than for sleptons, due to their dependence on α_3. The expected mass hierarchy between flavours for the first two generations is then

$$m_{\tilde{q}_{\mathrm{L}}} \geqslant m_{\tilde{q}_{\mathrm{R}}} \geqslant m_{\tilde{l}_{\mathrm{L}}} \geqslant m_{\tilde{l}_{\mathrm{R}}}.$$

In several models of gravity-mediated supersymmetry breaking based on superstrings, such as the dilaton-dominated or the no-scale models, it is expected that $m_{1/2}$ be appreciably larger than m_0 [1]. In this case, it can be expected that $M_{\tilde{g}}$ is larger than any of the sfermion masses, but, due to the contribution of α_3 to the squark masses, we expect at most $m_{\tilde{g}} \simeq 1.2 m_{\tilde{q}}$. Nevertheless, they are taken in phenomenological studies as independent parameters which reflect our ignorance of supersymmetry breaking.

5.5.2. Third family. To compute the masses of the third family scalars, the contributions from Yukawa couplings can no longer be neglected. Taking the example of the stop, an

Table 6. Coefficients for the masses of the third family of sfermions. The values of the c_i are determined from 1-loop RGEs for $\tan\beta = 10$, without including QCD corrections to the squark masses. The range of values quoted corresponds to a variation of $m_{1/2}$ from 50 (higher value) to 1000 GeV (lower value). The coefficients b_i and c_i are computed with SUSPECT2.0 [156].

Particle	b_i	c_i
$\tilde{t}_L$,$\tilde{b}_L$	0.62–0.69	3.2–5.0
$\tilde{t}_R$	0.28–0.33	2.4–3.7
$\tilde{b}_R$	0.83–0.96	3.5–5.5
$\tilde{\tau}_L$,$\tilde{\nu}$	0.99–1.0	0.41–0.48
$\tilde{\tau}_R$	0.98–1.0	0.11–0.14

F-term (28) of the form $h_t^2 H_u^{0*} H_u^0 \tilde{t}_L^* \tilde{t}_L$ is introduced, leading to m_t^2 after the Higgs field is replaced by its vev. These terms have been neglected for the first two generations, due to the smallness of the fermion masses. Furthermore, off-diagonal elements are generated in the mass matrix of $(\tilde{t}_L, \tilde{t}_R)$, from the F-term contribution in (30), of the form $-\mu h_t \tilde{t}_R^* \tilde{t}_L H_d^{0*} + \text{c.c.}$, and from a (scalar)^3 soft breaking contribution $A_t h_t \tilde{t}_R^* \tilde{t}_L H_u^0 + \text{c.c.}$. Together, they yield the off-diagonal term $v h_t (A_t \sin\beta - \mu \cos\beta)$. **The main effects of the Yukawa couplings can be summarized as follows. First, the effect of the RGE evolution is reduced, due to the opposite contributions of the Yukawa couplings compared with the gauge couplings. Second, a mixing of the left and right scalars is introduced, proportional to fermion mass m_f, and therefore potentially very important for the stop**. For stop and sbottom quarks the diagonal pieces of the mass matrix, including the Yukawa couplings in the RGEs, take the form

$$\tilde{m}_i^2 = m_{f_i}^2 + b_i m_{i,0}^2 + c_i m_{1/2}^2 + \Delta_i, \tag{93}$$

where Δ_i has been defined in equation (89) and the values of the coefficients evaluated at a scale $Q_{\text{EWSB}} \equiv \sqrt{m(t_L) m(t_R)}$ are summarized in table 6. The stop mass eigenstates $\tilde{t}_1$ and $\tilde{t}_2$ are given by

$$\tilde{m}_{t_{1,2}}^2 = \frac{1}{2}[m_{\tilde{t}_L}^2 + m_{\tilde{t}_R}^2 \mp \sqrt{(m_{\tilde{t}_L}^2 - m_{\tilde{t}_R}^2)^2 + 4 m_t^2 (A_t - \mu \cot\beta)^2}]. \tag{94}$$

This reduces further the mass of the lighter stop, especially for low values of $\tan\beta$, which is often found to be the lightest of all squarks. For large $\tan\beta$, the mixing effects can be quite important for the sbottom and the stau. Therefore, the stau is likely to be the lightest slepton. Their mass eigenstates are given by an equation similar to (94) after replacing $\cot\beta$ by $\tan\beta$.

Sum rules relating the masses of the third generation sfermion to the ones of the first two generations have also been derived in [157].

It is also observed from expression (94) that for large enough values of the trilinear coupling A_f at the electroweak scale (μ being fixed by the EWSB) the mass-squared of the sfermion can take a negative value, especially for third family particles where the fermion mass is largest. This may induce a minimum of the potential, implying that the sfermions acquires a vev, and breaking charge and colour will be discussed in more detail in section 8.4.

5.5.3. Radiative corrections to sfermion masses. The QCD corrections (one-loop) to squarks of the first two generations, evaluated in [104], vary between 1% for $m_{\tilde{g}} \ll m_{\tilde{q}}$ to 4–5% when $m_{\tilde{g}} \simeq m_{\tilde{q}}$. For the third generation, the QCD corrections are counteracted by the opposite sign corrections from Yukawa couplings. The stop mass receives corrections in the range of -5 to 2% and the sbottom mass in the range 0–3%. For sleptons, the corrections are typically in the range $\pm 2\%$.

The effect of radiative corrections to the $SU(2)$ breaking mass splittings in $SU(2)$ doublets has been computed in [158]. The tree level relation in equation (91) is corrected by $\leqslant \pm 0.05$ in terms of the effective $\cos 2\beta$ for a doublet for typical values of the SUSY parameters. For very heavy sfermions, the difference between the effective $\cos 2\beta$ for $\tilde{l}$ and for $\tilde{q}$ becomes large.

5.5.4. Non-universality of scalar masses. We would like to show here, in an example, how a departure from universality may lead to quite different experimental mass spectra. An example of non-universality of scalar masses at the GUT scale has been worked out for, e.g. $SO(10)$ grand unification [159]. We have seen in section 4.3.2 that the unification of families within $SO(10)$ implied, apart from the gauge coupling unification, that the Yukawa couplings are equal for all members of the family. Such equality does not need to apply also to the scalar masses, even if it is assumed that the soft SUSY-breaking masses take a universal value m_{16} and m_{10} for the **16** and **10** representations of $SO(10)$, respectively. The (direct) breaking of the gauge group from $SO(10)$ to $SU(3)_C \times SU(2)_L \times U(1)$ requires the breaking of the additional $U(1)_X$ factor, present in $SO(10)$, and induces D-terms for the scalar masses if the symmetry is spontaneously broken. The scalar masses at the GUT scale can then be parametrized as

$$\begin{aligned} m^2_{\tilde{q}} &= m^2_{\tilde{e}_R} = m^2_{\tilde{u}_R} = m^2_{16} + m^2_D, \\ m^2_{\tilde{d}_R} &= m^2_{\tilde{L}} = m^2_{16} - 3m^2_D, \\ m^2_{H_u, H_d} &= m^2_{10} \mp 2m^2_D, \end{aligned} \tag{95}$$

where m^2_D parametrizes the magnitude of the D-terms and can take positive or negative values. The coefficients reflect the quantum numbers of the scalar fields under the broken $U(1)_X$. Note that the mass splitting introduced by the D-terms preserves an $SU(5)$-type unification.

An analysis within this framework was performed in [160], confirming the results of [104] cited in section 4.3.3 that unification of the Yukawa couplings of $t - b - \tau$ occurs for $\tan\beta \simeq 50$ and $\mu < 0$. They obtain acceptable solutions (Yukawa unification to within 5%) for $m_{16} \leqslant m_{10} \leqslant 1.5m_{16}$ and $0.1m_{16} \leqslant m_D \leqslant 0.35m_{16}$. For too small m_D, there is not enough splitting between the Higgs soft masses for radiative EWSB to occur. Too large m_D yields third generation scalars below experimental limits or CCB minima in the scalar potential. They also find that these solutions require too large values of $B(b \to s\gamma)$, except for very large values of $m_{1/2}$.

For $\mu > 0$, solutions can also be obtained, but only at the expense of quite significant (several per cent) deviations from Yukawa unification [106, 161]. An approximate Yukawa unification, together with low energy constraints and radiative EWSB, imposes stringent limitations to the allowed SUSY spectra. It is found that typically $m_{16} > 1$ TeV, $m_{10} \simeq \sqrt{2}m_{16}$, similarly to the negative μ case. However, the acceptable solutions also require a large negative $A_0 \simeq -2m_{16}$ (which is not the case for $\mu < 0$). The sparticle spectrum corresponds to a radiatively driven 'inverted scalar hierarchy' [162], with scalars of the first two generations above 1 TeV, $\tilde{t}_1$ ∼(150–250) GeV as the lightest sfermion, $\tilde{b}_1$ ∼(450–650) GeV always heavier than $\tilde{t}_1$, $\tilde{\tau}_1$ ∼(200–500) GeV between the two and g ∼ (600–1200) GeV (numbers are from [106]). The chargino ∼(100–250) GeV is lighter than the $\tilde{\tau}_1$ and the LSP is the $\tilde{\chi}^0_1$ ∼(80–170) GeV. The light Higgs is in the region 115–130 GeV, as usual, whereas the heavy Higgses are not constrained by Yukawa unification.

It is also found in [106] that Yukawa unification with $\mu > 0$ is obtained more easily when only Higgs mass parameters are non-universal and split, but no D-terms are introduced for sfermions. This model, for which [106] gives some justification, leads to a similar spectrum to the above one.

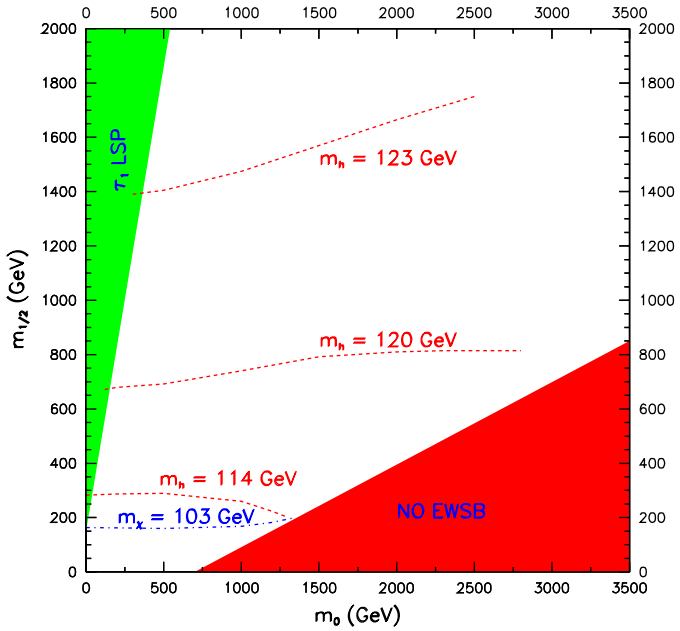

Figure 18. Allowed regions in the $(m_{1/2}, m_0)$ plane within the MSUGRA framework.

The value of $\tan\beta$ and the choice of the sign of μ has strong implications for rare decays, $(g-2)$ of muons and other low energy measurements, which will be further considered in section 6.

5.6. Examples of MSUGRA spectra

In the MSUGRA scenario with scalar and gaugino mass universality and the correct breaking of electroweak symmetry, the allowed parameter space is rather tightly constrained. This is illustrated in figure 18 in the $(m_0, m_{1/2})$ plane. The upper-left region (green) is excluded because the LSP would be the $\tilde{\tau}_1$. In the lower-right region (red) electroweak symmetry breaking cannot take place. The boundary of this region depends, however, very strongly on the mass of the top quark. For $m_t = 175\,\text{GeV}$ or more, it would occur at much larger m_0 values than shown in figure 18 where, for illustrative purposes, it is drawn for $m_t = 171\,\text{GeV}$ (more precise boundaries will be shown later). Also indicated are isomass curves for the light Higgs and the chargino. The mapping of these and other constraints will be discussed more thoroughly in section 12.

Moreover, the value of μ at the weak scale, derived from radiative electroweak symmetry breaking, for intermediate to large $\tan\beta$, depends little on m_0 and $\tan\beta$ and is almost linear in $m_{1/2}$, as was seen in section 5.3. This relation implies that, in most of the plane, the chargino and neutralino composition is gaugino-like, as $|\mu| > m_{1/2}$. Only for very large m_0, close to the boundary where no EWSB occurs, does the composition become of mixed type. This relation is quite sensitive to the value of the top quark mass.

Some examples of MSUGRA spectra are shown in figure 19. They fulfill additional requirements to be discussed later, including the LEP and Tevatron mass bounds from direct searches. The first three (cases 1 to 3) feature a rather low mass spectrum, with the gluino heavier than the squarks. The lightest charginos and neutralinos are in the gaugino-like region

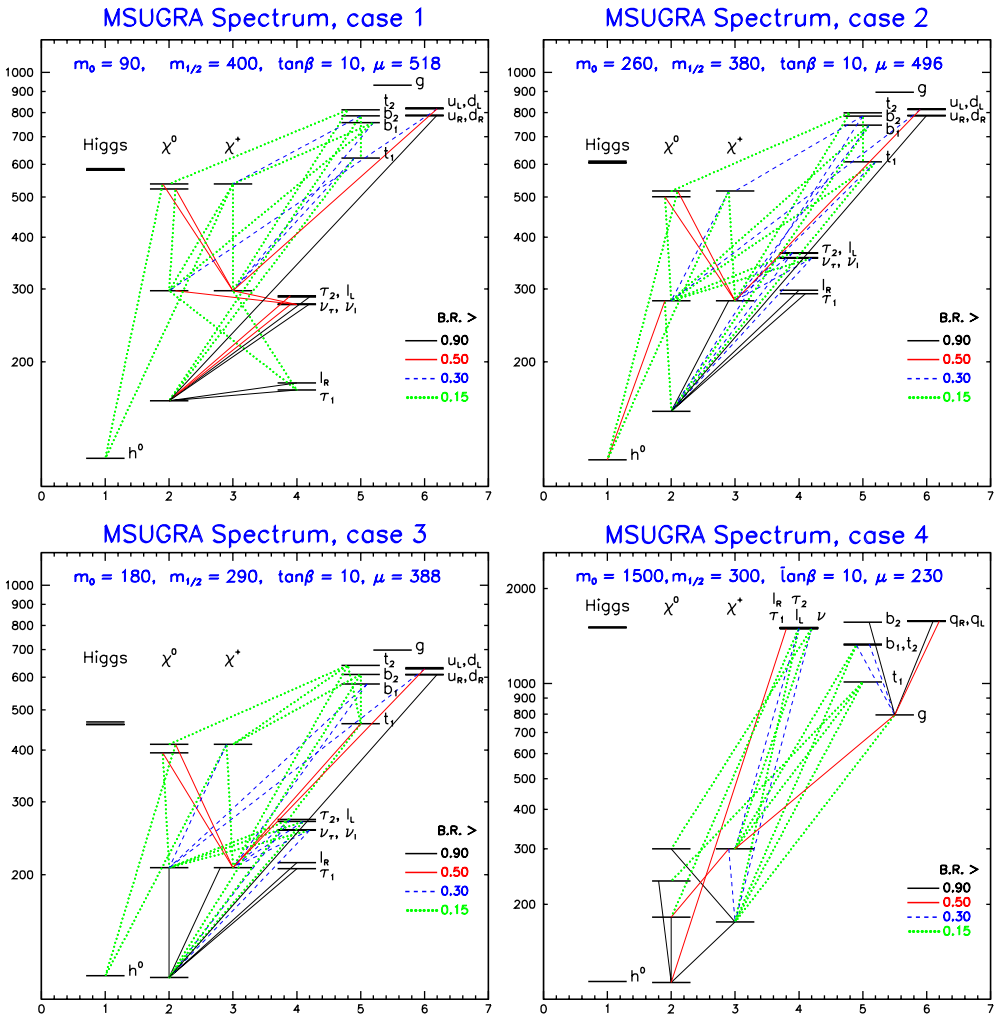

Figure 19. Examples of supersymmetric particle mass spectra in MSUGRA, computed with the program ISASUGRA7.69. Also indicated are the decays with branching ratios larger than 15%.

and the three cases differ by the relative position of the sleptons with respect to the $\tilde{\chi}_2^0$ and $\tilde{\chi}_1^\pm$, which affects the decay chains. In case 1 (point C from the 'post-LEP' benchmark points [143]), all slepton masses are between the LSP and the higher gaugino states. In case 2, the sleptons are heavier than $\tilde{\chi}_2^0$ and $\tilde{\chi}_1^\pm$ and the mass difference between the $\tilde{\chi}_2^0$ and $\tilde{\chi}_1^0$ is larger than the mass of the lightest Higgs. In case 3 (near the point of [163], a slightly modified version of the Snowmass SPS 1a [164]), sleptons are heavier than $\tilde{\chi}_2^0$ and $\tilde{\chi}_1^\pm$ (but lighter than the heaviest chargino and neutralinos) and the mass separation between $\tilde{\chi}_2^0$ and $\tilde{\chi}_1^0$ is less than m_h. In case 4 (point E from [143]), all scalars are heavy, due to the large value of m_0. The charginos and neutralinos are in the mixed region, where $M_2 \simeq |\mu|$. It is an example of the focus point scenario. The top mass was assumed to be 175 GeV for cases 1–3 and 171 GeV for case 4 (a bit low compared with the experimental value). A situation similar to case 4 with charginos and neutralinos in the mixed region can also be obtained for $m_t = 175$ GeV, but only for extremely large m_0 (e.g. $m_0 \simeq 3400$ GeV for the same $m_{1/2}$ as case 4). The values of

Table 7. Mass spectra in GeV for minimal SUGRA models calculated with ISASUGRA 7.69. The value of $|\mu|$ is estimated at the scale $Q = \sqrt{m_{\tilde{t}_1} m_{\tilde{t}_2}}$.

Model	Case 1	Case 2	Case 3	Case 4
$m_{1/2}$	400	380	290	300
m_0	90	260	180	1500
$\tan\beta$	10	10	10	10
sign(μ)	+	+	+	+
A_0	0	0	0	0
m_t	175	175	175	171
Masses				
$\|\mu\|$	514	491	385	227
h^0	117	116	114	114
H^0	584	609	464	1515
A^0	580	605	461	1505
$H^\pm$	590	614	470	1517
χ_1^0	158	151	112	113
χ_2^0	305	290	214	189
χ_3^0	518	496	390	237
χ_4^0	534	512	409	304
$\chi_1^\pm$	305	290	214	187
$\chi_2^\pm$	533	512	408	300
$\tilde{g}$	940	904	704	798
e_L, μ_L	293	370	272	1511
e_R, μ_R	179	298	214	1502
ν_e, ν_μ	277	358	258	1507
τ_1	172	293	208	1490
τ_2	294	371	274	1505
ν_τ	276	357	257	1501
u_L, c_L	860	856	662	1610
u_R, c_R	831	830	642	1608
d_L, s_L	864	860	667	1612
d_R, s_R	829	828	641	1608
t_1	653	640	488	1033
t_2	837	823	657	1363
b_1	790	779	603	1351
b_2	816	813	631	1573

the parameters and sparticle masses for all cases are collected in table 7[12]. All four cases give a h^0 mass within 2–3 GeV from the LEP limit.

The main features of the decays for the cases above will be discussed in section 9.7. Other benchmark points will be presented in section 15.4.

5.7. GMSB spectroscopy

The main characteristic of GMSB is that the LSP is always the gravitino, with a mass expected in the range of 1 eV to few hundred MeV. The GMSB spectroscopy, with masses defined at the messenger scale M, depends on two parameters, the scale Λ and the messenger index N. The evolution, through RGEs, down to the electroweak scale introduces an additional dependence on the other SUSY parameters.

[12] The differences between the mass values in table 7 and [143] for the same initial parameter values reflect the differences between various program codes.

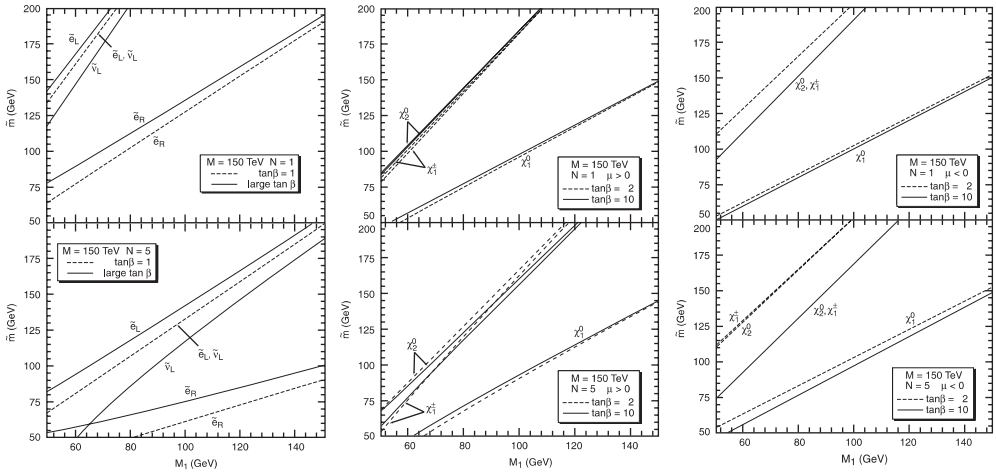

Figure 20. Supersymmetric particles masses in GMSB, from [131].

The gaugino masses take the simple form

$$M_a(t) = \frac{\alpha_a(t)}{4\pi} N\Lambda. \tag{96}$$

The scale at which they are defined is given by $t = \ln(M^2/Q^2)$. It is seen that their evolution is the same as encountered in the MSUGRA framework.

The masses of scalar particles at the messenger scale are obtained from

$$\tilde{m}^2 \simeq 2N\Lambda^2 \sum C_a \left(\frac{\alpha_a}{4\pi}\right)^2, \tag{97}$$

where the C_a are group constants, defined as $C_3 = 4/3$ for colour triplets and zero for singlets, $C_2 = 3/4$ for weak doublets and zero for singlets, $C_1 = 3/5(Y/2)^2$. These values have to be RGE-evolved down to the electroweak scale and the effect of mixing, as well as the D-term contribution, has to be included. The corresponding formulae can be found in Giudice and Rattazzi [131] (readers are warned that they do not use the canonical normalization for grand unification, used here and in [1]).

The dependence of the scalar and the gaugino masses as a function of the $U(1)$ mass parameter M_1 is displayed in figure 20 (from [131]). It is seen that GMSB, with this choice of parameter values, may lead to a rather light sparticle spectrum, observable with present day accelerators. The most striking feature in these plots is that for $N = 1$ the next-to-LSP (NLSP) is the $\tilde{\chi}_1^0$ (a bino), whereas for larger N it becomes the $\tilde{l}_R$ over most of the parameter space. The relative increase of the gaugino masses with N is due to their scaling like N, while scalar masses scale like $\sqrt{N}$. After including the effect of mixing, the best slepton candidate to become the NLSP is the $\tilde{\tau}_1$, especially at high $\tan\beta$ and/or large $|\mu|$ where the mixing is the largest. If mixing is negligible, the $\tilde{e}_R$ and $\tilde{\mu}_R$ will be close in mass with the $\tilde{\tau}_R$ and they are called 'co-NLSP'. Squark masses are, such as in MSUGRA, predicted to be much larger due to the contribution of α_3. An exception is $\tilde{t}_1$, which can even become the NLSP for small $\tan\beta$.

5.8. AMSB spectroscopy

In the minimal AMSB scenario, the gaugino and scalar mass parameters are determined from the gravitino mass $m_{3/2}$ and the universal scalar mass m_0. To leading order, they are given at

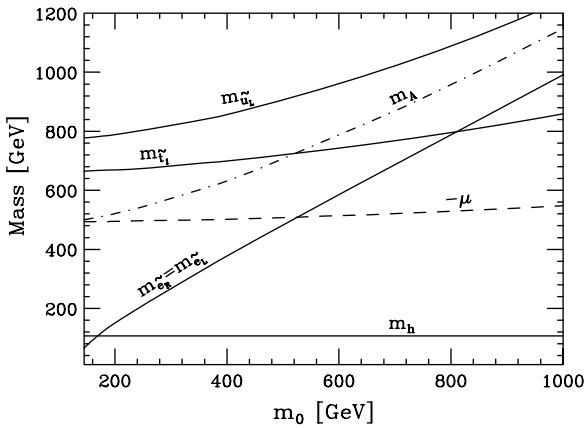

Figure 21. Example of supersymmetric particles masses in AMSB as a function of m_0, for $m_{3/2} = 36\,\text{TeV}$, $\tan\beta = 5$ and $\mu < 0$. Reprinted from [165]. Copyright 1999, with permission from Elsevier.

the GUT scale by

$$M_a = \frac{\beta_g}{g} m_{3/2} = b_a \frac{\alpha_a}{4\pi} m_{3/2},$$
$$\tilde{m}_f^2 = -\frac{1}{4}\left(\frac{\partial\gamma}{\partial g}\beta_g + \frac{\partial\gamma}{\partial y}\beta_y\right) m_{3/2}^2 + m_0^2, \tag{98}$$

where g are the gauge couplings, y the Yukawa couplings, β their respective beta functions and γ the anomalous dimension. The beta function for gauge couplings is simply $\beta_{g_a} = b_a g_a^3/16\pi^2$, where the coefficients $b_a = (33/5, 1, -3)$ are the same as encountered previously. The other functions are found in [165].

The next-to-leading-order (NLO) corrections to the gaugino mass parameters, also given in [165], are not negligible, especially for M_2. The mass ratios at NLO for $M_1 : M_2 : M_3$ are $2.8 : 1 : -7.1$. Hence, the winos are lighter than the bino, contrary to the situation in GMSB or in MSUGRA with gaugino mass universality. The neutral wino is found, including loop corrections dominated by the gauge bosons, to be lighter by few 100 MeV than the charged winos. Moreover, the value of $|\mu|$ derived from correct EWSB is typically 3–6 times larger than the wino mass. As a result, **the $\tilde{\chi}_1^0$ is expected to be wino-like, nearly degenerate with the lightest chargino and a good candidate LSP**.

The sfermion masses are obtained by evolving the parameters in equation (98) down from the GUT scale and adding the D-terms. An example is shown in figure 21 for illustration, with the parameters $m_{3/2} = 36\,\text{TeV}$, $\tan\beta = 5$ and $\mu < 0$. For this choice of parameters, $M_1 = 333\,\text{GeV}$, $M_2 = 119\,\text{GeV}$, $M_3 = 850\,\text{GeV}$. The squark masses are rather heavy, due to their dependence on α_S, and not very sensitive to the value of m_0. A striking feature of the slepton spectrum is the near degeneracy of the left and right charged sleptons of the two first generations. It turns out that, due to a numerical accident, their pure AMSB contributions are almost identical. The D-term contributions are also nearly the same, as can be seen in table 5. Moreover, neither of these contributions is very large. As a result, the sleptons are nearly degenerate and with mass close to m_0.

In the AMSB scenario, the LSP could in principle be the $\tilde{\chi}_1^0$, the $\tilde{\nu}$ or even the $\tilde{\tau}_1$, although a charged LSP is disfavoured by cosmology.

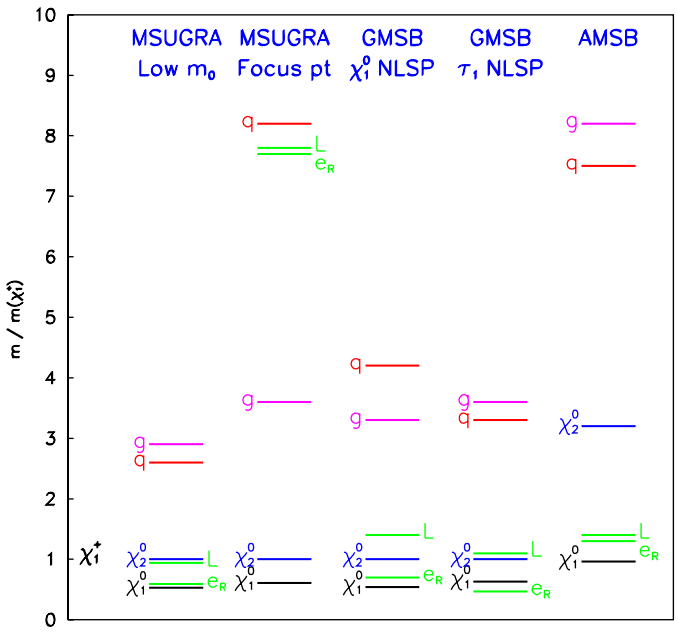

Figure 22. Main features of sparticle spectra for MSUGRA with low m_0, MSUGRA at a focus point, GMSB with neutralino NLSP, GMSB with $\tilde{\tau}_1$ NLSP, AMSB. All masses are normalized to the mass of the lightest chargino.

5.9. Gross features of the phenomenologies

The main features of the sparticle spectra expected for the different SUSY breaking scenarios are illustrated in figure 22. The particle masses on the vertical scale are normalized to the chargino mass. The two MSUGRA spectra are the ones from [143] encountered in figure 19, featuring a low m_0 and a focus point scenario. The two GMSB spectra are the points called MSSM1 and MSSM2 in [166]. The AMSB spectrum is the example discussed in section 5.8 with $m_0 = 200\,\text{GeV}$.

The different candidate MSSM models, MSUGRA, GMSB, AMSB or MSSM with breaking of R-parity, all lead to different experimental signatures. It is, therefore, mandatory to develop different experimental search strategies to be able to cope with all these situations.

Direct searches for SUSY particles in the context of MSUGRA rely on the fact that, for a large part of the MSUGRA parameter space, the neutralino is the LSP. If R-parity is conserved, it should be stable. Its interaction with matter is expected to be very weak (see Haber and Kane [167]), with a cross-section of the same order as the neutrino charged current cross-section. Therefore, the neutralino will escape undetected from electron or hadron collider detectors. As SUSY partners are produced in pairs and each of them will ultimately decay into a neutralino, the candidate events are signed by large missing energy.

Direct searches in the GMSB scenario are also based on a missing energy signature, due to the presence of a nearly massless gravitino-LSP ($\tilde{G}$) at the end of the decay chain. This signature is further complemented by a hard isolated photon if the next-to-LSP (NLSP) is a neutralino, decaying via $\tilde{\chi}_1^0 \rightarrow \gamma + \tilde{G}$, or by a tau in case the NLSP is a $\tilde{\tau}$, decay which is $\tilde{\tau} \rightarrow \tau + \tilde{G}$. Depending on the gravitino mass, the NLSP may appear as a long-lived particle.

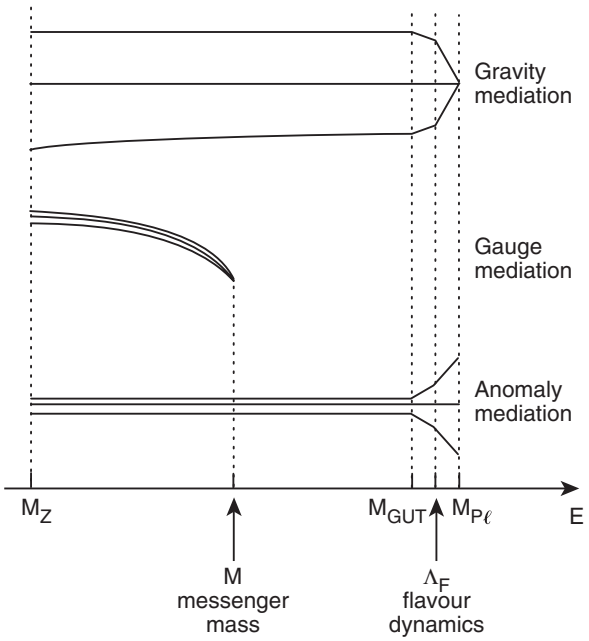

Figure 23. Schematic illustration of the energy dependence of the running squark masses of the three generations for various supersymmetric scenarios (see text). From [168].

In the AMSB scenario, the main signature is also missing energy, similar to the MSUGRA case. But, due to the near degeneracy of the lightest chargino and the neutralino, the dominant chargino decay is $\tilde{W}^{\pm} \rightarrow \pi^{\pm}\tilde{W}^{0}$ with a very soft pion. In a large fraction of the parameter space, the $\tilde{W}^{\pm}$ lifetime is long enough to produce visible decays in the detectors. Also, the degeneracy between the left and right sleptons is typical of AMSB.

Direct searches for SUSY particles if R-parity is violated cannot rely on a missing energy signature, as the LSP will decay, via a R-parity violating coupling, into normal SM particles. Nevertheless, they are recognizable by an anomalously large number of jets and/or leptons in the final state. In some cases, this may still be accompanied by a large missing energy when the decay involves neutrinos.

In conclusion, the various SUSY scenarios correspond to clear but diverse signatures and require very open search strategies to make sure that SUSY particles will not be missed provided their mass is kinematically within the reach of the experiments. At the same time, the diversity of searches for SUSY is such that several of them also cover other non-SUSY channels, related to technicolour, leptoquarks or compositeness. The main emphasis of the experimental searches should be less on models (which are numerous) than on specific topologies.

5.10. On the flavour problem and SUSY

The problem of the MSSM is not only the huge number of parameters (mostly belonging to the SB sector), but the fact that they must be highly fine tuned to match experimental observations on the FCNC processes and CP-violation phenomena.

We have presented in section 5.1 the various implementations of SUSY breaking and we discuss now their main features concerning the flavour problem [168], summarized by figure 23 which schematically illustrates the energy dependence of the running squark masses of the three different generations.

In gravity mediation the soft term sensitivity to ultraviolet physics implies that their flavour structure will retain the effects of any unknown flavour violation at very high energy. Even if we took mass degenerate squarks at $M_{\rm Pl}$, high energy flavour violations would induce large squark splittings, not correlated to Yukawa couplings, at low energy, a situation which is experimentally ruled out because it would induce unacceptably large contributions to Δm_K, ϵ_K, Δm_B, $b \to s\gamma$, $\mu \to e\gamma$, etc. To solve the flavour problem in this context requires the full control of the dynamics even beyond $M_{\rm Pl}$: its solution may lie in the properties of quantum gravity and its flavour symmetries.

However, in gauge mediated models the soft terms are insensitive to the far ultraviolet, above the messenger scale M. If M lies below any new flavour dynamics, then the Yukawa couplings provide the only source of flavour violations, which, in low energy processes, are fully under control.

Similarly, if the soft terms are dominated by the anomaly contribution, the mass relation giving the gaugino masses depends only on low energy coupling constants and makes no reference to the high energy boundary conditions. Although the soft terms are generated at very high energy scales, their RGE trajectories are determined in such a way that the low energy values of the soft terms are specified only by low energy parameters. This is appealing but should not mask the open problems of the AMSB quoted above.

Experiments searching for rare flavour violating or CP violating processes are of great value for discriminating between the above scenarios. In the latter (GMSB or AMSB) which satisfy a super-GIM mechanism, flavour and CP violation originate only from the CKM angles and phases. In the former (gravity mediation) there are necessarily new sources of flavour and CP violation in the symmetry breaking parameters.

Here, going beyond the case of SUSY, one can ask oneself in a more general way what is the minimum flavour violation (MFV) one can expect [168] in any model beyond the SM with non-trivial dynamics at the scale Λ, where Λ is the limit of validity of the corresponding effective theory approach. MFV essentially requires that all flavour and CP violating interactions are linked to the known structure of Yukawa couplings. For an effective theory derived from SUSY, the MFV definition coincides with the usual requirements of SUSY MFV: R-parity conservation, flavour universal soft scalar masses and trilinear terms proportional to the corresponding Yukawa couplings, as we saw in section 3.5. These requirements are not renormalization group invariant and usually taken to hold at a high energy scale Λ, whose value depends on the specific mechanism of SUSY breaking. As we just said, in SUGRA MFV in the soft terms requires that all dynamics up to the gravitational scale must satisfy MFV. The situation improves with GMSB and the problem is bypassed in AMSB.

In the latter, one can expect only moderate deviations from the SM predictions in flavour processes, except from processes which are accidentally suppressed in the SM ($B \to X_s\gamma$, ...), while in the former it is almost unavoidable that new effects appear just behind the present limits. B factories and improved searches for rare decays ($\mu \to e\gamma$, $\mu - e$ conversion) and e and n electric dipole moments will bring valuable information. For a theoretical perspective for SUSY in B-decays, see [169, 170].

FCNC and CP violation in physics involving $b \to s$ transitions still offer opportunities. The discrepancy between the amount of CP violation in the two B_d decay channels $J/\psi K_{\rm S}$ and $\Phi K_{\rm S}$, if confirmed, could be accounted for by the MSSM while respecting all the existing constraints in B physics. Then comes the measurement of ΔM_S. Finding it larger than $20\,{\rm ps}^{-1}$ would hint at new physics. The CP asymmetry in $B \to X_s\gamma$ is of greatest interest. Finally with large amounts of B_S, some processes which are mostly CP conserving in the SM, such as $B_S \to J/\psi\Phi$, can be quite rewarding. The possible impact of low energy measurements will be discussed in the next section.

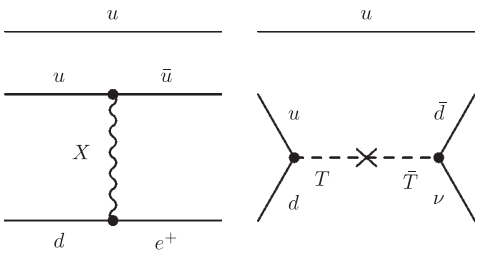

Figure 24. Examples of SM diagrams contributing to proton decay. (left) Dimension 6 t-channel exchange of a heavy gauge boson X. (right) Dimension 5 s-channel exchange of a heavy colour triplet Higgs T. This interaction is a dimension 6 operator, but due to the Higgs exchange, it is multiplied by $1/M_T$ which makes it effectively dimension 5.

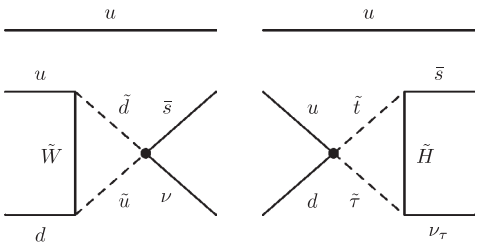

Figure 25. Examples of SUSY diagrams contributing to proton decay. The dot represents a dimension 5 s-channel exchange of a heavy colour triplet higgsino, analogous to the diagram of figure 24.

6. Low energy measurements and SUSY

6.1. SUSY GUT and proton decay

One major result from LEP is the demonstration of the accurate convergence of the three couplings of the SM at $M_{\mathrm{GUT}} \simeq 2 \times 10^{16}$ GeV in the frame of supersymmetry. This revived the interest in SUSY GUTs that, as we alluded to in section 4.3, provide a promising framework for physics beyond the SM. It is naturally expected in any GUT that protons must decay. A rather extensive discussion is found in [171].

Much effort is being put into the evaluation of the proton lifetime in such theories and the estimate of the dominant decay modes. We assume here R-parity conservation and therefore discard the corresponding dimension $d = 4$ operators (the dimension was explained in section 3.3). But operators of dimension $d = 5$, with a coefficient in $(\mathrm{mass})^{-1}$, or of $d = 6$, with a coefficient in $(\mathrm{mass})^{-2}$, may contribute. Examples involving only SM particles are displayed in figure 24. By raising M_X to $\sim 2 \times 10^{16}$ GeV, the SUSY GUT strongly suppresses the gauge-boson mediated $d = 6$ proton decay operators for which $\mathrm{e}^+\pi^0$ would have been the dominant mode. Second, they generate $d = 5$ proton decay operators [172], some examples being shown in figure 25. They are obtained from colour triplet Higgs exchange, which under some assumptions are found to provide the leading mechanism to proton decay, with dominant $\bar{\nu}K^+$ and comparable $\bar{\nu}\pi^+$ modes, and highly suppressed $\mathrm{e}^+\pi^0$, e^+K^0 and μ^+K^0 modes (see [88] for a simple explanation).

In SUSY unified theories based on $SO(10)$ or G (see section 4.3), a new source of $d = 5$ proton decay operators can be considered [173], actually linking proton decay to the masses and mixings of all fermions, including neutrinos.

Table 8. Values of the proton lifetime $\tau(K^+\bar{\nu})$ for a wide range of parameters [174]. Results are shown for the standard $d = 5$ operators, mediated by colour triplet higgsinos, in the MSSM and ESSM (see text) and for new $d = 5$ operators arising in the $G(224) = SU(4)_C \times SU(2)_L \times SU(2)_R$ unification group, related to the Majorana masses of the right-handed neutrinos.

	MSSM std $d = 5$		ESSM std $d = 5$		G(224) New $d = 5$
Parameters	$\tan\beta = 3$	$\tan\beta = 10$	$\tan\beta = 5$	$\tan\beta = 10$	any $\tan\beta$
Nearly central	0.2×10^{32} yr	1.6×10^{30} yr	0.25×10^{34} yr	0.7×10^{33} yr	0.50×10^{33} yr
Intermediate	0.7×10^{32} yr	0.6×10^{31} yr	$1. \times 10^{34}$ yr	2.8×10^{33} yr	$2. \times 10^{33}$ yr
Nearly extreme	0.3×10^{33} yr	2.6×10^{31} yr	$4. \times 10^{34}$ yr	1.1×10^{34} yr	$8. \times 10^{33}$ yr

In plain SUSY $SU(5)$ the inverse decay rate for the $\bar{\nu}K^+$ mode which is dominant is predicted to be less than $\sim 1.2 \times 10^{31}$ yr [174]. The superK preliminary 90% CL bound being [175],

$$\tau(\bar{\nu}K^+) > 1.9 \times 10^{33}\,\text{yr} \tag{99}$$

several authors conclude [176] that **minimal** SUSY $SU(5)$ is already excluded by a large margin.

The embedding of the MSSM in $SO(10)$ [177] is tightly constrained. As an example, an analysis made in the frame of $SO(10)$ [178] with a $U(2) \times U(1)^n$ family symmetry provides a theoretical upper bound

$$\tau(K^+\bar{\nu}) = 4.7 \times 10^{33}\,\text{yr}\left(\frac{0.015\,\text{GeV}^3}{\beta_{\text{lat}}}\right)^2\left(\frac{\tilde{M}_{\text{triplet}}}{8 \times 10^{19}\,\text{GeV}}\right)^2 \tag{100}$$

for $m_0 = 3$ TeV, $m_{1/2} = 175$ GeV and $\tan\beta \sim 54$, where β_{lat} is a strong interaction matrix element obtained from lattice calculations and $\tilde{M}_{\text{triplet}}$ is the effective colour triplet mass (see [171,178] for explanations). With the central estimate for β_{lat} and an exceptionally conservative upper limit for $\tilde{M}_{\text{triplet}}$ the results are barely consistent with the SuperK experimental limit. A representative set of results is presented in table 8 [174]. The MSSM with only standard $d = 5$ operators is nearly ruled out and, even with new operators, is close to the experimental bound. Allowing for an extended variant (ESSM) which introduces two extra vector-like families of quarks and leptons at the TeV scale (to be tested by LHC), the limit obtained is [174]

$$\tau_{\text{proton}} \leqslant (1/3 - 2) \times 10^{34}\,\text{yr} \tag{101}$$

with $\bar{\nu}K^+$ as dominant mode, but possibly μ^+K^0 and $e^+\pi^0$ being prominent.

Most authors agree on the fact that a next generation detector with 5–10 times more sensitivity than SuperK should give access to proton decay if SUSY GUTs are a valid description of nature, see for instance [179]. However, GUT realized in higher dimensions or some field theoretic constructions gives the possibility of evading such a conclusion [180]. Even in the minimal $SO(10)$ model, it is claimed in [181] that one can suppress p decay by a particular choice of Yukawa textures. This illustrates again the versatility of SUSY predictions and its practically unfalsifiable nature. On the other hand, the evidence of a positive signal of proton decay would still be a revolutionary advance in particle physics.

From an experimental side, it is conceivable to gain such an order of magnitude before hitting the irreducible background of atmospheric neutrinos [182]. However, this requires the observation of $\sim$1 megaton of matter and much work is still needed to prove that the background can be kept under control. Possible, although futuristic, solutions have been considered [182, 183], often in liaison with future ν programs. An ICARUS-like technique

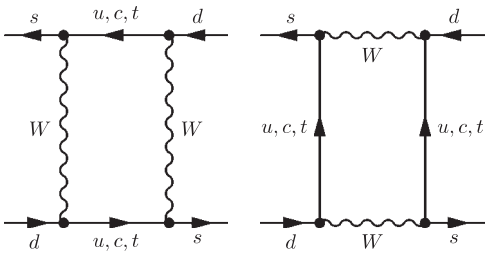

Figure 26. Examples of diagrams contributing to $K^0\bar{K}^0$ oscillations.

[184] using liquid argon may be ideal but the 600 t of a basic ICARUS module are far from the goal. **We cannot emphasize too much the importance of the topic and call for elaborate studies of future possibilities.**

6.2. $K^0\bar{K}^0$ oscillations

It was stated in section 3.5 that a general MSSM124 contains potentially dangerous terms if the GUT scale boundary conditions are non-universal in the generations. It is worth revisiting these arguments in slightly more detail.

The low energy measurement of $K^0\bar{K}^0$ oscillations induce strong bounds on the degeneracy of the squarks of the first two generations. In the SM, the $K^0\bar{K}^0$ oscillations are determined by box diagrams, shown in figure 26, involving the exchange of quarks and Ws. In the MSSM, there are additional contributions from, for example, the exchange of squarks and gluinos. For simplicity, let us consider the first two generations. On the basis where the Yukawa couplings of the d and s quarks are diagonal, there may be non-zero off-diagonal elements, Δ^2, in the mass squared matrix of the $\tilde{d}$ and $\tilde{s}$ squarks. Assuming that the squark masses are nearly degenerate with mass $\tilde{m}$, the existing constraints from Δm_K lead to the bound [69]

$$\frac{\Delta^2}{\tilde{m}^2} < 0.05 \left(\frac{\tilde{m}}{500\,\text{GeV}} \right), \tag{102}$$

and hence the off-diagonal Δ^2 must be small. Even more stringent bounds can be obtained from the $K^0\bar{K}^0$ mixing parameter ϵ_K [69]. This very strong bound can only be fulfilled if the squarks are highly degenerate and can be relaxed if the squarks are heavy. In the MSUGRA framework, this is achieved by assuming that they have a universal mass (and no mixing) at the GUT scale. As the Yukawa couplings of the first two generations are negligible, this degeneracy is preserved when running the masses down to low energy by the RGEs. For the third generation, the Yukawa couplings of the stop and possibly the sbottom (at large $\tan\beta$) affect the running of the mass and break their degeneracy with the first two generations, as seen in figure 12. This mass splitting does not, however, contradict the bound (102). **It is therefore likely that the squarks of the first two generations are quite heavy, while the stop and sbottom could be relatively light**, unless a SuperGIM mechanism is operative.

Bounds also exist on the mass difference for sleptons of the first two families. They are based on the measured limit for the process $\mu \to e\gamma$. This topic is further discussed in section 6.6.

6.3. $b \to s\gamma$ decays

The interest in testing the decay branching ratios of flavour changing neutral current (FCNC) processes, like the $b \to s\gamma$ decay, resides in the fact that such transitions do not

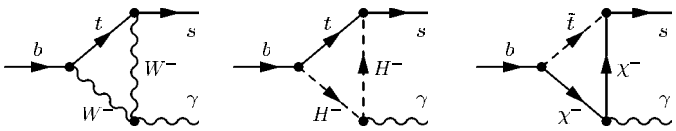

Figure 27. Examples of diagrams contributing to $b \to s\gamma$ decays.

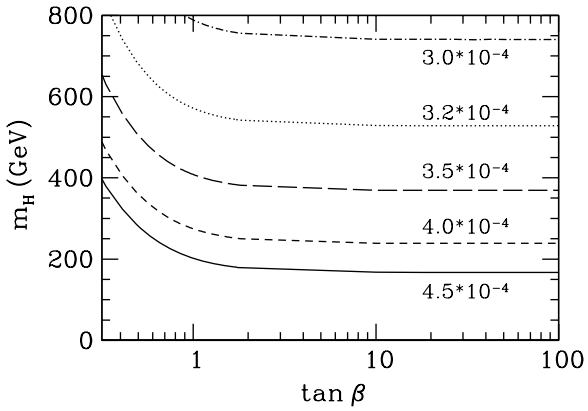

Figure 28. Charged Higgs mass versus $\tan\beta$ for several values of the $b \to s\gamma$ branching ratio, from [189].

exist at tree level in the SM, but can only proceed via loops. This allows, in principle, non-standard contributions to be of size comparable with the standard ones. Some diagrams which could contribute to the $b \to s\gamma$ decay are illustrated in figure 27.

A combination of the measurements of the inclusive branching ratio from ALEPH, BELLE, CLEO, BABAR by the heavy flavour averaging group (HFAG) [185] gives:

$$B(B \to X_s\gamma) = (3.54^{+0.30}_{-0.28}) \cdot 10^{-4}. \tag{103}$$

where the error includes statistical and systematic uncertainties, and contributions from the modelling of the photon spectrum.

6.3.1. Standard model expectation. In the SM this decay is mediated by penguin diagrams, dominated by the first diagram shown in figure 27, with exchange of a top quark. An overview of the steps involved in their calculation can be found in the lecture notes of Buras [186]. The most recent prediction of the branching fraction, including next to leading order (NLO) QCD corrections and QED corrections is [187, 188]

$$B(B \to X_s\gamma) \simeq (3.70 \pm 0.30)10^{-4}, \tag{104}$$

The prediction is in excellent agreement with the experimental result.

6.3.2. Extension with 2 Higgs doublets. In the SM with two Higgs doublets, one coupling to up-type fermions, the other to down-type fermions, (2HDM model II) and in the MSSM, there is an additional contribution from charged Higgses, like the one shown in the second diagram of figure 27. The amplitude contributing is of the same sign as for the $W - t$ loop, hence it increases the branching ratio. The Higgs contribution, which is known to full NLO [189, 190], is a function of $(m_t/m_{H^\pm})^2$ and $\tan\beta$. It decreases slowly with increasing $\tan\beta$ and saturates at $\tan\beta \sim 2$ and it decreases with increasing $m_{H^\pm}$, as shown in figure 28 from Borzumati

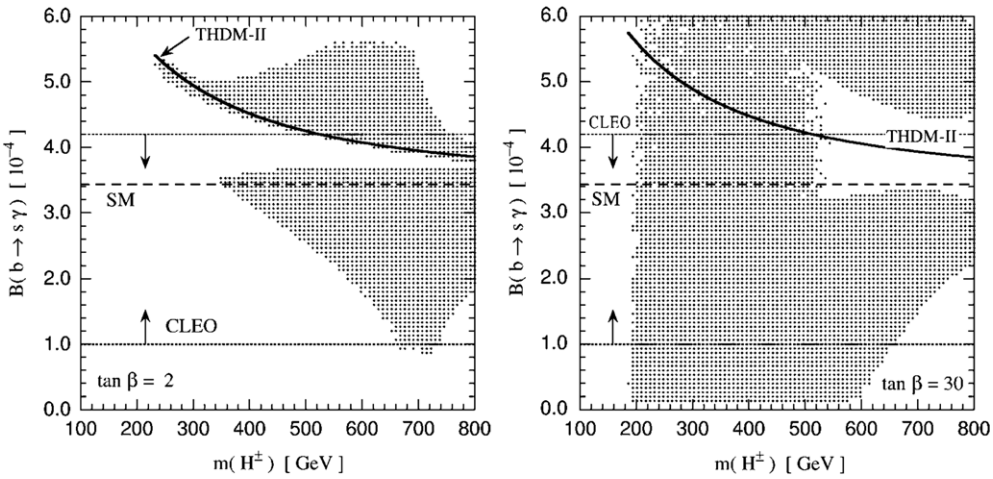

Figure 29. Branching ratio as function of the Higgs mass for the SM, the two Higgs doublet model, SUSY for $\tan\beta = 2$ and 30, reprinted with permission from [193]. Copyright 1998 by the American Physical Society. The darker region corresponds to strict MSUGRA universality conditions. For the lighter region, the Higgs universal mass parameters are allowed to differ from the other universal scalar masses.

and Greub [189]. The figure displays the minimum value of the branching ratio, obtained by varying simultaneously the input parameters within their errors, and is thus meant for establishing exclusions (average values would be about 10% higher).

6.3.3. Supersymmetry. Supersymmetry allows several additional transitions to take place, the dominant one involving a $\chi^- + \tilde{t}$ loop, as in the example of figure 27. The amplitude for a higgsino-like chargino at large $\tan\beta$ is approximately [191, 192]:

$$\propto \mu A_t \tan\beta. \tag{105}$$

Compared with the SM, the amplitude can be of the same sign if the SUSY parameters $\mu \cdot A_t > 0$, add to the effect of the charged Higgs. This case is presently disfavoured. The contribution can have an opposite sign if $\mu \cdot A_t < 0$, practically cancelling the charged Higgs contribution and thus close to (or even lower than) the SM expectation. In the MSUGRA model, the latter is realized for positive values of μ, as A_t tends to be negative at low energies [192]. This situation is illustrated in figure 29 from Goto, Okada and Shimizu [193]. The experimental range and the SM prediction differ from the values quoted in (103) and (104) because they represent the status of 1998. The continuous line corresponds to the two Higgs doublet model. In the left figure, for small $\tan\beta$, the dark area displays the MSSM solutions satisfying the experimental bounds on the SUSY particle masses, together with the assumptions of correct electroweak symmetry breaking and strict MSUGRA scalar mass universality at the GUT scale. For the lighter area, the universality condition is relaxed to a common value for all sparticles and another common value for the Higgs scalars. In the strict MSUGRA case, two branches are singled out. Either the allowed solutions are close to the two Higgs doublet model, hence the SUSY contributions are small due to the heaviness of the superpartners, or they are close to the SM, so that the charged Higgs contribution is cancelled by the SUSY contributions. With the relaxed universality condition, the allowed region is considerably extended. For large $\tan\beta$, the points allowed by the strict and the relaxed universality conditions cover the same area. As the SUSY contribution is proportional to $\tan\beta$, a large range of branching ratios is possible.

Table 9. Rare FCNC decays of b-quarks and s-quarks.

	Branching Ratio	
Decay	SM	Experimental
$b \to s e^+ e^-$	$(68.9 \pm 10.1)10^{-7}$ [196]	$(50 \pm 13)10^{-7}$, HFAG [185]
$b \to s \mu^+ \mu^-$	$(41.5 \pm 7.0)10^{-7}$ [196]	$(45 \pm 10)10^{-7}$, HFAG [185]
$B_s \to \mu^+ \mu^-$	$(3.4 \pm 0.5)10^{-9}$ [198]	$<3.4\,10^{-7}$, CDF+D0 (95% CL) [200]
$K^+ \to \pi^+ \nu \bar{\nu}$	$(7.7 \pm 1.1)10^{-11}$ [201]	$(1.47^{+1.30}_{-0.89})10^{-10}$, E787+E949 [202]
$K^0_L \to \pi^0 \nu \bar{\nu}$	$(2.6 \pm 0.5)10^{-11}$ [201]	$<5.9 \times 10^{-7}$, KTEV (90% CL) [203]
$K^0_L \to \pi^0 e^+ e^-$	$(3.2^{+1.2}_{-0.8}\ 10^{-11}$ [204]	$<2.8 \times 10^{-10}$ KTEV (90% CL) [205]

However, the authors of [194] examined squark–gluino loop effects on the process $b \to s\gamma$ in minimal SUSY with general flavour mixing in the squark sector. Stringent lower bounds on the mass scale of superpartners, which apply in the case of minimal flavour violation (see section 6.7), can be substantially reduced. The case of $\mu < 0$ can also become allowed for small $M_{\rm SUSY}$. One should therefore remember this caveat before drawing too strong conclusions from $b \to s\gamma$.

6.4. Other FCNC decays

Although the $b \to s\gamma$ decay has been the flagship of the rare decays, there are several other rare decays and low energy measurements which can bring valuable cross-checks and constraints on new particles. In the following, some of them will be presented, but without the ambition of being exhaustive. More complete accounts are found in lectures by Buras [186] or Nir [195].

Some of the more promising decays are listed in table 9. Their theoretical estimate is dominated by loop diagrams analogous to the ones of figure 27, with the photon replaced by a Z^0. As these are short distance effects, the estimates are rather accurate. The $b \to s l^+ l^-$ branching ratios have now been computed to NNLO accuracy [187, 196].

The $b \to s l^+ l^-$ branching ratios are more than an order of magnitude smaller than for $b \to s\gamma$, but the B-factories are reaching the sensitivity to test the SM. The preliminary results from BELLE, BABAR and CLEO, combined by the Heavy Flavor Averaging Group, are compatible with the SM expectation.

As an example of the possible effects of SUSY, figure 30 (left) shows the range of the branching ratio for $b \to s\mu^+\mu^-$ as a function of the $b \to s\gamma$ branching ratio at $\tan\beta = 30$ from Goto, Okada and Shimizu [193]. The $b \to s\mu^+\mu^-$ branching ratio is integrated over the lepton invariant mass spectrum below the J/ψ threshold to avoid the resonance peak. For large $\tan\beta$, the dilepton branching ratio can be increased by a factor two with respect to its SM value, even in a strict MSUGRA model. Moreover, when $b \to s\gamma$ has a branching ratio close to the SM expectation, the $b \to s\mu^+\mu^-$ ratio can be high. This occurs when the charged Higgs plus MSSM contribution to $b \to s\gamma$ is opposite to and about twice the SM value. It would indicate a negative value of $A\mu$. For low $\tan\beta$, the effect of SUSY on the dilepton decay width is negligible.

The $B_s \to \mu^+\mu^-$ branching ratio is rather small in the SM, compared with the existing bound from the Tevatron. However, supersymmetric loops involving charged higgsinos can also induce FCNC even in the minimum flavour violation (MFV) scenario through the diagram in figure 31 [207]. The coupling of $\tilde{H}^\pm_u$ to $\bar{s}_L \tilde{t}_R$ is proportional to $y_t V_{ts}$, where V_{ts} is the element of the CKM matrix, and the diagram generates a FCNC interaction $\bar{s}_L b_R H^\dagger_u$, induced solely by the mixing in the CKM matrix and without the need of inter-generational mixing in SUSY

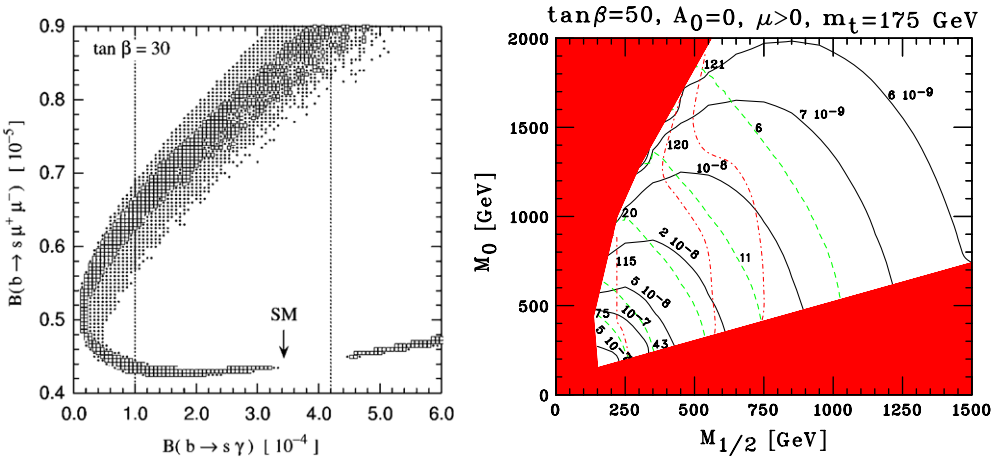

Figure 30. (left) Branching ratio of $b \to s\mu^+\mu^-$ versus $b \to s\gamma$ for the SM and for the MSSM with $\tan\beta = 30$, from [193]. The darker region corresponds to strict MSUGRA universality conditions. For the lighter region, the Higgs universal mass parameters are allowed to differ from the other universal scalar masses. The experimental range and the SM prediction differ from the values quoted in (103) and (104) because they represent the status of 1998. (right) Contour plots of $B_s \to \mu^+\mu^-$ (solid), $a_\mu^{\rm SUSY}$ (dashed) in units of 10^{-10} and light Higgs mass (dot-dashed) in the m_0 versus $m_{1/2}$ plane in the MSUGRA scenario, reprinted with permission from [199]. Copyright 2001 by the American Physical Society.

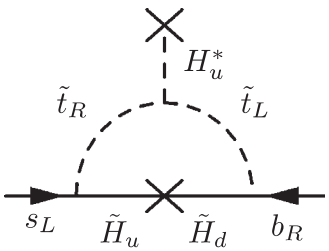

Figure 31. Supersymmetric contribution to $B_s \to \mu^+\mu^-$.

(which is typical of MFV). The contributions from supersymmetry, which are, in the large $\tan\beta$ approximation, proportional to $\tan^6\beta$, can increase its value by several orders of magnitude. They are also inversely proportional to the fourth power of the heavy Higgs mass, m_A^{-4}. The SUSY contribution can be further increased by including diagrams similar to the one in figure 31 where the higgsino is replaced by a gluino. The latter, however, requires inter generational mixing in the SUSY mass matrix (see e.g. [207]). The case of large $\tan\beta$ for a MSUGRA model is illustrated in the $(m_{1/2}, m_0)$ plane in figure 30 (right). Scaling the present Tevatron bound, which is based on $410\,\text{pb}^{-1}$, by the square root of the luminosity yields for $2\,\text{fb}^{-1}$/detector ($15\,\text{fb}^{-1}$/detector) the limits at 95% CL of $1 \times 10^{-7}(4 \times 10^{-8})$. Improvements in the signal selection and background rejection might further decrease these limits by about a factor of 2, which would make this decay accessible in a significant area of the m_0 versus $m_{1/2}$ plane (corresponding roughly to $m_h \lesssim 120\,\text{GeV}$ if $\tan\beta = 50$). In the future, the LHC experiments are expected to probe branching ratios at the level of the SM prediction [208]. Dimuon decays of B_d, which can be searched at B-factories, may also be interesting, but their branching ratios are suppressed relative to B_s by a factor $(V_{td}/V_{ts})^2 < 0.06$. The authors of [207] argue that the observation of an effect may allow a lower limit on $\tan\beta$ to be derived (as a function of m_A)

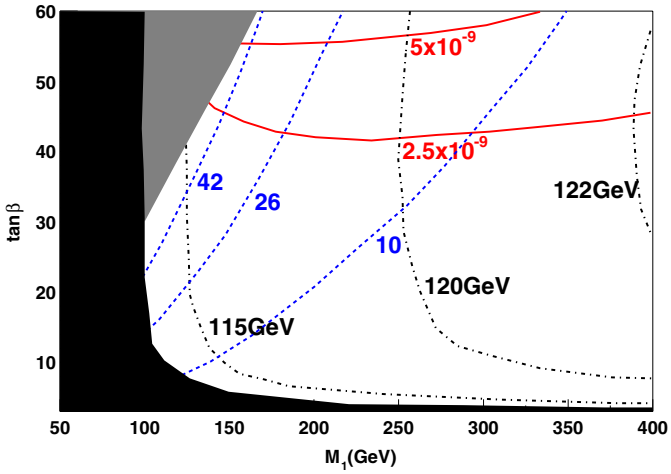

Figure 32. Branching ratio of $B_s \to \mu^+\mu^-$ (solid, red) in the plane tan β versus M_1 for the GMSB scenario with N=1 and $M = 10^6$ GeV, together with $a_\mu^{\rm SUSY}$ (dashed, blue) and light Higgs mass (dot-dashed, black). Reprinted with permission from [211]. Copyright 2002 by the American Physical Society.

and bring valuable information which is not easy to extract from the direct SUSY searches. Figure 30 (right) also displays the SUSY contribution to the anomalous magnetic moment of the muon $a_\mu^{\rm SUSY}$ (see section 6.5). It was pointed out in [199] that a strong correlation exists in the MSUGRA framework between an excess due to SUSY in B($B_s \to \mu^+\mu^-$) and in $a_\mu^{\rm SUSY}$, but it may be weakened in a more general MSSM [209]. A correlation of this branching ratio with the $B_s^0 - \bar{B}_s^0$ mass difference ΔM_s was emphasized in [210]. In [211] this correlation is studied for various SUSY breaking mechanisms. Figure 32 gives the expected contributions in the GMSB scenario. Another, potentially interesting decay mode is $B_s \to \tau^+\tau^-$. As the branching ratio is proportional to m_l^2, it is expected to be two orders of magnitude larger, but suffers from the more difficult detection of taus.

Also for the Kaon decays, large departures from the SM values are possible. The theoretical calculation of the branching ratios listed in table 9 is rather clean [186]. But their values in the SM are exceedingly small and these decays are even more difficult to access experimentally. The 'measurement' of $K^+ \to \pi^+\nu\bar{\nu}$ [202] is based on the observation of two events by E787 at BNL (in 6×10^{12} decays with an estimated background of 0.15 ± 0.05 events) and one more event in the first results of E949, an upgrade of E787. The other limits from KTeV (E799/E832) at Fermilab [203] are several orders of magnitude above the SM expectation. Moreover, a model independent bound from isospin symmetry based on the $B(K^+ \to \pi^+\nu\bar{\nu})$ yields the bound [186] $B(K_L^0 \to \pi^0\nu\bar{\nu}) < 2.6 \times 10^{-9}$ (90% CL), well below the KTeV limit. In the strict MSUGRA scenario, the effects are usually small. But in a relaxed MSSM framework, they may become sizeable (see for instance [212]). It is still difficult to quantify by how much, because some of the largest deviations estimated may not fulfil the constraints imposed by other decays and by CP-violation observables.

Looking into the future, further improvements on the B decays can certainly be expected from the B-factories. Also the sensitivity to $B_s \to \mu^+\mu^-$ is expected to be increased at the LHC to the level of the SM expectation. Concerning the $B(K^+ \to \pi^+\nu\bar{\nu})$, the experiment E949, the upgrade of E787, at Brookhaven was hoping to reach a sensitivity of $\sim 10^{-11}$/event and the experiment CKM (E921) [206], which was approved by Fermilab, was aiming at $\sim 10^{-12}$/event, which should have allowed a measurement of the branching ratio to 10% (100

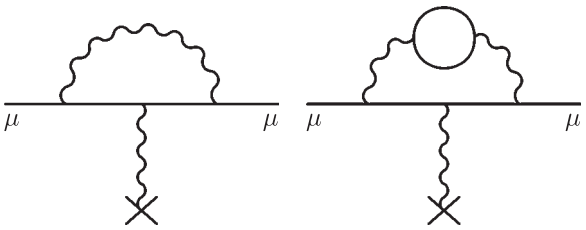

Figure 33. (left) Lowest order diagrams for SM contributions to $g_\mu - 2$. (right) LO hadronic contributions.

signal events on a background of <10). But both experiments were stopped. New proposals are currently being prepared: P940 for Fermilab and an extension of NA48 at CERN, both aiming at taking data in 2009, as well as a letter of intent for an experiment at J-PARC in Japan. For the $B(K_L^0 \to \pi^0 \nu\bar{\nu})$, the KEK experiment E391a, which started taking data in 2004, should reach a sensitivity of $\sim 10^{-10}$/event (and might be upgraded for J-PARC to reach $\sim 3 \times 10^{-13}$/event) and the KOPIO experiment (E926) at Brookhaven expects to reach $\sim 2 \times 10^{-12}$/event.

6.5. $g - 2$ *measurements*

The slight departure of the muon g factor, relating the magnetic moment to the spin, from its canonical Dirac value of 2 is due to the fact that the electromagnetic interaction of a muon and a photon is perturbed by the exchange of one (or more) additional photon(s), as illustrated in figure 33 (left).

After the completion of the CERN measurement some 20 years ago [213], a new measurement of the muon $g - 2$ is taking place at BNL (E821) [214]. It started in 1997 and its most recent results are [215] $a_{\mu^+} \equiv (g_\mu - 2)/2 = 11659204(7)(5) \times 10^{-10}$, based on statistics of about 4 billion μ^+ decays collected in 2000 and [216] $a_{\mu^-} = 11659214(8)(3) \times 10^{-10}$ from μ^- decays collected in 2001. The experimental principle is similar to that of the final CERN experiment and uses the 'magic' momentum of muons for which the precession frequency does not depend on the electric field, which allows the electrostatic quadrupole field to be used for vertical beam focusing. The new result is compatible with and dominates the results based on about 1 billion decays collected in 1999 [217, 218] and with the earlier results, yielding the new world average

$$a_\mu^{\text{exp}} = (11659208.0 \pm 5.8) \times 10^{-10}. \tag{106}$$

From the theoretical point of view, the current status, which is, however, still evolving, is summarized in table 10 (see e.g. [219] for a review). The QED contribution has been evaluated up to 4 loops and includes an estimate of the 5 loop contribution. The electroweak corrections, dominated by exchange of W and Z^0, have a theoretical error that includes an estimate of the higher order contributions, but remains small, anyhow. The hadronic vacuum polarization contribution, shown in figure 33 (right), involves the strong interaction at low energy and thus cannot be computed from first principles. Instead, it is determined from a dispersion integral over the e^+e^- cross-section and is dominated by the energy region $\sqrt{s} \leqslant 1.4\,\text{GeV}$. Several estimates exist in the literature for the LO contribution. They differ by the inputs used (inclusion of τ data, usage of perturbative QCD at higher energies) and/or by the integration method. The most recent LO results, are moderately compatible with each other and the numbers quoted in table 10 correspond to their highest and lowest values obtained. Earlier estimates [228, 229], computed in 2002 before the re-analysis of the e^+e^- cross sections by

Table 10. List of the radiative corrections contributing to a_μ. The value of the total published by Davier *et al* differ slightly from the total value in the table, due to their use of slightly different estimates for the EW or light-by-light contributions. The value of Melnikov *et al* is slightly different from the one in their paper and was quoted in Davier *et al*. All errors have been added in quadrature.

Source	$a_\mu \times 10^{11}$	Remarks
QED	116584719.6 ± 1.4	Kinoshita *et al* [220]
EW	154 ± 2	Czarnecki *et al* [221]
LO hadronic	6934 ± 64	Davier *et al* [222] e^+e^-
	7110 ± 58	Davier *et al* [224] τ decays+CVC
NLO hadronic	-100 ± 6	Alemany+Davier+Höcker [225], Krause [226]
Light-by-light	120 ± 35	Melnikov *et al* [227]
Total a_μ	116591827.6 ± 73.3	using Davier *et al* e^+e^-
	116592003.6 ± 68.0	using Davier *et al* τ decays

CMD-2 [230], showed larger discrepancies, e.g. Hagiwara *et al* [229] found a LO hadronic contribution of $(6831 \pm 62)10^{-11}$ derived from inclusive e^+e^- cross sections. More recent results based on e^+e^- include $(6963 \pm 72)10^{-11}$ from Davier *et al* [224], $(6948 \pm 86)10^{-11}$ from Ghozzi and Jegerlehner [231], $(6996 \pm 89)10^{-11}$ from Ezhela *et al* [223] and $(6935 \pm 59)10^{-11}$ from de Troconiz and Yndurain [232]. They agree with each other and with the value quoted in the table, which also uses new data from the KLOE experiment [233] based on the technique of radiative return. However, this apparent moderate disagreement on a_μ hides much larger incompatibilities between some experimental inputs: between the inclusive e^+e^- cross-section and the sum of exclusive channels in the region $\sqrt{s} = 1.4$–$2\,\mathrm{GeV}$ [229]; between the sum of the $\pi^+\pi^-$ channel in e^+e^- and the expectation from τ decays based on CVC in the region $\sqrt{s} = 0.85$–$1.8\,\mathrm{GeV}$ [224]. More work is needed to understand these differences, which is the reason why we quote the two extreme values in table 10. It was recently argued in [234] that some additional contributions from the putative scalar mesons $\sigma(0.60)$ and $f_0(0.98)$ ought to be included, although this is very controversial.

Another new fact is the re-evaluation in 2002 of the hadronic light-by-light scattering contribution [227], dominated by the $\gamma^*\pi\gamma^*$ interaction, and for which there was previously an error of sign.

After revision of the SM prediction for a_μ, the most recent estimates, taking into account the VEPP CMD-2 e^+e^- results, are shown together with the BNL measurements, in figure 34. The present result is

$$a_\mu^{\mathrm{exp}} - a_\mu^{\mathrm{SM}} = (8 \pm 9) \times 10^{-10} \text{ to } (25 \pm 9) \times 10^{-10} \tag{107}$$

for the two extreme values of the hadronic LO corrections and with all errors added in quadrature. It should be interpreted with care as the dominant errors are systematic. The experimental result is 0.9 to 2.7 σ higher than the SM prediction. Note that the estimate from Hagiwara *et al* [229] in 2002 based on the previous e^+e^- cross sections, compared with the μ^+ measurement, gave $a_\mu^{\mathrm{exp}} - a_\mu^{\mathrm{SM}} = (36 \pm 11) \times 10^{-10}$, hence a $3.3\,\sigma$ effect. It decreased to $2.0\,\sigma$ in 2003 using the updated estimate from Davier *et al* [224] and increased again slightly after the publication of the μ^- results. This shows a clear evolution of the results with time and, before drawing any conclusion, it is wise to let the situation settle.

SUSY, like other sources of new physics, could lead to a discrepancy between experiment and the SM prediction of $g_\mu - 2$ [235, 218]. The basic loop contributions to $g_\mu - 2$ in supersymmetry are given in figure 35. For the CP conserving case, the chargino–sneutrino loop

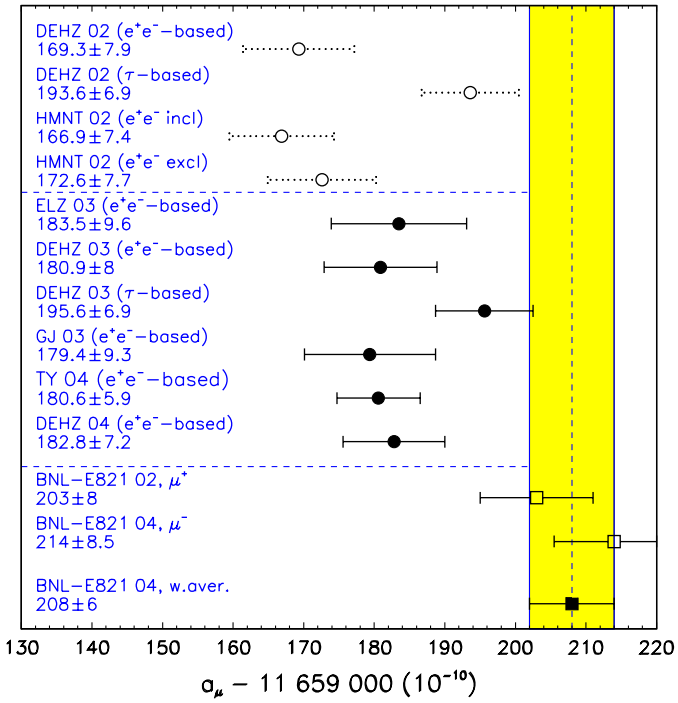

Figure 34. Comparison of the most recent estimates of a_μ and of the measurements [215, 216] by experiment E821. The labels refer to Davier *et al* [228] (DEHZ02), Hagiwara *et al* [229] (HMNT02), Ezhela *et al* [223] (ELZ03), Davier *et al* [224] (DEHZ03), and Ghozzi and Jegerlehner [231] (GJ03), de Troconiz and Yndurain [232] and Davier *et al* (presented by Höcker) [222].

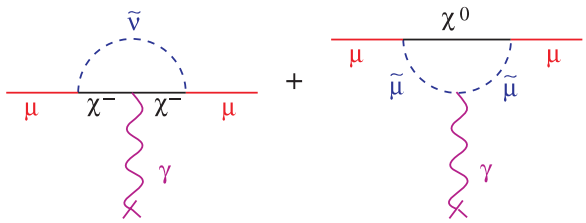

Figure 35. Lowest order diagrams for SUSY contributions to $g_\mu - 2$, from [218].

contribution is usually the largest and its expression for large $\tan\beta$ is approximately [235, 218]

$$a_\mu^{\mathrm{SUSY}} \simeq \frac{\alpha(M_Z)}{8\pi \sin^2\theta_W}\frac{m_\mu^2}{\tilde{m}^2}\tan\beta\,\mathrm{sign}(\mu) \simeq 130\,10^{-11}\left(\frac{100\,\mathrm{GeV}}{\tilde{m}}\right)^2\tan\beta\,\mathrm{sign}(\mu) \qquad (108)$$

(the numerical factor includes a small contribution from neutralino exchange) where $\tilde{m}$ represents a common mass for the contributing SUSY particles (else, it is approximately the heavier mass). Hence, the magnitude of a_μ^{SUSY} is proportional to the square of the muon mass. This shows that the anomalous magnetic moment of a muon is about 40 000 times more sensitive than an electron in new physics. It is also proportional to $\tan\beta$ and its sign is generally the same as the sign of the parameter μ [236]. Some effort in recent years was devoted to the computation of SUSY two-loop effects [237]. In particular the chargino–neutralino two-loop contributions can be important for small $\tilde{m}$ and large $\tan\beta$.

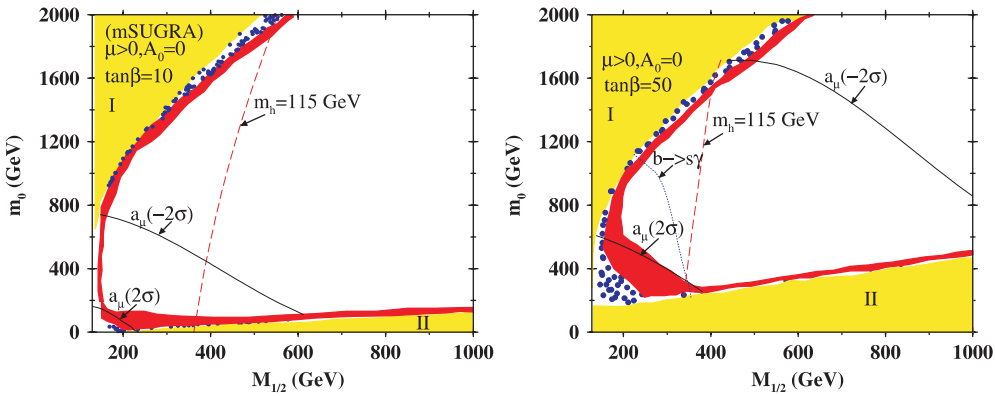

Figure 36. Region in the m_0 versus $m_{1/2}$ plane compatible with the $g_\mu - 2$ measurement, reprinted with permission from [238]. Copyright 2002 by the American Physical Society.

If the difference in equation (107) is attributed to supersymmetry, it implies that negative values of the parameter μ are disfavoured. An analysis in the MSUGRA framework [238] shows that by imposing, for instance, a $2\,\sigma$ constraint, taking as deviation $a_\mu^{\rm exp} - a_\mu^{\rm SM} = (26 \pm 10) \times 10^{-10}$ near the upper value of (107), one can get lower and upper limits in the $m_0 - m_{1/2}$ plane as illustrated by figure 36 in the case of $\tan\beta = 10$ and 50. The light grey (yellow) regions are theoretically disallowed and the dark grey (red) region is cosmologically preferred (see more on this in section 12.2.1). The upper limit on sparticle masses for large $\tan\beta$ is on the borderline of (or exceeds) the reach for LHC. The naive approximation (108) would lead, for $\tan\beta = 50$, to an upper bound on $\tilde{m}$ of about 1.1 TeV, while the MSUGRA analysis finds a limit of ∼2.5 TeV for squarks of the third generation and of ∼3 TeV for gluinos and squarks of the first two generations. This $2\,\sigma$ deviation would correspond to $1\,\sigma$ if the higher SM expectation in (107) had been used. It is also observed in figure 36 that at high $\tan\beta$ the $b \to s\gamma$ decay imposes a strong constraint on the parameter space.

The experiment E821 hopes to obtain more running time, aiming to collect an extra 6 billion events. Their final goal is to reduce the measurement error to $\pm 40 \times 10^{-11}$. It is estimated in [229] that the error on the LO correction can be lowered to about 1×10^{-10}. A third source of information about low energy e^+e^- hadronic states will come in the future from radiative return measurements by B-factories [239] and other low energy colliders. One has however to reach a normalization accuracy of 1% and a mastering of the radiative process [240], which is challenging [241]. In these conditions, it will be important to also lower the (rather conservative) error on the light-by-light scattering contribution in table 10, a result which could be achieved by lattice calculations.

6.6. Lepton flavour violating decays

Lepton flavour violating (LFV) interactions, like $\mu \to e\gamma$ or $\mu - e$ conversion in nuclei have been searched for since the evidence that the muon is a lepton [242]. The strongest experimental bound on $B(\mu \to e\gamma)$ is from the MEGA experiment at LAMPF [243]

$$B(\mu \to e\gamma) < 1.2 \times 10^{-11} \tag{109}$$

at 90% CL.

This process is forbidden in the SM by conservation of the lepton family number. Even with LFV in the neutrino sector, the branching ratio remains exceedingly small [244]. However,

several SUSY models have been proposed in which LFV is strongly enhanced and could occur at experimentally accessible levels. Moreover, the diagrams inducing $\mu \to e\gamma$ decay are closely related to the ones in figure 35 which affect the muon $(g-2)$. Assuming, for example, that the off-diagonal entry $(m^2_{\tilde{l}})_{\tilde{e}\tilde{\mu}}$ between selectron and smuon in the left-handed slepton mass matrix is non-zero, the following approximate relation is obtained [244] from

$$B(\mu \to e\gamma) \simeq 3\,10^{-5} \left(\frac{a_\mu^{\mathrm{SUSY}}}{10^{-9}}\right)^2 \left(\frac{(m^2_{\tilde{l}})_{\tilde{e}\tilde{\mu}}}{\tilde{m}^2}\right)^2 \tag{110}$$

For $a_\mu^{\mathrm{SUSY}} \simeq 10^{-9}$, the present bound would imply $(m^2_{\tilde{l}})_{\tilde{e}\tilde{\mu}}/\tilde{m}^2 \lesssim 6\,10^{-4}$, which already constitutes a serious constraint on model building. Further improvements on the $\mu \to e\gamma$ decay may be expected from the MEG experiment [245] at PSI which has planned to start taking in data in 2006 and aims at a sensitivity of $\sim 10^{-14}$/event.

There is the experiment SINDRUM2 at PSI looking for the $\mu - e$ conversion in nuclei which has set a preliminary limit of $<8 \times 10^{-13}$ at 90% CL for conversion on gold. It is anticipated that this experiment may further improve its sensitivity by at least a factor of 10. A proposal has been submitted at BNL for the MECO experiment (BNL E940) [247] aiming at reaching a sensitivity per event of 2×10^{-17}. In a more distant future, it has been estimated that at a CERN neutrino factory (NUFACT) a sensitivity of $\sim 10^{-19}$/event could be reached [248].

6.7. SUSY and CP violation

The presence of SUSY particles in loop diagrams gives flavour violating contributions, which may or may not involve CP violation. SUSY CP violation in the flavour sector will depend on the way the SUSY induced flavour violating effects are kept under control: universality, heavy squarks, alignment. Only the latter [249] seems to offer the hope of measurable effects. Present data from B-physics are in good agreement with the CKM model, but within the present accuracy they constrain only the squark mass splittings and mixing angles in the gluino couplings. There is presently no evidence from heavy flavour physics for the need of any extra phase, besides the large CKM one which by itself explains phenomena of very different magnitudes ($\epsilon \sim \epsilon'/\epsilon \sim 10^{-3}$, $a_{B\to\psi K_S} \sim 1$).

However, another manifestation of CP violation, the baryon asymmetry of the universe, is a reality and calls for something more beyond MFV: new CP violating sources or new flavour structure beyond the Yukawa matrices [250]. The same will be true if the value of the CP asymmetry of $B \to \phi K_S$ is confirmed since in MFV it should not differ from the $B \to J/\psi K_S$ one. Belle and Babar CP asymmetries in $B \to \phi K_S$ and $B \to \eta' K_S$ indicate a possible deviation from the SM (2.4 and 2.7 σ for Belle and Babar, respectively). It has been proposed that SUSY contributions may explain the result. In [251] it has been shown that EDM constraints (see next section) severely restrict the flavour mixings between second and third generations and provide guidance in the possible interpretations.

More information is needed to go further but none is easy to get: more precise data in B physics, CP violating couplings of Higgs, neutrino physics to determine θ_{13} and possibly CP violation. A major input will be the confirmation or refutation of electroweak baryogenesis (m_h at the edge of discovery and light stop). If however it is refuted and if the CP phase responsible for the baryon asymmetry is connected to phases in the heavy Majorana neutrinos sector, it may be unfortunately difficult to relate them to possible low energy CP violating phenomena in the neutrino sector, through ν oscillations or $0\nu\beta\beta$ decay.

6.8. Electric dipole moments (EDM)

Electric dipole moments (EDM), defined for a fermion as

$$\mathcal{L} = -\frac{i}{2} \mathrm{d}_f \bar{f} \sigma_{\mu\nu} \gamma_5 f F^{\mu\nu} \tag{111}$$

violate parity (P) and time reversal (T) and are hence a signature of CP violation, under the assumption of conservation of CPT. They are due to loop diagrams similar to those contributing to $g-2$. In the SM, at 1-loop level, amplitudes are real and EDM appear only at the 3-loop level. They are expected to be many orders of magnitude smaller than the foreseeable experimental sensitivity. A measurable value would therefore be a clear sign of CP violation beyond the CKM phase.

New physics contributes to the $(g-2)$ and EDM via operators which are closely related, e.g. the loops of figure 35 in the case of supersymmetry, involving gluino, chargino and neutralino exchange. The SUSY contribution to the electron EDM is due to 1-loop chargino and neutralino exchange. To the EDMs of quarks one should add 1-loop gluino exchange and 2-loop gluino–quark–squark diagrams. Considering the neutron EDM, assumptions about the neutron structure are necessary to express it in terms of quark EDMs. The chiral quark model, the parton quark model, QCD sum rules and the chiral Lagrangian approach [252] give different relationships between the neutron and quark EDMs, in particular concerning the contribution of the s-quark. The quark EDMs themselves may receive contributions from electric and chromoelectric dipole operators and the Weinberg three-gluon operator. Gluino, chargino and neutralino are involved.

In SUSY models there are many new CP violating phases beyond δ_{CKM}. But in MSUGRA only two of these are physical: Φ_A, related to the relative phase between the A-terms and the gaugino mass terms, and Φ_μ, related to the relative phase between the μ-term and the B-term. The problem is to keep the SUSY CP violating induced effects below the limits presently existing. For instance, the neutron EDM is expected to be [249]

$$d_n \sim 300 \left(\frac{100\,\mathrm{GeV}}{\tilde{m}} \right)^2 \sin\Phi\, 6.3 \times 10^{-26}\, e \cdot \mathrm{cm}, \tag{112}$$

where $\tilde{m}$ is a typical spartner mass and Φ a CP violating phase in the SUSY breaking terms. So, unless $\tilde{m}$ is very large this crude formula shows that the present limits on EDMs (and *a fortiori* the foreseen ones) *a priori* put very strong constraints on the phases.

No EDMs have yet been found yet. The experimental limits are

$$\begin{aligned} |d_n| &< 6.3 \times 10^{-26}\, e \cdot \mathrm{cm}\ (90\%\mathrm{CL}) \\ |d_\mathrm{e}| &< 1.6 \times 10^{-27}\, e \cdot \mathrm{cm}\ (90\%\mathrm{CL}) \\ |d_{\mathrm{Hg}}| &< 2.1 \times 10^{-28}\, e \cdot \mathrm{cm}\ (90\%\mathrm{CL}) \end{aligned} \tag{113}$$

where the bound on d_n is from [253], on d_e, obtained from atomic thallium, from [254] and on d_{Hg} from [255]. Experiments using ultra cold neutrons and new techniques are planned to gain 2 to 3 orders of magnitude on the latter [256].

The only limit from a dedicated search for a permanent muon EDM available is still the 1979 result of the CERN experiment [213].

$$d_\mu = (3.7 \pm 3.4) 10^{-19} e \cdot \mathrm{cm}. \tag{114}$$

It has been emphasized in [257] that the BNL experiment E821 measuring the spin precession frequency of the muon is sensitive to both the anomalous magnetic moment and the muon EDM. The excess observed could be partly or entirely attributed to the EDM and provides in fact the most stringent bound which, for the largest deviation in equation (107) would be

$d_\mu < 3.4 \times 10^{-19}\, e\cdot$ cm at the 2σ level. This motivates more sensitive searches for the muon EDM, like the proposed new experiment at BNL [258], aiming at a sensitivity of $10^{-24}\, e\cdot$ cm, or the NUFACT proposal for a neutrino factory [259] at CERN, which quotes a sensitivity of $5 \times 10^{-26}\, e\cdot$ cm.

In most models, the lepton EDMs scale, i.e. are proportional to the lepton mass. The current measurement of the electron EDM [260] $d_e = (0.69 \pm 0.74)10^{-27} e\cdot$ cm, which gives a 95% CL upper bound of $d_e < 1.9 \times 10^{-27} e\cdot$ cm, implies that $d_\mu < 3.9 \times 10^{-25} e\cdot$ cm under the hypothesis of scaling. This is beyond the sensitivity of the BNL experiment.

A priori the SUSY phases are strongly constrained by the above limits. In SUSY models the EDM can be suppressed by the following.

1. Small SUSY CP-phases ($\leqslant 10^{-2}$). This can be motivated by approximate CP-symmetry which also implies that the CKM phase is small.
2. Heavy SUSY sfermions of the first two generations. This is hard to realize without much fine tuning, as done in split supersymmetry, see section 5.3.4. For instance in a MSUGRA model with maximal CP phases the EDM constraints require m_0 to be around 10 TeV, which is very unnatural.
3. EDM cancellations between the chargino and neutralino loops [261]. These are still possible in MSUGRA, but require small Φ_μ and suppressed $|A|$, i.e. one is back to small phases.
4. Flavour off-diagonal CP violation. This allows for significant SUSY effects in B and K physics [262, 250].

The first and fourth options are the most attractive ways to avoid overproduction of the EDMs in SUSY models. With the inclusion of non-universalities, it is found [257] that non-degeneracy of selectron and smuon masses or flavour violation at a level still acceptable by the current limits may enhance the muon EDM to values $d_\mu \sim 10^{-22} e\cdot$ cm, observable by the proposed BNL experiment.

6.9. Atomic parity violation (APV)

Parity non conservation in atomic cesium ^{133}Cs, a field pionneered by Bouchiat and Bouchiat [263], has been measured at Boulder [264] with an uncertainty of ∼0.6%. In such measurements, one determines a parity violating signal $E_{\rm PNC}$

$$E_{\rm PNC} = K_{\rm PNC} Q_W \tag{115}$$

The parameter $K_{\rm PNC}$ multiplying the weak charge Q_W needs sophisticated atomic-structure calculations and its accuracy remains the limiting factor of the determination of the weak charge.

In the past it was claimed that the caesium weak charge differs from the SM expectation [264]. Several improved theoretical calculations [265] suggest on the contrary that the agreement is correct. Taking at face value the claim of [264], the SM prediction of $Q_W^{\rm SM}$ would be larger than the experimental value $Q_W^{\rm exp}$

$$(Q_W^{\rm exp} - Q_W^{\rm SM})/Q_W^{\rm SM} = -0.016 \pm 0.006, \tag{116}$$

and one can speculate at what new physics could cause the discrepancy. For the sake of illustration of the power of APV, for instance in scenarios with extra neutral gauge bosons, the bounds obtained [266] on a Z' would then be $630 \leqslant M_{Z'} \leqslant 1470$ GeV, where the lower bound is from the Tevatron [267]. But with the new status of the theory giving

$$(Q_W^{\rm exp} - Q_W^{\rm SM})/Q_W^{\rm SM} = -0.005 \pm 0.007 \tag{117}$$

the authors of [268] show the present lower limits on various types of Z' and compare them to the LEP and Tevatron bounds. For example, the 95% CL lower limits on a Z' in a left–right model are 665 GeV from APV, compared with 630 GeV (804 GeV) from CDF (LEP); in a sequential SM they are 1010 GeV from APV and 690 GeV (1787 GeV) from CDF (LEP).

These are of the same order, which illustrates the power of APV. However in the future direct searches at the LHC will be much more performant.

If one focuses only on APV and in case of a discrepancy, it is clear that SUSY is not the first kind of new physics to be suspected. But at the same time, measurements of superallowed nuclear Fermi β-decay provide the most precise measurement of V_{ud} and an averaging over several decays gave [269]

$$(|V_{ud}|^2_{exp} - |V_{ud}|^2_{SM})/|V_{ud}|^2_{SM} = -0.0029 \pm 0.0014, \tag{118}$$

where a discrepancy seemed to appear. While an additional neutral weak gauge boson could be the culprit behind an APV deviation [266], it would not help to account for the β-decay result.

In reference [269], it had been shown that in extensions of the MSSM having R-parity violation, there exists a small but non-vanishing region of the parameter space of couplings and sfermions masses which may account for both. Observable consequences in other processes were deduced. However V_{ud} was estimated assuming the unitarity of the CKM triangle applied to its first line, taking V_{us} from the existing data. It appeared later that the culprit of this apparent discrepancy was V_{us} [270] rather than V_{ud}. One can therefore consider the problem as solved.

Clearly, a new independent measurement of APV in caesium or francium with an error at the level of Boulder would be interesting. However, to be competitive in the LHC era, the APV programme should now aim at errors at the per mille level. Since the final publication of Boulder results on Cs [264], the Cs activity has been ongoing in LKB (Laboratoire Kastler Brossel at Ecole Normale Supérieure) with a different approach [271]. The present activities and ideas for the future of APV are described in [272]. In particular, programmes involving francium are under investigation [273, 272]. In this field as well, theoretical activity is crucial and abundant. In [274] it is shown that a comparison of the weak charges of the electron and the proton, obtained from fixed-target parity violating electron scattering experiments, can reveal the effect of SUSY loop contributions and help distinguish between different SUSY scenarios.

6.10. LEP/SLC precision measurements

A wealth of electroweak observables have been measured with very high accuracy, by the e^+e^- experiments on the Z^0 resonance at LEP and SLC, as well as up to 208 GeV at LEP2. The theoretical expectations have been computed in the framework of the SM, including quantum corrections, and are generally found to be in good agreement with the measurements combined by the LEPEWWG [275] (see also [276]), as summarized in figure 37 (left) by the pulls (in absolute value) on the individual observables. The pull for observable 'x' is defined as $(x_m - x_f)/\sigma$, where x_m is the measured value, x_f the fitted one and σ the experimental error. A pull of +2.9 is, however, found for the νN neutral to charged current cross section ratio from NuTeV [277]. The fit including all data has a χ^2/d.o.f. = 25.4/15, i.e. a rather low probability of 4.5%, but improves to 16.7/14 (28%) without the NuTeV result. Only two observables, $A_{FB}(b)$ and $A_l(SLD)$ are slightly above the 2 sd level, indicating that none of the measurements is really anomalous. We will see in section 8.1 that their 2.8σ disagreement is nevertheless embarrassing concerning the Higgs mass. A similar fit was made recently by [278], who do not include the NuTeV result but do include the measurements of $g_\mu - 2$ and of $B \to X_s\gamma$, with the results shown in figure 37 (right). The obtained χ^2 probablility

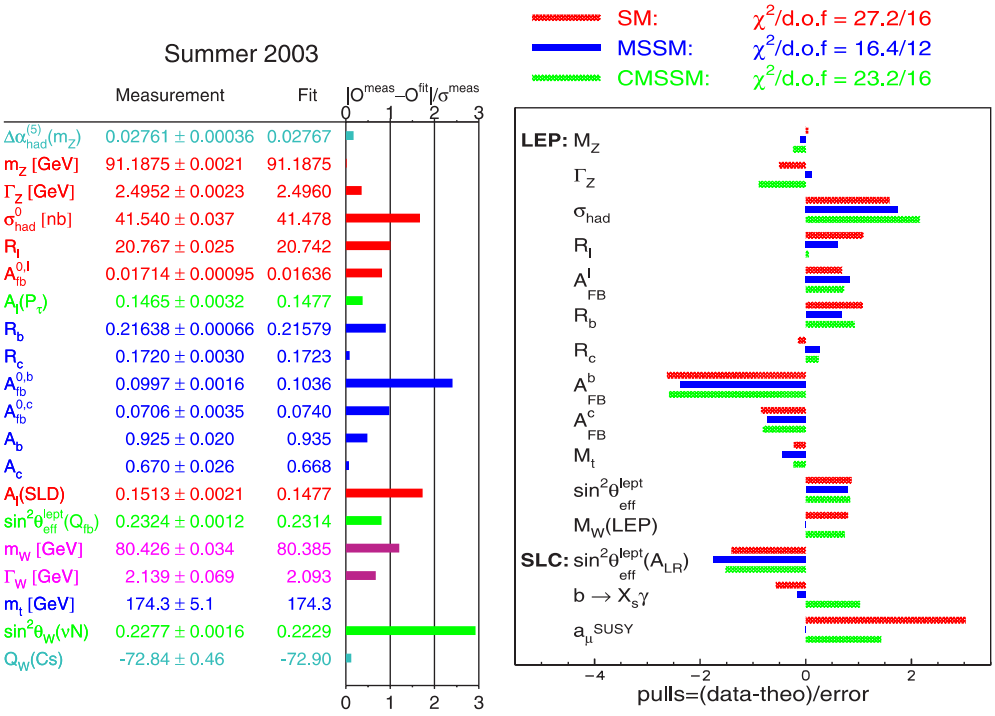

Figure 37. Results from a fit to the electroweak observables. (left) Fit to the SM by the LEPEWWG [275]. (right) Fit to the SM, to the MSSM and to CMSUGRA (called CMSSM on the figure) reprinted from [278]. Copyright 2004, with permission from Elsevier.

is not very good (∼5%), largely due to the inclusion of $g_\mu - 2$, for which the authors use the deviation $\Delta a_\mu = (339 \pm 112) \cdot 10^{-11}$. Apart from this, their results are nearly the same as the ones from the LEPEWWG.

The expectations from the SM are modified by the inclusion of the superpartners in the loop corrections and the question arises whether the achieved precision is sufficient to allow sensitivity to such deviations, given the existing lower bounds on sparticle masses from direct searches.

A second fit was made by [278] in the framework of a MSSM with the GUT universality assumption for M_1 and M_2, a common GUT mass for the sleptons, one for the stop and one for the other squarks. The results of the fit are also shown in figure 37 (right). The resulting χ^2 is reduced compared with the SM fit, mainly from a better agreement for a_μ, but also the number of degrees of freedom is smaller and the fit probability is not improved much (18% versus 5% for the SM).

Finally a fit was made in the MSUGRA framework (labelled CMSSM) with universality of the gauge and the scalar masses at the GUT scale and radiative electroweak symmetry breaking. The χ^2 increases, compared with the MSSM fit, but the probability remains similar due to the increase in the number of degrees of freedom.

The allowed departures with respect to the SM are found to be small in all cases, less than one standard deviation. Moreover, the figures do not show the correlations between observables in the fit. For example, bringing $A_{\rm FB}(b)$ closer to its measured value would lead to a worse value for R_b. The conclusion is that, **at the existing level of precision, the observables show little sensitivity to the SUSY particles beyond the limits of direct searches and that the**

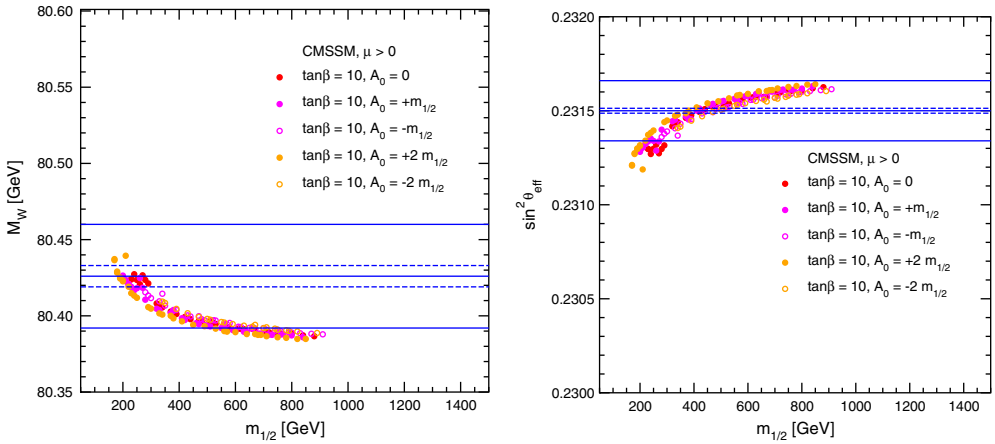

Figure 38. MSUGRA+WMAP prediction for the electroweak observables as a function of $m_{1/2}$. (left) For M_W, (right) for $\sin^2\theta_W$, from [281].

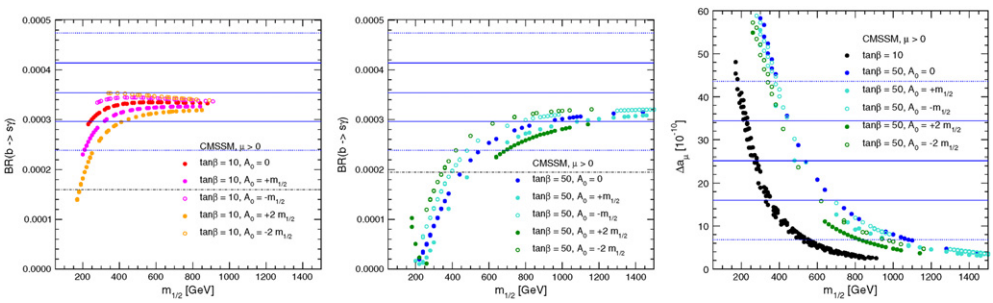

Figure 39. MSUGRA+WMAP prediction for $BR(b \to s\gamma)$ at $\tan\beta = 10$ (left), $\tan\beta = 50$ (centre) and (right) a_μ as a function of $m_{1/2}$, from [281].

SUSY models do not improve the fit quality over the SM. The same conclusion was reached previously from a similar fit to the LEP/SLC data of 1998 [279]. An exception is the $b \to s\gamma$ branching ratio which, for the SUSY parameter $\mu > 0$, allows strong constraints to be put on the MSSM spectrum. These have been discussed in section 6.3. Allowing both signs of μ, a small portion of the SUSY parameter space, e.g. in the $m_{1/2}$ versus m_0 plane, can nevertheless be excluded [280] and Erler and Pierce [279] conclude that the mass of the CP-odd Higgs has to be larger than 150 GeV, which would imply that h^0 is always very much SM-like.

Another analysis of the constraints was carried out [281] under the assumption of MSUGRA with the additional constraint that the relic density in the universe, measured by WMAP, is constituted by the LSP (see more details in section 12.2.1). The allowed parameter space is then shrunk to narrow lines in the m_0 versus $m_{1/2}$ plane for fixed $\tan\beta$, sign(μ) and A_0, enabling m_0 to be expressed as a function of $m_{1/2}$. Figure 38 displays the allowed values of M_W (left) and of $\sin^2\theta_W$ (right) versus $m_{1/2}$ for various values of A_0 and fixed $\tan\beta = 10$, $\mu > 0$. The horizontal full lines show the present central value and the $\pm 1\,\sigma$ band from the electroweak measurements. The narrow regions delimited by dashed lines are projections into the future, assuming improved measurements of the electroweak parameters [281]. At the present level of accuracy they favour a range of $m_{1/2}$ from 300 to 600 GeV at the $1-\sigma$ level, but all values of $m_{1/2}$ are allowed at the 90% confidence level. Similar plots are shown for the $BR(b \to s\gamma)$ and $a_\mu = (g-2)_\mu$ (using $\Delta a_\mu = (25.2 \pm 9.2)10^{-10}$) in figure 39.

The dotted lines show the $2-\sigma$ range. The dash-dotted lines for $BR(b \to s\gamma)$ is the 95% CL exclusion taking into account the experimental errors and the uncertainty existing in the SUSY loop calculation. The constraint from $BR(b \to s\gamma)$ imposes a lower bound on $m_{1/2}$ for $\tan\beta = 50$, but allows all values of $m_{1/2}$ for $\tan\beta = 10$. The 'discrepancy' on a_μ again favours the range $m_{1/2} \sim 200$–$400\,\text{GeV}$ when $\tan\beta = 10$, which shifts to 400 to 800 GeV for $\tan\beta = 50$. But, as emphasized in section 6.5, the latter has to be interpretaed with care. Finally, a least squares fit was performed including all constraints, showing a preference for $m_{1/2} \sim 300\,\text{GeV}$ and negative A_0 when $\tan\beta = 10$. However, the increase of the χ^2 with increasing $m_{1/2}$ is dominated by the a_μ constraint. For $\tan\beta = 50$, the preferred value of $m_{1/2}$ is about 200–300 GeV higher and A_0 remains negative. In consequence, the best fit values at $\tan\beta = 10(50)$ for the LSP and the $\tilde{\tau}_1$ are $\sim$100(250) GeV, for the $\tilde{\chi}_2^0$ and $\tilde{\chi}_1^\pm$ around 200(400) GeV, the squarks around 600(1000) GeV, except the $\tilde{t}_1$ which is expected around 500(900) GeV (with a significant dependence on A_0). It also leads to $m_A \gtrsim 300(400)\,\text{GeV}$, confirming the result of [279].

In the LEP/SLC results one may however underline the discrepancy between the two most accurate measurements of $\sin^2\theta_W$, from A_{FB}^b and A_{LR}, and play various games around that fact. For instance, discarding the former one gets an embarrassingly light Higgs, well below the LEP direct lower limit. The authors of [282] find then that the inclusion of light superpartners at the limit of LEP direct exclusion could improve the situation. However, by including LEP2 results it goes the other way around [283].

Conclusion. in spite of the attractivemess of accurate measurements and the successful and spectacular prediction of the top mass by LEP (see figure 1), one is forced to admit that they are not a panacea. Low energy measurements like $g-2$ or B rare decay, except $b \to s\gamma$, have not yet reached the required sensitivity and still suffer from various ambiguities. Even if disagreements with the SM are established, identifying the physics responsible may be difficult, unless a typical pattern emerges. As for the LEP/SLC electroweak observables, although they seem to indicate a light Higgs, they do not offer much information about SUSY, which by construction is mimicking closely the SM and could still be close to the limit without being noticed. **The conclusion is that nothing can replace a direct exploration of the phenomena.**

7. Machines and programs involved

7.1. Accelerator experiments

The majority of the results on searches for new particles were obtained by the experiments at LEP (Aleph, Delphi, L3 and Opal), at the Tevatron (CDF and D0) and at HERA (H1 and Zeus). The main parameters affecting the reach for searches, the centre-of-mass energy and the integrated luminosity recorded by the experiments, are (approximately) summarized in table 11. The results presented below are based on these data. Further improvements can be expected in the near future, from the following approved projects.

- **Tevatron** has increased its energy to 2 TeV. The aim was to accumulate in run II 2–3 fb^{-1} by the end of 2004, a factor of 20 increase over the present integrated luminosity. A further increase in luminosity by a factor of 10 could yield up to 5 fb^{-1} per year and per experiment. The Tevatron collider run II began in March 2001 after several major changes were made, in particular the construction of the main injector and of the recycler ring.
  Actually, progress has been slower than expected, as can be seen from figure 40. The luminosity in June 04 was $\sim$ a quarter of the run II design (7×10^{31} instead of 29×10^{31}),

Table 11. High energy machines contributing to searches.

Machine	Reaction	Experiment	$\sqrt{s}$, GeV	pb^{-1}/exp
LEP	e^+e^-	ADLO		
		1989–95	91	150
		1995–97	130–183	80
		1998	189	175
		1999	192–202	230
		2000	204–208	215
Tevatron (run I)	$\bar{p}p$	CDF, D0	1800	110
HERA	$e^{\pm}p$	Zeus, H1		
		1993–97	300	50
		1998–00	318	83

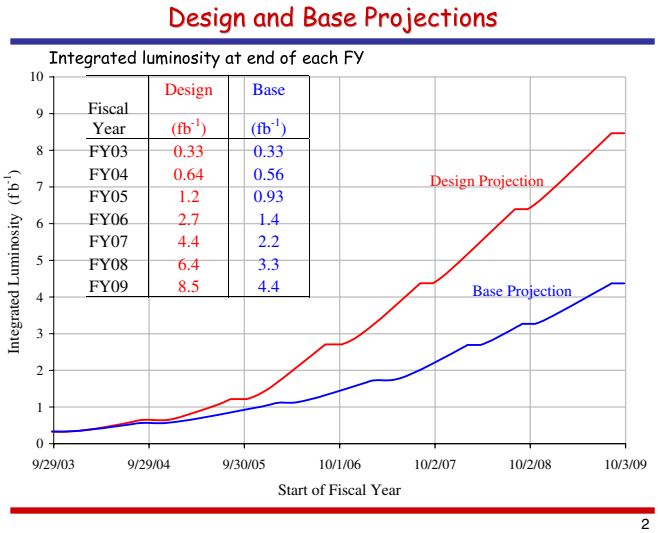

Figure 40. Tevatron projection of integrated luminosity until 2009, From [284].

with 550 pb^{-1} integrated luminosity registered. The rate of antiprotons is still low and has to improve. As a base projection for 2007 one could gain a factor ∼2.5 on the luminosity per week, giving ∼4.4 fb^{-1} accumulated by 2009. The DOE review panel views this goal as having a good probability of being met or even exceeded [284]. But meeting the design goal of 8.5 fb^{-1} by the end of 2009 remains very challenging.

- **HERA I** (1992–2000) has delivered ∼190 pb^{-1} of which ∼140 pb^{-1} was collected by the experiments (e.g. ZEUS). A shutdown for HERA II started in autumn 2000. After delays due to a high level of background, the programme has restarted and from 2003 to March 2005 an additional ∼120 pb^{-1} was delivered by the machine (see figure 41), from which ∼70 pb^{-1} was collected by ZEUS. The programme should continue up to ∼2007 at the same e+p energy of 27.5 + 920 GeV with the hope of accumulating about 1 fb^{-1}/exp, giving thus a factor ∼5 increase in luminosity. Moreover, the electron beam will be polarized ($P_e \simeq 0.6$–0.7).
- **LHC**, planned to start in 2007, should run at 14 TeV and expects to collect ∼10 fb^{-1}/year for the first 2–3 years, after which a high luminosity phase with ∼100 fb^{-1}/year would follow, yielding a total of up to 300 fb^{-1} per experiment.

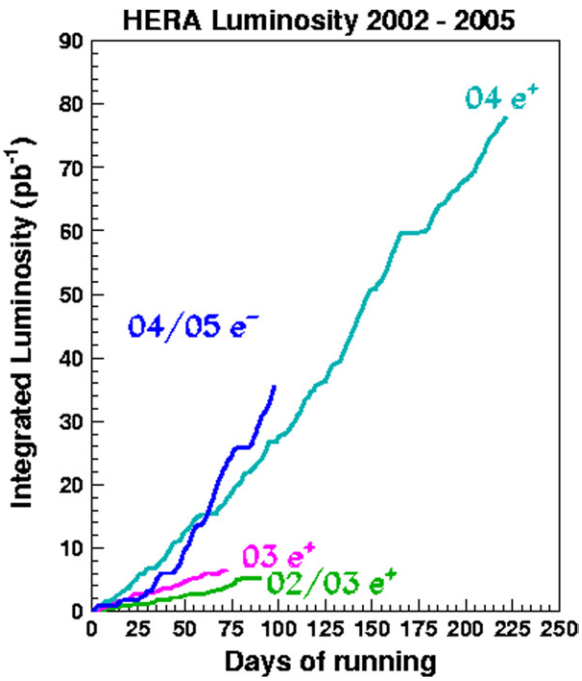

Figure 41. Hera integrated luminosity, from [285].

One should point out, as a general remark, valid for all evaluations of sensitivities, that 100 fb^{-1}/yr, for instance, means 10^{34} times 10^7 second, namely the nominal luminosity during $\sim$ 4 months. **With such an estimate, LEP for instance should have registered $\sim\pi$ times more integrated luminosity than it did.**

The challenge of LHC is well known. LHC will collide 7 TeV protons, providing parton collisions in the TeV CM region. The interesting cross-sections scaling as $1/E^2$, one will need 100 times more luminosity than at LEP, i.e. $10^{34}\,\text{cm}^{-2}\,\text{s}^{-1}$. To achieve that, proton bunches will encounter every 25 ns (nearly 1000 times more frequent than LEP bunches did). Per crossing $\sim$20 interactions will occur, giving overall 10^9 interactions per second (at LEP1 one had 1 Z^0 every 3 seconds and, with Bhabhas, this represented a large fraction of the total rate). To cope with the high level of irradiation (up to 100 Mrad), to keep the detector occupancy at an acceptable level, to achieve the trigger selectivity (10^{-7}) and to deal with the flux of information ($\sim$1 Tbyte/day), one must build for LHC quite sophisticated detectors with a large number of channels (tens of millions for tracking) and involving many forefront technologies. This challenging situation already makes LHC a very interesting project. An impressive amount of R&D has been completed in the last decade. LHC success also relies heavily on the steady progress of several technologies in the surrounding industrial world. The comparison with the 'easiness' of LEP physics is impressive. However several other programs (Tevatron, B factories, fixed target experiments,..) have already been successful in quite challenging conditions.

LHC upgrades. Several possible upgrades of the LHC have already been contemplated [286]. The first one concerns a further increase in luminosity from $\sim 10^{34}$ to $\sim 10^{35}\text{cm}^{-2}\,\text{s}^{-1}$, which

could be envisaged at the earliest for ∼2012. *A priori* this seems to require only modest changes to the machine: increasing the crossing angle by $\sqrt{2}$ for half the nominal β^* to keep the same small contribution of long-range collisions to the beam–beam effect, increasing the bunch number (one every 12.5 ns) and population up to the ultimate intensity (1.7×10^{11} protons per bunch), upgrading the injectors to deliver beams with higher brilliance and halving the bunch length. This would provide $\sim 4.7 \times 10^{34}\,\mathrm{cm}^{-2}\,\mathrm{s}^{-1}$. Considerable hardware changes in the injectors, to increase the brilliance and inject at higher energy, would allow for further steps. One should not underestimate the difficulties of this upgrade, actually an 'upgrade of an upgrade', and the question marks are still open: can one really stand a bunch separation of 12.5 ns? Could the shorter luminosity lifetime reduce the expected gain? What about the activation level of the central part of the detector? And major detector upgrades would be needed to fully benefit from the luminosity upgrade as discussed below.

Another possibility considered is to increase the LHC energy. This case is less demanding on the experiment side, but a strong R&D program on new magnets (niobium–tin) and a complete rebuilding of the machine would be necessary, which implies a big investment, a very long shutdown and therefore a substantial disruption of the physics programme. It is unrealistic to consider that this could happen in the near future.

Future machines. In a more distant future the next step is to be expected from projects under discussion, like a sub TeV e^+e^- linear collider or, even further away, a multi-TeV version of it, a muon collider or a VLHC. A summary of the current situation has been presented in [287]. **None of these should be decided before seing the first solid LHC results, meanwhile vital R&D programmes should be pursued vigorously.**

Electron colliders. An important physics community is evaluating the physics potential and performing hardware tests in view of building a linear e^+e^- collider (LC). The machine parameters are summarized in figure 42. Two kinds of LC are presently considered, on different time-scales: a ∼500 GeV version, which may be extendable to the TeV region (ILC for International Linear Collider), and CLIC which is considered as a genuine multi-TeV collider (3 TeV CM energy, maybe 5 TeV at the end of its possible expansion). In the former version, one can contrast the supraconducting design of TESLA [288] to the warm versions of JLC [289] and NLC [290]. The beam time structures are quite different, although all of these machines will collide on the order of 10 000 bunches per second with $\sim 10^{10}$ particles per bunch. All of them have to realize collisions of bunches having a vertical size of one to a few nanometres and the issue of alignment and stability is a key one. Among other important points, one can say the folowing.

- TESLA depends much on the performances of the SC RF cavities, working at 1.3 GHz, hence of smaller size than LEP ones. Accelerating fields with beams of $\sim 22.4\,\mathrm{MV\,m}^{-1}$ have been achieved, and $25\,\mathrm{MV\,m}^{-1}$ have been measured in the cryostats without couplers. Further improvements have shown that $35\,\mathrm{MV\,m}^{-1}$, as required for 800 GeV operation, can be obtained. The time structure of the TESLA beam with its long pulses and large spacing between bunches is quite favourable from the detector side. TESLA has submitted a TDR [288] in 2001.
- The JLC and NLC, aiming at 500 GeV, later possibly 1 TeV, use a higher frequency (11.4 GHz) and higher gradient in normal conducting structures. They depend greatly on the performances of their numerous (several thousand) klystrons which must reach 75 MW for a couple of microseconds. The use of periodic permanent magnet focusing, instead of a solenoid, to decrease the power consumption, is an example of important ongoing

TABLE 2: Summary of Machine Parameters

	TESLA		JLC-C		JLC-X/NLC[a]		CLIC	
Center of mass energy [GeV]	500	800	500	1000	500	1000	500	3000
RF frequency of main linac [GHz]	1.3		5.7	5.7/11.4[b]	11.4		30	
Design luminosity [10^{33} cm^{-2}s^{-1}]	34.0	58.0	14.1	25.0	25.0 (20.0)	25.0 (30.0)	21.0	80.0
Linac repetition rate [Hz]	5	4		100	150 (120)	100 (120)	200	100
Number of particles/bunch at IP [10^{10}]	2	1.4		0.75	0.75		0.4	
$\gamma\varepsilon_x^*$ / $\gamma\varepsilon_y^*$ emit. at IP [m·rad $\times$ 10^{-6}]	10 / 0.03	8 / 0.015		3.6 / 0.04	3.6 / 0.04		2.0 / 0.01	0.68 / 0.01
β_x^* / β_y^* at IP [mm]	15 / 0.40	15 / 0.40	8 / 0.20	13 / 0.11	8 / 0.11	13 / 0.11	10 / 0.05	16 / 0.07
σ_x^* / σ_y^* at IP before pinch[c] [nm]	554 / 5.0	392 / 2.8	243 / 4.0	219 / 2.1	243 / 3.0	219 / 2.1	202 / 1.2	60 / 0.7
σ_z^* at IP [μm]	300		200	110	110		35	
Number of bunches/pulse	2820	4886		192	192		154	
Bunch separation [nsec]	337	176		1.4	1.4		0.67	
Bunch train length [μsec]	950	860		0.267	0.267		0.102	
Beam power/beam [MW]	11.3	17.5	5.8	11.5	8.7 (6.9)	11.5 (13.8)	4.9	14.8
Unloaded/loaded gradient[d] [MV/m]	23.8 / 23.8[e]	35 / 35	41.8/31.5	41.8/31.5 / 70/55	65 / 50		172 / 150	
Total number of klystrons	572	1212	4276	3392/4640	4064	8256	448	
Number of sections	20592	21816	8552	6784/13920	12192	24768	7272	44000
Total two-linac length [km]	30	30	17.1	29.2	13.8	27.6	5.0	28.0
Total beam delivery length [km]	3			3.7	3.7		5.2	
Proposed site length [km]	33			33	32		10.2	33.2
Total site AC power[f] [MW]	140	200	233	300	243 (195)	292 (350)	175	410
Tunnel configuration[g]	Single			Double	Double		Single	

[a]Numbers in ( ) for the JLC-X/NLC correspond to the NLC design with 120 Hz repetition rate.

[b]The 1 TeV JLC-C collider uses a C-band rf system for the first 200 GeV of each linac followed by an X-band rf system for the remaining 300 GeV of acceleration—the X-band rf system would be identical to that described for the JLC-X band collider.

[c]For all designs except CLIC, the IP spot sizes are calculated as usual from the emittances and beta functions. With the design emittances in CLIC, nonlinear aberrations in the final focus system increase the final spot size by 20 to 40%.

[d]The main linac loaded gradient includes the effect of single-bunch (all modes) and multibunch beam loading, assuming that the bunches ride on crest. Beam loading is based on bunch charges in the linacs, which are slightly higher than at the IP.

[e]With the present site layout for TESLA, 23.4 MV/m was the required energy gain per meter of accelerator structure. A detailed analysis by the ILC-TRC revealed that the gradient has to be increased to 23.8 MV/m when rf phasing, especially for BNS damping, is taken into account.

[f]Total site power includes AC for linac rf and cooling systems as well as power for all other beam lines and site facilities.

[g]The single tunnel layout has both the klystrons and accelerator structures in the main linac tunnel while the double tunnel layout places the klystrons and modulators in a separate enclosure. In the CLIC scheme, the main linac uses a single tunnel since there are no klystrons or modulators associated with it. The 300 m-long CLIC drive beam accelerator is located in a tunnel with a separate klystron gallery on the surface.

Figure 42. Electron collider parameters.

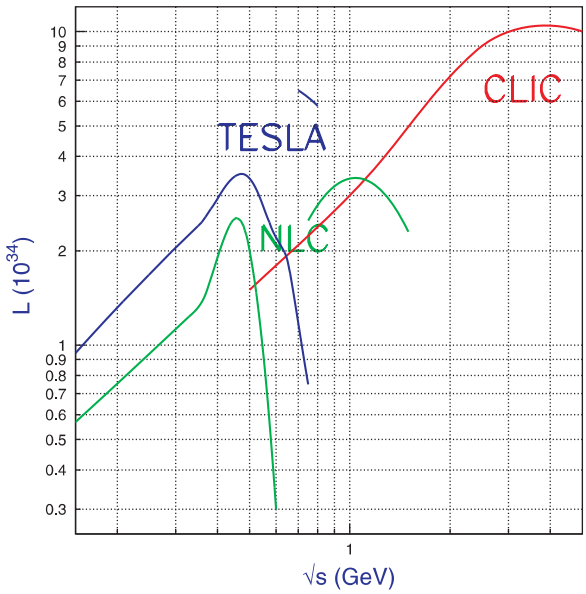

Figure 43. Luminosity spectra for future e^+e^- linear colliders.

development on these klystrons. Long structures have been experiencing pitting around irises under the effect of high fields but solutions exist to overcome this problem [291]. In 2004 an international panel has recommended for the sub-TeV ILC (International Linear Collider) the choice of cold technology, along the line of but not identical to TESLA.

- CLIC [292] aims at CM energies ranging from 0.5 to 5 TeV. It uses very high frequency (30 GHz) normal accelerating structures powered by a high intensity, low energy parallel drive beam. The goal is to reach a gradient of 150 MV m^{-1} over 30 km. Here too, the copper cavities have been suffering from high gradient testing, but recently it has been shown that accelerating cavities with tungsten and molybdenum irises and an optimized geometry can stand such gradients without any damage, at least for pulses of shorter duration than the actual ones, 16 ns instead of 130 ns [293]. CLIC has to go on demonstrating the validity and viability of its principle and assessing the performances of two-beam acceleration, which is likely to be the road towards multi-TeV collisions. Very promising results on the way to a validation of the technique have been obtained [294] from several successive test set-ups. A third test facility, CTF3, is starting its activity to demonstrate the key concepts of the RF power generation scheme and allow a full-scale test of the cavities: it will bring its answers in the next (three) years. It is vital that this goes on at the right level and pace, so that one could have a clear answer about its feasibility when LHC will give its first indications.

The 500 GeV machines are planned to accumulate up to 1000 fb^{-1} over several years. CLIC could also accumulate some 1000 fb^{-1} in about 3 years. The luminosity spectra are shown in figure 43.

For all these machines, a photon–photon or electron–photon option is also contemplated, with the photons obtained by Compton backscattering of laser light: CLIC Higgs experiment and CLIC 3 TeV gamma collider [295], TESLA [296]. Much more work is needed to reach a viable design. It would be interesting to know whether part of the CLIC drive beam can provide an adequate FEL beam for the photon–photon option.

An excellent introduction to e^+e^- (and muon) colliders and their physics can be found in [297][13].

Muon colliders. The idea of using muons, unstable particles, instead of electrons may sound odd. However, it has been recognized for many years [298, 299] that, since they live relatively long, ∼2 microsecond, which allows them to make ∼300 B_{tesla} turns in a collider, a muon collider could be a viable option if one can accumulate and concentrate enough of them in phase space.

A muon collider can do nearly everything an electron collider can do. There are, however, a few weak points: a somewhat lower luminosity, backgrounds due to muon decay, neutrino radiation when the energy becomes large and no possibility of turning the collider into a gamma–gamma collider. On the other hand the potential advantages of muons are as follows.

(1) They do not radiate 'externally' (the internal radiation, logarithmic in mass, is however not so different from electrons). The beam energy resolution can thus be excellent. The rate of synchrotron radiation loss per turn is $(200)^4$ times smaller than for electrons and thus negligible.
(2) They are coupled $(200)^2$ more to the Higgs boson(s) than electrons. One can then produce it (them) in the s-channel. The excellent beam resolution, and the possibility of measuring it accurately, as well as the beam energy, allow an optimal exploitation of this advantage. Naturally the Higgsstrahlung process is present as well.

One can conceive a large span of colliders [300, 302], ranging from a light Higgs factory ($E_{\text{cm}} \sim 115$ GeV) to a really multiTeV machine (we will consider 4 TeV of E_{cm}). The luminosity has to scale as E^2. We will assume it to be $L \sim 0.7 \times 10^{34}\ E^2_{\text{CM}}$, with E in TeV. This represents 70 E^2_{CM} fb^{-1} per 'year'. Concerning the resolution in energy, 0.1% can be considered as a standard feature, but, at the expense of luminosity, one can hope to reach 0.003% if needed.

The size of the muon collider complex, if one folds it on itself, is not too unreasonable. However, the road to a muon collider requires an enormous amount of R&D in several sectors, in particular the capture and cooling of the muons, and one is still far from a proven design. The proton source is another concern, and a substantial step compared with existing machines has to be taken to reach, for instance, the 16 GeV with 4 MW on target required by one of the schemes. These aspects are obviously relevant also for neutrino factories (NF) but at a slightly less frightening level: concerning muon cooling an order of magnitude has to be gained in both emittances from a NF to a Higgs factory.

The Liouville theorem states that the normalized emittance of a beam is a constant of motion. So beam cooling requires a 'violation' of this theorem, which is made possible by means of dissipative forces such as energy loss. This 'ionization cooling' is the only method which acts fast enough for muons.

The idea of transverse cooling is quite simple [303]. By ionization muons lose momentum along their flight direction, while some RF system gives them back momentum along the beam axis. Hence cooling occurs, provided multiple scattering does not ruin the beneficial effect. The beam energy has to be low (200–300 MeV c^{-1}) to ensure a cost effective re-acceleration. The radiator must be of low Z: the best choice is liquid hydrogen (8.7 m of radiation length), which raises the technical problem of its containment (very thin windows, ability to stand the heat deposition of up to 10^{14} muons s^{-1}). The beam to be cooled has initially a large transverse size: hence, besides big RF cavities, large magnetic apertures, for instance of the

[13] See P Janot's WEB site.

focusing solenoids, are needed. Field 'flipping' is required to cancel the bad effects of fringe fields.

However transverse ionization cooling increases the longitudinal emittance. Direct longitudinal cooling is impractical and the only way is to use emittance exchange, by suitably shaped absorbers located in a lattice point where there is momentum dispersion. A natural idea is thus to combine both coolings and repeat them in a ring.

The MUCOOL program [304] at Fermilab includes engineering tests of the cooling components, but no actual demonstration of the cooling of a beam. Such a demonstration is the purpose of the proposed international MICE program [305] which was submitted at the end of 2002.

VLHC. A very large hadron collider, is also being discussed [306]. The current thinking is that it could be built in two stages, first a pp machine running at 40 TeV with a luminosity of $1 \times 10^{34}\,\mathrm{cm}^{-2}\,\mathrm{s}^{-1}$ with 'reasonable' 2 Tesla magnets already well studied; afterwards a machine reaching 200 TeV with $2 \times 10^{34}\,\mathrm{cm}^{-2}\,\mathrm{s}^{-1}$ luminosity and requiring a strong R&D for its magnets. The effect of synchrotron radiation would become quite serious.

7.2. Progress in detectors

Progress in the detectors and experimental techniques is mandatory to guarantee the future. The amount of R&D which was needed before the final design and realization of the LHC experiments is most impressive. For some of their aspects one is still relying, as we said, on the steady technical progress and cost reduction of industrial technologies in the surrounding world. A new fact, for the machine components as well as for the experiments, is the time scales involved which may be long compared with the period of stability of industrial firms.

The LHC experiments are constructed under strong time pressure and there is presently no more room for much innovation concerning the first phase of the programme. However, for a possible second phase of LHC (with a luminosity approaching 10^{35}), a well targeted programme of R&D has to continue, especially for the inner tracking systems, including radiation-hard front-end electronics and optical links, but also probably concerning part of the forward calorimetry and muon systems.

A detector for the ILC, and *a fortiori* for CLIC and a muon collider, also needs a substantial R&D programme. While its details depend on the energy span, on the time structure of the machine and on the dominant backgrounds, one can identify common requirements for all future colliders.

Generally speaking, and in the field of tracking and microvertexing, the future belongs probably to all-silicon detectors, fast and radiation-hard, as for CMS at LHC, but possibly thinner [50], to reduce the material budget, and provide 3-D information (and not stereo information) as pixels (micro- or macro-pixels) do, or CCD's if the time structure of the machine allows them. As the energy increases, the radius of the microvertex should increase as well, since a 1 TeV B meson flies ∼10 cm. New flavour tag techniques, like multiplicity counting at various depths, will be required. New effects may have to be taken into account: for instance in 1.5 m of 4 Tesla field, a 1 TeV electron loses ∼60 GeV by synchrotron radiation, as a large number of O (1 GeV) photons, which will convert in the tracker. Landau–Migdal–Pomeranchuk effects may start to play a non-negligible role as well.

Considering calorimetry, all efforts should be made to avoid the two usual defects: either a solenoid coil or a large inactive volume between electromagnetic and hadronic components. The TESLA design [309] of a dense and highly segmented W(Cu)–Si calorimeter goes in that direction. If the cost allows it, a limiting case could be a 'digital' calorimeter in which the

energy is given by hit counting. The impact of an improved energy resolution in physics is important: below some value of its resolution, calorimetry allows the separation of the two-jet decays of W and Z, a capability of great interest for instance in the study of strong electroweak symmetry breaking, as discussed below.

Many other beneficial features may be looked for. At a LC an excellent time stamp of the event would allow it to be isolated as much as possible from neighbouring ones. **A high quality time-of-flight measurement may be another strong asset, in case heavy quasi-stable interacting particles exist**, as in one of the scenarios described in section 2.

7.3. SUSY Monte Carlo programs

There exist several publicly available codes to compute the SUSY spectra, decay branching ratios and production cross-sections for the various scenarios and types of machines. Some of the most heavily used are listed here. More details are provided, for example, in [310].

ISAJET 7.69 [133]: uses ISASUGRA for the calculation of the supersymmetric spectra in the MSUGRA, GMSB or AMSB scenarios, with decay rates computed by ISASUSY. It allows one to cope with pp, $\bar{\mathrm{p}}\mathrm{p}$ and $\mathrm{e}^+\mathrm{e}^-$ interactions with or without beam polarization. It includes independent jet fragmentation.

SUSYGEN 3.00 [311]: calculates the sparticle masses from the MSUGRA conditions, with the possibility of overriding some constraints, or for GMSB. Strict MSUGRA with correct electroweak symmetry breaking is implemented via the SUSPECT code [156]. The decays incorporate the R-parity conservation or not. It handles interactions in $\mathrm{e}^+\mathrm{e}^-$, hadron and e–p colliders, with or without beam polarization and includes spin-correlations. It is interfaced to JETSET/PYTHIA for parton fragmentation.

PYTHIA 6.2/00 [312]: uses semi-analytical expressions in SPYTHIA to compute the sparticle spectra and is, therefore, less accurate. But it is easily interfaced with another parton-level generator to provide the JETSET fragmentation part. Other publicly available programs to compute sparticle spectra include SDECAY [313] (which includes SUSPECT for the spectra), SOFTSUSY1.7 [314] (written in C++) and SPHENO2.0 [315] and a frequently used program for parton fragmentation is HERWIG6.5 [316].

Both packages, ISASUGRA and SUSPECT, follow the same logic, which we outline here for the MSUGRA case. They start with the evaluation of the gauge couplings and the third generation Yukawa coupling at the scale M_Z. These parameters are evolved to the GUT scale, defined by the crossing of the electroweak coupling constants g_1 and g_2, where the high scale boundary conditions are imposed. All couplings and mass parameters are then run down to the weak scale. The RGEs are of two-loop order for the gauge and Yukawa couplings and of one- or two-loop order for the soft masses and A-parameters. The one-loop effective scalar potential is evaluated at the electroweak symmetry breaking scale, chosen as $M_{\mathrm{EWSB}} = \sqrt{m_{\tilde{t}_1} m_{\tilde{t}_2}}$ to minimize the scale dependence. Radiative electroweak symmetry breaking is then imposed, which determines the values of $|\mu|$ and B (and some checks are performed on the validity of the solution). The whole SUSY spectrum is computed, including radiative corrections, and the mass matrices for the third generation sfermions and the gauginos are diagonalized to obtain the physical masses. Finally, as the radiative corrections depend on the sparticle masses, the procedure is iterated by running all parameters to the GUT scale and back, including the decoupling when sparticle threshold are crossed, until a stable solution is reached.

The mass spectra of ISASUGRA7.69, SUSPECT2.1, SOFTSUSY1.7 and SPHENO2.0 agree at the level of $\lesssim$5%, measured by the rms deviation of the four programmes, for not too extreme conditions [317]. But larger deviations are found for large values of the parameters m_0

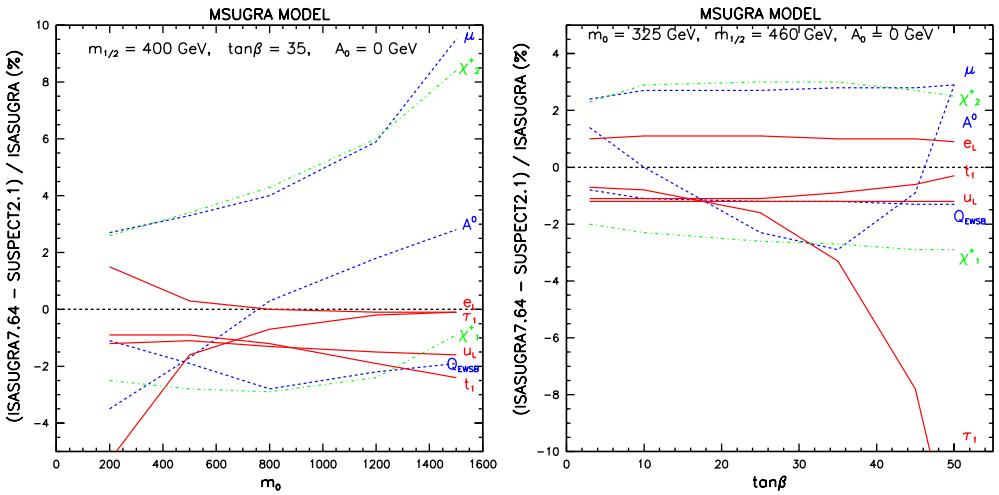

Figure 44. Relative difference between the masses computed in a MSUGRA model by ISASUGRA7.69 and SUSPECT2.1 as function of m_0 and of tan β.

(focus point region) or tan β, for instance, where some particle properties depend sensitively on the implementation of higher order corrections, in particular for the top quark Yukawa coupling. The relative difference between the mass values computed by ISASUGRA7.69 and SUSPECT2.1 is illustrated for a few representative quantities in figure 44. Moreover, the decays are treated at different levels of sophistication and, depending on the program, some may be missing (especially to or from the Higgses). In view of the fact that the precision on mass measurements at the LHC (and even more so at a lepton collider) is expected to be less than 10% and usually much better, the present situation of the software is still not really satisfactory, although it should be recognized that improvements are continuously being implemented by the authors in the most recent versions.

8. The Higgs sector in SUSY

This chapter will be devoted to the problem of EWSB in SUSY. Since this topic is abundantly documented the presentation will be concise and insist mostly on the most striking and robust aspect of SUSY phenomenology, the existence of a light Higgs boson. A detailed review of the Higgs search phenomenology is found in the paper by Spira and Zerwas [318], by Haber [319] or in [320] (and references therein). The experimental search strategy at LEP1 and LEP2 is clearly described by Janot [321].

8.1. Indirect indication in the frame of the SM

As noted already, the neutral current sector of the SM is in numerical agreement with the data to the per mille level or better. These accurate data, interpreted in the frame of the SM, predict the existence of a light Higgs boson, lighter than ∼250 GeV at 95% CL and the limit would become ∼280 GeV if $m_t = 180$ GeV. A word of caution has already been said on this point. As one can see from figure 45 the information on the Higgs mass, once the top mass is known, is mostly due to the accurate knowledge of $\sin^2\theta_w$. Unfortunately the use of an average for all measurements of $\sin^2\theta_w$ masks the fact that the two most accurate of them differ by 2.8σ,

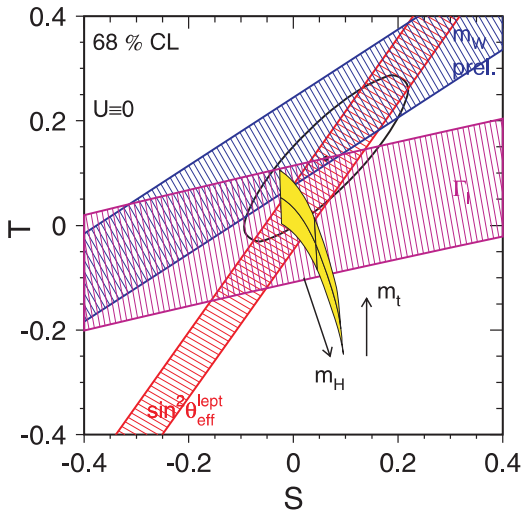

Figure 45. Constraints from precision measurements on the variables S and T from Peskin and Takeuchi [322].

without any chance of discriminating between them in the foreseeable future. The A_{LR} from SLC leads to a very light Higgs mass (smaller than the present direct limit at 95% CL) while A^b_{FB} from LEP still allows for a Higgs mass of a few hundred GeV. Note that a somewhat higher top mass would decrease the discrepancy. The usual attitude is to ignore this discrepancy and consider only the mean value, which provides the limit quoted above. Even so, one can ask oneself whether this result represents the truth or could be the result of a conspiration in which the effect of a heavy Higgs on electroweak observables is compensated by some new effect beyond the SM. For a quite complete survey of this legitimate question we refer to [323]. The conclusion is that, while such conspirations are possible, they occur in rather contrived or speculative scenarios. **The most natural attitude for the time being is thus to give priority to the search for a light boson**.

8.2. The avenues beyond the SM

There are many reasons, as we said, which push to go beyond the SM and we gave in section 2 a brief survey of the possible routes.

To do so, the two classical avenues are to add either new forces, for instance a new strong interaction between vector bosons, and/or constituents, like in technicolour, or to add more symmetry, like in supersymmetry, the choice we develop in this review. **Technicolour** breaks electroweak symmetry by condensates of new fermions and does not contain elementary Higgs scalars. *A priori* it is not favoured by accurate measurements. But the situation may be more complex and we refer to [34] for a review of the situation of technicolour. **Supersymmetry, on the contrary, justifies the existence of elementary scalars and predicts sharply a crucial feature of the Higgs sector: the existence of one light boson at least**. It also predicts a spectrum of superpartners, however less constrained as far as masses are concerned. It agrees with present data as well as the SM does, as we saw in section 6.10.

As we said in section 2, a third avenue appeared more recently [42, 43]: the possible existence of **extra–dimensions** at energy scales much lower than expected, maybe down to the TeV scale. As we saw in section 2, in these models, the apparent hierarchy between the

electroweak and Planck scales is due to the geometry of these extra spatial dimensions, either because they occupy a large volume (ADD) [42] or because of a strong curvature of the extra dimensional space (RS) [43]. We will not discuss here the *'bien-fondé'* of such assumptions, but it is certainly interesting and motivating to study whether they have testable consequences, in particular in the Higgs sector, for instance through the effect of the hypothetical radion in the RS model. We refer to [39] for a summary of the collider signatures and existing constraints.

Similarly, the **little Higgs** scenario may allow for a somewhat heavier Higgs boson through a conspiration with its new boson Z'.

It is worthwhile repeating here that, whatever the fashionable theories, the first duty of an experimentalist is to keep ones eyes wide open and to explore systematically all accessible channels.

8.3. The 'how' of the Higgs mechanism in SM

In the standard model, the potential of the Higgs field, ϕ, has the form:

$$V(\phi) = -\mu^2|\phi|^2 + \lambda|\phi|^4. \tag{119}$$

The quartic coupling λ has to be positive to ensure that the potential is bounded from below. If the first term is also positive or zero the potential has a trivial monotonic behaviour. **The ad-hoc solution of the SM, which has no physical justification, is to choose it as negative.** The potential displays then a characteristic minimum leading to a vev, v, for the Higgs field. The Higgs mass is given by $m_H^2 = 2v^2\lambda(v)$ where the value of the vev, $v \simeq 175\,\text{GeV}$, is determined from the mass of the W vector boson. The coupling λ varies with the energy scale due to radiative corrections and its RGE, neglecting gauge couplings, is

$$\frac{\mathrm{d}\lambda(t)}{\mathrm{d}t} = \frac{3}{4\pi^2}(\lambda^2 + \lambda h_t^2 - h_t^4), \tag{120}$$

with $t = \ln(\Lambda/v)$, Λ being the scale at which λ is evaluated and h_t representing the top Yukawa coupling, related to the top mass by $m_t = h_t \cdot v$.

If $\lambda(v)$ is large compared with h_t^2, it dominates the RGE evolution and may eventually drive $\lambda(\Lambda)$ into a non-perturbative regime. If one insists in avoiding this regime, an upper limit on the Higgs mass is derived depending on the scale, Λ, up to which the standard model remains perturbative (called triviality bound).

Conversely, if $\lambda(v)$ is small compared with h_t^2, the h_t^4 term can drive λ negative so that the potential (119) becomes unbounded from below. The condition of vacuum stability up to the scale Λ determines a lower limit on the Higgs mass. One can extend this condition to a condition of sufficiently long metastability.

These limits are displayed in figure 46 for a top mass $m_t = 175\,\text{GeV}$. If the SM is to be valid up to the Planck scale, the Higgs mass is constrained to lie in the range $130 < m_H < 180\,\text{GeV}$. A 115 GeV boson would correspond to the metastability lower bound provided the top mass is on the low side of its present measurement. However, as recalled by figure 46 (right), this requires an increasingly embarassing fine tuning[14] (note that the fine tuning definition used here is the reverse of our definition (72)).

8.4. The 'why' of the Higgs mechanism in MSSM

In the MSSM, two doublet Higgs fields are necessary, H_d and H_u, defined in table 2. The form of the neutral Higgs potential was given in equation (35). When running down the mass-squared parameters $m_{H_\mathrm{d}}^2$ and $m_{H_\mathrm{u}}^2$ of the Higgs fields, their RGEs contain a positive contribution

[14] See Kolda *et al* in [323].

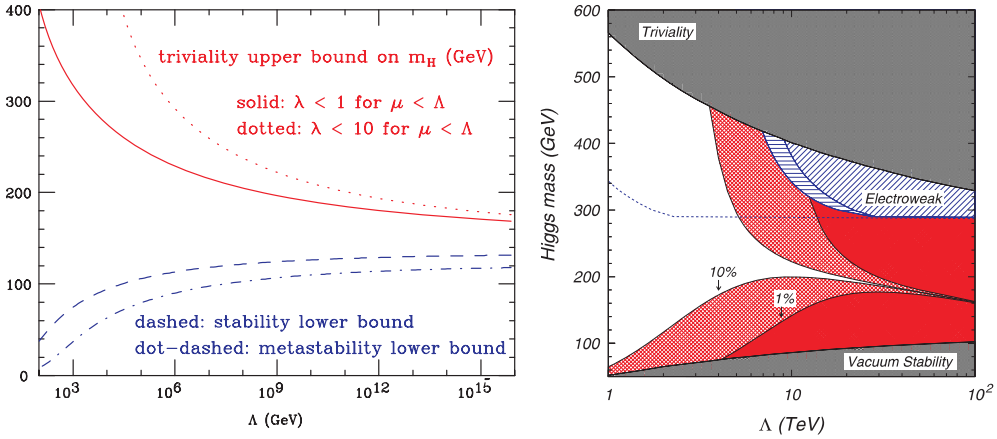

Figure 46. (left) SM Higgs mass bounds from perturbativity and vacuum stability, from [324]. (right) The level of (inverse) fine tuning needed in the $m_H - \Lambda$ plane, from Kolda and Murayama in [323].

from the gauge couplings and a negative contribution from the Yukawa couplings. As the top mass is large, its Yukawa coupling is also typically large and dominates the evolution of $m^2_{H_u}$. **This drives $m^2_{H_u}$ negative somewhat above the electroweak scale.**

This fact was first noticed in [20] and at that time the requirement that the top should be heavy was formulated. However $M_{\rm top}$ larger than ∼50 GeV would be sufficient in this respect. Furthermore this fact explains the 'why' of the Higgs mechanism. In the SM one had to choose as negative the first 'mass' term of the potential, which looked quite odd. **Here one can choose the corresponding term as positive at a high energy scale, which is a normal situation, and it is then naturally driven to a negative value at low energy.**

The minimization of the neutral Higgs potential with respect to the two Higgs fields induces two constraints among the weak scale parameters. The first one was given, at tree level, in equation (71). In the MSUGRA model, where $m_{H_d} = m_{H_u} = m_0$ at the GUT scale, it is frequently used to determine the absolute value of μ as a function of the remaining parameters. The second condition allows the GUT scale parameter B_0 to be exchanged with the electroweak scale parameter $\tan\beta$.

The potential (35), leading to the 'physical' minimum which determines the gauge boson masses, contains only the Higgs fields. But in the MSSM, there exist additional scalar fields in the potential which may give rise to other disconnected minima, local or global, with charge and/or colour breaking (CCB) or to directions in field space where the potential is unbounded from below (UFB). To give a hint of how this happens, we can follow the toy example (first mentioned in [325]), simply demonstrated in [326], assuming that only the stop quarks, i.e. the most dangerous ones because of their large Yukawa coupling, contribute to the potential. Consider the term $h_t \tilde{t}_L \tilde{t}^C_L H^0_u$ in the superpotential (22) and the associated soft breaking contributions. The scalar potential then consists of the F-terms from (28) and the soft term including $A_t h_t \tilde{t}_L \tilde{t}^C_L H^0_u + \text{c.c.}$ as well as the scalar mass contributions given in (34). When this potential is examined along the direction $|\tilde{t}_L| = |\tilde{t}^C_L| = |H^0_u|$ (which cancels their D-terms), it is found to develop a local minimum, unless the following condition $A_t^2 < 3(m^2_{\tilde{t}_L} + m^2_{\tilde{t}^C_L} + \mu_2^2)$ is fulfilled. Hence, it imposes a condition among the soft mass parameters and, in particular, puts an upper limit on the acceptable values of the A-parameter. The full treatment of this problem is, however, considerably more involved and the above condition is neither necessary

nor sufficient. A review is found in [327]. To find the solutions in the general case, a numerical method is indispensible. The authors of [328] perform a scan over the MSUGRA parameter space and, taking one-loop corrections to the scalar potential into account, find that the low m_0 region is severely affected by CCB global minima.

It is altogether not clear whether the conditions to be imposed should avoid completely the existence of such disconnected minima. It is indeed found that the universe is most likely driven to the charge and colour conserving 'physical' minimum and that the tunnelling time from our 'physical' vacuum to the CCB minima can easily be large compared with the age of the universe [329].

8.5. Phenomenology MSSM, NMSSM

Since this aspect is particularly well documented, we will, here again, be brief and focus mostly on the properties of the lightest boson, h^0.

8.5.1. Higgs mass in the MSSM. In the MSSM, there are two weak isospin doublet Higgs fields H_d and H_u, hence 8° of freedom. Three are needed to provide mass to the $W^\pm$ and Z^0. The remaining degrees of freedom give rise to 5 physical particles: two neutral CP-even, h^0 and H^0, one neutral CP-odd, A^0, and a pair of charged scalars, $H^\pm$. The neutral Higgses are given as a function of the fields H_d and H_u (expanded around their ground state) by:

$$\begin{aligned} H^0 &= \mathrm{Re}(H_\mathrm{d}^2)\cos\alpha + \mathrm{Re}(H_\mathrm{u}^1)\sin\alpha, \\ h^0 &= -\mathrm{Re}(H_\mathrm{d}^2)\sin\alpha + \mathrm{Re}(H_\mathrm{u}^1)\cos\alpha, \\ A^0 &= \mathrm{Im}(H_\mathrm{d}^2)\sin\beta + \mathrm{Im}(H_\mathrm{u}^1)\cos\beta, \end{aligned} \tag{121}$$

where α is a mixing angle of the scalar Higgses, related to the other parameters by

$$\tan 2\alpha = \tan 2\beta \frac{m_A^2 + M_Z^2}{m_A^2 - M_Z^2} \text{ with } -\frac{\pi}{2} < \alpha < 0. \tag{122}$$

The Higgs masses derived from the scalar potential are, at tree level,

$$m_{H^\pm}^2 = M_W^2 + m_A^2, \tag{123}$$

$$m_{H,h}^2 = \frac{1}{2}(m_A^2 + M_Z^2) \pm \frac{1}{2}[(m_A^2 + M_Z^2)^2 - -4m_A^2 M_Z^2 \cos^2 2\beta]^{1/2}, \tag{124}$$

and are expressible in terms of two parameters, which can be chosen as m_A and $\tan\beta$. The mass m_A, usually treated as a free parameter, can be expressed in terms of the SUSY parameters evolved down to the electroweak scale,

$$m_A^2 = \frac{2\mu B}{\sin 2\beta} = \frac{m_{H_\mathrm{d}}^2 - m_{H_\mathrm{u}}^2}{\cos 2\beta} + M_Z^2 \tag{125}$$

at tree level. By construction $m_h < m_H$.

Some extreme cases are worth mentioning. For small $\tan\beta \simeq 1$ the solutions of equation (124) are $m_h = 0$ and $m_H^2 = m_A^2 + M_Z^2$, the h is expected to be light. For large $\tan\beta$ the solutions are $m_h, m_H = \min, \max(M_Z, m_A)$, with degeneracy of h and A in the region where $m_A < M_Z$. For any $\tan\beta$, when $m_A \simeq 0$, the lightest Higgs also has $m_h \simeq 0$.

The mass of the lightest Higgs is limited by:

$$0 \leqslant m_h \leqslant M_Z |\cos 2\beta|. \tag{126}$$

For large values of m_A the light Higgs saturates the upper bound (126) and the three heavy Higgses become nearly degenerate.

However these relations are no longer valid after including radiative corrections, and this is the point we develop next.

8.5.2. Lightest Higgs mass with radiative corrections. The radiative corrections were computed for the first time in 1991 [330] and numerically nearly finalized in 1995 [331]. They increase the tree level value of m_h^2 by approximately (for $v = 174\,\mathrm{GeV}$) [330]

$$\Delta(m_h^2) = \frac{3m_t^4}{4\pi^2 v^2} \ln\left(\frac{m_{\tilde{t}_1} m_{\tilde{t}_2}}{m_t^2}\right), \tag{127}$$

which can be substantial, due to the heaviness of the top quark. Since one knows semi−accurately the top mass, the bulk of the correction is known as well. But the exact upper limit of the h^0 mass depends on $\tan\beta$ and on the details of the stop sector. It also depends on the level of approximation of the calculation and of the method used. Radiative corrections have been computed using different techniques: effective potential approach, direct diagrammatic calculation and effective theories with renormalization group (RG) tools. The best way to proceed is to combine the three, retaining the virtues of each approach.

The complete one-loop radiative corrections to $\mathrm{m}_{h^0}^2/\mathrm{m}_t^2$ have been calculated [332][15]. The dominant leading-logarithmic contribution gives the log term of (127). The most important finite non-logarithmic correction is

$$\Delta(m_h^2) = \frac{3m_t^4}{4\pi^2 v^2}\left(\frac{X_t^2}{m_{\tilde{t}}^2} - \frac{X_t^4}{12m_{\tilde{t}}^4}\right), \tag{128}$$

where $X_t = A_t + \mu\cot\beta$ is the top-squark mixing parameter. The maximum value of the correction is obtained for $X_t^2 = 6m_{\tilde{t}}^2$, called the maximum mixing situation. The most important part of the higher order radiative corrections can be collected and resummed using RG techniques and have been computed up to second order in $\alpha_t = h_t^2/4\pi$. See [331, 333] for a nearly complete list of references. Making use of RG resummation it is possible to get compact analytical approximations for $\mathrm{m}_{h^0}^2$. For example we give here the one of[16]:

$$\begin{aligned}\Delta(m_h^2) = \frac{3}{4\pi^2 v^2}&\left[\bar{m}_t^4(Q_t)\ln\frac{m_{\tilde{t}}^2(Q_{\tilde{t}})}{\bar{m}_t^2(Q_t')} + \bar{m}_t^4(Q_{th})\left(\frac{X_t^2(Q_{th})}{m_{\tilde{t}}^2(Q_{th})} - \frac{X_t^4(Q_{th})}{12m_{\tilde{t}}^4(Q_{th})}\right)\right] \\ &+\frac{\alpha_S m_t^4}{2\pi^3 v^2}\left[-\frac{2X_t}{m_{\tilde{t}}} - \frac{X_t^2}{m_{\tilde{t}}^2} + \frac{7X_t^3}{3m_{\tilde{t}}^3} + \frac{X_t^4}{12m_{\tilde{t}}^4} - \frac{X_t^5}{6m_{\tilde{t}}^5}\right].\end{aligned} \tag{129}$$

One recognizes the two terms quoted above, as well as additional corrections. The quantities are evaluated at different scales ($Q_t^2 = m_t m_{\tilde{t}}$ and, for instance, $Q_{\tilde{t}} = Q_t' = Q_{th} = m_{\tilde{t}}$) with simple formulae of evolution like

$$\bar{m}_t^2(Q) = \bar{m}_t^2(Q')\left(1 + \frac{2\alpha_S}{\pi}\ln\frac{Q'^2}{Q^2}\right). \tag{130}$$

The most complete formulae available so far, including $\alpha_b = h_b^2/4\pi$ corrections up to second order, can be found in [334]. At very large $\tan\beta$ the role of the b quark becomes crucial. The agreement between the various calculations is at the $\sim$2 GeV level. They all confirm the fact known for a long time[17] that **in the MSSM the lightest boson has to be lighter than $\sim$130 GeV. As a rule of thumb an increase of 1 GeV on m_{top} translates into a 1 GeV increase of the bound on m_h.**

Although one should not expect substantial differences, since the main feature stems from equation (35), one can investigate the mass distribution of h^0 in the framework of the three most prominent SUSY-breaking scenarios. For the central value of the top mass the authors of [335]

[15] See Pierce *et al* [104].
[16] Espinosa and Navarro and Zhang in [333].
[17] see Carena *et al* 1995 in [331] and references therein.

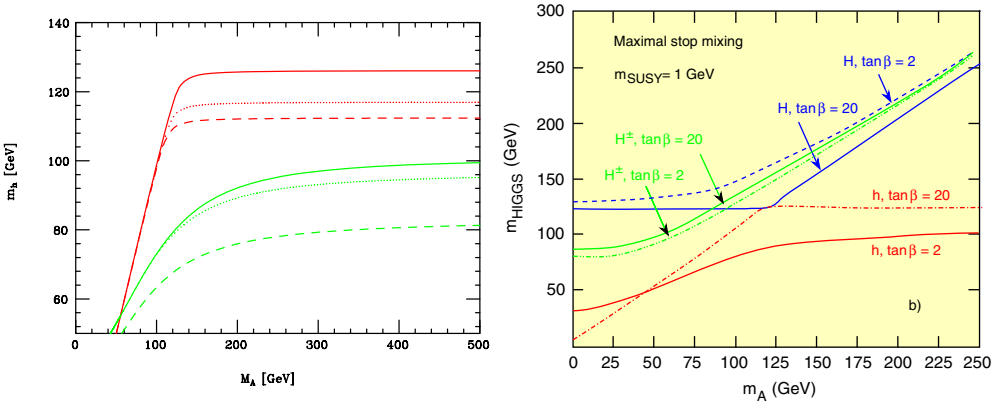

Figure 47. Higgs masses as function of m_A, from Carena *et al* 1995 in [331] and [338]. (left) Mass of the lighter Higgs with radiative corrections for different values of tan β stop mixing and $m_t = 175$ GeV. (right) Masses of neutral and charged Higgses.

found $m_{h^0} \leqslant 124$, 119 and 122 GeV in the mSUGRA, mGMSB and mAMSB, respectively, while it is ∼130 GeV in the unconstrained MSSM. We refer to [335] for the description of the input parameters ranges and other information. The authors of [336], adopting $m_t = 178$ GeV, also find a limit < 130 GeV for the three scenarios. In the unconstrained version (*a priori* 22 free parameters), by looking systematically for the 'maximum maximorum', adding linearly uncertainties (on m_t and theoretical) and taking the stop masses at 2.5 and 1.25 TeV, they manage to reach a value near 150 GeV. The naturalness of such a solution is not discussed. One sees that specific models do not allow the 'maximum maximorum' value of the general scenario to be reached. We will see it again when exploring SUSY benchmarks in section 12.2.1.

There exist several publicly available programs to compute the Higgs masses including radiative corrections, some examples being FeynHiggs2 [337] and SuSpect2.1 [156].

If m_A is large, say larger than ∼100 GeV, h^0 is SM-like. If m_A is very large, one can conceive a limiting case, the 'heavy MSSM', where, apart from h^0, all other bosons, degenerate with A^0, and the superpartners are heavy.

In figure 47 (left) from Carena *et al* 1995 in [331], the lower set of curves is for tan $\beta = 1.6$, the upper set for tan $\beta = 15$, a value above which m_h saturates as function of tan β. Within each set, the dashed line represents the case of minimal mixing, $X_t = 0$, and the full line the maximal effect of mixing, given by $X_t^2 = 6m_t^2$. The masses of the heavier Higgses are shown in the right part. At large tan β, either the lighter Higgs, h^0, or the heavier CP-even Higgs, H^0, is degenerate with the CP-odd Higgs A.

It is interesting to compare the mass bounds obtained in the SM and in the MSSM. Figure 48, shows the SM lower bound from vacuum stability (steep curve) and the MSSM upper bound as function of the top mass. At the measured top mass of 175 GeV, they almost cross each other and the regions allowed for the SM and the MSSM are mutually exclusive. If a Higgs exists near 115 GeV, the SM is deemed to break down before the Planck scale, as shown by the continuous lines in figure 48 (right), unless the top mass is substantially lighter than the present central value (dotted curve).

8.5.3. The effect of phases. The question should be raised whether the above conclusions on a light Higgs boson are affected by the possible existence of phases in SUSY parameters. The phenomenological consequences of CP-violating phases in the Higgs sector have been

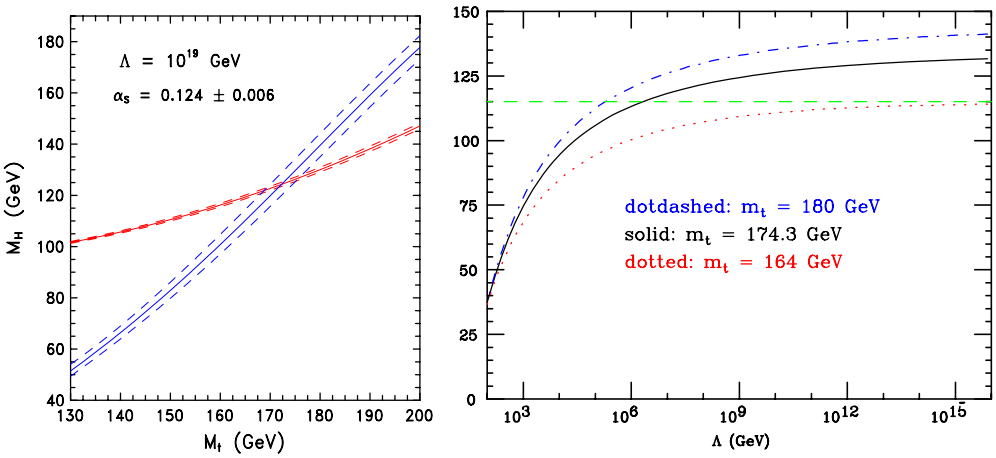

Figure 48. (left) Lighter Higgs mass bounds in SM and MSSM from [339]. (right) SM Higgs metastability lower bound from [324].

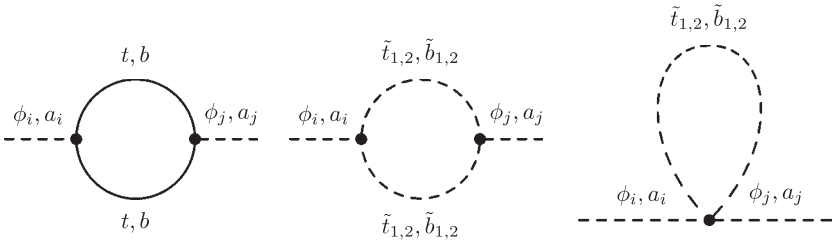

Figure 49. Examples of diagrams inducing CP violation. The fields ϕ_i and a_i represent respectively the real and imaginary parts of the Higgs fields.

investigated in early papers by Pilaftsis and Wagner [340][18] and later by Carena *et al* [333] (see references therein). CP-violation is induced radiatively by loops involving the trilinear couplings of Higgs bosons and stop or sbottom (complex A_t and A_b), examples being shown in figure 49. The loops induce transitions between the real part, ϕ_i, and the imaginary part, a_i, of the Higgs fields. As a result, the CP-even Higgs states h^0 and H^0 mix with the CP-odd state A^0. The masses of the eigenstates H_1, H_2 and H_3 (ordered in increasing mass) are most conveniently expressed in terms of the mass m_{H^+} of the charged Higgs, instead of the parameter m_A of the CP-conserving case. The upper bound on the mass of H_1 is almost identical to the one obtained for h^0 in the CP-invariant theory for both low and high $\tan\beta$ values.

The values of the couplings normalized to their SM value, follow the rules:

$$g_{H_kVV} = \epsilon_{ijk} g_{H_iH_jZ}$$
$$g^2_{H_1ZZ} + g^2_{H_2ZZ} + g^2_{H_3ZZ} = 1, \tag{131}$$

with $V = W^{\pm}, Z^0$. The three couplings to ZZ cannot simultaneously be small.

For a heavy charged Higgs, with mass above 200–300 GeV, the CP-violating phase has little effect and the lightest neutral Higgs, H_1, behaves SM-like for all values of $\tan\beta$. However, in the low to intermediate $\tan\beta$ region, the coupling $g^2_{H_1ZZ}$ of the lightest Higgs to the gauge boson can be drastically reduced compared with its SM value when the charged

[18] see Pilaftsis and Wagner in [333].

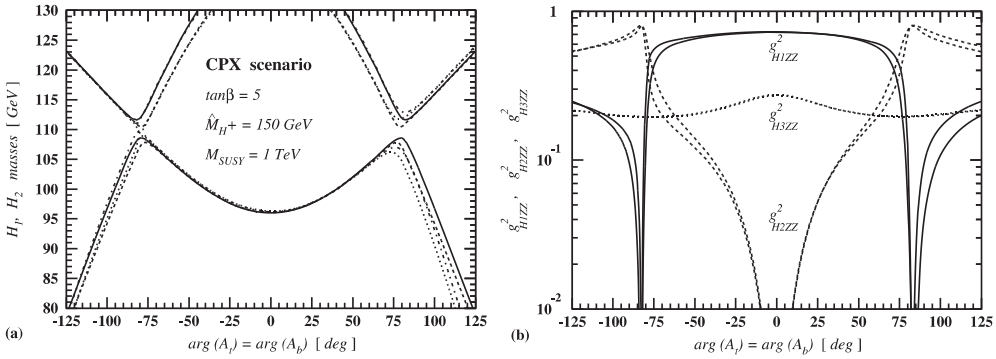

Figure 50. Coupling of the lightest Higgs to ZZ and mass of H_1 and H_2 as function of the CP-violating phase, for $\tan\beta = 5$, reprinted from Carena *et al* 2002 in [333]. Copyright 2002, with permission from Elsevier.

Higgs is lighter. This happens at maximal CP-violation (phase $\simeq 90^\circ$) and, for a relatively light charged Higgs boson, $m_{H^+} \simeq 150$ GeV, it may even decouple from the Z^0 for a specific choice of the CP-violating phase, as illustrated in figure 50. Hence, the Higgsstrahlung cross-section may become too small to provide sensitivity to the lightest Higgs. Some sensitivity can be recovered as the next-to-lightest Higgs, H_2, is light in the same region of the CP-violating phase and it has a large coupling to ZZ. Moreover, the associated production (see [340], see footnote 21) H_1H_2 and H_1H_3, which may be within the kinematical reach given the low mass of the H_1, also has a sizeable coupling to the Z^0.

For large values of $\tan\beta$**, the CP-violating contributions are severely constrained by the electric dipole moments of the electron and neutron** (see section 6.8) and no major modifications are expected to the Higgs phenomenology with respect to the CP-conserving case.

So far, no systematic analysis of the possible implications of CP-violating phases has been reported by the LEP experiments. It is clear from figure 50 that a somewhat higher centre of mass energy ($\sim$220 GeV) would allow the question to be answered since in such a case at least one Higgs boson is always accessible.

For LEP running at $\simeq$206 GeV, the mass range accessible via Higgsstrahlung may be somewhat reduced, compared with the CP-conserving case. The associated Higgs production also remains accessible for not too heavy H_1 and H_2, i.e. not too heavy charged Higgs. It would, however, require a dedicated search, as the approximate equality of masses $m_h \simeq m_A$ assumed in standard hA analyses can no longer be applied, and a huge integrated luminosity.

8.5.4. Evading the MSSM Higgs theoretical mass bounds in the NMSSM. The upper bound on the mass of the lightest Higgs is, as we saw, quite robust in the MSSM, whatever the SUSY breaking scheme and one needs additional Higgs fields, like in the NMSSM, and additional matter fields to obtain a higher bound.

In the NMSSM the Higgs phenomenology is more complicated than in the MSSM. In its minimal version, the NMSSM assumes the existence of a single scalar, S, which transforms as a singlet under the gauge groups. The additional pieces in the superpotential and in the neutral Higgs potential were described in section 3.5.2. Once the electroweak symmetry is broken, the scalar component of S acquires a vacuum expectation value $\langle S\rangle$, thus generating an effective μ term. Two new states, a CP-even (real part of S) and a CP-odd (imaginary part of S) neutral

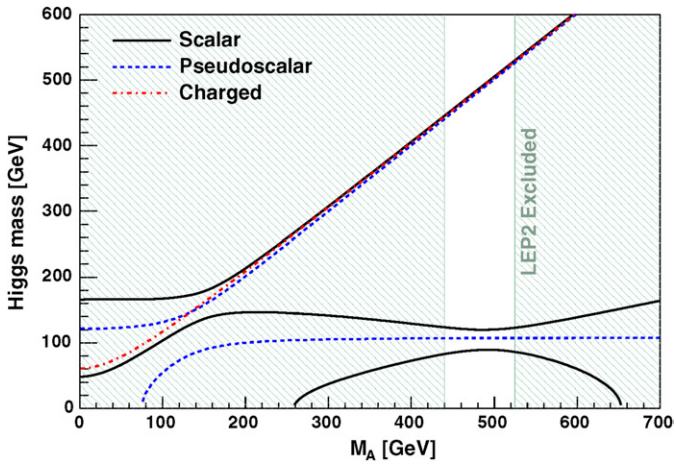

Figure 51. Higgs masses as a function of m_A for the NMSSM with parameter values $\lambda = 0.3$, $\kappa = 0.1$, $\mu = 157$ GeV, $\tan\beta = 3$ and $A_\kappa = -60$ GeV. From [341].

Higgs appear. They usually mix with the corresponding MSSM states, giving three CP-even and two CP-odd neutral Higgs states. Observing three light Higgs bosons but no light charged one at future colliders would be the signature. A strongly broken PQ symmetry may lead to decoupled scenarios more difficult to distinguish from the MSSM.

The requirement of perturbativity up to the GUT scale imposes a bound on the NMSSM couplings λ and κ which was given in equation (41). Analytical formulae for the Higgs masses have been obtained in [341] in the approximation where the Peccei–Quinn symmetry is exact or slightly broken ($\kappa = 0$ or $\kappa \lesssim \lambda^2$). The mass of the SM-like Higgs (h_2^0) remains $\leqslant$130–135 GeV, after including loop corrections, like in the MSSM. An example of the Higgs mass spectrum as a function of m_A (the MSSM-like CP-odd scalar a_2) for a set of NMSSM parameters is shown in figure 51. An interesting feature of the small κ scenario is that the lighter CP-odd Higgs (a_1) becomes very light and the decay $h_2 \to a_1 a_1$ may be important. The spectrum of the non-singlet Higgses resembles closely the one of the MSSM Higgses of figure 47.

The phenomenologies are different depending on whether one assumes universality of the soft breaking terms or not.

Assuming universality, the authors of [342] have scanned the 4 free parameters space ($m_0/m_{1/2}$, $A_0/m_{1/2}$, λ and κ) and found that the doublet Higgs sector is basically MSSM-like and that the singlet sector is quasi-decoupled. Assuming also the existence of one neutral CP-even boson with mass $\sim$115 GeV (see section 8.6) puts further constraints: one finds that the 115 GeV state is a quasi-pure SM-like H_u state ($\tan\beta > 4$, $m_A > 160$ GeV, etc). Concrete prospects exist both at the Tevatron (if the luminosity increases substantially) and especially at the LHC to detect, besides those of the MSSM-like doublet Higgs sector, at least one neutral state with a dominant singlet component.

In non-universal scenarios, the outcome can be different [343]. Further discussions of the Higgs sector and a representative sample of NMSSM solutions can be found in [73]. The mixing of the MSSM-like Higgses with the singlet states may reduce sizeably the couplings, and hence the production cross sections and/or decay branching ratios of the standard LHC search channels. In spite of establishing a 'partial no-lose theorem' for NMSSM Higgs boson discovery at LHC [343], it is conceivable that the detection of the $h \to aa$ decay could be

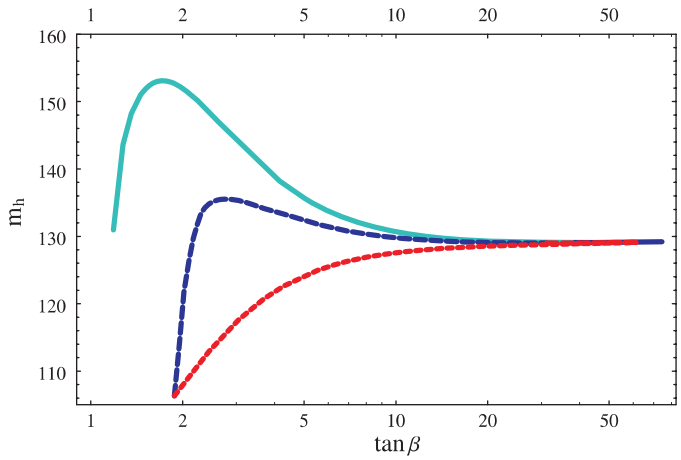

Figure 52. Higgs mass bounds as function of $\tan\beta$ for the MSSM (lower curve), the MSSM with an extra scalar singlet (middle curve) and with 4 families of intermediate particles in $5 + \bar{5}$ representations and a singlet (upper curve). Reprinted with permission from [346]. Copyright 1998 by the American Physical Society.

difficult. Here h is any CP-even boson and a is a light CP-odd one, and this is supposed to be the only available channel. Scanning over the 6 free NMSSM parameters in regions where the usual LHC detection modes have all significances below 5σ and where decay modes like $h \to aa$ are allowed, it is concluded in [344] that a signal in the $jj\tau\tau$ mass distribution is observable, though on the tail of a steeply increasing $t\bar{t}$ background. The observability hence depends entirely on the accuracy with which the background shape can be controlled.

Having as an objective to illustrate the complementarity of LHC and a sub-TeV linear collider one can naturally invent quite peculiar situations. The authors of [345] choose the parameters of the NMSSM leading to the spectrum shown in figure 51, with corresponding branching ratios and cross sections (see their paper) as a function of m_A. If m_A is around 500 GeV one can conclude that LEP200 has missed the MSSM scalar (115–130 GeV) and that LHC, which will discover it, may miss the lightest singlet dominated scalar, so that a LC is needed to establish the NMSSM nature of the situation.

Can one still go higher in upper mass limit for the light Higgs? A test case of next to minimal supersymmetry standard model (NMSSM) was studied by Masip *et al* [346] who assume the existence of a scalar, S, which transforms as a singlet under the gauge groups. Introducing a coupling of the form $\lambda H_u H_d S$ into the superpotential leads to an additional term $\lambda^2 v^2 \sin^2 2\beta$ in the Higgs mass bound. The results are displayed in figure 52. Depending on the assumptions made one can raise the bound to ∼135 (if only a single singlet is added) or even ∼155 GeV (if one also adds 4 families of intermediate particles). Note that in minimal NMSSM, when only a singlet is added, the largest value of the bound occurs at $\tan\beta \lesssim 2.5$, a region where in the MSSM the bound is low and will be excluded by LEP2. For $\tan\beta \gtrsim 20$ the bounds are indistinguishable from the MSSM one. It was also shown that including weak isospin triplets [347] one can even raise the bound to ∼195 GeV.

Many non-SUSY theories beyond the SM predict additional $U(1)'$ symmetries broken near the electroweak scale [348]. They bring a solution to the μ problem, but one needs to make the Z' sufficiently heavy. Different mechanisms [349] have been proposed to ensure a large $U(1)'$ breaking scale. A class of these involves [350] an ordinary sector of symmetry breaking fields, including two Higgs doublets and an $SU(2)$ singlet, similar to the NMSSM

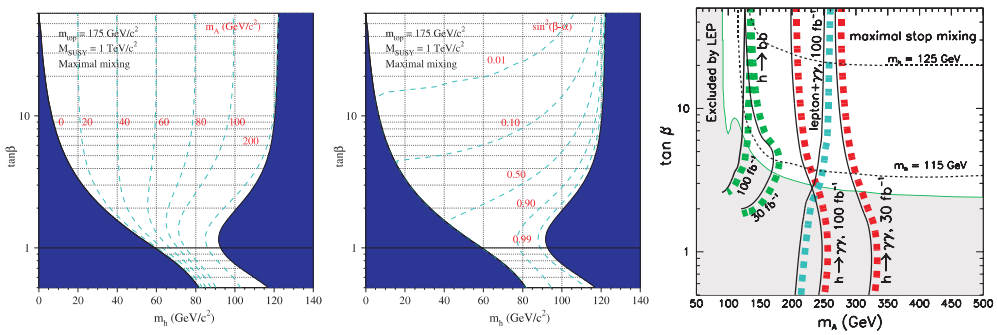

Figure 53. $\tan\beta$ versus m_h plane showing (left) isomass curves for m_A and (right) constant $\sin^2(\beta-\alpha)$ for the case of a maximal effect of mixing. From [321].

but with a quite different choice of parameters, and a secluded sector involving three $SU(2)$ singlet fields. The spectrum of the symmetry breaking sector is very rich and one can avoid the usual bound on the lightest CP-even boson.

8.5.5. MSSM Higgs composition and couplings. The main results which interest us here are summarized in figure 53 from which the following consequences emerge, concerning the h_0.

(1) For large m_A, the lightest Higgs mass m_{h^0} is forced to lie close to its upper bound for a given $\tan\beta$ and the heavier Higgses to be nearly degenerate with A, in particular $m_{H^0} \simeq m_A$. The light Higgs h^0 couples to the vector bosons with its SM strength ($\sin^2(\beta-\alpha) \simeq 1$). The coupling of h^0 to quarks and leptons also reaches its SM value, proportional to the quark or lepton mass. **The lighter Higgs, h^0, behaves in all respects SM-like, the process to be considered at LEP is the Higgsstrahlung one, and the conclusions drawn from the SM Higgs search remain valid in the MSSM case**. The $\tan\beta$–m_A plane is shown in the case of maximal stop mixing with iso-m_h curves and the bounds expected from LHC. **Note that the whole upper-right part corresponds to the last few GeV of** m_h and that a 'small step' in m_h is a 'huge step' in other relevant SUSY variables, as will be abundantly shown in many subsequent plots.

(2) For $\tan\beta$ large and $m_A \leqslant 120$ GeV, one sees from figure 47 (left) that $m_{h^0} \simeq m_A$. Now the H^0, which is quite light, behaves in a SM-like way, whereas the h^0 decouples from the vector bosons and has a maximal coupling g_{hAZ}. This implies that the associated production mechanism $e^+e^- \to h^0A^0$ has now to be considered as well. Both h^0 and A have large ($\propto \tan\beta$) couplings to down-type fermions and strongly suppressed couplings to up-type fermions.

8.5.6. Impact of the limits on m_h in the domain of SUSY parameters. Once m_t is known and for a given $\tan\beta$, the value of m_h in the MSSM is given by the stop sector (see section 8.5.2): it is therefore through this sector that the limit on m_h has an impact on the SUSY parameters. In the $\tan\beta$–m_A plot, one can read it directly from the iso-m_h curves. In the $m_0 - m_{1/2}$ plane, such h^0 isomass curves will be indicated as well. We recall that 1 GeV increase of the top mass increases m_h by 1 GeV (or less) and that the theoretical uncertainty on the m_h limit may be a couple of GeV.

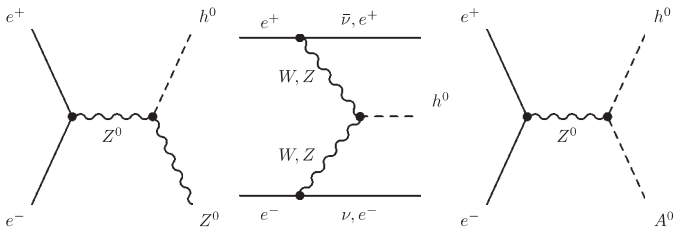

Figure 54. Examples of diagrams contributing to the Higgs production. (left) Higgsstrahlung, (centre) fusion, (right) associated production.

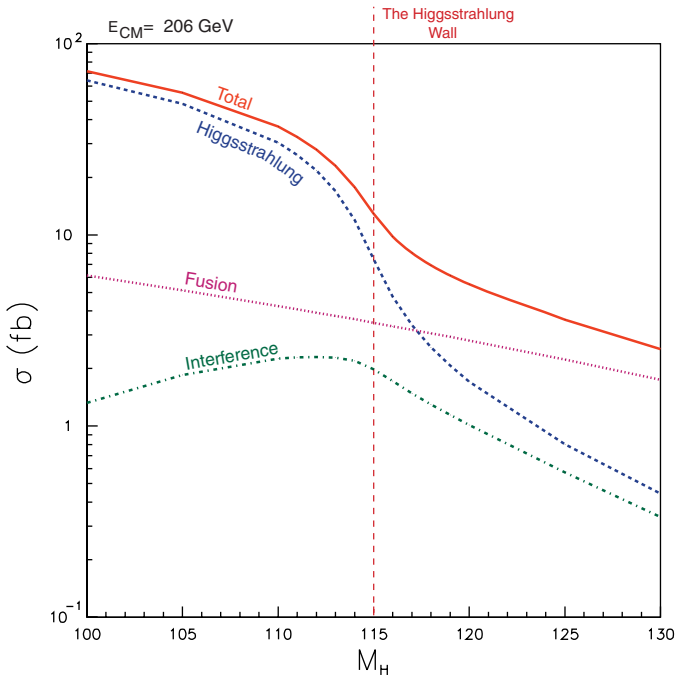

Figure 55. The various components of the H ν ν channel near the 'kinematical limit' [351].

8.6. Searches at LEP

The Higgs boson searches at LEP have been described in such detail [338] that we will only summarize the situation and focus on the highest accessible mass region. A SM or SM-like boson, like h^0 under the conditions given above, is produced in association with a Z^0 by the Higgsstrahlung (HS) process, shown in figure 54 (left). The possibility of exploring Higgs masses near and beyond the Z^0 mass, thanks to b-tagging, have been realized since 1990 and the corresponding discovery limit rule-of-thumb clearly formulated. The HS hits a kinematical barrier when sqrt(s) equals M_Z+M_H: tails beyond this barrier reflect the tail of the Z^0 Breit–Wigner. At and beyond the kinematic limit, the fusion process, shown in figure 54 (centre), and its interference with HS can be used in the H $\nu\nu$ channel, as seen in figure 55 [351], but the cross-section is tiny. **So LEP was a threshold machine and the goal was to run at the highest possible energy to maximize the chances of discovery**. An increase in energy pushes up the kinematic limit. For a given Higgs mass it allows the Higgs production cross-section to

approach its maximal value. In case of a possible signal, it gives a chance to check its stability and therefore its reality.

Unfortunately in 2000 LEP has reached the maximum energy, ∼206 GeV, allowed by its park of 285 SC RF cavities, running beyond their design accelerating voltage, at 7.5 MV m^{-1} instead of the 6 MV m^{-1} foreseen. ∼15 GeV in CM energy could have been gained by filling the equipped zones with cavities, reaching an amount of ∼380 of them overall [352], but this option had not been retained.

Given the three generic channels of Z^0 decay, the Higgs boson was searched for in all hadronic mode (4 or 5 jets, two from beauty), missing energy mode (the Z^0 into neutrinos) and dilepton–dijet (the jets being b-jets from the Higgs boson). The last one is the cleanest, but has the smallest branching ratio.

The missing energy channel considers events with two jets and missing energy. Even close to the Higgsstrahlung kinematical limit, these two jets are still substantially acolinear and acoplanar. This is also obviously true for the case of fusion. The analysis uses rescaling of the missing mass to the Z^0 mass. A dangerous background is due to double radiative return to the Z^0 in a quasi-symmetric way. This produces a Z^0 roughly at rest and the procedure of rescaling automatically brings its mass to a value close to the kinematic limit $\sqrt{s} - M_Z$, i.e. 115 GeV at $\sqrt{s} = 206$ GeV. The main weapon against this background is a cut in acoplanarity,[19] because such a Z^0, with both photons in the beam pipe, is roughly coplanar with the beam. Another background is due to normal beauty–antibeauty two-jet events, produced at full energy, but which present a large missing energy because of a strong emission of neutrinos (for instance if the B decays to τ-ν) and possibly other reasons (like some energy lost in cracks): but such events are nearly collinear and can be discarded without much loss in acceptance for the signal. For a high mass Higgs, one can also require that the measured hadronic mass is clearly above what one expects for a Z. With few other precautions this channel can be made rather background-free for a high mass search.

The four jet channels are more difficult. WW, ZZ and QCD all contribute to the background, up to the highest masses that even WW and ZZ can populate through mis-pairing of jets. A very strong rejection of WW is obtained through b-tagging (figure 56 left), the limit coming in particular from our inability to distinguish totally c from b jets, and from some tiny content of beauty in WW events. Figure 56 (right) shows the evolution of the background in 4-jet with the severity of the cuts, hence, for a decreasing efficiency to the signal. As expected, the ZZ background is the most resistant, in particular because 44% of ZZ have one $b\bar{b}$ at least and 74% have $b\bar{b}$ or $c\bar{c}$. Besides the resolution of the mass determination procedure (actually some analyses use a rescaling and $m_h = \sum_{1,2} M_{\text{pair}} - M_Z$) and the natural tail of a Breit–Wigner distribution, tails towards high masses are due to mis-pairings of jets and to initial state radiation: the latter, being generally unnoticed, leads to rescale to an energy higher than the one at which the ZZ event occured, and thus to inflate masses. If the ISR photon is detected and incorporated into the final state, one similarly gets masses higher than one should.

The traditional statement is that 'all these effects are present in the simulation': indeed a tremendous effort has been put into the understanding and modelling of these various effects and no manifest discrepancy was seen between data and simulation at intermediate stages of the analyses. But when one deals with the few last events, after having achieved rejection factors of up to a few hundred, one may fear that reality and simulation have diverged, especially close to the kinematic limit.

[19] The coplanarity is the angle between two particles or jets in the plane perpendicular to the beam. The acoplanarity is 180° minus the coplanarity.

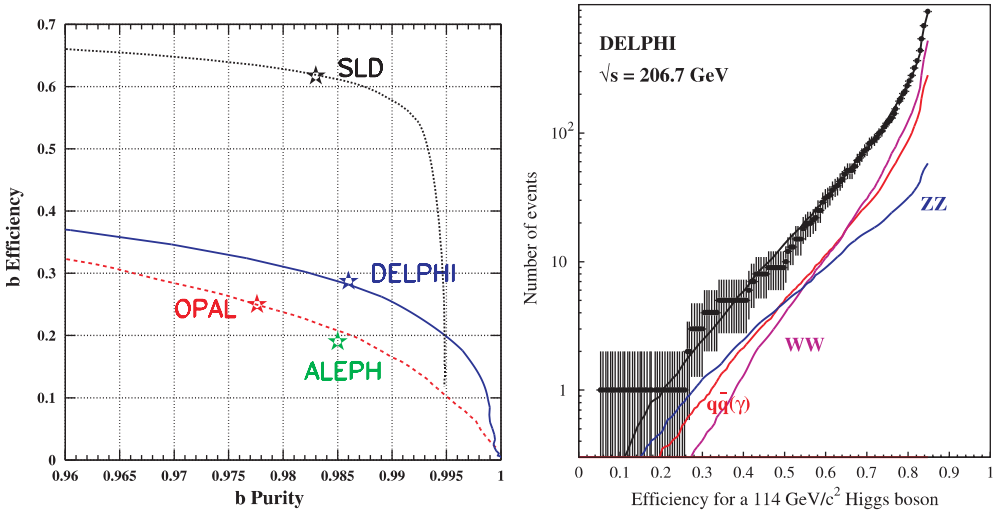

Figure 56. (left) The rejection due to b-tag at LEP2. (right) The evolution of the data and of various backgrounds when the severity of the cuts is increased.

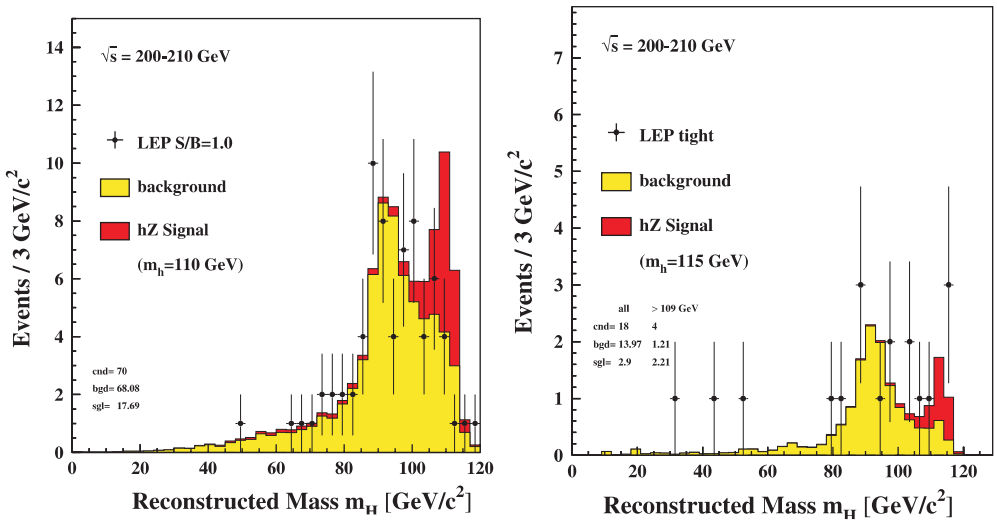

Figure 57. (left) Mass spectrum of Higgs candidates, in summer 2000 [353]. (right) Same for final LEP results.

Having excluded lower masses, up to 112.3 GeV, in the summer of 2000 [353] (see figure 57, left) the LEP search in the few last months of running focused on the highest accessible mass, at the kinematical limit of the Higgsstrahlung process, namely ∼114/115 GeV for an ultimate CM energy of ∼206 GeV. Under such conditions, for a mass of 115 GeV, the total Higgs cross-section is ∼50 fb only (it would be 5 times higher with 10 GeV more in the cms), compared with 1 picobarn for ZZ.

Some candidate events, appearing at such masses, and visible in figure 57 (right), generated a lot of excitement. However, no appreciable gain in energy was foreseable and the decision to stop LEP by the end of 2000 was maintained.

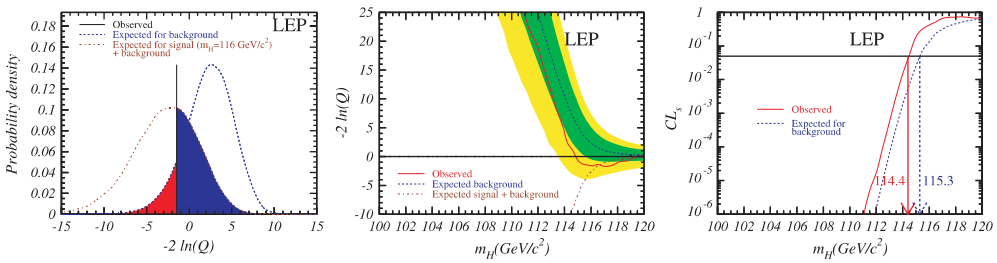

Figure 58. (left) Probability density distributions for the background and background+signal hypotheses at a fixed Higgs mass. (middle) Value of the test statistic $-2lnQ$ as a function of the Higgs mass for the combined data of the four LEP experiments. The solid (red) line represents the observation. The dashed and dash-dotted lines show the median background and background+signal expectations. The dark (green) and light (yellow) bands are the 68% and 95% probability bands about the median. (right) Confidence level CL_s for the signal+background hypothesis, with the same conventions as previous figure. From [355].

Table 12. Confidence levels for a Higgs mass of 116 GeV. From [355].

	$1-CL_b$	CL_{s+b}
ALEPH	2.4×10^{-3}	0.956
DELPHI	0.874	0.033
L3	0.348	0.408
OPAL	0.543	0.208
LEP	0.099	0.369

After the end of LEP, the situation can be summarized [354] by figure 58. The confidence levels are evaluated from the ratio, Q, of likelihoods for the signal+background to background only hypotheses, where the likelihood is a function of the Higgs mass and of several event observables, like the b-tagging, the event kinematics, etc. The probability density distributions of the test statistic $-2lnQ$ is displayed in figure 58 (left) for a Higgs mass of 116 GeV. The integral of the distribution from $-\infty$ to the observed value, $1-CL_b$ (light grey area) quantifies the probability that an event would be more signal-like than the observation for a large number of events from background only. The integral from the observation to $+\infty$, CL_{s+b} (dark grey area), is the probability that events from signal+background experiments are more background-like than the observation. Evidence for a signal would correspond to a small $1-CL_b$ and large CL_{s+b}. The results from the individual experiments for a Higgs mass of 116 GeV are summarized in table 12.

In brief, most of the effect comes from the fact that one experiment (ALEPH) sees an excess in one channel (the four-jets, largely through three notorious events). ALEPH quotes 2.4×10^{-3} as the probability to be more signal-like in the absence of a real signal. Combining all four experiments, this becomes 9.9%. **The future will tell whether this indication is a true effect or not. The final LEP limit on a SM-like neutral boson is 114.1 GeV. This is also the limit for the MSSM h^0 in the (likely) case where $m_A \geqslant 100$ GeV.**

The canonical MSSM Higgs search, exploiting both the HS mode and the associated production mode can be summarized by figure 59, given in the case of a mixing in the stop sector leading to $m_h^{\max}$, the most conservative case, and the case of no mixing in the stop sector. The no mixing scenario is almost completely ruled out. Lower limits for m_h and m_A, as well as excluded values for $\tan\beta$ (for $m_t = 174.3$ GeV), are given in table 13 for two scenarios of mixing. **The final truth will depend on the actual m_t value.**

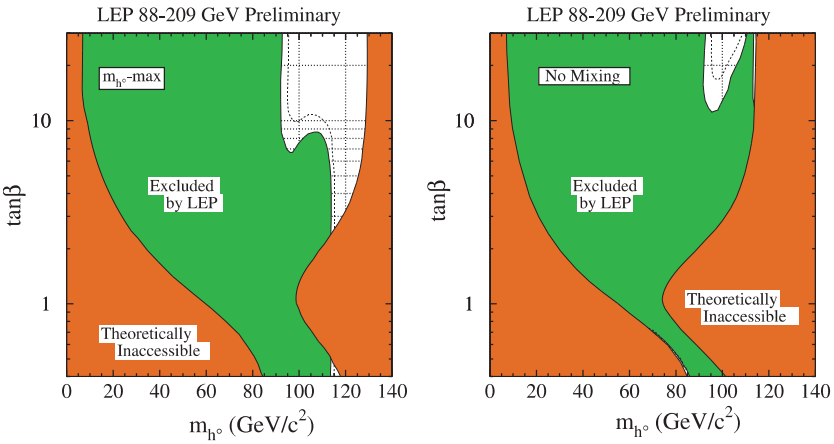

Figure 59. Excluded regions in the plane of m_h versus $\tan\beta$ for (left) the $m_h^{\max}$ case and (right) the no-mixing case. From [355].

Table 13. Obtained and expected (in parentheses) exclusion limits at 95% CL on Higgs masses and $\tan\beta$ from the combination of LEP experiments. From [355].

Scenario	m_h bound (GeV)	m_A bound (GeV)	$\tan\beta$ range excluded
$m_h^{\max}$	91.0 (94.6)	91.9 (95.0)	0.5–2.4 (0.5–2.6)
no mixing	91.5 (95.0)	92.2 (95.3)	0.7–10.5 (0.8–16.0)

Among all searches for non-conventional Higgs bosons [355], let us quote first the invisible one. There may be several reasons why it could be so. The boson could decay into neutralinos, although this is almost excluded for the MSSM with universality. One may also invoke TeV gravity, Higgs decay into majorons [356] or the SM with a singlet. For LEP, detecting such a boson is not much of a problem, since the bilan of energy–momentum can be properly done. The main background is ZZ, with one Z decaying in neutrinos, and the possibility of reducing it through b-tagging is lost. The ADLO limit is presently 114.2 GeV, assuming the SM cross-section and that the Higgs decays exclusively into invisible final states.

For what concerns a flavour-blind search, relevant for alternative scenarios, like those which involve the radion hypothesis [48,50], the combined LEP limit is presently $\geqslant$ 112.9 GeV.

LEP epilogue: a look at figure 53 (or equivalently to several other figures of this review showing h^0 iso-mass curves) shows that, concerning the MSSM, 10 to 15 GeV more in the centre of mass energy (i.e. 1.33 times the number of RF cavities in the equipped straight sections) would have been needed to get a meaningful answer about its validity, if the top mass is not far from its assumed value of 175 GeV.

The non-observation of h^0 up to the present limit has been analysed in terms of the degree of fine tuning required among the SUSY parameters, as discussed in 5.3.3. We note, however, that this was done in the spirit of low $\tan\beta$, an assumption which was then prevailing, but has no very solid justification. **The conclusion to be drawn from LEP is rather that the MSSM is still a viable possibility, but with intermediate or large** $\tan\beta$.

Supersymmetry offered the possibility of achieving **baryogenesis at the electroweak scale** by providing a potentially stronger electroweak phase transition and larger CP violating phases. The situation is summarized in [357]. In the MSSM, in addition to a particular tuning

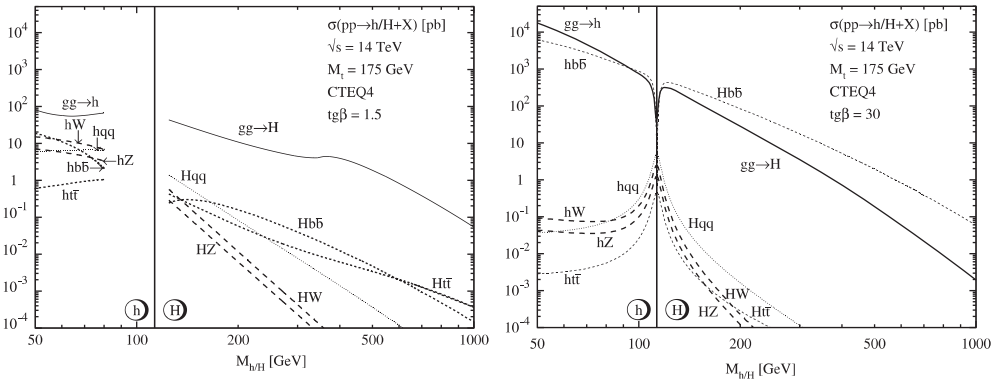

Figure 60. SM Higgs production cross-section in pb for various processes at the LHC as a function of the Higgs mass. From [318].

of parameters, electroweak baryogenesis requires a light h^0: with the present limit on m_h, it still works (up to $m_h \simeq 120\,\text{GeV}$) provided the right-handed stop mass is very light ($< m_t$) and the left-handed stop heavy. The idea is not yet ruled out, but is close to being so. Here again, the exploration of a few more GeV for the h^0 mass would have been decisive. On the contrary, 'life is easier' in the NMSSM [358], where a singlet Higgs field is present and where it is not difficult to make the electroweak phase transition stronger. As stated previously, the present trend is to favour another version of the baryogenesis scenario, as a consequence of leptogenesis at a much higher scale.

8.7. Higgs production at hadron colliders

The most important processes for Higgs production at hadron colliders are gluon fusion, vector boson fusion, $q\bar{q}$ or qq scattering and Higgs radiation off top and bottom quarks, for which the production cross sections at the LHC are summarized in figure 60.

The dominant Higgs production mechanism is the gluon fusion $gg \to H$ through top-quark loops. The resulting leading order (LO) cross-section is a function of α_S^2 and exhibits a strong dependence of the renormalization scale μ. This scale dependence is reduced by evaluating the next-to-leading order (NLO) contributions, but this increases the cross-section by approximately 70%. It is therefore important to calculate it at the NNLO [359, 360] to increase the confidence in the result. These higher order calculations include new diagrams, some of which involve the emission of real gluons and affect not only the total cross-section, but also the topologies by introducing additional jets. Figure 61 compares the cross-sections as a function of the mass of a SM Higgs m_H, computed to LO (dotted curve), NLO (dot–dashed curve) and NNLO (solid line). The two curves for each case correspond to the choices of scale $\mu = m_H/2$ and $\mu = 2m_H$ and illustrate the reduced scale dependence of the NNLO calculation. The increase in cross-section from the NLO to the NNLO results is still about 30% and the global K-factor (ratio of NNLO to LO cross-section) is approximately 2 for the LHC and 3 for the Tevatron. A similar behaviour with the same increases in the cross-section from LO to NNLO calculations has been found for the production of the pseudoscalar Higgs A by gluon fusion [361] for $m_A \lesssim 300\,\text{GeV}$. The results for the production of the bosons H and A are valid for small and moderate tan β, else they are significantly affected by loops involving b-quarks.

For the Higgsstrahlung off top quarks, the cross-section is much smaller, as illustrated by figure 62. In this case, the QCD corrections computed at NLO decrease the cross-section

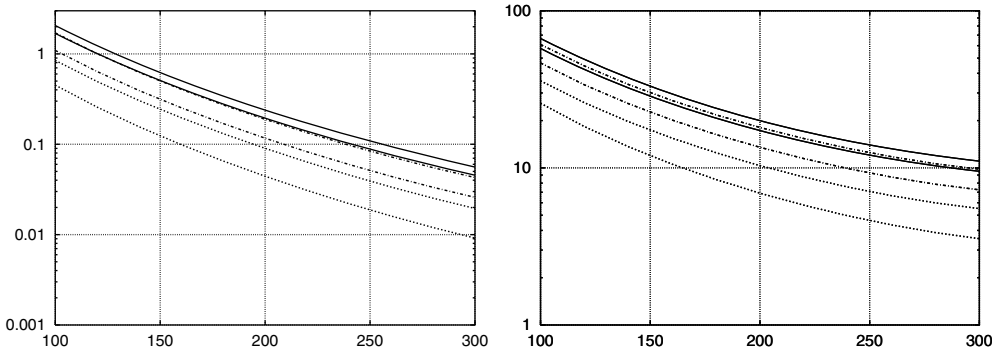

Figure 61. Higgs production cross-section in pb from gluon fusion at the Tevatron (left) and LHC (right) as function of the Higgs mass in GeV. Reprinted from [360]. Copyright 2002, with permission from Elsevier.

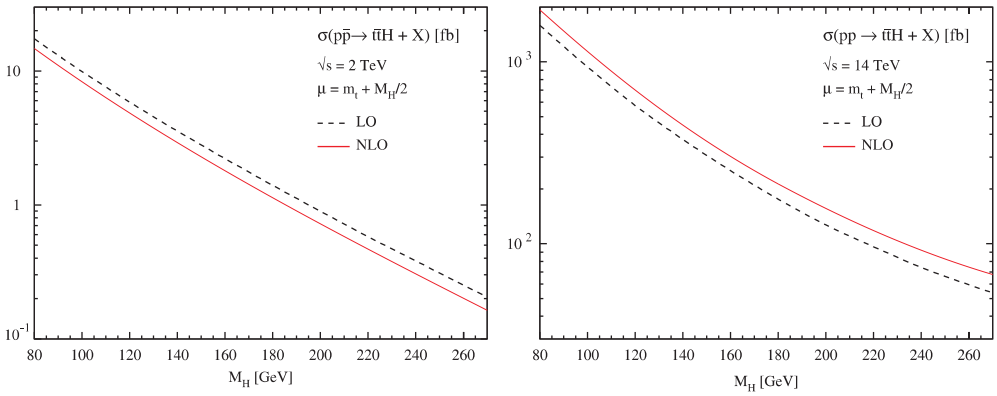

Figure 62. Higgs production cross-section in pb via Higgsstrahlung off top quarks at the Tevatron (left) and LHC (right) as a function of the Higgs mass [362].

at the Tevatron by about 20% and increase it at the LHC by 20–40%. The remaining scale dependence for the NLO result is not very large and it is considered [362] that the production rate is under proper theoretical control.

8.8. EWSB at the Tevatron

At the Tevatron the dominant production mode of the Higgs boson is through gluon–gluon fusion. This is not exploitable for $m_H \lesssim 130$ GeV, where the main decay mode is $h/H \to b\bar{b}$, because of the rate of background, but becomes usable for heavier Higgses whose decay is dominated by $h/H \to WW^*$. For low Higgs masses, one has to use the smaller production rate of the boson in association with a W or a Z, due to $q\bar{q} \to Wh/H$.

For a low mass boson, below 130 GeV, beauty is still the dominant decay and the modes looked for are those of LEP, plus $\mathrm{l}\,\nu\,\mathrm{b}\,\bar{\mathrm{b}}$ from WH production. Obviously proton and antiproton remnants are also present in the final state. Above 130 GeV, simpler modes like $\mathrm{l}^+\mathrm{l}^-\,\nu\,\nu$, coming from H decay into W W*, are searched for.

Preliminary results have been made available from run II [363] which, per experiment, are typically 50 times above the SM expectation (for $M_H = 120$ GeV) (figure 63 left). One must therefore gain a large cumulative factor in the effective integrated luminosity. The gain

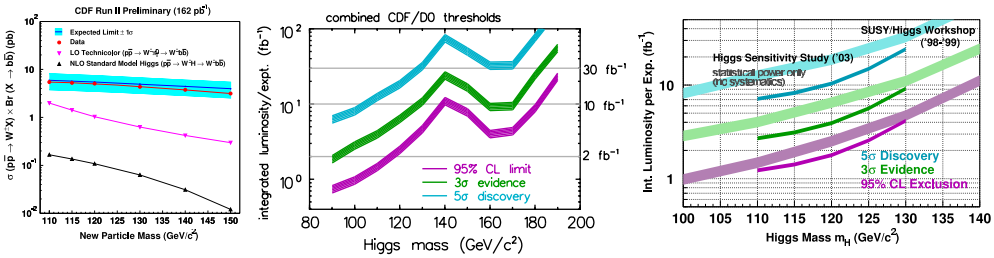

Figure 63. (left) Limits on the SM Higgs from CDF Run II [363]. (centre) The expected reach of the Tevatron in SM-like Higgs search [364]. (right) The same for the light Higgs mass region [365].

expected in run II from increasing the luminosity, combining the two experiments, increasing their geometrical acceptance as well as their b-tagging and trigger efficiencies, improving the di-jet mass resolution and refining the analyses is indeed quite impressive, of the order of 600 [364] compared with run I. Figure 63 (right) summarizes the expected reach of the Tevatron. If this is achieved, the 95% CL exclusion limit for the Higgs would be 115 GeV for $2\,\mathrm{fb}^{-1}$. With $10\ \mathrm{fb}^{-1}$, this exclusion limit can be pushed to 180 GeV. A 5 sigma discovery is possible for 110 GeV and a 3σ evidence up to 130 GeV and in the range 155–175 GeV. Needless to say, this will not be an easy task, but it may be feasible and the numbers above represent one of several estimates. We mentioned in section 7.1 that such integrated luminosities, given the present problems of the Tevatron, are even beyond the optimistic side, unless the programme lasts much longer.

One should add that in SUSY some coverage of the parameter space at large $\tan\beta$ will be ensured through the study of the 4 b-jet channel, from the Higgsstrahlung production $b\bar{b}h$ [366]. It is, however, likely that at the Tevatron cascading from heavier sparticle states will not contribute to the h^0 rate.

It is clear that for the EWSB study at the Tevatron the best preparation, besides the detector improvements, consists in front line QCD studies, refining the cross-section estimates as well as several key distributions [367].

8.9. EWSB at the LHC

Here again the literature is abundant [368–370]. In brief, the discovery potential of LHC is wide, but, except for very simple channels, experimentation will be difficult. LHC will collide 7 TeV protons, providing parton collisions in the TeV CM region. The LHC programme opens the possibility of making a decisive step in our understanding of EWSB, by producing Higgs bosons, as well as superpartners, if any, or indicating what alternative to EWSB has been chosen.

A list of channels commonly investigated for the (SM-like) Higgs search is:

- $gg \to h/A \to \gamma\gamma$
- $gg \to h \to ZZ^{(*)} \to lll'l', llv\nu, lljj$
- $gg \to h \to WW^{(*)} \to lvlv, lvjj$
- $gg, q\bar{q} \to t\bar{t}h, h \to \gamma\gamma, W \to lv$
- $gg, q\bar{q} \to t\bar{t}h, h \to b\bar{b}\ W \to lv$
- $gg, q\bar{q} \to W/Zh, h \to \gamma\gamma$, leptonic decay of W, Z
- $gg, q\bar{q} \to W/Zh, h \to b\bar{b}$, leptonic decay of W, Z
- $qq \to qqWW \to qqh, h \to \gamma\gamma$

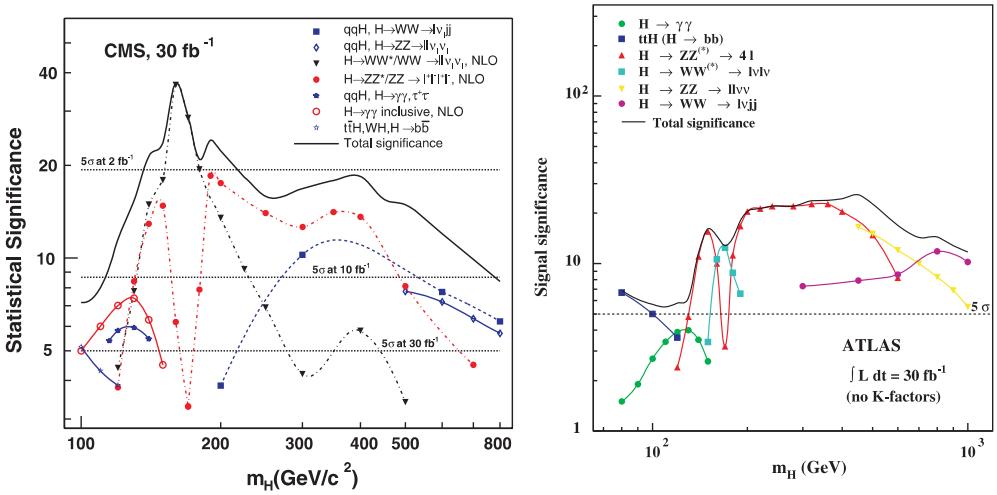

Figure 64. (left) Luminosity required for a 5σ discovery of a SM-like Higgs at LHC in CMS [369]. (right) Significance of the Higgs signal with 30 fb^{-1} in ATLAS [371].

- $qq \to qqWW \to qqh, h \to WW^{(*)} \to lvlv, lvjj$
- $qq \to qqWW \to qqh, h \to \tau\tau$
- $qq \to qqWW \to qqh, h \to \tilde{\chi}_1^0\tilde{\chi}_1^0$ (invisible).

The SM-like Higgs boson is produced singly by gluon–gluon interaction via a heavy quark loop and also in association with vector bosons and $t\bar{t}$, as illustrated in figure 60. For a light object, one decay mode exploited is the small (BR$\sim 10^{-3}$) mode gamma–gamma, a loop process. For recent NLO evaluations of its production, of the irreducible $\gamma\gamma$ background and about the treatment of the reducible one, see [359, 372]. The dominant $b\bar{b}$ decay mode is also exploited, but only for associated production like $t\bar{t}H$. More study is needed about the complementary $h^0 \to Z\gamma$ mode. At higher masses the WW and ZZ modes always dominate the t–$\bar{\text{t}}$ mode. Very elaborate studies have shown that, with $\sim$30 fb^{-1} (about three years at a luminosity of $10^{33}\,\text{cm}^{-2}\,\text{s}^{-1}$), one gets a significant signal over the full range of mass, as shown in figure 64.

An significant breakthrough fact was to realize the importance of the H to the WW channel, where both W decay leptonically: exploiting angular distributions, one can enhance the S/B and provide a very significant signature in the mass domain around 170 GeV [373], which could be covered with only a few fb^{-1}. **Another novelty was the exploitation of vector boson fusion (VBF)** (labelled qqH in figure 64 (left)), extended to the low mass region, where the Higgs boson is produced, accompanied by two forward jets. Figure 64 (left) shows the improvement obtained in this low mass region.

Yet another potential source for discovery could be provided by the production of squarks and gluinos. **If the hadronic sparticles are sufficiently light, they are produced abundantly and may have a sizeable branching ratio to h^0 in cascade decays via neutralinos.** In the MSUGRA framework, this is possible in a large part of the parameter space. It has even been shown that in a more general MSSM this process could also lead to the detection of the heavier Higgses, H^0 and A^0 [374].

With more luminosity, say 300 fb^{-1} per experiment (the nominal $10^{34}\,\text{cm}^{-2}\,\text{s}^{-1}$ during three 'years' of 10^7 s), one can start to give measurements of the SM Higgs mass ($\sim$0.1%) and of the Higgs width (better than 10%, for masses above 250 GeV) [375].

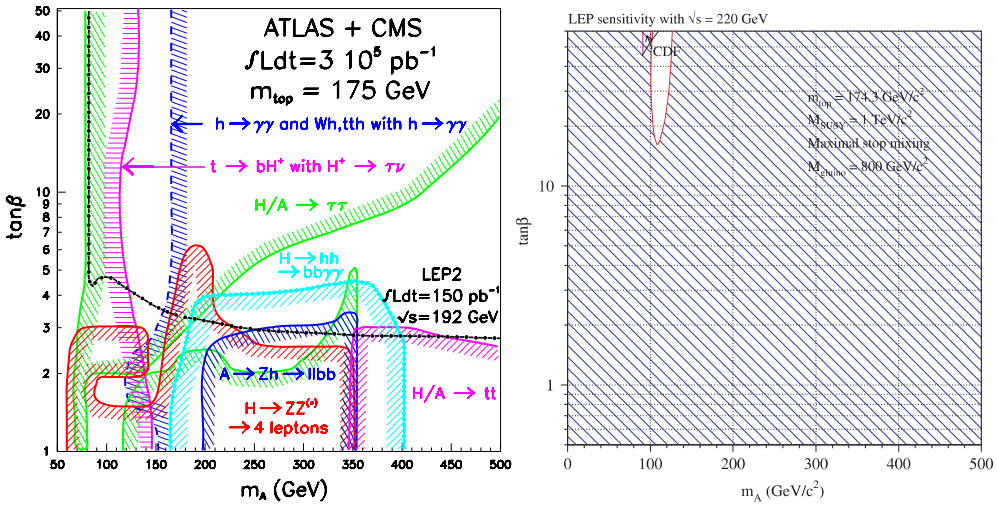

Figure 65. (left) Regions for Higgs discovery by the explorations of various final states at the LHC, from [368]. (right) The coverage of the same plane by a would-be 220 GeV LEP, from [376].

A complete coverage of the MSSM tan β–M_A plot can be achieved for a similar luminosity, by combining a large set of measurements (figure 65 left). LEP, if it had been pushed to ∼220 GeV, would have provided a larger coverage than LHC (figure 65 right), but could only discover the h^0. Given what has been actually achieved with the final LEP energy, there will exist some regions in the MSSM plane (say $M_A \sim 300$ GeV, $\tan\beta \sim 10$) where only one object in the Higgs sector (here the h^0) will ever be observed. There will also exist a region ($80 \leqslant M_A \leqslant 170$ GeV, $\tan\beta \gtrsim 4$) where the h^0, which is the only one for which a strong upper bound exists in the MSSM, is not accessible. In this case, the hope would be to discover it in the decay of a SUSY particle. As discussed in section 15.2, the LHC should generally see some of the superpartners, a chance of discovery of SUSY as well as a potential contribution to the h^0 yield.

If nature has chosen the composite way, the LHC also offers the possibility of studying vector boson scattering. The difficulty will depend on its behaviour, resonant or not. At LHC, one will have to use the gold-plated signature of VB leptonic decays, thus decreasing the available statistics. The authors of [30, 377] have given rates for various scenarios. For a ρ_T of $N = 4$ TC of 1.8 TeV (2.5 TeV), the author of [377] guesses a minimum luminosity of 200 (150) fb^{-1} to get a significance in the like-sign WW channel and of 44 (320) to get it in WZ. For a 4 TeV rho one needs 110 fb^{-1} in like-sign WW and there is no way in the WZ channel. See [377] for the details of the assumptions. The rates, for such an example, are clearly not overwhelming and it is likely that LHC will then only give a hint of what is going on. A VLHC or a multi-TeV lepton collider would be the right machine to say more about such a scenario.

8.10. EWSB at linear colliders

Figure 66 shows the physics scenery at a LC. At a few hundred GeV, one recognizes well the familiar LEP200 situation, with some increase in the role played by the rising fusion processes. But the differences will increase with energy and the CLIC multiTeV scenery may be very new compared with what we know, with events having many jets, b-hadrons flying up to 20 cm, boosted events, large backgrounds, etc.

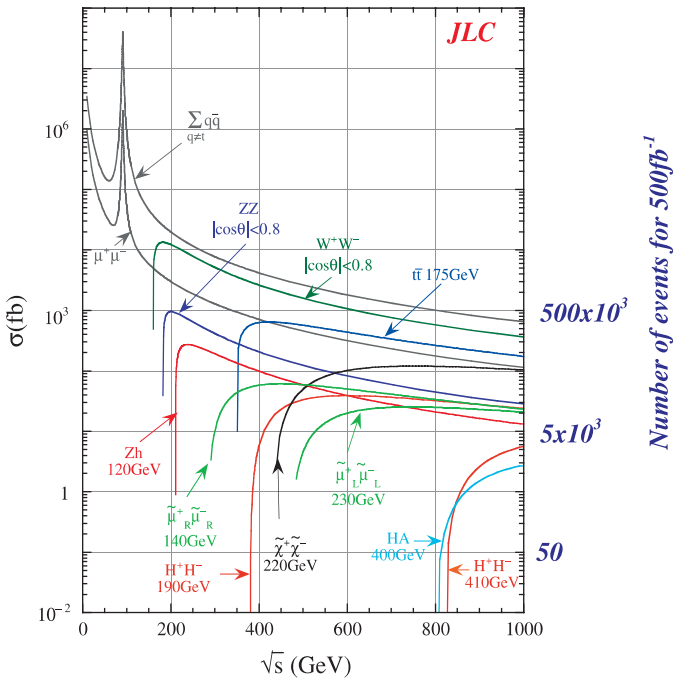

Figure 66. Scenery at a LC. From [378].

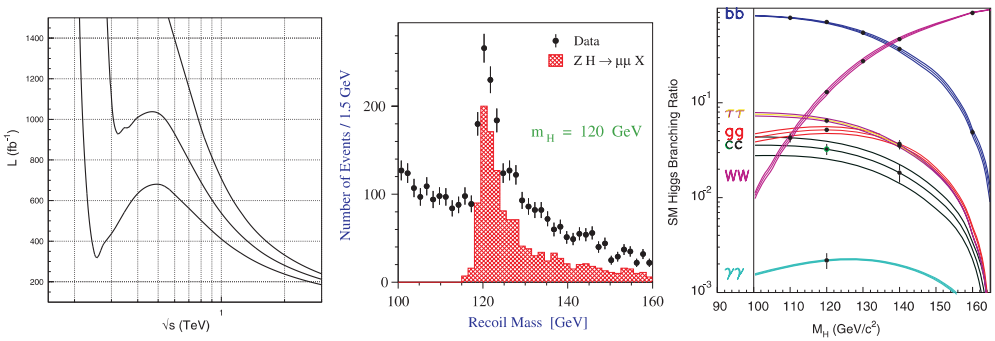

Figure 67. (left) Luminosity needed to produce 10^5 SM-like Higgs bosons at a LC. Masses considered are 120, 180 and 240 GeV. (centre) How this boson would appear. (right) Measurement of the Higgs branching ratios at a LC. From [380].

A first merit of a sub TeV LC [379] would be to provide the top mass with great accuracy, ∼150 MeV, from a threshold scan. Remember in particular that, through radiative corrections, $\Delta M_h \sim \Delta M_{\rm top}$.

Figure 67 (left) gives the luminosity needed to produce 10^5 SM-like Higgs bosons and figure 67 (centre) shows how such a boson would appear from a recoil mass measurement to $\mu\mu$ pairs. Let us note that, for a Higgs boson of ∼100 GeV, the fusion process takes over the Higgsstrahlung at $E_{\rm cm}$ ∼500 GeV. However the main role of a LC should be, once the boson has been discovered, which is likely to happen beforehand, to provide accurate measurements of its properties. Figure 67 (right) gives the accuracy with which one can obtain the Higgs

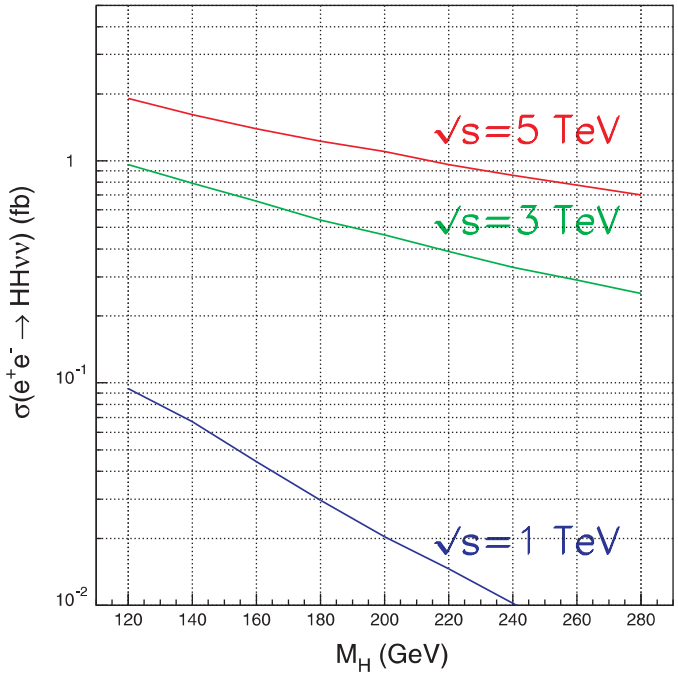

Figure 68. Cross-section of double Higgs production by fusion at e^+e^- colliders of various energies. From [382].

branching ratios, with 500 fb^{-1} (say two 'years' at nominal luminosity). The main systematic errors would come from our limited knowledge of basic quantities like the b and c running masses or α_S.

Several papers [323] have discussed the possibility of conspirations, in which some new effects beyond the SM mimic the effect of a light Higgs boson, while in reality the boson is heavier or composite: in the scenarios considered up to now, one always finds, given the constraints of the accurate measurements, that a boson should nevertheless exist below ∼500 GeV: the consensus is that a subTeV LC, maybe helped by a GigaZ, is thus likely to be sufficient to disentangle any of these possibilities.

In case light supersymmetry is a reality, it has also been shown that a LC would be a splendid machine to discover and measure most of what exists within its energy range [381], as we shall illustrate later. **A multiTeV collider can however add important information even to the properties of a light Higgs**, by reconstructing the potential of the Higgs field, for instance allowing the study of the triple Higgs coupling in the fusion process ee→HH$\nu\nu$ [382]. Figure 68 shows indeed the huge increase in the corresponding cross-section with CM energy. The multiTeV option may also be required to study rare Higgs decays and heavy Higgs states, if they happen to lie beyond 1 TeV. The $\gamma\gamma$ version of a multi TeV e^+e^- collider can produce these heavy Higgs states in the s-channel.

In the case of a dynamical symmetry breaking, if Nature is unkind to us and does not provide light conspicuous resonances, the situation may be more difficult: figure 69 (left), referring to vector boson scattering, and figure 69 (right), referring to W pair production, show the clear advantage of reaching higher energies. To fix the ideas, the ILC, at a CM energy of 500 (800) GeV, should see a 3.5 (6) standard deviation effect even in the case of a low energy

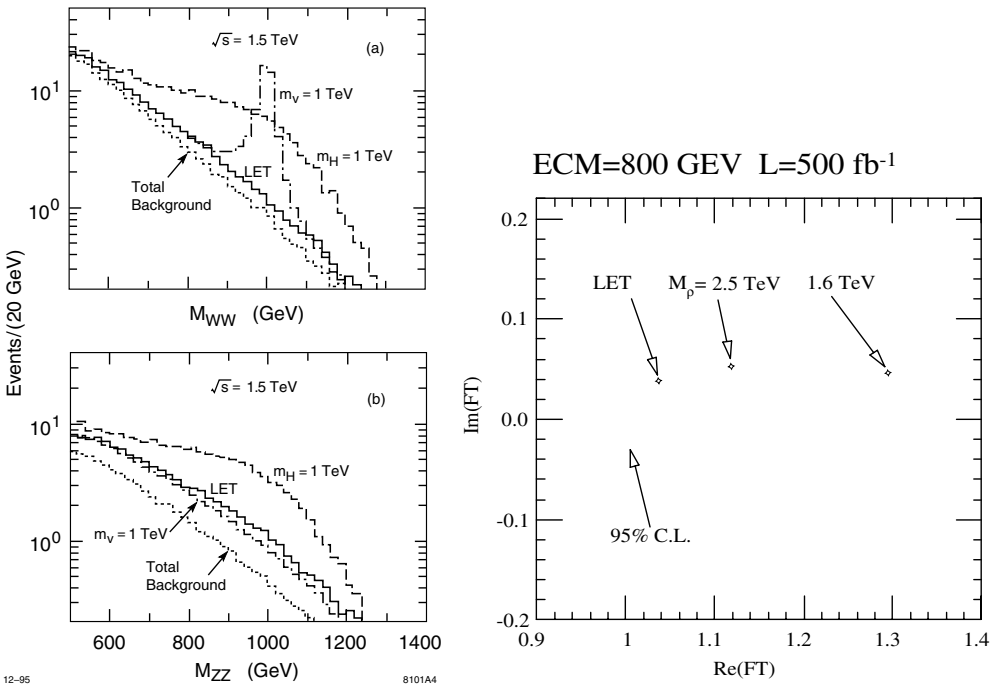

Figure 69. (left) The rate of events at a 1.5 TeV LC in WW and ZZ scattering, for 200 fb^{-1}: the scenarios are the LET, SM and chirally-coupled vector models. From [383]. right separability of the LET scenario and various technirho hypotheses from the SM at a 0.8 TeV LC. F_T is the technipion form factor. The contour around the point SM with light Higgs is at 95% confidence level. From [384].

Table 14. Summary of the reach of various accelerators. From [385].

Process	LHC 14 TeV 100 fb^{-1}	SLHC 14 TeV 1000 fb^{-1}	28 TeV 100 fb^{-1}	VLHC 40 TeV 100 fb^{-1}	VLHC 200 TeV 100 fb^{-1}	LC 0.8 TeV 500 fb^{-1}	LC 5 TeV 1000 fb^{-1}
Squarks	2.5	3	4	5	20	0.4	2.5
$W_L W_L$	2σ	4σ	4.5σ	7σ	18σ	6σ	90σ
Z'	5	6	8	11	35	8	30
Extra-dim ($\delta = 2$)	9	12	15	25	65	5–8.5	30–55
q^*	6.5	7.5	9.5	13	75	0.8	5
Λ compositness	30	40	40	50	100	100	400

theorems scenario. But a multiTeV machine would then be required to decipher the case as shown in table 14 from [385]. Similarly, the accuracy one can obtain on TGC's improves with the CM energy as one can read from figure 70. A goal one could aim at is to reach the level of the SM radiative corrections around few per mille.

8.11. EWSB: summary

Concerning details on Higgs studies at machines beyond the LHC we refer to [381, 379] for linear colliders and to [386, 387] for muon colliders for detailed discussions. Let us give here a crude summary of the potential of all the programmes.

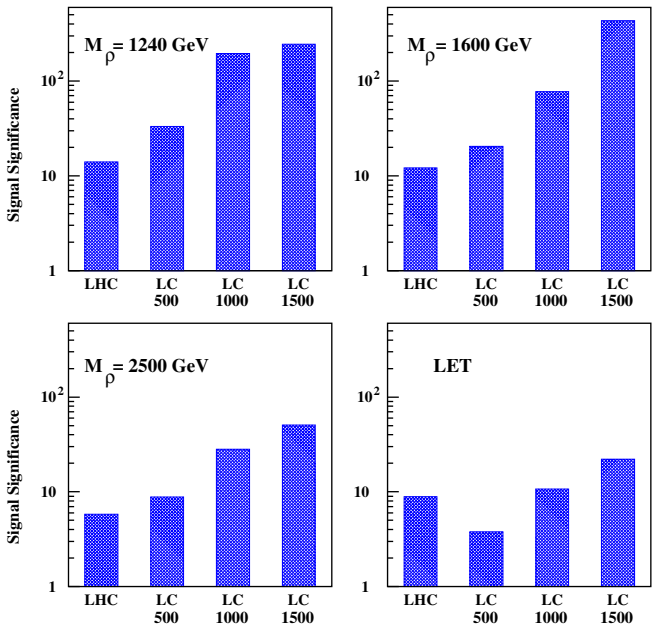

Figure 70. Strong symmetry breaking: signal significance at various collider energies. From [29].

For the SM-like Higgs we saw that, if it is not discovered at the Tevatron, it will be at LHC, with ∼10–30 fb^{-1} depending on the mass. With 100 fb^{-1} one can envisage at LHC some measurements of its mass, its width and, at ∼10%, of its production times decay rate into gamma–gamma and ZZ. At the LHC [388, 389], the non-vanishing of the Higgs self-coupling λ can be established at 95% CL but only for $150 \leqslant M_H \leqslant 200\,\text{GeV}$.

A 500 GeV LC can discover the boson up to 350 GeV, but this will have been done previously at the LHC. With 500 fb^{-1}, the LC can provide: its mass to 0.05%, its spin and parity, the Higgsstrahlung cross-section, therefore the ZZH coupling, to a couple of percent. Most of its decay fractions will be measured with good statistical precision: the dominant systematics will come from the uncertainty on b and c running masses and from α_S. Its total decay width can be estimated from its branching ratio into WW and the knowledge of the WWH coupling (from ZZH), with a ∼6% uncertainty. At a 500 GeV linear collider, for $M_H = 120\,\text{GeV}$, one can get a 20% measurement of the self-coupling λ with an extremely high luminosity ($2ab^{-1}$).

Much later a μ–μ collider could measure the Higgs boson line shape [386], as shown in figure 71. With 1000 pb^{-1} per year, for a 110 GeV boson, it would give the mass to ±0.1 MeV, the width to ±0.5 MeV, the cross-section to ±5%, without the systematic errors quoted previously.

For the MSSM we saw that LHC with 300 fb^{-1} will cover the whole parameter plane, as would a e^+e^- machine slightly above LEP energy. H and A bosons can only be discovered in parts of the parameter space. A LC and a μ–μ collider can then provide the needed precision studies.

For $V_\text{L}\ V_\text{L}$ strong scattering, the possibilities depend much on the scenario, resonant or non-resonant [31]. LHC or a 800 GeV LC may observe it, or have a hint of what goes on. For instance, as we said, at a 800 GeV linear collider, a 6σ effect is expected in the non-resonant LET case. But it is not unlikely that the right machine to perform quantitative work on such a

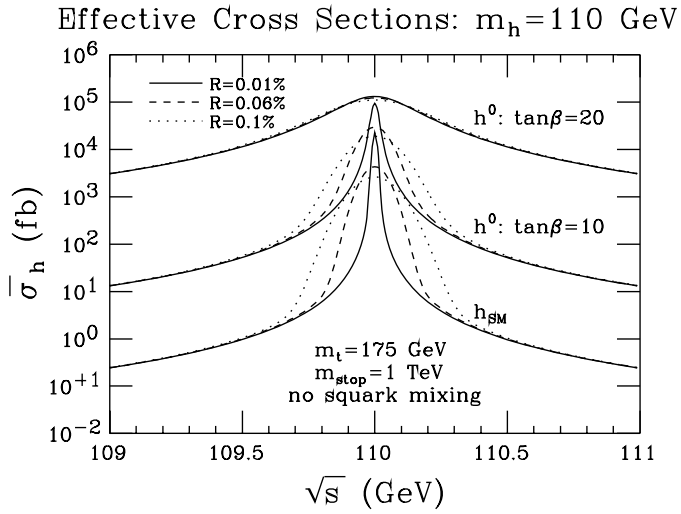

Figure 71. Higgs cross section at a muon collider for several assumptions of the beam resolution $R = \Delta E_b/E_b$. From [386].

scenario, especially if no resonance shows up, has to be a multi-TeV lepton collider, CLIC, a μ–μ collider or a very large hadron collider (VLHC).

Let us hope that nature will not leave us waiting for so long, that the indirect indications of a light Higgs are correct and that such an object will reveal itself in the next machine.

9. SUSY particle decays and signatures[20]

9.1. Sfermion mixing

The left and right sfermion **interaction eigenstates** can mix, due to an off-diagonal term in their mass matrix which is given by $a_u m_u = m_u(A_u - \mu \cot\beta)$ or $a_d m_d = m_d(A_d - \mu \tan\beta)$ for up-type and down-type states, respectively. For the first two generations, the fermion masses are small and the mixing can, therefore, be neglected. For the third generation leptons and quarks, the mixing may be important. This will shift the mass of the lighter mass eigenstate down and possibly make it the lightest sfermion.

Most expressions in this section will be written for sfermions in general, as they equally apply to sleptons and squarks. Moreover, when refering to chargino and neutralino states, their numbering will be in order of increasing mass.

The mass eigenstates of sfermions are related to their interaction eigenstates by:

$$\begin{pmatrix} \tilde{f}_1 \\ \tilde{f}_2 \end{pmatrix} = \begin{pmatrix} \cos\theta_{\tilde{f}} & \sin\theta_{\tilde{f}} \\ -\sin\theta_{\tilde{f}} & \cos\theta_{\tilde{f}} \end{pmatrix} \begin{pmatrix} \tilde{f}_L \\ \tilde{f}_R \end{pmatrix},$$

where the mixing angle $\theta_{\tilde{f}}$ can be expressed in terms of the masses and mixing parameters, see [390].

The decay branching ratios can be computed by programmes like SDECAY [313] or any of the other SUSY generators.

[20] In this report, when considering neutralinos and charginos, the tilde, signalling a sparticle, is frequently omitted for simplicity.

9.2. Slepton decay

The sleptons can decay according to

$$\tilde{l}^{\pm} \to l^{\pm}\chi_i^0,\ \tilde{l}^{\pm} \to \nu\chi_i^{\pm}. \tag{132}$$

The decay of $\tilde{e}$ or $\tilde{\mu}$ is rather simple as there is no mixing between L and R states and the Yukawa couplings are negligible. It corresponds to a $(\lambda\phi\psi)$ transition (figure 3) to a gaugino-like χ^0 or $\chi^{\pm}$ with a width given in [391] and its phenomenology is easily read off from figure 15.

- In the deep gaugino region, $M_2 \ll |\mu|$, the LSP $= \chi_1^0$ is mostly bino-like and the χ_2^0 and $\chi_1^{\pm}$ are mostly wino-like. The $\tilde{l}_{\mathrm{R}}$ coupling to the χ_2^0 or $\chi_1^{\pm}$ is suppressed, even if they are kinematically accessible and the decay is predominantly to the bino LSP. On the contrary, the $\tilde{l}_{\mathrm{L}}$ has a non-negligible branching ratio into χ_2^0 and $\chi_1^{\pm}$ if they are kinematically accessible. Hence, cascade decays with additional leptons and/or hadrons will play an important role. A somewhat unexpected consequence might be a large hadronic branching ratio in slepton decay.
- In the higgsino region, $|\mu| < M_1$, the LSP $= \chi_1^0$ and the $\chi_1^{\pm}$ are both higgsino-like, whereas the χ_2^0 (or $\chi_{3,4}^0$ when M_2 is large) is gaugino-like. If allowed by kinematics, the sleptons decay preferentially to χ_2^0 (or $\chi_{3,4}^0$). This is the region where the branching ratio for $\chi_2^0 \to \chi_1^0 + \gamma$ is important.

The $\tilde{\tau}$ decay is more complicated as it can be mediated by a vertex of the type $(\lambda\phi\psi)$ (figure 4), leading to a gaugino, or a Yukawa coupling $(\tilde{H}\phi\psi)$, leading to a higgsino. The $\tilde{\tau}$ decay phenomenology will therefore vary strongly with the composition of the low mass neutralinos and chargino. The $\tilde{\tau}$ decay branching ratios can be understood qualitatively as follows, assuming that the gaugino mass unification holds.

- In the deep gaugino region, $\tilde{\tau}$ decays are dominated by their gauge couplings and their phenomenology is the same as for $\tilde{e}$ or $\tilde{\mu}$.
- In the higgsino region, $M_2 \gg |\mu|$, the LSP $= \chi_1^0$ and the $\chi_1^{\pm}$ are both higgsino-like and nearly mass degenerate. Decays to these states through gauge couplings are suppressed and the dominant contribution is from Yukawa couplings, especially when $\tan\beta$ is large. For a $\tilde{\tau}_{\mathrm{R}}$, the branching ratios to χ_1^0 and to $\chi_1^{\pm}$ are of comparable magnitude. For a $\tilde{\tau}_{\mathrm{L}}$, the coupling $\tilde{\tau}_{\mathrm{L}} - \nu_\tau - \chi_1^{\pm}$ vanishes due to the chirality flip of the higgsino coupling. The branching ratio is about 100% into the LSP. Although the decay to χ_2^0 is not phase space suppressed (χ_2^0 is nearly degenerate with χ_1^0 and $\chi_1^{\pm}$) it plays no role in the decay of $\tilde{\tau}_{\mathrm{L}}$ nor $\tilde{\tau}_{\mathrm{R}}$ [390].

The $\tilde{\nu}$ decays to a neutralino or chargino through a reaction similar to (132). When it decays directly to $\nu\tilde{\chi}_1^0$, it remains unobservable. However, it may have a significant branching ratio to charginos or heavier neutralinos as soon as they are kinematically accessible, making it detectable.

9.3. Squark decay

Squarks have a large number of potential decay modes, depending on their masses relative to the other SUSY particles. If the gluino is lighter than the squark, the decay

$$\tilde{q} \to q + \tilde{g} \tag{133}$$

proceeds at strong interaction strength and will predominate. In the MSUGRA scenario, this condition is met in the region approximately defined by $m_0 \gtrsim m_{1/2}$ (for the first two

generations), as can be verified using the mass relations (90) and (79). Otherwise, squarks will decay through electroweak interactions.

$$\tilde{q} \to q\tilde{\chi}_i^0, \tilde{q} \to q'\tilde{\chi}_i^{\pm}. \tag{134}$$

For the first two generations, the decays are determined by the gauge couplings and are rather simple. In the gaugino-like region, the right squarks decay according to $\tilde{q}_R \to \tilde{\chi}_1^0 q$ with 100% branching ratio and the left squarks to $\tilde{q}_L \to \tilde{\chi}_2^0 q$ and $\tilde{q}_L \to \tilde{\chi}_1^{\pm} q'$ in ratios of approximately 1/3 and 2/3, respectively.

If the mass differences between the sfermions are sufficiently large, they may decay into each other

$$\tilde{q} \to \tilde{q}' + W^{\pm}, H^{\pm}, \tilde{q}_2 \to \tilde{q}_1 + Z^0, H^0, \tag{135}$$

where the decay to a vector bosons proceeds via a $(A\phi\phi)$ gauge coupling, whereas the decay to a Higgs corresponds to a Yukawa coupling (and thus depends strongly on $\tan\beta$). These decays are most relevant for the third generation sfermions.

For the squarks of the third generation, decays mediated by Yukawa couplings cannot be neglected [392]. They will reduce the branching ratio for the decay to gluino, even if it is lighter than the squarks, and enhance decays to charginos and neutralinos. They have non-negligible branching ratios to the heavier neutralinos and chargino (higgsino-like in MSUGRA), giving rise to cascades. For sufficient mass separation, the heavier squarks may have large decay branching ratios to the $\tilde{t}_1$ with the emission of a W, a Z^0 or a h^0.

SUSY-QCD corrections to the squark decays have been calculated, see [393] (and references therein).

9.3.1. Stop decay modes. If kinematically allowed, the decay $\tilde{t}_1 \to t + \tilde{g}$ predominates. If the $\tilde{g}$ is too heavy to participate in the $\tilde{t}$ decay, the weak decays

$$\tilde{t} \to b\chi_1^+, \qquad \tilde{t} \to t\tilde{\chi}_i^0 \tag{136}$$

can take place. The decay modes with a top quark in the final state require a heavy stop, not observable at LEP. For large stop mixing the $\tilde{t}_1$ can be lighter than the top quark and the decay could proceed through

$$\tilde{t}_1 \to b\chi_1^+, \qquad \tilde{t}_1 \to c\chi_1^0. \tag{137}$$

At LEP, the direct decay into chargino, if kinematically allowed, would have close to 100% branching ratio. This decay is limited to region I of figure 72. If $m(\tilde{t}_1) < m(\tilde{\chi}_1^{\pm}) + m(b)$, the flavour changing decay into $c + \tilde{\chi}_1^0$ will have pratically 100% branching ratio. This decay proceeds through loop diagrams (see [394]) mediated by a pair $(b\tilde{W})$ or $(\tilde{b}W)$. These loops involve the electroweak coupling twice and the CKM matrix element K_{bc}. The width is then expected to be small compared with $\Gamma_{had} \simeq 200\,\text{MeV}$, the width corresponding to the hadronization time of order 10^{-23} s. Hence, the $\tilde{t}_1$ would hadronize into colourless $(\tilde{t}_1\bar{q})$ or $(\tilde{t}_1 qq)$ s-hadrons before decaying, as is the rule for quarks in the SM. Such decays dominate in region III of figure 72. Decays to χ_2^0 can also take place in region II.

If $m(\tilde{l}) < m(\tilde{t}_1)$ or $m(\tilde{\nu}) < m(\tilde{t}_1)$, the three-body decays $\tilde{t}_1 \to b\tilde{l}^+\nu$ or $\tilde{t}_1 \to b\tilde{\nu}l^+$, mediated by the exchange of a $\tilde{\chi}_1^{\pm}$, may compete with the $c\tilde{\chi}_1^0$ decay.

If the mass differences are sufficient, other decays with usually small branching ratios, may also participate, like $\tilde{t}_i \to \tilde{b}_j W^+(H^+)$ or $\tilde{t}_2 \to \tilde{t}_1 Z^0(h^0, H^0, A^0)$.

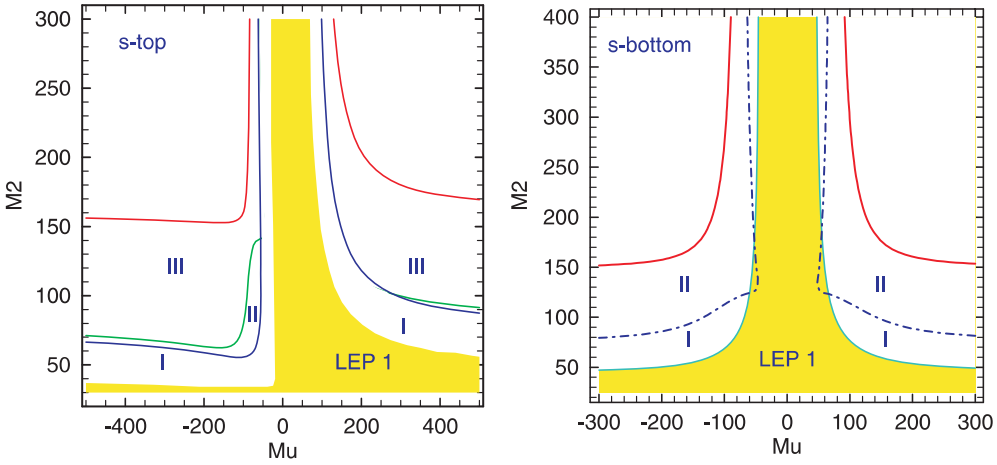

Figure 72. Decay modes of stop (left) for $\tan\beta = 2$ and sbottom (right) for $\tan\beta = 40$ in the M_2 versus μ plane, from [338]. A squark mass of 80 GeV is assumed.

9.3.2. Sbottom decay modes. Assuming the gluino to be heavier than the sbottom, the main decay mode expected is

$$\tilde{b}_1 \to b\tilde{\chi}_1^0. \tag{138}$$

The decay into χ_2^0 is also possible in the parameter region approximately given by M_2 or $|\mu|$ less than $m(\tilde{b}_1) - m(b)$ (region I of figure 72). This will give rise to cascade decays. The phenomenology of $\tilde{b}$ decays is very similar to the one encountered for the $\tilde{\tau}$.

As for the $\tilde{t}_1$, the decay width of $\tilde{b}_1$ can also be less than the hadronization width, especially for large $|\mu|$ where the (weak) gauge couplings determine the decay strength or when the Yukawa couplings are not enhanced by a large $\tan\beta$.

As the $\tilde{t}_1$ is often the lightest squark, the decay mode

$$\tilde{b} \to \tilde{t}_1 W^- \tag{139}$$

may also contribute significantly.

Other decays with smaller branching ratios, analogous to the ones for the $\tilde{t}$, may also contribute.

9.4. Gluino decays

If the gluino is heavier than at least one squark, the decay proceeds as

$$\tilde{g} \to \tilde{q} + \bar{q} \tag{140}$$

with democratically distributed branching ratios into the various flavours and chiralities. As the $\tilde{t}_1(\tilde{b}_1)$ is often considerably lighter than the other squarks, its branching ratio may be enhanced by phase space.

If the gluino is lighter than any squark, the main decays are through weak interactions mediated by a virtual $\tilde{q}$

$$\tilde{g} \to \tilde{\chi}_i^{\pm} q\bar{q}', \tilde{g} \to \tilde{\chi}_i^0 X, \tag{141}$$

where X is $q\bar{q}$ or g (the latter being a loop decay). These decays have been studied neglecting Yukawa couplings or taking into account the top Yukawa coupling for decays into quarks of

the third generation. In [392], the case of large tan β has been treated completely, including the bottom Yukawa coupling, as well as $\tilde{b}$ and $\tilde{t}$ mixing.

In well chosen mass windows, special modes are selected, such as, $\tilde{g} \to \tilde{b}_1\bar{b}$ when $m_{\tilde{b}_1} + m_b < M_{\tilde{g}} < m_{\tilde{q}}$, where $\tilde{q}$ is any other squark than $\tilde{b}_1$. One can even have a situation where a three-body decay mode, like $\tilde{g} \to \tilde{t}_1\bar{b}W^-$, is important or dominant if the necessary mass hierarchy is satisfied [395].

When squarks are very heavy, like in the split supersymmetry scenario, the above decay modes which are all mediated by squarks will be strongly suppressed (see section 5.3.4). The gluino lifetime, given approximately by formula (74), can be long enough [146] to hadronize before decaying and to form colourless bound states, called R-hadrons, of the types $\tilde{g}q\bar{q}$ (R-mesons), $\tilde{g}qqq$ (R-baryons) or $\tilde{g}g$ (R-gluons), which can be charged or neutral. They will propagate through the detector losing energy by hadronic interactions or by ionization if they are charged. They may also undergo charge exchange interactions (e.g. $\tilde{g}d\bar{d} + uud \to \tilde{g}uud + d\bar{d}$) which flip their charge between charged and neutral possibly several times along their flight path. The hadronic interaction probability of the gluino itself with the quarks in the detector material is small, as it is suppressed by the inverse square of the mass. Hence it can be viewed as the interaction of the cloud of light partons surrounding the gluino [396,146]. In this picture, the mean energy loss $\langle \Delta E \rangle$ per interaction depends only on the velocity β of the R-hadron. As a consequence, the fraction of energy lost per interaction will be very small. Using simple models for the cross section calculation [146], it is expected that $\langle \Delta E \rangle \simeq k\gamma$ ($\gamma = E/m$) with, for instance, k around 0.3 GeV and an interactions length of about 19 cm in iron. In a typical hadron calorimeter of about 1 m thickness, a R-hadron of 200 GeV mass and 800 GeV energy would lose only 6 GeV. A slow charged R-hadron will also undergo energy loss by ionization, which follows the usual Bethe–Bloch formula and dominates over nuclear interactions in the region $\gamma \lesssim 1.5$.

9.5. Chargino and neutralino decays

The two-body decays of the charginos and neutralinos are presented below. They are usually dominant. But there exist regions of the parameter space where they are suppressed and the decays are dominantly three-body, e.g. $\tilde{\chi}^{\pm} \to \tilde{\chi}^0_1 f \bar{f}'$ and $\tilde{\chi}^0_2 \to \tilde{\chi}^0_1 f \bar{f}$.

9.5.1. Chargino decay modes. **Decays into sleptons.** Provided the chargino contains at least a small wino component it may decay, similarly to the W in the SM, into a (fermion, scalar) pair with a coupling ($\lambda\phi\psi$) of weak interaction strength. Since the squarks are usually heavier than the sleptons, the most likely decay will be into a (lepton, slepton) pair:

$$\chi_i^{\pm} \to \tilde{\nu} + l, \tilde{l} + \nu \tag{142}$$

(assuming the slepton to be lighter than the chargino). In the gaugino region, it will predominate over the decays mediated by a W, as in case 1 of figure 19. As the coupling in the decay (142) is exclusively to winos, only left sleptons and leptons are obtained. The sleptons will further decay into their lepton partner and a neutralino. This reaction could, therefore, significantly increase the leptonic branching ratio above the value of 1/3 expected for Ws. Conversely, a lower branching ratio would be obtained in case squarks would be lighter than the chargino.

Even if the decays to sfermions are not allowed kinematically, the slepton diagrams can still contribute and interfere with the decays via W and they have to be included in the calculation of the branching ratios. For example, in the region $-\mu \simeq M_2 \leqslant 100$ GeV, the leptonic branching ratio may become very small due to destructive interference [397].

When the chargino is pure higgsino, it can still decay into sleptons, but only via a $(\tilde{H}\phi\psi)$ Yukawa coupling. It would almost exclusively lead to $\tilde{\nu}_\tau\tau_R$ and $\tilde{\tau}_R\nu_\tau$ final states and can become competitive with the decays into vector bosons only for large $\tan\beta$.

Decays into SM vector bosons . A wino-like chargino may decay through a $(A\lambda\lambda)$ gauge coupling to a vector boson and a wino. A higgsino-like chargino has a $(A\psi\psi)$ vertex leading to a vector boson and a higgsino. Both have electroweak strength:

$$\begin{aligned}&\tilde{\chi}_i^\pm \to \tilde{\chi}_j^0 + W^\pm,\ W^\pm \to f\bar{f}'\\&\tilde{\chi}_2^\pm \to \tilde{\chi}_1^\pm + Z^0,\ Z^0 \to f\bar{f}\end{aligned} \tag{143}$$

and the decay takes place via an on- or off-shell W or Z^0. Transitions from gaugino-like (higgsino-like) charginos to higgsino-like (gaugino-like) neutralinos are suppressed. This decay is dominant in the higgsino-like region. In the gaugino-like region, the gaugino mass universality condition $M_2 \simeq 2M_1$ implies that the lightest chargino and the lightest neutralino are respectively wino- and bino-like, as can be verified in figure 15, and this decay is not favoured. It may nevertheless take place via the (possibly small) wino component of the lightest neutralino if other decay modes, e.g. to sleptons, are suppressed.

If sfermions are heavy, like in case 2–4 of figure 19, the lightest chargino decays directly to χ_1^0 and a (possibly virtual) W, giving a (jet+jet) or a (charged lepton+neutrino) pair with the W branching fractions.

There is a region approximately defined by $-M_2 \leqslant \mu \leqslant -M_1$ where $M(\chi_2^0) < M(\chi_1^+)$ (see figure 15), the χ_1^+ and χ_2^0 are both higgsino-like and the χ_1^0 is gaugino-like. In this region, the χ_1^+ can first decay into χ_2^0 which will in turn decay to χ_1^0. When M_2 is not too large ($\leqslant$200 GeV), these cascade decays can reach 30% branching ratios. They yield final states involving more leptons and/or jets. For small $\tan\beta$, the χ_2^0 decays in part of this region preferentially into $\chi_1^0 + \gamma$, giving instead topologies with a hard isolated photon. For larger values of M_2, the χ_1^+ becomes nearly degenerate with the χ_2^0 and the cascade decays are suppressed by phase space.

The heavier chargino, χ_2^+, could also decay directly into χ_1^0, but in most of the parameter space, when the χ_2^+ is dominantly gaugino the χ_1^0 is dominantly higgsino and viceversa. This enhances the branching fraction for the decay via χ_1^+ or χ_2^0 which would again give rise to cascade decays with complicated final state topologies.

Decays into Higgses. Finally, charginos could decay via a $(\lambda\phi\psi)$ gauge coupling into Higgses:

$$\begin{aligned}&\chi_i^\pm \to \chi_j^0 + H^\pm,\ H^\pm \to f\bar{f}'\\&\chi_2^\pm \to \chi_1^\pm + H^0,\ H^0 \to f\bar{f}.\end{aligned} \tag{144}$$

Such vertices induce transitions from gaugino to higgsino states and vice versa. The experimentally most favourable decay would be the second one in (144) with H^0 being the h^0, the lightest of all Higgs states. This decay might dominate over the decay via vector bosons in the region where $|\mu| > M_2$, provided the h^0 is sufficiently light [398]. Examples of $\tilde{\chi}_2^\pm$ decays to h^0 are found in cases 1 to 3 of figure 19. But, given the excluded mass range for the h^0, this would require a too heavy chargino to be observable at LEP.

The decays will end into a χ_1^0 LSP either directly or through cascading.

In the case of heavy scalars, like in split supersymmetry (see section 5.3.4), the only available decay modes will be through vector bosons or the light Higgs.

9.5.2. Neutralino decay modes. **Decays into sleptons.** The zino component of the neutralino can give rise to a decay, similar to a Z^0 in the SM, into a (fermion, scalar) pair with a coupling

($\lambda\phi\psi$) of weak interaction strength. Assuming the sleptons to be lighter than the squarks and lighter than the neutralino, the most likely decay will be into a (lepton, slepton) pair:

$$\chi_i^0 \to \tilde{l} + l, \tilde{\nu} + \nu \tag{145}$$

This decay is important for a χ_2^0 in the deep gaugino region. In case of large $\tilde{\tau}$ mixing, the decay to $\tilde{\tau}_1$ may be favoured over the other sleptons by phase space. The sleptons will further decay into their SM partner and the LSP, leading to final states where both leptons are of the same flavour. A contribution from this decay is the only possibility to obtain a sizeable ($\geqslant$ 10%) leptonic branching ratio. Note that the $\tilde{\nu} + \nu$ final state will often be invisible.

Decays into Z^0s. The higgsino component of a neutralino may trigger a decay via the ($A\psi\psi$) coupling to

$$\chi_i^0 \to \chi_j^0 + Z^0, Z^0 \to f\bar{f}, \tag{146}$$

the Z^0 being on- or off-shell. The gaugino component of a neutralino cannot induce such a decay as the coupling of a ($A\lambda\lambda$) vertex is zero. This decay is dominant for the χ_2^0 in the higgsino-like region, but is suppressed elsewhere. It may nevertheless take place in the gaugino-like region when all other χ_2^0 decays are closed. It may also be important in the gaugino-like region for the heavier neutralinos, e.g. $\chi_3^0 \to \chi_2^0 + Z^0$. For this decay mode, the branching ratio into jets is about 70% and into charged leptons about 10%. Both leptons are of the same flavour.

Decays into Ws . Alternatively, the gaugino or higgsino component of a heavy neutralino can induce a decay through, respectively, a ($A\lambda\lambda$) or a ($A\psi\psi$) vertex into:

$$\chi_i^0 \to \chi_1^\pm + W^\mp, \qquad W^\pm \to f\bar{f}' \tag{147}$$

with an on- or off-shell W. It gives rise to cascade decays, via the decay of the $\chi_1^\pm$, with 4 fermions in the final state and an accompanying χ_1^0: 4 jets+χ_1^0 (with BR=4/9), $l\nu$+2 jets+χ_1^0 (with BR=4/9) or $2l + 2\nu + \chi_1^0$ (with BR=1/9). In the $2l$ final state, the $e\mu$ will be twice more abundant than the ee or the $\mu\mu$. This decay may be dominant for the heaviest neutralinos.

Decays into Higgses. The neutralinos can also decay into Higgses through a ($\lambda\phi\psi$), e.g. a ($\tilde{Z}\tilde{H}^0H^0$), coupling:

$$\begin{aligned} &\chi_i^0 \to \chi_j^0 + H^0, \;\; H^0 \to f\bar{f} \\ &\chi_i^0 \to \chi_j^\pm + H^\mp, H^\pm \to f\bar{f}' \end{aligned} \tag{148}$$

Examples of $\tilde{\chi}_4^0$ decays to h^0 are found in cases 1 to 3 of figure 19. A sizeable branching ratio for the decay of $\tilde{\chi}_2^0$ into h^0 is also found in case 2, showing that the decays to Higgs usually dominate over decays with Z^0 when they are kinematically allowed. But for the same reasons as presented in the chargino decay, these are not kinematically the most favoured ones at LEP energies, but **they may be useful at LHC where they could even help discovering the Higgs**.

All decays encountered so far, except the one into Higgs, are transitions from gaugino into gaugino or from higgsino into higgsino states. If the final state particles are kinematically allowed to be on-shell (two-body final states) they will dominate over the others. However, two-body transitions between two higgsino states are not possible in any region of the parameter space, due to the small spacing in mass. They can exist between gaugino states, but are phenomenologically relevant only when the production cross-section is not negligibly small. The dominant decay modes at LEP are, therefore, expected to be three-body decays over most of the parameter space.

Radiative neutralino decay. In certain regions of the parameter space, the above decays can be suppressed by kinematics or by dynamics. Dynamical suppression occurs when χ_1^0 is purely gaugino and χ_2^0 purely higgsino or vice versa. It may also take place when χ_2^0 is

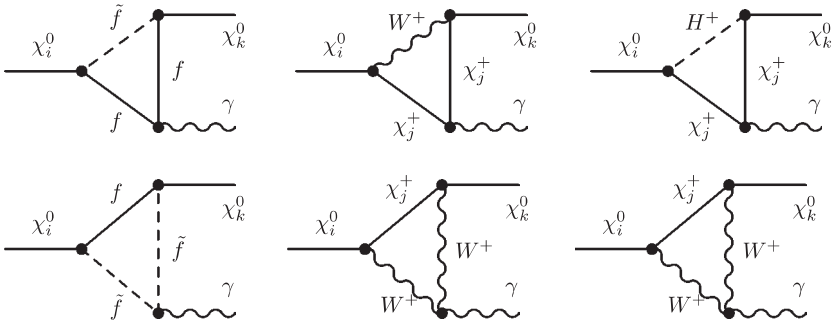

Figure 73. Radiative decays of neutralinos.

Table 15. Summary of slepton and squark decays.

Sleptons		Squarks	
		$\tilde{q} \to \tilde{g} + q$	Strong, $m(\tilde{q}) > m(\tilde{g})$
$\tilde{l} \to \tilde{\chi}_i^{\pm} + \nu, \tilde{\chi}_i^0 + l^{\pm}$	$(\lambda\phi\psi)$	$\tilde{q} \to \tilde{\chi}_i^{\pm} + q', \tilde{\chi}_i^0 + q$	$(\lambda\phi\psi)$
$\tilde{\tau}_i \to \tilde{\nu}_\tau + W^-, H^-$	$(A\phi\phi)$, Yukawa	$\tilde{b}_i \to \tilde{t}_j + W^-, H^-$	$(A\phi\phi)$, Yukawa
$\tilde{\nu}_\tau \to \tilde{\tau}_i + W^+, H^+$	$(A\phi\phi)$, Yukawa	$\tilde{t}_i \to \tilde{b}_j + W^+, H^+$	$(A\phi\phi)$, Yukawa
$\tilde{\tau}_i \to \tilde{\tau}_j + Z^0, H^0$	$(A\phi\phi)$, Yukawa	$\tilde{t}_i \to \tilde{t}_j + Z^0, H^0$	$(A\phi\phi)$, Yukawa
		$\tilde{b}_i \to \tilde{b}_j + Z^0, H^0$	$(A\phi\phi)$, Yukawa
		$\tilde{t}_1 \to \tilde{\chi}_1^0 + c$	Loop
		$\tilde{g} \to \tilde{q} + \bar{q}$	Strong, $m(\tilde{q}) < m(\tilde{g})$
		$\tilde{g} \to \tilde{\chi}^{\pm} + q + \bar{q}', \tilde{\chi}^0 + q + \bar{q}$	$m(\tilde{q}) > m(\tilde{g})$
		$\tilde{g} \to \tilde{\chi}^0 + g$	$m(\tilde{q}) > m(\tilde{g})$, loop

dominantly gaugino and the decay (145) to sfermions is suppressed by a large sfermion mass. Another type, called kinematical suppression, occurs when the χ_2^0 and χ_1^0 are nearly degenerate in mass. As discussed in [399], the decay rates to Z^0 or sfermions may become very small and one-loop decays, like

$$\chi_2^0 \to \chi_1^0 + \gamma \tag{149}$$

may then play an important role. Such decays proceed through Feynman diagrams like the ones depicted in figure 73 (the complete set of diagrams is given in [400]). Apart from the diagrams on the left, the others can induce transitions between gaugino and higgsino states. As these decays have an additional factor $\alpha_{\rm em}$ in their coupling, their branching ratios are normally of the order of few per cent. However, they may become dominant when tree-level processes are suppressed. They are most relevant in the region $\mu \simeq -M_1$ at low $\tan\beta$. For large $\tan\beta$ their contribution is negligible.

In the case of heavy scalars, like in split supersymmetry (see section 5.3.4), the only available decay modes will be through vector bosons or the light Higgs.

9.6. Summary of sparticle decays

The main slepton and squark decays are summarized in table 15.

If mass differences are too small for the above decays, the lighter stop can give rise to 3-body decays, like

$$\tilde{t}_1 \to W^+ b\tilde{\chi}_1^0, H^+ b\tilde{\chi}_1^0, b\tilde{l}_i^+ \nu_j, b\tilde{\nu}_i^+ l^+$$

Table 16. Summary of chargino and neutralino decays.

Chargino		Neutralino	
$\tilde{\chi}_i^{\pm} \to \tilde{l} + \nu, \tilde{\nu} + l$	$(\lambda\phi\psi)$	$\tilde{\chi}_i^0 \to \tilde{l} + l, \tilde{\nu} + \nu$	$(\lambda\phi\psi)$
$\tilde{\chi}_2^{\pm} \to \tilde{\chi}_1^{\pm} + Z^0$	$(A\lambda\lambda), (A\psi\psi)$	$\tilde{\chi}_i^0 \to \tilde{\chi}_j^0 Z^0$	$(A\psi\psi)$
$\tilde{\chi}_i^{\pm} \to \tilde{\chi}_i^0 + W^{\pm}$	$(A\lambda\lambda), (A\psi\psi)$	$\tilde{\chi}_i^0 \to \tilde{\chi}_j^{\pm} W^{\mp}$	$(A\lambda\lambda), (A\psi\psi)$
$\tilde{\chi}_2^{\pm} \to \tilde{\chi}_1^{\pm} + H^0$	$(\lambda\phi\psi)$	$\tilde{\chi}_i^0 \to \tilde{\chi}_j^0 H^0$	$(\lambda\phi\psi)$
$\tilde{\chi}_i^{\pm} \to \tilde{\chi}_j^0 + H^{\pm}$	$(\lambda\phi\psi)$	$\tilde{\chi}_i^0 \to \tilde{\chi}_1^{\pm} H^{\mp}$	$(\lambda\phi\psi)$
		$\tilde{\chi}_2^0 \to \tilde{\chi}_1^0 \gamma$	Loop decay

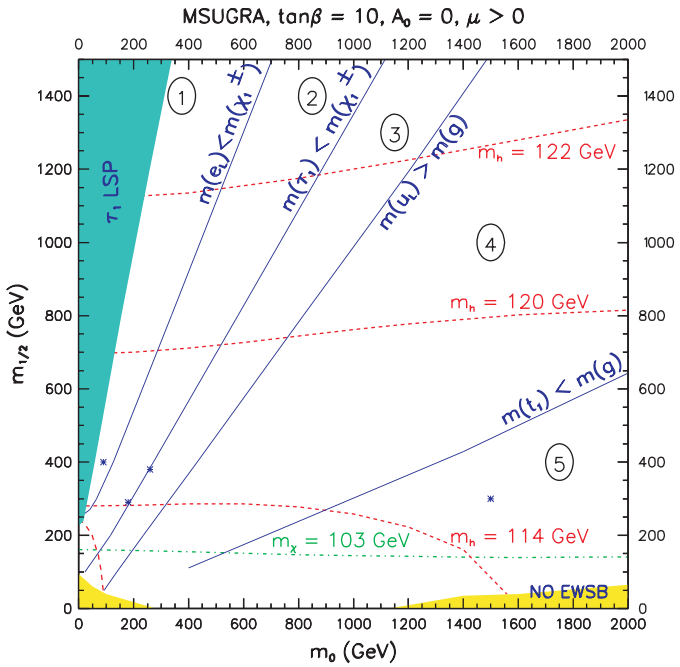

Figure 74. Regions of the m_0 versus $m_{1/2}$ plane displaying different relations between the masses of sparticles. Also shown as crosses are the cases presented in figure 19: dashed lines (red) are isomass curves for the light Higgs and dash-dotted line (green) is an isomass curve for $\tilde{\chi}_1^{\pm}$. Masses are computed with ISASUGRA7.69 for $\tan\beta = 10$, $A_0 = 0$ and $\mu > 0$, $m_t = 175$ GeV.

(mediated by a chargino), and even 4-body decays, like

$$\tilde{t}_1 \to b f \bar{f}' \tilde{\chi}_1^0$$

(mediated by a virtual chargino and W).

The main chargino and neutralino decays are summarized in table 16.

9.7. MSUGRA signatures

In the MSUGRA framework, the $\tilde{\chi}_1^0$ is the LSP and invisible. The signature is missing energy. In addition, the final state topologies are largely characterized by the relative positions of:

- $m(\tilde{\chi}_1^{\pm}) \simeq m(\tilde{\chi}_2^0)$ versus $m(\tilde{l})$
- $m(\tilde{g})$ versus $m(\tilde{q})$

The regions in the m_0 versus $m_{1/2}$ plane delimited by these conditions are outlined in figure 74.

- In region 1, all sleptons are lighter than the $\tilde{\chi}_1^{\pm}$ (and $\tilde{\chi}_2^0$) and the latter, either directly produced or resulting from a cascade decay, will decay to slepton–lepton pairs rather than to the LSP. Final states will be rich in leptons. Note that a non-negligible fraction of the decays will be to a $\tilde{\nu}$ which will itself decay to the LSP and remain invisible. An example is case 1 of figure 19.
- In region 2, only the $\tilde{\tau}_1$ (and possibly the $\tilde{l}_R$) remains lighter than the $\tilde{\chi}_1^{\pm}$ and $\tilde{\chi}_2^0$. Their decays will now involve only taus in the final state, although direct decays to the LSP may also have an important branching ratio.
- In regions 3, 4 and 5 no sleptons are lighter than the $\tilde{\chi}_1^{\pm}$ or $\tilde{\chi}_2^0$, hence the decays to sleptons are closed. If kinematically allowed, the $\tilde{\chi}_1^{\pm}$ and $\tilde{\chi}_2^0$ will dominantly decay to the LSP with the emission of a h^0. An example is case 2 of figure 19. Else, the dominant decays will be to the LSP with the emission of a $W^{\pm}$ or a Z^0. Final states with charged leptons amount typically to about 10%. An example is case 3 of figure 19. In principle, 3-body decays could also occur when the mass difference with the $\tilde{\chi}_1^0$ is less than the $W^{\pm}$ or Z^0 mass. In strict MSUGRA, a large part of this region is by now excluded by the LEP bound on the h^0 mass. But it would remain allowed if the GUT universality of the Higgs masses is abandoned (CMSSM). Note that the heavier chargino and neutralinos also have very small branching ratios to sleptons, as they are dominantly composed of higgsinos.
- In regions 1 to 3, all squarks are lighter than the gluino. The gluino, if produced, decays democratically into $\tilde{q}\bar{q}$ (both L and R squarks). The $\tilde{q}_R$ states decay directly to the LSP, whereas the $\tilde{q}_L$ states decay preferentially through the charginos and (heavier) neutralinos. There is even a non-negligible branching ratio to the heaviest chargino and neutralino, leading to long cascade decay chains.
- In region 4, some squarks are heavier than the gluino and will decay to it, although the electroweak decays to charginos and neutralinos may still remain important.
- In region 5, all squarks are heavier than the gluino. Most of them will, in a first step, decay to their partner quark plus a gluino. Subsequently, the gluino decays through electroweak interactions. An example is case 4 of figure 19.
- Decays to h^0 also occur with non negligible branching ratios for the heavy states $\tilde{\chi}_2^{\pm}$ and $\tilde{\chi}_4^0$, as seen in figure 19 for cases 1 to 3. In strict MSUGRA, decays of charginos and neutralinos into heavy Higgses H^0, A^0 and $H^{\pm}$ are not kinematically possible. They may become important, however, if the universality of the Higgs mass parameter is abandoned.

These conclusions have been established in a strict MSUGRA framework. Their main features will, however, hold in a less constrained scenario, provided an (even approximate) universality of sfermion and of gaugino masses is assumed and the chargino and neutralino composition remains gaugino-like in most of the plane.

9.8. The effect of phases

Work has been done on the construction of CP-sensitive observables in SUSY particle reactions. The definition of appropriate T-odd asymmetries were proposed for sfermion decay, neutralino production and decay, chargino production. In particular, [401] studied the CP-asymmetry involving the transverse polarization of the τ lepton in the decay of the neutralino into τ and $\tilde{\tau}$. It is sensitive to the phase of the trilinear coupling parameter A_τ.

The phase dependence of CP-even observables was also investigated. In the MSSM with complex parameters SUSY particle masses, decay branching ratios, production cross sections, etc. may depend on the phases of the SUSY parameters involved. In [402] the impact of CP phases on the searches and decays of stop and sbottom was analysed, and in particular how

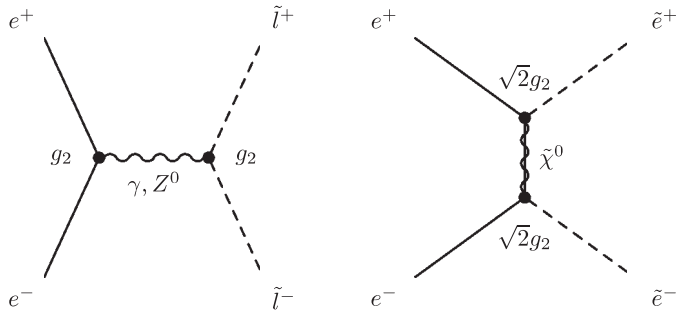

Figure 75. Slepton production in e^+e^- interactions.

and with what accuracy one can extract information on the complex μ, M_1, A_t andA_b from fermionic and bosonic decays of $\tilde{t}_{1,2}$ and $\tilde{b}_{1,2}$.

The effect of CP phases on the phenomenology of SUSY particles is summarized in [132]. The strong phase dependence of CP-even observables in heavy squark physics has to be taken into account in SUSY searches at future colliders and will affect the determination of the underlying MSSM parameters. The T-odd asymmetries in the gaugino sector can be large and will be an important tool for the search of CP violation in SUSY and the determination of the phases of SUSY parameters.

10. Sparticle production

We will first review sparticle production in e^+e^- collisions. Since the results come from LEP200, we will emphasize its energy domain. But we will also describe what one expects in a LC in which, if kinematically accessible, the various sparticles are 'democratically' produced. Next we will consider hadronic interactions. In these, the main source of most, if not all, sparticles is through the decay of squarks and gluinos. We will, therefore, put the emphasis on the production of these strongly interacting sparticles. But we will also mention exceptional cases.

10.1. Sparticle production in e^+e^- *interactions*

10.1.1. Sfermion production in e^+e^- *interactions.* In e^+e^- interaction, the sleptons can be produced in association through s-channel Z^0 or γ exchange

$$e^+e^- \to \tilde{l}^{\pm}\tilde{l}^{\mp} \tag{150}$$

with both sleptons belonging to the same family. The s-channel Z^0 or γ exchange proceeds through a $(A\phi\phi)$ coupling according to the first Feynman diagram of figure 75. The photon couples to the charge $Q = -1$ for both mass eigenstates defined in section 9.1 and the Z^0 to $\tilde{f}_L$ and $\tilde{f}_R$ with a coupling $(I^3 - Q\sin^2\theta_W)$. As only the $\tilde{f}_L\tilde{f}_L$ interaction final state contributes with non-zero isospin, it introduces a factor $\cos^2\theta_{\tilde{f}}$ for the $\tilde{f}_1\tilde{f}_1$ final state, $\sin^2\theta_{\tilde{f}}$ for the $\tilde{f}_2\tilde{f}_2$ final state and $2\sin\theta_{\tilde{f}}\cos\theta_{\tilde{f}}$ for the $\tilde{f}_1\tilde{f}_2$ final state. Both left and right states contribute equally to the $Q\sin^2\theta_W$. The Z^0 then couples to the $\tilde{f}_1\tilde{f}_1$ final state with strength $(I^3\cos^2\theta_{\tilde{f}} - Q\sin^2\theta_W)$. The total cross-section for production of $\tilde{f}_1\tilde{f}_1$ at tree level is given in Bartl *et al* [390]. Some examples are illustrated in figure 76 where the effects of initial state radiation are included. It displays the typical β^3 threshold suppression for scalar particles, with $\beta^2 = 1\text{–}4m^2_{\tilde{f}1}/s$. Furthermore, it develops a minimum as function of the mixing angle

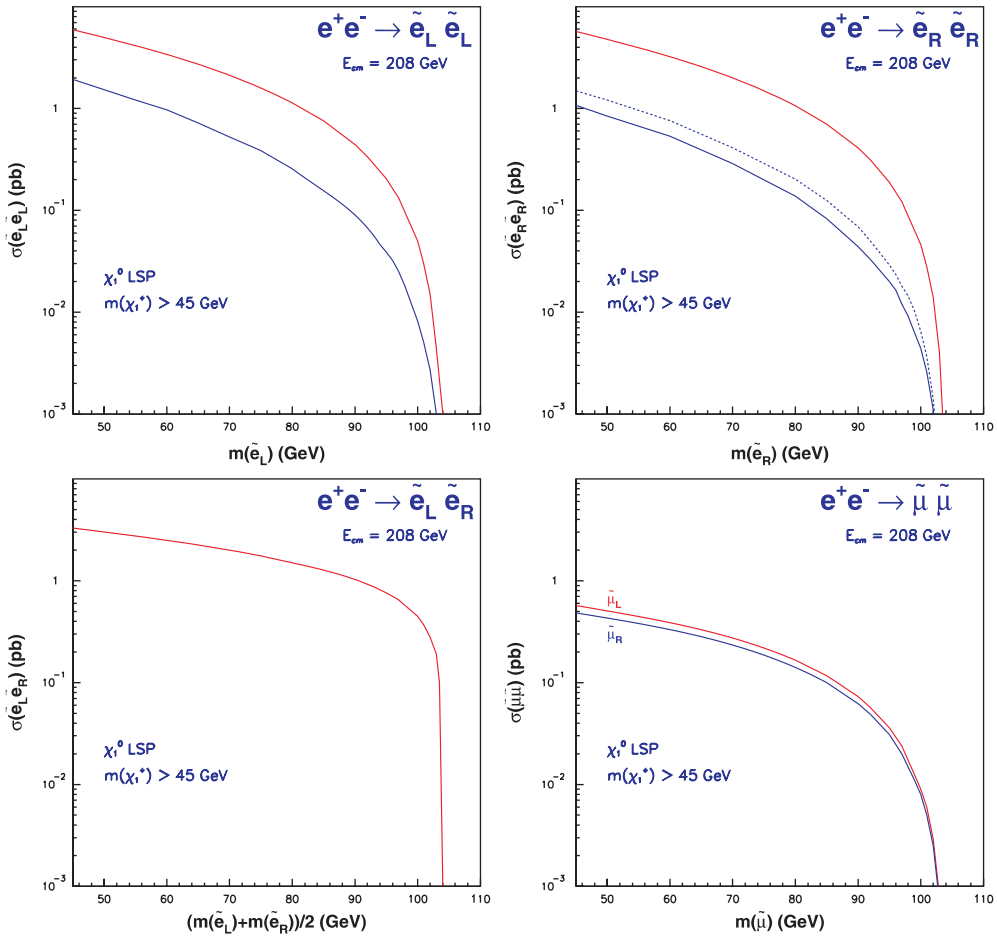

Figure 76. Production cross-sections for selectrons LL, RR and LR and for smuons at $\sqrt{s}$ = 208 GeV, including initial state radiation. Cross-sections are computed with SUSYGEN3.00 [311].

for (v_e and a_e are the vector and axial vector couplings for electrons):

$$\cos^2\theta_{\tilde{f}}|^{\min} = \frac{Qs_W^2}{I^3}\left[1 + 2\frac{v_e}{v_e^2 + a_e^2}c_W^2\left(1 - \frac{M_Z^2}{s}\right)\right], \tag{151}$$

which, for an energy at the Z^0 peak, corresponds to the decoupling from the Z^0. For energies large compared with M_Z the $\gamma - Z^0$ interference contribution shifts the dip in $\cos^2\theta_{\tilde{f}}$ towards about 75% of this value.

The tree level production angular distribution exhibits the familiar shape for scalar particles:

$$\frac{d\sigma^{\text{tree}}}{d\cos\theta} = \frac{3}{4}\sin^2\theta\sigma^{\text{tree}} \tag{152}$$

$\tilde{\mu}\tilde{\mu}$ **production**. Due to the smallness of the μ Yukawa coupling, the $\tilde{\mu}$ is not expected to exhibit any significant mixing. Its production cross-section is therefore fully determined once its mass is known and is independent of the SUSY parameters. As the $\tilde{\mu}\tilde{\mu}$ final state arises from a $(A\phi\phi)$ vertex, both smuons will have the same chirality. The production cross-section

is computed for either a left state, with $I^3 \cos^2\theta_{\tilde{f}} = -1/2$, or a right state, with $I^3 \cos^2\theta_{\tilde{f}} = 0$. The couplings for left and right smuons are almost the same, leading to nearly equal cross-sections. In the region $\sqrt{s} \simeq M_Z$, the reaction is completely dominated by the Z^0 resonance production. For $\sqrt{s} = 208\,\text{GeV}$ the cross-section, including ISR corrections, decreases from about 0.1 pb to 0.01 pb for smuon masses from about 85 to 100 GeV, reflecting its approximate β^3 dependence.

$\tilde{e}\tilde{e}$ **production**. Like for the smuons, no mixing is expected between the left and right states. Hence, the s-channel diagrams will lead to $\tilde{e}_L\tilde{e}_L$ or $\tilde{e}_R\tilde{e}_R$ mass eigenstates. The $\tilde{e}\tilde{e}$ final state can also be produced by t-channel exchange of a χ^0 [391], shown in the second diagram of figure 75, which occurs through a $(\lambda\phi\psi)$ vertex and is therefore determined by the gaugino component of the neutralinos. In principle, the higgsino component of the neutralino also gives a contribution, but, being a Yukawa coupling, it can be ignored for electrons. The t-channel diagram gives rise to LL and RR final states and, in addition, to LR final states even in the absence of mixing. At energies close to M_Z, the cross-section is again dominated by s-channel Z^0 exchange, leading to large numbers of events in the LL and RR channels with little dependence on the MSSM parameters. Above the Z^0, the magnitude of the cross-section is strongly affected by the t-channel contribution and, hence, very sensitive to the neutralino mass and composition. The upper and lower values of the cross-section, shown as two curves in figure 76, are determined as follows.

- The LSP is supposed to be the lightest neutralino. The LEP1 constraint on the chargino mass, $M(\tilde{\chi}_1^{\pm}) \geqslant 45\,\text{GeV}$, is imposed, as well as gaugino mass universality at the GUT scale. It is also assumed that the selectron masses arise from soft masses at the GUT scale, without imposing scalar mass universality. Using the relation (90) for running masses, implies that

$$\begin{aligned} m^2_{\tilde{e}_L} &\simeq m^2_{0,L} + 0.77 M_2^2 + \Delta_L, \\ m^2_{\tilde{e}_R} &\simeq m^2_{0,R} + 0.23 M_2^2 + \Delta_R, \end{aligned} \tag{153}$$

  where both the D-terms are positive.
- The cross-section is maximal when the mass of the lightest gaugino-dominated neutralino is smallest, which enhances the t-channel contribution. A zero-mass neutralino (i.e. $M_2 = 0$) is allowed by the LEP1 constraint $M(\tilde{\chi}_1^{\pm}) \geqslant 45\,\text{GeV}$ for $\tan\beta \simeq 1$ in the region $|\mu| \leqslant 100\,\text{GeV}$, as seen in figure 16. The upper curves in figure 76 are obtained for $\mu = -100\,\text{GeV}$.
- The cross-section is minimal when the lightest gaugino-dominated neutralino is the heaviest. This suppresses the t-channel exchange amplitude and, as can be verified from the formulae in [391], it also yields the strongest negative interference between the s-channel and t-channel diagrams. The largest value which the neutralino mass can reach for a fixed selectron mass is determined by the largest value of M_2 compatible with the relations (153), hence for $m_0 = 0$ and $\tan\beta = 1$ (zero D-terms). For $\tilde{e}_L$ pair production, the minimal cross-section is practically independent of the parameter μ, i.e. it is the same in the gaugino- and higgsino-like regions. For the $\tilde{e}_R\tilde{e}_R$ production, the minimum of the cross-section in the gaugino-like region is, due to the smallness of the coefficient of M_2 in relation to (153), determined by the condition $m(\tilde{\chi}_1^0) \leqslant m(\tilde{e}_R)$ and is shown as a dashed line in figure 76. The absolute minimum is reached in the higgsino-like region, where $m(\tilde{\chi}_1^0)$ can be kept low as it is given by μ, and the lightest gaugino-dominated neutralino is $\tilde{\chi}_2^0$ (or $\tilde{\chi}_3^0$) which mass is bounded by (153). The larger mass of $\tilde{\chi}_2^0$ allowed in this case explains the lower minimal cross-section for $\tilde{e}_R\tilde{e}_R$ than for $\tilde{e}_L\tilde{e}_L$.
- It is worth emphasizing that the extrema obtained for the cross-sections do not rely on the universality of scalar masses.

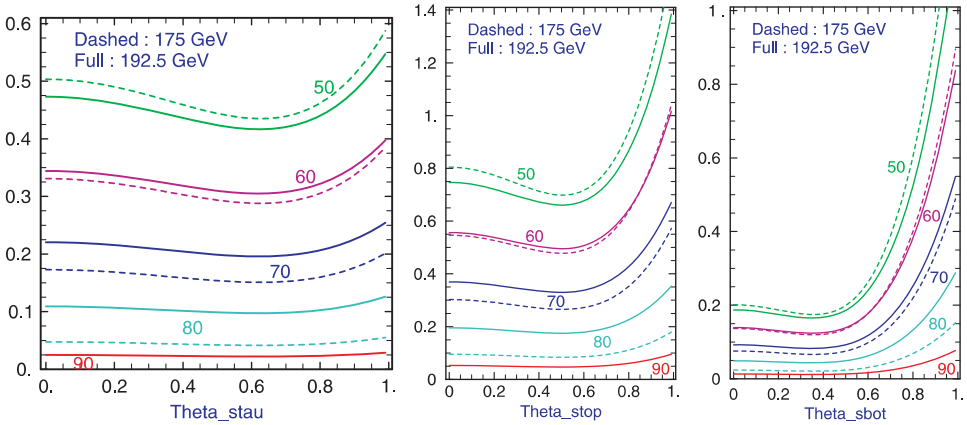

Figure 77. Production cross-sections (in pb) as function of the cosine of the mixing angle, for stau (left), stop (centre) and sbottom (right), from [338].

The cross-section can still reach several pb but, depending on the MSSM parameters, it can be several orders of magnitude lower for the LR final state (whose minimum is below the scale shown in figure 76).

$\tilde{\tau}\tilde{\tau}$ **production**. For the $\tilde{\tau}$ the left–right mixing may be important, especially if $\tan\beta$ is large. Consequently, the $\tilde{\tau}_1\tilde{\tau}_1$ production cross-section depends on the mixing, as seen in figure 77 (left). But, like for smuons, the difference between left and right production is small and the minimum in the cross-section, corresponding to equation (151), is not very pronounced. Cross-sections are very similar for $\tilde{\tau}$ and $\tilde{\mu}$.

$\tilde{\nu}\tilde{\nu}$ **production**. The $\tilde{\nu}$ is expected to be lighter than its corresponding charged slepton and is potentially an interesting candidate to be searched for, provided its decay is not predominantly into $\tilde{\nu} \to \chi_1^0\nu$ which is not observable. The $\tilde{\nu}\tilde{\nu}$ proceeds through s-channel Z^0 exchange and the $\tilde{\nu}_e\tilde{\nu}_e$ has also a contribution from t-channel exchange of charginos (a $(\lambda\phi\psi)$ vertex).

$\tilde{t}\tilde{t}$ **and** $\tilde{b}\tilde{b}$ **production**. The production cross-section is also illustrated in figure 77.

The cross-section for associated production of stop shows a marked difference between right and left states. At about 190 GeV, for masses varying from 50 to 80 GeV, the cross-section for right stop goes from 0.8 pb to 0.2 pb, whereas for left ones it drops from 1.4 pb to 0.35 pb.

For sbottom the difference between the production of left and right states is even more pronounced. The left states have a cross-section similar to the stop left states and the right sbottom is about a factor of 4 less than the right stop. The latter can be understood from the fact that for right states the Z^0 coupling is determined by the hypercharge. Then, there is a factor of 2 from the charge for the photon exchange and a factor 2 from the hypercharge ($Y_{\tilde{t}} = -4/3$ versus $Y_{\tilde{b}} = 2/3$), leading to a factor of 4 on the cross-section. The cross-section for right states is close to the LEP experimental sensitivity.

10.1.2. Chargino production in e^+e^-. Charginos are a mixture of charged winos and higgsinos. They are produced in e^+e^- interactions by the reaction:

$$e^+e^- \to \chi_i^{\pm}\chi_j^{\mp}. \tag{154}$$

It is instructive to view the production and decay processes in terms of the fundamental interactions from which they are constituted. The production proceeds through the two Feyman diagrams of figure 78.

The gauge interaction mediated by s-channel Z^0 **or** γ **exchange gives rise to gaugino and to higgsino final states**. The gauginos are produced via the $(A\lambda\lambda)$ vertex, the

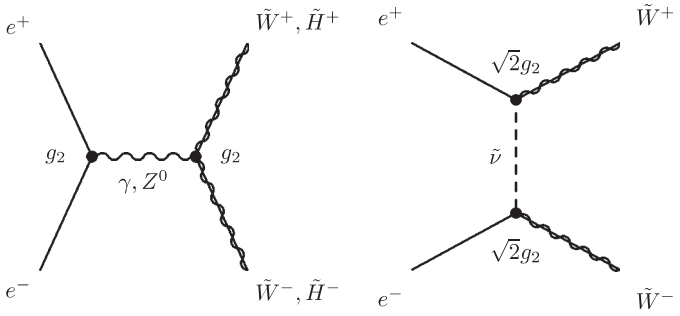

Figure 78. Chargino production in e^+e^- interactions.

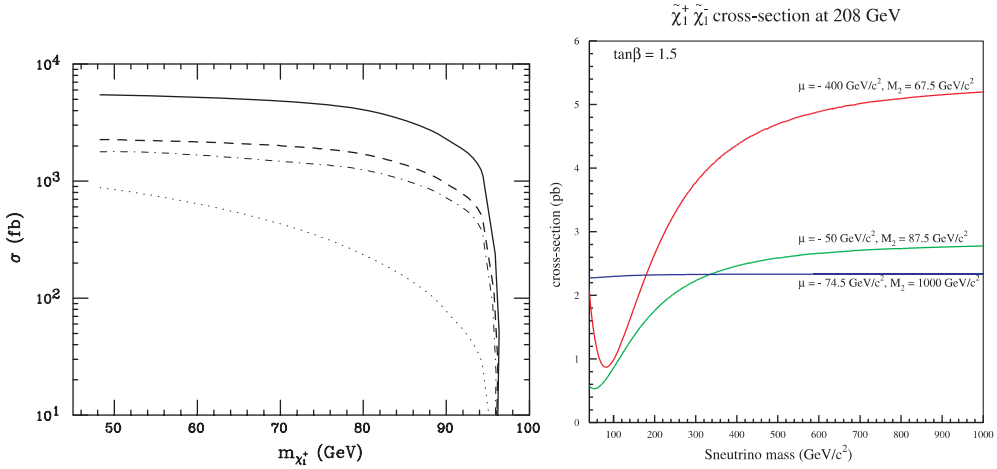

Figure 79. (left) Production cross-section for gaugino-like charginos at 190 GeV [338]. (right) Variation of the chargino production cross-section with the sneutrino mass at 208 GeV [151].

supersymmetric analogue of the SM ($W^0W^+W^-$) gauge couplings. The higgsinos originate from a ($A\psi\psi$) coupling, the same as the ($Af\bar{f}$) of the SM. The photon couples to the charge, eQ, and hence produces mass eigenstates. The Z^0 couples to the combination ($I^3 - Q\sin^2\theta_W$), where ($I^3 = 1$, $Q = +1$) for winos and ($I^3 = 1/2$, $Q = +1$) for higgsinos, with the same strength for left and right states. **The production of higgsinos from Z^0 exchange is therefore suppressed compared with winos**.

The t-channel production occurs through $\tilde{\nu}$ exchange (via a ($\lambda\phi\psi$) vertex) and can only lead to winos in the final state. In principle, a ($\psi\psi\phi = e\tilde{h}\tilde{\nu}$) vertex leading to higgsinos in the final state also contributes, but its magnitude being determined by a Yukawa coupling, it is negligible for electrons.

The complete cross-section formulae can be found in [403].

$\chi_1^+\chi_1^-$ production. Charginos are produced in both wino and higgsino states. If the t-channel exchange is small (very large $\tilde{\nu}$ mass), the total cross-section reaches a level of several pb, except when chargino masses approach the kinematical limit, as shown in the example of figure 79 (full curve in left figure). For the same chargino mass, it is larger in the gaugino-like region than in the higgsino-like region. This is due to the isospin coupling to the Z^0 which introduces the factor of 1/2 for higgsinos, see equation (14).

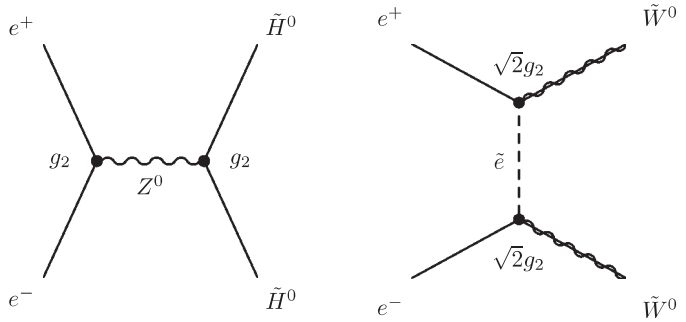

Figure 80. Neutralino production in e^+e^- interactions.

In the total cross-section, the interference of the t-channel $\tilde{\nu}$ exchange with s-channel γ and Z^0 exchanges gives rise to two negative contributions. As t-channel exchange produces only winos, charginos which are dominated by their gaugino component may have a drastic reduction of their cross-section in the case of light sneutrinos. This behaviour is illustrated by the full line in figure 79 (right). Higgsino-like charginos will not be affected, as the t-channel contribution is negligible in this case. An example is given by the dotted line in figure 79 (right). The same effect is shown in figure 79 (left), where the dashed, dash-dotted and dotted lines correspond, respectively, to sneutrino masses of 2000 GeV, 200 GeV and 45 GeV. For small sneutrino masses, the cross-section can be near the experimental sensitivity at LEP.

10.1.3. Neutralino production in e^+e^-. Neutralinos are a mixture of neutral wino, bino and higgsinos. They can be pair produced in e^+e^- interactions by:

$$e^+e^- \to \chi_i^0 \chi_j^0, \tag{155}$$

which proceed through the Feynman diagrams of figure 80 (see Bartl *et al* [404]).

In the s-channel, no neutral gauginos can be produced (the coupling for the $(A\lambda\lambda)$ vertex is zero). Neutral higgsinos can be made by the $(A\psi\psi)$ coupling to the Z^0 with a coupling constant proportional to I^3 (as $Q = 0$).

The t-channel production occurs through $\tilde{e}$ exchange (via a $(\lambda\phi\psi)$ vertex) and only leads to winos and binos in the final state.

$\chi_2^0\chi_1^0$ **production.** An interesting aspect of this reaction is that, as $M(\chi_1^0) < M(\chi_2^0) \simeq M(\chi_1^\pm)$, the reachable search limits translated in the μ versus M_2 plane can extend somewhat beyond the kinematic limit of chargino production. The general features of the production cross-section can be understood qualitatively (see also Ambrosiano and Mele [405]). Under the assumption that $M_2 \simeq 2M_1$, the following statements can be made.

- In the deep higgsino region ($|\mu| \leqslant M_1$), both χ_1^0 and the second (or third) lightest neutralino (labelled solution 3 in figure 15) are dominantly higgsino-like and the s-channel Z^0 exchange makes a sizeable contribution. The t-channel contribution is negligible and the interference is small (but positive). Typical cross-sections of 1–5 pb at $\sqrt{s} = 190$ GeV are obtained, practically independent of the selectron mass. At threshold, the cross-section increases very fast, approximately as β. The decay of the χ_2^0 leads to a typical signature of $Z^0 + 2\chi_1^0$ final states.
- In the deep gaugino region ($|\mu| \gg M_2$), both χ_1^0 and χ_2^0 are dominantly gaugino-like and the s-channel contribution is negligible. The t-channel contribution is not large either, except for very light selectron masses and the interference is small (but positive). Even for selectron masses of 100 GeV, the cross-section is typically 0.1–0.2 pb at $\sqrt{s} = 190$ GeV

for masses $M(\chi_1^0) \simeq 50\,\text{GeV}$ and $M(\chi_2^0) \simeq 100\,\text{GeV}$. For larger selectron masses the cross-section is even lower. Above threshold, the cross-section increases slowly with energy.

- In the region where $M_1 \leqslant \mu \leqslant M_2$, the χ_1^0 is dominantly gaugino (and χ_2^0 higgsino). The s-channel contribution remains small, the t-channel and the (positive) interference contributions are both about equal but not very large. Now the cross-section is only of $\leqslant 0.1\,\text{pb}$, below the experimental sensitivity at LEP. Also in this case the cross-section decreases with increasing selectron mass.

These results are rather insensitive to the value of $\tan\beta$.

$\chi_1^0\chi_1^0$ **production.** This gives rise, for stable neutralinos, to undetectable final states. The production cross-section is not very large, a maximum of a few pb for small $|\mu|$. This is too small to trigger the events by means of initial state radiated photons. In addition, no limit can be derived from the Z^0 invisible width, as the neutralino can decouple from the Z^0 if it is gaugino-like. Therefore, **limits on the lightest neutralino mass can only be obtained indirectly** (see below). It may, of course, give a detectable final state if R-parity is not conserved.

$\chi_2^0\chi_3^0$ **production.** In the intermediate region where $M_1 \leqslant |\mu| \leqslant M_2$, both χ_2^0 and χ_3^0 are dominantly higgsino-like (see figure 15). Such heavier neutralino states can be accessible at LEP provided M_2 is not too large. Their s-channel production yields a cross-section of 0.1–0.7 pb and allows the coverage of regions in the parameter space where the sensitivity is insufficient to detect the $\chi_1^0\chi_2^0$ final state. They give rise to interesting signatures, including cascade decays and photons in the final state.

Other cascade decays, from $\chi_1^0\chi_{3,4}^0$ or from $\chi_2^0\chi_4^0$ can also contribute in some regions of the parameters, as illustrated in figure 81.

10.1.4. e^+e^- *interactions: strategies and problematic areas.* With much simplification, one can summarize the e^+e^- situation concerning gauginos in LEP type searches in the following way. In section 10.2 we will consider the promises of a linear collider. For the discovery of the chargino, the most promising reaction is clearly $e^+e^- \to \chi_1^+\chi_1^-$, associated production of the lightest chargino. In most of the SUSY parameter space, the decay of the lightest chargino leads directly to a LSP and a W, giving 2 jets or a (charged lepton+neutrino) pair. Chargino events will then contain two unobserved neutralinos, giving rise to a large missing energy and mass and the visible system will consist of jets (BR = 4/9), a jet and a lepton (BR = 4/9) or two leptons (BR = 1/9). In the latter case, the leptons may belong to different generations and there will be two times more $e\mu$ pairs than ee or $\mu\mu$. Branching ratios may differ from the above values if the sneutrino mass is low or if there exist important contributions from cascade decays, but the kinematical characteristics of signal events are not drastically affected. Cascade decays may lead, in addition, to a topology with isolated photons from the decay $\chi_2^0 \to \chi_1^0 + \gamma$.

The most promising discovery reaction for the neutralino is $e^+e^- \to \chi_1^0\chi_2^0$, followed by the decay $\chi_2^0 \to \chi_1^0 + Z^0$ (if higgsino-like) or $\chi_2^0 \to \tilde{l}+l$ (if gaugino-like and the $\tilde{l}$ is sufficiently light) or for some regions of parameter space $\chi_2^0 \to \chi_1^0 + \gamma$.

At LEP2, the dominant backgrounds are $q\bar{q}\gamma$, four-fermion and 2–γ interactions. The $q\bar{q}\gamma$ background can largely be removed by cuts on acoplanarity. In some kinematical regions, the WW, $We\nu$ or 2–γ interactions can lead to irreducible backgrounds.

Problematic areas. There are some weak spots in the detection of charginos and neutralinos.

- A reasonable detection efficiency can only be maintained when the deposited energy and p_T are sufficient to separate the signal events from the 2–γ background. This requires

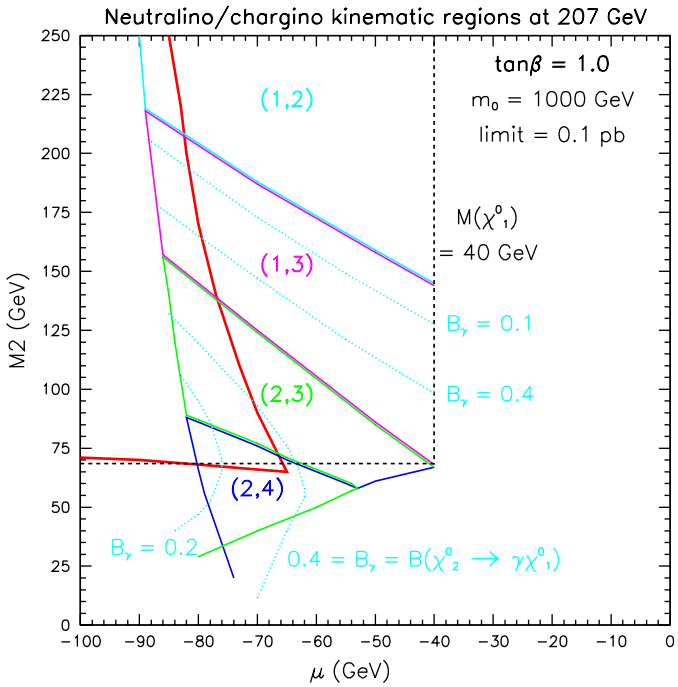

Figure 81. Regions of the (μ, M_2) where various neutralinos are produced in association at 207 GeV with cross-sections above 0.1 pb, together with the chargino kinematic limit. Regions where the branching ratio B_γ for $\chi_2^0 \to \chi_1^0\gamma$ is significant are also indicated. The values $\tan\beta = 1$ and $m_0 = 1$ TeV are assumed.

the mass difference, ΔM, between the parent particle and the LSP to remain above a threshold, typically 3–5 GeV for the standard searches at LEP. But the efficiency already starts to drop from $\Delta M \simeq 10$ GeV. In the deep higgsino region the $\chi_1^\pm$ and the χ_2^0 are nearly degenerate with the LSP. A similar situation arises if the sneutrino is lighter than and nearly degenerate with the chargino or if the $\tilde{\tau}_1$ is lighter than the chargino and nearly degenerate with the LSP. Furthermore, if the sneutrino is lighter than the χ_2^0, the decay may become invisible. All LEP experiments have designed specific selection criteria to improve the sensitivity in the low ΔM region.

- In the region of small $M(\chi_1^0)$ and large ΔM, where the $\chi_1^\pm$ and the χ_2^0 masses are close to the W mass, the background from 4-fermion production is important, forcing stronger anti-W cuts to be applied and resulting in lower efficiencies. For charginos, the non-negligible branching ratio into the background free photonic final states compensates for this loss.

10.2. Brief overview of sparticle physics at linear colliders (LC)

For e^+e^- interactions, although some considerations were quite general, we have focused up to now mostly on LEP200. We now turn to the higher energies of a linear collider.

As we said in section 10.1, sleptons are the lightest observable superpartners in many models. Slepton pair production proceeds through s-channel gauge boson exchange. For the first generation there are also contributions of t-channel exchange of chargino and neutralino. If lepton number is conserved, there is no t-channel contribution for the next generations. In the

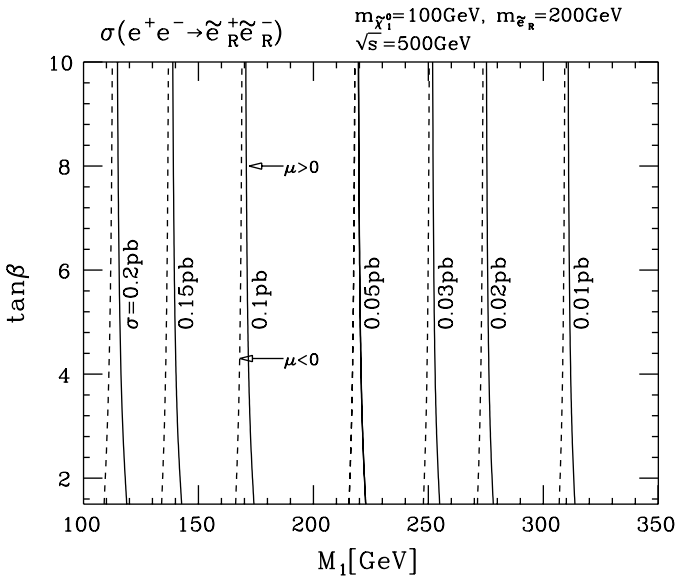

Figure 82. Contours of $\sigma(e^+e_R^- \to \tilde{e}_R^+\tilde{e}_R^+)$ for $m(\tilde{e}_R^+) = 200\,\text{GeV}$ and $\sqrt{s} = 500\,\text{GeV}$ in the $(M_1, \tan\beta)$ plane. At each point in the plane, μ is chosen so that $m(\tilde{\chi}_1^0) = 100\,\text{GeV}$. Reproduced with permission from [568]. Copyright 1996 by the American Physical Society.

simplest case of SUGRA with R-parity conservation, where a charged lepton is the next-to-LSP (NLSP) and the $\tilde{\chi}_1^0$ is the LSP, we have the usual signal of same flavour opposite sign dileptons. The W^+W^- background is very peaked forward. Furthermore, beam polarization can greatly reduce it. The two-photon background can largely be eliminated by $\not{p}_T$ and acoplanarity cuts. Slepton masses can be obtained with high accuracy through kinematic endpoints, minimum mass method and threshold scans, as shown in section 15.3.

The case of selectron pair production has interesting properties related to the existence of t-channel amplitudes. Figure 82 gives an example of the cross sections to be expected. The polarization of any lepton from slepton decay carries information about the SUSY parameters: this can be exploited in the case of stau decay.

Considering gaugino studies, the relevant production processes proceed through s-channel Z exchange and t-channel selectron exchange for neutralinos: s-channel exchange of γ and Z and t-channel exchange of $\tilde{\nu}_e$ for charginos (see section 10.1). As for sleptons, the dominant backgrounds are SM gauge boson processes, as WW and ZZ, and are removed similarly. However, in the case of pair production of wino-like states, a right polarized electron beam reduces both the signal and the background. An example of cross sections for $\chi_1^+\chi_1^-$ production is given in figure 83. We show in section 15.3 what can be deduced from a thorough study of chargino including the beam polarization.

One can show from a specific example the complementarity of a LC and LHC. In [407], the authors adopt a case study based not on MSUGRA but on a SUSY $SO(10)$ GUT. Such a case would be discovered by LHC and distinguished from MSUGRA, but it will be left to a LC to provide model independent mass measurements: this therefore illustrates the complementary roles of such machines. Figure 84 gives the SUSY pair production cross sections for the two machines. See [407] for the model parameters. Some masses are $m(\tilde{g}) = 649\,\text{GeV}$, $m(\tilde{t}_1) = 531\,\text{GeV}$, $m(\tilde{b}_1) = 240\,\text{GeV}$, $m(\tilde{\chi}_{2(1)}^0) = 131(85)\,\text{GeV}$ and $m(\tilde{\chi}_1^\pm) = 120\,\text{GeV}$. The ordering of states according to the cross section is quite different for the two machines. At a LC the chargino pair production leading to a 2-jet + 1 + $\not{E}_T$ can give a very accurate measurement

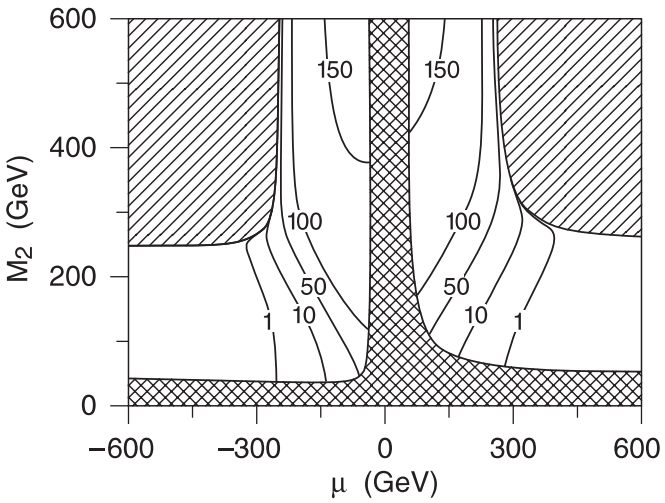

Figure 83. Contours of $\sigma(e^+e_R^- \to \chi_1^+\chi_1^-)$ (in fb) in the (μ, M_2) plane for fixed $\tan\beta = 4$ and $\sqrt{s} = 500\,\text{GeV}$. The cross-hatched region is excluded by LEP and the hatched region is kinematically inaccessible at this energy. From [406].

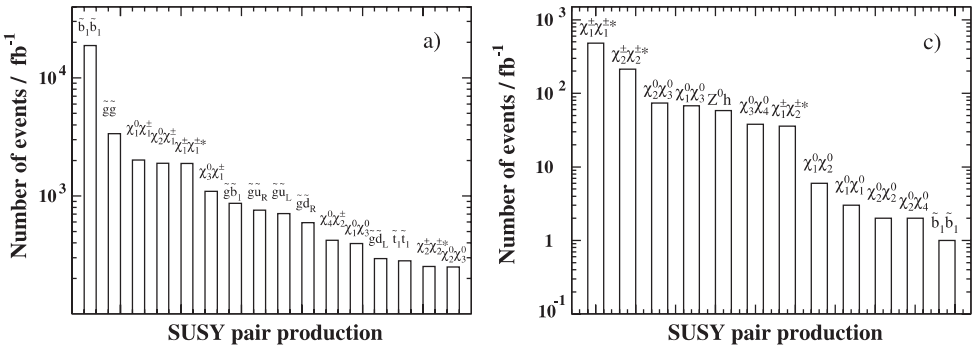

Figure 84. Production cross sections for various SUSY channels at LHC (left) and LC (right). From [407].

of $m(\tilde{\chi}_1^0)$ and $m(\tilde{\chi}_1^\pm)$ through the 2-jet energy distribution. LHC data can be re-analysed with the use of this information to improve the masses of heavier objects.

10.3. Sparticle production in hadron colliders

Squarks and gluinos can be copiously produced at hadron colliders via strong interactions. Some limits from the Tevatron are reported in the next section. Let us note that, with the possible exception of neutralino–chargino and slepton pair production, **squarks and gluinos, through their decay which may involve complex cascading, will be the main source of all SUSY particles in hadron colliders**. For example, charged sleptons can be produced at hadron colliders through their couplings to γ, Z^0 and W bosons. The production cross-sections at the Tevatron are, however, small (tens to hundreds of fb) and the backgrounds are important. So far, none of the Tevatron experiments has reported results from slepton searches in the MSUGRA framework [408]. Their observation from cascade decays is more promising and is presented in section 15.

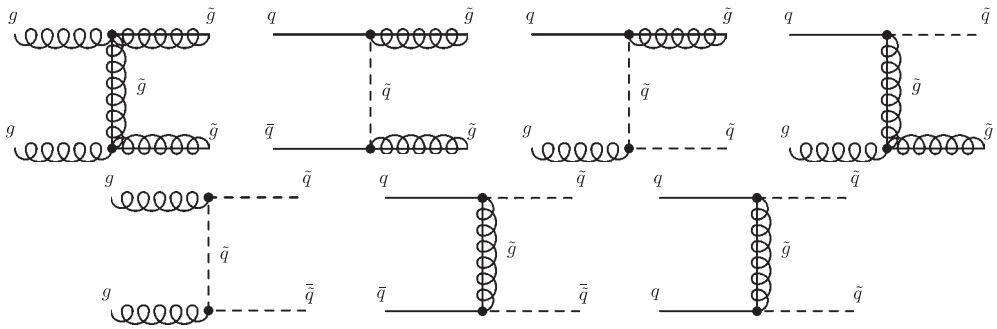

Figure 85. Examples of Feynman diagrams contributing to the hadron production of squarks and gluinos.

10.3.1. Production of squarks and gluinos. Squarks and gluinos can be produced in four different processes:

$$p\bar{p}/pp \to \tilde{q}\tilde{q}, \tilde{q}\bar{\tilde{q}}, \tilde{g}\tilde{g}, \tilde{q}\tilde{g} + X. \tag{156}$$

The calculation of LO cross-sections was performed a long time ago. The different subprocesses are

$$\begin{aligned} qq' &\to \tilde{q}\tilde{q}', \\ gg, q\bar{q} &\to \tilde{g}\tilde{g}, \tilde{q}\bar{\tilde{q}}, \\ q\bar{q}' &\to \tilde{q}\bar{\tilde{q}}', \\ gq &\to \tilde{g}\tilde{q}. \end{aligned} \tag{157}$$

and the underlying tree level Feynman diagrams are displayed in figure 85. The LO hadronic cross-sections are obtained by convoluting the partonic ones with the corresponding parton densities. The LO scale dependence leading to a 50% uncertainty for the cross-section, a complete NLO calculation is needed. In [409,362] the evaluation of the full QCD corrections is described in detail. They enhance the cross-section by 10–90%. The scale dependence, which serves as an estimate of the theoretical uncertainty, is decreased to ∼15%. The production cross-sections for $\tilde{q}$ and for $\tilde{g}$ are summarized in figure 86 as function of the sparticle mass for $\sqrt{s} = 1.8$ TeV. The cross-section assumes degenerate masses for five flavours of $\tilde{q}$s. For squark production, the gluino mass was set to 200 GeV, for gluino production the squark mass was set to 200 GeV. For the production of $\tilde{q}\tilde{g}$, in (a) M_X is the $\tilde{q}$ mass and the $\tilde{g}$ mass was assumed to be 200 GeV; in (b) M_X is the $\tilde{g}$ mass and the $\tilde{q}$ mass was assumed to be 200 GeV.

The production cross-sections of squarks and gluinos at the LHC computed at LO and NLO [410] are illustrated in figure 87. At LHC, for $m_{\tilde{q}}/m_{\tilde{g}} = 0.9, 1.2, 5.0$, the total cross-sections, in pb, computed with the program PROSPINO [411] are given in table 17. The shape of the NLO transverse momentum and rapidity distributions are only slightly modified, compared with the LO. A simple rescaling of the LO distributions by the K factors of the total cross-sections is a good approximation. Some examples of transverse momentum distributions of $\tilde{q}$ and $\tilde{g}$ for the various production proceses, computed with PROSPINO at NLO, are given in figure 88.

A SLHC of 28 TeV would gain an order of magnitude on the cross-section for the 1 TeV mass region, a factor 50–100 for 2 TeV [412]. Or, for a cross-section of 1 pb, the gain in mass would be ∼1.5.

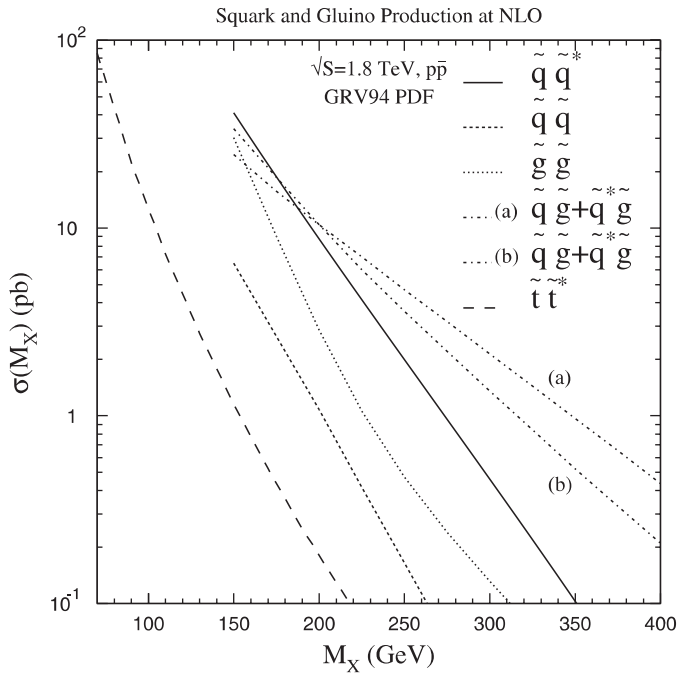

Figure 86. Production cross-sections for $\tilde{q}$ and $\tilde{g}$ at the Tevatron, from [408].

10.3.2. Production of stop pairs. Since the light stop, in the case of strong mixing, can be the lightest of all SUSY sfermions, it is interesting to study its production in a hadron collider. The picture emerging from such NLO studies [413] can be summarized as follows.

- The cross-section for production of diagonal pairs $\tilde{t}_1\tilde{t}_1$ or $\tilde{t}_2\tilde{t}_2$ depends essentially only on the masses of the stop particle produced and little on other SUSY parameters, in particular the $\tilde{g}$ mass. The SUSY–QCD corrections increase the cross-section by about 40% and leave a scale dependence of about 10–15%. In the SUGRA inspired scenario of [413] at the Tevatron (1.8 TeV) the $\tilde{t}_1\tilde{t}_1$ cross-section is ∼2 pb for $m(\tilde{t}_1) = 200$ GeV. At the LHC, the same cross-section is obtained for a mass of ∼400 GeV. It is about ten times smaller at ∼600 GeV.
- The mixed stop pair production is only possible at NLO and beyond. It is suppressed by $\mathcal{O}(\alpha_S^2)$ with respect to diagonal pair production and can be neglected.

An example of stop pair production cross-sections for the Tevatron and LHC at $\sqrt{s} = 2$ TeV is shown in figure 89.

10.3.3. Slepton pair production at hadron colliders. At a hadron collider the slepton pair production proceeds through a Drell–Yan interaction mediated by a Z^*, yielding $\tilde{l}_L\tilde{l}_L$, $\tilde{l}_R\tilde{l}_R$ or $\tilde{\nu}\tilde{\nu}$ pairs, or by a W^*, yielding $\tilde{l}_L\tilde{\nu}$. As these are electroweak processes, their cross-sections are much smaller than for the production of squarks. Production cross-sections with QCD radiative corrections have been computed at NLO [414] and were found to be enhanced by 35% to 40% at the Tevatron and 25% to 35% at the LHC compared with the LO results. The NLO cross-sections are displayed in figure 90 as a function of the slepton mass for the Tevatron and the LHC. The NLO contributions of virtual squarks and gluinos, not included in [414], have been added by [416] and were found to modify only slightly the earlier results.

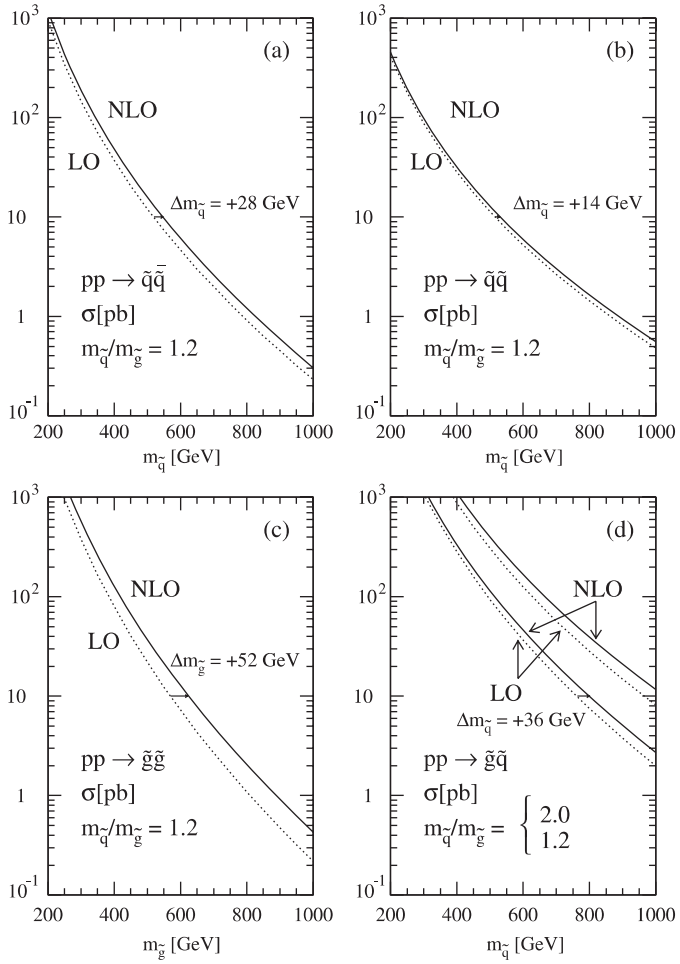

Figure 87. Production cross-sections for $\tilde{q}$ and $\tilde{g}$ at the LHC, reprinted from [410]. Copyright 1997, with permission from Elsevier.

It has been recently emphasized [415] that pair production of sleptons by gauge boson fusion also needs to be considered. Although its cross-section is much smaller than for Drell–Yan production at small slepton masses, it decreases less steeply with increasing slepton mass and becomes dominant for masses above ∼250–300 GeV. It may extend the reach for the slepton pair production at the LHC.

For $\tilde{l}\tilde{l}$ events, the signature is two same flavour leptons with missing energy. The total cross-section of diagonal production of $\tilde{t}\tilde{t}$ at the LHC is given in table 18.

10.3.4. Chargino/neutralino direct production at hadron colliders. The direct search channel for charginos and neutralinos at hadron colliders consists of the production via

$$q\bar{q}' \to \tilde{\chi}_2^0 \tilde{\chi}^{\pm} \tag{158}$$

followed by the decays

$$\tilde{\chi}_2^0 \to \tilde{\chi}_1^0 l^+ l^-, \qquad \tilde{\chi}^{\pm} \to \tilde{\chi}_1^0 l^{\pm} \nu. \tag{159}$$

Table 17. Partonic total cross-sections, in pb, computed with the program PROSPINO [411] for LHC, assuming $m_{\tilde{q}}/m_{\tilde{g}} = 0.9, 1.2, 5.0$. For squarks, the cross-section is the sum over the first five flavours assumed degenerate.

$m_{\tilde{q}}/m_{\tilde{g}} =$	Channel	$m(\tilde{q}) = 400$	$m(\tilde{q}) = 600$	$m(\tilde{q}) = 1000$	$m(\tilde{q}) = 2000$	$m(\tilde{q}) = 1000$
0.9	$\tilde{q}\bar{\tilde{q}}$	48.2	5.98	0.294	0.001	—
	$\tilde{q}\tilde{q}$	27.2	4.99	0.459	0.007	0.001
	$\tilde{g}\tilde{g}$	67.3	6.18	0.185	0.000	—
	$\tilde{g}\tilde{q}$	146.	18.6	0.940	0.004	—
1.2	$\tilde{q}\bar{\tilde{q}}$	48.2	6.09	0.305	0.001	—
	$\tilde{q}\tilde{q}$	31.8	5.95	0.554	0.008	0.001
	$\tilde{g}\tilde{g}$	337.	37.1	1.57	0.007	0.001
	$\tilde{g}\tilde{q}$	336.	46.3	2.72	0.019	0.002
	Channel	$m(\tilde{q}) = 2000$	$m(\tilde{q}) = 4000$	$m(\tilde{q}) = 6000$	$m(\tilde{q}) = 8000$	$m(\tilde{q}) = 10000$
5.0	$\tilde{q}\bar{\tilde{q}}$	0.001	—	—	—	—
	$\tilde{q}\tilde{q}$	0.008	—	—	—	—
	$\tilde{g}\tilde{g}$	138.3	2.37	0.139	0.013	0.002
	$\tilde{g}\tilde{q}$	1.09	0.004	—	—	—

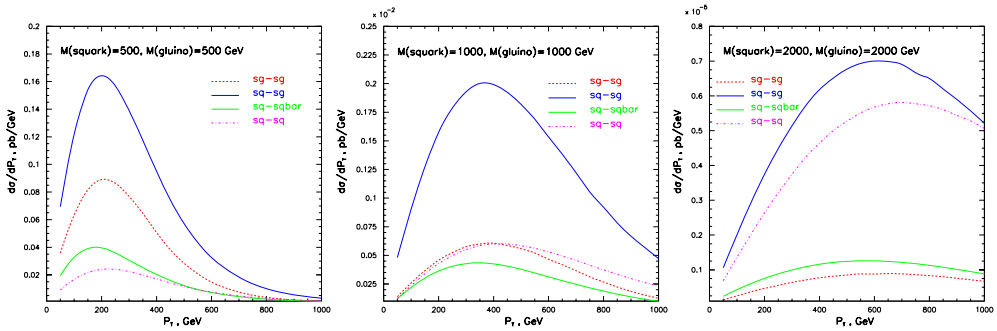

Figure 88. Production cross-sections for $\tilde{q}$ and $\tilde{g}$ processes as a function of the transverse momentum at the LHC.

The production proceeds through s-channel exchange of a W^* and t-channel exchange of a $\tilde{q}$. This channel leading to di- and tri-lepton states, without jets, is searched for at the Tevatron and is discussed in section 15.1. Reference [416] gives the cross-sections for these reactions in the next-to-leading order SUSY QCD. The basic diagrams and SUSY QCD corrections are the ones given by figure 91 (left). They enhance the cross-section by about 10–40%. Figure 91 (right) summarizes the cross-sections for various pair productions in a typical MSUGRA case at the Tevatron and LHC. However, at LHC, the main source of charginos and neutralinos will usually be cascading from squark and gluino decay. Nonetheless, at large m_0 where the squark production is suppressed, the direct chargino/neutralino production may be very important.

10.3.5. Associated production of gluinos and squarks with gauginos. The cross-sections for the associated production of gluinos with charginos or neutralinos can be sizeable [362, 417] at the Tevatron and the LHC if the gluino mass is less than about 400–500 GeV. They proceed in leading order through a q–$\bar{q}$ initial state with the t- or u-channel exchange of a squark, as shown by the diagrams in figure 92. The SUSY–QCD corrections have been computed and are found to decrease the cross-section by about 3% at the Tevatron and increase it by about

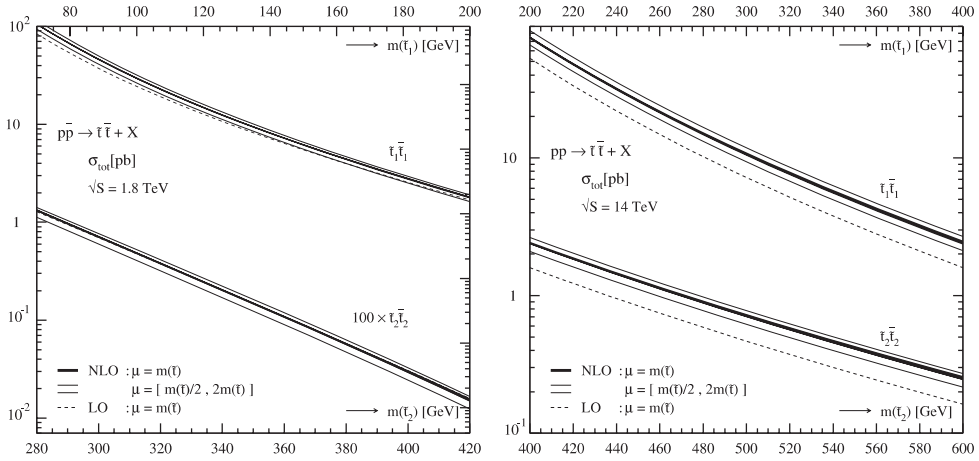

Figure 89. Production cross-sections of stop pairs at the Tevatron (left) and LHC (right) as a function of the mass of $\tilde{t}_1$ or $\tilde{t}_2$. Reprinted from [413]. Copyright 1998, with permission from Elsevier.

Table 18. Partonic total cross-sections for diagonal $\tilde{t}\tilde{t}$ production, in pb, computed with the program PROSPINO [411] for LHC, assuming a heavy $\tilde{q}$ and $\tilde{g}$.

$m(\tilde{t})$ (GeV)	200	400	600	800	1000	1200
	78.9	2.63	0.279	0.048	0.011	0.003

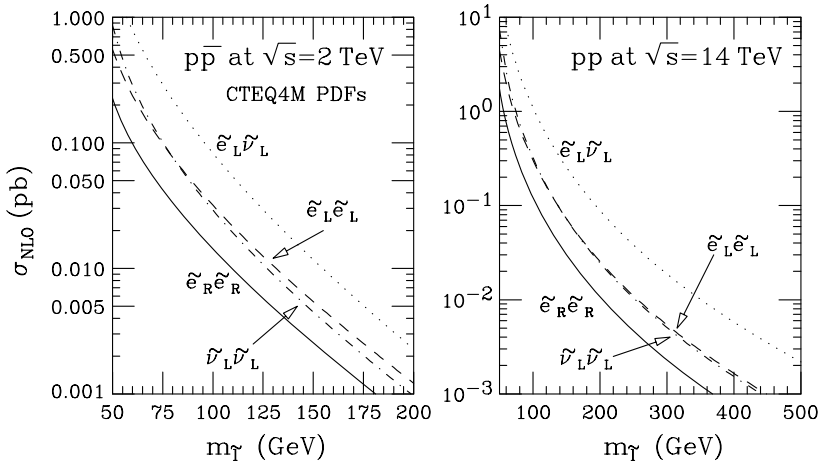

Figure 90. Production cross-sections of slepton pairs at the Tevatron (left) and the LHC (right). Reprinted with permission from [414]. Copyright 1998 by the American Physical Society.

10–20% at the LHC. The scale dependence is reduced to 10–15%, which signals a stabilization of the theoretical prediction.

11. Present limits

Limits on the mass of some superpartners have been derived from the measured Z^0 width at LEP1, compared with the SM expectation. It puts a limit of about 45 GeV on the masses of

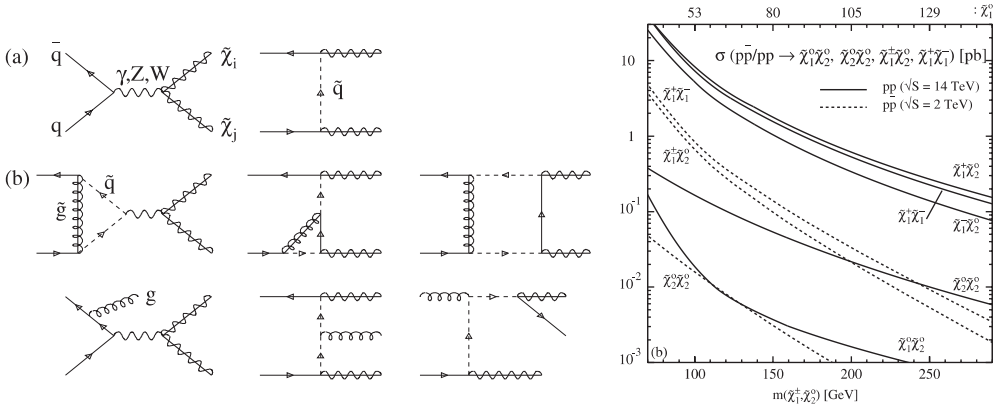

Figure 91. Left: production diagrams for chargino/neutralino at hadron colliders and their QCD corrections. Right: summary of cross-sections in pb at the Tevatron and LHC. Reprinted with permission from [416]. Copyright 1999 by the American Physical Society.

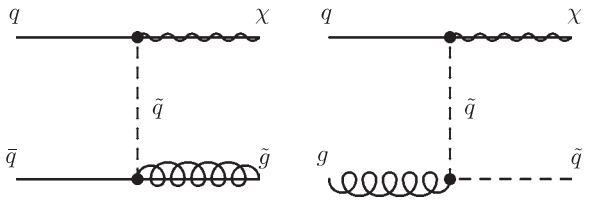

Figure 92. Feynman diagrams contributing to the associated production of squarks and gluinos with gauginos.

the $\tilde{e}$, $\tilde{\mu}$, $\tilde{q}$ of the first two generations and $\tilde{\chi}_1^\pm$. The same limit holds for the third generation sfermions $\tilde{\tau}_1$, $\tilde{t}_1$ and $\tilde{b}_1$, provided they do not decouple from the Z^0. These limits are superseded by the direct searches at other machines and at LEP2. The mass bound on the $\tilde{\nu}$ will be discussed in section 11.3.

11.1. Searches at HERA

At HERA, the dominant MSSM process is the production of a selectron and a squark via a t-channel exchange of a neutralino

$$eq \to \tilde{e}\tilde{q} \tag{160}$$

followed by $\tilde{e} \to e\tilde{\chi}^0$, $\tilde{q} \to q\tilde{\chi}^0$. The signature is a high P_T electron, a jet and $\not{E}$. The limit set on $(m_{\tilde{e}} + m_{\tilde{q}})/2$ at 77 GeV [418] is not competitive with those of LEP2 and Tevatron. **The strength of HERA is rather in the exploration of R-parity violating scenarios** that we discuss in section 14.

11.2. Tevatron results on gluinos and squarks

The production cross-sections for $\tilde{q}$ and for $\tilde{g}$ have been summarized in figure 86 as function of the sparticle mass for $\sqrt{s} = 1.8$ TeV.

The decay reactions are

$$\begin{aligned} &\text{if } m(\tilde{q}) > m(\tilde{g}) : \tilde{q} \to q\tilde{g}\,;\ \tilde{g} \to q\bar{q}\tilde{\chi}_i^0, q\bar{q}'\tilde{\chi}_i^\pm, \ldots, \\ &\text{if } m(\tilde{q}) < m(\tilde{g}) : \tilde{g} \to q\tilde{q}\,;\ \tilde{q} \to q\tilde{\chi}_i^0, q'\tilde{\chi}_i^\pm. \end{aligned} \tag{161}$$

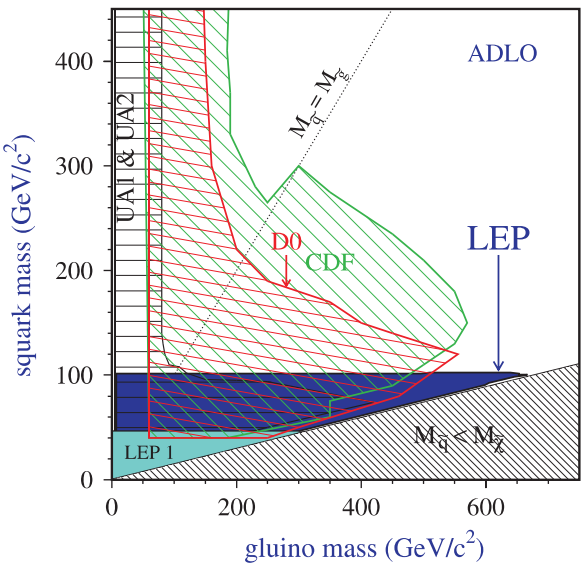

Figure 93. Exclusion limits at 95% CL from CDF [419] and D0 [420] experiments. Also included is the squark mass bound from LEP at 208 GeV [422].

Interesting signatures are (multi-jets with missing energy) or (leptons plus jets plus missing energy). A particularly clean signature comes from

$$2\tilde{g} \to \tilde{\chi}^{\pm}\tilde{\chi}^{\pm} + \cdots \to l^{\pm}l^{\pm} + \cdots \tag{162}$$

with two like-sign leptons in the final state, accompanied by jets and missing energy. The results [408] from D0 and from CDF are presented in figure 93. For $m(\tilde{q}) \gg m(\tilde{g})$, the only production contributing to the cross-section is $\tilde{g}\tilde{g}$. The resulting limit is then independent of the squark mass. When $m(\tilde{q}) \simeq m(\tilde{g})$, the cross-section is increased by the contribution of $\tilde{g}\tilde{q}$ production, which improves the limits and creates the 'nose' seen in the figure. The strongest limits on the gluino mass are from the multi-jets and missing energy channel and a scan over the MSUGRA parameter space yields the values of 195 GeV for CDF [421] and 190 GeV for D0 [420] (the latter is for $\tan\beta = 2$, $\mu < 0$). Limits on squarks have also been presented, but they vary with the relative value of the squark and gluino masses. The stop and sbottom exclusions are shown in section 11.3.4. However, the Tevatron limits depend strongly on the SUSY parameters. Hence, **these searches provide excellent discovery opportunities but make it hard to set significant mass limits**.

11.3. Sfermion mass limits

11.3.1. Sneutrino search limits from LEP. Supposing that the $\tilde{\nu}$ decays entirely into $\nu + \chi_1^0$, it will not be directly observable in the detector. However, indirect searches can be performed, based on the accurate measurement of the number of neutrino species in e^+e^- interactions at the Z^0 peak. The partial width for the decay of the Z^0 into a pair $\tilde{\nu}\tilde{\nu}$ of a single flavour is [423]

$$\frac{\Gamma(Z^0 \to \tilde{\nu}\tilde{\nu})}{\Gamma(Z^0 \to \nu\nu)} = \frac{1}{2}\left(1 - \frac{4m_{\tilde{\nu}}^2}{m_Z^2}\right)^{3/2}. \tag{163}$$

The invisible width of the Z^0 determined by the Electroweak Group, combining the results from the four LEP and the SLD experiments, has a 95% CL (one-sided) upper limit of

$\Delta\Gamma_{\rm inv} < 2$ MeV [275]. As the SM value for the neutrino partial width is $\Gamma(\nu\bar{\nu}) = 167.23$ MeV, the resulting lower limit on the sneutrino mass is

$$m_{\tilde{\nu}} > 43.7\,\text{GeV} \tag{164}$$

if it is completely assigned to a single flavour. As the sneutrinos of the different generations are expected to be nearly degenerate in the MSSM, the limit could optimistically be improved to $m_{\tilde{\nu}} > 44.7$ GeV for three degenerate $\tilde{\nu}$ pairs (neglecting the t-channel exchange in $\tilde{\nu}_{\rm e}$ production).

A legitimate question [424] is whether $\tilde{\nu}$s with mass between 45 GeV and the kinematic limit of LEP2 are not buried in LEP data. It would be interesting, using the single γ spectrum of ADLO, to derive a limit on their production.

The above decay is usually the most favourable one, but at large $\tan\beta$ it is also possible to have $\tilde{\nu}_\tau \to \tilde{\tau}_1\tau\nu_\tau$ when $\tilde{\tau}$ mixing is large, lowering the mass of $\tilde{\tau}_1$.

Finally, indirect limits on the sneutrino mass can be derived from the bounds on charged slepton masses, by using the relations (90).

11.3.2. Sfermion decay kinematics in e^+e^-. At LEP, the sfermion search is mostly based on the direct decay into a neutralino LSP. Such events are characterized by final states composed of two leptons with the same flavour or two jets, acoplanar with the beam, and large missing energy and momentum.

The energy distribution of the final state leptons in the e^+e^- rest frame is constant due to the slepton two-body decay and is limited by

$$E_l^{\rm max,min} = \frac{E_{\rm b}}{2}\left(1 - \frac{M_\chi^2}{M_{\tilde{l}}^2}\right)\left[1 \pm \sqrt{1 - \frac{M_{\tilde{l}}^2}{E_{\rm b}^2}}\right] \tag{165}$$

with $E_{\rm b}$ being the beam energy. For slepton production close to threshold, the energy distribution is very narrow. For small $\Delta M = M_{\tilde{l}} - M_\chi$, the visible energy is small. Similar conclusions hold for the jets from squark two-body decays.

Sfermion detection is made difficult in some areas. For small ΔM, there is a huge background of $\gamma\gamma$ interactions, which can be rejected only at the expense of lowering the efficiency. At LEP, for $\Delta M \lesssim 3$ GeV, the efficiency drops essentially to zero. Another difficulty is that, for small M_χ, when $M_{\tilde{f}}$ approaches M_W, the events are indistinguishable from WW events. Finally, in some regions of the SUSY parameter space, cascade decays may contribute with a non-negligible branching ratio. Until now, this is usually taken into account (conservatively) by assuming zero efficiency for cascades.

11.3.3. Charged slepton search limits at LEP. The results from a combination of the four LEP experiments up to 208 GeV by the LEP SUSY Working Group [422] are shown in figure 94. These limits are computed under the assumption that $\mu = -200$ GeV and $\tan\beta = 1.5$, which is primarily important for the selectron cross-section, but also affects the $\tilde{l} \to l\tilde{\chi}^0$ branching ratios for all sleptons. This point was chosen because it is a region where the slepton limits play a crucial role for the exclusion of the LSP (see section 12). The mass limits in the region where $\Delta M \equiv (m_{\tilde{l}} - M_{\rm LSP}) > 10$ GeV are summarized in table 19. The bounds for $\tilde{e}$ and $\tilde{\mu}$ apply to the most conservative case of right sleptons and for $\tilde{\tau}$ at the minimal production cross-section, near to the point where it decouples from the Z^0. Although these limits are given for a specific point, they remain essentially valid for the whole gaugino-like region $\mu \ll M_2$. For smaller values of μ, the limits may be invalidated due to the existence of cascade decays. As we will see below, this is a region excluded by the chargino and neutralino searches. Apart

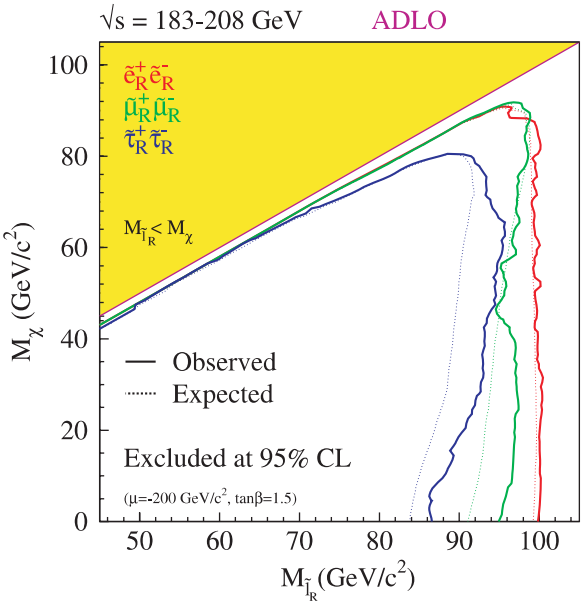

Figure 94. LEP 208 GeV combined slepton mass exclusion limits at 95% CL, from [422], under the assumption that $\mu = -200$ GeV and $\tan\beta = 1.5$.

Table 19. Mass exclusion limits for sleptons at 95% CL, assuming that $\mu = -200$ GeV and $\tan\beta = 1.5$.

Channel	$m(\tilde{l}) >$
$\tilde{e}$	99.4 GeV
$\tilde{\mu}$	94.9 GeV
$\tilde{\tau}$	85.0 GeV

from this, the slepton limits are very robust: they do not rely on scalar universality and, strictly speaking, not on gaugino universality either, as the only requirement is that the $\tilde{\chi}^0_1$ be lighter than the sleptons.

No limits from the LEP SUSY Working Group exist for $\Delta M = m_{\tilde{l}_R} - m_{\rm LSP} < 3$ GeV nor in regions of the parameter space where sleptons undergo cascade decays via $\tilde{l} \to l\tilde{\chi}^0_2$. The ALEPH experiment [425] covered the small ΔM by a dedicated search of $\tilde{e}_R\tilde{e}_L$ in the single electron topology. They also excluded the region of small $\tan\beta$, $|\mu|$ and m_0, leading to a light $\tilde{\chi}^0_2$, by their searches for charginos and for the production of $\tilde{\chi}^0_1\tilde{\chi}^0_3$. They derive the limit $m(\tilde{e}_R) > 73$ GeV at 95% CL. Stronger bounds are also obtained by imposing the limits from the Higgs search or in a strict MSUGRA framework.

Furthermore, as the $\tilde{\tau}$ can decouple from the Z^0, the bound of 45 GeV obtained from Z^0 data is not valid for any mixing. A dedicated search was carried out by DELPHI [426] to retrieve events with low mass $\tilde{\tau}$s which are highly boosted and therefore fail to satisfy the acoplanarity cuts applied in the standard analyses. A lower limit on the stau mass was established at 25.1 GeV for $\Delta M = m_\tau$, improving to 39.7 GeV at $\Delta M = 4$ GeV, for any $\tilde{\tau}$ mixing. For larger ΔM, the bound increases smoothly to the value listed in table 19.

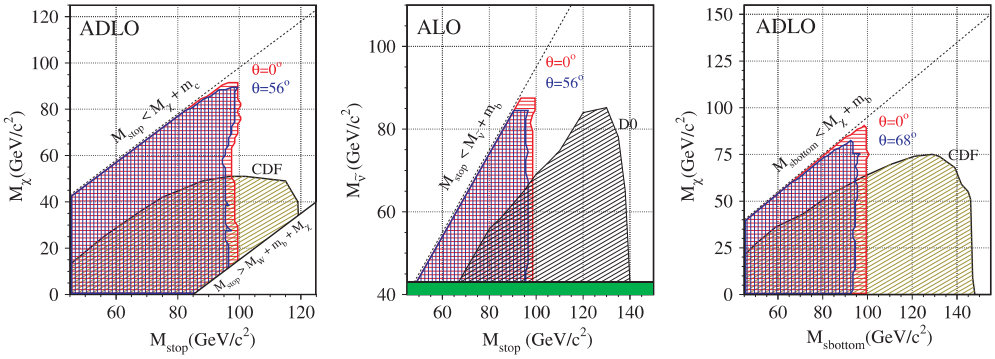

Figure 95. LEP 208 GeV combined squark mass exclusion limits at 95% CL, from [422].

Table 20. LEP 208 GeV mass exclusion limits for squarks at 95% CL.

Channel	$\theta = 0$	$\theta_{\min}$
	$M(\tilde{q}) >$	
$\tilde{t} \to c\tilde{\chi}_1^0$	98 GeV	95 GeV
$\tilde{t} \to bl\tilde{\nu}$	99 GeV	96 GeV
$\tilde{b} \to b\tilde{\chi}_1^0$	99 GeV	94 GeV

11.3.4. Stop and sbottom search limits at LEP and Tevatron. At LEP, squarks have been searched for in topologies corresponding to their two- and three-body decays. The difficult regions for their detection are similar to the ones for sleptons.

The mass exclusion limits at 95% CL obtained by combining the data up to 208 GeV from the LEP experiments in the LEP SUSY Working Group [422] are plotted in figure 95 for $\tilde{t} \to c\tilde{\chi}_1^0$, $\tilde{t} \to bl\tilde{\nu}$ and $\tilde{b} \to b\tilde{\chi}_1^0$ from left to right. Limits corresponding to the no mixing case and to the mixing yielding the minimal cross-section are both shown. For the decay $\tilde{t} \to c\tilde{\chi}_1^0$, the triangular region where $\Delta M > M_W + m_b$ is not excluded, as the decay of stop is dominated by the $\tilde{t} \to bW^+\tilde{\chi}_1^0$ channel. The excluded mass regions for right squarks with $(m_{\tilde{q}} - M_{\mathrm{LSP}}) > 20$ GeV are summarized in table 20. In addition, ALEPH has combined the $\tilde{t} \to c\tilde{\chi}_1^0$ search with searches for long lived stop hadrons, determining an absolute lower limit on the stop mass of 63 GeV [427]. This limit holds for any value of ΔM, stop lifetime or decay branching ratios.

It is instructive to compare the LEP results to the exclusion limits obtained by the Tevatron experiments. The CDF results on searches for $\tilde{t} \to c\tilde{\chi}_1^0$ and $\tilde{b} \to b\tilde{\chi}_1^0$ [428] and the D0 results on $\tilde{t} \to bl\tilde{\nu}$ [429] are also reproduced in figure 95. **It is clear that Tevatron experiments have a much larger reach in squark mass, but are unable to cover as small values of ΔM as LEP**.

A more general limit on the sbottom mass, valid for any hadronic decay, has been derived in [430]. Such a light sbottom should increase the $e^+e^- \to hadrons$ cross section by about 2% far from the Z^0 and 5% at the Z^0 peak. The author compiled the cross section results between 20 and 209 GeV from PEP, PETRA, TRISTAN, LEP1, SLC, LEP2. When combining these with the values of Γ_Z, R_l and R_b from LEP1 and SLC into a global fit, a lower limit of 8.5 GeV is set on the sbottom mass for any mixing and any hadronic decay to light quarks.

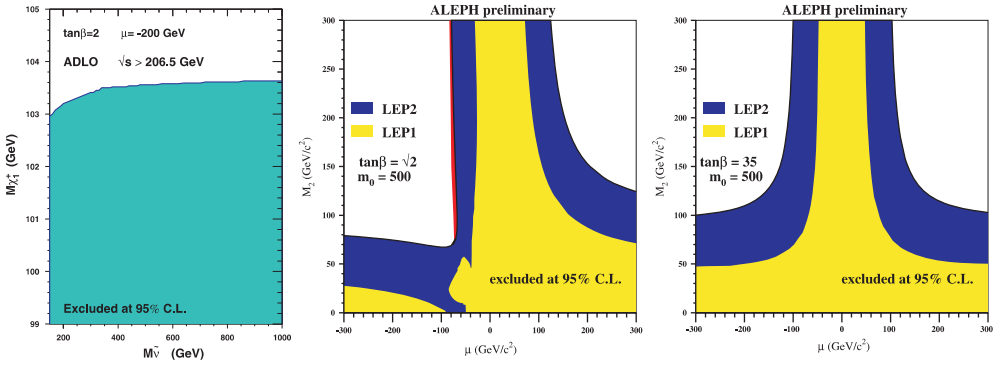

Figure 96. Left: chargino mass exclusion limits as a function of $m(\tilde{\nu})$, from combined LEP experiments at 206–208 GeV [422]. Chargino limits for $\tan\beta = \sqrt{2}$ and 35, from ALEPH at 189 GeV [431].

11.4. LEP results on charginos and neutralinos in MSUGRA

The chargino mass depends on the parameters M_2, μ and $\tan\beta$. However, the detection capability also depends on the MSUGRA parameter m_0, as the latter intervenes in the value of the sneutrino mass. We first consider the simplest cases where the search results from charginos and neutralinos suffice to establish limits on the masses of these particles. These are

(a) for large m_0 and hence heavy sleptons, so that chargino production cross-sections are large;
(b) for small $\Delta M = m(\tilde{\chi}_1^{\pm}) - m(\tilde{\chi}_1^0)$, which in the hypothesis of gaugino mass universality $M_2 \simeq 2M_1$ corresponds to the deep higgsino region.

The case of the lightest neutralino, likely to be the LSP, is discussed at length in section 12.

11.4.1. Mass limits for large m_0. The chargino pair production is an ideal channel for LEP, as the production cross-section is large and a few pb^{-1} luminosity could be sufficient to make a discovery. All four LEP experiments have looked for the lightest chargino in the topologies with leptons, leptons plus jets and jets. The results from these channels were combined by the SUSY Working Group [422] under the assumption that the charginos decay via a W^*. **This is the only decay allowed at LEP for $\tilde{\chi}_1^{\pm}$ under the assumption of heavy sfermions and compatible with the Higgs exclusion limit**. Limits on the mass were obtained from a scan over the MSSM parameters. The exclusion limits from 206–208 GeV data are shown in figure 96 (left). Under the assumption that $m(\tilde{\nu}) > 300$ GeV, chargino masses are bounded in the range $M(\tilde{\chi}_1^{\pm}) > 103.5$ GeV, this limit being set by the $\sim$35 pb^{-1} of data collected by the four experiments together at 208 GeV.

It is instructive to display the excluded range in the space M_2 versus μ (for fixed $\tan\beta$), as illustrated by the ALEPH results at 189 GeV [431] in figure 96 (centre and right) for $\tan\beta = \sqrt{2}$ and 35. The light grey area was excluded by the LEP1 results. The black area is the additional excluded region from LEP2 searches for charginos. The narrow dark grey region at low $\tan\beta$ and $\mu < 0$ represents the further exclusion by searches for neutralinos, which illustrates the fact that the reach in the $\tilde{\chi}_i^0\tilde{\chi}_j^0$ (and cascades) search exceeds slightly the chargino kinematical limit at low $\tan\beta$. In fact, the $\tilde{\chi}_1^0\tilde{\chi}_2^0$ search determines the exclusion for $M_2 > 100$–120 GeV. The exclusion for lower values of M_2 results from searches for cascade decays like $\tilde{\chi}_2^0\tilde{\chi}_3^0$ and $\tilde{\chi}_2^0\tilde{\chi}_4^0$.

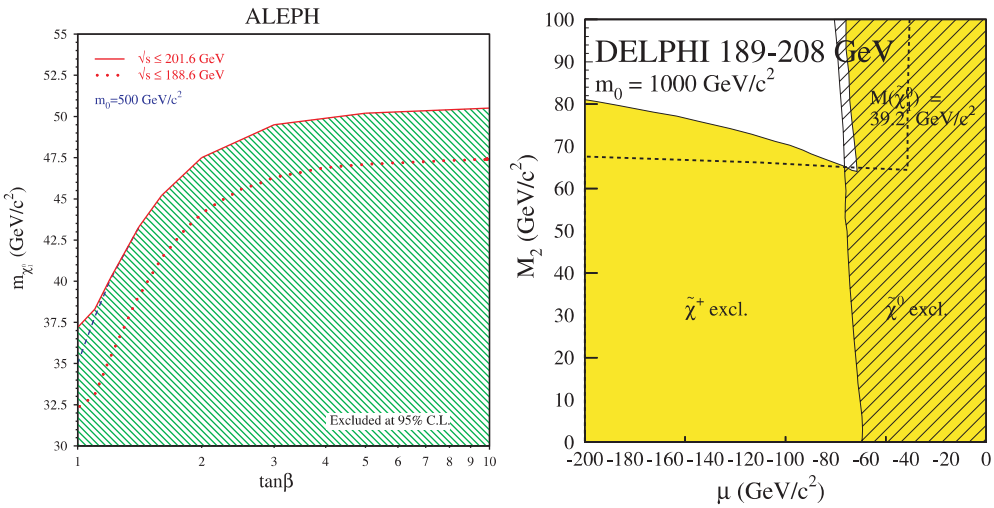

Figure 97. Neutralino mass exclusion curves as function of tan β for $m_0 = 500$ GeV, from ALEPH at 202 GeV [432]. Excluded regions in the M_2 versus μ plane from DELPHI at 208 GeV [426].

The parameter space excluded in the M_2 versus μ plane allows the extraction of an indirect limit on the $\tilde{\chi}_1^0$ mass, under assumption that $M_2 = 2M_1$. Figure 16 displays isomass curves for the $\tilde{\chi}_1^0$. The leftmost curve is the chargino kinematic limit for $M(\chi_1^{\pm}) = 104$ GeV. It is seen that for $\tan\beta \simeq 1$, the chargino kinematic limit bites into low $\tilde{\chi}_1^0$ masses along the $\mu \simeq -M_2$ diagonal (for larger $\tan\beta$ this effect is less severe; it also diminishes with increasing energy). As seen from figures 96 and 81, this is the region where some help can be expected from the neutralino searches, especially the cascade decays.

An example of the dependence of the limit on the lightest neutralino mass as a function of $\tan\beta$ is displayed in figure 97 (left) from the ALEPH analysis at 202 GeV [432]. The dashed line shows the exclusion limit if only the chargino search were included. The neutralino searches improve the limit by ∼2 GeV, but the limit is still obtained for $\tan\beta = 1$. The limit derived by the DELPHI experiment from the data up to 208 GeV [426], shown in figure 97 (right) is $M(\tilde{\chi}_1^0) \geqslant 39$ GeV, under the assumption of heavy sleptons. This limit is based solely on the chargino and neutralino searches and arises for $\tan\beta = 1$ and $\mu < 0$. Allowing for light sleptons would affect this limit very significantly.

11.4.2. Chargino mass limits for small ΔM. If the universality of gaugino masses at the unification scale is assumed, the small ΔM region corresponds to higgsino-like states, where the $\tilde{\chi}_1^{\pm}$, $\tilde{\chi}_2^0$ and $\tilde{\chi}_1^0$ are nearly degenerate with a mass close to $|\mu|$. This near degeneracy is illustrated by the lines of constant ΔM in figure 98 (left). The LEP1 data allowed the mass range $M(\tilde{\chi}^{\pm}) \leqslant 45$ GeV to be excluded for any value of ΔM. As we already mentioned, the standard chargino search loses sensitivity at small ΔM, typically $\Delta M \lesssim 3$ GeV, and hence at large M_2.

To reach yet smaller values of ΔM, dedicated searches have been developed. Such a search was conducted by the four LEP experiments and the result of their combination by the LEP SUSY Working Group at 189–208 GeV is displayed in figure 98 (right). The standard search reaches down to $\Delta M \simeq 3$ GeV. In the region 3 GeV $\geqslant \Delta M \geqslant$ 200 MeV, the visible products from the chargino decay carry little energy and missing p_T and the search is based on **events with a photon from initial state radiation (ISR) in the detector**, as originally

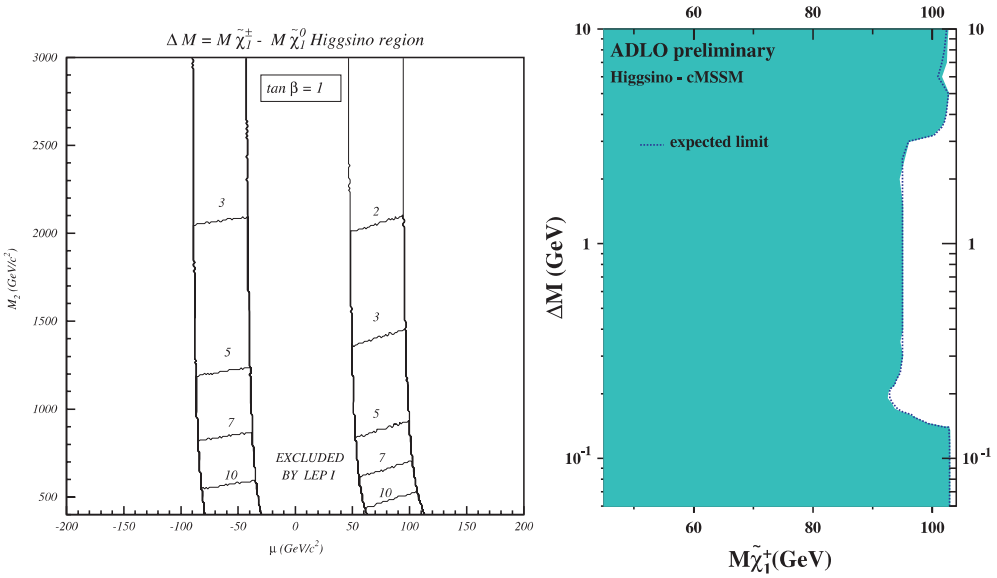

Figure 98. Left: regions of small ΔM in the M_2 versus μ plane [433]. The numbers indicate the mass spacing $\Delta M = M_{\tilde{\chi}_1^\pm} - M_{\tilde{\chi}_1^0}$ in GeV. Right: Exclusion limits at 95% CL on ultra-degenerate charginos in the higgsino-like region from the combination of LEP experiments [422].

proposed in [434]. This reduces strongly the background from $\gamma\gamma$ interactions, which is otherwise overwhelming. The excluded mass range remains smaller than for the standard search due to the lower efficiency resulting from the requirement of an ISR photon. Below 200 MeV a good sensitivity is recovered by the **search for long-lived particles**, which is discussed in section 13.2 on stau search in the GMSB framework. It is seen that the search with ISR photons allows the gap between the standard search and the search for a long-lived chargino to be closed completely. The reach in chargino masses is of ∼92.4 GeV, slightly lower than for the standard search, and it implies a strong bound on the neutralino mass, as they are approximately degenerate.

11.5. LEP results on charginos in AMSB

In SUSY with AMSB, it is found that $M_2 < M_1$ (see section 5.8), contrary to the expectation from gaugino mass universality. This also leads to near degeneracy of $\tilde{\chi}_1^\pm$ and $\tilde{\chi}_1^0$, like in the small ΔM region of MSUGRA. However, the degeneracy occurs in the gaugino-like region and implies different production diagrams. As a result, the selection efficiency is slightly different and the cross-section is larger, provided the sneutrino is heavy. Using the same search strategies as for MSUGRA with small ΔM, the results from the four LEP experiments were combined by the SUSY Working Group and the obtained limit is shown in figure 99. The obtained bound for gaugino-like degenerate charginos is $M(\tilde{\chi}_1^\pm) > 91.9$ GeV under the assumption that $m_{\tilde{\nu}} \geqslant 500$ GeV.

For smaller sneutrino masses, the production cross-section decreases and the mass limit deteriorates. In an analysis from DELPHI [435], it is found that when $M(\tilde{\chi}_1^\pm) \simeq m(\tilde{\nu})$, no bound is obtained beyond the one of LEP1 for $\Delta M < 200$ MeV. When the sneutrino is lighter than the chargino, the decay $\tilde{\chi}_1^\pm \to \tilde{\nu} l^\pm$ has practically 100% branching ratio. The standard chargino analysis for leptonic final states can then be used for the search. The region of the

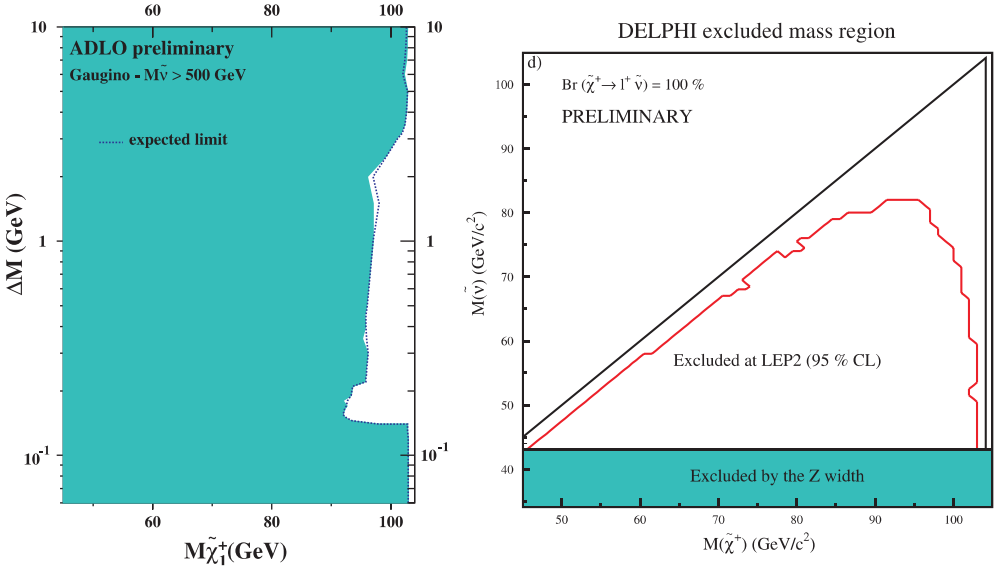

Figure 99. Left: exclusion limits at 95% CL on ultra-degenerate charginos in the gaugino-like region for $m_{\tilde{\nu}} = 500\,\text{GeV}$, from the combination of LEP experiments [422]. Mass bounds for $M(\tilde{\chi}_1^{\pm}) \geqslant m(\tilde{\nu})$ from DELPHI at 208 GeV [435].

$M(\tilde{\chi}_1^{\pm})$ versus $m(\tilde{\nu})$ plane excluded by DELPHI [435] from the data up to 208 GeV is shown in figure 99 (right).

11.6. A light gluino?

Up to now, we have discussed lower limits for sparticles ranging from $M_Z/2$ to a few hundred GeV. It is however often said that a very light gluino is still an open possibility. At first glance, it looks surprising that a strongly produced particle of a few GeV or so could have been missed. The direct searches, interpreted within the standard picture of such a particle, have been negative. Another argument against a light gluino is that its existence would slow the running of α_S: this is a delicate test and the answer was obscured for several years by possible discrepancies between low and high energy α_S determinations. Recently it has been claimed [436] that the 95% CL limit of $\Delta\Gamma_{\text{had}} < 3.9\,\text{MeV}$ applied to the $e^+e^- \to q\bar{q}\tilde{g}\tilde{g}$ process leads to $m_{\tilde{g}} > 6.3\,\text{GeV}$ at the 95% CL.

From the theory side [437], in a theory which has no dimension-3 SUSY breaking operators, the gluino and lightest neutralino are massless in the tree level approximation. The gluino obtains mass at one-loop from virtual quark–squark pairs and, within our present knowledge, can still be quite light. New light predicted hadrons [438] are mainly a $\tilde{g}-\tilde{g}$ bound state and its superpartner, a gluon–gluino bound state, discussed in section 9.4. The latter R^0 would be the lightest R-hadron, possibly long-lived or even stable.

Let us summarize the situation, following [439]:

(a) **Recent analyses of α_S running**: these seem to show consistency with standard QCD [439,440]. For instance, if one relies on QCD in τ decay and on the LEP measurements of $\alpha_S(M_Z)$, there is little room for a light gluino. However, discarding part of the information or increasing systematic errors may lead to different conclusions. To explain the reported excess of b-quark hadroproduction (however an anomaly which seems to fade away), it

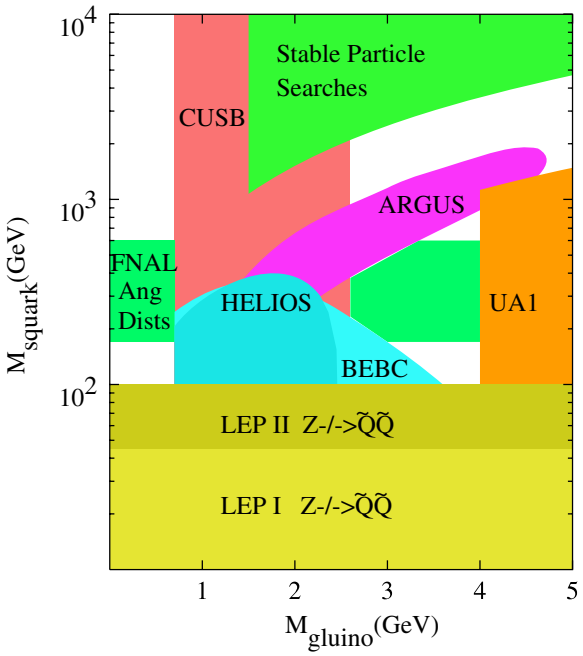

Figure 100. Map of excluded regions from light gluino searches, from [439].

has been recently proposed [441] that a light gluino (12–16 GeV) combined with a light $\tilde{b}$ (2–5.5 GeV) could play a role. This would affect the running of α_S and raise $\alpha_S(M_Z)$ by $\sim 0.013 \pm 0.001$ [442]. Combining sources of uncertainty at low and high mass scales, one cannot exclude such a possibility. Prospects for improvements are discussed in [442].

(b) **Direct searches for** R^0: the latest searches performed at Fermilab in KTeV [443] and E761 [444] turned out to be negative. Figure 100 (from [439]) summarizes the constraints on gluino mass in the current standard picture of gluino decay.

(c) **Concomitant predictions**: in the gravity mediated MSSM, the existence of a light gluino entails the existence of a light Higgs and light neutralino and chargino ($\mathcal{O}(M_W)$). With the present limits, the scenario is ruled out, unless there are perturbations to these mass predictions or gaugino mass universality is broken.

A list of the constraints to be met for a light gluino to be viable is found in [445]. In spite of the counter indications, one may still be able to invent scenarios involving such a particle. For instance [439] describes a scenario, guided by GMSB ideas, which could avoid the problems presented above, including the negative conclusion of the searches, while preserving the potential positive indications. In particular, it has been advocated that the CDF inclusive jet transverse energy cross-section at Fermilab [446] suggests an anomalous behaviour, in line with what one could expect in the light gluino scenario, in conjunction with a $\tilde{q}$ in the 100 GeV region. However the effect, if any, can have more mundane explanations and the results of run II at the Tevatron should clarify the situation.

12. The LSP and its phenomenology

When R-parity is conserved, a condition which is not imperative but guarantees conservation of L and B quantum numbers, the LSP is stable and weakly interacting. If it has been produced in the early universe and has not been annihilated, it will exist as a relic particle. At accelerators, its production contributes to the missing energy signature. Given its potential importance for cosmology, it is worth studying which limits can presently be set on the LSP mass. The bounds vary strongly with the experimental inputs included in the analysis and with the model assumptions. First, the limits achieved solely by the negative results from searches at accelerators will be reviewed. Then, further constraints including the estimated amount of dark matter in the universe and the low energy measurements will be discussed. Finally, direct and indirect searches without accelerators will be discussed. The future at accelerators will be quoted but treated in section 15.

12.1. Limits from negative searches at accelerators

12.1.1. Combining various searches from LEP. The chargino and neutralino search results do not allow by themselves a determination of an absolute exclusion limit on the chargino nor on the LSP when slepton masses are allowed to become small. The LEP results for the higgsino region remain unaffected, but important effects are expected in the gaugino and in the mixed regions.

- Chargino searches are weak in the gaugino-like region when the $\tilde{\nu}$ is light, due to the lowering of the production cross-section by interference with the t-channel exchange diagram, as discussed in section 10.1.2. This effect is compensated by the increase in the neutralino cross-section due to a lower $\tilde{e}$ mass.
- The assumption of scalar mass universality, for which the strongest constraint is from $\tilde{e}_{\mathrm{R}}$:

$$m^2_{\tilde{e}_{\mathrm{R}}} = m_0^2 + .23M_2^2 - 0.27M_Z^2 \cos 2\beta, \tag{166}$$

  allows the exclusion of low regions of M_2 for fixed m_0 and $\tan\beta$ by using the $\tilde{e}_{\mathrm{R}}$ mass limits. Its exclusion is strongest at low $\tan\beta$.
- The bound on the mass of the lightest Higgs is naturally a crucial one. The LEP limit allows the region of low $\tan\beta$ to be ruled out. This constraint is due to the dependence of the Higgs mass on the sparticle masses via the loop corrections, particularly the stop, and is thus sensitive to the SUSY parameters.
- When the $\tilde{\nu}$ mass is below but nearly degenerate with the chargino mass, the final state becomes undetectable. At the same time, $\tilde{\chi}_2^0 \to \tilde{\nu}\nu$, an invisible final state. This narrow region in the plane of chargino mass versus m_0 has been called the 'corridor'. Since the corridor corresponds to small $\tilde{\nu}$ masses, the slepton search results can impose constraints.
- At large $\tan\beta$, the $\tilde{\tau}$ mixing becomes important. It may lead to a situation where the $\tilde{\tau}_1$ is lighter than the chargino and nearly degenerate with the neutralino LSP, which makes the dominant chargino decay $\tilde{\chi}_1^{\pm} \to \tilde{\tau}_1\nu_\tau$ undetectable. This may be recovered by looking for the $\tilde{\chi}_2^0 \to \tilde{\tau}_1\tau$ decay with one soft and one harder τ in the final state.

12.1.2. LEP results interpreted in CMSSM. LSP mass bounds have been derived in a CMSSM framework, where **GUT unification of gaugino masses and of sfermion masses is assumed. Higgs mass parameters are not supposed to be unified**. The free parameters are then $\tan\beta$, M_2, m_0, μ, m_A and A_t.

At $\tan\beta \simeq 1$, the constraint (166) from the slepton search is very strong for small m_0. For increasing m_0, the limit from sleptons first decreases steeply and then joins smoothly

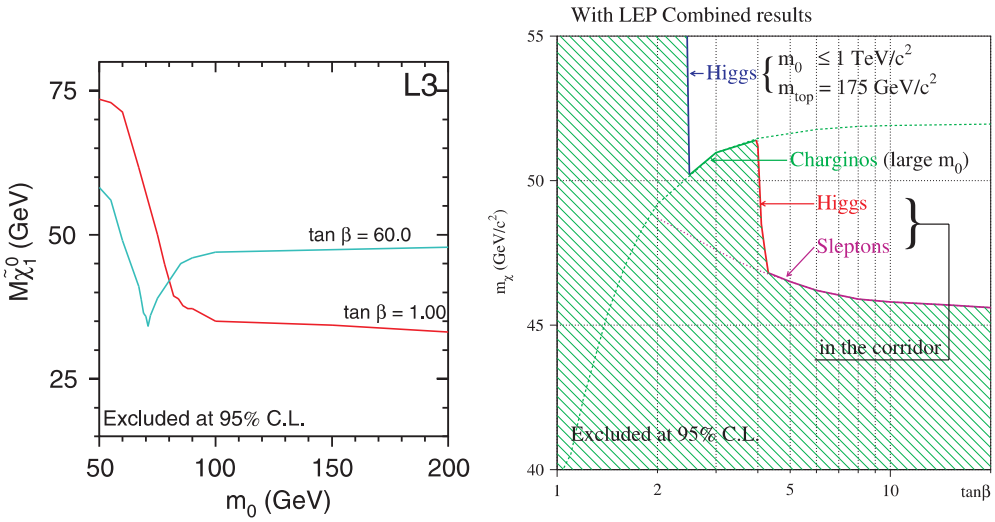

Figure 101. Mass exclusion limit at 95% CL for the lightest neutralino. Left: illustration of the dependence of the mass bound on m_0 for small and large values of tan β, from L3 at 189 GeV [447]. Right: mass bound on the LSP as function of tan β from the combination of the LEP experiments up to 206 GeV by the LEP SUSY Working Group [422].

the exclusion by charginos and neutralinos obtained for large m_0. This behaviour is clearly illustrated in figure 101 (left). At larger tan β, the constraint from the slepton searches at small m_0 is still important but weaker than for small tan β, as also seen in figure 101 (left). At large m_0, the exclusion from the chargino and neutralino searches is stronger than for low tan β due to a different relation between the masses of $\chi_1^\pm$ and $\tilde{\chi}_1^0$. In the intermediate region, $m_0 \simeq 70$–80 GeV, there is a minimum in the exclusion, related to the degeneracy of a gaugino-like chargino with the sneutrino.

The excluded range of LSP masses as function of tan β, from the combination of the LEP experiments by the LEP SUSY Working Group [422], is shown in figure 101 (right). For given values of tan β, m_0 and M_2 the maximum predicted Higgs mass, $m_h^{\max}$, is computed for $m_A = 2$ TeV and by maximizing the effect of stop mixing by varying A_t–$\mu \cot \beta$. For such large values of m_A, the MSSM Higgs behaves as the SM Higgs and the bound $m_h > 114$ GeV has been used. This excludes completely the region of low tan $\beta < 2.5$, as shown in table 13. The range excluded in the plot depends quite strongly on the assumed value of $m_{\text{top}} = 175$ GeV and the upper limit of the scan $m_0 < 1$ TeV. In the region $2.5 < \tan \beta < 4$ the LSP exclusion is determined by the chargino search limit for large m_0. For tan $\beta > 4$, there is a small region for tan $\beta < 4.2$ where the Higgs mass bound still contributes and above this, the LSP limit is set by the slepton searches in the chargino–sneutrino corridor.

In this CMSSM scenario, the lower limit on the LSP mass is found for large tan β at about 45 GeV.

12.1.3. LEP results interpreted in MSUGRA. Limits on the LSP mass have also been obtained in a strict MSUGRA framework. Correct breaking of the electroweak symmetry was imposed, which determines the value of m_A and the absolute value of μ as function of the other parameters. The free parameters are now tan β, M_2, m_0, sign(μ) and A_0. The common trilinear coupling A_0 was first supposed to be zero at the GUT scale. The excluded range of LSP masses as function of tan β, from the combination of the LEP experiments by the SUSY

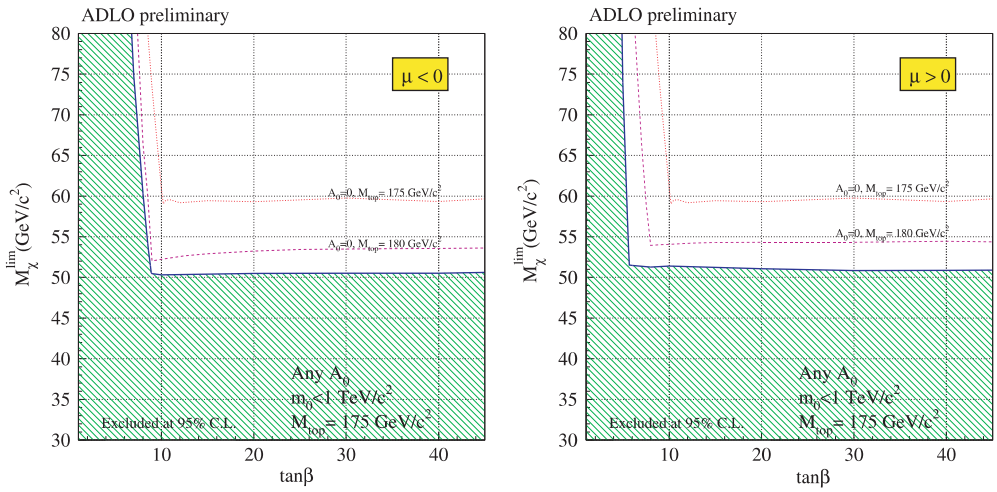

Figure 102. Mass bound on the LSP as function of tan β in the MSUGRA scenario for positive and negative values of μ. The dotted and dashed lines (red) show the limits obtained for $A_0 = 0$ and a top mass of 175 GeV and 180 GeV, respectively. The dashed area (green) represents the excluded region for any A_0 and $m_t = 175$ GeV. From the LEP SUSY Working Group [422].

Working Group [422], is shown in figure 102. The impact of the Higgs limit extends to much larger values of tan β in this case than in CMSSM. This is due to the fact that within MSUGRA, the stop mixing is never maximal. For higher tan β values, the limit is set by the chargino search. In this region of high tan β, the stau mixing may be important, leading to $\tilde{\tau}_1$ lighter than the chargino and hence the dominant decay $\tilde{\chi}_1^{\pm} \to \tilde{\tau}_1 \nu$. In the case of stau–neutralino degeneracy, the sensitivity of the chargino search is lost. It is recovered by the search for $\tilde{\chi}_2^0 \to \tilde{\tau}_1 \tau$ cascade decays from $\tilde{\chi}_1^0 \tilde{\chi}_2^0$ and $\tilde{\chi}_2^0 \tilde{\chi}_2^0$ production, so that the LSP bound is again set by the charginos at large m_0 over the whole range. However, the figure also illustrates the sensitivity of the LSP bound to the value of the top mass. This dependence on m_t can be traced back to a variation of the parameter μ due to the top Yukawa coupling which enters its RGE, which affects the neutralino composition [21].

The MSUGRA interpretation puts a bound on the LSP mass $M(\tilde{\chi}_1^0) > 58.6$ GeV, valid for $m_0 < 1$ TeV, $A_0 = 0$, $m_t = 175$ GeV and negative μ. For $m_t = 180$ GeV, the limit is lowered to 52.0 GeV. For positive μ, the corresponding bounds increase by 1–2 GeV.

The limit on the LSP mass is also sensitive to the value of A_0. A scan has been performed on the GUT scale value of A_0 which extends typically from -2 to +2 TeV. The bound on the LSP mass is set for large m_0 and large negative values of A_0. The results from the LEP SUSY Working Group are also shown in figure 102 as function of tan β. The limit is lowered to $M(\tilde{\chi}_1^0) > 50.3$ GeV for negative μ and $m_t = 175$ GeV. It becomes $M(\tilde{\chi}_1^0) > 50.8$ GeV for positive μ and the same top mass.

12.1.4. LEP results in AMSB. Like for MSUGRA, bounds can be derived on the AMSB spectrum from a scan over the parameters $m_{3/2}$, m_0, tan β and sign(μ) (enforcing radiative electroweak symmetry breaking) by imposing constraints from the following.

- The Higgs search. In AMSB, the relation $m_A \gg M_Z$ is always fulfilled. Therefore, the light Higgs h^0 is SM-like and the corresponding mass bound, given in section 8.6, can be

[21] We thank G Ganis for providing us with this information.

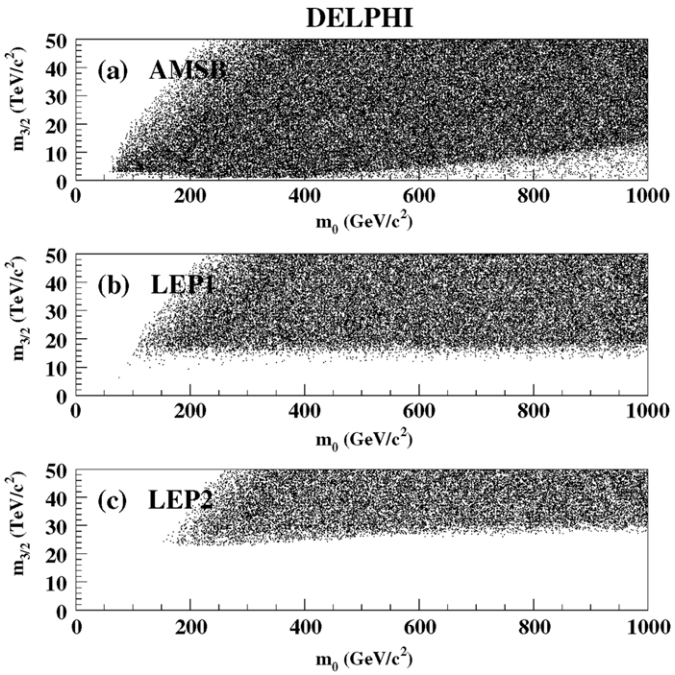

Figure 103. Allowed points for the AMSB scenario in the $m_{3/2}$ versus m_0 plane (upper). The bands at large m_0 reflect the resolution of the scan over the parameter space. Middle: points remaining after imposing the experimental bounds on the chargino and sneutrino masses and (lower) after all bounds are applied. From [435].

applied. However, in some regions of the parameter space, h^0 decays to SUSY particles are allowed. Important decay modes are $h^0 \to \tilde{\chi}_1^0\tilde{\chi}_1^0$, $\tilde{\chi}_1^\pm\tilde{\chi}_1^\pm$, $\tilde{\nu}\tilde{\nu}$, for which the results from invisible Higgs can be used. Finally, the decay $h^0 \to \tilde{l}\tilde{l}$ may also contribute.

- The search for charginos, discussed in section 11.5.
- The search for stable $\tilde{\tau}_1$, nearly mass degenerate with the $\tilde{\chi}_1^0$.

As an example, a scan over the AMSB parameters performed by DELPHI [435] is displayed in the upper figure 103 as a function of $m_{3/2}$ and m_0, with $1.5 \leqslant \tan\beta \leqslant 35$ and both signs of μ. The empty region at low m_0 is excluded because sleptons would be tachyonic. The middle plot shows the points remaining after imposing the LEP1 bounds on the charginos and sneutrinos. A further improvement on LEP2 searches is visible in the lower figure. This is mainly due to the constraints from the SM and the invisible Higgs. A small contribution at low $m_{3/2}$ is due to the chargino search and at low m_0 to the slepton search. Altogether, neutralinos are excluded below 70 GeV and sneutrinos below 100 GeV.

12.1.5. Gluino LSP scenario. There are several models, with appealing theoretical motivations, in which the LSP is a gluino. The very light gluino case has been discussed in section 11.6. Even if one has to consider a substantial mass, it is unwise to simply assume that the gluino cannot be the LSP or NLSP [448]. Present and future experiments can find or exclude it in a significant range of $m_{\tilde{g}}$.

A gluino LSP is expected to be stable and to fragment into R-hadrons, either neutral $R^0(\tilde{g}g, \tilde{g}u\bar{u}, \ldots)$ or charged $R^\pm(\tilde{g}u\bar{d}, \ldots)$. The charged state can be identified by anomalous

ionization and the neutral one by its partial energy deposit in the calorimeters, which lead to a lower missing energy than for the $\tilde{\chi}_1^0$ LSP of SUGRA with R-parity conservation [448]. A search was made by DELPHI [449] for gluino pair production by gluon splitting. As the production rate is too low at higher energies, the Z^0 data from LEP were used. They exclude a stable gluino with mass between 2 and 18 GeV. Another analysis searched for the decays $\tilde{t}_1 \to c\tilde{g}$ and $\tilde{b}_1 \to b\tilde{g}$ in the 189–208 GeV data. It resulted in the exclusion limits $m_{\tilde{t}_1} > 87$ GeV and $m_{\tilde{b}_1} > 82$ GeV, independent of the stop and sbottom mixing angles.

12.2. Cosmological constraints

Barring an alternative explanation involving a modification of Newton's law at very large scale [450] or modified newtonian dynamics (MOND), there is strong evidence [451] for a large amount of dark matter in the universe, which means matter whose existence has been inferred only through its gravitational effects. It may be baryonic (made of baryons which are not seen) and non-baryonic. Non-baryonic dark matter is called hot (HDM) or cold (CDM), depending on its status, relativistic or non-relativistic, at the time relevant for galaxy formation. With the usual inputs, galaxy formation models require primarily CDM. The two most studied candidates for CDM are the axion [451] and the LSP of R-parity conserving supersymmetry, although other possibilities exist, as we saw in section 2.3. Besides DM, converging evidence from supernova studies, CMB and galaxy surveys show that either a negative-pressure component or some HDM is required in addition. The pressure of component i is defined by $p_i \equiv w_i \rho_i$, where the energy density is $\rho_i \equiv \Omega_i \rho_c$ with ρ_c the critical density. For instance, a model with $\Omega_{\rm CDM} = 0.3$, $\Omega_{\rm HDM} = 0$, $\Omega_X = 0.7$ with $w_X = -0.6$ (where X represents the dark energy due to the cosmological constant or quintessence) fits all data. Let us note that a negative-pressure component contributes to the acceleration of the expansion of the universe through its indirect gravitational effect. One should also point out that there exist alternative explanations to the data quoted above, for instance [452] as well as some conflicting sets of data [453].

The key question is the predicted value of $\Omega_{\rm CDM}$. If the particle is its own antiparticle or if particles and antiparticles are present in equal numbers, and if these particles were in thermal equilibrium with radiation at least until they became non-relativistic, their relic abundance is determined by their annihilation cross-section $\sigma_{\rm ann}$.

$$\Omega_{\rm CDM} \simeq 7 \times 10^{-27}\,{\rm cm}^3\,{\rm s}^{-1}/\langle\sigma_{\rm ann} v_{\rm rel}\rangle \tag{167}$$

where $v_{\rm rel}$ is their relative velocity. The value of the bracket needed for $\Omega_{\rm CDM} = 1$ would correspond to a weakly interacting particle (WIMP) of mass $m_{\rm DM} = 100$ GeV:

$$\langle\sigma_{\rm ann} v_{\rm rel}\rangle \sim \alpha^2/8\pi m_{\rm DM}^2 \sim 3 \times 10^{-27}\,{\rm cm}^3\,{\rm s}^{-1}. \tag{168}$$

The LSP of the MSSM qualifies as such a WIMP, with its mass expected in the range of tens to hundreds of GeV. In minimal SUGRA, which has a greatly reduced parameter space compared with the MSSM, it is possible to have parameters agreeing with all data and satisfying $\Omega_{\rm CDM} = 0.3$.

For a long time, most studies adopted as cosmologically acceptable the range

$$0.1 < \Omega_{\rm LSP} h^2 < 0.3, \tag{169}$$

where $h \simeq 0.7$ is the present Hubble expansion rate in units of $100\,{\rm km\,s^{-1}\,Mpc^{-1}}$. However, measurements of fluctuations in the cosmic microwave background radiation in particular by the Wilkinson microwave anisotropy probe (WMAP) [454] yield more accurate determinations of the cosmological parameters. They quote a total matter density $\Omega_m h^2 = 0.135^{+0.008}_{-0.009}$ and a

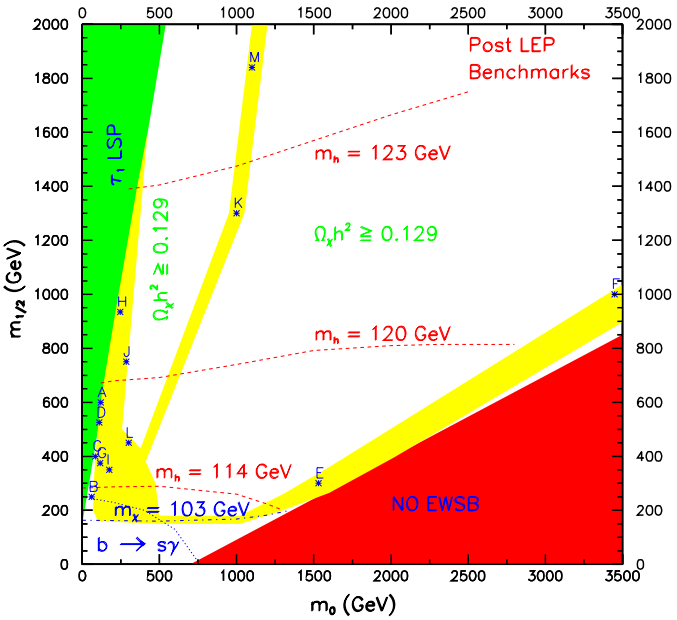

Figure 104. Illustration of the constrained MSUGRA regions for various constraints.

baryon density $\Omega_b h^2 = 0.0224 \pm 0.0009$ from which the range of CDM density at 2 standard deviations is derived as

$$0.094 < \Omega_{\rm LSP} h^2 < 0.129 \tag{170}$$

considerably narrowing the allowed range. The lower bound is optional since there could be other sources of CDM besides the LSP. We will discuss in more detail the impact of these constraints in section 12.2.3.

12.2.1. Constrained MSUGRA. There exist various versions of the constrained MSUGRA (also called constrained MSSM in some papers), which differ by the constraints imposed. Most of them assume mass universality at the GUT scale and impose radiative electroweak symmetry breaking. They differ in the additional requirements whose effect is best viewed in a plot of m_0 versus $m_{1/2}$ for fixed $\tan\beta$ and a chosen sign of μ. The parameter A_0 is often set to zero at the GUT scale. For further information, we refer, for example, to the lecture notes [455, 456].

Some constraints are illustrated in figure 104. The extension of the regions is qualitative only, as their actual boundaries depend on $\tan\beta$, A_0 and the top mass. Accurate plots, including the $\tan\beta$ dependence, are found in section 12.2.3. Their gross features can be summarized as follows.

Some regions are excluded by the model itself. In the lower right dark shaded (red) region no correct electroweak symmetry breaking can be achieved, as we discussed in section 5.3. The actual boundary of this region is quite sensitive to the details of the calculation and varies considerably between different programs. In the upper left shaded (green) region the LSP would be a $\tilde{\tau}_1$.

Stringent constraints are provided by direct searches at LEP. In most of the parameter space, the strongest constraint is from the Higgs mass bound $m_h \geqslant 114\,\text{GeV}$ (section 8.6),

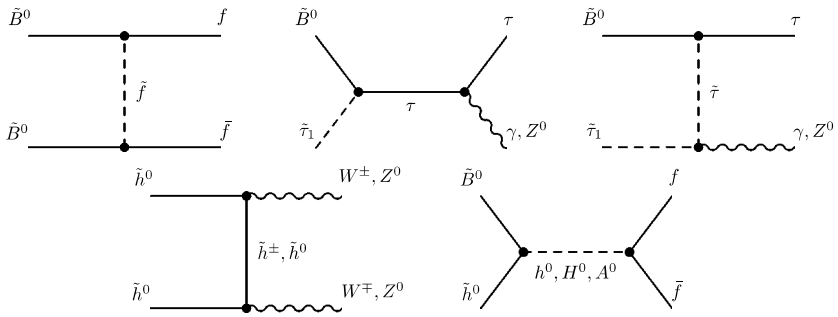

Figure 105. Examples of diagrams contributing to neutralino annihilation.

which applies for most parameter choices as the light Higgs is almost always SM-like in the MSUGRA. Since m_h is sensitive to the stop mass via the radiative corrections, formula (127), its bound implies a constraint, e.g. the dashed (red) line in figure 104, which affects mostly $m_{1/2}$. The excluded region in the $(m_0, m_{1/2})$ plane also depends on $\tan\beta$ and decreases with increasing $\tan\beta$. The sensitivity to m_h is particularly important at large $m_{1/2}$, say $m_{1/2} > 500$ GeV, where a shift of 1 GeV on m_h corresponds to several hundred GeV on $m_{1/2}$, as seen from the curves at various Higgs masses (computed with ISASUGRA for $\tan\beta = 10$). This constraint relies on strict universality of all scalar masses. It is, therefore, useful to also display constraints from other processes, which may be weaker but depend on different assumptions. One such constraint comes from the bound $M(\tilde{\chi}_1^\pm) > 103.5$ GeV (section 11.4), seen as a dash–dotted (blue) contour in figure 104, at nearly fixed $m_{1/2}$. This constraint is only weakly dependent on $\tan\beta$ and the sign of μ. The selectron limit $m_{\tilde{e}} > 99$ GeV also allows the exclusion of a small region (not shown) in the plane for small values $m_0 < \sim 100$ and $m_{1/2} < \sim 250$ GeV.

Among the low energy measurements, an important constraint is due to the $B(b \to s\gamma)$ which, being compatible with the SM prediction (section 6.3), excludes low mass charginos and charged Higgses and is shown as the dotted (blue) line. Its effect is typically stronger for large than for low $\tan\beta$ and for $\mu < 0$ than for $\mu > 0$. The measured muon anomalous magnetic moment (section 6.5), together with the new evaluation of the SM expectation, given in equation (107), could also exclude the low mass corner of the $m_0/m_{1/2}$ plane (not shown) at the 2σ level, provided the largest value is taken for the discrepancy. For $\mu < 0$, its exclusion is slightly stronger than for $\mu > 0$.

Further constraints can be imposed under the assumption that the remnants of the lightest neutralinos left over from the Big Bang form (or at least contribute to) the CDM of the universe, see section 12.3, whose density is bounded by the ranges (169) or (170). The upper bound is mandatory [456]: a larger value of the relic density would overclose the universe. The lower bound is optional, since there could be contributions, other than the LSP, to the relic density. The neutralino relic density is controlled by the annihilation cross-section of neutralinos and without annihilation, the relic density would by far exceed the upper bound. Some contributing diagrams are displayed in figure 105. In a vast area of the MSUGRA parameter space, the LSP is bino-like and two neutralinos annihilate by t-channel exchange of sfermions, shown in the top-left diagram. This forms the 'bulk' of the CDM region (light-shaded, yellow) drawn in figure 104. Since the cross-section is sizeable only for light sfermions, this region is restricted to low m_0 and $m_{1/2}$. The allowed region extends in the $m_0/m_{1/2}$ plane along several filaments. At larger $m_{1/2}$ and low m_0 the $\tilde{\tau}_1$ is light, nearly degenerate with the neutralino, and coannihilation of $\tilde{\tau}_1\tilde{\chi}^0$ (as well as the other right-handed sleptons which are also close in mass) takes place due to s- and t-channel exchange depicted in the upper central and right diagrams.

Another possibility arises at large m_0, near the area where EWSB is no longer possible. In this 'focus point' region and for intermediate to large $\tan\beta$, the neutralinos have an important higgsino component, giving rise to annihilation into gauge bosons according to the lower-left diagram. Finally, there is a narrow region where $M(\tilde{\chi}_1^0) \simeq m_{\text{Higgs}}/2$ or $M_Z/2$, the 'funnel' where rapid annihilation takes place via s-channel poles, an example being the lower-right diagram. This process is only important for large $\tan\beta$, else the higgsino component is too small.

Another constraint which is sometimes invoked is the 'fine tuning'. It will not be discussed here, as its significance is very debatable: there is no consensus on how large a fine tuning is acceptable and the input variables, which are treated as independent, may well be correlated in a more complete theory, hence modifying the value of the fine tuning measure.

It is interesting to see how the regions allowed by the DM constraint are affected by the universality assumption. Such an exploratory analysis was made in [457] by allowing for non-universal Higgs mass parameters (NUHM). Hence, μ and m_A become free parameters, in addition to the usual CMSUGRA ones. A striking difference with the CMSUGRA scenario is that there now exists a DM allowed strip from rapid annihilation via s-channel A and H poles (the funnel), even for moderate $\tan\beta$, due to the increased higgsino content of the $\tilde{\chi}_1^0$. Unlike in CMSUGRA, where the funnel follows approximately along the diagonal, it occurs in NUHM around a fixed value of $m_{1/2}$, corresponding to $m_{\tilde{\chi}_1^0} \simeq m_A/2$ and reflecting the fact that the CMSUGRA relation between m_A and m_0 is lost. By varying m_A it becomes now possible to sample different regions in the $(m_0, m_{1/2})$ plane.

12.2.2. LSP limits in a general MSSM. An obvious question is to know how light the LSP can be in a more general context than the CMSUGRA. In [458] the authors consider a general R-parity conserving MSSM. They only require that the LSP be the lightest neutralino, that it be responsible for the observed relic density, which they take in the range $0.05 \leqslant \Omega h^2 \leqslant 0.3$, and that the MSSM respect the LEP2 limits, summarized as all scalar leptons and charginos being heavier than 103 GeV (a bit optimistic for sleptons). Actually, this implies an $SU(2)$ relation (91) between the mass of the left slepton and the sneutrino in each generation. Moreover, the LEP1 limit on the invisible Z^0 decay width, already used for bounding sneutrino masses in section 11.3, strongly limits the higgsino component of a light $\tilde{\chi}_1^0$, as this would couple to a Z^0 with gauge coupling strength. A light $\tilde{\chi}_1^0$ is thus expected to be dominantly gaugino-like, its annihilation to proceed via the t-channel exchange of a slepton and the slepton to be light enough to reach the required level of dark matter. Hence, the LEP2 exclusion of light sleptons, combined with the CDM constraint, may exclude a very light LSP. Figure 106 shows the results of a complete scan. If the relic density $\Omega h^2 = 0.2$ is allowed to be reached, a minimal LSP mass of ∼18 GeV is obtained. However, if the WMAP central value of ∼0.11 is taken, the neutralino mass lower limit is much higher. On the other hand, a reduced slepton mass limit $m(\tilde{\tau}_1) > 80$ GeV would only exclude an LSP mass $\lesssim 10$ GeV. The lowest value of the LSP mass requires all sleptons and charginos to be just above the LEP2 limit.

A similar analysis was performed in [459], which imposes more realistic limits from LEP2, in particular $m(\tilde{\tau}_1) > 86$ GeV. It confirms that, for a relic density $\Omega h^2 < 0.3$, a lower limit $m(\tilde{\chi}_1^0) \gtrsim 10$ GeV is obtained. However, when combined with the constraint from g_μ–2 (using $\delta a_\mu > -21 \times 10^{-10}$), the lower bound is raised to $m(\tilde{\chi}_1^0) \gtrsim 18$ GeV for $\mu > 0$ and about 2 GeV more for $\mu < 0$, both for $\tan\beta = 10$.

12.2.3. LSP limits in constrained MSUGRA. An analysis [460] was made in the constrained MSUGRA framework with the free parameters m_0, $m_{1/2}$, $\tan\beta$, $\text{sign}(\mu)$ and fixed values

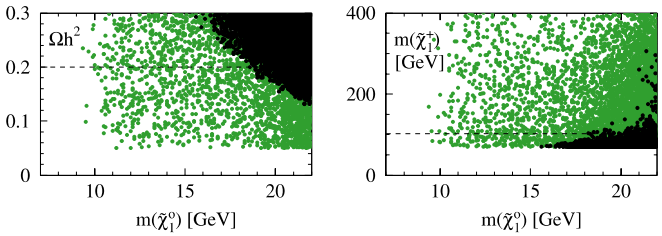

Figure 106. MSSM points in the plane of the neutralino LSP mass and either the relic density (left) or the lighter chargino mass (right). In grey (green) are all points with $0.05 \leqslant \Omega h^2 \leqslant 0.3$ and in black the ones obeying the limit $m(\tilde{\tau}_1) > 103$ GeV. The dashed lines are the experimental chargino mass limit and a possibly improved limit on the relic density. Reprinted from [458]. Copyright 2003, with permission from Elsevier.

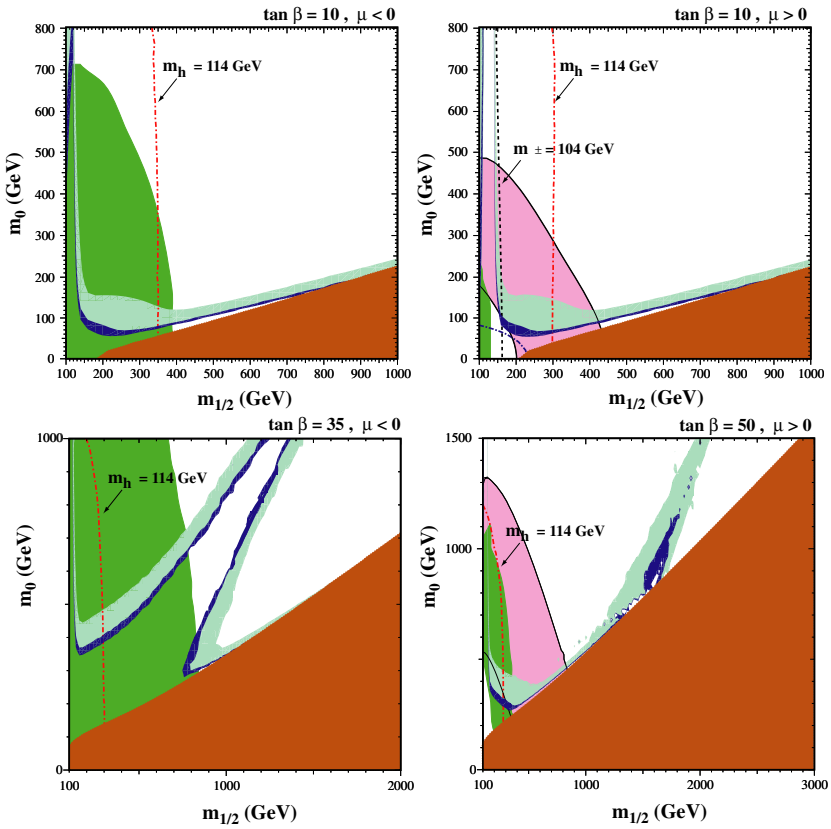

Figure 107. Allowed regions in the $(m_0, m_{1/2})$ plane. See the text for explanations of the constraints. Reprinted from [460]. Copyright 2003, with permission from Elsevier.

$A_0 = 0$ and $m_t = 175$ GeV. The allowed regions are presented in figure 107. Indicated are the regions excluded by the LEP2 lower limits on m_h (red dash–dotted line), $m(\tilde{\chi}_1^\pm)$ (black dashed line), $m(\tilde{e})$ (black dotted line, only visible in the $\tan\beta = 10$, $\mu > 0$ panel), as well as those ruled out by the $\tilde{\tau}_1$-LSP in dark grey (red), the $b \to s\gamma$ decay in medium grey (green) and the region favoured by g_μ–2 at the 2–σ level, assuming the SM value based on e^+e^- data, in lighter

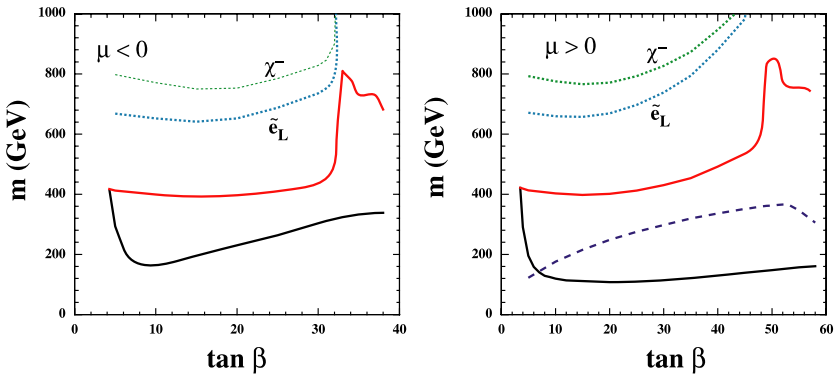

Figure 108. Lower and upper bounds on $m(\tilde{\chi}_1^0)$ compatible with the new cosmological constraint, equation (170) and the experimental limits. The lower limit on $m(\tilde{\chi}_1^0)$ is drawn as a fat (black) continuous line. The upper limits on $m(\tilde{\chi}_1^0)$ are shown without (red solid line) and with (blue dotted line) the g_μ–2 constraint. Also shown are the $\tilde{e}_L$ and $\tilde{\chi}^\pm$ masses at the tips of the coannihilation tails. Reprinted from [460]. Copyright 2003, with permission from Elsevier.

grey (pink). Also shown are the regions allowed by the older cosmological constraint (169) in light shading (cyan) and by the newer one (170) in dark shading (blue). It is immediately seen that the cosmological regions are much narrower and that the 'bulk' region has almost disappeared once the experimental constraints from WMAP are imposed. The largest value allowed for $m_{1/2}$, and hence for the mass of the $\tilde{\chi}_1^0$, is reached in the coannihilation region for low $\tan\beta$ and in the rapid annihilation funnel for large $\tan\beta$, both of which have now a much reduced extension in $m_{1/2}$. The position and extension of these strips varies with $\tan\beta$. They lead to lower and upper bounds on the lightest neutralino mass displayed in figure 108, which can be summarized as

$$\begin{aligned} 108 < m(\tilde{\chi}_1^0) < 500\,\text{GeV for} \mu > 0 \,\text{and}\, \tan\beta < 40 \\ 160 < m(\tilde{\chi}_1^0) < 430\,\text{GeV for} \mu < 0 \,\text{and}\, \tan\beta < 30. \end{aligned} \tag{171}$$

The upper bound weakens considerably for larger values of $\tan\beta$. If the g_μ–2 constraint is included, the upper bound for $\mu > 0$ becomes $m(\tilde{\chi}_1^0) < 370\,\text{GeV}$. The lower bound is set at large $\tan\beta$ by the $b \to s\gamma$ constraint for both signs of μ. At lower $\tan\beta$ it is higher and is set by the Higgs limit.

These new reduced upper bounds improve the prospects for discovering supersymmetry at the LHC, assuming the validity of this rather restrictive model, discarding large values of $\tan\beta$ and ignoring the focus point region. It should, however, be borne in mind that the allowed bands may be shifted in the plane or broadened by several effects. For example the shift due to a non-zero value of A_0 can be very significant, especially at large $\tan\beta$ and was considered in [281,461]. The uncertainty on the mass of the top quark also broadens the strips [281,462]: e.g. the shift introduced by moving m_t from 175 to 178 GeV is equivalent to changing $\tan\beta$ from 35 to 40 for $\mu < 0$ and from 50 to 57 for $\mu > 0$. Significant shifts in the position of the strips are also observed between the different SUSY programs available [463], due to the different approximations made to compute the sparticle spectrum. Their magnitude often amounts to values comparable to or even larger than the experimental uncertainty on the relic density. Furthermore, in the NUHM scenario of section 12.2.1 larger values of $m(\tilde{\chi}_1^0)$ can be reached for a suitable choice of the m_A and μ parameters, unless the g_μ–2 constraint is applied.

12.3. Neutralino non-accelerator searches

Experiments show that, within the Milky Way, the amount of dark matter (DM) is

$$\rho_{\mathrm{DM}} \simeq (0.3\text{–}0.5\,\mathrm{GeV})\,\mathrm{cm}^{-3}. \tag{172}$$

As we said, SUSY with R-parity conservation possesses a natural candidate for cold dark matter, the lightest neutralino $\tilde{\chi}_1^0$. We focus here more generally on the search for SUSY weak interacting massive particles (WIMPS), of which the neutralino is a special case. See figure 1 of [464] for a broader point of view.

One may either perform direct searches for relic neutralinos through their interaction with ordinary matter, in appropriate detectors, or indirect ones through their pair annihilations in the halo or in celestial bodies (Earth or Sun) [465]. We discuss the former in section 12.3.1, the latter in 12.3.2.

12.3.1. Direct searches. Direct searches aim at the measurement of the energy released by a $\tilde{\chi}^0$ to a target nucleus. The detection rate is given by the $\tilde{\chi}^0$-nucleus cross-section, convoluted with the phase-space distribution function of the $\tilde{\chi}^0$ in the galactic halo. The uncertainties of the latter are substantial. The former can either be coherent ($\sim A^2$) or spin-dependent. In the case of a $\tilde{\chi}^0$ with coherent interaction with matter [466] the range of cross-section under current exploration (called stage 1) is [467, 468]

$$10^{-6}\,\mathrm{pb} \lesssim \xi\sigma_{\mathrm{scalar}}^{\mathrm{nucleon}} \lesssim 2\times 10^{-5}\,\mathrm{pb} \tag{173}$$

for a $\tilde{\chi}^0$ in the mass range 30–270 GeV, with the best limits obtained by CDMS [469], EDELWEISS [470] and ZEPLIN1 [471]. The constant ξ is a scaling parameter which accounts for the fraction of DM to be attributed to the candidate $\tilde{\chi}^0$. Let us note that a comparison of results from experiments using different target nuclei is only meaningful under the assumption that the interaction is dominantly coherent. Spin-dependent interactions require special nuclei such as ^{23}Na, ^{127}I, ^{73}Ge and ^{129}Xe.

Experimental challenges for the detection of such nuclear recoils, which are expected to be in the range 1–100 keV, are the following.

- To reach conditions of ultra-low background (shielding, radiopurity of the detector).
- To use methods discriminating electron recoils (from radioactivity) from nuclear recoils (from WIMPs). They can be either statistical (pulse shape analysis) or on an event-by-event basis (for instance, by measuring simultaneously ionization and heat).
- To exploit kinematical features characteristic of the galactic WIMP signal, such as the annual modulation of the rate and the front–back asymmetry of nuclear recoil, as well as the nuclear target dependence of the rates.

The next round of experiments (stage 2), such as CRESST2 [472], CDMS2, EDELWEISS2 and ZEPLIN2, should have a reach of the order of 10^{-8} pb.

The various options for the future include the use of germanium detectors, NaI scintillators, xenon scintillation detectors, time projection chambers, metastable particle detectors and cryogenic particle detectors. The exploration of the coherent interaction cross-sections with the required sensitivity is a far reaching goal, implying substantial improvements in all sectors: nuclear recoil discrimination efficiency reaching 99.9%, improved radiopurity and shield, lower E_{vis} thresholds and the use of quite massive detectors. Future experiments (stage 3), summarized in table 21 [467], are expected to reach cross-sections of 10^{-10}–10^{-11} pb and could achieve the goal. Figure 109 summarizes the techniques involved in such searches and illustrates the fact that **generally two independent signatures are required to discriminate signal from backgrounds.**

Table 21. Future experiments (>2003–2007) and their prospect for the detection of dark matter. From [467].

Experiment	Technique	Sensitivity (pb)
CUORE [473]	TeO_2 phonons 760 kg	5×10^{-8}
GENIUS 100 [474]	Ge ioniz 100 kg	5×10^{-8}–2×10^{-9}
GEDEON [475]	Ge ioniz 28–112 kg	10^{-7}–10^{-8}
DRIFT 10 [476]	Xe 10 m^3 TPC	10^{-8}
ZEPLIN-IV [477]	Xe Two-Phase	10^{-10}
GENIUS [478]	Ge ioniz 1–10 Tons	10^{-9}–10^{-10}
CryoArray [479]	Ge ioniz+phonons 1 Ton	6×10^{-10}
DRIFT-1 ton [476]	Xe 1 Ton TPC	10^{-10}–10^{-11}

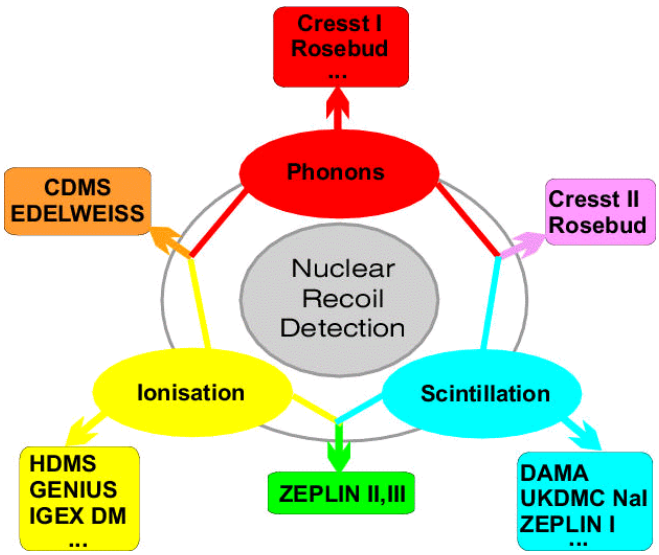

Figure 109. Reprinted from [480]. Copyright 2003, with permission from Elsevier.

Direct search signals depend also on the velocity distribution of the dark matter. In the standard assumption of virialized DM, with gaussian velocity distribution and zero average velocity, the earth motion around the sun produces an annual modulation. However, we have no direct evidence for the DM velocity distribution and it could be quite different: co- or counter-rotating DM around the centre of the galaxy or DM falling into the galaxy and oscillating in and out [481], leading to an annual modulation phase opposite to the one usually expected.

Up to now, the only announced signal is a possible annual modulation seen in DAMA (∼100 kg of NaI in Gran Sasso) [482, 483]. Such a result seems contradicted by further experiments (CDMS, Edelweiss, ZEPLIN I), as seen in figure 110. However, this conclusion should be taken with caution, in particular due to the very low threshold used by DAMA and the different nuclei involved in the various experiments [480].

The important question is whether present sensitivities are enough to explore parts of the SUSY parameter space. The authors of [484] consider an effective MSSM with a set of assumptions implemented at the electroweak scale which reduces the number of parameters to seven (M_2, μ, $\tan\beta$, m_A, $m_{\tilde{q}}$, $m_{\tilde{l}}$, A). All existing experimental constraints are taken into account. Figure 111 tells that present experiments (sensitivity between horizontal lines) explore

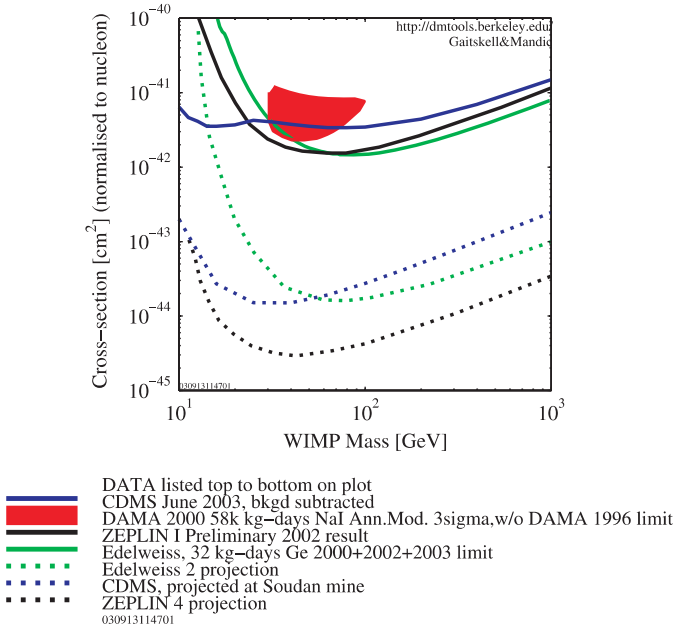

Figure 110. Some selected spin-independent exclusion limits including the DAMA evidence region. From [485].

significant regions of the parameter space, in particular in interesting relic neutralino sectors. However, it is also clear that several orders of magnitude in sensitivity would be needed to cover most of the expected domain.

In MSUGRA, as we have seen above, the allowed amount of dark matter restricts the SUSY parameter space to a narrow band in the $m_0 - m_{1/2}$ space, except at very large $\tan\beta$. Figure 112 (left) summarizes existing and expected bounds. Few GeV more on m_h will be decisive, as well as the clarification of a_μ and the measurement of $B_s \to \mu\mu$. Concerning the direct search, the authors of [487] have performed a most systematic scan of the parameter space. Figure 112 (right) summarizes their findings, confirming the above statement. It is remarkable that the region corresponding to the focus point scenario (see section 5.3) seems covered by the third generation of searches. Dark matter detection cross-sections are $\geqslant 10^{-10}$ pb and within the range of the most ambitious planned detectors. Models with non-universal Higgs mass parameters introduce new regions allowed by the DM constraint and can significantly increase the DM cross-section [486].

12.3.2. Indirect neutralino detection. Cosmic rays as γ, $\bar{p}$ and e^+ can be produced by neutralino DM pair annihilation in the galaxy and may be observed by space or balloon-borne experiments [488]. To estimate the flux one needs the density profile ρ of DM in our galaxy. Various parametrizations exist, even distributions with a singular profile at the centre of the galaxy. The DM pair annihilation rate is proportional to ρ^2 and the γ ray flux for instance from $\chi\chi \to \gamma X$ is proportional to the integral of ρ^2 along the line of sight. If the integration from 0 (galaxy centre) is infinite one admits that all DM particles in the region $r < r_{\rm cut}$ have already pair annihilated.

The γ component consists of a continuum coming from $\chi\chi$ annihilation into $f\bar{f}$, WW, ZZ etc and a monochromatic component from $\chi\chi \to \gamma\gamma, \gamma Z$ radiative processes which are

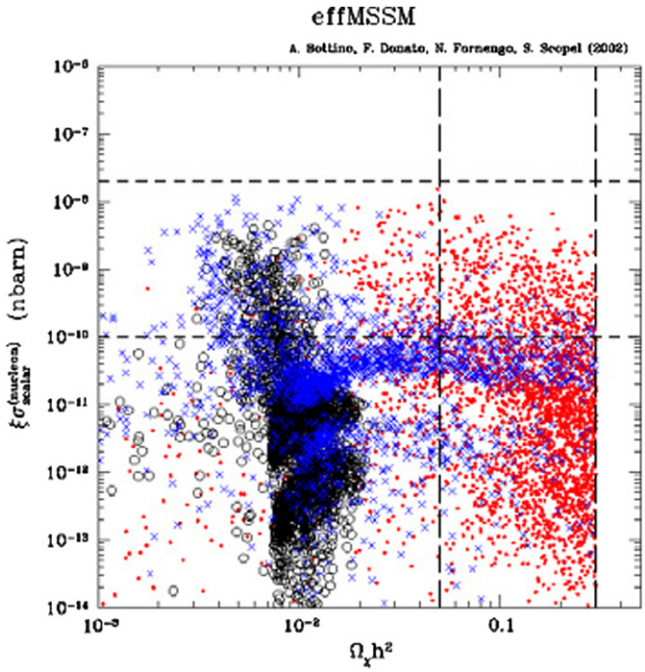

Figure 111. Scatter plot of $\sigma^{\text{nucleon}}_{\text{scalar}}$ versus $\Omega_\chi h^2$ in an effective MSSM model. Dots denote gauginos, circles denote higgsinos and crosses denote mixed configurations. Reprinted from [484]. Copyright 2002, with permission from Elsevier.

however suppressed. The continuum would give a kink in the background spectrum. The monochromatic signal, if any, is robust.

From EGRET [489] to GLAST [490] and ground based airshower Cerenkov telescopes, the progress is described by table 22. For the continuum component (10–40 low energy photons per annihilation for $m_\chi = 500\,\text{GeV}$) from the centre of the galaxy, EGRET would be sensitive to $m_\chi < 500\,\text{GeV}$ for one of the singular profiles [494]. An overview of the sensitivity of the various detectors is displayed in figure 113 assuming a 5σ signal from a point source after one year data taking for the wide field detectors EGRET and GLAST and with at least 10 events collected during 50 h for the Cerenkov telescopes. In the future, the GLAST [490] space telescope will be the most sensitive detector in the range of $\sim 10^{-1}$–10 GeV. Larger point source sensitivity can be reached by ground based Cerenkov telescopes, at the expense of a higher energy threshold. The intermediate range ∼10–100 GeV will be covered by MAGIC [491] and the upper range ∼100 GeV–10 TeV by HESS [492] and, in the future, by VERITAS [493].

Concerning the gamma line, the signal flux may be detectable for a wino-like (as in AMSB) or higgsino-like neutralino. The pair cross-section for this is

$$\sigma(\chi\chi \to 2\gamma) \sim \frac{\alpha^2\alpha_2^2}{M_W^2} \tag{174}$$

and does not have the usual $1/m_\chi^2$ dependence (because the mass of the chargino in the loop is about m_χ). For a complete evaluation of this, see [495].

Antiparticle searches are also improving. Antiprotons from the centre of the galaxy propagate to our solar system without too much loss. On the other hand, positrons lose energy by synchrotron radiation and inverse Compton scattering and can only come from nearby local clumps.

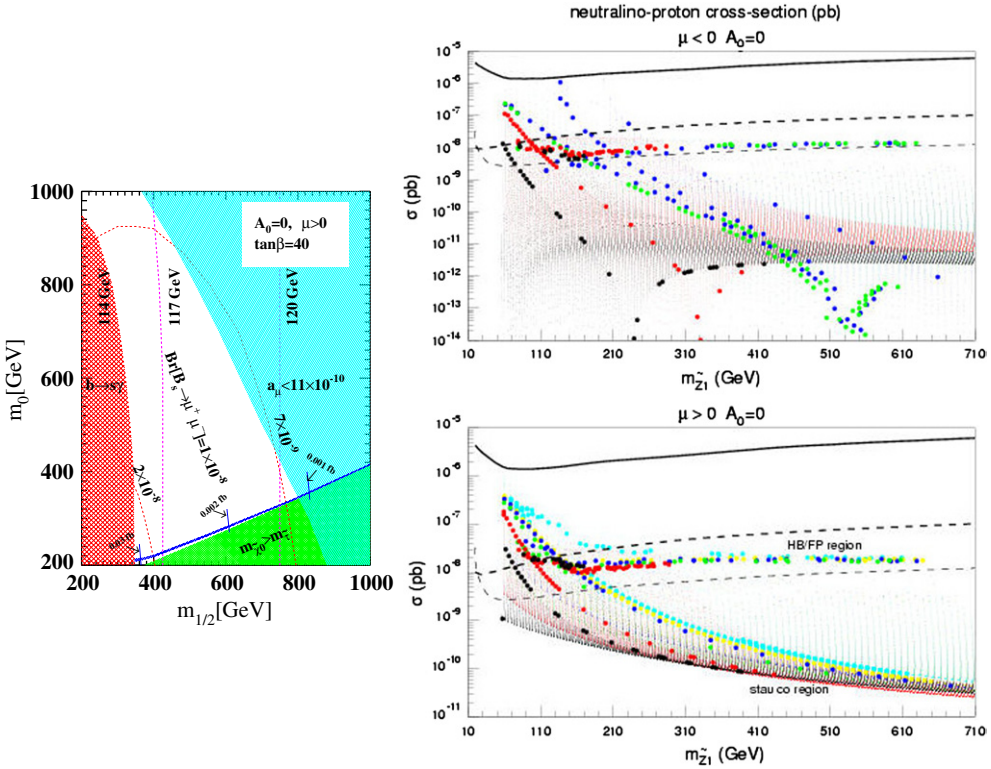

Figure 112. Left: summary of expectations in the $(m_0, M_{1/2})$ plane for $\tan\beta = 40$ and $\mu > 0$. Shown are the regions excluded by $b \to s\gamma$ (green shaded), the isomass curves for the h^0 (red full lines) and the branching ratios for $B_s \to \mu\mu$ (red dashed lines). The DM region is defined by $0.07 < \Omega_{\rm CDM}h^2 < 0.21$. The lower and upper short vertical lines correspond to $\sigma_{\tilde{\chi}_1^0 p} = 3 \times 10^{-8}$ pb and 1×10^{-9} pb, respectively. From [486][22]. Right: spin independent cross section as a function of the neutralino mass, from [487]. Points corresponding to the focus point scenario follow an approximately horizontal line (HB/FP region). The regions delimited by a full, a fat dashed and a thin dashed line are accessible by first, second and third generation of experiments, respectively.

Table 22. EGRET compared with future experiments (>2003–2007) and their sensitivity. From [488].

Point source	EGRET	GLAST	MAGIC	VERITAS, HESS
Sensitivity $\mathrm{cm}^{-2}\,\mathrm{s}^{-1}$	10^{-8}	$> 10^{-10}$	10^{-12}	10^{-13}–10^{-14}
E_γ	0.01–30 GeV	0.1–300 GeV	10 GeV–1 TeV	50 GeV–10 TeV
E or ang.resol.	0.4°	$\Delta e_\gamma \sim 10\%$		

As past and future actors, let us quote HEAT [496] and the space experiment AMS which, after the shuttle flight [497], will be installed on the international space station (ISS). The balloon-borne experiment BESS [498] will move to Antartica, fly longer and be sensitive to $\bar{p}$ with $E_{\rm kin} > 300$ MeV but should offer long term operation.

Exploiting the existing results on gammas from EGRET, on positrons from AMS and HEAT and on antiprotons from BESS, the authors of [499] claim that the observed spectra

[22] We thank the authors of [486] for a recent update of this figure.

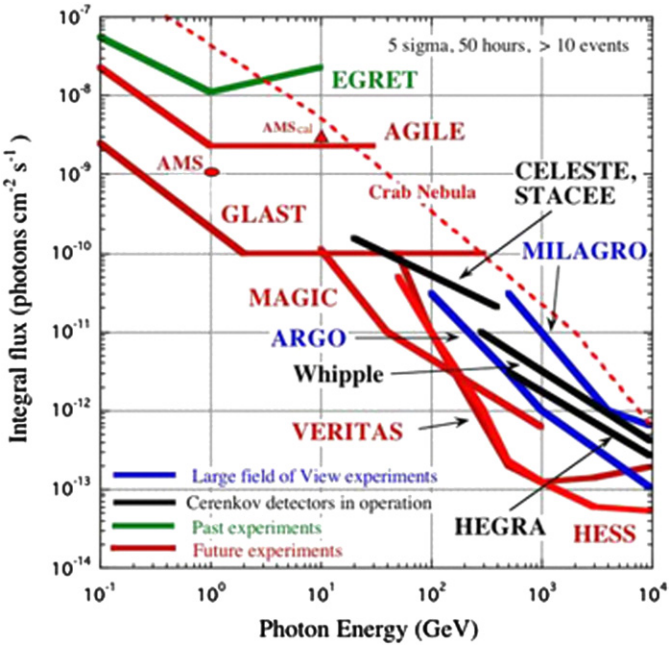

Figure 113. Sensitivity of present and future detectors in the gamma-ray astrophysics. Reprinted from [490]. Copyright 2002, with permission from Elsevier.

are better reproduced if one adds additional sources due to the annihilation of neutralinos satisfying the WMAP constraint, with a typical mass of 50–100 GeV. Other authors [500] on the contrary consider that the positron excess observed by HEAT would require very unlikely conditions of local substructure to be accounted for by neutralino dark matter. A more mundane explanation, namely a readjustment of the galactic average proton spectrum used in the cosmic ray propagation model, was also found to fit the EGRET energy spectrum [501].

12.3.3. Conclusion on non accelerator searches. From our discussion on the direct and indirect detection of WIMPS and for instance from figure 112 (right), we can conclude that **it may be possible, with some luck, to observe a signal,** as advocated by [499]. In particular, it is interesting that the focus point scenario, which may lead to a difficult situation at colliders [502] (see figures 104 and 143) is on the contrary the most favourable one for non-accelerator searches. **On the other hand, if no signal is observed it will be impossible to falsify the theory.**

The special case of gravitino dark matter, as in GMSB and too weakly interacting to be directly detectable, poses also some conceptual problems discussed in [488].

Let us recall that the universal extra dimensions scenario is also proposing a cold dark matter candidate, the lightest Kaluza–Klein particle. Its non accelerator search is discussed in [503].

Let us also quote for completeness another possible piece of evidence for 'light' (a few to 100 MeV) dark matter [504] which *a priori* would have nothing to do with SUSY nor any usually considered scenario. Their existence was conjectured as an explanation of the 511 keV gamma ray line from the galactic bulge detected by the SPI spectrometer of the INTEGRAL satellite [505].

12.4. Search for LSP at future accelerators

This will be part of sections 15.2 and 15.3. In R-parity conserving scenarios the LHC, through the missing transverse energy signal, will 'discover' the LSP. Under favourable conditions its mass can be obtained with limited accuracy, see table 27.

A linear collider can obviously deal numerically with the standard scenarios. But it can also certainly tackle quite peculiar and elaborate situations. An example is given in [506]: the authors examine the case of AMSB models with a neutral wino as LSP, nearly mass degenerate with the lighter chargino, and pinpoint a special trigger topology providing a distinct and unique signal.

13. Gauge mediated supersymmetry breaking

13.1. GMSB decays and signatures

Supersymmetric particles can decay to their SM partner and a gravitino through the diagrams of figure 9. But **as the coupling to the goldstino remains small compared with gauge couplings, they will preferably decay first in the same way as for MSUGRA until they reach the NLSP, which will then decay to a gravitino**. The decay rate for the NLSP, called $\tilde{X}$, to its SM partner X is

$$\Gamma(\tilde{X} \to X\tilde{G}) = \kappa_X \left(\frac{m_{\tilde{X}}}{100\,\mathrm{GeV}}\right)^5 \left(\frac{100\,\mathrm{TeV}}{\sqrt{\langle F\rangle}}\right)^4 2 \times 10^{-3}\,\mathrm{eV}. \tag{175}$$

These decays give rise to quite distinctive signatures from the MSUGRA case.

13.1.1. Neutralino NLSP. When the neutralino is the NLSP, its dominant decay mode is

$$\chi_1^0 \to \gamma\tilde{G} \tag{176}$$

provided χ_1^0 has non-vanishing photino component, its photino content being measured by κ_X in formula (175). This is expected to be satisfied, as the value of $|\mu|$ determined from the electroweak symmetry breaking tends to be large and the neutralino is therefore mainly bino. For a suitable composition of the χ_1^0 other decays could also contribute, such as $\tilde{\chi}_1^0 \to Z^0\tilde{G}$ and $\tilde{\chi}_1^0 \to h^0\tilde{G}$. However, these decays have a strong phase space suppression factor β^8 which makes them practically irrelevant, unless the neutralino is very heavy or if it is mainly bino-like (in which case $\kappa_Z/\kappa_\gamma = 0.3$ but κ_h/κ_γ is negligible). It is often assumed that the neutralino decay into a photon has a branching ratio of 100%. **The experimental signature of the neutralino NLSP scenario with prompt decay consists of isolated photons with missing energy**.

13.1.2. Stau NLSP. When the stau is the NLSP, it decays according to

$$\tilde{\tau} \to \tau\tilde{G} \tag{177}$$

with $\kappa_X = 1$ in formula (175) and 100% branching ratio. Other sparticles will decay into $\tilde{\tau}$, so for example $\tilde{\chi}_1^0 \to \tilde{\tau} + \tau$. **The experimental signature of the $\tilde{\tau}$ NLSP scenario consists of multi-τ final states with missing energy carried away by the gravitino (and neutrinos from the τ decay)**.

In the co-NLSP scenario, each of the other sleptons decays preferably to its lepton partner and a gravitino. The experimental signature for a prompt decay is then multi-lepton final states with missing energy.

Table 23. Search strategies for GMSB.

Decay /	$\tilde{\chi}_1^0$ **NLSP**	$\tilde{\tau}$ **NLSP**
Production	$\tilde{\chi}_1^0 \to \gamma + \tilde{\mathbf{G}}$	$\tilde{\tau} \to \tau + \tilde{\mathbf{G}}$
PROMPT	γ **pointing**	**Decay at vertex**
$\tilde{\chi}_1^0 \tilde{G}$	1γ (MSSM)	2τ
$\tilde{\chi}_1^0 \tilde{\chi}_1^0$	2γ (MSSM)	4τ
$\tilde{\tau}^+ \tilde{\tau}^-$	$2\tau + 2\gamma$	2τ (MSSM)
$\tilde{\chi}_1^+ \tilde{\chi}_1^-$	$2W^* + 2\gamma$	2τ (MSSM)
INSIDE		
Detector	γ **not pointing**	**Impact Parametes or kinks**
$\tilde{\chi}_1^0 \tilde{\chi}_1^0$	1 or 2 γ	2τ+1 or 2 IP/kinks
$\tilde{\tau}^+ \tilde{\tau}^-$	2 τ+1 or 2 γ	1 or 2 IP/kinks
$\tilde{\chi}_1^+ \tilde{\chi}_1^-$	$2W^*$+1 or 2 γ	1 or 2 IP/kinks
OUTSIDE		
Detector	**No** γ	**Heavy stable charged**
$\tilde{\chi}_1^0 \tilde{\chi}_1^0$	-	2τ+1 or 2 heavy
$\tilde{\tau}^+ \tilde{\tau}^-$	2 τ (MSSM)	1 or 2 heavy
$\tilde{\chi}_1^+ \tilde{\chi}_1^-$	$\tilde{\chi}_1^+ \tilde{\chi}_1^-$ (MSSM)	1 or 2 heavy

13.1.3. Finite decay length. The decay length for the NLSP is obtained from equation (175) as

$$L_{\mathrm{cm}} = \frac{1.76 \times 10^{-3}}{\kappa_X} \sqrt{(E_{\tilde{X}}^2/m_{\tilde{X}}^2) - 1} \left(\frac{m_{\tilde{X}}}{100\,\mathrm{GeV}}\right)^{-5} \left(\frac{m_{\tilde{G}}}{1\,\mathrm{eV}}\right)^2 \mathrm{cm}. \tag{178}$$

The decay length is fairly sensitive to the gravitino mass. A light gravitino gives rise to prompt decays or to decays with an observable length in the detector. For $m_{\tilde{G}} \geqslant 1\,\mathrm{keV}$, the NLSP will escape the detector before decaying. If the NLSP is the χ_1^0, the experimental signature is missing energy, like in the case of MSUGRA. If the NLSP is a $\tilde{\tau}$, it will appear as a heavy charged particle, identifiable by its $\mathrm{d}E/\mathrm{d}x$ or in RICH counters, without being accompanied by missing energy.

It is seen from equation (175) that a measurement of the NLSP mass and lifetime allows $\sqrt{F}$ to be determined directly.

13.1.4. GMSB search strategy. In order to cope with the various signatures of the GMSB scenario, it is indispensable to design dedicated search strategies. An overview is sketched in table 23. For some channels, flagged as '(MSSM)', the results obtained in the SUGRA searches can be directly reinterpreted in the GMSB scenario. The others, which need a specifically designed analysis, have been covered to a varying degree by LEP experiments. Some examples are given in later sections.

13.2. LEP results on GMSB with stau NLSP

The characteristic feature of this scenario is that the decay chain of sparticles will end in staus, which themselves decay into τ according to reaction (177) and lead to final states with several taus and missing energy.

13.2.1. Stau pair production. The simplest case is the associated production

$$\mathrm{e}^+\mathrm{e}^- \to \tilde{\tau}\tilde{\tau}. \tag{179}$$

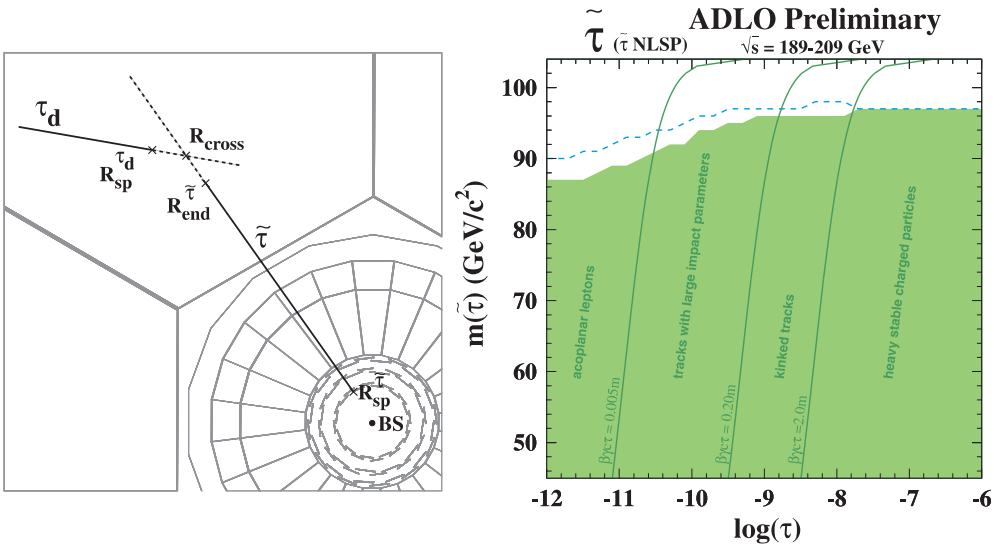

Figure 114. Left: stau decay visible in the detector. Right: exclusion limit on the stau mass as function of the stau lifetime, from [422]. The regions where different search methods are applied are indicated.

The final state is expected to contain two acoplanar taus. As the stau mean decay length depends strongly on the masses of the stau and of the gravitino, several searches have to be conducted in parallel in order to cover all possible configurations.

When the stau mean decay length is short, the MSUGRA search results for prompt decays can be reinterpreted in the GMSB framework. **The GMSB limit corresponds to the situation with** $m(\tilde{\chi}_1^0) = 0$. In this region, the exclusion is rather poor, due to the irreducible background from WW production followed by leptonic decays.

When the stau decay length is observable in the detector, specific search algorithms need to be developed. The principle is sketched in figure 114. If the decay occurs inside the volume of the tracking chambers, it is observable as a kink on the track or as a secondary decay vertex. If it happens too early in the detector to allow the primary track to be reconstructed, the extrapolation of the decay track may give rise to a measurable impact parameter with respect to the interaction point. Most SM backgrounds from $ll\gamma$, $\gamma\gamma \to \tau\tau$ or 4-fermions as well as cosmics background are strongly suppressed by cuts on missing transverse momentum, acoplanarity, acollinearity and decay angle for kinks. The background remaining at the end of the selection affects mostly the impact parameter search and amounts typically to one (or a few) events. It is mostly of instrumental origin, being due to reconstruction problems or hadronic interactions in the detector material.

Finally, if the decay takes place outside the tracking devices, the stau will appear as a heavy charged particle. It can be recognized by the $\mathrm{d}E/\mathrm{d}x$ in the central detectors or by the non-emission of Cerenkov light in RICH counters. Also for this search, the remaining background is of the order of one event.

These various analyses have been combined to obtain exclusion limits at 95% CL on the mass of the sleptons over a large range of mean decay lengths or equivalently of gravitino masses. The limits obtained for the stau after combining the LEP experiments in the LEP SUSY Working Group [422] using data up to 208 GeV are exhibited in figure 114 (right). It is seen that the weakest exclusion is in the region of prompt (MSUGRA-like) decays.

The same experiments carried out similar analyses looking for associated production of selectrons and smuons, to also cover the co-NLSP scenario. The results are comparable to the ones from the stau analysis.

13.2.2. Neutralino pair production. Another clean signature could be observed from the reaction

$$e^+e^- \to \tilde{\chi}_1^0\tilde{\chi}_1^0, \tag{180}$$

where the $\tilde{\chi}_1^0$ decays via

$$\tilde{\chi}_1^0 \to \tilde{\tau}\tau \tag{181}$$

giving rise to four-tau final states with missing energy. This topology, which has a very low background, has been investigated by Delphi [507] and Aleph [508]. Both also studied the possibility of co-NSLSP which could give rise to two pairs of leptons with the same or with different flavours.

13.3. LEP results on GMSB with neutralino NLSP

An interesting aspect of GMSB is that **the neutralino associated production could give rise to observable final states, provided its lifetime is not too long**. A neutralino as NLSP, produced in the reaction

$$e^+e^- \to \tilde{\chi}_1^0\tilde{\chi}_1^0 \tag{182}$$

appears as an event with two acoplanar photons. As the neutralino is expected to be gaugino-like, its associated production proceeds through t-channel exchange of a selectron (see section 10.1.3).

13.3.1. Prompt neutralino decays. The recoil mass spectrum to the di-photon system obtained by combining the four LEP experiments and including the energies up to 208 GeV is presented in figure 115. The figure shows a stage of preselection in the analysis based on loose cuts in order to verify the SM modelling of the backgrounds. The background, consisting mainly of $e^+e^- \to \nu\nu\gamma\gamma(\gamma)$, exhibits clearly the radiative return peak to the Z^0 which decays into $\nu\bar{\nu}$. No anomalous production of acoplanar photon pairs is observed and combined exclusion limits, shown in figure 116, are computed. The plot on the left gives the excluded cross-section limit at 95% CL for a pure bino neutralino and two values of the selectron mass. As the neutralino production is dominated by selectron exchange in the t-channel, the cross-section shows some sensitivity to the selectron mass. This is displayed in the figure on the right as an exclusion in the plane of the neutralino versus the selectron mass. The tooth-shaped area is the region kinematically compatible with the CDF $ee\gamma\gamma$ event [509]. The whole area is now excluded.

13.3.2. Delayed neutralino decays. Other analyses have been designed to look for long lived neutralinos. As the requirements on the photon pointing to the primary vertex are not very stringent in the acoplanar di-photon analysis, it can still be used in the region of moderate decay length. For larger decay length, at least one of the neutralinos is likely to escape detection. To obtain any sensitivity to the neutralino decay, the high SM background of single photon events from initial state radiation is to be drastically reduced, which is achieved by requiring **a photon not pointing to the interaction region**. Results from this search have been reported by Delphi [510] and Aleph [508]. The complementarity between the two-photon and the non-pointing single photon searches is illustrated by the excluded cross-section limit from Delphi using data from 183 and 189 GeV, shown in figure 117. A considerable gain in sensitivity from the single photon search is observed at long decay distances.

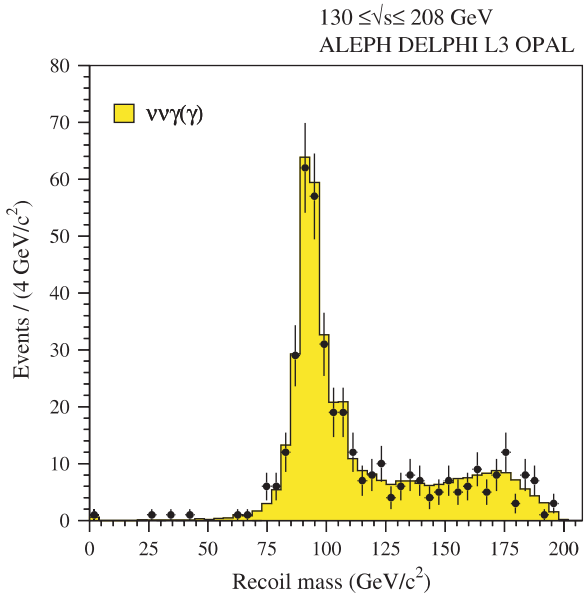

Figure 115. Di-photon recoil mass spectrum, from the LEP SUSY Working Group [422].

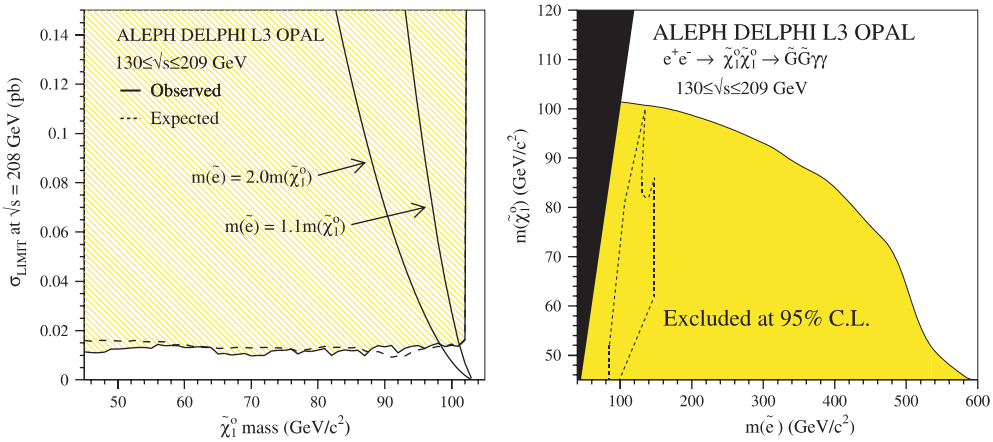

Figure 116. Exclusion limits on the neutralino cross-section (left) and in the neutralino versus selectron mass plane (right), from the LEP SUSY Working Group [422].

13.3.3. Charginos with neutralino NLSP. The GMSB topologies are the same as for the chargino search with isolated photons conducted in the MSUGRA framework. The presence of additional photons makes these events more easy to separate from the SM backgrounds. The reach is somewhat better (1–2 GeV) than in the MSUGRA search. The sensitivity extends up to the kinematic limit and covers the whole range of $\Delta M \geqslant 1$ GeV.

13.4. LEP combined results on GMSB

The LEP results on the neutralino NLSP and slepton NLSP can be combined to provide limits on the GMSB parameter space. The results from the LEP SUSY Working Group are shown in

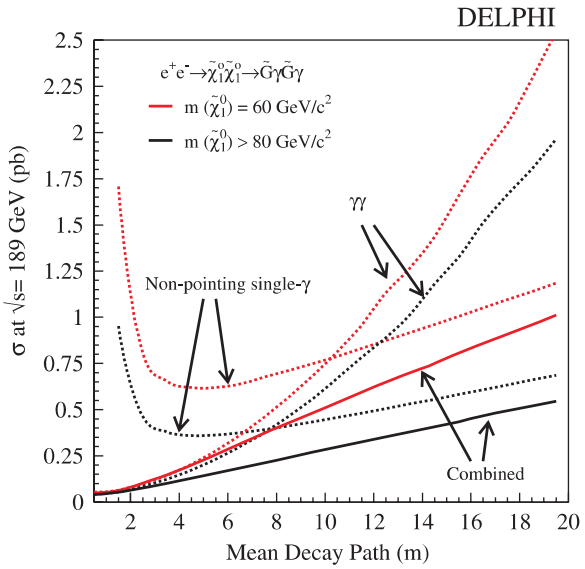

Figure 117. Exclusion limits on the neutralino cross-section as function of the mean decay length, from Delphi [510].

figure 118. The dark grey region is excluded by LEP1 searches and the regions excluded by the slepton and acoplanar photon searches are shown separately. The grey regions to the right are not excluded or kinematically not accessible at LEP2.

13.5. Tevatron results on GMSB with neutralino NLSP

The lightest neutralino decays into a photon and a gravitino. So any pair of produced sparticles will yield a pair of photons and missing E_T. A systematic search of events $\gamma\gamma X$ [509,511] has been performed for different photon energy thresholds. The number of observed events was found in agreement with the SM. One can thus exclude a region of the M_2 versus $\tan\beta$ plane for each sign of μ: typically $M_2 > 120$–150 GeV. The bounds from CDF/D0 are 65/77 GeV for the neutralino and 120/150 GeV for the chargino.

Another example is the search for a superlight $\tilde{G}$, with all other sparticles heavy and inaccessible to the Tevatron, leading to large missing E_T and high E_T jets performed by CDF. Limits are set on the production of gravitino pairs ($\sigma(\tilde{G}\tilde{G}) \propto 1/M_{\tilde{G}} \propto 1/F$), hence on the $\tilde{G}$ mass ($M_{\tilde{G}} > 1.2 \times 10^{-5}$ eV) and on $\sqrt{F}$($\sqrt{F} > 221$ GeV).

The future of GMSB searches at run II is described in detail in [512]. Interesting and sometimes spectacular signatures for bino-like NLSP, higgsino-like NLSP and stau NLSP have been identified. Besides photons in the final state, they may include in particular cascades to and decay of $\tilde{\chi}_1^0$ NLSP including a h^0 boson, 'displaced' objects and kinks, due to NLSP macroscopic decay length and quasi-stable heavy particles. Some features of the upgraded detectors (D0 preradiator, CDF TOF, etc) are welcome to identify them.

14. R-parity violation

The notion of R-parity and the R_p violating terms in the superpotential have been introduced in section 3.6. Here, we will examine the main phenomenological consequences of and the

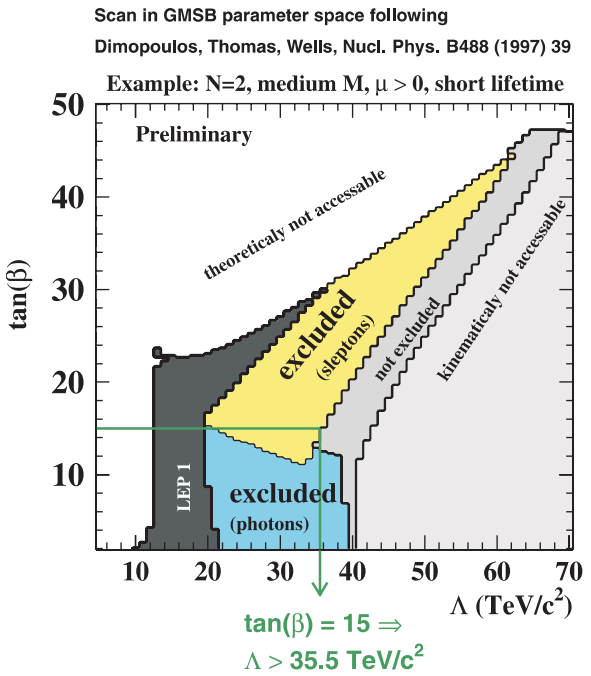

Figure 118. Excluded regions in the $(\Lambda, \tan\beta)$ plane for the parameter values $N = 2$, $M = 250$ TeV and $\mu > 0$, from [422].

existing limits on RPV. For an extensive discussion of R_p violation, the reader can consult, for example, the review [26].

14.1. Low energy limits on Rp violation

A wealth of low energy phenomena allows bounds to be put on the RPV couplings. They have been summarized by Dreiner [513].

The low energy constraints allow bounds which are in most cases at the level of a few% or worse to be obtained. Only the couplings λ_{133} (from the ν_e mass) and λ'_{111} (from neutrinoless double-β decay) are at the level of per mille and λ''_{112} (from nucleon decay) and λ'_{113} (from $n - \bar{n}$ oscillations) at 10^{-6} and 10^{-5}, respectively. This leaves space for improvement by high energy experiments. For reference, a coupling of electromagnetic strength, defined by $\lambda^2/4\pi = \alpha_{em}$, would correspond to $\lambda \simeq 0.3$.

Some products of couplings are, nevertheless, very strongly constrained by the low energy results [514]. For example, tree level transitions which would induce proton decay put a bound $\lambda'_{11k}\lambda'_{11k} < 10^{-24}$. Other products, which enter only at the 1-loop level, are limited to $\lambda'_{ijk}\lambda'_{lmn} < 10^{-10}$. The non-observation of the decay $\mu \to 3e$ yields the bound $\lambda_{1j1}\lambda_{1j2} < 7 \times 10^{-7}$.

R-parity violation in the supersymmetric SM can be the source of neutrino Majorana masses and mixing, through either bilinear or trilinear violation. In the former, the bilinear terms induce sneutrino vacuum expectation values which allow the neutrinos to mix with neutralinos. In the latter, products of trilinear λ and/or λ' couplings generate a neutrino mass matrix through one–loop self-energy graphs, like the one in figure 119. Conversely, information on neutrino properties, like the one obtained from WMAP, can constrain R_p violating couplings.

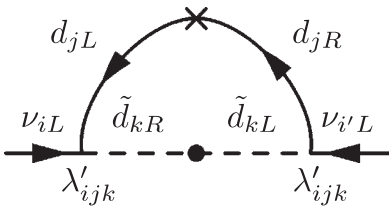

Figure 119. Example of R_p violating graph contributing to a neutrino Majorana mass.

When the WMAP limit $\sum m_i < 0.71\,\text{eV}$ (95% CL) is saturated, $m_i < 0.24\,\text{eV}$ for each neutrino mass. On the other hand, oscillation studies provide a lower bound on the heaviest neutrino mass of 0.03 eV. The heaviest neutrino mass is thus known to an order of magnitude

$$0.03 < m_3 < 0.24\,\text{eV}\,(95\%\text{CL}). \tag{183}$$

From such bounds the authors of [515] were able to deduce bounds on products of trilinear couplings, like for instance

$$\lambda'_{i33}\lambda'_{i'33} < 3.6 \times 10^{-8} \tag{184}$$

with heavy fermions inside the loops. The limits are more stringent than existing ones by an order of magnitude. Similarly for the μ_i bilinear terms.

14.2. Phenomenologies

R-parity violation introduces new decay patterns and new production modes. Depending on which is the LSP, two scenarios can be envisaged.

14.2.1. Indirect decays. If the LSP is the $\tilde{\chi}_1^0$, sparticles will preferably decay first to the $\tilde{\chi}_1^0$, like in MSUGRA, as the RPV couplings are expected to be small compared with the gauge couplings. At the end of the decay chain, the $\tilde{\chi}_1^0$ will decay by an RPV transition, as illustrated in figure 5 (right) via the exchange of a virtual $\tilde{l}$ or $\tilde{q}$. The following decays can take place:

$$\begin{aligned}
\tilde{\chi}_1^0 &\to l + \tilde{l} \;\to l + l + \nu, (\lambda)\\
&\to l + \tilde{l} \;\to l + q + q, (\lambda')\\
&\to \nu + \tilde{\nu} \to \nu + l + l, (\lambda)\\
&\to \nu + \tilde{\nu} \to \nu + q + q, (\lambda')\\
&\to q + \tilde{q} \to q + l + q, (\lambda')\\
&\to q + \tilde{q} \to q + \nu + q, (\lambda')\\
&\to q + \tilde{q} \to q + q + q, (\lambda'),
\end{aligned} \tag{185}$$

where particles and antiparticles are not explicitly distinguished to simplify the notation. The purely leptonic decays always involve a neutrino, so that the missing energy signature is not completely spoiled. Furthermore, the dilepton final states will most often contain lepton pairs of the same family as well as from different families, the latter providing a useful experimental signature.

14.2.2. Direct decays. If the LSP is a sfermion, it will predominantly decay directly via an RPV transition. Some examples are displayed in figure 120. Direct decays of sleptons can occur through a λ or λ' coupling and squark direct decays via λ' or λ' vertices. The direct

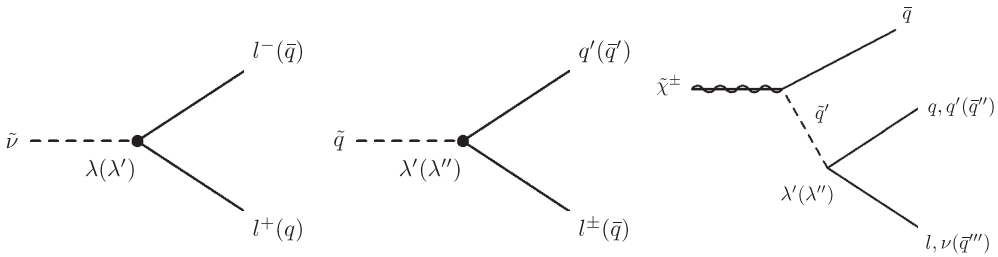

Figure 120. Examples of R_p violating direct decays.

decay of a neutralino or chargino can be mediated by an on-shell sfermion, the LSP in this framework.

It is important to realize that **a single non-zero Yukawa coupling is at the origin of several interaction vertices**. For instance, the term $\lambda_{1j1}\tilde{L}_1\tilde{L}_j\tilde{E}_1^C$ with $j = 2, 3$ governs

$$\begin{aligned}
\tilde{e}_R^- &\rightarrow e_L^- + \nu_\mu, e_L^- + \nu_\tau \\
\tilde{\nu}_\mu, \tilde{\nu}_\tau &\rightarrow e_R^- + e_L^+ \\
\tilde{e}_L^- &\rightarrow e_R^- + \bar{\nu}_\mu, e_R^- + \bar{\nu}_\tau \\
\tilde{e}_R^- &\rightarrow \nu_e + \mu_L^-, \nu_e + \tau_L^- \\
\tilde{\mu}_L^-, \tilde{\tau}_L^- &\rightarrow e_R^- + \bar{\nu}_e \\
\tilde{\nu}_e &\rightarrow e_R^- + \mu_L^+, e_R^- + \tau_L^+
\end{aligned} \tag{186}$$

as well as the time-reversed process, the s-channel production of sneutrinos

$$e^+ + e^- \rightarrow \tilde{\nu}_\mu, \tilde{\nu}_\tau, \tag{187}$$

where μ is associated to the coupling λ_{121} and τ to λ_{131}. This example illustrates clearly the fact that, **if an effect is detected in any given decay or production reaction, there should be several other reactions also exhibiting a signal and allowing the discovery to be confirmed (or contradicted)**.

14.2.3. Measurable decay lengths. So far, searches for RPV have only been carried out assuming that the particles decay promptly. However, when the Yukawa couplings become sufficiently small, the RPV decays may give rise to long decay lengths to which present searches are blind. The mean decay length for a neutralino or chargino LSP is given by [516]

$$L(\text{cm}) = 0.3(\beta\gamma)\left(\frac{m_{\tilde{f}}}{100\,\text{GeV}}\right)^4\left(\frac{1\,\text{GeV}}{m_{\tilde{\chi}^0}}\right)^5\frac{1}{\lambda^2}, \tag{188}$$

where $\beta\gamma = p_{\tilde{\chi}^0}/m_{\tilde{\chi}^0}$ is a Lorentz factor for the LSP. For a crude estimate, it is assumed that the efficiency is not violently affected for a decay length below about 1 cm. This implies a sensitivity in the range $|\lambda| > 10^{-4}$ if the LSP is a $\tilde{\chi}_1^0$ and $|\lambda| > 10^{-7}$ if it is a $\tilde{f}$. It also implies that the analyses are not sensitive to neutralino masses below 10–15 GeV. Obviously, this range could be extended by dedicated searches for long-lived particles, like the ones designed for GMSB, in case the above limits were reached.

14.3. Types of analyses

14.3.1. Associated production. **The sparticles are still expected to be pair produced via R_p conserving couplings, provided they are kinematically accessible. The cross-sections**

Table 24. Final states expected for various RPV couplings. Cascade decays like $\tilde{f} \to f + \tilde{\chi}^{\pm}$ are not included.

Topology	$\tilde{\chi}_1^0\tilde{\chi}_1^0$	$\tilde{\chi}_1^0\tilde{\chi}_2^0$	$\tilde{\chi}_1^+\tilde{\chi}_1^-$	$\tilde{l}^+\tilde{l}^-$	$\tilde{\nu}\bar{\nu}$	$\tilde{q}\bar{q}$
$4l$					λ^D	
$6l$			λ^D			
$2l + \not{E}$			λ^D	λ^D		
$4l + \not{E}$	λ^D	λ^D, λ^I	λ^D		λ^I	
$6l + \not{E}$		λ^I	λ^I	λ^I		
$2l + 2j$						λ'^D
$2l + 4j$	λ'^D	λ'^D	λ'^D			
$2l + 6j$		λ'^I, λ'^I		λ'^I		λ'^I
$2l + 8j$			λ'^I			
$4l + 4j$		λ'^I		λ'^I		
$1l + 2j + \not{E}$						λ'^D
$1l + 4j + \not{E}$	λ'^D	λ'^D, λ'^I	λ'^D		λ'^I	
$1l + 6j + \not{E}$		λ'^I	λ'^I			λ'^I
$1l + 8j + \not{E}$			λ'^I, λ'^I			
$2l + 4j + \not{E}$		λ'^I	λ'^I	λ'^I	λ'^I	
$2l + 6j + \not{E}$			λ'^I, λ'^I			
$3l + 4j + \not{E}$		λ'^I	λ'^I	λ'^I		
$3l + 6j + \not{E}$			λ'^I			
$4l + 2j + \not{E}$		λ^I				λ^I
$4l + 4j + \not{E}$			λ^I, λ'^I			
$5l + 2j + \not{E}$			λ^I			
$4j$				λ'^D	λ'^D	λ'^D
$6j$	λ'^D	λ'^D	λ'^D			
$8j$		λ'^I				λ'^I
$10j$			λ'^I			
$2j + \not{E}$						λ'^D
$4j + \not{E}$	λ'^D	λ'^D, λ'^I	λ'^D		λ'^I	
$6j + \not{E}$		λ'^I, λ'^I			λ'^I	λ'^I
$8j + \not{E}$			λ'^I			

are the same as in the MSUGRA scenario. The RPV interactions then only enter in the sparticle decays. This implies that the rates are independent of the RPV coupling constants, but the mass reach is kinematically limited by $\sqrt{s}/2$. Several such searches were conducted by the LEP and the Tevatron experiments.

The effects of $R_{\rm p}$ violation can here only be diagnosed by the distinct signatures that it produces. As an illustration, the final states reached from various e^+e^- initiated production reactions are shown in table 24, assuming that only one RPV coupling is non-zero at a time and that the decays occur either directly (D) or indirectly (I). It shows rather convincingly the huge variety of topologies with anomalously large numbers of leptons and/or jets expected if R-parity is not conserved. True or not, RPV SUSY is an excellent incentive to adopt on what should be the right attitude, namely to explore all accessible topologies in a systematic way.

14.3.2. Single sparticle production. Apart from the associated production, another production mechanism is made possible by violation of $R_{\rm p}$, namely **the direct s-channel or t-channel production of a single sparticle**. Some types of transitions are listed in table 25.

Table 25. Single sparticle production reactions via R_p violating vertices.

$e^+e^- \to \tilde{\nu}_{Lj}$	$L_1 L_j \bar{E}_1$	LEP
$e^- u_j \to \tilde{d}_{Rk}$	$L_1 Q_j \bar{D}_k$	HERA, LEP
$e^- \bar{d}_k \to \tilde{\bar{u}}_{Lj}$	$L_1 Q_j \bar{D}_k$	HERA, LEP
$\bar{u}_j d_k \to \tilde{e}^-_{Li}$	$L_i Q_j \bar{D}_k$	Tevatron
$d_j \bar{d}_k \to \tilde{\bar{\nu}}_{Li}$	$L_i Q_j \bar{D}_k$	Tevatron
$\bar{u}_i \bar{d}_j \to \tilde{d}_{Rk}$	$\bar{U}_i \bar{D}_j \bar{D}_k$	Tevatron
$d_j d_k \to \tilde{\bar{u}}_{Ri}$	$\bar{U}_i \bar{D}_j \bar{D}_k$	Tevatron

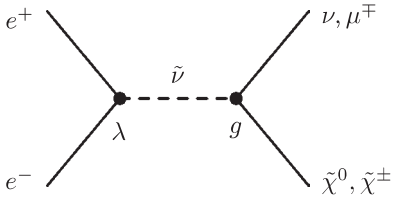

Figure 121. s-channel production of a sneutrino at LEP.

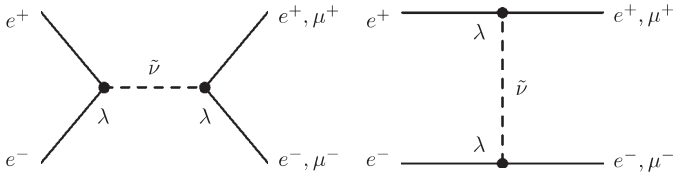

Figure 122. RPV interactions leading to the same final state as in the SM.

R_p violation offers, for example, the possibility to produce the sneutrino as an s-channel resonance at LEP, according to the graph of figure 121. The production of the sneutrino occurs through a coupling λ_{1j1}, where $j = 2, 3$ from the requirement of $SU(2)$ conservation (see section 4.2), hence leading to a $\tilde{\nu}_\mu$ or a $\tilde{\nu}_\tau$. The decay of the sneutrino can proceed via usual MSUGRA-type gauge couplings, leading to final states with ($\tilde{\chi}^0 + \nu_\mu$ or ν_τ) or the kinematically less likely ($\tilde{\chi}^\pm + \mu^\mp$ or $\tau^\mp$). Because of its RPV coupling to the initial state, the production rate is suppressed by a factor proportional to $|\lambda_{1j1}|^2$, compared with typical associated production rates, but the single production allows a larger mass range to be probed, limited only by $\sqrt{s}$. If it is assumed that only one Yukawa coupling is non-zero, the $\tilde{\chi}^0$ will decay leptonically and the final state consists of two charged leptons (ee, eμ or eτ) and two neutrinos.

There is also the possibility that by a double RPV vertex, the final state is the same as from a SM reaction, an example being displayed in figure 122. For s-channel exchange, a single non-zero λ_{1j1} coupling yields e^+e^- final states, while a $\mu\mu$ final state can be obtained provided both λ_{131} and λ_{232} differ from zero. With t-channel exchange, a single coupling allows the production of either ee or $\mu\mu$ final states: however the t- and u-channel contributions are negligible compared with the s-channel for sneutrino masses and couplings consistent with low energy data. The existence of RPV can only be observed in these final states by deviations from the expectations of the SM. The rates are, however, suppressed by a factor proportional to $|\lambda|^4$, so they are not expected to be large, except on resonance where the cross-section is given by the unitarity limit.

More recently, the possibility was suggested of studying single sneutrino production in an e^+e^- collider by means of the eγ interaction [517]. The contributing Feynman diagrams are

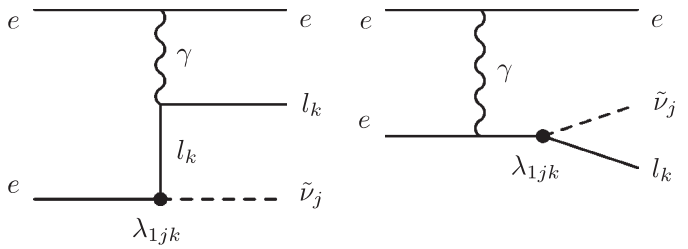

Figure 123. Feynman diagrams for γe production of sneutrinos in e^+e^- interactions.

Table 26. Correspondence between some leptoquarks and squarks. From [519].

LQ	sQuark	Q	Decay mode	BR $e^{\pm}j$	Coupling
			$e_L u$	1/2	g_L
S_0	$\tilde{d}_R$	$-1/3$	$\nu_L d$	0	$-g_L$
			$e_R u$	1	g_R
$\tilde{S}_{1/2}$	$\tilde{\bar{d}}_L$	+1/3	$\nu_L \bar{d}$	0	g_L
	$\tilde{\bar{u}}_L$	$-2/3$	$e_L \bar{d}$	1	g_L

drawn in figure 123. The interest of this production reaction is that it may probe λ_{1jk} couplings not accessible by means of the other s-channel sneutrino production processes.

14.4. Connection with leptoquarks

Leptoquarks (LQ) appear in all theories attempting to relate leptons and quarks. They carry the quantum numbers of both objects. Their phenomenology is complex [518,519]. LQ can be scalars or vectors. The search is limited to pure chiral couplings of the LQ, given the features of pseudoscalar meson decays: there are 14 species of such chirally coupled LQ. Those accessible to accelerators are assumed to couple only to one generation to avoid problems with FCNC processes. LQ carry a fermion number 0 (in the case of $\bar{e}q$, as in HERA e^+q collisions) or 2 (in the case of e^-q).

Actually, **in the case where both production and decay occur through the same λ'_{1jk} squarks and scalar leptoquarks behave similarly**. The leptoquark interaction l–q–$\tilde{q}$ is derived from the R-parity violating $LQ\bar{D}$ type of superpotential term. As table 26 shows, the correspondence is for instance between the LQ $\tilde{S}_{1/2}$ and a $\tilde{u}_L$. The results on leptoquark searches [520] can then be interpreted in terms of R-parity violation production of squarks and vice versa.

14.5. Limits from associated production at LEP

As in associated production the signal rate is independent of the Yukawa couplings, the non-observation of a sparticle can be translated into the exclusion of a mass range. For the latter to hold generally, all possible couplings for direct and indirect decays have to be investigated. The mass exclusion is then determined by the worst limit. The LEP results based on data taken up to 208 GeV have been reported by the four LEP experiments in [521, 522]. So far, not all earlier results of all experiments have been updated.

14.5.1. Chargino and neutralino limits. It was seen in table 24 that the associated production of charginos and of neutralinos at LEP can give rise to a vast number of topologies, involving multi-lepton and multi-jet final states. If m_0 is assumed to be large, the sleptons and squarks will be heavy and only the $\tilde{\chi}_1^0$ is expected to give rise to three-body direct decays listed in (185), with di-leptons, lepton+jets and multi-jet topologies. The heavier neutralinos and the charginos will decay dominantly into $Z^*\tilde{\chi}_1^0$ and $W^*\tilde{\chi}_1^0$ (indirect decays), respectively, followed by the decay of the $\tilde{\chi}_1^0$. They will lead to additional leptons and/or jets. **The experiments at LEP2 have designed searches to cover all such topologies**.

At LEP1, the precision measurement of the Z^0 width yields a 95% exclusion for charginos $M(\tilde{\chi}^{\pm}) > 45$ GeV, for any R-parity violating couplings. No similar exclusion can be derived for neutralinos, as they may decouple from the Z^0.

Based on data taken up to 208 GeV, the LEP experiments obtain a chargino mass exclusion of about $M(\tilde{\chi}^{\pm}) \gtrsim 103$ GeV, reaching close to the kinematic limit. This exclusion limit is independent of the type of Yukawa couplings considered. It is valid in the MSSM for any value of $\tan\beta$ and m_0. For the lightest neutralino, the mass range $M(\tilde{\chi}_1^0) \lesssim 40$ GeV is excluded by Delphi and L3 for λ and λ'' couplings.

14.5.2. Sfermion limits. At LEP1, the precision measurement of the Z^0 width yields 95% exclusions, applicable to any R-parity violating couplings, of $M(\tilde{l}) > 38$ GeV, $M(\tilde{\nu}) > 41$ GeV and $M(\tilde{q}_{\mathrm{L}}) > 44$ GeV.

The experiments at LEP2 have developed techniques to explore the kinematically accessible mass range for pair produced sfermions. In the absence of a signal, the exclusion of a sparticle at any given mass requires probing all possibilities of direct and indirect decays with the different types of allowed couplings and family indices. Given the huge number of final states involved, no attempt will be made here to cover them systematically. Rather, we will concentrate on the example of sleptons with a λ coupling. Pair produced charged leptons will, as seen from (186), give rise through direct decays to a pair of charged leptons, possibly from different families, and two neutrinos. The experimental topologies to investigate are ee, $\mu\mu$, $\tau\tau$, eμ, eτ and $\mu\tau$ accompanied by missing energy. Indirect decays will, through the decay of the neutralino (185), produce six leptons and missing energy.

The associated production of sneutrinos, which may be unobservable in the MSUGRA scenario, can also be detected if R_{p} is violated. The direct decay of $\tilde{\nu}_i\bar{\tilde{\nu}}_i$ gives $\mathrm{e}_j\bar{e}_j\mathrm{e}_k\bar{e}_k$ with $j \neq i$ and k unrestricted. The expected signatures are eeee, ee$\mu\mu$, ee$\tau\tau$, $\mu\mu\mu\mu$, $\mu\mu\tau\tau$ and $\tau\tau\tau\tau$ without missing energy. The leptons come in particle–antiparticle pairs, unless more than one non-zero Yukawa coupling is invoked. Indirect decays of sneutrinos produce eight final state leptons, of which four are neutrinos. The same charged lepton configurations are found as for direct decays but with missing energy.

As an example, the cross-sections excluded by Aleph at 208 GeV [521] for the $llll$, $ll\tau\tau$ and $\tau\tau\tau\tau$ final states are presented in figure 124 (left). The observed final states can be reached via λ couplings. The comparison with the expected signal cross-sections, also displayed in the figure, allows the derivation of an excluded mass range for each case and the weakest limit is retained. In figure 124 (right), the result of the search for indirect decays is shown. After the same procedure is repeated for all couplings, the weakest of all exclusions determines the final sneutrino mass limit. For $\tilde{\nu}_{\mathrm{e}}$ the lower limits on the mass range from 89 to 100 GeV and for $\tilde{\nu}_{\mu,\tau}$ from 70 to 90 GeV.

The limits obtained individually by the LEP experiments at 208 GeV for charged sfermions are approximately the same as the corresponding limits in the R_{p} conserving case. For example, the lower mass limits for $\tilde{e}$ range from 89 to 99 GeV (at $\tan\beta = 1.5$ and $\mu = -200$ GeV) and for $\tilde{\mu}$ from 81 to 96 GeV, depending on the type of coupling.

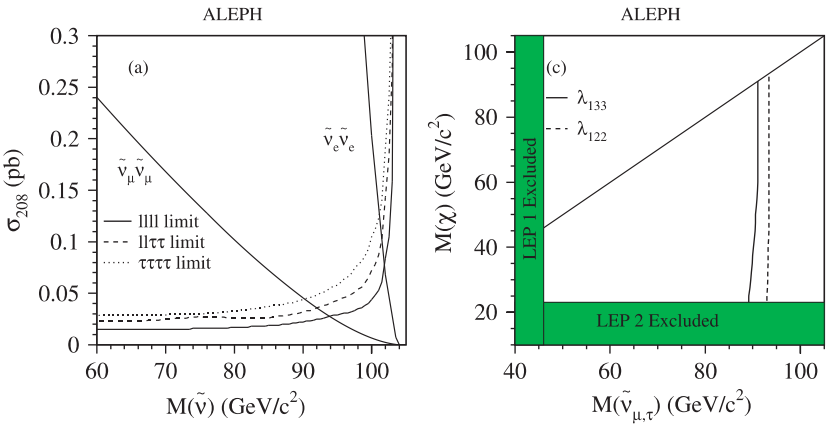

Figure 124. Exclusion plots at 95% CL from [521]. Left: excluded cross-section for direct decays. Right: excluded mass range for indirect decays of sneutrinos.

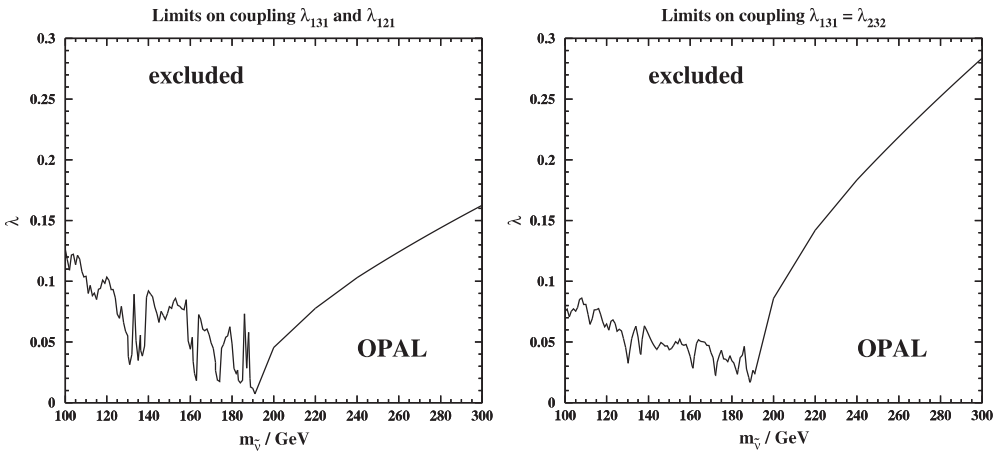

Figure 125. Limits at 95% CL on the λ couplings as function of the $\tilde{\nu}$ mass, (left) from the e^+e^- final state analysis and (right) from the $\mu^+\mu^-$ final state analysis, both from Opal [523] at 189 GeV.

14.6. Limits from s-channel sparticle production

14.6.1. Limits from SM final states at LEP. At LEP2, the production $e^+e^- \to \tilde{\nu}_{Lj} \to l^+l^-$ is allowed by the $L_1 L_j \bar{E}_1$ operator, through s-channel and t-channel exchange, illustrated by the diagrams in figure 122. Two examples of results are displayed in figure 125. The figure on the left, from Opal [523], shows the results obtained from the study of the reaction $e^+e^- \to e^+e^-$ at 189 GeV. This is sensitive to the couplings $|\lambda_{1j1}|$ with $j = 2, 3$. As the same final state is produced by SM interactions, cuts on the production polar angle θ are applied to reduce the Bhabha background. The inclusion of events with initial state radiation allows a large range of centre of mass energies to be scanned, after reconstructing the effective interaction energy $\sqrt{s'}$. The existence of a sneutrino would be observable as a peak at a value $s' = m^2_{\tilde{\nu}}$. The comparison of the spectrum of selected events with the expected SM background allows 95% CL limits to be established on the signal cross-section and hence on the RPV couplings. The obtained limit is more severe than the exclusion from low energy measurements mentioned in section 14.1.

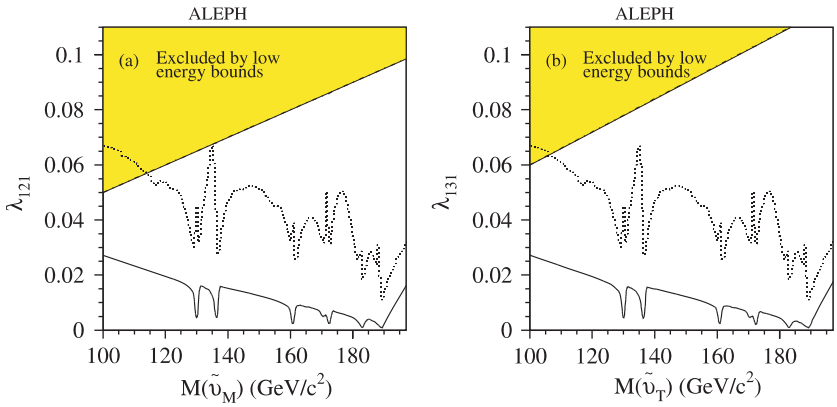

Figure 126. Limits at 95% CL on the couplings λ_{1j1} as function of the $\tilde{\nu}$ mass, from [524].

The figure on the right shows the result of a similar analysis applied to the $e^+e^- \to \mu^+\mu^-$ channel by Opal at 189 GeV [523]. The RPV interpretation of this reaction involves the product of couplings $|\lambda_{131}\lambda_{232}|$. If the assumption is made that $|\lambda_{131}| = |\lambda_{232}|$, the analysis of the s' spectrum yields the 95% CL limit shown in the figure.

14.6.2. Sneutrino limits from SUSY decays at LEP. Searches can also be conducted for s-channel production of sparticles with non-standard model decays of the sparticles.

Assuming one of the couplings $\lambda_{1j1} \neq 0$ at a time allows the following sequence of reactions to take place

$$e^+e^- \xrightarrow{\lambda} \tilde{\nu}_{Lj} \to \tilde{\chi}^0\nu_j, \qquad \tilde{\chi}^0 \to \nu_k\tilde{\nu}_k^*, \tilde{\nu}_k^* \xrightarrow{\lambda} e^\pm l^\mp \tag{189}$$

in the hypothesis that the $\tilde{\chi}^0$ is the LSP (indirect decays). If $\lambda_{121} \neq 0$, the final states will be $e^+e^-\not{E}$ or $e^\pm\mu^\mp\not{E}$; if $\lambda_{131} \neq 0$, they are $e^+e^-\not{E}$ or $e^\pm\tau^\mp\not{E}$. The signature is events with two acoplanar leptons and missing energy.

The results of an anaysis by Aleph [524] including all data taken from $\sqrt{s} = 130$–189 GeV are displayed in figure 126. The exclusions (full line) are evaluated in the gaugino region at $\mu = -200$ GeV and $\tan\beta = 2$. The obtained limits are stronger than from the electroweak fits of previous section, shown as the dotted line, and stronger than from the low energy measurements.

Results including the 208 GeV data have been published by Delphi [525].

14.6.3. Sneutrino limits from $e\gamma$ interactions at LEP. Final states from $e\gamma$ production of single sneutrinos at LEP have been investigated by Aleph [526] using data from 189 to 208 GeV. They obtain upper limits on the couplings λ_{122}, λ_{123}, λ_{132}, λ_{133}, λ_{231}, which are stronger than the ones from the low energy measurements mentioned in section 14.1. A similar search for single squark production mediated by a λ' coupling was carried out by Opal [527]. Limits at 95% CL slightly less than 200 GeV on squark masses are derived for λ' couplings of electromagnetic strength.

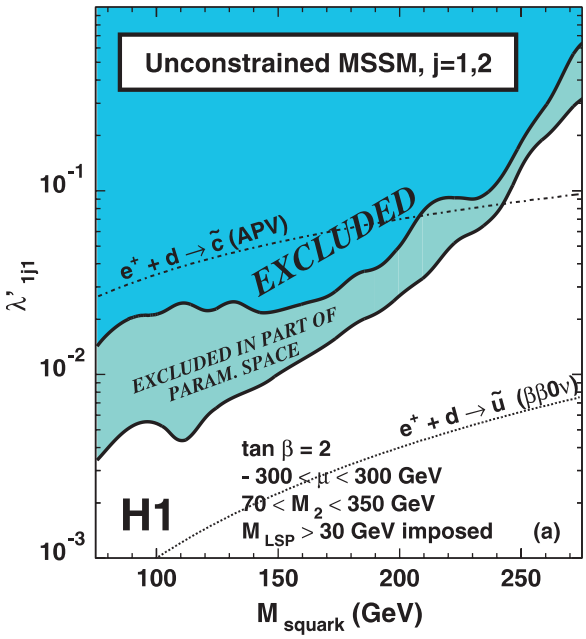

Figure 127. Limits at 95% CL on the couplings λ'_{1j1} as function of the $\tilde{q}$ mass, from H1 [528].

14.7. Squark limits from HERA

The HERA experiments are the ideal place to probe the direct production of squarks via $\lambda'_{1jk} \neq 0$ couplings in the s-channel fusion reactions:

$$\begin{aligned} &e^+ d_k \to \tilde{u}_j, \tilde{u}_j \to e^+ d_k, \\ &e^+ \bar{u}_j \to \tilde{\bar{d}}_k, \tilde{\bar{d}}_k \to e^+ \bar{u}_j, \bar{\nu}_e \bar{d}_j, \end{aligned} \tag{190}$$

for which the mass reach extends in principle to $\sqrt{s}$. Especially the first reaction with couplings $\lambda'_{1j1} \neq 0$ is of interest, since it corresponds to scattering from valence quarks. An e^- beam would probe mainly $e^- + u \to \tilde{d}_{Rk}$, produced via λ'_{11k} couplings.

For direct decays, also given in (190), the signature consists of events with $e^+(\bar{\nu}) +$ jet, which look like charged current (CC) or neutral current (NC) deep inelastic scattering. Hence, they are difficult to extract from the bulk of events and a mass dependent angular cut (cut on y) is applied. If it is assumed that also the coupling $\lambda'_{3jk} \neq 0$, the signature can be $\tau^+(\bar{\nu}_\tau) +$ jet, which is more easily distinguished from the background.

Furthermore, there can be indirect decays where the $\tilde{q}$ first decays via gauge couplings to a $q\tilde{\chi}^0_n$ state (or $q\tilde{\chi}^\pm$). The neutralino will subsequently undergo the RPV decay $\tilde{\chi}^0_n \to e^\pm q\bar{q}'$ or $\tilde{\chi}^0_n \to \nu q\bar{q}$, with branching ratios depending on the SUSY parameters. The heavier neutralinos and the charginos can either decay directly through an RPV coupling or indirectly into a $\tilde{\chi}^0_1$ by emission of a gauge boson. The topologies consist of a high P_T lepton and multi-jets. They are again difficult to distinguish from the CC and NC events, except the 'wrong' sign events with an e^- which can be cleanly selected.

By combining the results from the searches for the direct and indirect decays, H1 [528] derived limits, based on a luminosity of 37 pb^{-1}, on the coupling constants λ'_{1j1} as function of the squark mass. As example, figure 127 shows the excluded regions for λ'_{111} and λ'_{121}. They are comparable or more severe than the ones from the low energy results, based on

atomic parity violation. On the contrary, the very stringent low energy limit on λ'_{111} from neutrinoless double beta decay remains at least an order of magnitude better than obtained from H1. Similar exclusions have been obtained by Zeus [529]. Squark masses less than 260 (H1) to 269 (ZEUS) GeV are excluded at the 95% CL for a coupling of electromagnetic strength.

The reach in the above searches is limited to $\sqrt{s}$. This range can be extended to higher masses by including both s-channel and u-channel exchange diagrams which can be probed in contact interaction studies. The sensitivity is less but extends to about 400 GeV for $\lambda' \lesssim 1$.

14.8. Limits from Tevatron

At a hadron machine, the $\bar{p}p$ interactions can give rise to the associated production:

$$gg, q\bar{q} \to \tilde{q}\bar{\tilde{q}}, \tilde{g}\bar{\tilde{g}} \tag{191}$$

with relative cross-sections to squark or gluons depending on their mass. These production reactions were discussed in section 11.2.

In the scenario where a $\tilde{q}$ is the LSP, the $\tilde{g}$ first decays through strong interactions into a $\tilde{q}$, followed by the RPV direct decay of the $\tilde{q}$. The eventuality where $\lambda'_{121} \neq 0$ would simultaneously allow the decays $\tilde{c}_j \to e^+ d_k$, $\tilde{s}_j \to \nu_e d_k$, $\tilde{d}_k \to e^- c_j$ and $\tilde{d}_k \to \nu_e s_j$. Assuming approximately equal masses for $\tilde{c}_L$, $\tilde{s}_L$ and $\tilde{d}_R$ would lead to equal production rates for these squarks and thus branching ratios to $e^\pm$ and to ν of 1/2 each. An interesting signature comes from the production $\bar{p}p \to \tilde{g}\tilde{g}$, where both gluinos decay into $\tilde{g} \to \tilde{q}\bar{q}$ or both into $\tilde{g} \to q\bar{\tilde{q}}$ in 50% of the cases. Combined with the electron branching ratio squared, **this yields like-sign** $e^\pm e^\pm$ + jets **events 1/8 of the time, a topology affected by small SM backgrounds**.

In the scenario where $\tilde{\chi}^0_1$ is the LSP, indirect decays will take place with $\tilde{q} \to q\tilde{\chi}^0_1$ followed by RPV decay of $\tilde{\chi}^0_1$. Assuming again that $\lambda'_{121} \neq 0$ would give $\tilde{\chi}^0_1 \to c\bar{d}e^-$, $d\bar{c}e^+$, $d\bar{s}\nu$ and $s\bar{d}\nu$, through virtual exchange of squarks ($\tilde{c}$, $\tilde{s}$ or $\tilde{d}$) or of sleptons ($\tilde{e}$ or $\tilde{\nu}$). The branching ratios depend on the SUSY parameters, but for the analysis, they are assumed equal for $e^\pm$ and for ν. Since each $\tilde{\chi}^0_1$ decays, due to its Majorana nature, with equal probability to an e^+ and an e^-, the like-sign $e^\pm e^\pm \geqslant 2j$ events would then have a branching ratio of 1/8. To prevent decays to charginos, which could dominate over the $\tilde{\chi}^0_1$ decays, the chargino is assumed to be heavier than the squarks. Although the interpretation of these analyses introduces some model dependence, the results are independent of the value of the λ' couplings, unlike the case of HERA.

The CDF experiment has presented results from its like-sign dilepton search. The case of associated production of stop with indirect decays of $\tilde{t}_1 \to c\tilde{\chi}^0_1$ is shown in figure 128 for neutralino masses in the range $M(\tilde{\chi}^0_1) \geqslant M(\tilde{t}_1)/2$ to prevent stop decays into charginos. The comparison with the theoretical expectation, which is independent of the size of the λ'_{121} coupling, leads to the constraint $M(\tilde{t}_1) \geqslant 120$ GeV. Since the analysis does not distinguish quark flavours, the results remain valid for any coupling $\lambda'_{1jk} \neq 0$ where j is 1 or 2 and k is 1, 2 or 3. Under the same conditions as above, the mass limit for 5 degenerate squarks becomes $M(\tilde{q}) \geqslant 200$ GeV.

Decays mediated by a λ'_{1jk} were also searched by the D0 experiment, looking for events with ee + jets, $e\nu$ + jets and $\nu\nu$ + jets [532], originating from direct decays. For squarks of the type $\tilde{u}_{Lj}$, which can only decay to $e\tilde{d}_{Rk}$, a mass limit of 204 GeV is derived. For $\tilde{d}_{Rk}$ type squarks, which have equal branching ratios to $e\tilde{u}_{Lj}$ and to $\nu_e\tilde{d}_{Lj}$, the mass bound is 225 GeV.

Direct decays via a λ'_{2jk} coupling were also probed. They yield final states like in the previous example with the electron replaced by a muon. From the $\mu\mu$ + jets search, CDF and D0 derive a lower limit on $\tilde{u}_{Lj}$ type squarks of 202 GeV and 200 GeV, respectively. Based on

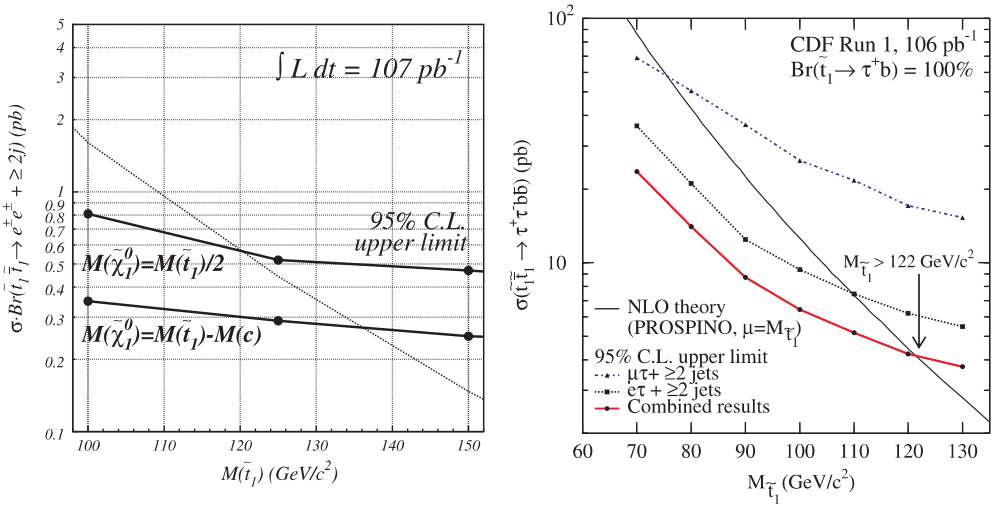

Figure 128. Limits at 95% CL on the branching ratio times the cross-section for the production of stop as function of the $\tilde{t}$ mass. Left: for indirect decays via λ'_{121} couplings from CDF. Reprinted with permission from [530]. Copyright 1999 by the American Physical Society. Right: for direct decays with λ'_{33k} coupling from CDF. Reprinted with permission from [531]. Copyright 2004 by the American Physical Society.

the same final state, the CDF limit for $\tilde{d}_{Rk}$ type squarks is 160 GeV. By including $\mu\nu$ + jets and $\nu\nu$ + jets searches, D0 improves this limit to 180 GeV.

Recently, CDF has presented results on a search for λ'_{33k}, observable as $\tilde{t}_1$ pair production followed by the decay $\tilde{t}_1 \to \tau$ + jet [531]. The search is based on events where one tau decays leptonically, the other hadronically into 1 or 3 prongs. Their result, displayed in figure 128 (left) gives the constraint $m(\tilde{t}_1) > 122$ GeV.

14.9. Summary

Some of the indirect limits from low energy measurements remain fully competitive, especially on products of couplings.

The associated sparticle production at LEP is the only case allowing mass limits to be derived for all three couplings, λ, λ' and λ'. Limits have been obtained for gauginos, sleptons and squarks and are comparable to the ones for the R_p conserving framework, or even stronger in the case of sneutrinos.

The strongest mass bounds on squarks have been obtained at the Tevatron in the case of λ' couplings. But hadron machines have no sensitivity to the λ or λ' couplings via direct decays.

HERA can, through direct production or contact interactions probe a large mass range for squarks for λ' couplings. But, as the production itself depends on λ', a mass range can only be excluded as a function of the value of the coupling. An example of excluded regions in the plane of the coupling λ' versus the squark mass is shown in figure 129.

15. Future searches

We will not be able to cover exhaustively all future searches which have been studied for the upgraded Tevatron, the LHC and a LC. There exist several rather complete reports for each of these machines. We will present some of the major issues and refer to the literature for more complete presentations.

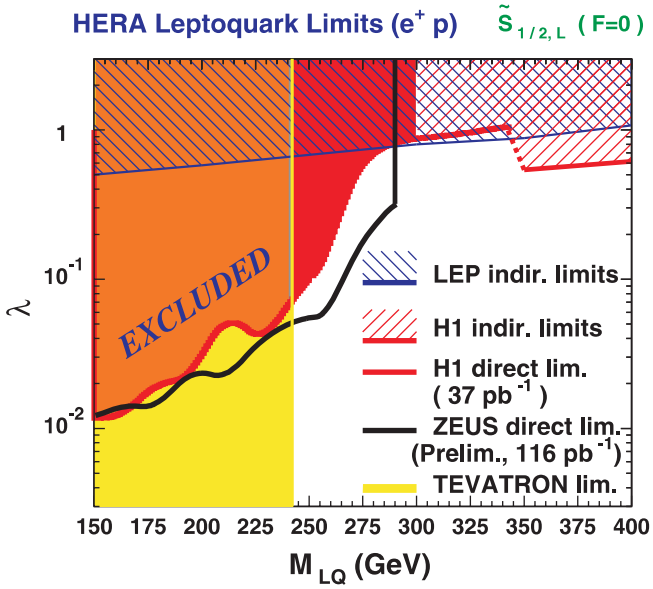

Figure 129. Limits at 95% CL on λ' couplings versus the squark mass (M_{LQ}) comparing different experiments, from [520].

15.1. SUSY searches at the Tevatron run II

The reach of the upgraded Tevatron CDF and D0 experiments for run II has been extensively described in [71]. We give a few examples.

One of the most promising SUSY search channels is and will still be the trilepton plus $\not\!\!E_T$ channel, mostly populated by $p\bar{p} \to \tilde{\chi}_2^0 \tilde{\chi}_1^{\pm}$ with the decays $\tilde{\chi}_2^0 \to l^+ l^- \tilde{\chi}_1^0$ and $\tilde{\chi}_1^{\pm} \to l^{\pm} \nu \tilde{\chi}_1^0$ (with l = e or μ). Assuming an (optimistic) integrated luminosity of about 20 fb^{-1}, charginos, for instance, could be discovered up to about 200 GeV. For large tan β, charginos and neutralinos preferentially decay to third generation fermions (taus) and possibly sfermions. The rate for multilepton signals, in particular trileptons, is much reduced. New signatures involving tau detection, have been studied extensively. The reach in the $m_0 - m_{1/2}$ plane is described by figure 130.

The first two generation squarks and the gluino can be probed by means of the $\not\!\!E_T$ + jets channel up to 350 (to 400) GeV with an integrated luminosity of 2 (to 30) fb^{-1} [71]. For stop pair production, the $bl\not\!\!E_T$ and at least 1 additional jet (from $\tilde{t} \to \tilde{\chi}_1^{\pm} b$), $c\bar{c}\not\!\!E_T$ (from $c\tilde{\chi}_1^0$) and $jl^+l^-\not\!\!E_T$ (from $b\tilde{l}\nu$ or $bl\tilde{\nu}$) event topologies will allow masses to be probed up to 185 GeV, 160 GeV, 190 GeV, respectively, for 2 fb^{-1} already and 250 GeV for 20 fb^{-1}. Figure 131 gives a summary of the combined SUSY reach in the MSUGRA framework. However, for tan $\beta > 35$, the improvements due to the new signatures (see preceding figure) have to be included.

To keep SUSY hidden from the Tevatron when sparticles are light, one seems to need two separate deviations from the canonical MSUGRA framework: one to suppress the $\not\!\!E_T$ signal, another one to reduce the cross-section for isolated multilepton events.

15.2. SUSY searches at the LHC

The first SUSY signal to look for at the LHC will be through an inclusive search relying on the large production cross-sections for gluinos and squarks. Various topologies with $\not\!\!E_T$, jets with

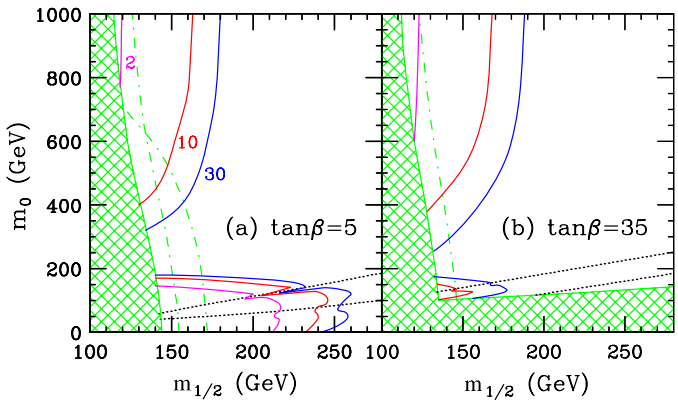

Figure 130. Tevatron reach in the trilepton signal for a fixed value $A_0 = 0$ and $\mu > 0$. The reach is shown for integrated luminosities of 2, 10 and 30 fb^{-1}. From [71].

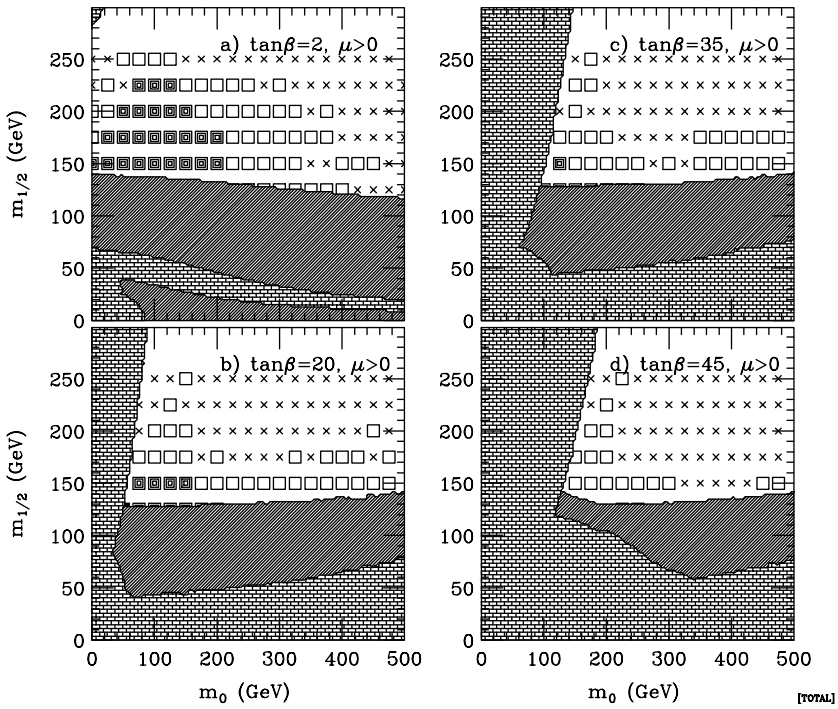

Figure 131. Tevatron SUSY reach, after combining all searches, in the $m_0 - m_{1/2}$ plane with 2 fb^{-1} (grey squares) and 25fb^{-1} (hollow squares). The bricked (hatched) areas are theoretically (experimentally) excluded. From [71].

large p_T and 1 to 4 leptons in the final state will allow the exploration, already after the first year of running, of a region of the parameter space extending well beyond the Tevatron reach. If SUSY is discovered, more detailed studies and cross checks will be made possible through the analysis of specific signatures, several of which should be simultaneously observable. If the squarks and gluinos decay through long enough cascade chains, it will also be possible to reconstruct the sparticle masses from the measurement of end points in the effective mass distributions.

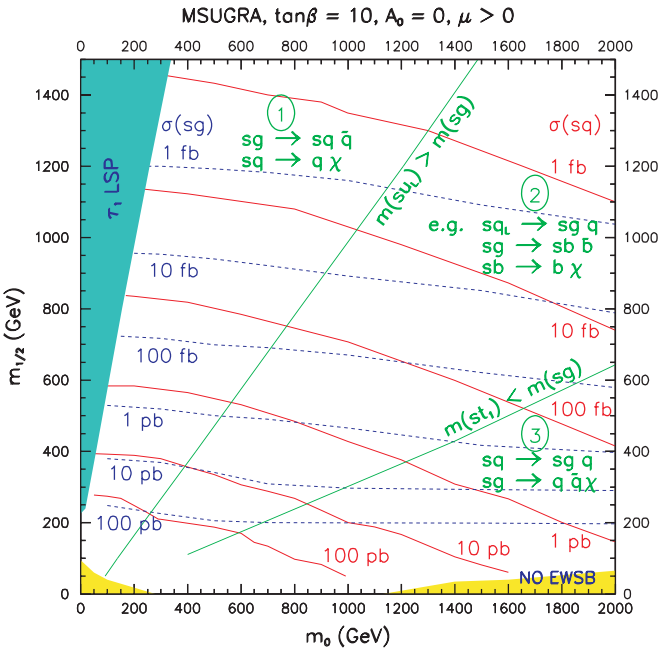

Figure 132. Production cross-sections at the LHC in the $(m_0, m_{1/2})$ plan for squarks, except stop, as full (red) lines labelled on the right and for gluinos as dashed (blue) lines labelled on the left. The nearly diagonal (green) lines delimit the regions with the different mass hierarchies between gluinos and squarks (see text).

15.2.1. Signatures based on $\not{E}_T$ and $E_T^{\rm sum}$. **The most promising discovery channels are related to squarks and gluinos which are copiously pair-produced through strong interactions**, as we saw in section 10.3 where values for the NLO cross-sections of various subprocesses were quoted. The NLO cross-sections computed with PROSPINO are displayed in figure 132 in the $(m_0, m_{1/2})$ plane assuming the MSUGRA scenario. The numerical value of the cross-sections obviously depends on the masses of $\tilde{g}$ and $\tilde{q}$ and is $\mathcal{O}(1\,\text{pb})$ at the TeV level. For the third generation squarks, the amount of mixing is a crucial element. The lighter squarks and gluinos will dominate the production. The heavier ones will mostly decay through strong interactions, via $\tilde{g} \to \tilde{q}\bar{q}$ for $m(\tilde{g}) > m(\tilde{q})$ or $\tilde{q} \to \tilde{g}q$ for $m(\tilde{q}) > m(\tilde{g})$. This is indicated in figure 132 by the nearly diagonal (green) lines which delimit three regions.

- Region 1: in this region, the gluinos are heavier than any of the squarks. The decay chains of the produced sparticles are expected to be
$$\tilde{g} \to \tilde{q}\bar{q}, \tilde{q} \to q\chi.$$
- Region 2: in this region some squarks are heavier, others are lighter than the gluino. Hence, rather complicated decay chains are possible, for instance
$$\tilde{q}_L \to \tilde{g}q, \tilde{g} \to \tilde{b}\bar{b}, \tilde{b} \to b\chi$$
as the $\tilde{q}_{\rm L}$ of the first two generations are expected to be among the heaviest squarks and the $\tilde{b}_1$ (and $\tilde{t}_1$) among the lightest.
- Region 3: in this region, the gluinos are lighter than any of the squarks. A typical decay chain is then
$$\tilde{q} \to \tilde{g}q, \tilde{g} \to q\bar{q}\chi,$$
where the gluino gives rise to a three-body decay.

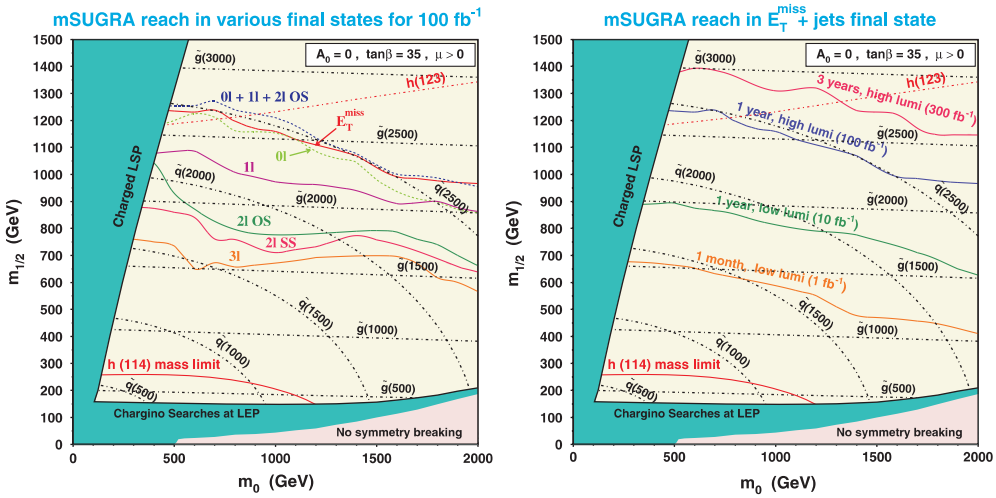

Figure 133. Left: CMS sensitivity for squarks and gluinos for $\tan\beta = 35$ from [535]. Full lines show the 5σ discovery regions, dot–dashed lines the isomass curves for squarks and gluinos. The labels nl indicate the number of leptons in the topology, with SS for same sign and OS for opposite sign dileptons. Right: CMS reach as function of luminosity for $\tan\beta = 35$.

The expected reach for sparticles at LHC has been studied by simulation of the ATLAS [371] and CMS [534,535] experiments. An example of the reach for the various topologies in the plane of $m_{1/2}$ versus m_0 is presented in figure 133 for the MSUGRA scenario.

For gluino decays, we saw in section 10.3 that the key point is whether the gluino is heavier than any squark (the most frequent case in the benchmarks of [143] but by no means necessary) or not. Anyway, a cascade will occur, down to the lightest sparticle, which in SUGRA is the neutral and invisible LSP $\tilde{\chi}_1^0$, leading to the missing E_T signature. As seen from figure 133, **the $\not{E}_T$ signature would allow squarks and gluinos to be discovered up to 2.5 TeV with an integrated luminosity of** $300\,\text{fb}^{-1}$. This would cover the whole region compatible with WMAP for $\tan\beta < 40 (\mu > 0)$ and $\tan\beta < 30 (\mu < 0)$, presented in section 12.2.3, provided MSUGRA is the correct scenario. The LHC experiments are sensitive to squark and gluino masses up to about 2 TeV with a luminosity of $100\,\text{fb}^{-1}$. Already with $\sim$1–$10\,\text{fb}^{-1}$ (1 year of LHC running) masses up to $\sim$1.5 TeV could be reached thanks to the large production cross sections. As emphasized in [536], for such an early discovery of SUSY the prerequisites will be a good understanding of the detector (calibrations, jet energy resolution, weak areas in the detector) as well as of the numerous backgrounds. The latter require detailed studies of the data and comparison with Monte Carlo simulation (in Z+jets, QCD multijet, $t\bar{t}$, ...) in signal-free regions, e.g. at low $\not{E}_T$, to predict the background in the signal region, e.g. at large $\not{E}_T$. Crucial to this will be the correct description of the physics by the Monte Carlo generator programs.

The main question concerns the number of steps in the cascade and whether, besides the $\not{E}_T$, one or more distinctive features can be observed and measured. A step in the cascade like

$$\tilde{g} \to \tilde{q}q, \tilde{q} \to q\tilde{\chi}_i^0 \text{ or } \tilde{g} \to q\bar{q}\tilde{\chi}_i^0 \tag{192}$$

can give one or more high p_T jets, allowing the transverse energy sum E_T^{sum} (also called 'effective mass', M_{eff}) variable to be built:

$$E_T^{\text{sum}} = \not{E}_T + \sum_{i=1}^{4} p_{T,i} \tag{193}$$

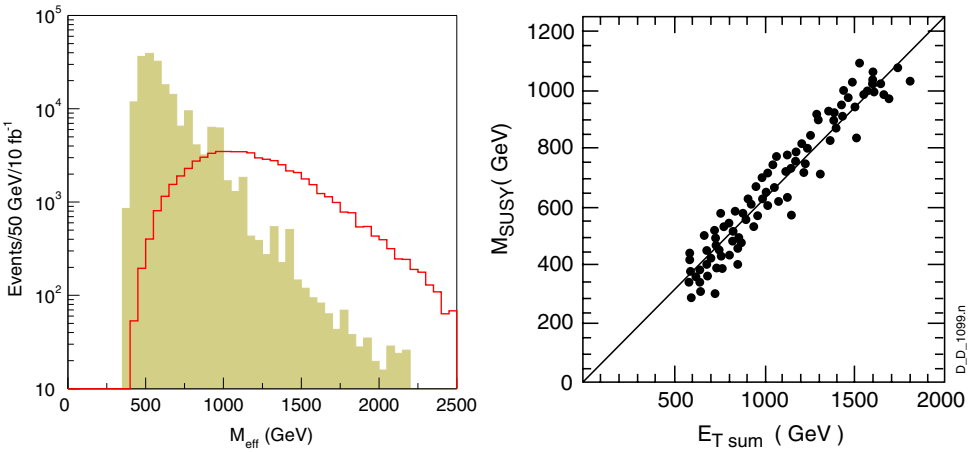

Figure 134. Left: distribution of $E_T^{\rm sum}$ (called $M_{\rm eff}$) for a point with squark and gluino masses of about 700 GeV (red line) and the SM background (shaded) from ATLAS [388]. Right: correlation between the peak value of $E_T^{\rm sum}$ and the SUSY mass scale $M_{\rm SUSY}$, defined as $\min(m_{\tilde g}, m_{\tilde q})$, from [535].

computed from the missing energy and the four hardest jets. The study of its distribution is usually sufficient in $R_{\rm p}$-conserving scenarios to reveal the presence of SUSY particles in the final state. The difference between the distribution in $E_T^{\rm sum}$ for a signal with squark and gluino masses of about 700 GeV and the SM background is shown in figure 134 (left) after multijet and $\not\!\!E_T$ cuts. A clear excess due to SUSY events, about an order of magnitude above the SM background, is observed at large $E_T^{\rm sum}$. Moreover, the peak value of the $E_T^{\rm sum}$ distribution provides a first estimate of the SUSY mass scale, defined as $\min(m_{\tilde g}, m_{\tilde q})$, within the MSUGRA scenario. This is seen in figure 134 (right) where the points represent the values obtained from a random scan over the MSUGRA parameters [535]. The $E_T^{\rm sum}$ variable provides an excellent illustration of the need of higher order QCD calculations in the Monte Carlo predictions of multijet states at hadron colliders. The above figure was based on multijet production by means of a shower Monte Carlo. More recently, the ALPGEN program was made available [537], which includes the matrix elements for multi-parton emission. This exact calculation shows that the production cross section is higher and that variables like $E_T^{\rm sum}$ are strongly affected. The $E_T^{\rm sum}$ distribution from $Z(\to \nu\bar\nu + 4$jets extends to much larger $E_T^{\rm sum}$ values and becomes almost indistinguishable from the SUSY production [536, 538]. The $\not\!\!E_T$ signature remains, however, viable [538].

In conclusion, the missing E_T signature is certainly the first signal to be expected at the LHC for the discovery of SUSY, thanks to the large production cross-sections for squarks and gluinos. It does not, however, single out unambiguously SUSY as the origin and other explanations, like universal extra dimensions, could equally be invoked. To distinguish between the possible origins, a detailed reconstruction of the particles involved will be indispensable. However, to separate the many different channels from SUSY cascade decays and to get handles from which one can hope to evaluate the masses of the particles involved, more specific features must be identified and measured.

15.2.2. Additional signatures. Useful signatures may result from the following electroweak decay chains:

- $\tilde g \to \tilde\chi^{\pm}_{1,2} q\bar q'$ or $\tilde\chi^0_i q\bar q$

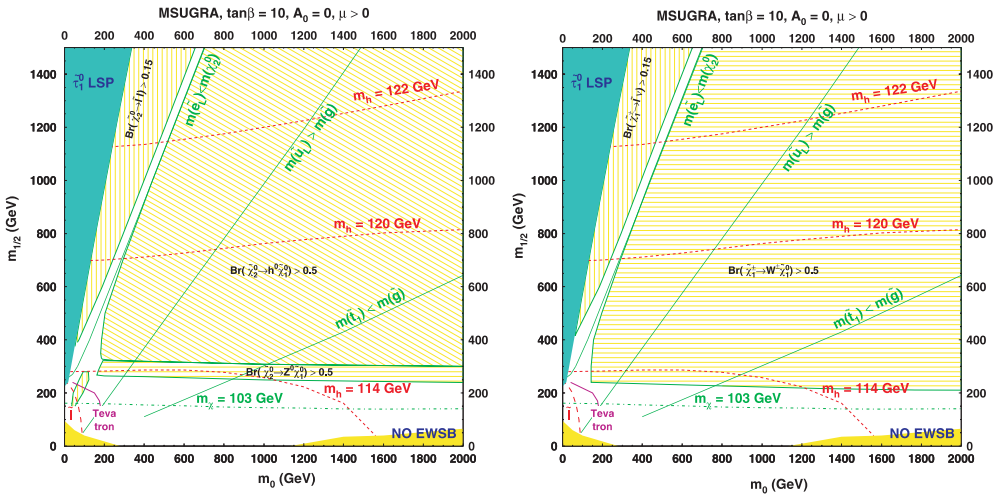

Figure 135. Left: regions of the $(m_{1/2}, m_0)$ plane where various decay modes of the $\tilde{\chi}_2^0$ have important branching ratios in the MSUGRA scenario for $\tan\beta = 10$ and $\mu > 0$. Also shown as heavy (green) lines are the kinematic relations between sparticle masses, as already discussed in figure 74. Right: same for the $\tilde{\chi}_1^{\pm}$ decay. The spectra were computed with ISASUGRA7.69.

- $\tilde{q} \to \tilde{\chi}_1^{\pm} q'$ or $\tilde{\chi}_{1,2}^0 q$
- $\tilde{\chi}_2^0 \to \tilde{l}^{\pm} l^{\mp}$ or $l^+ l^- \tilde{\chi}_1^0$ or $Z^0 \tilde{\chi}_1^0$ or $h^0 \tilde{\chi}_1^0$
- $\tilde{\chi}_1^{\pm} \to \tilde{l}^{\pm} \nu$ or $\tilde{\nu} l^{\pm}$ or $l^{\pm} \nu \tilde{\chi}_1^0$ or $W^{\pm} \tilde{\chi}_1^0$

which lead to events with multi-jets+missing E_T; multi-jets+missing E_T + $(n = 1, 2, 3, 4)$ isolated leptons with large P_T, originating from cascade decays through charginos and neutralinos; multi-jets+missing E_T+lepton pairs of the same charge, a signature also used at the Tevatron. The presence of high P_T isolated leptons and large missing E_T provides an efficient veto against the main backgrounds from $W^+W^-X \to l^+\nu l^-\bar{\nu}X$, $Z^0WX \to l^+l^-l'\nu X$ and $t\bar{t} \to W^+W^-b\bar{b} \to l^+\nu l^-\bar{\nu}X$. An example of the reach expected for the various inclusive leptonic topologies is shown in figure 133 (left). The mass range up to about 1.5–2 TeV is covered by several topologies and will allow a detailed study of branching ratios from which the decay chain can be inferred.

The most striking signatures are provided by the decay of $\tilde{\chi}_2^0$ when it appears at the end of the cascade decay chain. The type of signature which will dominate depends on the SUSY parameters. This is illustrated for $\tan\beta = 10$ and $\mu > 0$ in the $(m_{1/2}, m_0)$ plane in figure 135 (left). The following main regions can be identified.

- A triangular area, extending to the right of the region where the $\tilde{\tau}_1$ would be the LSP, where $\tilde{\chi}_2^0 \to \tilde{l}l$ (with l = e or μ) has a branching ratio > 15%. In the larger part of this region, the $\tilde{l}$ branching ratio is dominated by decays to left sleptons, which corresponds to a gauge interaction coupling of a wino to a $\tilde{l}_L l$ pair and dominates in MSUGRA if it is kinematically allowed. The invisible decays to $\tilde{\nu}\nu$ and $\tilde{\tau}_1\tau$ decays have usually large contributions and limit the maximum branching ratio achievable for the $\tilde{l}l$ decay. This region is accompanied by an area at small m_0 and $m_{1/2} \simeq 200$ GeV where >15% branching ratio is reached for the decay to $\tilde{l}_R$.
- In the largest part of the plane the decays to sleptons are kinematically forbidden and $m_{1/2}$ is sufficient to yield mass differences of $\tilde{\chi}_2^0$ and $\tilde{\chi}_1^0$ allowing the neutralino to decay into

$h^0\tilde{\chi}_1^0$. This corresponds to a gaugino–higgsino transition and thus requires a non-zero higgsino component in at least one of the two neutralinos. This decay easily reaches branching ratios larger than 90%.

- For smaller values of $m_{1/2}$, the decay to h^0 is kinematically forbidden, but in a narrow area the $Z^0\tilde{\chi}_1^0$ is possible, also leading to branching fractions above 90%. This decay is suppressed compared with the h^0 decay because it couples to the higssino component of both neutralinos.
- At yet smaller values of $m_{1/2}$, the three-body decay (through an off-shell Z^0) becomes dominant and, for low m_0, the 3-body decay to $ll\tilde{\chi}_1^0$ (mediated by an off-shell slepton) may be important.

The exact boundaries delimiting these regions depend on $\tan\beta$ and on the sign of μ, but the gross features described above are rather generic, as they reflect the gauge couplings of the theory. An exception to the above picture is a narrow range around $\tan\beta \simeq 4$ for $\mu < 0$ where the h^0 decouples from the $\tilde{\chi}_2^0$. In this case, the large area with dominant $\tilde{\chi}_2^0 \to h^0\tilde{\chi}_1^0$ becomes dominated by the decay $\tilde{\chi}_2^0 \to Z^0\tilde{\chi}_1^0$.

As seen in figure 135 (right), the chargino gives rise to leptonic decays $\tilde{\chi}_2^0 \to \tilde{l}\nu$ or $\tilde{\nu}l$ with branching ratios totalling $> 15\%$ in the same triangular region where $\tilde{\chi}_2^0 \to \tilde{l}l$. As the Higgs decay of the chargino would lead to a $H^\pm$ which is heavy in MSUGRA, this decay mode is closed. Instead, the regions with dominant decay of $\tilde{\chi}_2^0$ into h^0 or Z^0 correspond to $\tilde{\chi}_1^\pm \to W\tilde{\chi}_1^0$.

Another striking signature may be provided by the gluino decay into a chargino. When a gluino pair is produced, both gluinos may decay into charginos of the same charge, due to the Majorana nature of the gluino. If the chargino decays leptonically, $\tilde{\chi}^\pm \to l^\pm\nu\tilde{\chi}_1^0$, this yields events with two same sign leptons, a very clear signature with little SM background. This signature is relevant in the whole region of figure 135 where $m(\tilde{g}) < m(\tilde{t}_1)$. It may even extend to lower m_0 and higher $m_{1/2}$, as seen from the same sign di-lepton reach of figure 133 (left). In this case, they occur mostly via the decay chain $\tilde{g} \to \tilde{t}_1 t$, $\tilde{t}_1 \to \tilde{\chi}^\pm b$, $\tilde{\chi}^\pm \to W^\pm\tilde{\chi}_1^0$ with a leptonic decay of the $W^\pm$.

At the LHC, sleptons can also be directly pair produced by a Drell–Yan mechanism (by γ or Z^0 exchange) and by gauge boson fusion. The most interesting signature is from the decay $\tilde{l} \to l + \tilde{\chi}_1^0$, giving rise to two isolated leptons of the same flavour with opposite charge and missing transverse momentum. The dominant backgrounds from $t\bar{t}$ and $WW + X$ production, as well as from other SUSY processes, are partly vetoed by the requirement of no additional jets. Simulation studies of the Drell–Yan production by CMS have shown [539] that, for a luminosity of $100\,\mathrm{fb}^{-1}$, the mass reach extends from about 100 to 400 GeV. At low masses the limitation comes from a low signal to background ratio and at the high mass end from the small signal rate. This would correspond to a roughly circular region of radius $\lesssim 400$ GeV in figure 133 (left). So far, the contribution from gauge boson fusion has not yet been included and, as seen in section 10.3, it is expected to increase the reach to larger masses.

As yet another mechanism, it would be possible to look for the direct production of $\tilde{\chi}_2^0\tilde{\chi}_1^\pm$, to be detected by means of its trilepton signature, like is currently done at the Tevatron. The present conclusions from simulation studies [539] indicate that large statistics could be accumulated at the LHC, allowing detailed analyses of their properties and that the accessible mass range would cover the region $m_{1/2} \lesssim 200$ GeV. As seen from figure 135 (left), for larger $m_{1/2}$ the $\tilde{\chi}_2^0$ decays into h^0 (or Z^0).

15.2.3. Sparticle mass reconstruction. Determining the sparticle masses on an event by event basis is not feasible, the kinematical constraints being insufficient due to the presence of two

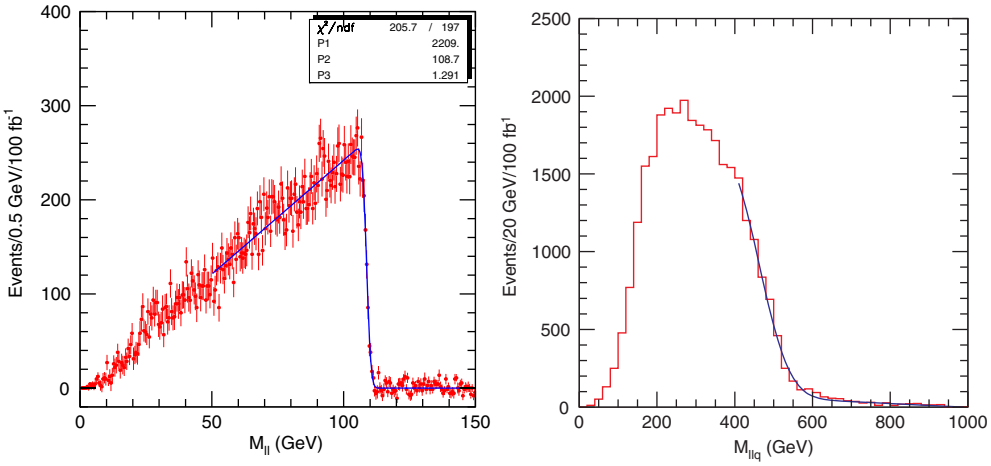

Figure 136. Left: di-lepton mass distribution for events with a decay $\tilde{\chi}_2^0 \to \tilde{l}^{\pm} l^{\mp}$ after subtraction of $e^{\pm}\mu^{\mp}$ masses. From ATLAS [388]. Right: distribution of the llq mass for the minimum mass obtained by combining the di-lepton system of the left figure with a hard jet.

invisible neutralinos in every event. However, mass distributions of the leptons and/or quark jets for specific final states will allow the measurement of sparticle masses [388, 540]. Given the complexity of the events, the search for a signature starts from the bottom of a decay chain.

As an example, we can take the decay chain $\tilde{q} \to \tilde{\chi}_2^0 q \to \tilde{l}^{\pm} l^{\mp} q \to \tilde{\chi}_1^0 l^+ l^- q$, for which detailed analyses exist in [541, 542]. **The end point of the same flavour dilepton mass distribution from the decay of $\tilde{\chi}_2^0$ carries useful information on the sparticle masses**. An example is provided in figure 136 for events with cuts on $E_T^{\rm miss}$ and the p_T of jets and leptons. In case the end point is blurred by other decays, e.g. from charginos or top, it can be improved by using the flavour subtracted combination $e^+e^- + \mu^+\mu^- - e^{\pm}\mu^{\mp}$ which cancels most backgrounds. For the three-body $\tilde{\chi}_2^0$ decay, the end point measures directly the mass difference between the parent $\tilde{\chi}_2^0$ and the resulting $\tilde{\chi}_1^0$. For the two-body decay via a slepton, it has a different shape with a very sharp edge. The triangular shape is a direct reflection of the spin-zero nature of the intermediate state $\tilde{l}$ which decays isotropically. The end point position also depends on the slepton mass and is given by

$$M_{ll}^{\rm max} = \sqrt{\frac{(m^2_{\tilde{\chi}_2^0} - m^2_{\tilde{l}})(m^2_{\tilde{l}} - m^2_{\tilde{\chi}_1^0})}{m^2_{\tilde{l}}}}. \tag{194}$$

On its own, this equation does not allow the masses to be determined. Further constraints can be derived, e.g. from the relative magnitude of the two lepton momenta, which allows the mass of the LSP to be constrained from its effect on the decay kinematics. By combining further with, for example, the quark jet from the squark decay, information on the masses of all members of the decay chain can eventually be obtained. For example, the mass distribution of (llq) also exhibits an end point, shown in figure 136 (right), which values constrains the mass of the parent $\tilde{q}$. Moreover, end points are observable in the $M(lq)$ distribution. In this case, two end points can be extracted, one for the lepton from the $\tilde{\chi}_2^0$ decay $(l1)$ and one for the lepton from the $\tilde{l}$ decay $(l2)$. Together, these provide 4 end points which allow, in principle, a model independent determination of the 4 unknown masses of the $\tilde{q}$, $\tilde{\chi}_2^0$, $\tilde{l}$ and $\tilde{\chi}_1^0$. Expressions of the end points as a function of the sparticle masses are summarized, together with the corresponding kinematical configurations in figure 137. To simplify the formulae, the

following symbols are used for the masses: $M_Q = m_{\tilde{q}}$, $M_X = m_{\tilde{\chi}_2^0}$, $M_R = m_{\tilde{l}}$, $M_0 = m_{\tilde{\chi}_1^0}$. Several difficulties are apparent from this figure. Some are related to the association of the correct formula to a given end point. So far, this was frequently done based on the *a priori* knowledge of the masses injected in the simulation, which introduces 'model dependence'. An alternative, used in [542], is to try all physically meaningful combinations and keep only those which solutions give the correct sparticle mass hierarchy. Another possibility would be to look at correlations between the effective masses, as the end points occur for specific kinematical configurations. First, the two leptons from $\tilde{\chi}_2^0$ and from $\tilde{l}$ decays cannot be distinguished. Nevertheless, the end points in $M(l1q)$ and $M(l2q)$ can in principle be distinguished thanks to their different configurations and corresponding $M(ll)$ regions to which they are related, as seen in figure 137. Similarly, the correct formula for the $M(llq)$ end point could be identified by correlations with the $M(ll)$ and $M(lq)$ distributions.

Another difficulty is that the second and third formula for $M(llq)$ are not independent of the other ones. In this case the above four end points are not sufficient to determine the sparticle masses. But additional end points can be measured, like from the $M(l1q) + M(l2q)$ distribution. In some cases it is also possible to observe an end point at the lower edge of the mass distribution, for instance for the (llq) mass after selecting (ll) masses near the end point. If the only available leptonic two-body decay is $\tilde{\chi}_2^0 \to \tilde{\tau}_1\tau \to \tilde{\chi}_1^0\tau\tau$, for instance at large $\tan\beta$, this most difficult case may nevertheless lead to measurements of masses, although less precise than for e or μ.

In conclusion, for long enough decay chains, the number of constraints from the end points is sufficient to determine all masses involved. But as more end points can be determined, the extraction of the mass values is most easily done by randomly generating the masses (or the MSUGRA parameters) to compare the obtained end points to the experimental ones and, for example, performing a χ-squared minimization.

Apart from studying final states with leptons, **there is a possibility to detect the Higgs in the decay chain $\tilde{\chi}_2^0 \to h^0\tilde{\chi}_1^0 \to b\bar{b}\tilde{\chi}_1^0$, which may have a substantial branching ratio**. The requirements of two b-tagged jets, not too separated (as m_h is small) and large missing E_T removes most of the SM backgrounds and a clear h^0 mass peak can be observed, which allows its mass to be reconstructed, as shown in figure 138 (left). Like the di-lepton signal, the h^0 can also be combined with additional jets and the end point in the $M(h^0q)$ distribution, shown in figure 138 (right), serves to constrain the $\tilde{q}$ mass [388]. A similar approach can be adopted for the decay $\tilde{\chi}_2^0 \to Z^0\tilde{\chi}_1^0$, where the Z^0 is usually reconstructed from its di-lepton decay. If, in these cases, the decay originates from a squark, the cascade is too short to allow the determination of the masses involved, as only the $M(h^0q)$ mass distribution is available. The masses can be reconstructed if the decay originates from a gluino, giving access to additional mass distributions, or if other decay chains are simultaneously detectable (e.g. with di-leptons).

It should be noted that several of these decay modes may be simultaneously present and that the same decay may originate from a $\tilde{\chi}_2^0$ as well as from a heavier neutralino state. In the latter case, more than one end point may be observed in the same distribution.

Most end points can be measured with good accuracy, of order of a few GeV or less. A model independent, apart from the assumed decay chain, calculation of the sparticle masses is possible yielding uncertainties ranging from 1 to ~10% according to [541]. An example of masses computed from the end points for the benchmark point SPS1A assuming an integrated luminosity of 300 fb^{-1} in ATLAS [543] is given in table 27.

Of course, much more information on the SUSY particles will be available than just the end points, for example several branching ratios and cross-sections. They will also help in testing the models.

1. $(\mathbf{ll})^{\mathbf{max}}$

$$M_{ll}^{max} = M_X\sqrt{(1-\tfrac{M_R{}^2}{M_X{}^2})(1-\tfrac{M_0{}^2}{M_R{}^2})}$$

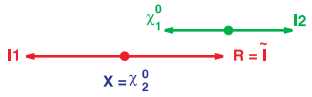

2. $(\mathbf{ll})^{\mathbf{min}}$ (parallel leptons)

$$E_{l2}/E_{l1} = (M_R^2 - M_0^2)/(M_X^2 - M_R^2)$$

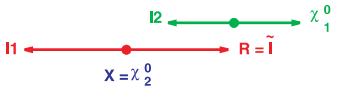

3. $(\mathbf{l1q})^{\mathbf{max}}$ (1st lepton)

$$M_{l_1q}^{max} = M_Q\sqrt{(1-\tfrac{M_X{}^2}{M_Q{}^2})(1-\tfrac{M_R{}^2}{M_X{}^2})}$$

4. $(\mathbf{l2q})^{\mathbf{max}}$ (2nd lepton)

$$M_{l_2q}^{max} = M_Q\sqrt{(1-\tfrac{M_X{}^2}{M_Q{}^2})(1-\tfrac{M_0{}^2}{M_R{}^2})}$$

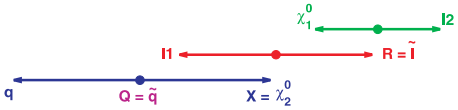

5. $(\mathbf{llq})^{\mathbf{max}}$

$$M_{llq}^{max} = M_Q\sqrt{(1-\tfrac{M_X{}^2}{M_Q{}^2})(1-\tfrac{M_0{}^2}{M_X{}^2})}$$
for $\frac{M_X}{M_Q} < \frac{M_0}{M_X}$

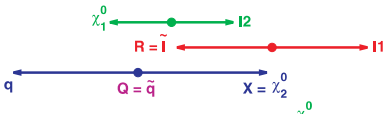

$$M_{llq}^{max} = M_Q\sqrt{(1-\tfrac{M_R{}^2}{M_Q{}^2})(1-\tfrac{M_0{}^2}{M_R{}^2})}$$
for $\frac{M_0}{M_R} < \frac{M_R}{M_Q}$

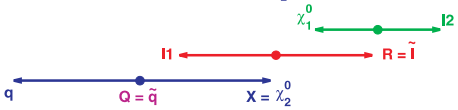

$$M_{llq}^{max} = M_Q\sqrt{(1-\tfrac{M_R{}^2}{M_X{}^2})(1-\tfrac{(M_X M_0)^2}{(M_Q M_R)^2})}$$
for $\frac{M_R}{M_X} < \frac{M_X}{M_Q}\frac{M_0}{M_R}$

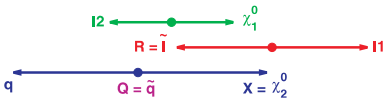

$$M_{llq}^{max} = M_Q - M_0 \qquad \text{otherwise}$$

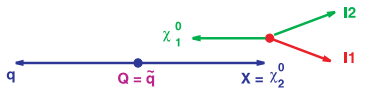

6. $(\mathbf{l1q} + \mathbf{l2q})^{\mathbf{max}}$

$$(M_{l1q} + M_{l2q})^{max} = M_{l1q}^{max} + \sqrt{(M_{llq}^{max})^2 - (M_{l1q}^{max})^2}$$

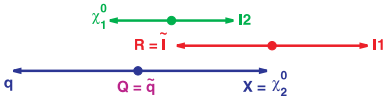

7. $(\mathbf{llq})^{\mathbf{min,max}}$ versus $(\mathbf{ll})$

$$(M(llq)^{min,max})^2 = M_Q^2 + M_0^2 - \tfrac{1}{2}M_Q^2(1+\tfrac{M_X{}^2}{M_Q{}^2})(1+\tfrac{M_0{}^2}{M_X{}^2}) + \tfrac{M_Q^2}{2M_X^2}(1+\tfrac{M_X{}^2}{M_Q{}^2})M_{ll}^2$$
$$\mp \tfrac{M_Q^2}{2}(1-\tfrac{M_X{}^2}{M_Q{}^2})\sqrt{(1-\tfrac{M_0^2}{M_X^2}-\tfrac{M_{ll}^2}{M_X^2})^2 - 4\tfrac{M_0^2}{M_X^2}\tfrac{M_{ll}^2}{M_X^2}}$$

Figure 137. End point formulae and kinematical configurations. See text for explanations.

SUSY may lead to quite complex events [544]. In the MSUGRA region close to the focus point boundary [143], with heavy squarks, the production of $\tilde{g}\tilde{g}$ pairs dominates and the largest $\tilde{g}$ branching ratios are for $\tilde{g} \to \chi_i^- t\bar{b}$. The final state is certainly spectacular (12 to 16 jets and/or leptons), but sorting out the combinatorial background is certainly challenging.

15.2.4. Beyond MSUGRA. Several MSUGRA points have been explored. However, another question is to see what happens when one leaves the strict MSUGRA scenario and allows

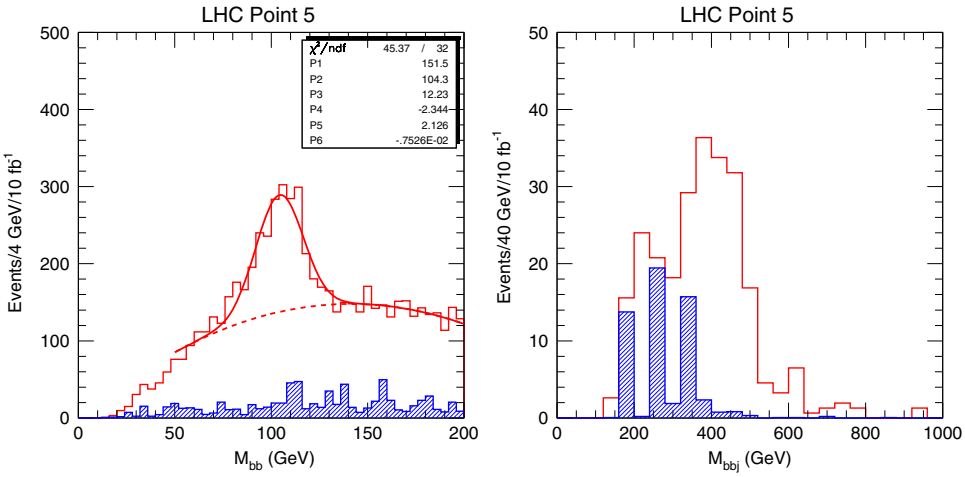

Figure 138. (left) Mass of b-jet pairs from a signal (open histogram) and sum of backgrounds (shaded histogram). (right) The smaller of $(b\bar{b}j)$ masses for signal and background for events with the $(b\bar{b})$ mass selected in the peak of the figure on the left. From ATLAS. Reprinted with permission from [540]. Copyright 1997 by the American Physical Society.

Table 27. Anticipated measurements and precision of sparticle masses at LHC, from [543]. The generated mass quoted for $\tilde{q}_R$ is for $\tilde{u}_R$ and for $\tilde{q}_L$ is the average of $\tilde{u}_L$ and $\tilde{d}_L$.

Particle	Measurements + errors	Generated value
$\tilde{\chi}_1^0$	96.16 ± 4.76	96.05
$\tilde{\chi}_2^0$	176.9 ± 4.66	176.80
$\tilde{\chi}_4^0$	377.9 ± 5.11	377.83
$\tilde{g}$	595.1 ± 8.05	595.5
$\tilde{q}_R$	520.4 ± 11.8	520.5
$\tilde{q}_L$	540.3 ± 8.79	540.14
$\tilde{b}_1$	491.9 ± 7.45	491.92
$\tilde{b}_2$	524.5 ± 7.93	521.
$\tilde{l}_R$	143.1 ± 4.75	143.00
$\tilde{l}_L$	202.3 ± 5.03	202.12
$\tilde{\tau}_1$	132.5 ± 6.25	133.39

for some degree of non-universality. An example is given by [545] describing models with effective SUSY where the third generation of squarks is light, the first two are heavy and the general case of non-universal gaugino masses is considered. The visibility of a SUSY signal is found to depend strongly on the relation between LSP, $\tilde{\chi}_2^0$, $\tilde{g}$ and $\tilde{q}$ masses and may turn out to be quite low in some unfavourable scenarios, where the LSP mass is close to the third generation squark masses.

Another example of a departure from MSUGRA is described in [407], which adopts a case study based on a SUSY $SO(10)$ GUT without universality within the generations. In this scenario, the LHC would discover SUSY and distinguish it from MSUGRA. However, this example illustrates the complementary role of a linear collider to obtain accurate estimates of the masses.

We have seen that in the MSUGRA scenario the h^0 can appear in cascade decays, resulting from the $\tilde{\chi}_2^0$ decay. The heavier Higgses are, however, quite heavy in MSUGRA and are not expected to be produced from cascades. But they can be made lighter in a more general MSSM and can be produced in cascades involving charginos and neutralinos. This may even become

an interesting discovery channel for favourable SUSY parameter values [374], as we already mentioned in section 8.9.

In GMSB models, in which the $\tilde{G}$ is the LSP, the phenomenology depends on the nature of the NLSP. Hard isolated photons or long-lived particles can provide further handles to isolate and identify SUSY final states. Reference [546] examined signals for sparticle production at LHC with a low SUSY breaking scale for four different models leading to different signatures. Starting with the canonical $\not{E}_T$ and multilepton channels, they consider special features related to the nature of the NLSP, for instance the presence of hard isolated gammas or $h \to b\bar{b}$ (but with the conservative assumption that the NLSP decay is prompt), which could further enhance the signal over background. They find that the SUSY reach measured in terms of $m_{\tilde{g}}$ is at least as large as in the MSUGRA framework: in particular in the best case of the co-NLSP scenario, the reach extends to $m_{\tilde{g}} \geqslant 3$ TeV with 10 fb^{-1}. The study [371] of a few points in the GMSB parameter space has shown that, also in this case, the reconstruction of the sparticle masses from end points in the effective mass distributions is possible.

Following other studies, [547] investigates the discovery potential for the minimal AMSB scenario in which, as we said in section 5.1.4, a conformal anomaly in the auxiliary field of the supergravity multiplet transmits SUSY breaking to the observable sector. The parameters of minimal AMSB are $m_{3/2}$ (gravitino mass), m_0 (universal scalar mass introduced to cure the slepton negative mass squared), $\tan\beta$ and $\mathrm{sign}(\mu)$. The classic AMSB prediction of a wino-like LSP nearly mass degenerate with the lightest chargino means that the latter may have a long lifetime. Reference [547] generates minimal AMSB spectra on a grid 100 GeV–5 TeV in the m_0–$m_{3/2}$ plane for $\tan\beta = 10$ and $\mu > 0$ and determines the reach of the LHC with a realistic (ATLAS) detector simulation, optimized but generic SUSY cuts on 10 variables and 100 fb^{-1}. The 5σ (and $\geqslant 10$ events) discovery reach shows that the LHC will be able to distinguish minimal AMSB from SM in various multi-lepton with $\not{E}_T$ channels over a large range of parameters with the reach extending to $m_{\tilde{q}} \sim 2.8$ TeV or $m_{\tilde{g}} \sim 2.1$ TeV, whichever is the lower. The Snowmass point SPS9 lies well within the discovery region. The near degeneracy of a $\tilde{\chi}_1^{\pm}$ and LSP leading to a more or less long-lived chargino is a strong signature for AMSB (even beyond the minimal version). In [547], a range of model points is defined for the most difficult regime of shorter lifetimes ($0.2 \leqslant \Delta M_{\tilde{\chi}_1^{\pm}} \equiv m_{\tilde{\chi}_1^{\pm}} - m_{\tilde{\chi}_1^0} \leqslant$ a few GeV), with a decay before the first tracking layer and soft tracks, and explores methods to probe this region. They conclude that selecting events with large $\not{E}_T$ and identifying tracks from chargino decays the wino-like nature of the LSP can be determined and $\Delta M_{\tilde{\chi}_1^{\pm}}$ can be measured over a large range of parameters. Evidence for this class of models can be obtained even in cases where the chargino is shorter lived than predicted in minimum AMSB.

With R-parity violation the large $\not{E}_T$ signature is lost but it provides multiple leptons and/or very high jet multiplicities. The latter is, however, a signal difficult to extract from the QCD background. The R-parity violation with $\tilde{\chi}_1^0 \to qqq$, in particular $\tilde{\chi}_1^0 \to cds$, is another example of complex signature, with a few or no b-jet and small $\not{E}_T$ and with a QCD background which is not well known. The searches for R-parity violation will be further discussed in section 15.5.

15.3. SUSY searches at lepton colliders

If the machine energy is sufficient, superpartners may also be observed and their masses measured at lepton colliders [548]. The fixed energy of the pair produced final state sparticles is then very advantageous. It allows, for example, the measurement of both the lower and upper edge of the energy distributions in two-body decays, see formula (165), which determine the masses of the parent and of the $\tilde{\chi}_1^0$. Expected accuracies are of the order of a few 0.1%.

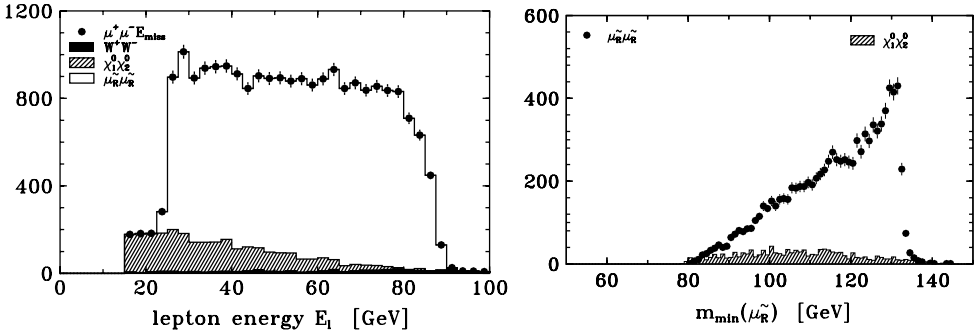

Figure 139. (left) Muon energy distributions from $\tilde{\mu}_R$ pair production. (right) Minimum mass distribution. The energy is supposed to be $\sqrt{s} = 320$ GeV, the integrated luminosity 160 fb^{-1} and the sparticle masses are $m(\tilde{\mu}_R) = 132$ GeV and $M(\tilde{\chi}_1^0) = 71.9$ GeV. From [406].

Further improvements on the mass determination can be achieved through threshold scans. As an example, figure 139 (left) gives the muon energy distribution from $\tilde{\mu}_R$ pair production, as well as the backgrounds. The $\tilde{\mu}$ and $\tilde{\chi}_1^0$ masses are determined by measuring the two end points. Figure 139 (right) gives, for the same process, the minimum mass distribution [406], defined as the minimum slepton mass compatible with the slepton momenta for a postulated $\tilde{\chi}_1^0$ mass. It is sharply peaked at the actual $\tilde{\mu}$ mass and allows an accurate determination of the slepton mass, assuming that the $\tilde{\chi}_1^0$ mass is well measured from another process, such as chargino production.

Another advantage is the availability of beam polarization, which allows the determination of the spin and coupling of the sleptons. It may select a specific process, e.g. an e_R^- beam selects the production of $\tilde{\mu}_R\tilde{\mu}_R$, suppressing the $\tilde{\mu}_L\tilde{\mu}_L$ and also suppressing the WW background. This may help distinguishing nearly mass degenerate states.

Lepton colliders are, therefore, expected to provide more accurate measurements than achievable at the LHC. On the other hand, it is easily seen from figure 133 that a reach for squarks comparable to the one of LHC would require a very high energy machine.

Charginos and neutralinos are among the lightest superpartners, so among the most likely to appear at a LC. Focusing on chargino pair production, as an example, the flexibility of a LC allows all the involved parameters to be disentangled by measuring

$$M(\tilde{\chi}_1^{\pm}), \sigma_R, A_R^{FB}, \sigma_L, A_L^{FB}, \tag{195}$$

where L and R denote the left- and right-polarized e^- beam. The mass measured by kinematic end points or threshold scans provides essentially a measurement of M_2 or $|\mu|$, whichever is smaller. The right-polarized quantities provide complementary information on chargino mixing. The left ones are sensitive to the mass of the exchanged sneutrino.

Figure 140 gives the two chargino mixing angles (entering the diagonalization matrices for the chargino masses) obtained by exploiting some of the measurements quoted above.

A LC allows the dependence of various CP-conserving observables (cross-sections, masses, decay distributions) on the phases of SUSY parameters μ and M_1 to be measured. This is illustrated in figure 141. As evident from the examples given, **even if only a few superpartners are accessible, the LC should provide model independent measurements of several soft SUSY breaking parameters**. We will see in section 16.2 how this information can be extrapolated to high energy scales to get an idea of the scenario involved.

As an example, table 28 summarizes, for a MSUGRA point (slight modification of Snowmass point SPS1a [164]), a sample of masses and expected accuracies, where the

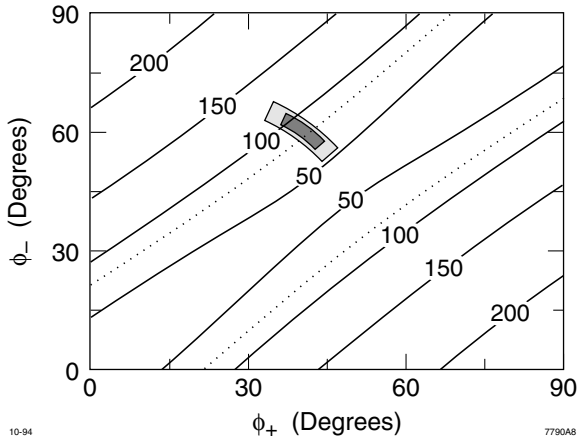

Figure 140. Chargino mixing angles. Reprinted with permission from [549]. Copyright 1995 by the American Physical Society.

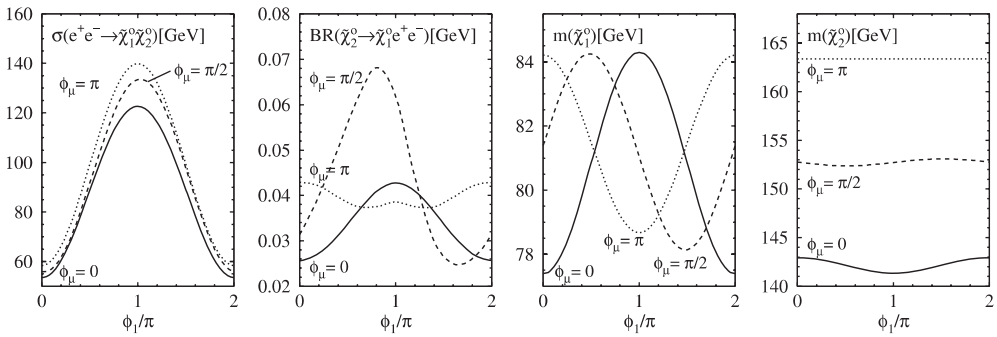

Figure 141. Dependence of various observables on CP-violating phases for the parameters μ and M_1, assuming MSUGRA with $m_0 = 100\,\text{GeV}$, $m_{1/2} = 200\,\text{GeV}$, $A_0 = 0$, $\tan\beta = 4$ and $\mu > 0$. Reprinted with permission from [569]. Copyright 2001 by the American Physical Society.

contributions of LC, LHC and CLIC are added. LHC should discover all particles. For this favourable scenario, the LC has access to six sparticles (plus naturally the h^0). Only CLIC will give access to the heavy Higgses.

15.4. Post-LEP benchmarks

Benchmark points have often been used in the past to evaluate the potentialities of new machines and experiments. An example is given by the benchmark points suggested by the LHC Committee in 1996 and used by ATLAS [371] and CMS [535]. As the older ones often fail to fulfil the LEP constraints from direct searches, in particular from the light Higgs, a series of new post LEP benchmarks were proposed. One example is shown in figure 104, the 'Cern' benchmarks (drawn as stars) originally proposed in [143] and recently updated to comply with the WMAP results in [550]. Other examples, among several, are the 'points d'Aix' from [166] or the Snowmass points and slopes (SPS) from [164], already mentioned earlier. The principal aim of [143, 550] was to choose points which are compatible with the aforementioned constraints, including CDM, and which span a wide area of the allowed SUSY parameter space. The proposed points range over $\tan\beta$ values from 5 to 50. Five are in the

Table 28. Anticipated measurements and precision of sparticle masses, from [163].

Particle	Measurements + errors	
$\tilde{\chi}_1^{\pm}$	183.05 ± 0.15	LC
$\tilde{\chi}_2^{\pm}$	383.28 ± 0.28	LC
$\tilde{\chi}_1^0$	97.86 ± 0.20	LC
$\tilde{\chi}_2^0$	184.65 ± 0.30	LC
$\tilde{e}_{\mathrm{R}}$	224.82 ± 0.15	LC
$\tilde{e}_{\mathrm{L}}$	269.09 ± 0.28	LC
$\tilde{u}_{\mathrm{R}}$	572 ± 10	LHC+CLIC
$\tilde{u}_{\mathrm{L}}$	589 ± 10	LHC+CLIC
$\tilde{g}$	598 ± 10	LHC
h^0	113.38 ± 0.05	LHC+LC
A^0	435.5 ± 1.5	CLIC

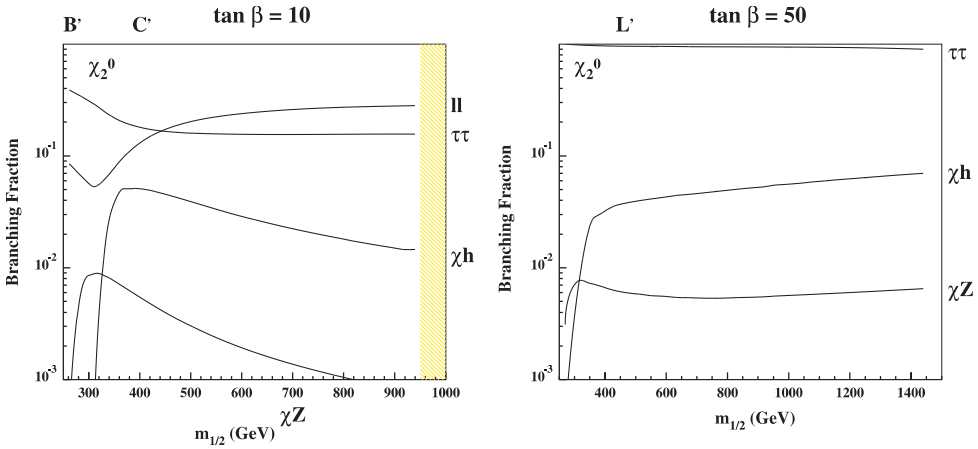

Figure 142. Decay branching ratios of $\tilde{\chi}_2^0$ along WMAP lines for $\tan\beta = 10$ and 50 with $\mu > 0$. From [550].

'bulk' region, four are spread along the coannihilation 'tail', two are in the 'focus point' region and two are in the rapid annihilation 'funnels'. The values for m_h are compatible with the LEP limit, within uncertainties, but never more than ~10 GeV above it.

It is clear that by relaxing the model constraints, e.g. allowing non-universal Higgs mass parameters, the forbidden region with $\Omega_\chi h^2 > 0.129$ would become acceptable. However, it is seen from figure 104 that the chosen points would still remain representative of a broad variety of SUSY scenarios. It should, nevertheless, be emphasized that the points do not provide an unbiased statistical sampling of the constrained MSUGRA parameter space.

Given the narrow region still allowed after imposing the CDM constraint from WMAP, seen in figure 107, it is possible to define 'lines' for constant $\tan\beta$ in the $(m_0, m_{1/2})$ plane where all constraints are fulfilled. The idea is that, following the suggestion of the Snowmass slopes [164], it may be interesting to check the observability of SUSY and the reconstruction of the spectrum along these lines with increasing $m_{1/2}$. A parametrization of the lines is found in [550]. The main decay branching ratios of the $\tilde{\chi}_2^0$, the starting point for mass reconstruction, are shown in figure 142 for $\tan\beta = 10$ and 50. For low to intermediate $\tan\beta$ the decays of $\tilde{\chi}_2^0$ to $\tilde{l}l$ and to $\tilde{\tau}\tau$ are both important, whereas for large $\tan\beta$ the branching ratio to $\tilde{\tau}\tau$ approaches 100%, due to its increased Yukawa coupling. The decays to $h^0\tilde{\chi}_1^0$ and $Z^0\tilde{\chi}_1^0$ never exceed 5–6% and 1%, respectively. The strong constraints forbid the region in parameter space where

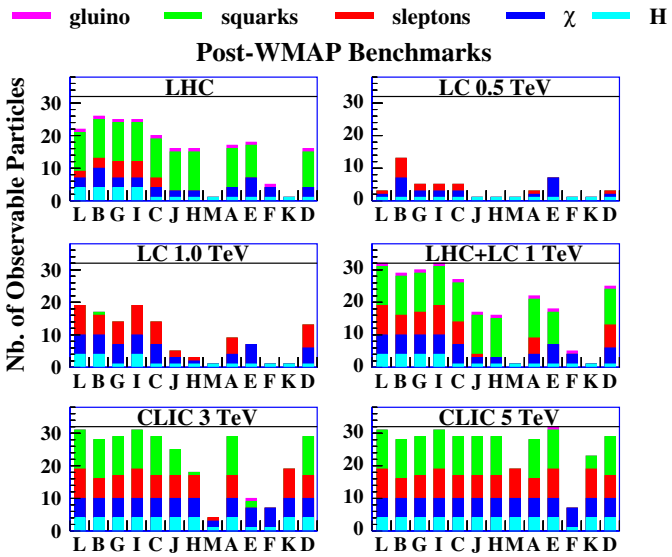

Figure 143. Summary of sensitivities for various accelerators. From [550].

large branching ratios to h^0 or Z^0 are reached. Again, this may be relaxed by allowing for non-universality. But a lesson of this constrained MSUGRA is perhaps that the final states with $\tilde{\tau}\tau$ will play a crucial role in the discovery of SUSY.

A crude estimation of the discovery potential of various accelerators for the benchmark points of [550] was made. The results are summarized in figure 143.

The potentiality of the LHC experiments was estimated on the basis of existing studies from CMS [534] and ATLAS [371]. The lightest Higgs, whose mass is below 125 GeV in all scenarios, is always found. Also squarks and gluinos are usually discovered, although there are some benchmark points where all sparticles are too heavy to be detected at the LHC, points K′ and M′ located in the funnels. The weakly interacting sparticles are mostly observable only as decay products of squarks and gluinos and are often missed. This is the case of charginos, neutralinos, sleptons and heavier Higgses.

For lepton colliders, the potential was based on the assumption that the discovery of sparticles required a cross-section time branching ratio into visible particles of $\geqslant 0.1\,fb$, corresponding to about 100 produced sparticles in the total data sample of $1 ab^{-1}$. The lightest Higgs is observable here as well, but in addition, a linear collider allows an accurate determination of its mass and branching ratios. A 1 TeV linear collider would be able to discover and study several weakly interacting sparticles in many scenarios and appears complementary to the LHC in this respect. The $\gamma\gamma$ option of the linear collider would also allow the s-channel production of heavy Higgses via $\gamma\gamma \rightarrow H^0$ or A^0. However, there are some points where neither a 1 TeV linear collider nor the LHC can discover supersymmetry. Only a multi-TeV linear collider like CLIC, or a muon collider, seems able to cover all benchmark points.

The prospects for the direct detection of neutralinos from astrophysical origin through their spin-independent elastic scattering have been studied in [551] for the benchmark points of [143]. The conclusion is that the projected sensitivities of CDMS II, CRESST and GENIUS would probably allow the detection of neutralinos for several of the benchmarks. Unfortunately, the most difficult ones for LHC (K and M) would also remain undetectable by these experiments.

15.5. Searches for R-parity violation

R-parity violating SUSY will be searched for at future colliders.

At hadron colliders, as one can guess, this will not be an easy task. It will probably be impossible to be exhaustive. The goal is to select the topologies which are likely to be measurable and, in the case of a signal, to distinguish it from other possible sources.

The Tevatron [552] will study resonant single slepton production and resonant stop production, under various conditions for their subsequent decay, either a direct RPV decay or a cascade to a RPV decaying LSP. It will also study pair production of gluinos, squarks and other MSSM particles, in particular cascading to the LSP which then has an RPV decay.

A relatively simple way is to focus on a well-defined experimental signature, such as the rate of single leptons e and μ in the final state in case of non-zero λ couplings [553], the flavour content of jets in case of baryon number RPV couplings λ'' [554] or the details of the production of $\mu^+\mu^-$ pairs [555]. Concerning the latter, the study of Drell–Yan at the LHC could be a significant tool since RPV, through the presence of λ'_{ijk}, can distort the differential cross-section: λ'_{2jk} would lead to an additional u-channel diagram for $\bar{u}_j u_j \to \mu^+\mu^-$ with $\tilde{d}^k_{\mathrm{R}}$ exchange and a t-channel one for $\bar{d}_k d_k \to \mu^+\mu^-$ with $\tilde{u}^j_{\mathrm{L}}$ exchange. **This is one more incentive to perform an accurate measurement of this 'standard' channel.**

Many other possibilities can be thought of and should be explored, like single top (i.e. $t\bar{c}$ or $t\bar{b}$) production. The study of single top quark production at hadron colliders shows that the LHC is better at probing the baryon violating coupling λ'', whereas the Tevatron and the LHC have similar sensitivity to λ' couplings. In [556] a feasibility study was carried out to detect single top production through RPV at the LHC measuring the $tb \to l\nu bb$ final state (a high p_T lepton and $\not{E}_T$) obtained by u-channel slepton exchange ($\lambda' \neq 0$) or s-channel squark exchange ($\lambda'' \neq 0$). The $t\bar{t}$ background is reduced by a strong jet veto on the third jet. At the chosen value of the coupling constants ($\sim 10^{-1}$) a significant signal over background ratio is obtained in the channel considered if the exchanged sparticle is a squark with narrow width ($\sim$1 GeV). With 30 fb^{-1} the $\lambda'_{123}\lambda'_{323}(\tilde{s}$ exchange) combination can be probed down to 10^{-2}–10^{-3} (the λ'_{112} is already too low to be relevant). In case of absence of signal after 30 fb^{-1} one can lower the experimental limit on the quadratic combination of λ' couplings by an order of magnitude for narrow width quarks. In case of slepton exchange via $LQ\bar{D}$ couplings and for a $u\bar{d}$ partonic initial state, the $\lambda'_{k11}\lambda'_{k33}$ combination can be improved by a factor 2 compared with the current limit.

Reference [557] has studied the resonant production of sneutrinos at the LHC via λ'_{ijk} couplings from $pp \to \tilde{\nu}_i \to \tilde{\chi}^{\pm}_1 l_i$, $\tilde{\chi}^{\pm}_1 \to \tilde{\chi}^0_1 l^{\pm}\nu$, $\tilde{\chi}^{\pm}_1 \to l_i u_j \bar{d}_k$, through the tri-lepton signature which has a small SM background and allows mass reconstruction of the full $\tilde{\nu}$ decay chain. This signature can be detected for a broad class of SUSY models and for a wide range of values of several λ'_{ijk} coupling constants. In the framework of the MSUGRA model, for instance, a significant part of the $(m_0, m_{1/2})$ plane will be accessible for $\lambda'_{211} > 0.01$. The same analysis can bring interesting sensitivities on all couplings λ'_{2jk} and test most of the λ'_{1jk} couplings.

In [558] scenarios are studied where the $\tilde{\chi}^0_1$ decays in three quarks (λ''_{ijk}). The final state has no $\not{E}_T$ and a high jet multiplicity. Focusing on $\lambda'_{212} \neq 0$, $\tilde{q}_{\mathrm{L}} \to \tilde{\chi}^0_2 q \to \tilde{l}_{\mathrm{R}} lq \to \tilde{\chi}^0_1 llq$ with $\tilde{\chi}^0_1 \to 3$ jets as the experimentally most difficult case (no particular tag) they show that the $\tilde{\chi}^0_1$ and $\tilde{\chi}^0_2$ masses can be measured by 3-jet and 3-jet+lepton pair invariant mass combinations. A typical MSUGRA point (near SUGRA point 5) with $\lambda'_{212} = 0.005$ is studied in detail and the uncertainties on the $\tilde{\chi}^0_1$, $\tilde{\chi}^0_2$ $\tilde{l}_{\mathrm{R}}$ and $\tilde{q}_{\mathrm{L}}$ masses are given.

It is likely that one should build up a topological analysis identifying channels accessible at the LHC from which one can tell which RPV couplings can be probed.

SUSY with RPV leads to a rich phenomenology at a LC, provided it exists within its energy range. Examples among many others (the LEP program can be reconducted) include

single chargino production $e^+e^- \to \tilde{\chi}_1^{\pm}\mu^{\mp}$ via λ_{121} (with $\tilde{\nu}_{\mu L}$ in s-channel or $\tilde{\nu}_{eL}$ in t-channel). The RPV coupling is probed to a lower value than the existing low energy limits [559]. One can also quote pair production of LSP which decay for instance through λ''_{223} (6 jets signature including 2 b-jets): the signal can be extracted and the LSP mass measured.

16. Connection with GUT scale physics

16.1. Reconstructing electroweak scale MSSM parameters

Once supersymmetric particles would be discovered, the question arises of whether it will be possible to test the assumptions underlying the models and, above all, identify the mechanism of supersymmetry breaking.

A first hint may come from the study of the sparticle decay modes. We have seen that the MSUGRA (missing E_T), GMSB (γ, ...) or RPV (multi-jets, multi-leptons) scenarios each have their specific decay modes, which would allow their identification. But the type of spectra may also provide information on what happens at high energy scales [560], similarly to the unification observed experimentally for the gauge couplings. This might be done by performing a fit of the high scale parameters to the measured quantities. The results of such a fit may, however, be misleading if the model possesses pseudo-fixed point structures or if there are intermediate scales. A more promising approach may be a model independent determination of the fundamental MSSM parameters at the electroweak scale and their extrapolation to the high energy scales by means of their RGEs.

If sufficient measurements are available, it is possible to determine unambiguously the parameters of the SUSY theory. For example [561], at an e^+e^- collider with polarized beams, the measurement of the production cross-sections and left–right asymmetries of $\chi_1^+\chi_1^-$, $\chi_1^+\chi_2^-$ and $\chi_2^+\chi_2^-$ allow the mixing angles between the wino and higgsino components of the left and right chirality charginos to be computed. These, together with the chargino masses, determine the fundamental parameters $\tan\beta$, M_2 and μ of the MSSM. Moreover, the mass of the lightest neutralino (e.g. measured from the decay of the chargino) then allows M_1 to be computed. In lepton colliders with polarized beams, all parameters can be measured even in CP non invariant theories (μ complex).

However, seeing the discovery potential illustrated in figure 143 for the benchmark points, it seems more likely that, before long, only partial information will be available. Cases where less information is available have also been considered [562, 563]. But it is very difficult to design a realistic strategy before at least some of the SUSY particles have been discovered.

Programs reconstructing the SUSY parameters from the sparticle masses have been written. They can cope with partial information to determine the parameters of either constrained models, such as MSUGRA, or of more general MSSM ones.

16.2. Reconstructing high energy scale MSSM parameters

Assuming that the fundamental MSSM parameters $\tan\beta$, M_1, M_2 and μ, together with the slepton and squark masses, have been determined, they may be extrapolated from low energy to the high energy scales by means of their RGEs. This possibility was tested in [565] on an MSUGRA point yielding a rather low mass spectrum, such that all sparticles are observable at the LHC, as well as at a 1 TeV linear collider. Assuming the masses to be determined with the precision quoted in table 28, the evolution of the gaugino mass parameters and of the slepton and squark masses are shown in figure 144. In the two left most figures, the extrapolation is based on the precision achieved by LHC only. The two rightmost figures result from combining the LHC and the linear collider measurements. The gaugino mass

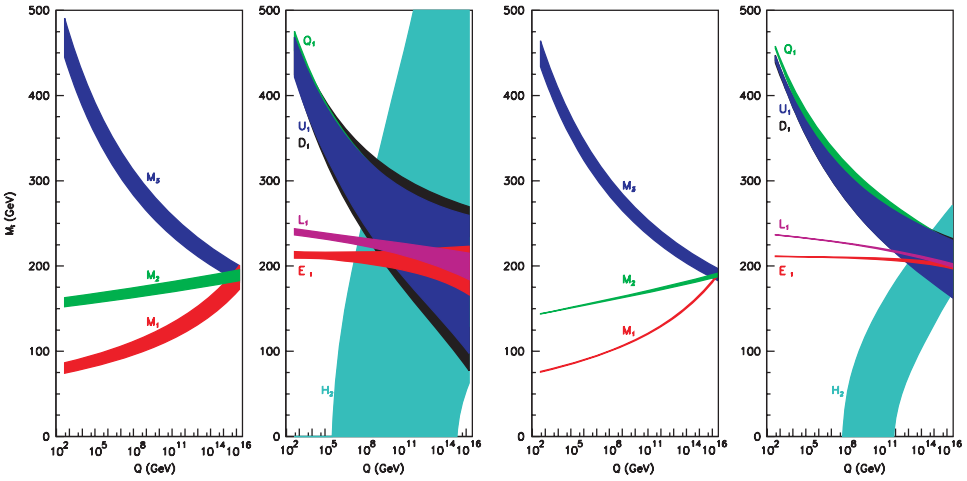

Figure 144. Extrapolation to high energy scales in a MSUGRA scenario. The two left figures are for LHC only, the two right figures are for LHC+LC. Reprinted with permission from [565]. Copyright 2001 by the American Physical Society. For an updated version of the LHC+LC figure, see [566].

parameters meet at the GUT scale, as expected. The value of $m_{1/2}$ is mostly determined by M_1 and M_2, since the uncertainty is much larger for M_3, reflecting the less precise measurement of the gluino mass. In the scalar sector, the mass parameter m_0 is mainly determined by the left and right sleptons. The considerably larger errors on the squark mass extrapolation are due to the large size of the coefficient multiplying $m_{1/2}$ in the approximate equations (90) and which magnify the uncertainty on $m_{1/2}$ in the solution for m_0. The even larger uncertainties in the extrapolation of the Higgs mass parameter m_{H_u} reflect its very weak dependence on m_0 (the 'focus point' behaviour mentioned earlier). In spite of the large uncertainties on some of the extrapolations, it is found in an example of GMSB scenario that the non-universality of the slepton and the squark masses remains clearly observable and would allow the two scenarios to be distinguished. It is, however, clear that the detection of possibly small non-universalities among the gaugino or the scalar masses requires very high precision data at the electroweak scale. This puts very stringent requirements on the measurements but also **highlights the need for further improvements in the calculation of the supersymmetric spectra, compared with the present status of the software**, as noted in section 7.3.

16.3. String effective field theories

In a string effective field theory [567] based on the heterotic string, the expected evolution of the gaugino masses is illustrated in figure 145 of [163]. The model also accounts for the small deviations of the gauge couplings at the GUT scale from their universal value at the string scale. An overall fit to masses and couplings gives the relevant parameters of the model. An exercise has shown that the reconstructed values, starting from quantities measured at colliders, are close to the ideal fundamental parameters.

17. Conclusions

We do not know presently whether supersymmetry has anything to do with reality, nor at which scale it will manifest itself. In spite of its very attractive features, only indirect and not fully conclusive indications exist in favour of light SUSY, such as the accurate convergence of gauge couplings in a supersymmetric scenario. The best one can say is that, because of

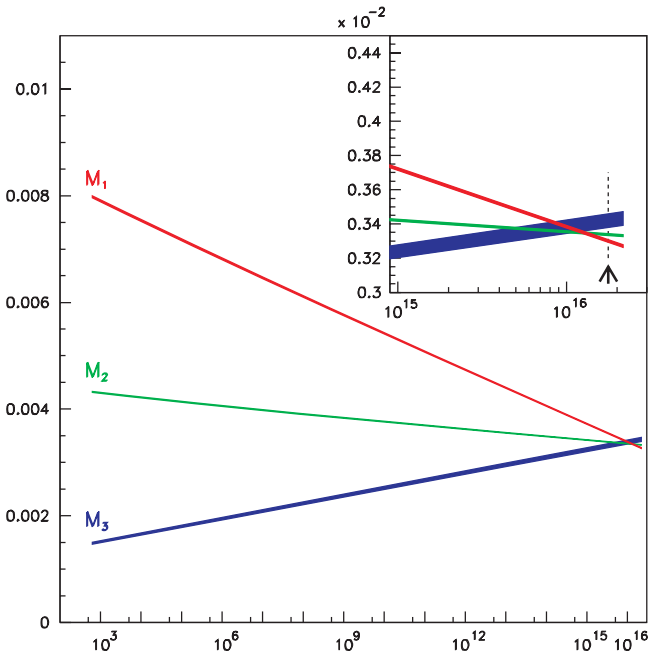

Figure 145. Extrapolation to high energy scales in an effective string scenario. From [163].

its discrete role in electroweak observables, no fact up to now contradicts the existence of a supersymmetric world at or near the electroweak scale. As has been known for a long time, the only outstanding prediction of SUSY, in its minimal version, is the existence of a light and very likely standard model-like h^0 boson. It is deeply regrettable that no resolute strategy was developed at LEP200 to give an answer to this precisely defined question: the answer will be delayed by a decade, waiting for the Tevatron or the LHC, while the MSSM is the overwhelmingly dominant paradigm beyond the standard model in the prospective studies of the LHC, as well as in the arguments put forward in favour of a next linear collider.

Besides this striking feature of the Higgs sector, the non-observation of SUSY partners up to now does not carry any strong message. A general consensus is that the spectrum of these, in order for SUSY to fulfil its main role, should be relatively light and accessible, at least partly, to LHC and a TeV linear collider, if not to the Tevatron. This statement is, however, vague and we have illustrated the large span of possible mass spectra. Some of the spartners can still be 'next door' and within reach of the Tevatron. However, part of them could also be heavy and out of reach of the most energetic machines foreseen.

Some low energy accurate measurements, such as EDM, $(g-2)_\mu$ and rare B decays, can in principle constrain SUSY. However, if deviations are observed, one will still have to wait for the next machines to bring the proof that these are due to SUSY. Also the discovery of a light $h^0 < 130\,\text{GeV}$ is a strong hint for but not a proof of SUSY.

If R-parity is conserved, SUSY offers a quite valuable candidate for cold dark matter, the amount of which is more and more accurately determined through cosmic microwave background studies. LEP exclusion of an LSP neutralino up to several tens of GeV is valid only in a restrictive set of parametrizations. Direct and indirect non-accelerator searches for WIMPS may reveal a signal but cannot lead to a definitive exclusion, because of too many unknowns in the distribution of cold dark matter and its exact nature. At colliders, the LSP provides the most striking signature of missing energy, which should be the way to discover R-parity

conserving SUSY. The hadron colliders should measure crudely the LSP mass, while a LC would provide it accurately.

The Tevatron, LHC and next LC studies have explored in detail a set of predetermined benchmark cases, thought to be representative. One can hope that in the case of SUSY conspicuous signals will appear: missing energy, jacobian peaks in di-lepton distributions, mass peaks of Z^0 and possibly h^0 in the final states. However, the variety of possible scenarios and, within a given class, the variety of possible sparticle spectra and of the corresponding intracascade transitions are such that **a more systematic approach, topology oriented, is probably required as well: this implies that for a set of final states as large as possible, the SM expectation as well as the various procedures, from trigger to analysis, are well mastered, so that one can reliably detect any discrepancy**.

The LHC has an excellent discovery potential for squarks and gluinos, up to about 2.5 TeV. For neutralinos, charginos and sleptons the reach is ∼0.5 TeV. An inspection of the various constrained MSUGRA benchmark points shows that LHC, besides the lightest Higgs boson, will generally detect a substantial number of supersymmetric particles, except in a few cases corresponding to the focus point region or to extreme cases allowed by the relic density constraints.

A TeV-scale linear collider has globally a more limited reach but may detect more sleptons and gauginos, complementing the LHC information, and especially it will provide a greater precision in the measurement of sparticle masses, decays and properties within its range of accessibility. This high precision will be crucial for the reconstruction of the underlying model and the identification of the SUSY breaking mechanism. The role of a multi-TeV collider like CLIC would be either to discover SUSY in the most problematic cases or to complete the spectrum and extend the accurate measurements, made at LHC and a TeV linear collider, to squarks and heavier sparticles. A $\gamma\gamma$ collider can also bring complementary information, for instance on gluino mass and couplings, which will be difficult to get in e^+e^- collisions, and on Higgs bosons of the MSSM which it can produce in the s-channel.

Acknowledgments

We are grateful to G F Giudice and F Zwirner for their comments and suggestions on the manuscript. We also thank G Dissertori, F Moortgat and F Pauss for their advice and encouragement.

References

[1] Martin S P 1998 *Perspectives in Supersymmetry* ed G Kane (Singapore: World Scientific) *Preprint* hep-ph/9709356

[2] Some lecture notes and reviews are listed here:
Raby S 2004 Desperately seeking Supersymmetry [SUSY] *Rep. Prog. Phys.* **67** 755 *Preprint* hep-ph/0411155
Chung D J H, Everett L L, Kane G L, King S F, Lykken J and Wang L-T 2005 The soft supersymmetry breaking Lagrangian: theory and applications *Phys. Rep.* **407** 1 *Preprint* hep-ph/0312378
Haber H E 2004 Review of particle physics *Phys. Lett.* B **592** 1003
Ellis J 2002 Limits of the Standard Model. Lectures given at *PSI Zuoz Summer School, Zuoz (Engadin, Switzerland, 18–24 August 2002*) *Preprint* hep-ph/0211168
Ellis J 2001 Supersymmetry for Alp hikers, Lectures given at *European School of High-Energy Physics (ESHEP 2001) (Beatenberg, Switzerland, 26 August–8 September 2001) Preprint* hep-ph/0203114
Gianotti F 2002 Searches for supersymmetry at high-energy colliders: the past, the present and the future *New J. Phys.* **4** 63.1
Murayama H 1999 *Supersymmetry Phenomenology*, UCB-PTH-00-05, LBNL-45321, Prepared for *ICTP Summer School in Particle Physics (Trieste, Italy, 21 Jun-9 Jul 1999) Preprint* hep-ph/0002232
Mohapatra R N 1999 Supersymmetric Grand Unification: an update, lectures given at *ICTP Summer School in Particle Physics (Trieste, Italy, 7 Jun-9 Jul 1999)* published in *Trieste 1999, Particle physics *Preprint* hep-ph/9911272

Zwirner F 1998 Beyond the Standard Model *1997 European School of High Energy Physics* ed N Ellis and M Neubert CERN 98-03
Gunion J F 1997 Searching for low-energy Supersymmetry *Proc. Int. Workshop on Quantum Effects in the Minimal Supersymmetric Standard Model (Barcelona, Spain, 9–13 September 1997)* ed J Sola (Singapore: World Scientific) *Preprint* hep-ph/9801417
Peskin M E 1996 Beyond the Standard Model. Lectures given at *The 1996 European School of High-Energy Physics (Carry-le-Rouet, France, 1–14 September 1996) Preprint* hep-ph/9705479
Dawson S 1997 The MSSM and why it works. Talk given at *Theoretical Advanced Study Institute (TASI 96) (Boulder, CO, 1–7 June 1997) Preprint* hep-ph/9712464
Arnowitt R and Nath P Perspectives on supersymmetry *Supergravity Unified Models* ed G L Kane *Preprint* hep-ph/9708254
Tata X 1997 *IX J.A.* Swieca Summer School *Preprint* hep-ph/9706307
Lykken J D 1996 Introduction to Supersymmetry. Talk given at *Theoretical Advanced Study Institute (TASI 97) (Boulder, CO, 2–28 June 1996) Preprint* hep-th/9612114
Drees M 1996 *An Introduction to Supersymmetry* APCTP-96-05, KEK-TH-501 *Preprint* hep-ph/9611409
Bagger J A 1995 *Weak-scale Supersymmetry: theory and practice*, prepared for *Theoretical Advanced Study Institute (TASI 95) (Boulder, CO, 4–30 June 1995) Preprint* hep-ph/9604232
Ramond P 1994 *Introductory lectures on low-energy Supersymmetry* prepared for *Theoretical Advanced Study Institute (TASI 94) (Boulder, CO) Preprint* hep-th/9412234
de Boer W 1994 Grand unified theories and supersymmetry in particle physics and cosmology *Prog. Part. Nucl. Phys.* **33** 201 *Preprint* hep-ph/9402266
Haber H E 1992 *Introductory low energy Supersymmetry* presented at *Theoretical Advanced Study Institute (TASI 92) (Boulder, CO, 3–28 June 1992) Preprint* hep-ph/9306207
Barbieri R 1988 *Riv. Nuovo Cimento* **11** 1
Sohnius M 1985 Introducing supersymmetry *Phys. Rep.* C **128** 39
Haber H E and Kane G L 1985 The search for supersymmetry: probing physics beyond the standard model *Phys. Rep.* C **117** 75
Nilles H P 1984 *Phys. Rep.* C **110** 1
Fayet P and Ferrara S 1977 *Phys. Rep.* C **32** 249
[3] Glashow S L 1961 *Nucl. Phys.* **22** 579
Weinberg S 1967 *Phys. Rev. Lett.* **19** 1264
Salam A 1968 *Proc. 8th Nobel Symp. (Stockholm 1968)* ed N Svartholm (Stockholm: Almqvist and Wiksells)
[4] Wilczek F 2001 Future summary *Int. J. Mod. Phys.* A **16** 1653
Wilczek F 2001 Future summary *Int. J. Mod. Phys.* A **16S1A** 129 *Preprint* hep-ph/0101187
[5] Wilczek F 2000 QCD made simple *Phys. Today*
[6] Englert F and Brout R 1964 *Phys. Rev.* **13** 321
Higgs P W B 1964 *Phys. Lett.* **12** 132
Kibble T W B 1964 *Phys. Rev.* **13** 585
[7] Veltman M 1977 *Acta Phys. Pol.* **8** 475
Veltman M 1977 *Nucl. Phys.* B **123** 89
Chanowitz M S, Furman M and Hinchliffe I 1978 *Phys. Lett.* B **78** 285
[8] Quigg C 1997 Top-ology *Phys. Today* **50N5** 20 *Preprint* hep-ph/9704332
Quigg C 2004 *Preprint* hep-ph/0404228, FERMILAB-CONF-04-049-T
[9] Witten E 1996 *Reflections on the fate of spacetime Phys. Today*
[10] Greene B 1999 *The Elegant Universe* (New York and London: Norton W W & Company)
[11] Schwarz J H 2000 *Introduction to Superstring Theory* CALT-68-2293, CITUSC/00-045 *Preprint* hep-ex/0008017
[12] Wess J and Zumino B 1974 *Nucl. Phys.* B **70** 39
Wess J and Zumino B 1974 *Nucl. Phys.* B **78** 1
Volkov D V and Akulov V P 1973 *Phys. Lett.* B **46** 109
Gol'fand Yu A and Likhtman E P 1971 *JETP Lett.* **13** 323
[13] Fayet P 1975 *Nucl. Phys.* B **90** 104
Fayet P 1976 *Phys. Lett.* B **64** 159
Fayet P 1977 *Phys. Lett.* B **69** 489
Fayet P 1979 *Phys. Lett.* B **84** 416
[14] Girardello L and Grisaru M T 1982 *Nucl. Phys.* B **194** 65
[15] Ferrara S, Freedman D Z and van Nieuwenhuizen P 1976 *Phys. Rev.* D **13** 3214
Deser S and Zumino B 1976 *Phys. Lett.* B **62** 335

Freedman D Z and van Nieuwenhuizen P 1976 *Phys. Rev.* D **14** 912
Cremmer E, Julia B, Scherk J, Ferrara S, Girardello L and van Nieuwenhuizen P 1979 *Nucl. Phys.* B **147** 105
Bagger J 1983 *Nucl. Phys.* B **211** 302
Cremmer E, Ferrara S, Girardello L and van Proeyen A 1983 *Nucl. Phys.* B **212** 413
For a review, see Nilles H P 1984 *Phys. Rep.* **110** 1
[16] Chamseddine A H, Arnowitt R and Nath P 1982 *Phys. Rev. Lett.* **49** 970
Ibañez L E 1982 *Phys. Lett.* B **118** 73
Barbieri R, Ferrara S and Savoy C A 1982 *Phys. Lett.* B **119** 343
Nilles H P, Srednicki M and Wyler D 1983 *Phys. Lett.* B **120** 346
Ellis J, Nanopoulos D V and Tamvakis K 1983 *Phys. Lett.* B **121** 123
Cremmer E, Fayet P and Girardello L 1983 *Phys. Lett.* B **122** 41
Alvarez-Gaumé L, Polchinski J and Wise M 1983 *Nucl. Phys.* B **221** 495
Hall L J, Lykken J and Weinberg S 1983 *Phys. Rev.* D **27** 2359
[17] Georgi H, Quinn H R and Weinberg S 1974 *Phys. Rev. Lett.* **33** 451
[18] Ellis J, Kelley S and Nanopoulos D V 1991 *Phys. Lett.* B **260** 131
Amaldi U, de Boer W and Fürstenau H 1991 *Phys. Lett.* B **260** 447
Langacker P and Luo M 1991 *Phys. Rev.* D **44** 817
Giunti C, Kim C W and Lee W W 1991 *Mod. Phys. Lett.* A **6** 1745
[19] Ibáñez L E and Ross G G 1982 *Phys. Lett.* B **110** 215
Inoue K, Kakuto A, Komatsu H and Yakeshita S 1984 *Prog. Theor. Phys.* **68** 927
Inoue K, Kakuto A, Komatsu H and Yakeshita S 1984 *Prog. Theor. Phys.* **71** 413
Alvarez-Gaumé L, Claudson M and Wise M 1982 *Nucl. Phys.* B **207** 96
Ellis J, Nanopoulos D V and Tamvakis K 1983 *Phys. Lett.* B **121** 123
[20] Ibáñez L E and Ross G G 1993 *Perspectives in Higgs Physics* ed G Kane (Singapore: World Scientific) *Preprint* hep-ph/9204201
[21] Diaz-Cruz J L and Mandez A 1992 *Nucl. Phys.* B **380** 39
[22] Farrar G and Fayet P 1978 *Phys. Lett.* B **76** 575
[23] Goldberg H 1983 *Phys. Rev. Lett.* **50** 1419
Ellis J, Hagelin J S, Nanopoulos D V, Olive K and Srednicki M 1984 *Nucl. Phys.* B **238** 453
Wolfram S 1979 *Phys. Lett.* B **82** 65
[24] Nobbenhuis S *Class. Quant. Grav.* submitted *Preprint* gr-qc/0411093
[25] Arkani-Hamed N and Dimopoulos S 2004 *Preprint* hep-th/0405159
Giudice G F and Romanino A 2004 *Nucl. Phys.* B **699** 65 *Preprint* hep-ph/0406088
Arkani-Hamed N, Dimopoulos S, Giudice G F and Romanino A 2004 *Preprint* hep-ph/0409232
[26] Barbier R *et al Phys. Rep.* submitted *Preprint* hep-ph/0406039
[27] Cheung K and Chiang C-W 2005 *Preprint* hep-ph/0501265 v2
[28] Herrero M J 1995 Talk given at *23rd Int. Meeting on Fundamental Physics: The Top Quark, Heavy Flavor Physics and Symmetry Breaking (Comillas, Spain, 22–26 May 1995) Preprint* hep-ph/9601286
[29] Barklow T L *et al* 2001 *SNOWMASS-2001-P350,eConf C010630* P1WG4
Barklow T L *et al* 2001 *eConf C010630* P350 *Preprint* hep-ph/0201243
[30] Dobado A, Herrero M J, Pelaez J R, Ruiz Morales E and Urdiales M T 1995 *Phys. Lett.* B **352** 400 *Preprint* hep-ph/9502309
[31] Han T 1996 *Strong W W Scattering Physics: A Comparative Study for the LHC, NLC and a Muon Collider* talk given at *Ringberg Workshop (Ringberg, Germany, 8–13 December 1996) Preprint* hep-ph/9704215
[32] Barklow T L 2001 *eConf C010630* E3067 *Preprint* hep-ph/0112286
[33] Dominici D 2001 *eConf C010630*P329
Dominici D 2001 *SNOWMASS-2001-P329 (October 2001)*
Dominici D 2001 *eConf C010630* P329 *Preprint* hep-ph/0110084
[34] Lane K 2002 *FERMILAB-PUB-02-040-T, BUHEP-02-15 Preprint* hep-ph/0202255
[35] Hill C T and Simmons E H 2003 *Phys. Rep.* **381** 235 (0203079)
[36] Weinberg S 1979 *Phys. Rev.* D **19** 1277
Susskind L 1979 *Phys. Rev.* D **20** 2619
[37] Cuevas J 2001 *7th Topical Seminar on the legacy of LEP and SLC (Siena, October 2001)*
Cuevas J 2002 *Nucl. Phys.* B **109** 256
[38] Antoniadis I 1990 *Phys. Lett.* B **246** 377
[39] Lykken J D 2005 Phenomenology Beyond the Standard Model *Preprint* hep-ph/0503148
Hewett J and Spiropulu M 2002 *Annu. Rev. Nucl. Part. Phys.* **52** 397 *Preprint* hep-ph/0205106
Hewett J and Sadri D 2002 *SLAC-PUB-9608 Preprint* hep-ph/0212111

Cheung K 2000 *Preprint* hep-ph/0003306
[40] Pasztor G and Rizzo Th G 2001 Report of the Snowmass Subgroup on extra dimensions *Snowmass 2001, eConf C010630* P333 *Preprint* hep-ph/0112054
[41] Uehara Y 2002 *Mod. Phys. Lett.* A **17** 1551 *Preprint* hep-ph/0203244
[42] Arkani-Hamed N, Dimopoulos S and Dvali G 1998 *Phys. Lett.* B **429** 263 *Preprint* hep-ph/9807344
[43] Randall L and Sundrum R 1999 *Phys. Rev. Lett.* **83** 3370 *Preprint* hep-th/9905221
Randall L and Sundrum R 1999 *Phys. Rev. Lett.* **83** 4690 *Preprint* hep-th/9906064
[44] Hannestad S and Raffelt G G 2003 *Phys. Rev.* D **67** 125008 *Preprint* hep-ph/0304029
[45] Giudice G F and Strumia A 2003 *Nucl. Phys.* B **663** 377 *Preprint* hep-ph/0301232
[46] Appelquist T, Cheng H and Dobrescu B 2001 *Phys. Rev.* D **64** 035002 *Preprint* hep-ph/0012100
[47] Cheng H-C, Matchev K T and Schmaltz M 2002 *Phys. Rev.* D **66** 056006 *Preprint* hep-ph/0205314
[48] Cheung K 2001 *Phys. Rev.* D **63** 056007 *Preprint* hep-ph/0009232
[49] Azuelos G, Cavalli D, Przysiezniak H and Vacavant L 2002 ATLAS Collaboration *Eur. Phys. J. Direct* C **4** 16
[50] Rizzo Th G 2002 *SLAC-PUB-9492Preprint* hep-ph/0209076
[51] Giudice G F, Plehn T and Strumia A 2005 *Nucl. Phys.* B **706** 455 *Preprint* hep-ph/0408320
[52] Hoyle C D, Kapner D J, Heckel B R, Adelberger E G, Gundlach J H, Schmidt U and Swanson H E 2004 *Phys. Rev.* D **70** 042004 *Preprint* hep-ph/0405262
Long J C, Chan H W, Churnside A B, Gulbis E A, Varney M C M and Price J C 2003 *Nature* **421** 922
Decca R S, Fischbach E, Klimchitskaya G L, Krause D E, D.López and Mostepanenko V M 2003 *Phys. Rev.* D **68** 116003 *Preprint* hep-ph/0310157
Lamoreaux S K 1997 *Phys. Rev. Lett.* **78** 5
Lamoreaux S K 1998 *Phys. Rev. Lett.* **81** 5475 (erratum)
[53] Dimopoulos S and Geraci A A 2003 *Phys. Rev.* D **68** 124021 *Preprint* hep-ph/0306168
[54] Abele H, Baessler S and Westphal A 2003 *Lect. Notes Phys.* **631** 355–66 *Preprint* hep-ph/0301145
[55] Barbieri R and Strumia A 2000 *Preprint* hep-ph/0007265
Strumia A 1999 *Preprint* hep-ph/9904247
[56] Barbieri R, Hall L and Nomura Y 2001 *Phys. Rev.* D **63** 105007 *Preprint* hep-ph/0011311
[57] Barbieri R, Marandella G and Papucci M 2002 *Phys. Rev.* D **66** 095003 *Preprint* hep-ph/0205280
[58] Arkani-Hamed N, Cohen A G, Gregoire T and Wacker J G 2002 *J. High Energy Phys.* JHEP0208 020 *Preprint* hep-ph/0202089
Arkani-Hamed N, Cohen A G, Katz E and Nelson A E 2002 *J. High Energy Phys.* JHEP07 034 *Preprint* hep-ph/0206021
Wacker J G 2002 *Proc. 31st Int. Conf. on High Energy Physics (ICHEP 2002) (Amsterdam, 24–31 July 2002) Preprint* hep-ph/0208235
[59] Burdman G, Perelstein M and Pierce A 2003 *Phys. Rev. Lett.* **90** 241802 *Preprint* hep-ph/0212228
[60] Dib C, Rosenfeld R and Zerwekh A 2003 *Preprint* hep-ph/0302068
[61] Hewett J L, Petriello F J and Rizzo T G 2003 *J. High Energy Phys.* JHEP0310 062 *Preprint* hep-ph/0211218
Csaki C, Hubisz J, Kribs G D, Meade P and Terning J 2003 *Phys. Rev.* D **67** 115002 *Preprint* hep-ph/0211124
Kribs G D *Preprint* hep-ph/0305157
[62] Deandrea A 2004 Talk given at *39th Rencontres de Moriond on Electroweak Interactions and Unified Theories (La Thuile, Aosta Valley, Italy, 21–28 March 2004) Preprint* hep-ph/0405120
[63] Logan H E 2004 *Eur. Phys. J.* C **33** S729 *Preprint* hep-ph/0310151
[64] Perelstein M, Peskin M E and Pierce A 2004 *Phys. Rev.* D **69** 075002 *Preprint* hep-ph/0310039
[65] Murayama H 2003 *Preprint* hep-ph/0307293
[66] Harnik R, Kribs G D, Larson D T and Murayama H 2004 *Phys. Rev.* D **70** 015002 *Preprint* hep-ph/0311349
[67] Dicus D A and Mathur V S 1973 *Phys. Rev.* D **7** 3111
Lee B W, Quigg C and Thacker H 1977 *Phys. Rev.* D **16** 1519
see also:
Marciano W, Valencia G and Willenbrock S 1989 *Phys. Rev.* D **40** 1725
Sirkka J and Vilja I 1993 *Phys. Lett.* B **316** 355–9 *Preprint* hep-ph/9307334
[68] Drees M 1996 *An Introduction to Supersymmetry*, APCTP-96-05, KEK-TH-501 *Preprint* hep-ph/9611409
[69] Murayama H 1999 *Supersymmetry Phenomenology* UCB-PTH-00-05, LBNL-45321. Prepared for *ICTP Summer School in Particle Physics (Trieste, Italy, 21 June–9 July 1999) Preprint* hep-ph/0002232
[70] Haber H E, *Supersymmetry* ed Hagiwara K *et al*
Haber H E 2002 Particle data group *Phys. Rev.* D **66** 010001 (http://pdg.lbl.gov/)
[71] Abel S *et al* 2000 *Report of the SUGRA Working Group for Run II of the Tevatron Preprint* hep-ph/0003154
[72] Giudice G F and Masiero A 1988 *Phys. Rev. Lett.* **206** 480

[73] Bastero-Gil M, Hugonie C, King S F, Roy D P and Vempati S 2000 *Phys. Lett.* B **489** 359 *Preprint* hep-ph/0006198
[74] Miller D J 2002 *2nd Workshop of the Extended ECFA/DESY Study (St Malo, April 2002)* www.desy.de/∼desch/higgs/stmalo/miller.ps
[75] Miller D J, Nevzorov R and Zerwas P M 2004 *Nucl. Phys.* B **681** 3 *Preprint* hep-ph/0304049
[76] Dimopoulos S and Sutter D 1995 *Nucl. Phys.* B **452** 496
[77] Haber H E 1998 *Nucl. Phys.* B **62** A–C 469
[78] Diaz M A 1997 *Preprint* hep-ph/9711435
[79] Porod W, Hirsch M, Romão J and Valle J W F 2001 *Phys. Rev.* D **63** 115004 *Preprint* hep-ph/0011248
Hirsch M, Porod W, Valle J W F, Díaz M A and Romão J C 2002 *Phys. Rev.* D **66** 095006 *Preprint* hep-ph/0207334
Díaz M A, Hirsch M, Porod W, Valle J W F and Romão J C 2003 *Phys. Rev.* D **68** 013009 *Preprint* hep-ph/0302021
[80] Hirsch M, Porod W, Valle J W F, Díaz M A and Romão J C 2000 *Preprint* hep-ph/0009127
Abada A, Bhattacharya G and Losada M 2002 *Phys. Rev.* D **66** 071701 *Preprint* hep-ph/0208009
[81] Georgi H and Glashow S L 1974 *Phys. Rev. Lett.* **32** 438
[82] Ward D R 2001 *Siena Workshop (October 2001)*
[83] Hinchliffe I 2004 Quantum chromodynamics *Review of Particle Physics*
Hinchliffe I 2004 *Phys. Lett.* B **592** 1 http://pdg.lbl.gov/
[84] Erler J and Langacker P 2004 Electroweak model and constraints on new physics *Review of Particle Physics*
Erler J and Langacker P 2004 *Phys. Lett.* B **592** 1 http://pdg.lbl.gov/
[85] Mattig P 2003 *38th Rencontres de Moriond on QCD and High-Energy Hadronic Interactions (Les Arcs, Savoie, France, 22–29 March 2003) Preprint* hep-ex/0312033
Neubert M 2002 *37th Rencontres de Moriond on QCD and Hadronic Interactions (Les Arcs, France, 16–23 March 2002) Preprint* hep-ph/0207357
[86] Amaldi U, Böhm A, Durkin L S, Langacker P, Mann A K, Marciano W J, Sirlin A and Williams H H 1987 *Phys. Rev.* D **36** 1385
[87] de Boer W 1998 *Search for SUSY and Higgs Particles* talk at *XVIII Phys. in Coll. (Frascati, 1998)*
[88] Raby S *Grand Unified Theories*
Hagiwara K *et al* 2002 Particle data group *Phys. Rev.* D **66** 010001 http://pdg.lbl.gov/
[89] Langacker P and Polonsky N 1995 *Phys. Rev.* D **52** 3081 *Preprint* hep-ph/9503214
Langacker P and Erler J 1997 *Preprint* hep-ph/9703428
[90] Anderson G, Chen C H, Gunion J F, Lykken J, Moroi T and Yamada Y 1996 *eConf C960625* SUP107 *Preprint* hep-ph/9609457
[91] Casas J A, Espinosa J R, Ibarra A and Navarro I 2001 *Phys. Rev.* D **63** 97302 *Preprint* hep-ph/0004166
Kowalska K 2002 *Acta Phys. Polon.* B **33** 1823 *Preprint* hep-ph/0203168
[92] Amaldi U, de Boer W, Frampton P H, Fürstenau H and Liu J T 1992 *Phys. Lett.* B **281** 374
[93] Dawson S and Georgi H 1979 *Phys. Rev. Lett.* **43** 821
Einhorn M B and Jones D R T 1982 *Nucl. Phys.* B **196** 475
[94] Mohapatra R N and Parida M K 1993 *Phys. Rev.* D **47** 264
Lee D G, Mohapatra R N, Parida M K and Rani M 1995 *Phys. Rev.* D **51** 229
[95] Dienes K R, Dudas E and Gherghetta T 1998 *Phys. Lett.* B **436** 55 *Preprint* hep-ph/9803466
Dienes K R, Dudas E and Gherghetta T 1999 *Nucl. Phys.* B **537** 47 *Preprint* hep-ph/9806292
[96] Carena M, Delgado A, Ponton E, Tait T M P and Wagner C E M 2003 *Phys. Rev.* D **68** 035010 *Preprint* hep-ph/0305188
[97] Ma E 2004 *5th Latin American Symp. on High Energy Physics (V-SILAFAE) (Lima, Peru, 12–17 July 2004) Preprint* hep-ph/0410023
[98] Pati J and Salam A 1973 *Phys. Rev.* D **8** 1240
[99] Barbieri R, Dvali G and Moretti M 1993 *Phys. Lett.* B **312** 137
[100] Dimopoulos S and Georgi H 1981 *Nucl. Phys.* B **193** 150
Sakai N 1981 *Z. Phys.* C **11** 153
[101] Georgi H and Jarlskog C 1979 *Phys. Lett.* B **86** 297
[102] Barr S M 1982 *Phys. Lett.* B **112** 219
[103] Georgi H 1974 *Proc. American Institute of Physics* ed C Carlson
Fritzsch H and Minkowski P 1975 *Ann. Phys.* **93** 173
Gell-Mann M, Ramond P and Slansky R 1978 *Rev. Mod. Phys.* **50** 721
For a review, see Mohapatra R 1999 *Preprint* hep-ph 9911272
[104] Pierce D M, Bagger J A, Matchev K T and Zhang R-J 1997 *Nucl. Phys.* B **491** 3 *Preprint* hep-ph/9606211

[105] Chattopadhyay U, Corsetti A and Nath P 2002 *Preprint* hep-ph/0204251
[106] Raby S 2002 *Preprint* hep-ph/0211025
Blažek T, Dermišek R and Raby S 2002 *Phys. Rev.* D **65** 115004 *Preprint* hep-ph/0201081
[107] Zwirner F 1998 Beyond the Standard Model *1997 European School of High Energy Physics* ed N Ellis and M Neubert, CERN 98-03
[108] Deser S and Zumino B 1977 *Phys. Rev. Lett.* **38** 1433
[109] Dine M and Nelson A E 1993 *Phys. Rev.* D **48** 1277
Dine M, Nelson A E and Shirman Y 1995 *Phys. Rev.* D **51** 1362
Dine M, Nelson A E, Nir Y and Shirman Y 1996 *Phys. Rev.* D **53** 2658
[110] Giudice G F, Luty M A, Murayama H and Rattazzi R 1998 *J. High Energy Phys.* JHEP12027 *Preprint* hep-ph/9810442
[111] Randall L and Sundrum R 1999 *Nucl. Phys.* B **557** 79 *Preprint* hep-th/9810155
[112] Boyda E, Murayama H and Pierce A 2002 *Phys. Rev.* D **65** 085028 *Preprint* hep-ph/0107255
[113] Nelson B D 2002 *Preprint* hep-ph/0211087
[114] Zwirner F 2002 Supersymmetry breaking with extra dimensions *Acta Phys. Pol.* B **33** 2463
[115] Scherk J and Schwarz J H 1979 *Phys. Lett.* B **82** 60
[116] Quiros M 2003 *Preprint* hep-ph/0302189
[117] Brignole A, Ibáñez L E and Muñoz C 1997 *Perspectives on Supersymmetry* ed G L Kane (Singapore: World Scientific) *Preprint* hep-ph/9707209
[118] Horava P and Witten E 1996 *Nucl. Phys.* B **460** 506 *Preprint* hep-th/9510209
[119] King S F and Rayner D A J 2002 *Preprint* hep-ph/0211242
[120] Giudice G F 2004 Theoretical predictions for collider searches *Int. J. Mod. Phys.* A **19** 835 *Preprint* hep-ph/0311344
[121] Csaki C, Grojean C, Murayama H, Pilo L and Terning J 2004 *Phys. Rev.* D **69** 055006 *Preprint* hep-ph/0305237
Hall L J and Nomura Y 2003 *Ann. Phys.* **306** 132 *Preprint* hep-ph/0212134
[122] Brignole A, Casas J A, Espinosa J R and Navarro I 2003 *Nucl. Phys.* B **666** 105 *Preprint* hep-ph/0301121
[123] Lopez J L and Nanopoulos D V 1996 *Int. J. Mod. Phys.* A **11** 3439 *Preprint* hep-ph/9412332
Lopez J L 1996 Supersymmetry: from the fermi scale to the Planck scale *Rep. Prog. Phys.* **59** 819 *Preprint* hep-ph/9601208
[124] Lopez J L, Nanopoulos D V and Zichichi A 1995 *Phys. Rev.* D **52** 4178 *Preprint* hep-ph/9502414
[125] Li T-J, Lopez J L and Nanopoulos D V 1997 *Mod. Phys. Lett.* A **12** 2647 *Preprint* hep-ph/9702237
[126] Komine S and Yamaguchi M 2001 *Phys. Rev.* D **63** 035005 *Preprint* hep-ph/0007327
[127] Komine S 2001 TU-610 *Preprint* hep-ph/0102030
[128] Kaplunovsky V S and Louis J 1993 *Phys. Lett.* B **306** 269
[129] Barbieri R, Louis J and Moretti M 1993 *Phys. Lett.* B **312** 451
[130] Casas J A, Lleyda A and Muñoz C 1996 *Phys. Lett.* B **380** 59
Casas J A, Lleyda A and Muñoz C 1996 *Phys. Lett.* **389** 305
Abel S A, Allanach B C, Quevedo F, Ibáñez L and Klein M 2000 *J. High Energy Phys.* JHEP0012026 *Preprint* hep-ph/0005260
[131] Giudice G F and Rattazzi R 1999 *Phys. Rep.* **322** 419 *Preprint* hep-ph/9801271
[132] Bartl A, Hesselbach S, Hidaka K, Kernreiter T and Porod W 2003 Contribution to *the extended joint ECFA/DESY Study on Physics and Detectors for a Linear Electron-Positron Collider Preprint* hep-ph/0306281
Bartl A and Hesselbach S 2004 *Preprint* hep-ph/0410237
[133] Baer H, Paige F E, Protopopescu S D and Tata X 2003 *Isajet 7.69: A Monte Carlo Event Generator for pp, $\bar{p}p$ and e^+e^- Reactions*, *Preprint* hep-ph/0312045 *Isajet 7.69* in http://paige.home.cern.ch/paige
[134] Carena M, Olechowski M, Pokorski S and Wagner C E M 1994 *Nucl. Phys.* B **426** 269 *Preprint* hep-ph/9402253
Drees M and Martin S P 1995 *Preprint* hep-ph/9504324
[135] Hill C T 1981 *Phys. Rev.* D **24** 691
Ibáñez L and Lopez C 1984 *Nucl. Phys.* B **233** 511
Hill C T, Leung C N and Rao S 1985 *Nucl. Phys.* B **262** 517
[136] Barger V, Berger M S and Ohmann P 1993 *Phys. Rev.* D **47** 1093
Barger V, Berger M S, Ohmann P and Phillips R J N *Phys. Lett.* B **314** 351
Bardeen W A, Carena M, Pokorski S and Wagner C E M 1994 *Phys. Lett.* B **320** 110 *Preprint* hep-ph/9309293
[137] Carena M and Wagner C E M 1995 *Nucl. Phys.* B **452** 45 *Preprint* hep-ph/9408253
[138] Jurčišin M and Kazakov D I 1999 *Mod. Phys. Lett.* A **14** 671 *Preprint* hep-ph/9902290
[139] Feng J L, Matchev K T and Moroi T 2000 *Phys. Rev. Lett.* **84** 2322 *Preprint* hep-ph/9908309
Feng J L, Matchev K T and Moroi T 2000 *Phys. Rev.* D **61** 075005 *Preprint* hep-ph/9909334
[140] Feng J L, Matchev K T and Wilczek F 2000 *Phys. Lett.* B **482** 388 *Preprint* hep-ph/0004043

Feng J L, Matchev K T and Wilczek F 2001 *Phys. Rev.* D **63** 045024 *Preprint* astro-ph/0008115
[141] Feng J L and Matchev K T 2001 *Phys. Rev.* D **63** 095003 *Preprint* hep-ph/0011356
[142] Ellis J, Enqvist K, Nanopoulos D V and Zwirner F 1986 *Mod. Phys. Lett.* A **1** 57
Barbieri R and Giudice G F 1988 *Nucl. Phys.* B **306** 63
[143] Battaglia M, De Roeck A, Ellis J, Gianotti F, Matchev K T, Olive K A, Pape L and Wilson G 2001 *Eur. Phys. J.* C **22** 535 *Preprint* hep-ph/0106204
[144] Kane G L, Lykken J, Nelson B D and Wang L-T 2003 *Phys. Lett.* B **551** 146 *Preprint* hep-ph/0207168
[145] Chankowski P H, Ellis J R, Olechowski M and Pokorski S 1999 *Nucl. Phys.* B **544** 39 *Preprint* hep-ph/9808275
[146] Hewett J L, Lillie B, Masip M and Rizzo T G 2004 *J. High Energy Phys.* JHEP0409 070 *Preprint* hep-ph/0408248
[147] Smith P F, Bennet J R J, Homer G J, Lewin J D, Walford H E and Smith W A 1982 *Nucl. Phys.* B **206** 333
Hemmick T K *et al* 1990 *Phys. Rev.* D **41** 2074
[148] Kilian W, Plehn T, Richardson P and Schmidt E 2004 *Preprint* hep-ph/0408088
[149] Gunion J F 1998 UCD-98-17 *Preprint* hep-ph/9810394
[150] Choi S Y, Kalinowski J, Moortgat-Pick G and Zerwas P M 2001 *Eur. Phys. J.* C **22** 563 *Preprint* hep-ph/0108117
[151] Alderweireld T 2002 *Thesis*
[152] Ellis J R, Falk T, Ganis G, Olive K A and Schmitt M 1998 *Phys. Rev.* D **58** 095002 *Preprint* hep-ph/9801445
[153] Pierce D and Papadopoulos A 1994 *Nucl. Phys.* B **430** 278 *Preprint* hep-ph/9403240
[154] Choi S Y, Miller D J and Zerwas P M 2005 *Nucl. Phys.* B **711** 83 *Preprint* hep-ph/0407209
[155] Ellwanger U, Gunion J F and Hugonie C 2004 *Preprint* hep-ph/0406215
[156] Djouadi A, Kneur J-L and Moultaka G 2002 *SuSpect: A Fortran Code for the Supersymmetric and Higgs Particle Spectrum in the MSSM*, *Preprint* hep-ph/0211331 http://www.lpm.univ-montp2.fr/ kneur/suspect.html
[157] Martin S P and Ramond P 1993 *Phys. Rev.* D **48** 5365
[158] Yamada Y 1996 *Phys. Rev.* D **54** 1150 *Preprint* hep-ph/9602279
[159] Kolda C and Martin S P 1996 *Phys. Rev.* D **53** 3871 *Preprint* hep-ph/9503445
[160] Baer H, Brhlik M, Diaz M A, Ferrandis J, Mercadante P, Quintana P and Tata X 2001 *Phys. Rev.* D **63** 015007 *Preprint* hep-ph/0005027
[161] Baer H and Ferrandis J 2001 *Phys. Rev. Lett.* **87** 211803-1 *Preprint* hep-ph/0106352
[162] Bagger J A, Feng J L, Polonsky N and Zhang R-J 2000 *Phys. Lett.* B **473** 264 *Preprint* hep-ph/9911255
[163] Zerwas P M, Kalinowski J, Freitas A, Blair G A, Choi S Y, Martyn H U, Moortgat-Pick G and Porod W 2002 *Preprint* hep-ph/0211076
[164] Allanach B C *et al* 2002 The snowmass points and slopes: benchmarks for SUSY searches *Eur. Phys. J.* C **25** 113
Allanach B C *et al* 2001 *eConf C010630* P125 *Preprint* hep-ph/0202233
[165] Gherghetta T, Giudice G F and Wells J 1999 *Nucl. Phys.* B **559** 27 *Preprint* hep-ph/9904378
[166] *Les Points d'Aix* http://www.desy.de/∼heinemey/LesPointsdAix.html
[167] Haber H E and Kane G L 1985 *Phys. Rep.* **117** 75
[168] Giudice G F 2000 *Int. J. Mod. Phys.* A **15S1** 440
Giudice G F 2000 *eConf C990809* 440 *Preprint* hep-ph/9912279
[169] Ali A 2002 *Preprint* hep-ph/0201120
[170] Ciuchini M, Franco E, Masiero A and Silvestrini L 2003 *eConf C0304052* WG307 *Preprint* hep-ph/0308013
Ciuchini M, Franco E, Masiero A and Silvestrini L 2003 *Phys. Rev.* D **67** 075016 *Preprint* hep-ph/0212397
[171] Raby S 2004 *Rep. Prog. Phys.* **67** 755 *Preprint* hep-ph/0411155 v2
[172] Weinberg S 1982 *Phys. Rev.* D **26** 287
Sakai N and Yanagida T 1982 *Nucl. Phys.* B **197** 533
[173] Babu K S, Pati J C and Wilczek F 1998 *Phys. Lett.* B **423** 337 *Preprint* hep-ph/9712307
[174] Pati J C *Preprint* hep-ph/0204240
[175] Shiozawa M 2000 *20th Int. Conf. on High Energy Physics (ICHEP2000) (Osaka, 27 July–2 August 2000)* (Singapore: World Scientific)
[176] Murayama H and Pierce A 2002 *Phys. Rev.* D **65** 055009 *Preprint* hep-ph/0108104
[177] Babu K S, Pati J C and Wilczek F 2000 *Nucl. Phys.* B **566** 33–91 *Preprint* hep-ph/9812538
[178] Dermíšek R, Mafi A and Raby S 2001 *Phys. Rev.* D **63** 035001 *Preprint* hep-ph/0007213
[179] Goh H S, Mohapatra R N, Nasri S and Siew-Phang Ng 2004 *Phys. Lett.* B **587** 105 *Preprint* hep-ph/0311330
[180] Barbieri R, Hall L J and Nomura Y 2002 *Phys. Rev.* D **66** 045025 *Preprint* hep-ph/0106190
[181] Dutta B, Mimura Y and Mohapatra R N 2004 *Preprint* hep-ph/0412105
[182] Suzuki Y *et al* (TITAND Working Group) 2001 *Preprint* hep-ex/0110005
[183] Jung C K 2000 *Preprint* hep-ex/0005046
[184] Rico J *et al* (ICARUS Collaboration) 2004 *Eur. Phys. J.* C **33** S840 *Preprint* hep-ex/0309023

Amoruso S *et al* (ICARUS Collaboration) 2004 *Eur. Phys. J.* C **33** 233 *Preprint* hep-ex/0311040
[185] Heavy Flavor Averaging Group (HFAG), see http://www.slac.stanford.edu/xorg/hfag/rare/
Barate R *et al* (ALEPH Collaboration) 1998 *Phys. Lett.* B **429** (1998) 169
Koppenburg P *et al* (BELLE Collaboration) 2004 *Phys. Rev. Lett.* **93** 061803 *Preprint* hep-ex/0403004
Abe K *et al* (BELLE Collaboration) 2001 *Phys. Lett.* B **511** 151
Chen S *et al* (CLEO Collaboration) 2001 *Phys. Rev. Lett.* **87** 251807 *Preprint* hep-ex/0108032 v3
Aubert B *et al* (BABAR Collaboration) 2002 *Preprints* hep-ex/0207074, hep-ex/0207076
[186] Buras A J 2000 *Lectures at the Erice Int. School of Subnucl. Phys. (August–September 2000)* TUM-HEP-402/01 *Preprint* hep-ph/0101336
[187] Ali A 2004 talk given at *ICHEP04 (Beijing, August 2004)* to appear in the proceedings, see http://www.ihep.ac.cn/data/ichep04/ppt/plenary/p13-ali-a.pdf
[188] Buras A J, Czarnecki A, Misiak M and Urban J 2002 *Nucl. Phys.* B **631** 219 *Preprint* hep-ph/0203135
Gambino P and Misiak M 2001 *Nucl. Phys.* B **611** 338 *Preprint* hep-ph/0104034 v2
[189] Borzumati F M and Greub C 1998 *ICHEP98 (Vancouver, 1998) Preprint* hep-ph/9810240
[190] Ciafaloni P, Romamnino A and Strumia A 1998 *Nucl. Phys.* B **524** 361 *Preprint* hep-ph/9710312
Ciuchini M, Degrassi G, Gambino P and Giudice G F 1998 *Nucl. Phys.* B **527** 21 *Preprint* hep-ph/9710335
[191] Degrassi G, Gambino P and Giudice G F 2000 *J. High Energy Phys.* JHEP0012 009 *Preprint* hep-ph/0009337
[192] Carena M, Garcia D, Nierste U and Wagner C E M 2001 *Phys. Lett.* B **499** 141 *Preprint* hep-ph/0010003 v2
[193] Goto T, Okada Y and Shimizu Y 1998 *Phys. Rev.* D **58** 094006 *Preprint* hep-ph/9804294
[194] Okumura K and Roszkowski L 2003 *J. High Energy Phys.* JHEP0310 024 *Preprint* hep-ph/0308102
[195] Nir Y 1998 *Lectures at 1998 European School of High Energy Physics (University of St Andrew, Scotland, 1998)* WIS-98/29/Oct-DPP *Preprint* hep-ph/9810520
[196] Ali A, Lunghi E, Greub C and Hiller G 2002 *Phys. Rev.* D **66** 034002 *Preprint* hep-ph/0112300
[197] Nishida S (BELLE Collaboration) 2002 *ICHEP02 (Amsterdam, 24–31 July 2002)*
[198] Buras A J 2003 *Phys. Lett.* B **566** 115 *Preprint* hep-ph/0303060
[199] Dedes A, Dreiner H K and Nierste U 2001 *Phys. Rev. Lett.* **87** 251804 *Preprint* hep-ph/0108037
[200] Herndon M 2004 talk given at *ICHEP04 (Beijing, August 2004)* see http://ichep04.ihep.ac.cn/db/paper.php
[201] Isidori G 2003 talk at *2nd Workshop on the CKM Unitarity Triangle (Durham, England, 5–9 April 2003) eConf C0304052* WG304 *Preprint* hep-ph/0307014
[202] Anisimovsky V V *et al* (E949 Collaboration) 2004 *Phys. Rev. Lett.* **93** 031801 *Preprint* hep-ex/0403036
Adler S *et al* (E787 Collaboration) 2002 *Phys. Rev. Lett.* **88** 041803 *Preprint* hep-ex/0111091
[203] Alavi-Harati A *et al* (KTeV Collaboration) 2001 *Phys. Rev. Lett.* **86** 397 *Preprint* hep-ex/0009030
Alavi-Harati A *et al* (KTeV Collaboration) 2000 *Phys. Rev. Lett.* **84** 5279 *Preprint* hep-ex/0001006
Alavi-Harati A *et al* (KTeV Collaboration) 2000 *Phys. Rev.* D **61** 072006
[204] Buchalla G, D'Ambrosio G and Isidori G 2003 *Nucl. Phys.* B **672** 387 *Preprint* hep-ph/0308008
[205] Alavi-Harati A *et al* (KTeV Collaboration) 2004 *Phys. Rev. Lett.* **93** 021805 *Preprint* hep-ex/0309072
[206] see CKM Collaboration http://www.fnal.gov/projects/ckm/Welcome.html
[207] Kane G L, Kolda C and Lennon J E 2003 *Preprint* hep-ph/0310042 and references therein
[208] Nikitenko A, Starodumov A and Stepanov N CMS NOTE 1999/039
Ball P *et al* 2000 CERN-TH-2000-101 *Preprint* hep-ph/0003238
[209] Isidori G and Retico A 2001 *J. High Energy Phys.* JHEP11 001 *Preprint* hep-ph/0110121
[210] Buras A J, Chankowski P H, Rosiek J and Slawianowska L 2002 *Phys. Lett.* B **546** 96 *Preprint* hep-ph/0207241
[211] Baek S, Ko P and Song W Y 2002 *Phys. Rev. Lett.* **89** 271801 *Preprint* hep-ph/0205259
[212] Isidori G 1998 *Int. Workshop on CP violation in K (KEK-Tanashi, Tokyo, December 1998) Preprint* hep-ph/9902235
Colangelo G and Isidori G 1998 *J. High Energy Phys.* JHEP09 009
[213] Bailey J *et al* 1979 *Nucl. Phys.* B **150** 1
[214] Danby G T *et al* 2001 *Nucl. Instrum. Methods* A **457** 151
Sedykh S A *et al* 2000 *Nucl. Instrum. Methods* A **455** 346
[215] Bennett G W *et al* (Muon (g-2) Collaboration) 2002 *Phys. Rev. Lett.* **89** 101804
Bennett G W *et al* (Muon (g-2) Collaboration) 2002 *Phys. Rev. Lett.* **89** 129903 *Preprint* hep-ex/0208001 v2 (erratum)
[216] Bennett G W *et al* (Muon (g-2) Collaboration) 2004 *Phys. Rev. Lett.* **92** 161802 *Preprint* hep-ex/0401008
[217] Brown H N *et al* 2001 *Phys. Rev. Lett.* **86** 2227 *Preprint* hep-ex/0102017
[218] Miller J P 2002 *Int. J. Mod. Phys.* A **17** 3318 *Preprint* hep-ex/0111036
[219] Knecht M 2003 Lectures given at *41st Int. Universitaetswochen fuer Theoretische Physik, Flavor Physics (IUTP 41) (Schladming, Styria, Austria, 22–28 February 2003) Preprint* hep-ph/0307239
[220] Kinoshita T and Nio M 2004 *Phys. Rev.* D **70** 113001 *Preprint* hep-ph/0402206

Czarnecki A and Marciano W J 2001 *Phys. Rev.* D **64** 013014 *Preprint* hep-ph/0102122
[221] Czarnecki A, Marciano W J and Vainshtein A 2003 *Phys. Rev.* D **67** 073006 *Preprint* hep-ph/0212229
Knecht M, Peris S, Perrottet M and De Rafael E 2002 *J. High Energy Phys.* JHEP0211 003 *Preprint* hep-ph/0205102
[222] Höcker A 2004 *Preprint* hep-ph/0410081
[223] Ezhela V V, Lugovsky S B and Zenin O V 2003 *Preprint* hep-ph/0312114
[224] Davier M, Eidelman S, Höcker A and Zhang Z 2003 *Eur. Phys. J.* C **31** 503 *Preprint* hep-ph/0308213
[225] Alemany R, Davier M and Höcker A 1998 *Eur. Phys. J.* C **2** 123 *Preprint* hep-ph/9703220
[226] Krause B 1997 *Phys. Lett.* B **390** 392 *Preprint* hep-ph/9607259
[227] Melnikov K and Vainshtein A 2004 *Phys. Rev.* D **70** 113006 *Preprint* hep-ph/0312226 (see also the comment in [222])
Nyffeler A 2002 CPT-2002-P-4341, *Preprint* hep-ph/0203243
[228] Davier M, Eidelman S, Höcker A and Zhang Z 2003 *Eur. Phys. J.* C **27** 497 *Preprint* hep-ph/0208177 v3
[229] Hagiwara K, Martin A D, Nomura D and Teubner T 2003 *Phys. Lett.* B **557** 69 *Preprint* hep-ph/0209187
[230] Akhmetshin R R *et al* (CMD-2 Collaboration) 2004 *Phys. Lett.* B **578** 285 *Preprint* hep-ex/0308008
[231] Ghozzi S and Jegerlehner F 2004 *Phys. Lett.* B **583** 222 *Preprint* hep-ph/0310181 v2
[232] de Troconiz J F and Yndurain F J 2004 *Preprint* hep-ph/0402285
[233] Aloisio A *et al* (KLOE Collaboration) 2005 *Phys. Lett.* B **606** 12 *Preprint* hep-ex/0407048
[234] Narison S 2003 *Phys. Lett.* B **568** 231 *Preprint* hep-ph/0303004
[235] Czarnecki A and Marciano W J 2001 *Phys. Rev.* D **64** 013014 *Preprint* hep-ph/0102122
[236] Lopez J L, Nanopoulos D V and Wang X 1994 *Phys. Rev.* D **49** 366
[237] Degrassi G *et al* 2004 *Acta Phys. Polon.* B **35** 2711
Heinemeyer S, Stockinger D and Weiglein G 2004 *Nucl. Phys.* B **699** 103 *Preprint* hep-ph/0405255
[238] Chattopadhyay U and Nath P 2002 *Phys. Rev.* D **66** 093001 *Preprint* hep-ph/0208012
[239] Solodov E P *et al* (BABAR Collaboration) 2001 *eConf C010430* T03 *Preprint* hep-ex/0107027
[240] Czyz H, Grzelinska A, Kuhn J H and Rodrigo G, *Preprint* hep-ph/0312217
[241] Davier M 2003 *Preprint* hep-ex/0312063
[242] Kuno Y and Okada Y 2001 *Rev. Mod. Phys.* **73** 151 *Preprint* hep-ph/9909265
[243] Brooks M L *et al* (MEGA Collaboration) 1999 *Phys. Rev. Lett.* **83** 1521 *Preprint* hep-ex/9905013
[244] Hisano J 2002 *Nucl. Phys. Proc. Suppl.* **111** 178 *Preprint* hep-ph/0204100
Hisano J and Tobe K 2001 *Phys. Lett.* B **510** 197 *Preprint* hep-ph/0102315 v2
[245] see http://meg.web.psi.ch/docs/index.html
[246] van der Schaaf A 2001 *4th Workshop on Neutrino Oscillations and their Origin (NOON2003) (Kanazawa, Japan, 10–14 February 2003)* see http://www-sk.icrr.u-tokyo.ac.jp/noon2003/
[247] see http://meco.ps.uci.edu/
[248] Äystö J *et al* 2001 *Preprint* hep-ph/0109217
[249] Ligeti Z and Nir Y 2002 *Nucl. Phys. Proc. Suppl.* **111** 82 *Preprint* hep-ph/0202117
[250] Khalil S and Sanz V 2003 *Phys. Lett.* B **576** 107 *Preprint* hep-ph/0306171
[251] Abel S and Khalil S 2004 *Preprint* hep-ph/0412344
[252] Hisano J and Shimizu Y 2004 *Phys. Rev.* D **70** 093001 *Preprint* hep-ph/0406091
[253] Harris P G *et al* 1999 *Phys. Rev. Lett.* **82** 904
[254] Regan B C, Commins E D, Schmidt C J and DeMille D 2002 *Phys. Rev. Lett.* **88** 071805
[255] Romalis M V, Griffith W C and Fortson E N 2001 *Phys. Rev. Lett.* **86** 2505 *Preprint* hep-ex/0012001
[256] Lamoreaux S 2003 *Lepton Moments Int. Symp. (Cape Cod, June 2003)* http://g2pc1.bu.edu/∼leptonmom/
[257] Feng J L, Matchev K T and Shadmi Y 2003 *Phys. Lett.* B **555** 89 *Preprint* hep-ph/0208106
Feng J L, Matchev K T and Shadmi Y 2001 *eConf* C010630 P307 *Preprint* hep-ph/0110157
Feng J L, Matchev K T and Shadmi Y 2001 *Nucl. Phys.* B **613** 366 *Preprint* hep-ph/0107182
[258] Semertzidis Y K *et al* 1999 *Proc. Int. Workshop on High Intensity Muon Sources (HIMUS99) (KEK, Japan, 1–4 December 1999) Preprint* hep-ph/0012087
[259] Äystö J *et al* 2001 *Preprint* hep-ph/0109217
[260] Abel S, Khalil S and Lebedev O 2001 *Nucl. Phys.* B **606** 151 *Preprint* hep-ph/0103320
Ibrahim T and Nath P *Preprints* hep-ph/0207213, hep-ph/0107325
Arnowitt R, Dutta B, Hu B and Santoso Y 2001 *Preprint* hep-ph/0108082
[261] Ibrahim T and Nath P 1998 *Phys. Rev.* D **58** 111301
Ibrahim T and Nath P 1998 *Phys. Rev.* D **60** 099902 *Preprint* hep-ph/9807501 (erratum)
Brhlik M, Good G J and Kane G L 1999 *Phys. Rev.* D **59** 115004 *Preprint* hep-ph/9810457
[262] Eyal G and Nir Y 1998 *Nucl. Phys.* B **528** 21 *Preprint* hep-ph/9801411
Babu K S, Dutta B and Mohapatra R N 2002 *Phys. Rev.* D **65** 016005 *Preprint* hep-ph/0107100

[263] Bouchiat M A and Bouchiat C 1997 *Rep. Prog. Phys.* **60** 1351
[264] Bennett S C and Wieman C E 1999 *Phys. Rev. Lett.* **82** 2484
[265] Derevianko A 2000 *Phys. Rev. Lett.* **85** 1618 *Preprint* hep-ph/0005274
Dzuba V A *et al* 2002 *Phys. Rev.* D **66** 076013 *Preprint* hep-ph/0204134
[266] Dominici D 1999 *Preprint* hep-ph/9909290
[267] Abe F *et al* (CDF Collaboration) 1997 *Phys. Rev. Lett.* **79** 2191
[268] Battaglia M, De Curtis S and Dominici D 2002 *J. High Energy Phys.* JHEP0212 004 *Preprint* hep-ph/0210351
[269] Ramsey-Musolf M J 2000 *Phys. Rev.* D **62** 056009 *Preprint* hep-ph/0004062
[270] Litov L (NA48 Collaboration) 2004 Talk given at *32nd Int. Conf. on High-Energy Physics (ICHEP 04) (Beijing, China, 16–22 August 2004) Preprint* hep-ex/0501048
Kessler R (KTeV Collaboration) 2005 *Nucl. Phys. Proc. Suppl.* **142** 304
[271] Bouchiat A M *et al* 1985 *Opt. Commun.* **56** 100
[272] Bouchiat A M and Frois B (ed) 1999 *Parity Violation in Atoms and Polarized Electron Scattering* (Singapore: World Scientific)
[273] Orozco L A 1996 *SILAFAE-1 (Merida, Mexico, 1996)*
[274] Kurylov A, Ramsey M J-Musolf and Su S 2002 *Preprint* hep-ph/0205183
[275] The LEP Collaborations ALEPH, DELPHI, L3, OPAL, The LEP Electroweak Working Group and the SLD Heavy Flavour Group 2003 LEPEWWG/2003-02, *Preprint* hep-ex/0312023
[276] Langacker P 2001 *Precision Electroweak Data: Phenomenological Analysis eConf C010630* P107 *Preprint* hep-ph/0110129
[277] Zeller G P *et al* (NuTeV Collaboration) 2002 *Phys. Rev. Lett.* **88** 091802
[278] de Boer W and Sander C 2004 *Phys. Lett.* B **585** 276 *Preprint* hep-ph/0307049
[279] Erler J and Pierce D M 1998 *Nucl. Phys.* B **526** 53 *Preprint* hep-ph/9801238
Erler J 1999 talk presented at *DPF99 (Los Angeles, 1999) Preprint* hep-ph/9903449
[280] Cho G C, Hagiwara K, Kao C and Szalapski R, UR-1558, ER/40685/927, KEK-TH-609 *Preprint* hep-ph/9901351
Pokorski S 1999 *Acta Phys. Polon.* B **30** 1759 *Preprint* hep-ph/9901427
[281] Ellis J R, Heinemeyer S, Olive K A and Weiglein G 2004 *Preprint* hep-ph/0411216
[282] Altarelli G, Caravaglios F, Giudice G F, Gambino P and Ridolfi G 2001 *J. High Energy Phys.* JHEP0106 018 *Preprint* hep-ph/0106029
[283] Marandella G, Schappacher C and Strumia A 2005 *Nucl. Phys.* B **715** 173 *Preprint* hep-ph/0502095
[284] DOE review panel closeout-February 2004, http://www-bdnew.fnal.gov/doereview04/RunII_Lum_Review 0204_closeout.pdf
[285] see http://www-zeus.desy.de/physics/lumi/lumi03/periods.html
[286] ed Gianotti F *et al* 2002 *Physics Potential and Experimental Challenges of the LHC Luminosity Upgrade* CERN-TH-2002-078 (*April 2002) Preprint* hep-ph/0204087
[287] Delahaye J P CERN-PS-99-061 (DI)
Carrigan R A JR *Fermilab-Conf-01/373-E* December 01
[288] Richard F, Schneider J R, Trines D and Wagner A *TESLA Technical Design Report* DESY 2001-011 http://tesla.desy.de/new_pages/TDR_CD/start.html
[289] Akasaka N *et al* 1997 *JLC Design Study*, *KEK Report* 97-1
[290] The NLC Collaboration *2001 Report on the Next Linear Collider* ed Nan Phinney, Fermilab-Conf-01-075-E, SLAC-R-571
Abe T *et al* (American Linear Collider Working Group Collaboration) *Linear Collider Physics Resource Book for Snowmass 2001*, SLAC-570 *Preprints* hep-ex/0106055, hep-ex/0106056, hep-ex/0106057, hep-ex/0106058
[291] Assmann R *et al* 2000 *SLC: the end game (Vienna 2000, EPAC 00)* pp 18–22
[292] The CLIC Study Team *A 3 TeV* e^+e^- *Linear Collider based on CLIC Technology* ed G Guignard G CERN 2000-008 (Proton Synchrotron Division).
[293] Braun H H *et al* 2001 Status of CLIC high gradient studies *IEEE Particle Accelerator Conf. (Chicago, IL, USA, 18–22 June 2001)* CERN-PS-2001-045-RF, CLIC-NOTE-489, PAC-2001-MPPH039, Jul 2001
[294] Wuensch W *CLIC Note* 532, CERN/PS 2002-059 (AE)
Braun H H, Döbert S, Syratchev I, Taborelli M, Wilson I and Wuensch W *CLIC Note* 535, CERN/PS 2002-062 (RF)
[295] Asner D *et al* 2001 *Higgs Physics with a Gamma Gamma Collider based on CLIC I* BNL-HET-01-32, CERN-PS-NOTE-2001-062-AE, CERN-SL-2001-055-AP, CERN-TH-2001-235, CLIC-NOTE-500, NUHEP-EXP-01-050, UCRL-JC-145692 *Preprint* hep-ex/0111056
Burkhardt H and Telnov V 2002 *CLIC 3 TeV photon collider option* CERN-SL-2002-013-AP, CLIC-NOTE-508

[296] Telnov V 2001 *Photon Collider at TESLA*, SNOWMASS-2001-T103
[297] Janot P, *La physique du Higgs aux collisionneurs* e + e− $\mu + \mu$ *Ecole de Gif 2001*
[298] Skrinsky A N 1996 Ionization cooling and muon collider *AIP Conf. Proc.* **372** 133
[299] Palmer R B 1998 Muon collider design *AIP Conf. Proc.* **441** 183
[300] By Muon Collider/Neutrino Factory Collaboration (M M Alsharoa *et al*) 2002 FERMILAB-PUB-02-149-E *Preprint* hep-ex/0111016
[301] Muon Colliders, http://www.fnal.gov/projects/muon_collider/ and http://muonstoragerings.web.cern.ch/; muonstoragerings/Welcome.html Autin *et al Prospective Study of Muon Storage Rings at CERN*, CERN 99-02
[302] Geer S 2002 *Int. J. Mod. Phys.* A **17** 3483 *Preprint* hep-ex/0111016
[303] Kaplan D M and Snowmass 2001 *Preprint* physics/0109061
MuCool Collaboration (Daniel Kaplan M for the collaboration), IIT-HEP-02, arXiv physics/0211017
[304] Kahn S A *et al* The instrumentation channel for the MUCOOL experiment New York 1999 Particle Accelerator vol 5 p 3026
[305] MICE Proposal, http://proj-bdl-nice.web.cern.ch/proj-bdl-nice/cool/proposal/proposal.pdf
[306] Very Large Hadron Collider, http://www.vlhc.org/
[307] Moretti S *Snowmass-P3-WG1/MC-001 (June 2001)*, http://zippy.physics.niu.edu/tools.ps
[308] Perl M L 1994 SLAC-PUB-6514, *Rencontres de Physique de la Vallee (La Thuile, Italy, 6-12 March 1994)*
[309] Brient J C *et al* 2001 LC-DET-2001-058 in *2nd ECFA/DESY Study 1998-2001* pp 2262–85
[310] Djouadi A SUSY calculation tools *Plenary talk at SUSY2002, DESY (Hamburg, 17–23 June 2002)* PM-02-42 *Preprint* hep-ph/0211357
[311] Ghodbane N, Katsanevas S, Morawitz P and Perez E *Susygen 3.0: A Monte Carlo Event Generator for Supersymmetric Particle Production at lepton, ep and Hadron Colliders Preprint* hep-ph/9909499 http://lyoinfo.in2p3.fr/susygen/susygen3
[312] Sjöstrand T, Lönnblad L and Mrenna S 2001 *Preprint* hep-ph/0108264 http://www.thep.lu.se/ torbjorn//Pythia.html
[313] Mühlleitner M, Djouadi A and Mambrini Y *SDECAY: a Fortran code for the decays of the supersymmetric particles in the MSSM*, CERN TH/2003-252, PM/03-22, PSI-PR-03-17, *Preprint* hep-ph/0311167
[314] Allanach B C 2002 SOFTSUSY1.7: a program for calculating supersymmetric spectra *Comput. Phys. Commun.* 143 305 *Preprint* hep-ph/0104145
[315] Porod W 2003 SPheno: a program for calculating supersymmetric spectra SUSY particle decays and SUSY particle production at e^+e^- colliders *Comput. Phys. Commun.* **153** 275 *Preprint* hep-ph/0301101
[316] Corcella G, Knowles I G, Marchesini G, Moretti S, Odagiri K, Richardson P, Seymour M H and Webber B R 2001 HERWIG 6.5 *J. High Energy Phys.* **0101** 010 *Preprint* hep-ph/0011363 *Preprint* hep-ph/0210213 http://hepwww.rl.ac.uk/theory/seymour/herwig/
[317] Allanach B C, Kraml S and Porod W 2003 JHEP **0303** 016 *Preprint* hep-ph/0302102
Allanach B C 2001 *Snowmass-2001/P3-19, eConf* C010630 P319 *Preprint* hep-ph/0110227
Ghodbane N and Martyn H-U, LC-TH-2001-079 *Preprint* hep-ph/0201233
[318] Spira M and Zerwas P lectures at Schladming 1997 *Preprint* hep-ph/9803257 CERN-TH/97-379, DESY 97-261
[319] Haber H E 1997 *Perspectives on Higgs Physics II* Kane G L ed (Singapore: World Scientific) *Preprint* hep-ph/9707213
[320] Gunion J F, Haber H E, Kane G L and Dawson S 1990 *The Higgs Hunter's Guide* (Reading, MA: Addison-Wesley)
Kane G L (ed) 1993 *Perspectives on Higgs Physics* (Singapore: World Scientific)
[321] Janot P 1997 *Perspectives in Higgs Physics II* ed G Kane (Singapore: World Scientific)
[322] Peskin M E and Takeuchi T 1990 *Phys. Rev. Lett.* **65** 964
Peskin M E and Takeuchi T 1991 *Phys. Rev.* D **46** 381
[323] Peskin M E and Wells J D 2001 *Phys. Rev.* D **64** 093003 *Preprint* hep-ph/0101342
Kolda C and Murayama H 2000 *J. High Energy Phys.* 0007 035 *Preprint* hep-ph/0003170
Kane G L, Wells J D, UCD-2000-09, LBNL-45356, LBL-45356, *Preprint* hep-ph/0003249
[324] Ridolfi G La Thuile 2001 *Results and perspectives in particle physics Preprint* hep-ph/0106300
[325] Frère J-M, Jones D R T and Raby S 1983 *Nucl. Phys.* B **222** 11
[326] Gunion J F, Haber H E and Sher M 1988 *Nucl. Phys.* B **306** 1
[327] Casas J A 1998 Perspectives on Supersymmetry ed G L Kane (Singapore: World Scientific) *Preprint* hep-ph/9707475
[328] Baer H, Brhlik M and Castaño D 1996 *Phys. Rev.* D **54** 6944 *Preprint* hep-ph/9607465
Brhlik M 2001 *Nucl. Phys.* B (*Proc. Suppl.*) **101** 395
[329] Kusenko A, Langacker P and Segre G 1996 *Phys. Rev.* D **54** 5824 *Preprint* hep-ph/9602414

[330] Early papers are: Ellis J R, Ridolfi G and Zwirner F 1991 *Phys. Lett.* B **275** 83
Okada Y, Yamaguchi M and Yanagida T 1991 *Prog. Theor. Phys.* **85** 1
Haber H E and Hempfling R 1993 *Phys. Rev.* D **48** 4280
[331] Hempfling R and Hoang A H 1994 *Phys. Lett.* B **331** 99 *Preprint* hep-ph/9401219
Carena M, Espinosa J R, Quiros M and Wagner C E M 1995 *Phys. Lett.* B **355** 209 *Preprint* hep-ph/9504316
Carena M, Quiros M and Wagner C E M 1996 *Nucl. Phys.* B **461** 407 *Preprint* hep-ph/9508343
[332] Brignole A 1992 *Phys. Lett.* B **281** 284
Chankowski P H, Pokorski S and Rosiek J 1992 *Phys. Lett.* B **274** 191
Dabelstein A 1995 *Z.Phys.* **C67** 495 *Preprint* hep-ph/9409375
[333] Haber H E, Hempfling R and Hoang A H 1997 *Z. Phys.* **C75** 539 *Preprint* hep-ph/9609331
Espinosa J R and Navarro I 2001 *Nucl. Phys.* B **615** 82 *Preprint* hep-ph/0104047
Pilaftsis A and Wagner C E M 1999 *Nucl. Phys.* B **553** 3 *Preprint* hep-ph/9902371
Carena M, Ellis J R, Pilaftsis A and Wagner C E M 2000 *Nucl. Phys.* B **586** 92 *Preprint* hep-ph/0003180
Carena M, Ellis J R, Pilaftsis A and Wagner C E M 2002 *Nucl. Phys.* B **625** 345 *Preprint* hep-ph/0111245 v2
Heinemeyer S, Hollik W and Weiglein G 1998 *Phys. Lett.* B **440** 296 *Preprint* hep-ph/9807423
Heinemeyer S, Hollik W and Weiglein G 1999 *Eur. Phys. J.* **C9** 343 *Preprint* hep-ph/9812472
Heinemeyer S, Hollik W and Weiglein G 1999 *Phys. Lett.* **B 455** 179 *Preprint* hep-ph/9903404
Zhang R-J 1999 *Phys. Lett* **B 447** 89 *Preprint* hep-ph/9808299
Espinosa J R and Zhang R-J 2000 *J. High Energy Phys.* JHEP0003 026 *Preprint* hep-ph/9912236
Espinosa J R and Zhang R-J 2000 *Nucl. Phys.* B **586** 3 (revised in *Preprint* hep-ph/0003246 v2)
Degrassi G, Slavich P and Zwirner F 2001 *Nucl. Phys.* B **611** 403*Preprint* hep-ph/0105096
Brignole A, Degrassi G, Slavich P and Zwirner F 2002 *Nucl. Phys.* B **631** 195 *Preprint* hep-ph/0112177
[334] Heinemeyer S, Hollik W, Rzehak H and Weiglein G 2005 *Eur. Phys. J.* **C39** 465 *Preprint* hep-ph/0411114
Dedes A, Degrassi G and Slavich P 2003 *Nucl. Phys.* B **672** 144 *Preprint* hep-ph/0305127
Brignole A, Degrassi G, Slavich P and Zwirner F 2002 *Nucl. Phys.* B **643** 79 *Preprint* hep-ph/0206101
[335] Dedes A, Heinemeyer S, Su S and Weiglein G 2001 *eConf* C010630 P305 *Preprint* hep-ph/0110219
[336] Allanach B C, Djouadi A, Kneur J L, Porod W and Slavich P 2004 *J. High Energy Phys.* JHEP0409 044 *Preprint* hep-ph/0406166
[337] Heinemeyer S, Hollik W and Weiglein G 2000 FEYNHIGGS: a program for the calculation of the masses of the Neutral CP even Higgs Bosons in the MSSM *Comput. Phys. Commun.* **124** 76 *Preprint* hep-ph/9812320 see http://wwwth.mppmu.mpg.de/members/heinemey/feynhiggs/
[338] G Altarelli *et al* (ed) 1996 *Physics at LEP 2* CERN 96-01
[339] Espinosa J R 1997 *Surveys High Energ. Phys.* **10** 279 *Preprint* hep-ph/9606316
See also Altarelli G and Isidori G 1994 *Phys. Lett.* B **337** 141 CERN-TH.7351/94
[340] Pilaftsis A 1998 *Phys. Lett.* B **435** 88 *Phys. Rev.* D58 096010
[341] Miller D J, Moretti S and Nevzorov R 2005 *Preprint* hep-ph/0501139
[342] Hugonie C and Moretti S 2001 *Snowmass 2001 eConf* C010630 P108 *Preprint* hep-ph/0110241
[343] Ellwanger U, Gunion J F and Hugonie C 2001 *Les Houches 2001, Physics at TeV colliders Preprint* hep-ph/0111179
[344] Ellwanger U, Gunion J F, Hugonie C and Moretti S 2003 *Preprint* hep-ph/0305109
[345] Miller D J and Moretti S 2004 *Preprint* hep-ph/0403137
[346] Masip M, Munoz-Tapia R and Pomarol A 1998 *Phys. Rev.* D **57** 5340 *Preprint* hep-ph/9801437
[347] Espinosa J R and Quiros M 1998 *Phys. Rev. Lett.* **81** 516*Preprint* hep-ph/9804235
Masip M 1998 *Phys. Lett.* B **444** 352 *Preprint* hep-ph/9810303
[348] Cvetič M and Langacker P 1996 *Phys. Rev.* D **54** 3570
Cvetič M and Langacker P 1996 *Mod. Phys. Lett.* **A11** 1247
Cvetič M and Langacker P 1998 *Perspectives in Supersymmetry* ed G Kane (Singapore: World Scientific)
[349] Cleaver G, Cvetič M, Espinosa J R, Everett L L, Langacker P and Wang J 1999 *Phys. Rev.* D **59** 115003
Everett L L, Langacker P, Plümacher M and Wang J 2000 *Phys. Lett.* B **477** 233
[350] Erler J, Langacker P and Li T-J 2002 *Phys. Rev.* D **66** 015002 *Preprint* hep-ph/0205001
[351] Gross E and Read A L CERN-EP-2000-034
[352] Myers S and Wyss C *Physics at LEP 2* ed G Altarelli *et al* CERN 96-01
[353] Read A for the LEP Higgs WG, LEPC 20/07/2000
[354] Igo Kemenes P 2001 *The Legacy of LEP and SLC (Siena, October 2001)* North (Amsterdam: Holland)
[355] LEP Higgs Working Group, the ALEPH, DELPHI, L3 and OPAL Experiments, Contributed paper for ICHEP'02 (Amsterdam, July 2002) see http://lephiggs.web.cern.ch/LEPHIGGS/papers/index.html
[356] Chikashige Y, Mohapatra R N and Peccei R D 1980 *Phys. Rev. Lett.* **45** 1926
Joshipura A S and Valle J W F 1993 *Nucl. Phys.* B **397** 105

Joshipura A S and Rindani S D 1992 *Phys. Rev. Lett.* **69** 3269
Diaz M A, Garcia-Jareno M A, Restrepo D A and Valle J W F 1998 *Nucl. Phys.* B **527** 44 *Preprint* hep-ph/9803362
[357] Cline J M 2000 *Pramana* **54** 1 *Preprint* hep-ph/0003029
Cline J M *COSMO-01*, *(Rovaniemi, Finland, 30 August–4 September 2001) Preprint* hep-ph/0201286
Murayama H 2002 *Nucl. Phys. Proc. Suppl.* **111** 136 *Preprint* hep-ph/0208005
[358] Huber S J and Schmidt M G *Marseille 2000, Strong and Electroweak Matter Preprint* hep-ph/0011059
[359] Harlander R V and Kilgore W B 2002 *Phys. Rev. Lett.* **88** 201801
Harlander R V and Kilgore W B 2002 *J. High. Energy Phys.* JHEP 0210 017
[360] Anastasiou C and Melnikov K 2002 *Nucl. Phys.* B **646** 220 *Preprint* hep-ph/0207004
[361] Anastasiou C and Melnikov K 2003 *Phys. Rev.* D **67** 037501 *Preprint* hep-ph/0208115
[362] Spira M *Preprint* hep-ph/0211145
[363] Wei-Ming Yao, (for D0 and CDF Collaborations) *32nd Int. Conf. High-Energy Physics (ICHEP 04) (Beijing, China, 16-22 August 2004) Preprint* hep-ex/0411053
[364] Carena M, Conway J S, Haber H E and Hobbs J D *Report of the Tevatron Higgs Working Group Preprint* hep-ph/0010338
[365] CDF and D0 Working Group (Babukhadia L *et al*) 2003 *Results of the Tevatron Higgs Sensitivity Study*, FERMILAB-PUB-03-320-E
[366] Affolder T *et al* 2001 (CDF Collaboration) *Phys. Rev. Lett.* **86** 4472
[367] Womersley J 2000 *Int. J. Mod. Phys.* A **15S1** 607
Womersley J 2000 *eConf C990809* 607 *Preprint* hep-ex/9912009
[368] Richter-Was E, Froideveaux D, Gianotti F, Poggioli L, Cavalli D and Resconi S 1998 *Int. J. Mod. Phys.* A **13** 1371 CERN-TH/96-111
[369] Abdullin S *et al* 2005 Summary of the CMS Potential for the Higgs Boson Discovery *Eur. J. Phys.* C **39** 41 CMS NOTE 2003/033 (10 December 2003)
[370] Del Duca V 2003 *eConf C030614* 016 *Preprint* hep-ph/0312184
[371] ATLAS Collaboration 1999 *ATLAS detector and physics performance Technical Design Report* CERN/LHCC 99-14/15
[372] Bern Z, Dixon L and Schmidt C 2003 *Nucl. Phys. Proc. Suppl.* **116** 178 *Preprint* hep-ph/0211216
[373] Pauss F and Dittmar M 1998 *Lectures at ASI Summer School (St.Croix, 1998)* ETHZ-IPP PR-98-09 *Preprint* hep-ex/9901018
Dittmar M 1998 *Lectures at* 30^{e} *Ecole d'Ete de Physiques des particules (7–11 September 1998 Marseille)* ETHZ-IPP PR-98-10 *Preprint* hep-ex/9901009
[374] Datta A, Djouadi A, Guchait M and Moortgat F 2004 *Nucl. Phys.* B **681** 31 *Preprint* hep-ph/0303095
[375] Gianotti F and Pepe-Altarelli M 2000 *Nucl. Phys. Proc. Suppl.* **89** 177 *Preprint* hep-ex/0006016
Gianotti F 2004 *Phys. Rep.* **403** 379
[376] Janot P private communication
[377] Chanowitz M S 2004 *The no-Higgs signal: strong WW scattering at the LHC*, talk given at Conf. on Physics at LHC (13-17 July 2004, Vienna, Austria) *Preprint* hep-ph/0412203
[378] Tauchi T *Physics plan at JLC*, KEK-PREPRINT-98-180, Nov. 1998, see also http://www-jlc.kek.jp
[379] Peskin M E *Physics goals of the Linear Collider Preprint* hep-ph/9910521
Bagger J *et al* (American Linear Collider Working Group), 2000 *The Case for a 500 GeV* e^+e^- *Linear Collider*, *Preprint* hep-ex/0007022
Heuer R D, Miller D, Richard F and Zerwas P M 2001 *Physics at an* e^+e^- *Linear Collider* TESLA Technical Design Report Part III http://tesla.desy.de/new_pages/TDR_CD/start.html
[380] Battaglia M *et al* 2002 *Experimental approaches at Linear Colliders*, SLAC-PUB-9144, SNOWMASS-2001-E3001, *Preprint* hep-ex/0201018 to appear in the *Proc. APS/DPF/DPB Summer Study on the Future of Particle Physics (Snowmass 2001) (Snowmass, Colorado, 30 June 21–July 2001)*
Battaglia M 2001 *Physics signatures at CLIC*, CERN-CLIC-NOTE-474, LC-PHSM-2001-072-CLIC, CLIC-NOTE-474, CERN-OPEN-2001-029 (January 2001), *Preprint* hep-ph/0103338
[381] Linear Collider Physics Resource Book for Snowmass 2001, Part 2: *Higgs and Supersymmetry Studies* (American Linear Collider Working Group), *Preprint* hep-ex/0106056
Murayama H, LBL-38891-REV, UCB-PTH-96-21, Invited talk at 3rd Workshop on Physics and Experiments with e+ e- Linear Colliders (LCWS 95), (8–12 Sep 1995: Iwate, Japan) published in Iwate Linear Colliders 1995:1–23 (QCD161:W579:1995) *Preprint* hep-ex/9606001
[382] 2004-2005 Report of the CLIC Physics Working Group, *Physics at the CLIC multi-TeV Linear Collider* ed Battaglia M *et al* CERN-2004-05 (10 June 2004)

[383] Barklow T L *et al* New directions for high-energy physics Snowmass 1996 SLAC-PUB-7397 CLNS-97-1473 pp 735–59
Barklow T L *et al* 1996 *eConf C960625* **STc118** *Preprint* hep-ph/9704217
[384] Barklow T L, SLAC-REPRINT-2000-107 prepared for *5th Int. Linear Collider Workshop (LCWS 2000) (24–28 Oct 2000 Fermilab, Batavia, Illinois)* Batavia 2000, Physics and experiments with future linear e+ e- colliders pp 568–572 See also [29]
[385] Gianotti F *Advanced Hadron Colliders (science case)*, presentation at the *ICFA Seminar-CERN (8-11 October 2002)* see http://dsu.web.cern.ch/dsu/of/Icfaprog1.html
[386] Gunion J F 1998 *Physics Motivations for a Muon Collider Preprint* hep-ph/9605396 *Physics at a Muon Collider AIP Conf. Proc.* **435** 37 *Preprint* hep-ph/9802258
[387] Blochinger C *et al* 2002 Physics Opportunities at Mu+ Mu- Higgs Factories *Report of the Higgs factory working group of the ECFA-CERN study on Neutrino Factory & Muon Storage Rings at CERN Preprint* hep-ph/0202199
[388] Branson J G, Denegri D, Hinchliffe I, Gianotti F, Paige F E and Sphicas P 2001 *High Transverse Momentum Physics at the Large Hadron Collider, The ATLAS and CMS Collaborations Preprint* hep-ph/0110021
[389] Baur U, Plehn T and Rainwater D 2002 *Phys. Rev. Lett.* **89** 151801 *Preprint* hep-ph/0206024
[390] Bartl A, Eberl H, Kraml S, Majerotto W and Porod W 1997 *Z. Phys.* C **73** 469 *Preprint* hep-ph/9603410
[391] Bartl A, Fraas H and Majerotto W 1987 *Z. Phys.* C **34** 411
[392] Bartl A, Majerotto W and Porod W 1994 *Z.Phys.* C **64** 499
Bartl A, Majerotto W and Porod W 1995 *Z.Phys.* C **68** 518 (erratum) and references therein
[393] Bartl A, Eberl H, Hidaka K, Kraml S, Majerotto W, Porod W and Yamada Y 1999 *Phys. Rev.* D **59** 115007 *Preprint* hep-ph/9806299
[394] Hikasa K and Kobayashi M 1987 *Phys. Rev.* D **36** 724
[395] Porod W J 2002 *High. Energy Phys.* **0205** 030 *Preprint* hep-ph/0202259
[396] Kraan A C 2004 *Eur. Phys. J.* C **37** 91 *Preprint* hep-ex/0404001
[397] Bartl A, Fraas H, Majerotto W and Mosslacher B 1992 *Z.Phys.* C **55** 257
[398] Gunion J F and Haber H E 1988 *Phys. Rev.* D **37** 2515
[399] Ambrosiano S and Mele B 1997 *Phys. Rev.* D **55** 1399
Ambrosiano S and Mele B 1997 *Phys. Rev.* D **56** 3157 (erratum) *Preprint* hep-ph/9609212
[400] Haber H E and Wyler D 1989 *Nucl. Phys.* B **323** 267
[401] Bartl A, Kernreiter T and Kittel O *Phys. Lett.* B 2004 **578** 341 *Preprint* hep-ph/0309340
[402] Bartl A, Hesselbach S, Hidaka K, Kernreiter T and Porod W 2004 *Preprint* hep-ph/0409347 and references therein
[403] Bartl A, Fraas H and Majerotto W 1986 *Z.Phys.* C **30** 441
[404] Bartl A, Fraas H and Majerotto W 1986 *Nucl. Phys.* B **278** 1
[405] Ambrosiano S and Mele B 1995 *Phys. Rev.* D **52** 3900 *Preprint* hep-ph/9503362
[406] Feng J L and Nojiri M M *Linear Collider Physics in the New Millenium*, ed D Miller *et al* (Singapore: World Scientific) *Preprint* hep-ph/0210390 at press
[407] Baer H, Balazs C, Mizukoshi J K and Snowmass 2001 (30 Jun-21 Jul 2001, Snowmass, Colorado) *eConf C010630* (2001) P348 *Preprint* hep-ph/0111029
[408] Carena M, Culbertson R L, Eno S, Frisch H J and Mrenna S 1998 *Perspectives in Supersymmetry*, ed G Kane (Singapore: World Scientific) *Preprint* hep-ex/9802006
[409] Spira M 1997 *Barcelona 1997 Quantum Effects in the Minimal Supersymmetric Standard Model Preprint* hep-ph/9711408
[410] Beenakker W, Hopker R, Spira M and Zerwas P M 1997 *Nucl. Phys.* B **492** 51 *Preprint* hep-ph/9610490
[411] Beenakker W, Hopker R and Spira M 1996 *PROSPINO, a program for the PROduction of Supersymmetric Particles In Next0to leading Order QCD*, *Preprint* hep-ph/9611232 http//people.web.psi.ch/spira/
[412] Azuelos G *et al* (ATLAS Collaboration) *Physics in ATLAS at a possible upgraded LHC*, ATL-PHYS-2001-002
[413] Beenakker W, Kramer M, Plehn T, Spira M and Zerwas P M 1998 *Nucl. Phys.* B **515** 3 *Preprint* hep-ph/9710451
[414] Baer H, Harris B W and Hall Reno M 1998 *Phys. Rev.* D **57** 5871 *Preprint* hep-ph/9712315
[415] Choudhury D, Datta A, Huitu K, Konar P, Moretti S and Mukhopadhyaya B 2003 *Phys. Rev.* D **68** 075007 *Preprint* hep-ph/0304192
[416] Beenakker W, Klasen M, Kramer M, Plehn T, Spira M and Zerwas P M 1999 *Phys. Rev. Lett.* **83** 3780 *Preprint* hep-ph/9906298
[417] Berger E L, Klasen M and Tait T M P 1999 *Phys. Lett.* B **459** 165 *Preprint* hep-ph/9902350
Berger E L, Klasen M and Tait T M P 2000 *Phys. Rev.* D **62** 095014 *Preprint* hep-ph/0005196
Berger E L, Klasen M and Tait T M P 2003 Erratum *Phys. Rev.* D **67** 099901 *Preprint* hep-ph/0212306
[418] Haller J 2002 *Acta Phys. Polon.* **B33** 3875

[419] Affolder T *et al* 2001 (CDF Collaboration) *Phys. Rev. Lett.* **87** 251803
[420] Abbott B *et al* (D0 Collaboration) *Phys. Rev. Lett.* 83 (1999) 4937, *Preprint* hep-ex/9902013
[421] Affolder T *et al* 2001 (CDF Collaboration) *Phys. Rev. Lett.* **88** 041801
[422] LEP SUSY Working Group, the ALEPH, DELPHI, L3 and OPAL Experiments, http://www.cern.ch/lepsusy/Welcome.html (and references therein)
[423] Barbieri R *Z Physics at LEP 1* ed G Altarelli *et al* CERN pp 89-08 vol 2
[424] Datta A and Datta A 2004 *Phys. Lett.* B **578** 165 *Preprint* hep-ph/0210218
[425] Heister A *et al* (ALEPH Collaboration) 2002 *Phys. Lett.* B **544** 73 *Preprint* hep-ex/0207056
[426] Abdallah J *et al* (DELPHI Collaboration) 2003 CERN-EP/2003-007 *Eur. Phys. J.* C**31** 421
[427] Heister A *et al* (ALEPH Collaboration) 2002 *Phys. Lett.* B **537** 5 *Preprint* hep-ex/0204036
[428] Affolder T *et al* (CDF Collaboration) 2000 *Phys. Rev. Lett.* **84** 5704
[429] Abozov V M *et al* (D0 Collaboration) 2002 *Phys. Rev. Lett.* **88** 171802 *Preprint* hep-ex/0108018
[430] Janot P 2004 *Phys. Lett.* B **594** 23
[431] The ALEPH Collaboration, Paper submitted to the *HEP'99 Conf. (Tampere, Finland, 15–21 July)* paper #7_415, ALEPH 99-011 CONF 99-006
[432] Barate R *et al* (ALEPH Collaboration) 2001 *Phys. Lett.* B **499** 67
[433] Gil I, Navas S and Rebecchi P (DELPHI Collaboration)1998 *DELPHI 98-56 CONF 129 (29 June 1998)*
[434] Chen C H, Drees M and Gunion J F 1996 *Phys. Rev. Lett.* **76** 2002 *Preprint* hep-ph/9512230
Chen C H, Drees M and Gunion J F 1999 Erratum *Phys. Rev. Lett.* **82** 3192 *Preprint* hep-ph/9902309
[435] Abdallah J *et al* (DELPHI Collaboration) 2004 *Eur. Phys. J.* C **34** 145 CERN-EP 2003-048
[436] Janot P 2003 *Phys. Lett.* B **564** 183 hep-ph/030207610.1016/S0370-2693(03)00539-2
[437] Farrar G 1996 *Phys. Rev. Lett.* **76** 4111 *Preprint* hep-ph/9603271
Farrar G 1998 *Nucl. Phys. Proc. Suppl.* **62** 485 and references therein
[438] Gutierrez T D, Vogt R and Gunion J F 2000 *Nucl. Phys.* B **591** 277 *Preprint* hep-ph/0002046
[439] Clavelli L 1999 *Preprint* hep-ph/9908342
[440] Dissertori G 1998 *Nucl. Phys. B Proc. Suppl.* **64** 46
[441] Berger E L, Harris B W, Kaplan D E, Sullivan Z, Tait T M P and Wagner C E M 2001 *Phys. Rev. Lett.* **86** 4231 *Preprint* hep-ph/0012001
[442] Chiang C-W, Luo Z and Rosner J L 2003 *Phys. Rev.* D **67** 035008 *Preprint* hep-ph/0207235
[443] Alavi-Harati A *et al* KTeV Collaboration 1999 *Phys. Rev. Lett.* **83** 2128 *Preprint* hep-ex/9903048
[444] Albuquerque I F M *et al* (E761 Collaboration) 1997 *Phys. Rev. Lett.* **78** 3252
[445] Murayama H 2002 *Light Gluino* ed K Hagiwara *et al* Particle data group *Phys. Rev.* D **66** 010001 (http://pdg.lbl.gov/)
[446] Clavelli L 1998 UA-HEP-98-12 *Preprint* hep-ph/9812340
[447] Acciari M *et al* 2000 (L3 Collaboration) *Phys. Lett.* B **472** 420 *Preprint* hep-ex/9910007
[448] Baer H, Cheung K and Gunion J F 1999 *Phys. Rev.* D **59** 075002 *Preprint* hep-ph/9806361
[449] Abdallah J *et al* (DELPHI Collaboration) 2003 *Eur. Phys. J.* C **26** 505
[450] Bekenstein J D 2004 *Preprint* astro-ph/0412652
Milgrom M 1983 *Astrophys. J.* **270** 365
Milgrom M 1983 *Astrophys. J.* **270** 371
Milgrom M 1983 *Astrophys. J.* **270** 384
[451] Srednicki M and Spooner N J C 2002 *Dark matter* ed K Hagiwara *et al* Particle data group *Phys. Rev.* D **66** 010001 (http://pdg.lbl.gov/)
[452] Kolb E W, Matarrese S, Notari A and Riotto A 2005 FERMILAB-PUB-05-024-A
[453] Blanchard A, Douspis M, Rowan-Robinson M and Sarkar S 2003 *Astron. Astrophys.* **412** 35 (astro-ph/0304237)
[454] Bennet C L *et al* (WMAP Collaboration) 2003 *Astrophys. J. Suppl.* **148** 1 (astro-ph/0302207)
Spergel D N *et al* (WMAP Collaboration) 2003 *Astrophys. J. Suppl.* **148** 175 (astro-ph/0302209)
[455] Ellis J 2002 *Supersymmetry for Alp Hikers*, CERN-TH/2002-052, *Preprint* hep-ph/0203114
[456] Olive K A 1999 *Introduction to Supersymmetry: Astrophysical and Phenomenological Constraints*, UMN-TH-1824/99, TPI-MINN-99/49 *Preprint* hep-ph/9911307
[457] Ellis J, Falk T, Olive K A and Santoso Y 2003 *Nucl. Phys.* B **652** 259 *Preprint* hep-ph/0210205
[458] Hooper D and Plehn T 2003 *Phys. Lett.* B **562** 18*Preprint* hep-ph/0212226
[459] Bélanger G, Boudjema F, Pukhov A and Rosier-Lees S 2002 *Preprint* hep-ph/0212227
[460] Ellis J, Olive K A, Santoso Y and Spanos V C 2003 *Phys. Lett.* B **565** 176 *Preprint* hep-ph/0303043
[461] Stark L S, Häfliger P, Biland A and Pauss F 2005 *Preprint* hep-ph/0502197
[462] Ellis J, Olive K A, Santoso Y and Spanos V C 2005 *Preprint* hep-ph/0502001
[463] Bélanger G, Kraml S and Pukhov A 2005 *Preprint* hep-ph/0502079
[464] Roszkowski L 2003 *Nucl. Phys. Proc. Suppl.* **124** 30 Also in **Marina del Rey 2002, Dark Matter** pp 30–37

[465] Mirabolfathi N 2004 *Preprint* astro-ph/0412103
[466] Bottino A *et al* DFTT 35/2000
Ellis J, Ferstl A and Olive K A 2001 *Phys. Rev.* D **63** 065016 *Preprint* hep-ph/0007113
Mandic V, Pierce A, Gondolo P and Murayama H 2000 *Preprint* hep-ph/0008022
Arnowitt R, Dutta B and Santoso Y 2002 *Phys. Atom. Nucl.* **65** 2218
Arnowitt R, Dutta B and Santoso Y 2002 *Yad. Fiz.* **65** 2281 *Preprint* hep-ph/0201194
[467] Morales A 2003 *Nucl. Phys. Proc. Suppl.* **114** 39 (astro-ph/0211446)
[468] Chardin G 2004 *Preprint* astro-ph/0411503
[469] Abrams D *et al* (CDMS Collaboration) 2002 *Phys. Rev.* D **66** 122003 (astro-ph/0203500)
[470] Benoit A *et al* (EDELWEISS Collaboration) 2001 *Phys. Lett.* B **513** 15 (astro-ph/0106094)
[471] Spooner N J C (ZEPLIN Collaboration) 2001 Snowmass 2001 *eConf C010630* E **108**
[472] Meunier P *et al* (CRESST Collaboration) 1999 *Appl. Phys. Lett.* **75** 1335 see also http://avmp01.mppmu.mpg.de/cresst/
[473] Arnaboldi C *et al* 2002 (CUORE Collaboration) *AIP Conf. Proc.* vol **605** 469
Arnaboldi C *et al* 2004 *Nucl. Instrum. Meth.* A **518** 775 *Preprint* hep-ex/0212053
[474] Baudis L *et al* (GENIUS Collaboration) 2002 *Nucl. Instrum. Meth.* A**481** 149 *Preprint* hep-ex/0012022
[475] Morales A *et al* (GEDEON Collaboration) 2001 *29th Int. Meeting on Fundamental Physics* (February 2001: Sitges) *Preprint* hep-ex/0111089
[476] (DRIFT Collaboration) Martoff C J, Snowden-Ifft D P, Ohnuki T, Spooner N and Lehner M 2000 *Nuclear Instruments Methods* in *Phys. Res.* A **440** 355 see also http://www.shef.ac.uk/physics/research/pa/DRIFT.html
[477] Cline D B *et al* (ZEPLIN Collaboration) 2003 *Nucl. Phys. B Proc. Suppl.* **124** 229
[478] Klapdor-Kleingrothaus H V, Majorovits B, Baudis L, Dietz A, Heusser G, Krivosheina I and Strecker H (GENIUS Collaboration) 2001 *Preprint* hep-ph/0103082
[479] Schnee R W, Akerib D S, Gaitskell R J (CryoArray Collaboration) 2003 *Nucl. Phys. B Proc. Suppl.* **124** 233 (astro-ph/0208326).
[480] Ramachers Y 2003 *Nucl. Phys. Proc. Suppl.* **118** 341 (astro-ph/0211500)
[481] Sikivie P, Tkachev I I and Wang Y 1997 *Phys. Rev.* D **56** 1863 (astro-ph/9609022)
[482] Bernabei R *et al* (DAMA Collaboration) 2000 *Phys. Lett.* B **480** 23
[483] Bernabei R *et al* (DAMA Collaboration) 2003 *Riv. Nuovo Cim.* **26** 1 (astro-ph/0307403) *Beyond the Desert (BEYOND 03) (9-14 Jun 2003: Castle Ringberg, Tegernsee, Germany) Preprint* astro-ph/0311046
[484] Bottino A, Donato F, Fornengo N and Scopel S 2002 *Nucl. Phys. Proc. Suppl.* **113** 50 *Preprint* hep-ph/0208273
[485] Green A M 2003 *IAU Symp. 220: Dark Matter in Galaxies (21-25 Jul 2003 Sydney, Australia) Preprint* astro-ph/0310215
[486] Arnowitt R and Dutta B 2002 *Preprint* hep-ph/0211042
[487] Baer H, Balazs C, Belyaev A and O'Farrill J 2003 *J. Cosmol. Astropart. Phys.* **0309** 007 *Preprint* hep-ph/0305191
[488] Nojiri M M 2004 *Pramana* **62** 335 *Preprint* hep-ph/0305192
[489] Nolan P L *et al* (EGRET Collaboration) 1992 *IEEE Transactions Nucl. Sci.* **39** 993
Hartman R C *et al* 1999 Astrophys.J.Suppl. **123** 79 see also http://lheawww.gsfc.nasa.gov/docs/gamcosray/EGRET/egret.html
[490] Morselli A *et al* (GLAST Collaboration) 2002 *Nucl. Phys. B Proc. Suppl.* **113** 213 (astro-ph/0211327)
Peirani S, Mohayaee R, de Freitas Pacheco J A 2004 *Phys. Rev.* D **70** 043503 (astro-ph/0401378)
[491] Barrio J A *et al The Magic Telescope*, MPI-PhE/98-5
Flix J, Martinez M and Prada F 2004 *Preprint* astro-ph/0401511 see also http://wwwmagic.mppmu.mpg.de/
[492] Konopelko A 1999 *Astropart. Phys.* **11** 263 see also http://www.mpi-hd.mpg.de/hfm/HESS/HESS.html
[493] Weekes T C *et al* 2002 *Astropart. Phys.* **17** 221 see also http://veritas.sao.arizona.edu/
[494] Moore B, Governato F, Quinn T, Stadel J and Lake G 1998 *Astrophys. J.* **499** L5 (astro-ph/9709051)
[495] Hisano J, Matsumoto S and Nojiri M M 2003 *Phys. Rev.* D **67** 075014 *Preprint* hep-ph/0212022
[496] Barwick S W *et al* (HEAT Collaboration) 1997 *Astrophys. J.* **482** L191 (astro-ph/9703192)
[497] Alcaraz J *et al* 2000 *Phys. Lett.* B **484** 10
[498] Maeno T *et al* (BESS Collaboration) 2001 *Astropart. Phys.* **16** 121 (astro-ph/0010381)
[499] de Boer W 2004 *Preprint* astro-ph/0412620
de Boer W, Herold M, Sander C and Zhukov V 2004 *Eur. Phys. J.* C **33** S981 *Preprint* hep-ph/0312037
[500] Hooper D, Taylor J E and Silk J 2004 *Phys. Rev.* D **69** 103509 *Preprint* hep-ph/0312076
[501] Strong A W, Moskalenko I V and Reimer O 2004 Astrophys.J. **613** 962 and 956
Moskalenko I V 2004 *Preprint* astro-ph/0410241
[502] Baer H, Belyaev A, Krupovnickas T and Tata X 2004 *J. High. Energy Phys.* JHEP **0402** 007 *Preprint* hep-ph/0311351

[503] Cheng H-C, Feng J L, Matchev K T 2002 *Phys. Rev. Lett.* **89** 211301 *Preprint* hep-ph/0207125
Servant G and Tait T M P 2002 *New J. Phys.* **4** 99 *Preprint* hep-ph/0209262
Bertone G, Servant G and Sigl G 2003 *Phys. Rev.* D **68** 044008 *Preprint* hep-ph/0211342
Hooper D and Silk J 2004 *New J. Phys.* **6** 023 *Preprint* hep-ph/0311367
[504] Boehm C, Hooper D, Silk J, Casse M and Paul J 2004 *Phys. Rev. Lett.* **92** 101301 (astro-ph/0309686)
[505] Knodlseder J *et al* astro-ph/0309442 *Astron. Astrophys.* submitted
Jean P *et al* 2003 *Astron. Astrophys.* **407** L55 (astro-ph/0309484)
[506] Ghosh D K, Roy P and Roy S 2000 JHEP **0008** 031 *Preprint* hep-ph/0004127
[507] Abdallah J *et al* 2003 (DELPHI Collaboration) *Eur. Phys. J.* C **27** 153
[508] Heister A *et al* (ALEPH Collaboration) 2002 *Eur. Phys. J.* C**25** 339 *Preprint* hep-ex/0203024
[509] Abe F *et al* (CDF Collaboration) 1999 *Phys. Rev.* D **59** 092002
[510] Ask S *et al* (DELPHI Collaboration) DELPHI 2003-040-CONF-660, contributed to EPS 2003 (Aachen) and LP 2003 (FNAL)
Abreu P *et al* (DELPHI Collaboration) 2000 *Eur. Phys. J.* C **17** 53
[511] Abbott B *et al* (D0 Collaboration) 1998 *Phys. Rev. Lett.* **80** 442
[512] Culbertson R *et al* (SUSY Working Group Collaboration) 2000 Part 3 of physics at Run II SUSY/Higgs report *Preprint* hep-ph/0008070
[513] Dreiner H 1997 in *Perspectives in Supersymmetry*, ed G Kane (Singapore: World Scientific) *Preprint* hep-ph/9707435
[514] Bhattacharyya G 1998 *Proc. Beyond the Desert 1997* ed H V Klapdor-Kleingrothaus and H Pas (Oxford: IOP Publishing) 114 *Preprint* hep-ph/9709395
Bhattacharyya G and Pal P B 1999 *Phys. Rev.* D **59** 97701 9, SINP/TNP/98-22 *Preprint* hep-ph/9809493
[515] Bhattacharyya G, Pas H, Song L-G, Weiler T J 2003 *Phys. Lett.* B **564**175 *Preprint* hep-ph/0302191
[516] Dreiner H and Ross G G 1991 *Nucl. Phys.* B **365** 597
Dawson S 1985 *Nucl. Phys.* B **261** 297
[517] Allanach B C, Dreiner H K, Morawitz P and Williams M D 1998 *Phys. Lett.* B **420** 307 *Preprint* hep-ph/9708495
[518] Buchmuller W, Rückl R and Wyler D 1987 *Phys. Lett.* B **191** 442
Buchmuller W, Rückl R and Wyler D 1999 Erratum *Phys. Lett.* **448** 320
[519] Kalinowski J *et al* 1997 *Z. Phys.* C **74** 595 *Preprint* hep-ph/9703288
[520] Zhang Z 2001 LAL-2001-30, *Preprint* hep-ex/0107017
[521] Heister A *et al* (ALEPH Collaboration) 2003 *Eur. Phys. J.* C**31** 1 *Preprint* hep-ex/0210014
[522] Abdallah J *et al* (DELPHI Collaboration) CERN-EP 2003-092 *Eur. Phys. J.* C**36** (2004) 1
Abdallah J *et al* (DELPHI Collaboration) 2004 Erratum *Eur. Phys. J.* C37 129
Achard P *et al* (L3 Collaboration) 2002 CERN-EP/01-068 *Phys. Lett.* B **524** 65
Abbiendi G *et al* (OPAL Collaboration) 2004 CERN-EP-2003-036 *Eur. Phys. J.* C**33** 149
[523] Abbiendi G *et al* (OPAL Collaboration) 2000 *Eur. Phys. J.* C **13** 553 CERN-EP/99-097
[524] Barate R *et al* (ALEPH Collaboration) 2001 *Eur. Phys. J.* C **19** 415 CERN-EP/2000-132
[525] Abdallah J *et al* (DELPHI Collaboration) *Eur.Phys. J.* C **28** (20031) **15** CERN-EP/2002-090
[526] Heister A *et al* (ALEPH Collaboration) 2002 *Eur. Phys. J.* C **25** 1 CERN-EP/2001-094
[527] Abbiendi G *et al* (OPAL Collaboration) 2002 *Phys. Lett.* B **526** 233 CERN-EP/2001-093 *Preprint* hep-ex/0112024 and 2002 *Eur. Phys. J.* C**23** 1 CERN-EP/2001-040 *Preprint* hep-ex/0106031
[528] Adloff C *et al* (H1 Collaboration) 2001 *Eur. Phys. J.* C**20** 639 *Preprint* hep-ex/0102050
[529] Breitweg J *et al* (Zeus Collaboration) 2000 *Eur. Phys. J.* C**16** 253 *Preprint* hep-ex/0002038 and 2001 *Phys. Rev.* D **63** 052002 *Preprint* hep-ex/0009059
[530] Abe F *et al* (CDF Collaboration) 1999 FERMILAB-PUB-98/374-E *Phys. Rev. Lett.* **83** 2133
[531] Acosta D *et al* (CDF Collaboration) 2004 *Phys. Rev. Lett.* **92** 051803 *Preprint* hep-ex/0305010
[532] Abbott B *et al* (D0 Collaboration) 1998 *Phys. Rev. Lett.* **80** 2051
[533] Schöning A 2000 Search for Leptoquarks *14th Workshop on Radiation Detectors and Their Uses* (1-3 Feb 2000: Tsukuba, Japan) *Preprint* hep-ex/0201011
[534] CMS Collaboration 1994 *Technical Proposal* CERN/LHCC 94–**38**
[535] Abdullin S *et al* 2002 Discovery potential for supersymmetry in CMS *J.Phys.* G **28** 469 *CMS NOTE* 1998/006 (April 1998) *Preprint* hep-ph/9806366 see also http://cmsdoc.cern.ch/cms/PRS/results/susybsm/susybsm.html
[536] Gianotti F and Mangano M L 2005 *Preprint* hep-ph/0504221
[537] Mangano M L, Moretti M, Piccinini F, Pittau R and Polosa A D 2003 *J. High Energy Phys.* JHEP **0307** 001 *Preprint* hep-ph/0206293
[538] Asai S *Studies of V+jets backgrounds to SUSY searches*, presented at the *TeV4LHC Workshop* (28-30 April, 2005: CERN) see http://conferences.fnal.gov/tev4lhc/

[539] Dittmar M CMS CR 1999/007, ETHZ-IPP PR-98-08 and references therein
[540] Paige F E 1997 Search for SUSY at LHC: Precision Measurements, *Int. Europhysics Conf. on High Energy Physics* (Jerusalem, 1997) *Preprint* hep-ph/9712402
Hinchliffe I, Paige F E, Shapiro M D, Soderqvist J and Yao W 1997 *Phys. Rev.* D **55** 5520 *Preprint* hep-ph/9610544
[541] Bachacou H, Hinchliffe I and Paige F E 2000 *Phys. Rev.* D **62** 015009 *Preprint* hep-ph/9907518
Allanach B C, Lester C G, Parker M A and Webber B R 2000 *HEP* **0009** 004 *Preprint* hep-ph/0007009
Paige F E *SUSY signatures at LHC*, SUSY02, (17-23 June 2002: Hamburg, Germany) *Preprint* hep-ph/0211017
Chiorboli M and Tricomi A Squark and Gluino reconstruction in CMS, *CMS NOTE*-2004/029 (22 November 2004)
[542] Gjelsten B K, Miller D J and Osland P 2004 *J. High Energy Phys.* JHEP **0412** 003 *Preprint* hep-ph/0410303 v2 and *Preprint* hep-ph/0501033
[543] Polesello G private communication quoted in [550] and presentation at the Les Houches Workshop, June 2003
[544] Paige F E 2002 *SUSY signatures at LHC*, SUSY02 (17–23 June 2002 Hamburg, Germany) *Preprint* hep-ph/0211017
[545] Bityukov S I and Krasnikov N V 2002 *Phys. Atom. Nucl.* **65** 1341
Bityukov S I and Krasnikov N V 2002 *Yad. Fiz.* **65** 1374 *Preprint* hep-ph/0102179
[546] Baer H, Mercadante P G, Tata X and Wang Y-L 2000 *Phys. Rev.* D **62** 095007 *Preprint* hep-ph/0004001
[547] Barr A J, Lester C G, Parker M A, Allanach B C and Richardson P 2003 *J. High Energy Phys.* JHEP **0303** 045 *Preprint* hep-ph/0208214
[548] Martyn H-U and Blair G A 1999 *Preprint* hep-ph/9910416
[549] Feng J L, Peskin M E, Murayama H and Tata X 1995 *Phys. Rev.* D **52** 1418 *Preprint* hep-ph/9502260
[550] Battaglia M, De Roeck A, Ellis J, Gianotti F, Olive K A and Pape L 2004 Updated Post-WMAP Benchmarks for Supersymmetry *Eur. Phys. J.* C**33** 273 *Preprint* hep-ph/0306219
[551] Ellis J, Feng J L, Ferstl A, Matchev K and Olive K A 2002 Prospects for Detecting Supersymmetric Dark Matter at Post-LEP Benchmark Points *Eur. Phys. J.* C **24** 311 (astro-ph/0110225)
[552] R parity Working Group Collaboration (Allanach B *et al*) 1999 *Part 4 of physics at Run II SUSY/Higgs report Preprint* hep-ph/9906224
[553] Mirea A and Nagy E 1999 *Preprint* hep-ph/9904354
[554] Allanach B C, Barr A J, Parker M A, Richardson P and Webber B R 2001 *J. High. Energy Phys. JHEP* **0109** 021 *Preprint* hep-ph/0106304
[555] Choudhury D, Godbole R M and Polesello G 2002 *J. High. Energy Phys. JHEP* **0208** 004 *Preprint* hep-ph/0207248
[556] Chiappetta P, Deandrea A, Nagy E, Negroni S, Polesello G and Virey J M 2000 *Phys. Rev.* D **61** 115008 *Preprint* hep-ph/9910483
[557] Moreau G, Perez E and Polesello G 2001 *Nucl. Phys.* B **604** 3 *Preprint* hep-ph/0003012
[558] Allanach B C, Barr A J, Drage L, Lester C G, Morgan D, Parker M A, Webber B R and Richardson P 2001 *J. High. Energy Phys. JHEP* **0103** 048 *Preprint* hep-ph/0102173
[559] Besançon M and Moreau G 1999 *4th Int. Workshop on Linear Colliders (LCWS 99) (28 Apr–5 May 1999, Sitges, Barcelona, Spain) Preprint* hep-ph/9909441
[560] Peskin M E 1997 *Beyond the Standard Model*, lectures given at The 1996 European School of High-Energy Physics (1-14 Sep 1996, Carry-le-Rouet, France) *Preprint* hep-ph/9705479
[561] Choi S Y, Djouadi A, Dreiner H, Kalinowski J and Zerwas P M 1999 *Eur. Phys. J.* C**7** 123 *Preprint* hep-ph/9806279
Choi S Y, Djouadi A, Song H S and Zerwas P M 1999 *Eur. Phys. J.* C**8** 669 *Preprint* hep-ph/9812236
[562] Kneur J L and Moultaka G 1999 *Phys. Rev.* D **59** 015005 *Preprint* hep-ph/9807336
[563] Choi S Y, Djouadi A, Guchait M, Kalinowski J, Song H S and Zerwas P M 2000 *Eur. Phys. J.* C**14** 535 *Preprint* hep-ph/0002033
[564] see contributions in the LHC/LC working group document, http://www.ippp.dur.ac.uk/ georg/lhclc/
Lafaye R, Plehn T, Zerwas D, *SFITTER: SUSY Parameter Analysis at LHC and LC*
Bechtle P, Desch K and Wienemann P *Fittino: A global fit of the MSSM parameters*
[565] Blair G A, Porod W and Zerwas P M 2001 *Phys. Rev.* D **63** 017703 *Preprint* hep-ph/0007107
Blair G A 2000 *Preprint* hep-ph/0011367
[566] Allanach B C, Blair G A, Freitas A, Kraml S, Martyn H U, Polesello G, Porod W and Zerwas P M 2004 *Nucl. Phys. Proc. Suppl.* **135** 107 *Preprint* hep-ph/0407067
[567] Binetruy P, Gaillard M K and Nelson B D 2001 *Nucl. Phys.* B **604** 32 *Preprint* hep-ph/0011081
[568] Nojiri M M *et al* 1996 *Phys. Rev.* D **54** 6756 (*Preprint* hep-ph/9606370)
[569] Barger V D *et al* 2001 *Phys. Rev.* D **64** 056007 (Preprint hep-ph/0101106)